Technische Universität München
TUM School of Natural Sciences

Studies on the Reactivity of Two Coordinate Acyclic Imino(silyl)silylene

Huaiyuan Zhu

Vollständiger Abdruck der von der TUM School of Natural Sciences der Technischen Universität München zur Erlangung eines

Doktors der Naturwissenschaften (Dr. rer. nat.)

genehmigten Dissertation.

Vorsitz: Prof. Dr. Torben Gädt

Prüfer*innen der Dissertation:

1. Prof. Dr. Shigeyoshi Inoue
2. Priv.-Doz. Dr. Felicitas Lips

Die Dissertation wurde am 12.01.2024 bei der Technischen Universität München eingereicht und durch die TUM School of Natural Sciences am 02.02.2024 angenommen.

Acknowledgments

I would first like to express my sincere appreciation to my supervisor Professor Shigeyoshi Inoue, for recruiting me into the research group and giving the opportunity to immerse me in the research. I am also grateful to him for his guidance, patience and support throughout my whole study period. Without his advice and help, I cannot finish my Ph.D thesis, even would never be a doctor of science in my life.

I am grateful to Dr. Felicitas Lips for acting as the examiner for this thesis, and Prof. Dr. Torben Gädt for accepting the invitation to be the chairman of the examination committee.

I would like to express my sincere thanks to my mentor Dr. Daniel Franz. I have learnt a lot of knowledge from him. Without his help, it would be tough for me.

I would like to thank Dr. Arseni Kostenko for his help with theoretical calculations and polishness of my article. I am very thankful to Dr. Franziska Hanusch, Dr. Shiori Fujimori, Dr. Christian Jandl, Dr. John A. Kelly and Mr. Sebastian Stigler for measuring crystals and for their help in solving the crystal structures. I would like to thank Dr. John A. Kelly for proof-reading and correcting this thesis. I thank Ms. Lisa Groll for translating the abstract.

I would also like to thank all the staff of the analytic department of Catalysis Research Center, Technische Universität München for their excellent work and strong support. I would like to thank Dr. Florian Tschernuth and Ms. Teresa Eisner for the VT-NMR measurements. I would also like to appreciate Olaf Ackermann for the melting point measurement. I would like to thank Dr. Maximilian Muhr and Mr. Tobias Weng for the LIFDI-MS measurements. In addition, I would like to thank Dr. Ammari Ulrike for the elemental analysis measurements.

I would like to thank all members of AK Inoue group for their support and help.

I would like to express my sincere thanks my families and friends for the support and encouragement throughout the four years.

I should finally thank the China Scholarship Council (CSC) for the financial support during my study in Germany.

List of Abbreviations

ΔE_{ST}	singlet-triplet energy gap [kcal/mol]
δ	chemical shift [ppm]
λ	wavelength [nm]
Ad	adamantyl
Ar	aryl
BCF	tris(pentafluorophenyl)borane
Bu	butyl
cf.	latin confer/conferatur: “compare”
cAAC	cyclic alkyl(amino) carbene
CGMT	“Carter-Goddard-Malrieu-Trinquier”
Ch	chalcogen
cHex	cyclohexyl
CHT	cycloheptatriene
Cp*	pentamethylcyclopentadienyl
CVD	chemical vapor deposition
d	day(s)
DFT	density functional theory
Dipp	2,6-diisopropylphenyl
^{Dipp}Ter	2,6-bis(2,6-^{i}Pr$_2$-C$_6$H$_3$)C$_6$H$_3$
DMAP	4-*N*,*N*-dimethylaminopyridine
DME	1,2-dimethoxyethane
E	element
EA	elemental analysis
e.g.	latin exempli gratia: “for example”
E_{Hybrid}	energy of hybridization [kcal/mol]
EPR	electron paramagnetic resonance
Et	ethyl
et al.	latin et alii: “and others”
etc.	latin phrase et cetera: “and others”
GIAO	gauge-including atomic orbitals
h	hour(s)

HOMO	highest occupied molecular orbital
HMPA	hexamethylphosphoric triamide
hypersilyl	tris(trimethylsilyl)silyl
i	iso
i.e.	latin (id est): “that is”
IDipp	1,3-bis(2,6-diisopropylphenyl)imidazolin-2-ylidene
IDippN	1,3-bis(2,6-diisopropylphenyl)imidazolin-2-iminato
I^{t}BuN	1,3-bis(*tert*-butyl)imidazolin-2-iminato
I^{i}Pr$_2$Me$_2$	1,3-diisopropyl-4,5-dimethylimidazolin-2-ylidene
IMe$_4$	1,3,4,5-tetramethylimidazolin-2-ylidene
in situ	latin: “on site”
IR	infrared
LUMO	lowest unoccupied molecular orbital
M	metal
m	*meta*
m.p.	melting point
Me	methyl
Mes	2,4,6-trimethylphenyl
^{Mes}Ter	2,6-bis(2,4,6-Me$_3$-C$_6$H$_2$)C$_6$H$_3$
Mes*	supermesityl | 2,4,6-^{t}Bu$_3$-C$_6$H$_2$
LIFDI–MS	Liquid injection field desorption ionization mass spectrometry
L$_n$M	transition metal complex
NAO	natural atomic orbital
nacnac	*β*-diketiminato
NBO	natural bond order
NHBO	*N*-heterocyclic boryloxy
NHC	*N*-heterocyclic carbene
NHI	*N*-heterocyclic imine
NHO	*N*-heterocyclic olefin
NHSi	*N*-heterocyclic silylene
NMR	nuclear magnetic resonance
NPA	natural population analysis
NRT	natural resonance theory
o	*ortho*

p	*para*
PDMS	poly(dimethylsiloxane)
Ph	phenyl
ppm	parts per million
Pr	propyl
QTAIM	quantum theory of atoms in molecules
R	substituent / functional group
r.t.	room temperature
SC-XRD	single-crystal X-ray diffractometry
silepin	sila-2,4,6-cycloheptatriene
supersilyl	tri-*tert*-butylsilyl
t	*tert*
Tbt	2,6-tris[bis(trimethylsilyl)methyl]phenyl
TEMPO	(2,2,6,6,-tetramethylpiperidin-1-yl)oxyl
THF	tetrahydrofuran
Tipp	2,4,6-triisopropylphenyl
TMS	trimethylsilyl
Tol	toluene
UV–vis	ultraviolet–visible
VT	variable temperature
WBI	*Wiberg* bond index
WCA	weakly coordinating anion
vide infra	latin: “see below”
vide supra	latin: “see above”
X	halogen
XRD	X-ray diffractometry

Publication List

- H. Zhu, A. Kostenko, D. Franz, F. Hanusch, S. Inoue, Room Temperature Intermolecular Dearomatization of Arenes by an Acyclic Iminosilylene. *J. Am. Chem. Soc.* **2023**, *144*, 1011-1021. https://doi.org/10.1021/jacs.2c10467

- H. Zhu, F. Hanusch, S. Inoue, Facile Bond Activation of Small Molecules by an Acyclic Imino(silyl)silylene. *Isr. J. Chem.* **2023**, *64*, e202300012. https://doi.org/10.1002/ijch.202300012

- H. Zhu, A. Kostenko, J. A. Kelly, S. Inoue, Substituent Exchange between an Imino(silyl)silylene and Aryl Isocyanides. *Chem* accepted.

Publications beyond the scope of this thesis:

- H. Zhu, S. Fujimori, A. Kostenko, S. Inoue, Dearomatization of C_6 Aromatic Hydrocarbons by Main Group Complexes. *Chem. Eur. J.* **2023**, e202301973 https://doi.org/10.1002/chem.202301973

Conference Contributions

- H. Zhu, D. Franz, A. Porzelt, S. Inoue, Synthesis, isolation and reactivity of acyclic iminosilylsilylenes, *19th International Symposium on Silicon Chemistry* **2021**, Toulouse, France (Online Conference); **Poster Presentation**.

- H. Zhu, A. Kostenko, S. Inoue, Small Molecules Activation by an Isolable Acyclic Imino(silyl)silylene, *International Conference on Phosphorus, Boron and Silicon* **2023**, Berlin, Germany; **Poster Presentation**.

- H. Zhu, A. Kostenko, S. Inoue, Isocyanides Mediated Aryl and Silyl Exchange of Acyclic Imino(silyl)silylene *via* Cleavage of Aryl C–N Bond, *10th European Silicon Days* 2023, Montpellier, France; **Poster Presentation**.

Abstract

In the current era there is a push for more sustainable chemistry, with the focus being on utilizing more abundant and less toxic materials, in the hopes to substitute the ubiquitous transition metal catalysts with more environmentally friendly elements. A prime example of such an element is silicon, which is the second most abundant element in the Earth's crust and is generally non-toxic. Therefore, this doctoral thesis is focused on the synthesis and reactivity study of isolable low oxidation state silicon compounds, in this case acyclic silylenes, with the aim to further reveal their potential application in metal-free catalysis.

First, the synthesis and isolation of a novel non-transient acyclic imino(silyl)silylene, bearing a bulky super silyl group (−Si^{t}Bu$_3$) and *N*-heterocyclic imine ligand with a methylated backbone, was presented. Initial studies revealed the intramolecular C−H activation of an aryl substituent occurs at elevated temperatures. Moreover, the imino(silyl)silylene exhibits an intermolecular Büchner-ring-expansion-type reactivity. The silylene is capable of dearomatizating arenes such as benzene and pyridine giving the corresponding silicon analogs of cycloheptatrienes and azacycloheptatrienes, *i.e*. silepins and azasilepins, respectively. Notably, the ring expansion reactions of the imino(silyl)silylene with benzene and 1,4-bis(trifluoromethyl)benzene are reversible. DFT calculations reveal an ambiphilic nature of the imino(silyl)silylene that allows the intermolecular aromatic C–C/N bond insertion to occur. Additional computational studies elucidate the inherent reactivity of the imino(silyl)silylene, the role of the substituent effect, and reaction mechanisms for the ring expansion transformations, are presented.

In a follow-up publication, the striking activation of various small molecules such as ethylene, dihydrogen, alkene, alkyne, silane and borane under mild conditions utilizing the imino(silyl)silylene was outlined. In addition, the re- and dearomative capabilities of the imino(silyl)silylene were demonstrated by the reaction with quinone and xanthone. Moreover, reactions with heavier chalcogens (S, Se, Te) allow the isolation of neutral three-coordinate Si=Ch complexes (S, Se, Te).

Finally, the reaction of various isocyanides with the acyclic imino(silyl)silylene was reported. Initial reaction with ^{t}BuNC resulted in the quantitative formation of the corresponding cyanosilane and isobutylene *via* cleavage of ^{t}Bu–NC bond and proton abstraction from the ^{t}Bu group. Moreover, the reaction with less bulky aryl isocyanides, led to C–N bond cleavage, and the transformation of aryl isocyanide to silylcyanide and diaryldiiminodisilene The reaction with bulkier aryl isocyanide afforded (imino)(iminoacyl)silylene reversibly *via* the migratory

insertion of isocyanide to Si–Si bond of the imino(silyl)silylene. A proposed reaction mechanism for the aryl and silyl group exchange, based on experimental evidence and supported by quantum chemical calculations, involves an initial insertion of aryl isocyanide into the Si–Si bond of imino(silyl)silylene and a subsequent aryl transfer to the silylene center *via* aryl C–N bond cleavage.

Kurzusammenfassung

In der gegenwärtigen Ära wird ein Vorstoß zu nachhaltigerer Chemie gemacht, wobei der Schwerpunkt auf der Nutzung häufiger vorkommender und weniger toxischer Materialien liegt, in der Hoffnung, die allgegenwärtigen Übergangsmetallkatalysatoren durch umweltfreundlichere Elemente zu ersetzen. Ein Paradebeispiel für ein solches Element istdas im allgemeinen ungiftige Silizium, das zweithäufigste Element in der Erdkruste. Daher konzentriert sich diese Doktorarbeit auf die Synthese und Reaktivitätsstudie isolierbarer Siliziumverbindungen mit niedrigem Oxidationszustand, in diesem Fall acyclischer Silylene, mit dem Ziel, deren potenzielle Anwendung in der metallfreien Katalyse weiterzuentwickeln.

Zunächst wurde die Synthese und Isolierung eines neuen stabilen acyclischen Imino(silyl)silylens vorgestellt, welches von einer sperrigen Supersilylgruppe (−Si^{t}Bu$_3$) und einen *N*-heterocyclischen-Imin-Liganden mit einem methylierten Rückgrat stabilisiert ist. Erste Studien zeigten, dass die intramolekulare C–H-Aktivierung eines Arylsubstituenten bei erhöhten Temperaturen erfolgt. Darüber hinaus zeigt das Imino(silyl)silylen die Fähigkeit zu intermolekularen Büchner-Ringerweiterungen. Das Silylen ist in der Lage, Arene wie Benzol und Pyridin zu de-aromatisieren, wodurch die entsprechenden Siliciumanaloga von Cycloheptatrienen und Azacycloheptatrienen entstehen, d. h. Silepine bzw. Azasilepine. Bemerkenswert ist, dass die Ringerweiterungsreaktionen des Imino(silyl)silylens mit Benzol und 1,4-Bis(trifluormethyl)benzol reversibel sind. DFT-Rechnungen zeigen die Ambiphilität des Imino(silyl)silylens, die die intermolekulare aromatische C–C/N-Bindungsinsertion ermöglicht. Zusätzliche theoretische Berechnungen verdeutlichen die grundlegende Reaktivität des Imino(silyl)silylens, die Rolle des Substituenteneffekts und Reaktionsmechanismen für die Ringerweiterungen.

In einer Folgepublikation wurde die bemerkenswerte Reaktivität des Imino(silyl)silylen gegenüber verschiedener kleiner Moleküle wie Ethylen, Diwasserstoff, Alken, Alkin, Silan und Boran unter milden Bedingungen beschrieben. Darüber hinaus wurden die Re- und Desaromatisierungsfähigkeiten des Imino(silyl)silylens durch die Reaktion mit Chinon und Xanthon demonstriert. Darüber hinaus ermöglichen Reaktionen mit schwereren Chalkogenen (S, Se, Te) die Isolierung neutraler dreifach koordinierter Si=Ch Doppelbindungskomplexe (S, Se, Te).

Schließlich wurde über die Reaktion verschiedener Isocyanide mit dem acyclischen Imino(silyl)silylen berichtet. Die Reaktion mit ^{t}BuNC führte zur quantitativen Bildung des entsprechenden Cyanosilans und Isobutylens *via* Spaltung der ^{t}Bu-NC-Bindung und

Protonenabstraktion von der ^{t}Bu-Gruppe. Darüber hinaus führte die Reaktion mit weniger sperrigem Arylisocyanid zur Spaltung der Aryl C–N-Bindung und zur Umwandlung von Arylisocyanid in Silylcyanid und Diaryldiiminodisilen. Die Reaktion mit sperrigerem Arylisocyanid erfolgte über die migratorische Insertion von Isocyanid in die Si–Si-Bindung des Imino(silyl)silylens und ergab reversibel (Imino)(iminoacyl)silylen. Ein vorgeschlagener Reaktionsmechanismus für den Aryl- und Silylgruppenaustausch, der auf experimentellen Beweisen basiert und durch quantenchemische Berechnungen gestützt wird, beinhaltet eine anfängliche Insertion von Arylisocyanid in die Si–Si-Bindung von Imino(silyl)silylen und einen anschließenden Aryltransfer auf das Silylen Zentrum über Aryl C–N-Bindungsspaltung.

Table of Contents

1. Introduction

Catalysis, that is a chemical term originated by the Jöns Jacob Berzelius in 1835 and defined by Wilhelm Ostwald based on reaction kinetics. Nowadays, catalysis is ubiquitous in the modern world with nearly 90% of commercially produced chemicals involving a catalyst at some stage of their manufacturing process.[1]

The fundamental steps associated with catalysis are oxidative addition and reductive elimination. As shown in Figure 1, the initial step is the addition of the substrate to the active catalyst affording an oxidized complex. Subsequent migratory insertion or σ-bond metathesis with other reagents, results in product formation. The final step is reductive elimination, releasing the desired product and regenerating the active catalyst.[2]

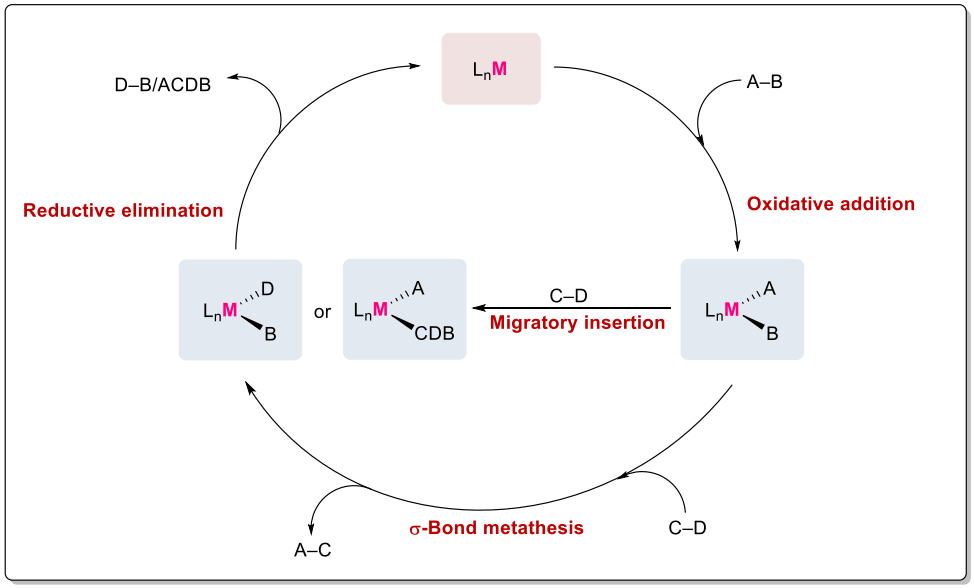

Figure 1. Representation of a conventional catalytic cycle and its most common elemental steps. A, B, C and D were substituents.

The biggest application of the oxidative addition and reductive elimination reaction pathway is cross-coupling reactions, catalyzed by transition metal, in which one of the most important reactions is the formation of C–E bonds (E = main group elements, usually carbon). Another important reaction is the catalytic hydrogenation of unsaturated bonds since it is relevant to commercial applications. In most cases, these type of reactions rely on precious metal catalysts composed of metals, such as platinum (Pt), palladium (Pd), ruthenium (Ru), rhodium (Rh), iridium (Ir). However, the use of these metals is limited by their high cost, low abundancy, and biological compatibility. Thus, the substitution of precious metal catalysts with economically

and ecologically friendly earth-abundant element catalysts is highly desirable in terms of sustainability.[2-3]

In 2005, Power and co-workers disclosed the first facile dihydrogen splitting by a heavy alkyne analogue (a digermyne) without the utilization of any catalyst, showcasing the similar reactivity between low oxidation state main group elements and transition metals.[4] Notably, they also showed the reversible reactions of ethylene with distannynes under ambient conditions, which first showed the oxidative addition/reductive elimination processes in main group compounds.[5] A year later, the Stephan group presented the reversible splitting of dihydrogen by a phosphino-borane, a so-called Frustrated Lewis Pair (FLP), which has emerged as an effective metal-free hydrogenation catalyst for unsaturated systems.[6-10] Since then, the field of main group based catalysis has been booming.

A very promising main group element for the substitution of transition metals is silicon, due to its very high abundancy and non-toxicity. So far, silicon-based catalysis has mainly focused on the utilization of the Lewis acidity of tetravalent organosilicon compounds.[11-12] Recently it has been shown that lox oxidation state silicon compounds have reactivity reminiscent of transition metals (*vide infra*) Thus, low-valent organosilicon compounds could be excellent candidates in catalytic reactions. However, reports on the applications of low-valent silicon-based catalysis such as silylenes, silyliumylidene cations, are still scarce and further intensive research is required.[13-19]

2. Organosilicon Chemistry

The metalloid silicon is the second most abundant elements in the Earth's crust after oxygen (46.4%) with a natural occurrence of 28.2% (Figure 2).[20] Elemental silicon was first discovered by Jöns Jakob Berzelius in 1824 *via* the reduction of hexafluorosilicate with elemental potassium. Silicon generally adopts an sp^3 hybridization bonding with four substituents, leading to a tetrahedral coordination sphere. For instance, orthosilicate (SiO_4^{4-}) is one of the most common forms of silicon in nature owing to the high oxophilicity of silicon.[21]

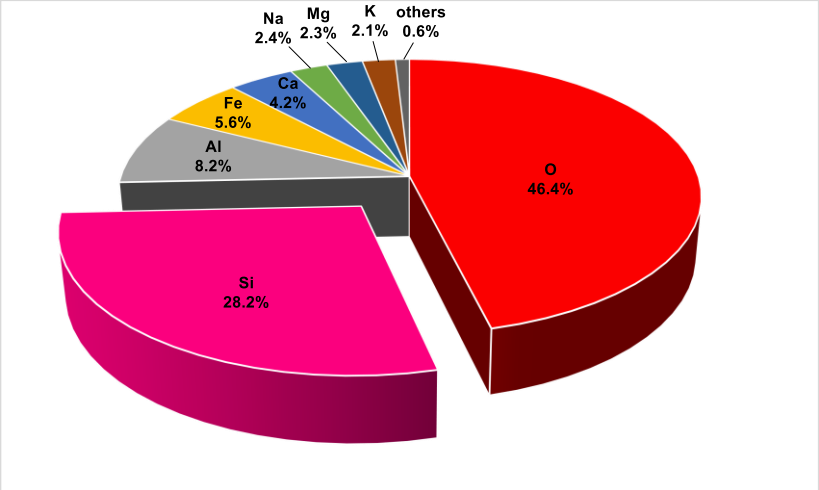

Figure 2. Abundance of chemical elements in the Earth's crust.

Another common existence forms is silica (SiO_2, exists as sand, quartz, amethyst *etc.*), which can be directly used in the formation of metallurgical-grade silicon (98.5–99.7% purity) *via* the reduction of quartz with carbon in an electric arc furnace at 2000 °C (Figure 3).[21] Moreover, this metallurgical-grade silicon can be directly used in the synthesis of organochlorosilanes *via* copper/silver-catalyzed reactions of alkyl/aryl halides with elemental silicon ("Müller-Rochow" process, Figure 3).[22] In addition, the polymerization of desired chlorosilane result in linear or cyclic oligo(siloxanes) *via* hydrolysis, which provide a lot of industrial applications, such as silicone oil, silicone grease and silicone rubbers.[23] The production of elemental silicon with higher purity was also achieved *via* the Siemens process (trichlorosilane is reduced by hydrogen on the surface of heated (1100 °C) silicon rods) and Czochralski method (monocrystalline silicon seed crystal is dipped into a crucible containing a 1420 °C hot polycrystalline silicon melt and pulled out under slow rotation,), which can be used in solar cells, semiconductors, integrated circuits *etc.*[21]

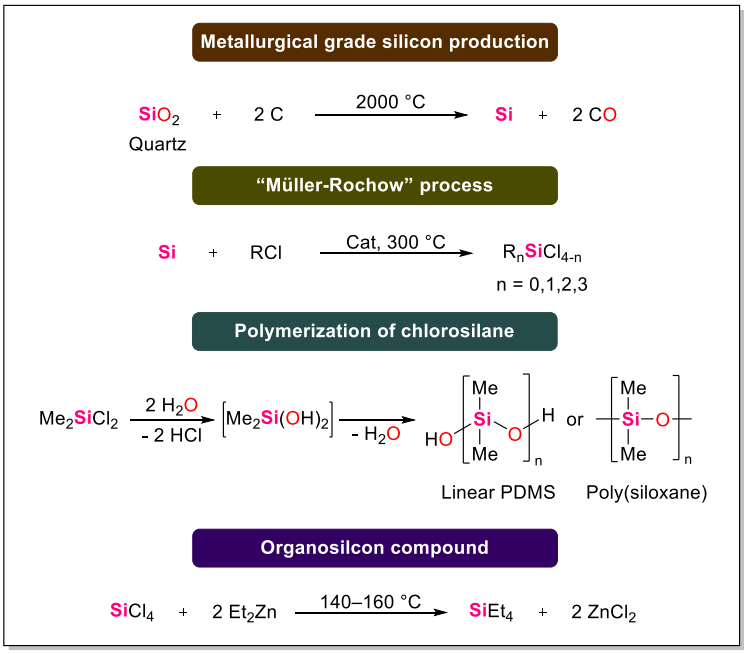

Figure 3. Production of metallurgical silicon via reduction of quartz, production of dimethyldichlorosilane *via* the Müller-Rochow process, preparation of poly(dimethylsiloxane) (PDMS) after hydrolysis of Me_2SiCl_2 and synthesis of the first compound containing a silicon-carbon bond (tetraethylsilane).

Another development of organosilicon chemistry was achieved by Friedel and Crafts in 1863 with the synthesis of tetraethylsilane *via* the reaction of silicon tetrachloride and diethylzinc in a sealed tube (Figure 3).[24] Since then, these small molecules are widely used in the synthesis of novel silicon-containing compounds, such as the formation of Si–E (E = other elements) bonds. Notably, the utilization of Grignard reagents for the synthesis of silanes becomes the most common synthetic method, which was implemented by Frederic Stanley Kipping in 1904.[25]

Today, organosilicon compounds are ubiquitous and have become indispensable in daily life and in the chemical industry. However, these organosilicon compounds are tetra-coordinate, in which the silicon nuclei is in the most stable oxidation state, *i.e.* Si(IV). As organosilicon chemistry has developed, the isolation of compounds containing silicon in lower oxidation states (+III – 0) became more and more viable.

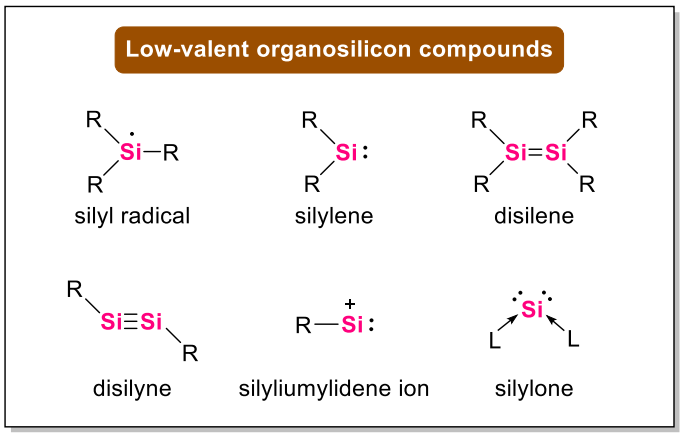

Figure 4. Low-valent organosilicon compounds.

Since the discovery of the first low oxidation state silicon compound, a disilene ($R_2Si=SiR_2$) in 1981 there has been an increasing number of reports for low-valent organosilicon compounds in oxidation states ranging from +III to 0.[26] Figure 4 outlines the various low-valent organosilicon compounds that have been synthesized and isolated at ambient temperature and have been used in small molecule activation and catalytic applications.[27-29] As the main focus of this thesis is on silylenes (heavy carbene analogues; R_2Si:) they will be discussed in more detail in the following chapter.

2.1 Silylenes

Carbenes are the divalent and neutral species with the general formula R_2C: (R^- is a monodentate (homo- or heteroleptic) or R_2^{2-} is a bidentate chelating σ- and/or π-donating ligands), in which the central carbon atom possesses six electrons in its valence shell. Carbenes were originally regarded as intermediary species until the isolation of first stable acyclic [bis(diisopropylamino)phosphino]trimethylsilylcarbene by Bertrand and co-workers in 1988.[30] Three years later, the Arduengo group described the first stable *N*-heterocyclic carbene (NHC).[31] Since then, the study of carbene chemistry is booming. Notably, NHCs have since become an indispensable part of modern chemistry and are widely applied in organocatalysis or as effective ligand in the stabilization of electron-poor elements.[32-37]

Silylenes (R_2Si:), the silicon analogs of carbenes, are one of the most important species among the low-coordinate organosilicon compounds. Despite the close relationship in the periodic table, the electronic properties of silylenes differ significantly from carbenes (Figure 5). The calculated molecular structure and electronic configuration of two divalent parent systems, *i.e.* methylene (H_2C:) and silylene (H_2Si:) revealed that methylene exhibits a triplet ground state with a negative singlet-triplet energy gap (ΔE_{ST} = –14.0 kcal mol^{-1}) resulting in the diradical character with spin-non-paired electrons in two sets of orbitals. In contrast, silylene favors the singlet ground state giving it an ambiphilic nature with a lone pair of electrons in 3s-orbital and a vacant $3p_z$-orbital due to the greater singlet-triplet energy gap (ΔE_{ST} = 16.7 kcal mol^{-1}).[38]

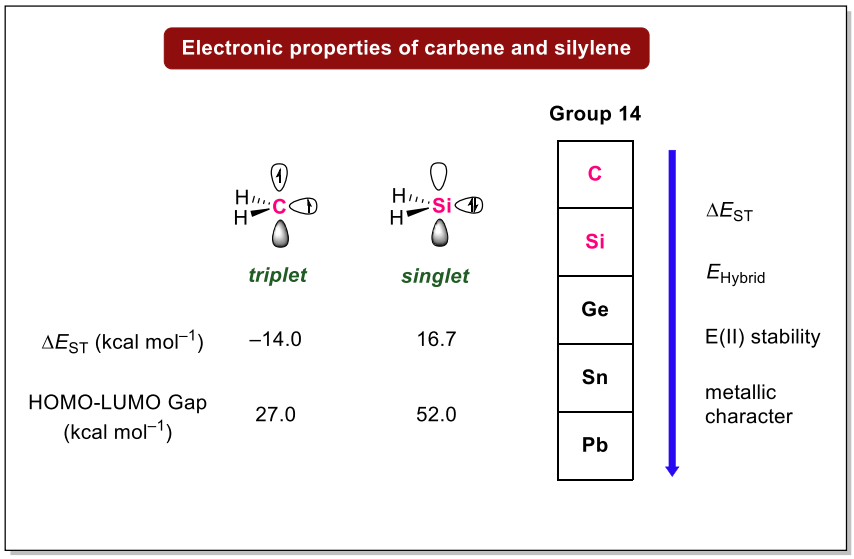

Figure 5. General trends of electronic properties of group 14 elements and schematic representation of the frontier orbitals of tetrylenes.

Moreover, the tendency to form hybrid orbitals generally decreases with the descent from carbon to lead in Group 14, which can be attributed to unfavorable overlap between s- and p-orbitals and higher effective nuclear charge resulting in an increase in the energy of hybridization (E_{Hybrid}) as the group is descended. [39] Another trend is that the heavier elements prefer lower oxidation states with an increase of the stability of tetrylenes (R_2E: E = tetrel elements). It can be explained by the inert pair effect, which suggests that electrons in valence s-orbitals of heavier group 14 elements are more tightly bound to the nucleus due to the weak shielding of the intervening d-orbitals and therefore need more energy to be ionized than electrons in p-orbitals. It means only the p-orbitals electrons can participate in chemical bonding.[40-41] Thus, the lone pair of electrons on silylene and heavier congeners possess a more pronounced s-character. It's also reflected in the decrease of H–E–H angle when descending the group (H_2C: 134°, H_2Si: 92.7°, H_2Ge: 91.5°, H_2Sn: 91.1°, H_2Pb: 90.5°).[38] In addition, the tetrylene lone pair of electrons generally represent the highest occupied molecular orbitals (HOMOs) and the vacant np-orbitals represent the lowest unoccupied molecular orbitals (LUMOs), as such the singlet-triplet energy gap is usually related to the HOMO-LUMO gap.[42]

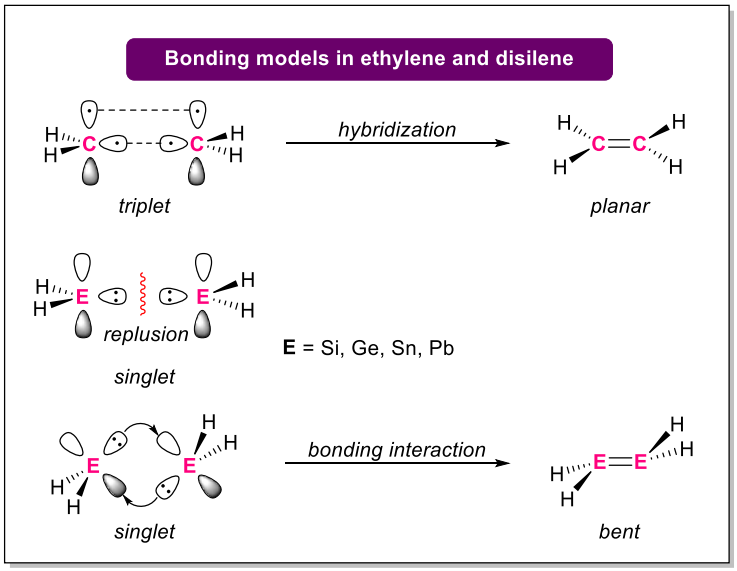

Figure 6. Bonding models for the dimerization of singlet and triplet tetrylene fragments.

Owing to the heavier group 14 element's poor propensity to hybridize, there is a significant difference in their ability to form multiple bonded compounds, compared to their lighter congener, carbon. Regarding the valence bond and structure theory of olefins, the planar structure of the C=C double bond is due to a complementary interaction between two sp^2 hybridized triplet carbenes (Figure 6).[43] In contrast, heavy tetrylenes, such as silylene, prefer the singlet ground state (*vide supra*), thus the combination of repulsion of the filled lone pairs

between both fragments and the Pauli repulsion between inner-shell electrons prohibit π-bond formation.[44] This type of principle is called "double bond rule". This means that heavier elements with a principal quantum number greater than 2 cannot form π-bonds, either with themselves or other elements.[45-46] However, this hypothesis was eventually disproven with the isolation of the several group 14 alkene analogues, such as digermene and distannene by Lappert,[47] disilene by West.[26] Accordingly, an adapted bonding model was developed by Carter, Goddard, Malrieu and Trinquier (CGMT),[48-49] in which the formation of ditetrylenes with double donor–acceptor type bond by electron donation from one sp^2-type lone pair orbital into a vacant p-orbital of another molecule. This type of bonding interaction led to the bent structure of ditetrylenes, which reflected in the bent angles. And the bent angles were strongly affected by the singlet-triplet energy gap of both tetrylene fragments (*vide supra*),[50-51] meaning that a small ΔE_{ST} affords a more planar structure and vice versa. Thus, the choice of the substituents can effectively adjust the singlet-triplet energy gap of tetrylenes manifesting in the bend angle of ditetrylenes.

As mentioned above, singlet ground state silylenes exhibit an ambiphilic nature, therefore they can act as Lewis bases and Lewis acids *via* their lone pair of electrons and their vacant $3p_z$-orbitals, respectively. However, silylenes are considered as electron deficient species and they easily undergo dimerization/oligomerization to form disilenes/polysilanes or react with small molecules *via* bond activation (*e.g.* Si–H, O–H) as a result of the unfulfilled octet rule caused by the empty $3p_z$-orbital.[38] Thus, reducing the electrophilicity of the silicon center is essential for the isolation of silylenes.

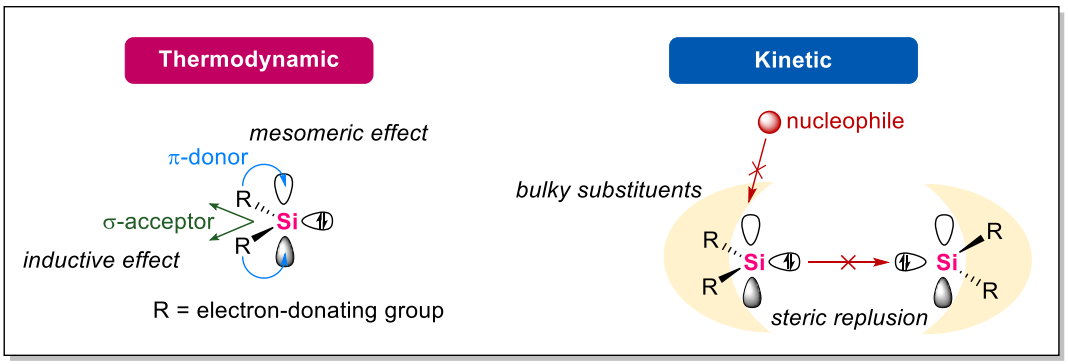

Figure 7. Thermodynamic and kinetic stabilization of divalent silylenes.

There are two general concepts in the attempted isolation of silylenes, that is thermodynamic and kinetic stabilization (Figure 7). In terms of the thermodynamic stabilization of silylenes, the use of electronegative substituents, such as amines, phosphines *via* π-electron-donation to the vacant $3p_z$-orbital (mesomeric effects), results in the reduction of electrophilicity. Also,

these electronegative substituents can act as a σ-acceptor to increase the s-character of the HOMO, thus promoting the singlet ground state and HOMO-LUMO gap.[38,44]

Kinetic stabilization is achieved by sterically demanding ligand frameworks that protect the silylene center from the attacks of nucleophiles and prevent the dimerization/oligomerization by steric repulsion. Utilizing both concepts has resulted in a plethora of substituents with bulky systems or specific electronic properties to be developed. It should be noted that with enough kinetic stabilization it has recently been shown that using electropositive substituents, like alkali metals, bulky silyl or boryl groups have been successfully applied in the synthesis of triplet silylenes,.[52-56]

2.1.1 Historic Milestones in Two-Coordinate Silylenes

The original study that hinted at the existence of silylenes can be traced back to one century ago, in which a silylene acts as an intermediate to form organosilane Si_4Ph_8 by Kipping.[57] Later in the 1930s, dichlorosilylene was detected by emission spectrum.[58-59] A few decades later, the highly reactive silylene species Me_2Si: was first trapped by trimethylsilane *via* Si–H insertion forming pentamethyldisilane, which was generated by reductive dechlorination of dimethlydichlorosilane with sodium/potassium vapor at 260 °C in 1964.[60] In 1979, the West and Michl group reported the UV-vis spectrum of dimethlysilylene (generated by the photolysis of dodecamethylcyclohexasilane) at 77 K with absorption bands at 453 and 650 nm, providing strong evidence for the existence of silylenes.[61] However, the isolation of silylenes was still elusive due to the lack of kinetic and thermodynamic stabilization.

The initial breakthrough in silylene chemistry was achieved by Jutzi in 1986 with the isolation of the first monomeric Si(II) compound, *i.e.* decamethylsiliconcene (**L1**, Figure 8).[62] However, **L1** cannot be considered as a genuine silylene since it isn't classically two coordinate, it possesses the two η^5-coordinating pentamethylcyclopentadienyl (Cp*) ligands, resulting in heightened nucleophilicity at the central silicon center inspired by the isolation of the first stable *N*-heterocyclic carbene (NHC) by Arduengo and co-workers,[31] the West and Denk group successfully reported the first isolable two-coordinate *N*-heterocyclic silylene (NHSi, $(HCN\textit{t}Bu)_2Si$: **L2**) in 1994 with five-membered aromatic ring stabilized by two adjacent amino group.[63] **L2** was prepared by the reductive dechlorination of the corresponding dichlorosilane with potassium at 60 °C. In contrast, the corresponding saturated analog of **L2** is less stable due to the lack of aromaticity.[64] An analogous silylene to **L2** but with a phenyl ring backbone (conjugated π-framework), i.e. **L3** was reported by Lappert one year later.[65] In the following years, NHSis were well developed and comprised the most abundant type of isolated silylenes.

In 1999, a milestone of silylene was achieved by Kira and co-workers with the isolation of carbocyclic dialkylsilylene, $(H_2CCTMS_2)_2Si$: **L4** (TMS = trimethylsilyl) stabilized by the four TMS group neighboring to the carbon (steric demand and *β*-silicon effect).[66] However, **L4** slowly decomposes in solution at room temperature to give to cyclic silene *via* 1,2-silyl migration. Furthermore, **L4** displayed a strong downfield shift in the ^{29}Si NMR spectrum at 567.4 ppm for central silicon, representing the closest chemical shift compared to calculated value of transient silylene H_2Si: (771.8 ppm) and Me_2Si: (739.6 ppm). By the ligand modification from TMS to bidentate alkyl substituent with 1,3-disilaindane moieties or aryl group, dialkylsilylenes $(H_2CC[\textit{o}\text{-}Ph(Me_2Si)_2]_2)Si$: **L11** and $(H_2CCAr_2)_2Si$: **L22** without the 1,2-substituent migration were reported by Iwamoto and co-workers in 2012 and 2019, respectively

(Ar = 3,5-bis(*tert*-butyl) methoxyphenyl).[67-68] Interestingly, silylene–disilene equilibrium was found in dialkylsilylene **L11** bearing bidentate alkyl substituent with 1,3-disilaindane moieties.[67]

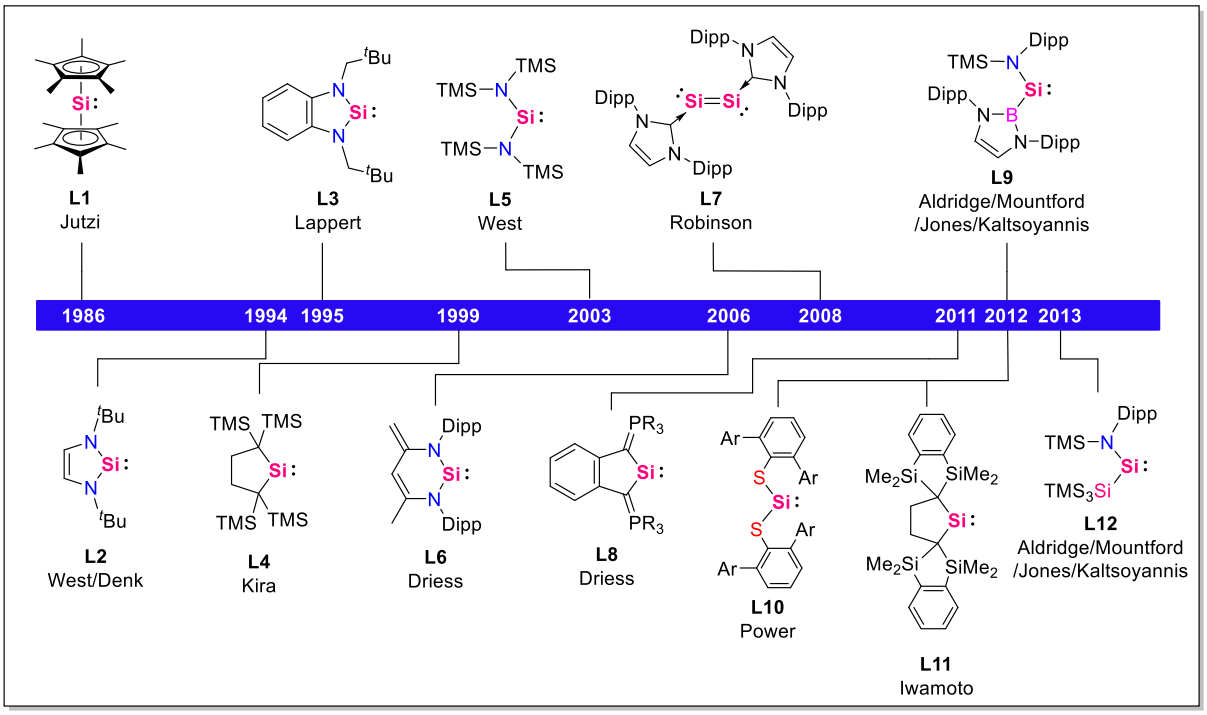

Figure 8. Timeline of historical milestones in the chemistry of divalent silicon species. Ar = Mes (2,4,6-trimethylphenyl), Dipp (2,6-diisopropylphenyl), Tipp (2,4,6-triisopropylphenyl), R = Ph or *m*-tol.

In 2003, the West group described the synthesis of acyclic bisaminosilylene $(TMS_2N)_2Si$: **L5** by the debromination of the corresponding dibromodiaminosilane with potassium graphite. However, L5 was only stable at –20 °C for 12 h.[69] The Driess group expanded the class of NHSis with the isolation of first conjugated six-membered NHSi, $HC[(C{=}CH_2)(CMe)(NDipp)_2]Si$: **L6** stabilized by *β*-diketiminate ligand (Dipp = 2,6-diisopropylphenyl).[70] They also revealed the zwitterionic, ylide-like property of diaminosilylene **L6**, which features high electrophilicity. Later in 2008, Robinson and co-workers set another milestone with the isolation of unique NHC-stabilized disilicon(0) compound, $[(IDipp)Si]_2$ **L7** by the reductive dechlorination of IDipp-$SiCl_4$ (IDipp = 1,3-bis(2,6-diisopropylphenyl)imidazolin-2-ylidene).[71] DFT calculations revealed the HOMO–2 of **L7** is one of the two nonbonding lone-pair of electrons, which was also verified by transition metal coordination reactions.[72-73] Moreover, analogs of cAAC-stabilized (cAAC = cyclic alkyl(amino) carbene) disilicon(0) and trisilicon(0) were reported by the Roesky group shortly .[74-75] An expansion of carbocyclic silylenes was achieved by Driess and co-workers in 2011 with the isolation of aromatic bisphosphorus yilde-stabilized silylene **L8**.[76] DFT

calculations revealed the strongly nucleophilic silicon center caused by additional π-donating from the zwitterionic phosphonium ylidic $R_3P^+–C^–$ moieties.

As already mentioned at the start of this chapter, the early attempts for the isolation silylenes are prone to the acyclic moieties, such as Me_2Si:, $^tBu_2Si$:, Mes_2Si:, $(TMS_2N)_2Si$: *et al*. Acyclic silylenes are an important class of silylene, made elusive by the fact that their heightened reactivity made isolation difficult. This was until 2012 which saw the synthesis of two acyclic silylenes (**L9** and **L10**), [77-78] Due to their high relevance to this thesis, the results related to acyclic silylene are separately addressed and discussed in detail in the following chapter.

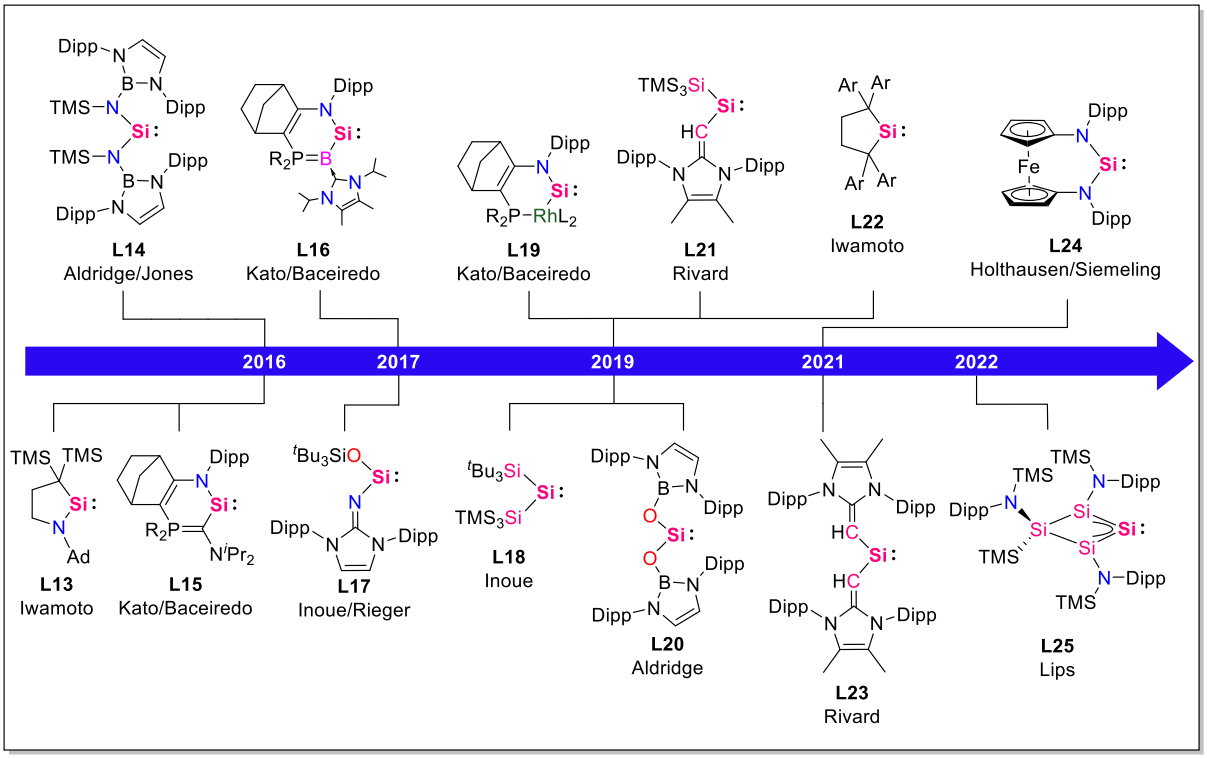

Figure 9. Timeline of historical milestones in the chemistry of divalent silicon species. Ad = adamantyl, Ar = 3,5-bis(*tert*-butyl) methoxyphenyl, R_2 = $Me_2Si(^tBuN)_2$, L_2 = $(H_2CPPh_2)_2$.

In 2016, the Iwamoto group reported the cyclic alkyl(amino) silylene $[(H_2C)_2(CAd)(NDipp)]Si$: **L13** (Ad = adamantyl),[79] the heavier analog of the cyclic alkyl(amino) carbene (cAAC) established by Bertrand and co-workers (Figure 9).[80] In contrast to the **L4**,[66] **L13** exhibits higher thermal stability and more selective reactivity, such as intermolecular benzylic C–H bond activation of toluene. The Kato and Baceiredo group reported two two-coordinate heterocyclic silylenes **L15** and **L16** in 2016 and 2017, respectively.[81-82] The introduction of a π-donating phosphonium-ylide or bora-ylide provides high thermal stability (150 °C for 2 days) and unique nucleophilicity. Remarkably, both silylenes **L15** and **L16** can be converted to the corresponding three-coordinate silanones upon

exposure to N_2O.[83-84] With the same ligand system, the first *N*-hetero-Rh^I-metallacyclic silylene **L19** with a distorted tetrahedral rhodium center was reported by Kato and co-workers in 2019.[85] DFT calculations revealed the tetrahedral geometry around rhodium increases the π-donating and σ-accepting character of the rhodium atom, thereby efficiently stabilizing the silylene center. In 2021, another entry into the NHSi library was achieved by the Siemeling and Holthausen group with the synthesis of NHSi **L24** with a 1,1'-ferrocenediyl backbone .[86] The neutral homocyclic silylene **L25** was successfully prepared by Lips and co-workers *via* initial amino group abstraction by potassium and followed by salt metathesis with TMSCl.[87]

So far, a plethora of stable silylenes with kinetic stabilization and/or thermodynamic stabilization has been prepared. Besides the aforementioned two-coordinate silylenes, some hyper-coordinate silylenes can also show interesting reactivity in small molecule activation and transition metal coordination. In the following chapter, selected typical acyclic silylenes and their reactivity will be presented according to this thesis.

2.1.2 Acyclic Silylens and General Reactivity

A major landmark in silylene chemistry was the isolation of the first acyclic silylenes, [Dipp(TMS)N](DippDAB)Si: **L9** (DippDAB = B(NDippCH)$_2$) and (MesTerS)$_2$Si: **L10a** (MesTer = 2,6-bis(2,4,6-Me$_3$-C$_6$H$_2$)C$_6$H$_3$) reported separately by the Aldridge/Jones group and the Power group in 2012 (Figure 10).[77-78] While aminoborylsilylene **L9** was prepared by the ligation and reduction of the corresponding aminoboryltribromosilane and boryl lithium reagent,[77] dithiolatosilylene **L10a** was synthesized by the reductive debromination of the corresponding dithiodibromosilane with Jones's magnesium(I) reagent[88] ((MesnacnacMg)$_2$, nacnac = HC(MeCNDipp)$_2$).[78] The isolation of **L9** and **L10a** disproves the long-held notion that acyclic silylenes are purely transient species, not being stable at ambient temperature.[69] Analysis of the molecular structure of **L9** and **L10a**, shows the R–Si–R angle is 109.7(1)° and 90.5(1)° (Table 1), respectively, with **L9** being significantly more obtuse compared to silylenes with a rigid cyclic framework. As we mentioned above, the R–Si–R angles of silylenes are directly related to the singlet-triplet energy gaps and the HOMO-LUMO gaps, which enhances the reactivities towards small molecules, such as selected bond activation. Accordingly, **L9** should be more reactive than **L10a** since the R–Si–R angle is more obtuse, in which theoretical calculations revealed narrower HOMO-LUMO gap (**L9**: 2.04 eV; **L10a**: 4.26 eV). Notably, the **L9** has an extremely electropositive boryl ligand, which will also have an effect on the HOMO-LUMO gap.

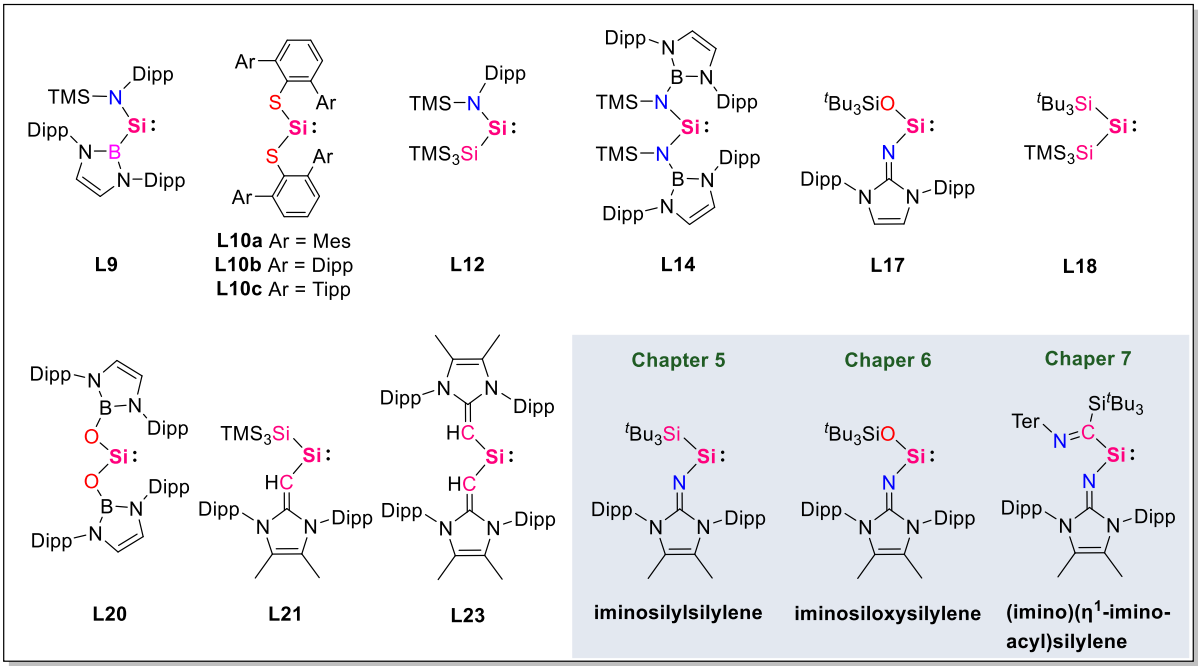

Figure 10. Structures of reported isolated two-coordinate acyclic silylenes and present work.

Table 1. Summary of Bonding angles and ^{29}Si NMR data of the central silicon atom of all reported isolated two-coordinate acyclic silylenes.

	L9	**L10a**	**L12**	**L14**	**L17**	**L18**	**L20**	**L21**	**L23**
R–Si–R [°]	109.7(1)	90.5(1)	116.9(7)	110.9	103.56	-	100.02	101.59	100.58
^{29}Si NMR [ppm]	439.7	285.5	438.2/467.4	204.6	58.9	-	35.5	432.9	272

The reactivity has been demonstrated and will be discussed in detail below. In 2013, both groups expanded the class of acyclic silylenes with the synthesis of silylaminosilylene, (TMS_3Si)[Dipp(TMS)N]Si: **L12** bearing more electropositive silyl group[89] and dithiolatesilylene, $^{Ar}TerS_2Si$: **L10b-c** (Ar = Dipp and Tipp, Tipp = 2,4,6-triisopropylphenyl) bearing bulkier aryl groups,[90] respectively. Remarkably, the R–Si–R angle of **L12** (116.91(5)°) is the widest reported as of writing this. The first isolable acyclic diaiminosilylene, [^{Dipp}DAB(TMS)N]$_2$Si: **L14**[91] was prepared by the group of Aldridge and Jones *via* salt metathesis between Roesky's IDipp-$SiCl_2$[92] and lithiated amino ligand in 2015. With the introduction *N*-heterocyclic imines into silylene chemistry, our group successfully reported the neutral three-coordinate silanones upon treating N_2O with transient acyclic iminosilylene,[93] in which the migratory insertion of oxygen into Si–Si bond occurred, forming the first acyclic iminosiloxysilylene (IDippN)(^{t}Bu$_3$SiO)Si: **L17** (IDippN = 1,3-bis(2,6-diisopropylphenyl)imidazolin-2-iminato).[94] In 2019, Recently, the isoelectronic *N*-heterocyclic olefins (NHOs) and *N*-heterocyclic boryloxy(NHBO) were also introduced into acyclic silylene chemistry with the isolation of dioxylsilylene, (^{Dipp}DABO)$_2$Si: **L20** by the Aldrige group,[95] and vinylsilylsilylene, (TMS_3Si)[(MeCDippN)$_2$C(H)C]Si: **L21**[96] and divinylsilylene, [(MeCDippN)$_2$C(H)C]$_2$Si: **L23**[97] by the group Rivard. Notably, our group disclosed the synthesis and isolation of equilibrium mixture containing the first isolable two-coordinate bissilylsilylene (^{t}Bu$_3$Si)(TMS_3Si)Si: **L18** and its isomeric tetrasilyldisilene (TMS)(^{t}Bu$_3$Si)Si=Si(TMS)$_2$ **L18'**. Supportive DFT calculations revealed a closer insight into the nature of the equilibrium and the bonding situation of **L18** and **L18'**.

Silylenes are considered as highly reactive species due to their ambiphilic nature. The Lewis basic character of silylenes has allowed them to play a significant role in coordination chemistry with transition metal and some low-valent main group compounds.[98-100] Furthermore, some silylene transition metal complexes are already used in some catalytic reactions.[98,100] However, the high reactivity of silylenes stems from their Lewis basic and Lewis acidic character (from the empty p-orbital). Due to these silylenes have been shown to be effective in bond activation reaction, whereby E–E bonds (E = s/p block elements) oxidatively add to the silylene center. This type of reaction is also well-known in transition metal chemistry, in which silylenes can

be considered as transition metal mimics. A prime example of this type of mimicry is the activation of the non-polar molecule, dihyrogen.[101] Among all the cyclic silylenes, only dialkylsilylene **L4** was able to split dihydrogen but only in the presence of Lewis acid or Lewis base.[102] In contrast, with the first isolation of acyclic silylene, the facile dihydrogen splitting forming corresponding silane **L9-1** was achieved with silylene **L9** at room temperature after 30 min or 0 °C within 2.5 h (Figure 11).[77] DFT calculations reveal the strong donation of electron density from σ bond (HOMO) of dihydrogen into the 3p-orbital (LUMO) of **L9**, and this splitting of dihydrogen is distinguished by a moderate energy barrier of 97.2 kJ mol^{-1}, that is markedly lower than those of computed bis(amino)silylenes (e.g. acyclic $Si(NH_2)_2$ 190.0 kJ mol^{-1} or cyclic $Si(NHCH)_2$) 277.8 kJ mol^{-1}).

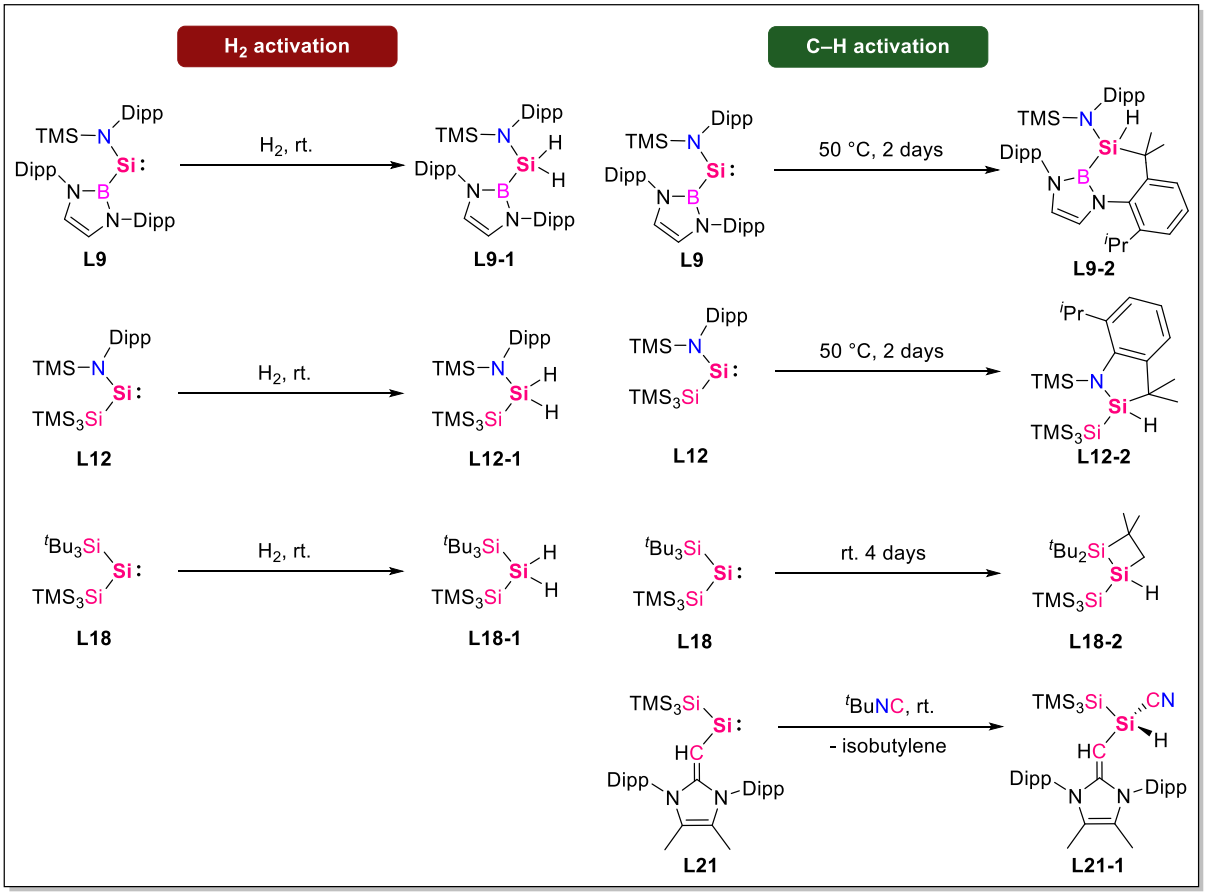

Figure 11. Dihydrogen and C–H bond activation by acyclic silylenes.

However, the simultaneously reported acyclic silylene **L10** cannot activate dihydrogen probably owing to the wider HOMO-LUMO gap (*vide supra*). In the next 10 years, the splitting of dihydrogen by simple acyclic silylene only was achieved by **L12** and **L18**.[89,103] Notably, intramolecular $C(sp^3)$–H splitting of substituent was accomplished by **L9**, **L12** and **L18** upon heating to 50 °C for 2 days or room temperature for 4 days,[77,89,103] which also demonstrated

by transient acyclic silylene (**L27**, *vide infra*).[104] These exemplify the high reactivity of acyclic silylenes. The first instance of C–H bond activation was achieved by the reaction of **L21** and ^{t}BuNC with the release of isobutylene and the formation of silyl cyanide **L21-1**.[96]

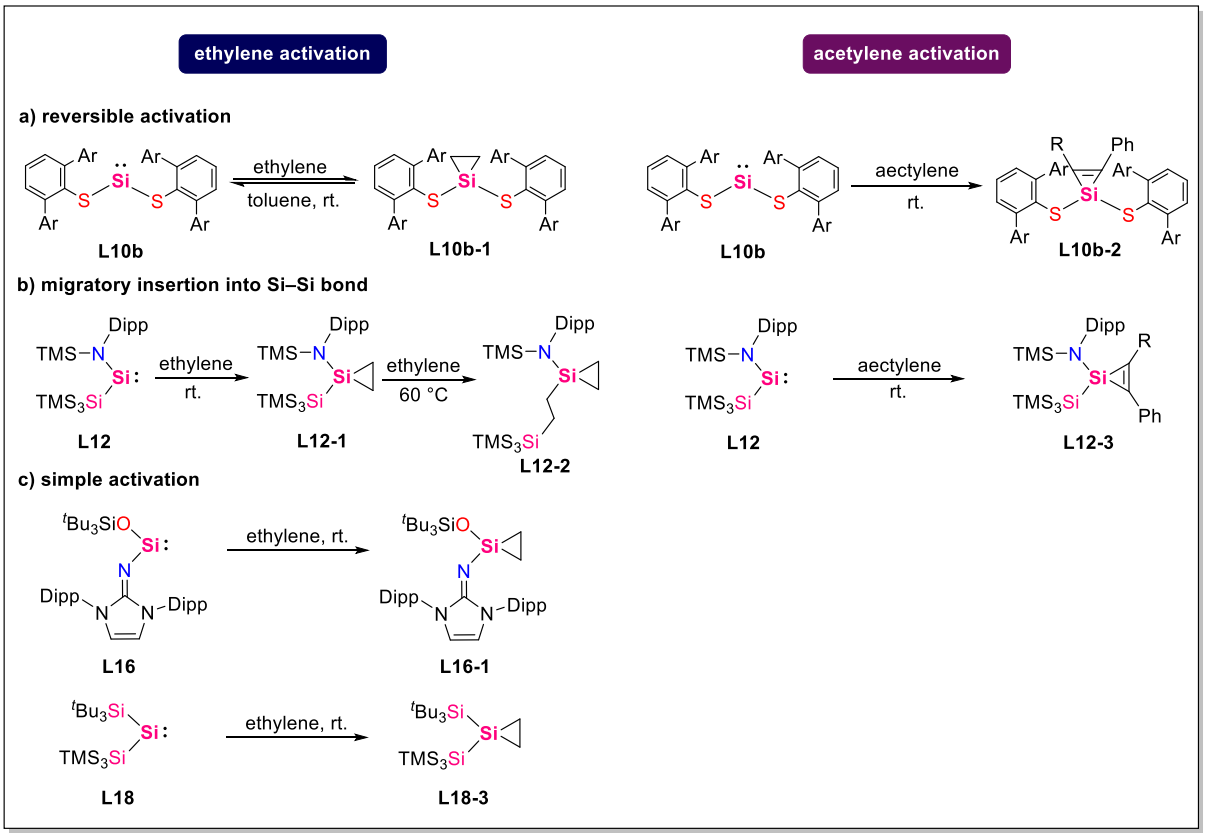

Figure 12. Ethylene and alkynes activation by acyclic silylenes. Ar = Dipp, R = H and Ph.

Despite **L10** being unable to activate dihydrogen, the mild cycloadditions with unsaturated bond systems were achievable, such as with alkenes and alkynes.[105-106] Interestingly, the combination of ethylene with **L10b** led to reversible cycloaddition forming corresponding silacycloprapane **L10b-1** (silirane), which can be considered as a side-on complexation of a C=C bond to a silylene center (Figure 12). Such a reversible activation was also demonstrated by distannynes[5] and silylene-phosphine complexes.[107] In terms of the potential for main group catalysis, this type of reversibility, oxidative addition and reductive elimination alternate with each other, are considered fundamental steps in a catalytic cycle. In contrast, the combination of ethylene with **L12** resulted in the corresponding silirane **L12-1** selectively[108]. When heating silirane **L12-1** to 60 °C in the presence of ethylene, unique migratory insertion of ethylene into Si–Si bond occurred, resulting in silirane **L12-2**. An NMR spectroscopic experiment using deuterated ethylene revealed the mechanism with migratory insertion of the coordinated ethylene into the Si–Si bond. Similar migratory insertion of ethylene with silylenes was reported by our group and the Kato group very recently.[109-110] And further facile

cycloaddition of **L12** with alkynes forming silacyclopropenes (silirenes **L12-3**) was also demonstrated.[111] In the shape contrast, the simple complexation of ethylene by **L16** and **L18** forming the corresponding silirane **L16-1** and **L18-3** was demonstrated by our group.

The mild transformation of C1 sources (CH_4, CO, CO_2, *etc*) into chemical building-blocks stands as a lucrative goal with the activation of C1 feedstocks being the first key step followed by further C–C coupling. In contrast with inert methane, carbon oxides are much easier to activate owing to the unsaturated and polar bond as well as its unique electronic structure.[112-113] There is growing interest in the activation and utilization of carbon dioxide (CO_2) due to its status as a major greenhouse gas. While the activation of CO_2 by carbenes generally forms carbene-CO_2 adducts, the reaction of silylenes with carbon dioxide goes via two pathways: oxygen abstraction with the release of carbon monoxide or cycloaddition with C=O moiety.[114-116] In contrast, carbon monoxide (CO) is harder to activate due to the C–O triple bond. However, owing to their carbenic structure, CO can act as electrophiles, nucleophiles or carbenes in organic synthesis and coordination chemistry.[117-120] The CO activation by specific silylenes is known. Despite the fixation of CO by highly reactive acyclic carbenes or cAACs forming ketenes was discovered in 2006,[121] the complexation of CO was independently achieved in 2020 by transient acyclic silylene $[L(Br)Ga]_2Si$: **L26** and **L18** by the Schulz and our group, respectively (Figure 13, L = nacnac).[122-123] DFT calculations revealed that both silylene-CO adducts (**L26-1** and **L18-4**) showed a strong interaction between the silylene center and CO moiety with CO→Si σ-donation and Si→CO π-back donation, resembling transition-metal carbonyls. Despite further homocoupling of CO with the silylene-CO adducts was unachievable until now, the reduction of our silylene-CO **L18-4** adduct resulted in the first sila-ketenyl anion.[124] The silylene-mediated first homologation of carbon monoxide was accomplished by silylene **L9** in 2019, forming $[C_2O_2]^{2-}$ moiety (**L9-3**) *via* the cleavage of Si–B bond.

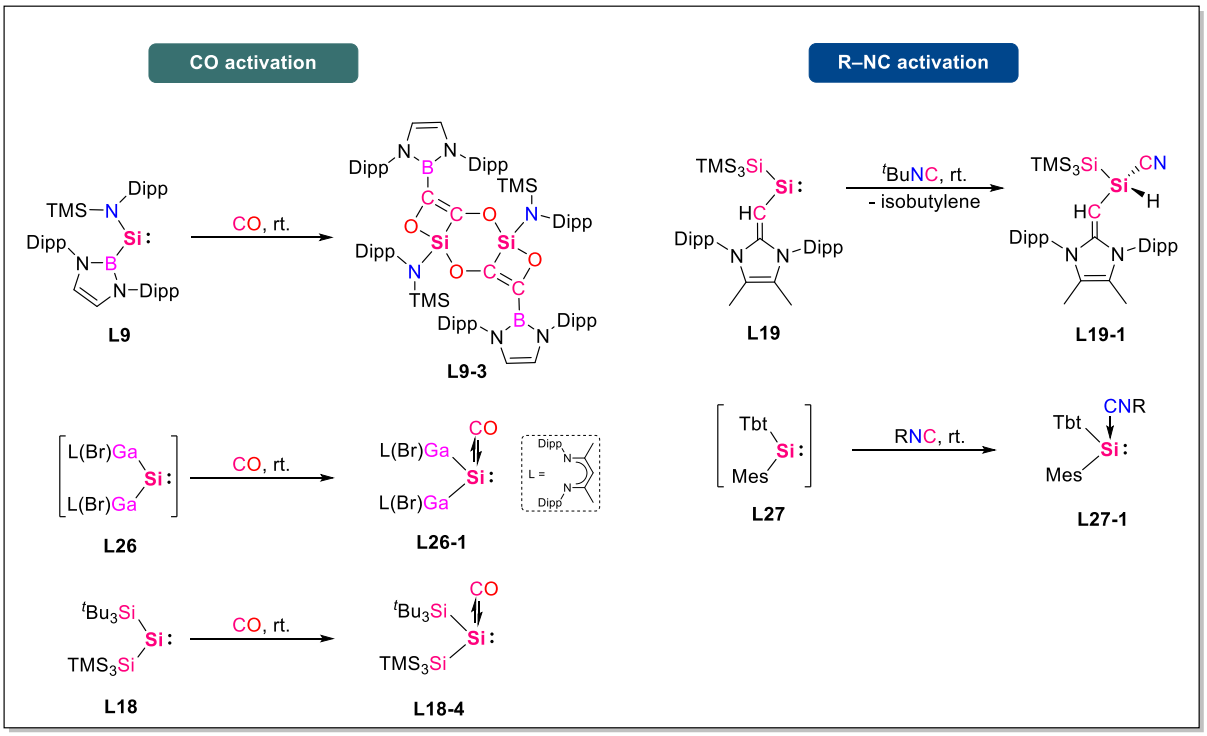

Figure 13. Carbon monoxide and isocyanides activation by acyclic silylenes. L = nacnac, R = Mes, Tipp, Tbt, Mes*, Tbt = 2,4,6-tris[bis-(trimethylsilyl)methyl]phenyl, Mes* = 2,4,6-$^{t}Bu_3$-C_6H_2.

Isocyanides (R–NC), are isoelectronic to carbon monoxide, but more reactive than carbon monoxide due to the adjustable steric and electronic properties by the modification of *N*-substituent. The study of the combination of isocyanides with silylenes was was first done with $^{t}Bu_2Si$: (generated in situ from a hexa(t-butyl)cyclotrisilane) with phenylisocyaide forming the corresponding transient silaketenimne in 1992, which dimerized to 1,3-disilacyclobutane-2,4-diimine with possesses a Si=C moiety.[125] The first stable silylene-isocyanide complex was first reported by Okazaki and co-workers in 1997 *via* complexation of aryl isocyanides and transient silylene (Tbt)(Mes)Si: **L27** (generated in situ from a disilene, Tbt = 2,4,6-tris[bis-(trimethylsilyl)methyl]phenyl).[126-127] Despite the activation or complexation of isocyanides by transient silylenes has been well established over the past 30 years,[128-129] the activation by isolable, two-coordinate silylenes is still rare.[96,130] Only the Kira group reported the synthesis of silaketenimines by the complexation of isocyanides with dialkylsilylene **L4** at room temperature in 2006[130] and the Rivard group disclosed the cyanation of silylene **L21** with the release of isobutylene upon treatment of **L21** with ^{t}BuNC at room temperature in 2019.[96]

2.2 Silepins

Büchner ring expansion, in which an *in situ* generated carbene undergoes [1+2] cycloaddition with an aromatic C–C bond in benzene derivatives, followed by the ring expansion to afford the corresponding cyclo-1,3,5-heptatrienes, was first discovered by Büchner and co-workers in 1885 (Figure 14).[131-132] Since then, Büchner ring expansion has played an important role as a method for synthesizing seven-membered rings in organic synthesis.[133-134] However, in general, Büchner ring expansion reactions without additives form hard-to-purify mixtures of isomeric cyclo-1,3,5-heptatrienes.[135] It was not until 1981 that regioselective transformations could be achieved in Rh(II) catalyzed reactions, providing control over arene ring expansion.[136]

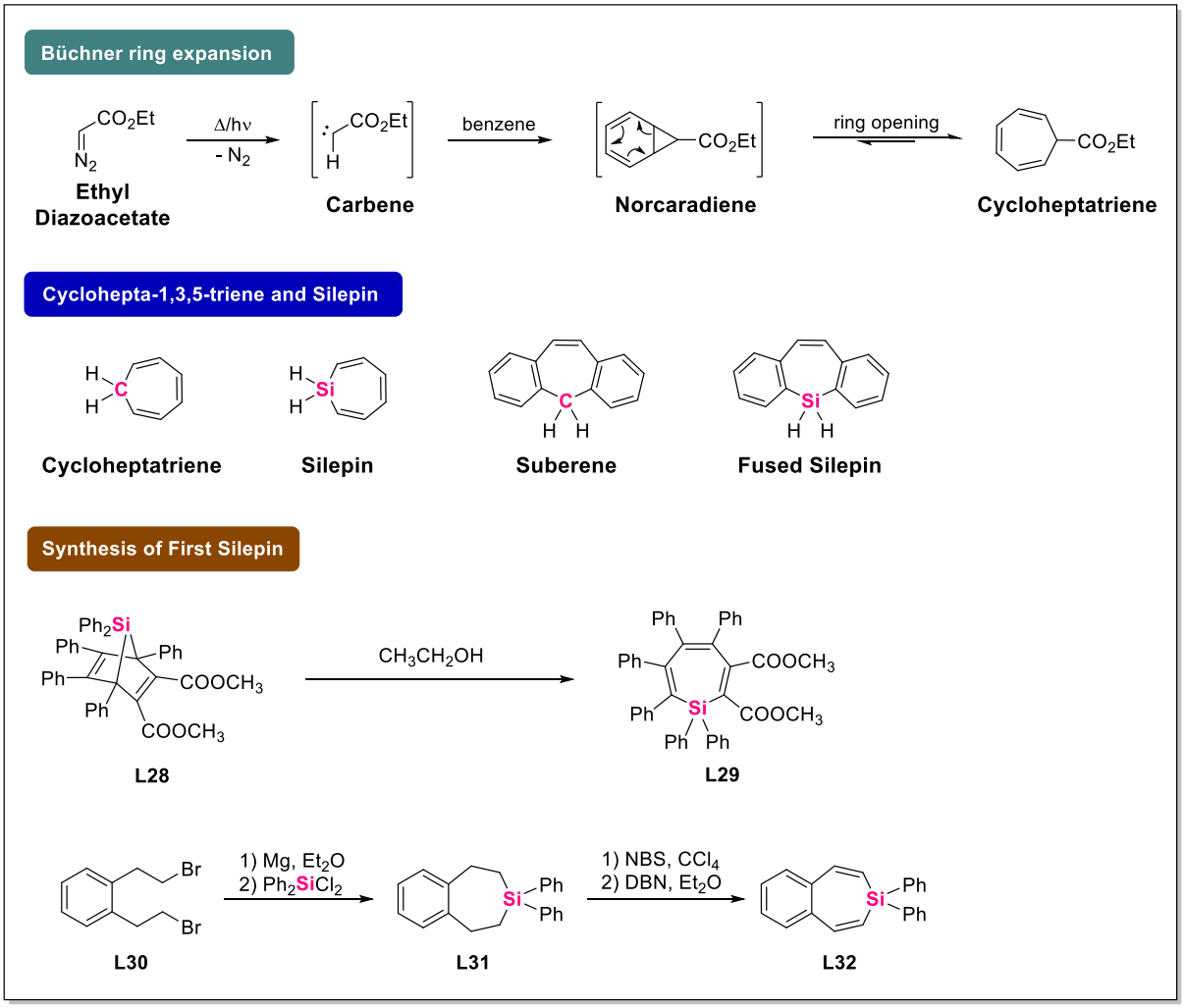

Figure 14. Büchner ring expansion, structure of cyclo-1,3,5-heptatriene and silepin (silacyclo-2,4,6-heptatriene) and synthesis of first silepin.

In contrast, silacyclo-2,4,6-heptatrienes (*i.e*. silepins), the heavier analogs of cyclo-1,3,5-heptatrienes, have for a long time been rather elusive owing to the extreme lability of the synthetic intermediate and methods until in the last decades with the development of more accessible modern synthetic tools.[137-138] Moreover, it's worth mentioning that the construction of fused silepins is more available than non-annulated silepins owing to the electron delocalization over the fused cycles. Therefore, despite the Gilman has tentatively suggested a fully substituted silepin **L29** as a possible product from decomposition of the 7-silanorbornadiene derivative **L28** in ethanol at an early stage,[139] the breakthrough in the silepin chemistry was set by Birkofer and Haddad *via* initial reaction of Grignard reagent derived from **L30** with diphenyldichlorosilane, followed with bromination and dehydrobromination affording bicycle fused silepin **L32** in 1969.[140] Since then, a plethora of silepins have been synthesized by dehydrogenation/dehalogenation of the corresponding silacyclo-2,6-heptadiene,[141-142] salt metathesis between lithium precursor and dichlorosilane,[143-146] or via catalytic reactions (intramolecular McMurry coupling, ring-closing metathesis, C–H/Si–H dehydrocoupling, *etc*).[147-153] Notably, fused silepins exhibit blue fluorescent in contrast with the all-carbon congener, which provides a potential application in new functional materials.[137-138,154] DFT calculations revealed the fluorescent possibly are due to the contribution from the Si–C σ bonds to the cycloheptatriene π system.[154]

The previous hypothesis that the vacant 3p orbital on silicon may be able to provide a conjugative π-interaction with carbon 2pπ orbitals, thereby leading to 4n + 2 π-electron neutral analog of the tropylium cation,[155-156] has been disproven so far by the reported silepins.[137-138] However, it still raises a question regarding the aromatic/antiaromatic nature of cycloheptatriene and silepin. Aside from cycloheptatriene **L33**, which possesses an essentially planar structure (Figure 15),[157] the so far structurally reported cycloheptatrienes and silepins exhibit a boat-shaped geometry (*C*s). In the boat-shaped cycloheptatrienes and silepins, the deviation from planarity can be expressed by the bow (α) and stern (β) tilt angles (Figure 15). The theoretical calculations gave α and β angles of 52.9° and 25.4°, respectively, which is in line with the experimental results.[158] Previous studies have concluded that cycloheptatriene is homoaromatic due to delocalization through space.[159] Low temperature ^{1}H NMR measurements showed that the homoaromatic, C_s-symmetrical, boat conformation of cycloheptatriene is prone to undergo a degenerate ring flip *via* a planar (α = 0°, β = 0°) antiaromatic C_{2v} transition with a free energy barrier of 5.7 kcal·mol^{-1} in $CBrF_3$ and 6.3 kcal· mol^{-1} in CF_2Cl_2.[160-161] And unlike the C_{2v} conformation of cycloheptatriene that is predicted to be homoaromatic, previous studies suggested that the planar transition state C_{2v}

structure possesses an antiaromatic character, due to the pseudo-2π-electron effect of the CH_2 group. Therefore, cycloheptatriene **L33** is antiaromatic as indicated by the positive NICS(0) (5.4 ppm), NICS(1) (2.0 and 2.2 ppm, respectively), and NICS(1)*zz* (9.0 and 9.7 ppm) of the seven-membered ring.[159]

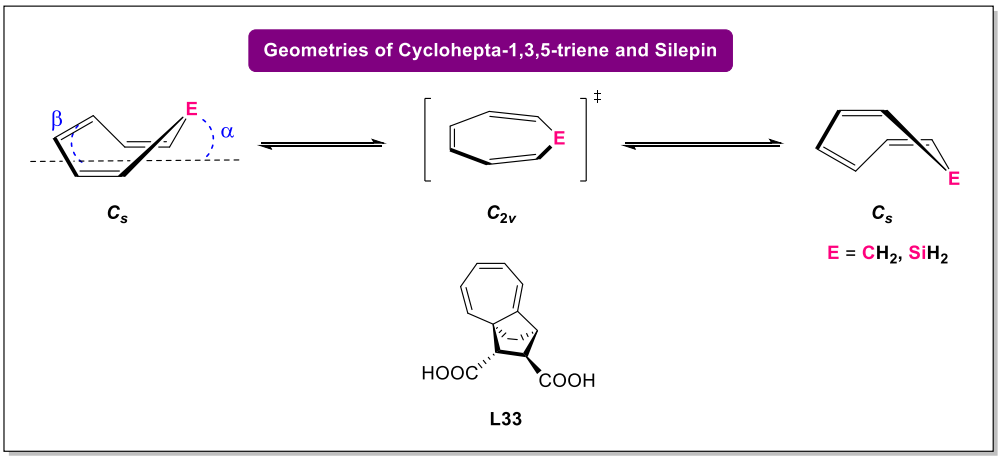

Figure 15. Geometries of cyclohepta-1,3,5-triene and silepin and planar cycloheptatriene.

With the development of silylene chemistry, it has been found that the ring expansion of benzene derivatives by silylenes in the Büchner-ring-expansion-type mechanism provides simpler methods and higher selectivity in the construction of silepins, especially the non-fused silepins, which was less studied so far. Notably, the potential reversibility between silepin and silylene can be consider as a "masked silylene" in terms of reactivity. Based on the relation of this thesis, in the following chapter, the synthesis of silepins from silylenes will be presented in detail.

2.2.1 Isolable Silepins from Silylenes

The first milestone of silepin derivative was set by Okazaki and co-workers in 1994 with the demonstration of the ring-expansion of benzene by a transient silylene **L27** (Figure 16).[162] Treatment of a transient silylene (generated *in situ* from a disilene) with benzene at elevated temperature resulted in the generation of the bicycle silepin derivative **L34**. They proposed that the formation of **L34** proceeds similarly to Büchner ring expansion, involving silanorcaradiene and silepin intermediates. However, the isolation of the silepin intermediate could not be accomplished in this case since the silepin is more reactive than benzene toward the silylene, resulting in the successive [1 + 2] cycloaddition to give **L34**. In the same report, the reaction with naphthalene yielded no ring expansion products, but rather two consecutive [1 + 2] cycloadditions, providing evidence for the existence of the proposed silanorcaradiene intermediate.

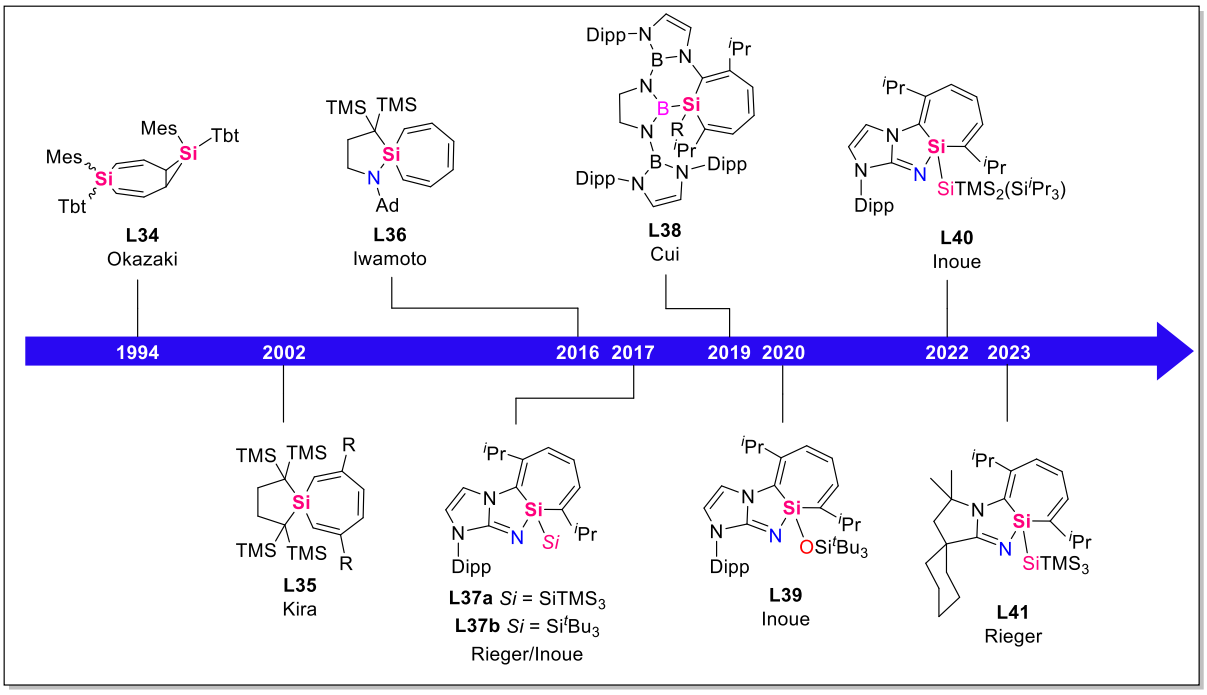

Figure 16. Timeline of historical milestones in the chemistry of silepins generated from silylenes. R = H, F, OMe, CF_3.

In 2002, the genuine silepins **L35** generated from silylene was reported by the Kira group *via* the photochemical reaction of benzene with the dialkylsilylene **L4**. The ring expansion of 1,4-benzene derivatives (*p*-xylene, 1,4-dimethoxybenzene, 1,4-difluorobenzene, *etc*) were also presented in the same report.[163] The follow-up quantum chemical calculations showed that, in the reaction with benzene, the singlet excited state of silylene, generated by irradiation, forms a 1,3-diradical reactive intermediate, which subsequently undergoes cyclization to silanorcaradiene and ring expansion to form the silepin **L35**.[164] A similar ring expansion reaction, in which the cyclic alkyl amino silylene **L13** activated benzene upon irradiation at λ=350 nm to form a silepin **L36**, was reported by the Iwamoto group in 2016.[79]

One year later, the first intramolecular ring expansion by transient acyclic iminosilylenes, forming silepins **L37**, was reported by our group in 2017.[93-94] In this process, the transient silylene insertion into the aromatic C−C bond of a Dipp substituent is reversible, as we demonstrated by the reactivity studies of **L37** and, directly, in the silepin **L40** reported by our group very recently, in which both isomers can be observed under ambient conditions (will be discussed in the following chapter in detail). On the other hand, the imino(siloxy)silylene **L17** can be isolated at ambient temperature, whereas irradiation (λ=340 nm) of **L17** in THF or benzene gave the corresponding silepin **L39** irreversibly. In 2019. Cui and co-workers also reported the ring-expansion products **L38** *via* the salt metathesis of the corresponding lithium silanorcardiene, which was obtained by the reduction dichlorosilacycle with lithium. Very

recently, silepin **L41** substituted with a modified imine ligand based on a cyclohexyl cyclic alkyl amino carbene was reported by the Rieger group, which also showed the reversibility between silepin and silylene during the reactivity investigation.[165]

2.2.2 General Reactivity of Silepins

Compared to low-valent silicon species, such as silylenes or silyl radicals, silepins are extremely stable after being exposed to air or high temperatures, , meaning reactivity studies are scarce.

In 2011, the first transformation of silepin **L42** to borepin **L42-1**was reported by the Piers group (Figure 17),[154] a reaction common with stannepins (tin analog of cycloheptatriene).[166] Similar transformation of silepin **L43** to bromoborepin **L43-1** and subsequent transmetalation to give to borepinium ions was also reported by Jäkle and co-workers in 2020.[167] In these types of reactions, the lower toxicity of silepins compared with organotin compound is the advantageous.

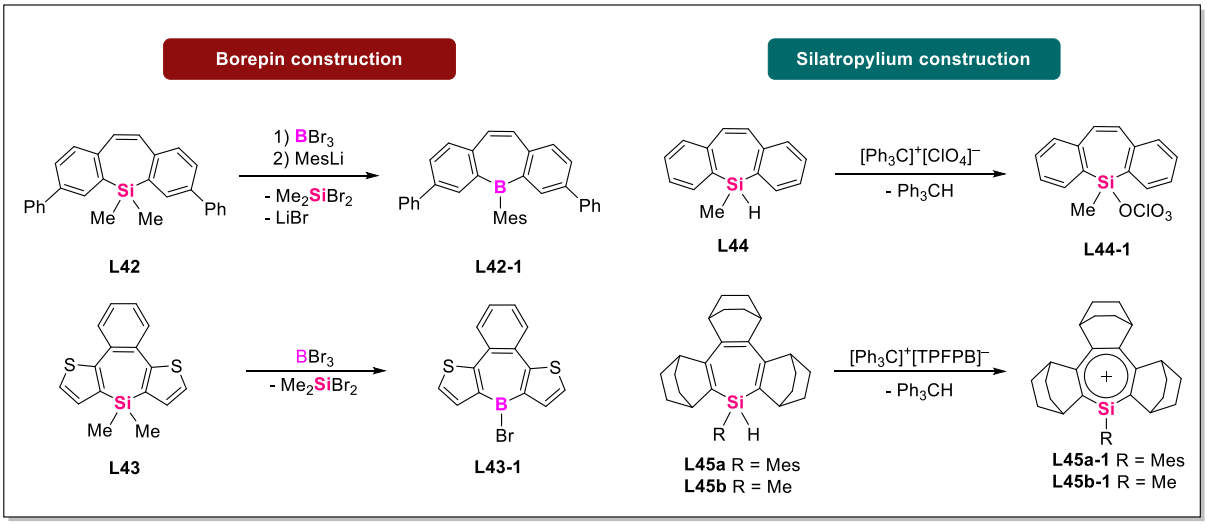

Figure 17. Reactivity of silepin for the construction of borepin and silatropylium.

With the isolation and wide application of tropylium ion ($C_7H_7^+$), interest in the silicon analog, *i.e.* silatropylium ions were grew and silepins were considered as a good candidate for their synthesis since dihydrogen/halogen in silicon center is promising. Previous studies suggested the silatropylium ion was more stable than its isomeric phenylsilyl cation in the gas phase.[168] Therefore, in 1992, the initial attempt of treating **L44** with trityl perchlorate ($[Ph_3C]^+[ClO_4]^-$) as a hydride abstracter formed a new silepin **L44-1** substituted with perchlorate instead of the formation of silatropylium ion.[169] Later in 2000, the Komatsu group reported the silatropylium ion annulated with a rigid σ-framework *via* the reaction of corresponding silepin **L45** with trityl borate ($[Ph_3C]^+[B(C_6F_5)_4]^-$) in DCM. However, both

silatropylium ions **L45a/b-1** were only observed at –50 °C in CD_2Cl_2 and slowly decomposed to dichlorosilepin at –50 °C within 12 h or benzene derivative at room temperature. The ^{29}Si NMR was observed at 142.9 ppm, indicating the formation of silylium cations.[170] The further attempt to isolate base stabilized silatropylium ion *via* treating acetonitrile with silatropylium ion failed.[146]

In terms of potential low-valent main group catalysis, oxidative addition/reductive elimination processes can be considered as key steps for a catalytic cycle. Therefore, the reversible conversion of silepin to silylene provides the potential functionalization of benzene derivatives. The first thermal conversion of silepin to silylene was reported by the Barton group in 1974 with the isolation of the first non-fused silepin **L46** (Figure 18).[156] When heating **L46** to 250 °C, *o*-terphenyl was cleanly formed, as detected by NMR spectroscopy. Despite there being no mention of the dimethylsilylene intermediate was not mentioned in this report, the observation of *o*-terphenyl can be considered as the tentative evidence for the conversion of silepin to silylene. Nearly half a century later, the fascinating reversibility between silepin and silylene was found by Rieger and our group. Transient acyclic iminosilylenes were observed at –78 °C, however, the intramolecular aromatic C–C bond activation compounds (**L37a/b**) were isolated at room temperature.[93-94] Interestingly, the silepin **L37** can be directly used as a silylene source in the further small molecule activation, such as with dihydrogen forming the corresponding silane,[93] with N_2O affording the silanone bearing a Si=O bond[94] or the construction of aluminata-silene.[171] And our recent report disclosed both silepin **L40** and corresponding silylene can be observed at ambient conditions with the modification of silyl substituent.[109] Similarly, silepin **L41** also showed the reversibility upon heating to 90 °C.[165]

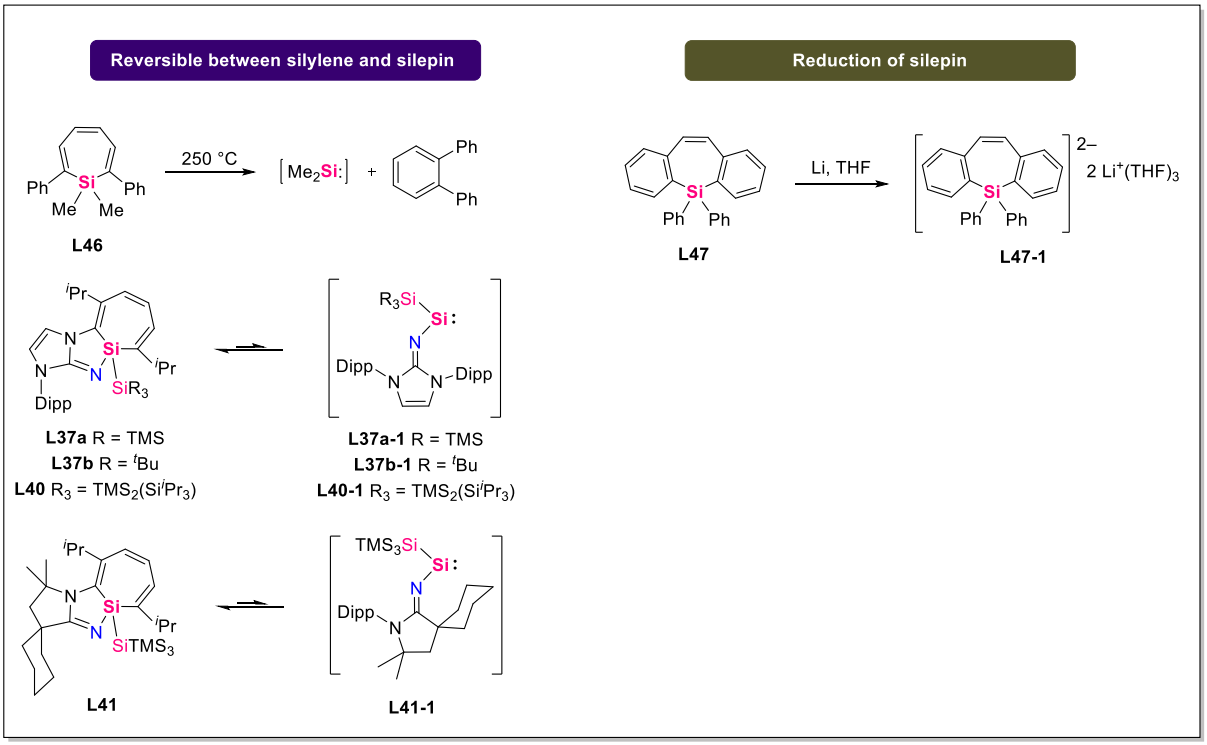

Figure 18. Reversibility between silepin and silylene and the reduction of silepin.

Owing to the π-conjugated system in silepins, the hyperconjugative (anti)aromaticity of these type compounds is also expected. Therefore, the reduction of fused silepin **L47** with lithium forming the corresponding silepin dianion **L47-1** was achieved by Kuwabara and co-workers. The dilithium dibenzosilepinide have a pseudo 16π-electron system involving negative hyperconjugation, which was also supported by DFT calculation with positive NICS value (NICS(–1)*zz* = 7.5 ppm) and paratropic ring currents in ACID.[172]

3. *N*-heterocyclic Iminato Ligand in Main Group Chemistry

Nitrogen donor ligands are ubiquitous in both transition metal and main group chemistry, they have been demonstrated to be potent ligands for the stabilization of a multitude of compounds. While amides $[NR_2]^-$ are already widely explored for the stabilization of main group elements, the class of imidazolin-2-imines, also named *N*-heterocyclic imines (NHIs), are far less studied. NHIs are composed of an NHC and an exocyclic nitrogen atom, and they can act as a strong 2σ and 2-4π electron donor for the thermodynamic stabilization of electron-poor species. Canonical form of anionic imidazolin-2-iminato ligand **A** possesses an ylene structure with a C_{NHC}=N_{imimo} bond and two potent electron pairs on the nitrogen atom, which can be considered as 2σ and 2π electron donor. And the ylide resonance structure **B** with two anionic charges and three potent electron pairs on the nitrogen atom, can be considered as a 2σ and 4π electron donor, in which the positive charge is delocalized over the NCN moiety (Figure 19). Relatively, NHI metal complexes may have canonical type **C** or significant metalla-2-aza-allene character (**D**) or metalimide (**E**) character. These properties were illustrated by an elongated C_{NHC}–N_{imimo} bond length and a shortened M–N bond length and a widening of the C–N–M angle toward the ideal 180° for an allene-type structure. Moreover, as a result of the adjustable imidazoline ring, NHI ligands can provide the specific requirements necessary to kinetically stabilize elusive compounds.[173]

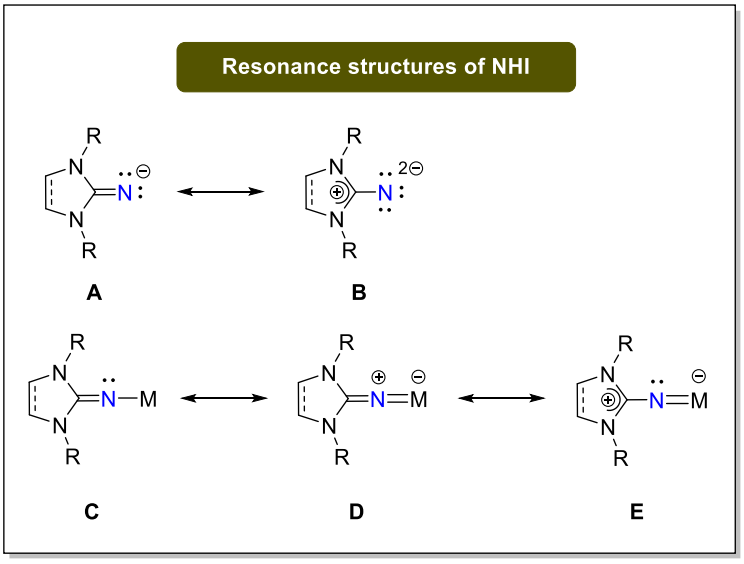

Figure 19. Selected resonance structures of NHI ligands and a model NHI-metal (M = metal, R = alkyl, aryl) complex.

Since the first discovery of NHI ligands by Kuhn and co-workers in 1995,[174-176] the utilization in the stabilization of transition-metal complexes is well established.[32,177] The

breakthrough for NHI ligands in terms of main group chemistry was achieved by Bertrand and co-workers with in the synthesis of carbene-stabilized phosphorus mononitride, which underwent one electron oxidation with trityl borate ($[Ph_3C]^+[B(C_6F_5)_4]^-$) forming the corresponding radical cation NHIPCAAC$^{+\bullet}$ **L48** (Figure 20).[178] DFT calculations revealed the delocalization of the single electron over the molecule in **L48**. The further utilization of NHI ligands by the same group in highly reactive pnictogen compounds was accomplished with the isolation of bis(imino)phosphinyl radical $(NHI)_2P^{\bullet}$ **L49**[179] and first isolable singlet phosphinonitrene $(NHI)_2PN$: **L50**.[180] It's worth mentioning that **L50** can be used as a nitrogen atom-transfer agent, its ambiphilic property was well illustrated by reactivity studies and complexation with transition metals.[181-183] This phosphinyl ligand was also used in stabilizing dicarbon species recently.[184]

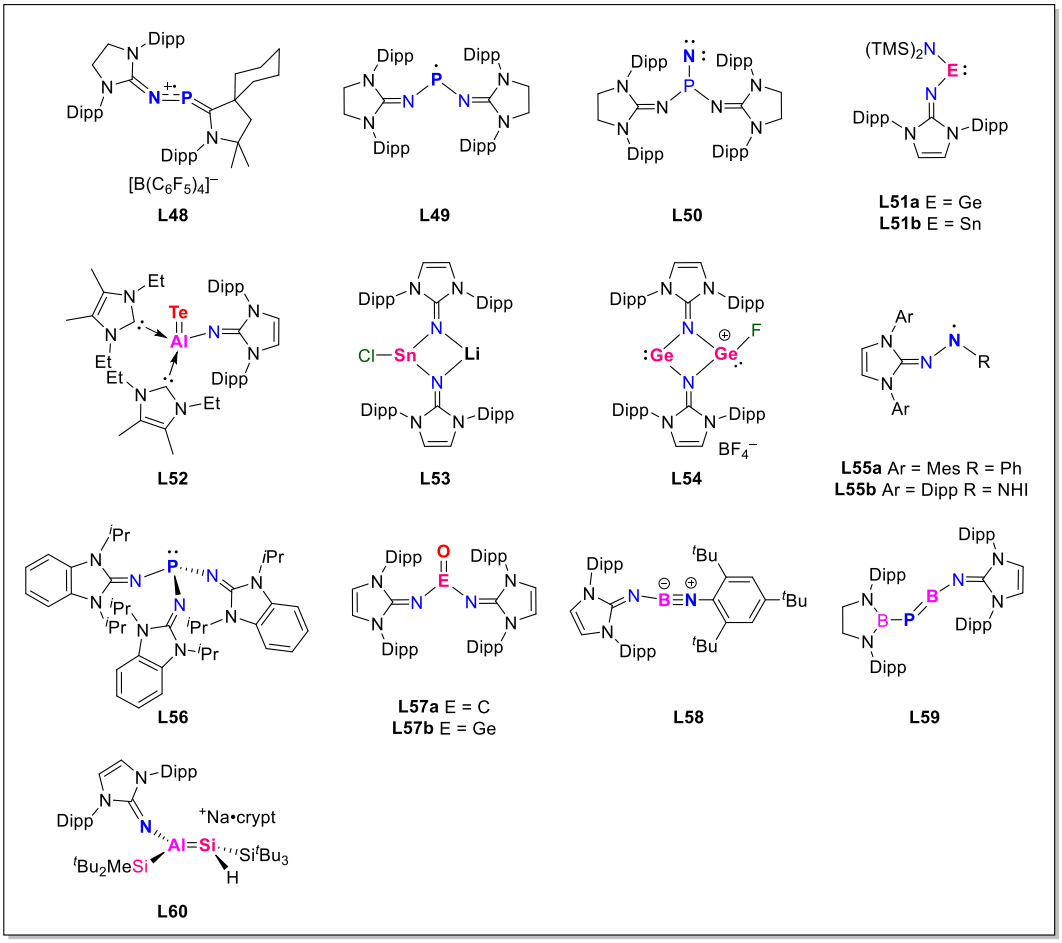

Figure 20. Selected examples of reported NHI-stabilized main group compounds.

From 2012, the implementation of NHI ligand for the synthesis of group 13 and 14 species was repotred by our group and Rivard group. For instance, NHIs have been used to isolate acyclic silylene **L61** (NHI substituted silicon species will be discussed below in detail),[185] aminoimino/bisiminotetrylene,[186-188] NHC-stabilized silaborene,[189] the elusive terminal

aluminum telluride **L52** with an Al=Te bond,[190] chlorostannylenoid **L53**[191] and bis(imino)germylene-germyliumylidene **L54**.[192] Meanwhile, NHI stabilized group 13 compounds were successfully utilized in the catalytic reaction, such as the hydroboration of alkynes and CO_2,[193-194] as well as the dehydrogenation of amino-boranes.[195-196]

The neutral aminyl radicals **L55** were isolated and reported by the Severin (**L55a**) and the Lee group (**L55b**) in 2015 and 2016, respectively. While the spin density was located on N_2 group in **L55a** bearing a phenyl group and an NHI, the spin density was delocalized over the N_3 moiety and its conjugated substituents in **L55b**, which bore two NHI ligands. In 2017, the Dielmann group reported the triiminophosphine $(NHI)_3P$ **L56**, which is highly electron-rich ligands for transition-metal catalysts and reversible carbon dioxide binding.[197-198] They also disclosed more chemistry with **L56** in the following years, such as triiminophosphine dications, which are isoelectronic with alanes and silylium cations,[199] and Lewis base free oxophosphonium ions.[200] The bisNHI substituted carbonyl $(NHI)_2C=O$ **L57a** and its heavier congener germanone $(NHI)_2Ge=O$ **L57b** were reported by Aldridge and our group, respectively.[201-202] The dearomative hetero-Diels-Alder-like reaction was demonstrated by Kong and co-workers by treating aryliminoborane **L58** and benzaldehyde.[203] In the same year, the Liu group disclosed the first free phosphaborene **L59** bearing π-donating NHI substituent on the boron center and a π-accepting *N*-heterocyclic boryl (NHB) substituent on the phosphine center *via* electron push-pull cooperation.[204] Very recently, our group described the synthesis and isolation of anionic aluminium–silicon core **L60**, which featured with alumanyl silanide (sequestered sodium cation) and aluminata-silene (separated ion pair) characteristics.[171]

As mentioned above, the first introduction of NHI ligands into silicon chemistry was accomplished by our group with the isolation of acyclic iminosilylene (NHI)(Cp*)Si: **L61** (Figure 21).[185] The reductive debromination of the precursor dibromosilane with KC_8 or sodium naphthalenide resulted in **L61** in only trace amounts. Instead the salt metathesis between IDippN-Li and silyliumylidene cation ($[Cp^*Si]^+[B(C_6F_5)_4]^-$) led to 57% yield of **L61**. The reductive debromination of dibromodiiminosilane by KC_8 afforded potassium amide **L62** *via* the migration of aryl moiety from nitrogen to silicon center, which can be described as over reduction of silylene intermediate.[186]

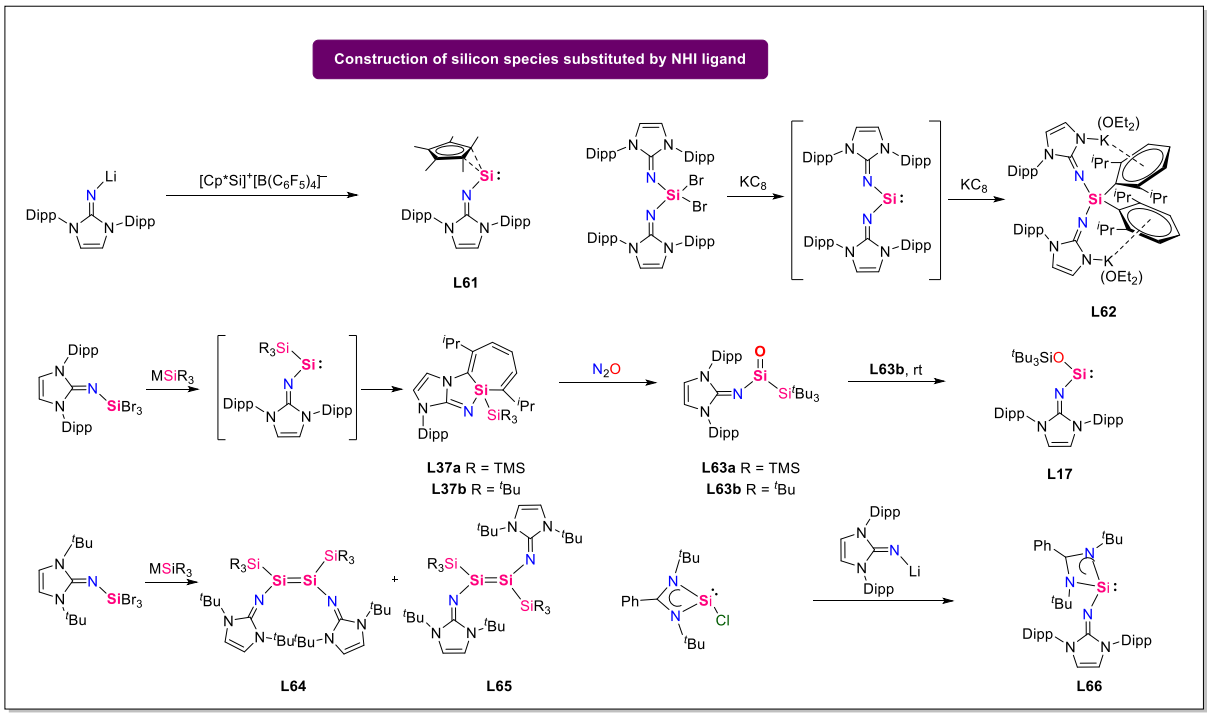

Figure 21. Construction organosilicon species substituted by NHI ligand.

The first isolation of two-coordinate acyclic silylene [(^{Dipp}DABB)(TMS)DippN]Si: **L9** provides a simple method for the construction of NHI-substituted acyclic silylene.[77] Therefore, in 2017, our group reported the synthesis of silepin **L37** generated from transient silylene *via* treatment with tribromoiminosilane with silanides. Exposing silepin **L37** to N_2O afforded silanone **L63** and followed the migration of oxygen to Si–Si bond forming iminosiloxysilylene **L17** (*vide supra*).[93-94] Utilizing the less bulky NHI (I^{t}BuN, 1,3-bis(*tert*-butyl)imidazolin-2-iminato) substituted tribromoiminosilane with silanides afforded the twisted disilene **L64** and **L65** with two different geometry (depends on the type of silanides).[205-207] Very recently, another salt metathesis between chlorosilyelene and IDippN-Li forming silylene **L66** was reported by Mo very recently, which can be used in the synthesis of disilicon(0) and ditin(0) complex.[208-209]

4. Scope of This Work

Main group chemistry has developed into a versatile field within the past decades, such as facile bond activation leading to novel compounds or remarkable catalytic applications. However, the related research and application of organosilicon species are still comparably limited, especially low-valent silicon species. Among these, silylenes, in particular acyclic, two coordinate silylenes have the highest potential due to their heightened reactivity (*vide supra*). As highlighted in the introduction, the oxidative addition/reductive elimination processes are key steps in conventional metal-catalyzed reactions, which are also demonstrated by silylene species. Thus, the catalytic application of silylenes is promising.

Accordingly, the most important initial task of this doctoral dissertation is the synthesis and isolation of novel acyclic, two-coordinate silylenes to gain more expertise in divalent organosilicon compounds. According to the previous report of the reactivity studies of silylenes, subsequently subject the synthesized silylene to diverse small molecules to choose the suitable molecules, which can undergo oxidative addition/reductive elimination processes in silylene center and provide potential catalytic application by silylene. Thus, strong small molecules, such as benzene, pyridine, methane, dihydrogen, carbon monoxide, isocyanides, dinitrogen, alkenes will be carried out.

To achieve this challenging task, the suitable substituents in silylenes should be considered first. With the deeper understanding of the ligand systems, we would utilize the excellent π-donating NHI ligand to thermodynamically stabilize the silylene center in combination with an electropositive silyl group that maintains the small frontier orbitals separation. Both advantages may lead to the unique reactivity toward extremely challenging molecules. Inspired by our previous report about the synthesis of transient silylene stabilized by none methylated NHI ligand and its intramolecular aromatic C–C activation forming corresponding silepins, we targeted the methylated-backbone NHI in combination with supersilyl group (Si^tBu_3) to prevent the intramolecular insertion of silylene center to aromatic framework. Similar synthesis route with the previous report, the reduction of corresponding $NHISiBr_3$ by two equivalents sodium silanide was implemented to yield stable acyclic imino(silyl)silylene **1** (Figure 22).

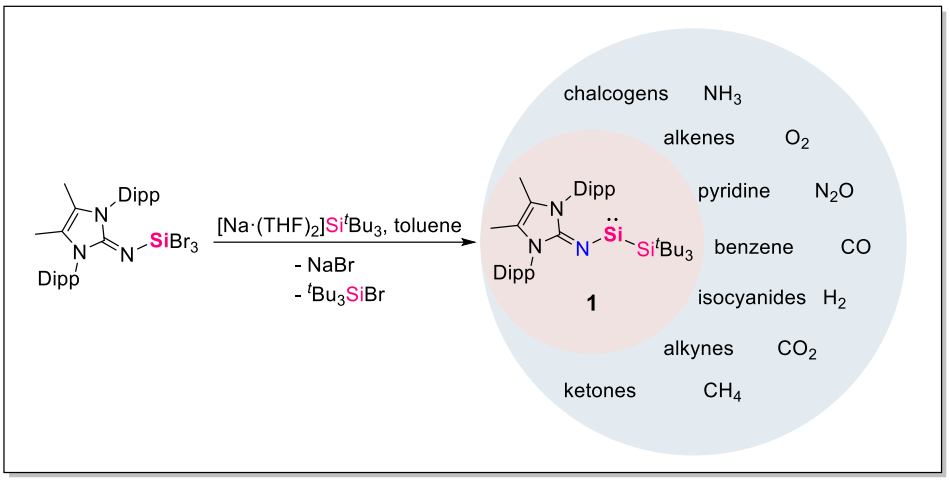

Figure 22. Planed synthesis route of acyclic imino(silyl)-silylene **1** potential small activation.

With the targeted compounds in hand, initial reactivity studies will be conducted to see if they have any dearomatization capacity. Thus, the reactions of **1** with benzene, benzene derivatives and pyridine were implemented.

Further reactivity studies will be conducted with other unsaturated systems, most prominently alkenes and alkynes. We will also treat silylene **1** with compounds possessing E–H bonds (E = Si, B, H) to observe how **1** interacts with such species. Inspired by the isolation of three-coordiate silanone, the reactions of **1** with oxygen-source reagent and elemental chalcogens will be implemented.

The isolation of silicon carbonyls by the reaction of transient silylenes with carbon monoxide prompts us to examine whether silylene **1** can react with carbon monoxide and its isoelectronic isocyanides to form stable silicon carbonyl or silylene isocyanide complexes. Thus, the reactions of **1** with carbon monoxide and variable isocyanides will be investigated.

Overall, this work is intended to gain a deep understanding of the silylene chemistry. To examine the fundamental differences and/or similarities between silicon and elements in the same periodic group (Group 14). With a deeper understanding of the reactivity of neutral silylenes, it should open up the possibility of implementing silylenes in more cataylic applications. Thus, particular attention will be paid to the investigation of the activated products for their potential reversibility.

5. Room Temperature Intermolecular Dearomatization of Arenes by an Acyclic Iminosilylene

Title: Room Temperature Intermolecular Dearomatization of Arenes by an Acyclic Iminosilylene

Status: Article; published online: January 4, 2023.

Journal: *Journal of the American Chemical Society* **2023**, *145*, 1011-1021.

Publisher: American Chemical Society (ACS)

DOI: 10.1021/jacs.2c10467

Authors: Huaiyuan Zhu, Arseni Kostenko, Daniel Franz, Franziska Hanusch, Shigeyoshi Inoue*

Reprinted with permission from the American Chemical Society. © 2023 American Chemical Society.

Content: A novel non-transient acyclic iminosilylene (**1**), bearing a bulky super silyl group (-Si^{t}Bu$_3$) and *N*-heterocyclic imine ligand (NHI) with a methylated backbone, was prepared and isolated. The methylated backbone is the feature of **1** that distinguishes it from the previously reported non-isolable iminosilylenes, as it prevents the intramolecular silylene center insertion into an aromatic C–C bond of an aryl substituent. Instead, **1** exhibits an intermolecular Büchner-ring-expansion-type reactivity; the silylene is capable of the dearomatization of benzene and its derivatives, giving the corresponding silicon analogs of cycloheptatrienes, *i.e.* silepins, featuring seven-membered SiC$_6$ rings with nearly planar geometry. The ring expansion reactions of **1** with benzene and 1,4-bis(trifluoromethyl)benzene are reversible. Similar reactions of **1** with *N*-heteroarenes (pyridine and DMAP, DMAP = 4-dimethylaminopyridine) proceed more rapidly and irreversibly forming the corresponding azasilepins, also with nearly planar seven-membered SiNC$_5$ rings. DFT calculations reveal an ambiphilic nature of **1** that allows the intermolecular aromatic C–C bond insertion to occur. Additional computational studies, that elucidate the inherent reactivity of **1**, the role of the substituent effect and reaction mechanisms behind the ring expansion transformations, are presented.

*H. Zhu and D. Franz planned and executed all experiments including analysis. H. Zhu wrote the manuscript. A. Kostenko designed and performed the theoretical analysis. F. Hanusch conducted the SC-XRD measurements and processed the corresponding data. All work was performed under the supervision of S. Inoue.

JACS
JOURNAL OF THE AMERICAN CHEMICAL SOCIETY
pubs.acs.org/JACS
Article

Room Temperature Intermolecular Dearomatization of Arenes by an Acyclic Iminosilylene

Huaiyuan Zhu, Arseni Kostenko, Daniel Franz, Franziska Hanusch, and Shigeyoshi Inoue*

Cite This: J. Am. Chem. Soc. 2023, 145, 1011−1021
Read Online
ACCESS | Metrics & More | Article Recommendations | Supporting Information

Downloaded via TU MUENCHEN on March 14, 2023 at 11:25:04 (UTC).
See https://pubs.acs.org/sharingguidelines for options on how to legitimately share published articles.

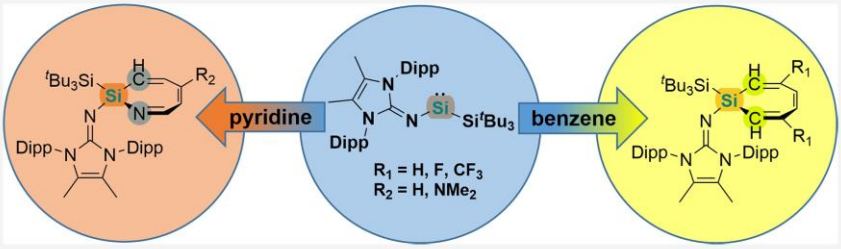

ABSTRACT: A novel nontransient acyclic iminosilylene (**1**), bearing a bulky super silyl group (−Si^{t}Bu$_3$) and *N*-heterocyclic imine ligand with a methylated backbone, was prepared and isolated. The methylated backbone is the feature of **1** that distinguishes it from the previously reported nonisolable iminosilylenes, as it prevents the intramolecular silylene center insertion into an aromatic C−C bond of an aryl substituent. Instead, **1** exhibits an intermolecular Büchner-ring-expansion-type reactivity; the silylene is capable of dearomatization of benzene and its derivatives, giving the corresponding silicon analogs of cycloheptatrienes, *i.e.* silepins, featuring seven-membered SiC$_6$ rings with nearly planar geometry. The ring expansion reactions of **1** with benzene and 1,4-bis(trifluoromethyl)benzene are reversible. Similar reactions of **1** with *N*-heteroarenes (pyridine and DMAP) proceed more rapidly and irreversibly forming the corresponding azasilepins, also with nearly planar seven-membered SiNC$_5$ rings. DFT calculations reveal an ambiphilic nature of **1** that allows the intermolecular aromatic C−C bond insertion to occur. Additional computational studies, which elucidate the inherent reactivity of **1**, the role of the substituent effect, and reaction mechanisms behind the ring expansion transformations, are presented.

INTRODUCTION

Büchner ring expansion, discovered in 1885,[1] in which an *in situ* generated carbene adds across an aromatic C−C bond to consequently form cycloheptatrienes, has played an important role as a method for construction of seven-membered rings in organic synthesis.[2] The natural outcome of Büchner ring expansion reactions are hard-to-purify mixtures of isomeric cycloheptatrienes (Scheme 1),[3] and it was not until 1981 that regioselective transformations could be achieved in Rh(II) catalyzed reactions, providing control over arene ring expansion.[4] Later, in 2017, the triplet ground state carbene chemistry was complemented by the discovery of reversible Büchner ring expansion featuring excited singlet diamidocarbenes.[2a,5]

The aromatic ring expansion chemistry feature of carbenes can also be expected from silylenes (R$_2$Si:)—the silicon analogs of carbenes—first example of which (*i.e.*, Cp*$_2$Si:) was reported by Jutzi only in 1986.[6] Since then, a plethora of highly reactive silylenes has been prepared.[7] Unlike carbenes, which can exist in the singlet or triplet ground state (depending on substituents), silylenes are generally closed shell, having a lone pair and vacant p-orbital,[7d,e,h,8] Thus, despite the high propensity of silylenes for small molecule activation,[7d,e,h]

Scheme 1. Büchner Ring Expansion

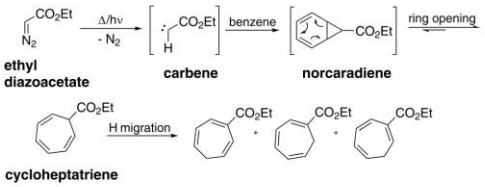

Received: October 2, 2022
Published: January 4, 2023

ACS Publications
© 2023 The Authors. Published by American Chemical Society

https://doi.org/10.1021/jacs.2c10467
J. Am. Chem. Soc. 2023, 145, 1011−1021

examples of silylene insertion into the aromatic C−C bonds are rare. The first intramolecular ring expansion by transient acyclic iminosilylenes **Ia** and **Ib**, forming silepins (silicon analogs of cycloheptatrienes) **IIa** and **IIb** (Scheme 2a), was reported by our group in 2017.[9] In this process, the silylene insertion into the aromatic C−C bond of a Dipp substituent is reversible, as we demonstrated by the reactivity studies of **IIa** and **IIb** and, directly, in the reaction of **Ic** ⇌ **IIc**, in which both isomers can be observed at ambient conditions.[10] The reversibility of the C−C insertion allows the silepins **IIa**, **IIb**, and **IIc** to act as synthetic equivalents of silylenes in small molecule activation.[9,10] Additionally, our group also reported the iminosiloxysilepin **IId**[11] that forms upon irradiation of the isolated iminosiloxysilylene **Id**[9b] (Scheme 2a).

Scheme 2. (a) Silylene Insertion into Aromatic C−C Bond; (b) Silylene Insertion into Aromatic C−N Bond; (c) Present Work

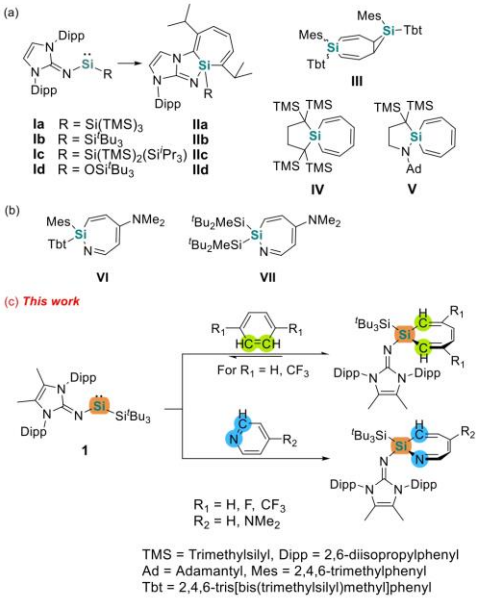

TMS = Trimethylsilyl, Dipp = 2,6-diisopropylphenyl
Ad = Adamantyl, Mes = 2,4,6-trimethylphenyl
Tbt = 2,4,6-tris[bis(trimethylsilyl)methyl]phenyl

The entropically more difficult intermolecular dearomatization of arenes by silylenes could also be achieved in a few cases. In 1994, Okazaki reported [1 + 2] cycloaddition of a silylene (generated *in situ* from a disilene) with benzene, forming a bicyclic compound **III** (Scheme 2a).[12] They proposed that the formation of **III** proceeds similarly to Büchner ring expansion, involving silanorcaradiene and silepin intermediates. However, the isolation of the silepin intermediate could not be accomplished in this case since the silepin is more reactive than benzene toward the silylene, resulting in the successive [1 + 2] cycloaddition to give **III**. In the same report, the reaction with naphthalene yielded no ring expansion products, but rather two consecutive [1 + 2] cycloadditions, providing evidence for the existence of the proposed silanorcaradiene intermediate. In 2002, Kira reported the silepin **IV**, formed in a photochemical reaction of benzene with a cyclic dialkylsilylene (Scheme 2a).[13a] The follow-up quantum chemical calculations showed that, in the reaction with benzene, the singlet excited state of silylene, generated by irradiation, forms a 1,3-diradical reactive intermediate, which subsequently undergoes cyclization to silanorcaradiene and ring expansion to form the silepin.[13b] Analogous formation of silepin **V** by an excited state cyclic alkyl amino silylene was demonstrated by Iwamoto (Scheme 2a).[14] Intermolecular dearomatization by silylenes of more reactive azulene or naphthalene was also reported by Iwamoto[15] and Chen et al.[16] Besides these examples, only few low-valent main group[17] and transition-metal complexes[18] capable of aromatic C−C bond cleavage were reported.

N-Heterocyclic arenes, like pyridine, can exhibit higher reactivity than benzene in certain cases due to the negative inductive effect of nitrogen, which not only prevents the electron delocalizing evenly over the ring but also causes lower aromatic resonance energy.[19] The permanent polarization of the π-system, which can be used for substitution of nitrogen to afford azinium salts (key intermediates of N-heterocyclic arene functionalization without catalyst),[20] makes it difficult for *N*-heterocyclic arene to undergo ring-opening under mild conditions. In low-valent transition-metal chemistry only a few examples were reported.[21] In main group chemistry a few scarce studies on silylene mediated C═N bond cleavage of pyridines, to give azasilepins **VI**[22] and **VII**[23] at elevated temperature, were reported by Tokitoh and our group (Scheme 2b).

One of the focuses of our research is the investigation of reactive capabilities of silylenes in relation to activation of small molecules and inert bonds. From this perspective, acyclic silylenes allow for enhanced reactivity, in comparison to cyclic silylenes, since they generally possess a smaller HOMO−LOMO gap with a low-lying excited state and are structurally more flexibile.[7d,24] Specifically, we have widely utilized *N*-heterocyclic imine (NHI) ligands in stabilization and reactivity explorations of low-valent main group element complexes.[25] Especially in silicon chemistry, NHI provided remarkable compounds and reactivities such as silepins mentioned above,[9−11] silanones,[9b,26] and disilenes.[27] Our studies have shown that the relative favorability of the intramolecular aromatic C−C insertion can be influenced by slight alternations of the iminosilylene substituents. Given our success in activation of intramolecular aromatic C−C bonds, we focused on developing an iminosilylene system capable of intermolecular aromatic C−C activation. Upon examination of the structural features of compounds **IIa**, **IIb**, and **IIc**, it came to our attention that the ^{i}Pr substituents of the silepin moieties are found in close proximity to the −CH═CH− bridge of the NHIs. Since the reactions of silylene insertion into the C═C bond of the Dipp substituent in these compounds are only slightly exergonic, we reasoned that methylation of the NHI will result in a higher steric repulsion between the ^{i}Pr substituent and the NHI, which could completely prevent the intramolecular aromatic C−C insertion. This scenario may not only allow for the isolation of a stable iminosilylene but also afford species capable of reacting with aromatic C−C bonds intermolecularly.

In this contribution, we present the synthesis and isolation of the acyclic imino(silyl)silylene **1**. The unique feature of **1** compared to previously described, nonisolable imino(silyl)-silylenes (**Ia**, **Ib**, and **Ic**) is the methylated backbone of the NHI substituent. This feature disfavors the intramolecular insertion of the silylene center into the aromatic C−C bond of

https://doi.org/10.1021/jacs.2c10467
J. Am. Chem. Soc. 2023, 145, 1011−1021

the Dipp substituent. Instead, **1** exhibits an extraordinary reactivity of intermolecular dearomatization of arenes at ambient temperatures (Scheme 2c).

RESULTS AND DISCUSSION

The synthesis of the imino(silyl)silylene **1** was accomplished by treatment of one equivalent of Si(IV) precursor methylated backbone *N*-heterocyclic iminosilicon tribromide with two equivalents of the silanide complex $[Na\cdot(THF)_2]Si^tBu_3$ in toluene at room temperature, affording a deep green solution with sodium bromide precipitate (Scheme 3).[9a] After washing

Scheme 3. Synthesis of Acyclic Silylene 1

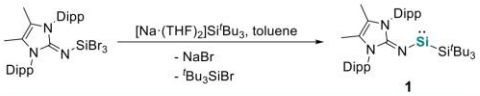

the crude product with cold hexamethyldisiloxane, **1** could be isolated in 60% yield as intensely blue powder. The $^{29}Si\{^1H\}$ NMR displays a signal at 454.0 ppm for the central silicon atom. This value lies in the range of known two-coordinated acyclic silylenes (35.5−467.5 ppm).[9b,28] The GIAO NMR calculated shift at 449.0 ppm is in a good agreement with the experiment (for additional information regarding the employed computational methods, see Supporting Information). In UV−vis spectroscopy, a characteristic low intensity band at 651 nm was observed (ε = 361 M^{-1} cm^{-1}, Figure S5). Accordingly, TD-DFT calculations show a transition at 626 nm, corresponding to the n → p excitation (Figures S50−S51 and Table S3). The molecular structure of **1** was determined by single crystal X-ray diffraction (SC-XRD) analysis (Figure 1) and it represents a rare example of structurally defined NHI-

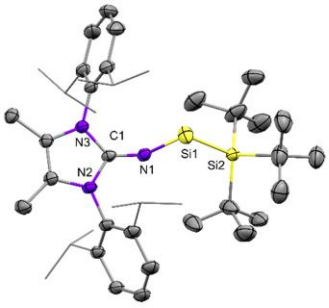

Figure 1. Molecular structure of **1**. Ellipsoids set at 30% probability to compensate for advanced thermal motion. Hydrogen atoms are omitted for clarity. Selected bond lengths [Å] and angles [deg]: Si1−Si2 2.4438(13), Si1−N1 1.665(2), C1−N1 1.297(3); N1−Si1−Si2 106.15(9), C1−N1−Si1 138.4(2).

silylenes.[9b,29] The Si1−N1 distance of 1.665(2) Å is similar to previous imino(siloxy)silylene (1.661(2) Å),[9b] but much shorter than known acyclic aminosilylenes (1.720(1)−1.750(10) Å).[28a,c,e] The N1−Si1−Si2 angle of 106.15(9)° is significantly more obtuse than the angles around the central Si atom typical for cyclic silylenes (86.94°−93.88(7)°),[14,30] implying higher reactivity,[24,28a] but it is still more acute than acyclic aminosilylsilylene $Si\{Si(SiMe_3)_3\}\{N(SiMe_3)Dipp\}$ (116.91(5)°).[28c]

The calculated electronic structure of **1** is essentially similar to that of the previously reported **Ic** and is described in detail in the Supporting Information (Figures S52−S54, S56).[10] The HOMO−LUMO gap of 3.22 eV (Figure S56) and the singlet−triplet energy gap ΔE_{ST} = 14.1 kcal mol^{-1} are slightly lower than those of **Ic** (3.25 eV, 18.2 kcal mol^{-1}) and the closely related, nonmethylated **Ib** (3.27 eV, 18.6 kcal mol^{-1}),[9a,10] which may point to increased ambiphilic reactivity. In order to assess the donor−acceptor abilities of **1** and compare them to other silylenes, the proton affinity (PA) and relative P−H rotational barrier (RRB) of **1** were calculated at the B97D//def2-TZVP//B97D/6-31G* level of theory, identically to the method used in the benchmark study by Szilvási.[31] **1** exhibits both a high PA of 1176 kJ mol^{-1} and high RRB of 0.508, compared with other reported silylenes, which reflect the high σ-donor and π-acceptor abilities. The σ-donor ability of **1** surpasses most of the three-coordinate silylenes, and its π-acceptor ability is greater than almost all of the donor-free silylenes mentioned in the benchmark study. In fact, the only other silylene on the list that has both a comparably high PA (1133 kJ mol^{-1}) and RBB (0.562) is the borylaminosilylene.[28a] The clearly ambiphilic nature of **1** enables the herein presented activation of arenes, as both the silylene lone pair interaction with the π^*-orbitals of an arene and the interaction between the vacant p-orbital with the arene π-system are crucial for the facile addition of a silylene to an aromatic C−C bond.[13]

Unlike the previously reported transient analogs of **1**, *i.e.* **Ia**, **Ib**,[9] or even the room temperature observable **Ic**,[10] which could not be isolated as silylenes since they undergo an intramolecular aromatic C−C bond insertion to form the corresponding silepins (Scheme 2a), **1** is persistent as silylene at ambient temperature. In the solid state, **1** is stable for more than half a year under an argon atmosphere, and in solution the intramolecular C−C insertion to form **1′** is not observed (Scheme 4a). DFT calculations show that the intramolecular

Scheme 4. Reactivity of Acyclic Silylene 1

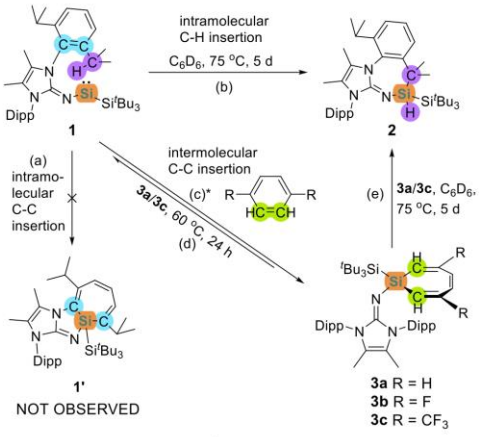

* benzene, rt, 1 month or 40 °C, 1 week gives **3a**.
1,4-difluorobenzene/benzene, rt. 2 weeks or 40 °C, 24 h gives **3b**.
1,4-bis(trifluoromethyl)benzene/benzene, rt. 2 days gives **3c**.

https://doi.org/10.1021/jacs.2c10467
J. Am. Chem. Soc. 2023, 145, 1011−1021

C−C insertion is energetically unfavorable in **1** (Figure 2, blue). This process is predicted to be endergonic by 7.6 kcal

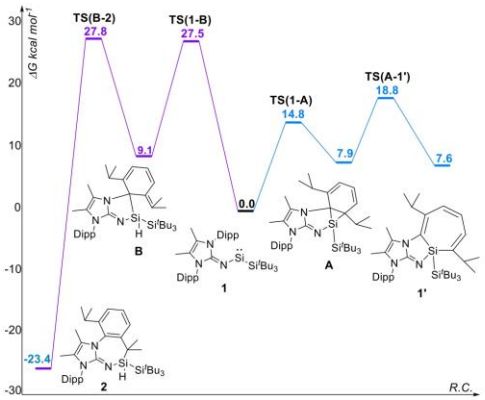

Figure 2. Calculated reaction pathway for the proposed mechanisms of the intramolecular insertion into the C═C (blue) and the C−H (purple) bonds in **1** at the PBE0-D3/def2-TZVP//PBE0-D3/def2-TZVP level of theory.

mol^{-1}. In comparison, the intramolecular C−C insertion is exergonic by 3.8 and 2.1 kcal mol^{-1} in the case of **Ia** and **Ib**, respectively. An insight into this phenomenon, which is attributed to the steric hindrance imposed by the presence of the methyl substituents on the NHI, can be provided by the comparison of **1′** with **IIb**, which are structurally identical with the exception of the methyl substituents. Natural steric analysis shows that the total steric exchange energy difference (ΔE_{Steric}) between the silylene and the silepin is 78.6 kcal mol^{-1} in the case of **1** → **1′** and 69.1 kcal mol^{-1} in the case of **Ib** → **IIb**. The ΔE_{Steric} = 9.5 kcal mol^{-1} correlates well the difference in Gibbs energies of the respective reactions (ΔG = 11.4 kcal mol^{-1}). The optimized structure of **1′** shows a close proximity between one of the NHI methyl groups and the closest isopropyl substituent of Dipp. Furthermore, in **1′** the second Dipp substituent is oriented in a way that leads to additional steric repulsion associated with the $^{i}Pr^{Dipp}$···$^{t}Bu_3Si$ interaction. All of these interactions are absent in **IIb**, since the NHI backbone is not methylated. The PNLMO overlaps and the corresponding pairwise steric exchange energies for the disjoint interactions present in **1′** and absent in **1** and **IIb** are shown in Figure S55. Based on these results, it is reasonable to suggest that the relative unfavorability of the formation of **1′** from **1**, in comparison to **Ib** → **IIb**, is due to the steric repulsions impelled by the methyl groups on the NHI backbone.

The calculated potential energy surface (PES) for the proposed mechanism of the intramolecular C−C activation is presented in Figure 2 (blue). The first step involves the reaction of the silylene across the aromatic C−C bond, dearomatizing the aryl and forming the Si(IV) silanorcaradiene intermediate (**A**) at 7.9 kcal mol^{-1}. At the second step, the single C−C bond is cleaved to form the silepin **1′** at 7.6 kcal mol^{-1}. The reaction barriers for both steps are relatively low (**TS(1-A)** at 14.8 kcal mol^{-1} and **TS(A-1′)** at 18.8 kcal mol^{-1}) and should be achievable at room temperature, resulting in **1**⇌**1′** room temperature thermodynamic equilibrium. However, due to the large energetic difference between the reactant and the product, **1′** cannot be observed (with a Gibbs energy difference of 7.6 kcal mol^{-1} at 25°C, the equilibrium constant for **1**⇌**1′** would be 4.5 × 10^{-6}).

Instead, upon heating a C_6D_6 solution of **1** to 75 °C for 5 days, an intramolecular Si(II) insertion into the C−H bond of the ^{i}Pr moiety of the NHI substituent takes place, giving the Si(IV) hydrosilane **2** (Scheme 4b), which features a seven-membered heterocycle. Similar aminosilylene C−H insertion reactivities were reported before.[28a,c] A new singlet Si−H resonance was observed at 4.93 ppm (J_{Si-H} = 177.2 Hz) in the ^{1}H NMR spectrum, and its corresponding ^{29}Si{^{1}H} was observed at −19.0 ppm (calculated −28.7 ppm). SC-XRD analysis revealed a seven-membered cyclic ring (Figure 3), with the newly formed Si1−C24 bond of 1.962(17) Å. The Si1−N1 distance of 1.713(13) Å is much longer than in **1**.

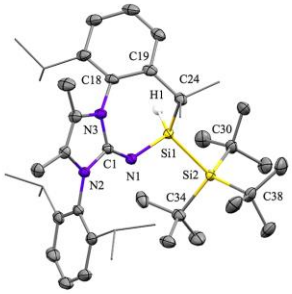

Figure 3. Molecular structure of **2**. Ellipsoids set at 50% probability. Hydrogen atoms are omitted for clarity, except for the respective Si−H nuclei of silane (H1). Selected bond lengths [Å] and angles [deg]: Si1−Si2 2.4168(6), Si1−N1 1.7135(13), Si1−C24 1.9623(17), C1−N1 1.2841(19), C1−N3 1.385(2); N1−Si1−Si2 108.44(5), C1−N1−Si1 126.03(11), N1−Si1−C24 106.03(7).

DFT calculations show that the intramolecular Si(II) insertion into the C−H bond of the ^{i}Pr moiety proceeds in two steps. The calculated PES for the proposed mechanism is presented in Figure 2 (purple). First, the silylene center abstracts a hydrogen from the isopropyl substituent and adds to the ipso-carbon of the aryl, forming the conjugated triene intermediate **B**. This step is endergonic by 9.1 kcal mol^{-1}. At the second step, a 1,3-silyl migration occurs, which leads to the Si−C^{ipso} bond cleavage, the Si−C^{iPr} bond formation, and rearomatization of the aryl. The high energy barriers for the two reaction steps, *i.e.* **TS(1-B)** at 27.5 kcal mol^{-1} and **TS(B-2)** at 27.8 kcal mol^{-1}, are concurrent with the elevated temperature and the protracted time required for the intramolecular C−H insertion to take place. The overall high exergonicity of the process (ΔG = −23.4 kcal·mol^{-1}), and the extremely high barrier for the reverse reaction (*i.e.*, **2** to **B**) of 51.2 kcal·mol^{-1}, make the C−H insertion irreversible.

Remarkably, leaving **1** at room temperature for a prolonged period in C_6D_6 or benzene solution leads to a slow reaction of the silylene with the solvent via the insertion into the aromatic C−C bond, which gives Si(IV) silepin **3a** in 20% conversion after 1 month (Scheme 4c). The silepin could also be isolated by heating a benzene solution of **1** at 40 °C for 1 week in 40% yield (50% conversion by ^{1}H NMR spectroscopy). **3a** is stable in solid state and solution (pentane, benzene, and THF) at

https://doi.org/10.1021/jacs.2c10467
J. Am. Chem. Soc. 2023, 145, 1011−1021

room temperature even under air over 1 week. Of particular interest, upon heating C_6D_6 solution of **3a** to 60 °C, **3a** was converted back to silylene **1** (Scheme 4d), as observed both by NMR spectroscopy and by color change from yellow to blue (Figure S35). This reversible benzene activation represents a rare example of reversible Büchner ring expansion in main group chemistry.[5,9a,17b] The reversibility of the benzene activation was further exemplified by heating a C_6D_6 solution of **3a** to 75 °C for 5 days, which led to the formation of the aforementioned hydrosilane **2** (Scheme 4e). The molecular structure of **3a** was determined by SC-XRD analysis (Figure 4), showing a nearly planar silepin seven-membered SiC_6 ring

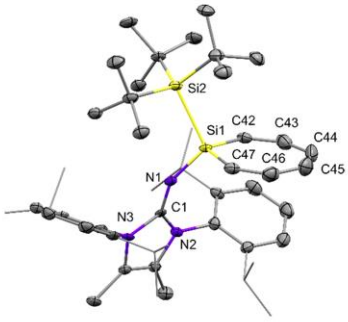

Figure 4. Molecular structure of **3a**. Ellipsoids set at 50% probability. Hydrogen atoms are omitted for clarity. Selected bond lengths [Å] and angles [deg]: Si1−Si2 2.3967(15), Si1−N1 1.689(3), Si1−C42 1.875(4), Si1−C47 1.877(4), C42−C43 1.336(5), C43−C44 1.452(7), C44−C45 1.359(7), C45−C46 1.432(5), C46−C47 1.338(6); N1−Si1−Si2 111.14(11), C42−Si1−C47 107.28(18).

with tilt angles $\alpha = 2.4°$, $\beta = 4.3°$ (for definition of tilt angles see Scheme 5). The Si1−C42 and Si1−C47 distances are

Scheme 5. Geometries of Cyclohepta-1,3,5-triene and Silepin

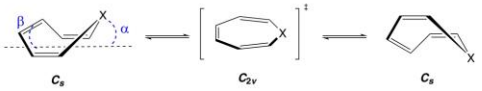

almost identical (1.875(4) and 1.877(4) Å) and much shorter than Si−C single bonds in **3a**. The C−C bond lengths in **3a** (1.336(5), 1.452(7), 1.359(7), 1.432(5), 1.338(6) Å) are consistent with alternating C═C double and C−C single bonds within a silepin ring.[13a] To the best of our knowledge, this is a rare example of intermolecular aromatic C═C double bond activation of benzene under mild conditions,[12,17b] and the first example of a silepin exhibiting a nearly planar geometry.[9a,13a,17e,32] The ^{1}H NMR signals of the seven-membered ring were observed at 5.56, 5.70, 5.99 ppm, and are much more upfield shifted than known silepin **IV** and **V**,[13a,14] indicating more paratropic ring current.[33] The central silicon atom displays a signal at −38.8 ppm (calculated −42.4 ppm), which is upfield shifted compared with known silepins **IV** (6.1 ppm)[13a] and **V** (−8.9 ppm),[14] presumably due to increased electron density.

Inspired by the intermolecular reversible C−C bond activation of benzene, we investigated similar reactivity of **1** toward other benzene derivatives. No reactivity of **1** toward toluene, anisole, or naphthalene was detected in toluene at ambient temperatures or 75 °C for 2 days when hydrosilane **2** has already started to accumulate. However, C−C bond cleavage of benzene derivatives featuring electron-withdrawing groups could be achieved under mild conditions. Upon treatment of **1** with fluorobenzene in C_6D_6 (C_6D_6/C_6H_5F = 1:1) at room temperature, 35% conversion was observed after 1 week by ^{1}H NMR. Heating the reaction mixture to 60 °C for 2 days resulted in full conversion of **1**, giving a mixture of two C−C insertion isomeric products (Figure S41a).

To avoid the formation of different isomers, 1,4-difluorobenzene and 1,4-bis(trifluoromethyl)benzene, in which only the addition across C_2-C_3 would be expected, were investigated (Scheme 4c). In the reaction of **1** with 1,4-difluorobenzene in benzene, 50% conversion was observed after 1 week at room temperature. Full conversion was achieved at 40 °C after 24 h exclusively furnishing the corresponding C_2-C_3 bond cleavage product, *i.e.* silepin **3b** (Scheme 4c). The ^{1}H NMR signals of the seven-membered ring were observed at 5.26, 5.35, 5.55 ppm (Figure S19), about 0.4 ppm upfield shifted compared to silepin **3a** due to the electron donation from fluoride lone pairs. The central ^{29}Si-{^{1}H} displayed a triplet signal at −49.6 ppm (calculated −54.2 ppm) with $^3J_{Si-F}$ = 17.6 Hz.

Similarly, upon treatment of **1** with an excess of 1,4-bis(trifluoromethyl)benzene in benzene for 2 days at room temperature, 70% conversion was observed by ^{1}H NMR monitoring. Two new singlet signals belonging to the bis(trifluoromethyl)benzene adduct appearing at 5.90 and 6.37 ppm, shifted approximately 0.4 ppm downfield compared with **3a**, which is consistent with the strong electron-withdrawing effect of the CF_3 substituent. The ^{29}Si{^{1}H} NMR displayed a singlet signal at −43.9 ppm (calculated −44.0 ppm) for the central silicon atom. Yellow crystals of **3b** were obtained by slow evaporation of benzene solution at ambient temperature, and orange crystals of **3c** were obtained by slow evaporation of pentane, THF, and toluene solution at −30 °C. Subsequent SC-XRD analysis revealed almost planar structures of silepin rings in **3b** and **3c** as well (Figure 5). The Si−C bond lengths (**3b**: 1.866(15) and 1.867(16) Å; **3c**: 1.875(13) and 1.867(14) Å) are similar to those of **3a**, but the C−C bond lengths of **3c** are slightly longer than those of **3a** and **3b**, possibly due to the steric hindrance of CF_3 groups.

Silepin **3b** and **3c** are stable in the solid state at ambient temperature under an argon atmosphere for at least one month. Silepin **3b** is also stable upon heating the benzene solution to 120 °C for 3 days in a J-Young sealed tube. However, **3c** shows slow reversibility in benzene solution to regenerate silylene **1** and 1,4-bis(trifluoromethyl)benzene at room temperature or a completely reversible reaction upon heating to 60 °C for 12 h (Scheme 4d and Figure S36).

To gain insight into the electronic structure, density functional theory was performed. DFT calculations show that the HOMO−1 of **3a** mainly corresponds to the conjugated triene system of the silepin moiety, and the HOMO corresponds mainly to the π-system of the five-membered ring of the NHI interacting with the C−N π^* orbital, while the LUMO corresponds to the π^*(C−C) orbitals of the silepin (Figure 6). The corresponding Wiberg bond indexes between the carbon atoms constituting the silepin ring (WBI($C^{42}-C^{43}$)

https://doi.org/10.1021/jacs.2c10467
J. Am. Chem. Soc. 2023, 145, 1011−1021

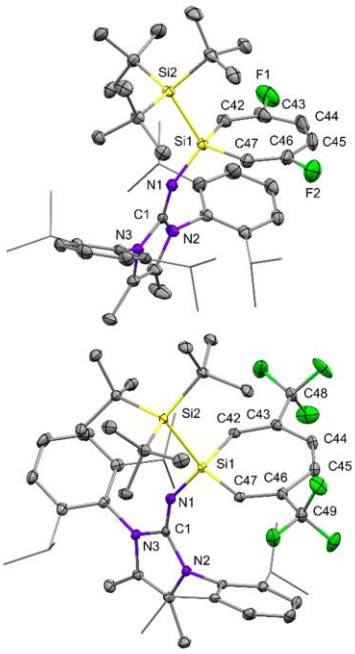

Figure 5. Molecular structures of **3b** and **3c**. Ellipsoids set at 50% probability. Hydrogen atoms are omitted for clarity. Selected bond lengths [Å] and angles [deg]: **3b** Si1−Si2 2.4051(5), Si1−N1 1.6837(12), Si1−C42 1.8660(15), Si1−C47 1.8674(16), C42−C43 1.333(2), C43−C44 1.437(3), C44−C45 1.335(3), C45−C46 1.442(3), C46−C47 1.327(2); N1−Si1−Si2 111.96(4), C42−Si1−C47 106.93(7); **3c**: Si1−Si2 2.4143(6), Si1−N1 1.6769(11), Si1−C42 1.8752(13), Si1−C47 1.8670(14), C42−C43 1.3423(18), C43−C44 1.4609(19), C44−C45 1.345(2), C45−C46 1.4647(19), C46−C47 1.3442(19); N1−Si1−Si2 114.18(4), C42−Si1−C47 108.08(6).

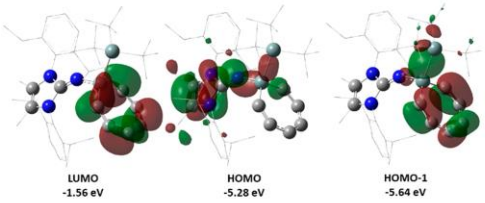

Figure 6. Frontier molecular orbitals of **3a** (iso = 0.03).

= 1.81, WBI(C^{43}−C^{44}) = 1.15, WBI(C^{44}−C^{45}) = 1.72, WBI(C^{45}−C^{46}) = 1.15, WBI(C^{46}−C^{47}) = 1.81) reflect the conjugated nature of the a planar triene system. Natural localized molecular orbitals depict the delocalization between the C−C π-bond and to the adjacent π^*(C−C)-orbitals. Second order perturbation analysis shows a significant amount of donor interaction from π(C^{42}−C^{43}) to π^*(C^{44}−C^{45}) of 16.0 kcal mol^{-1}, from π(C^{44}−C^{45}) to π^*(C^{42}−C^{43}) and π^*(C^{46}−C^{47}) of 14.9 and 15.7 kcal mol^{-1}, and from π(C^{46}−C^{47}) to π^*(C^{44}−C^{45}) of 15.3 kcal mol^{-1}. WBIs for the Si^1−C^{42} and Si^1−C^{47} bonds are both equal to 0.77.

The planar geometry, magnetic properties (NMR), and the electronic structure of the silepin moiety in **3a** raise a question regarding its aromatic/antiaromatic nature. The parent silepin is a silicon counterpart of a cyclohepta-1,3,5-triene (CHT) which exhibits a boat-shaped conformation as determined by electron diffraction, microwave studies, and quantum chemical calculations.[33,34] In the boat-shaped CHT and its heteroelement analogs (*e.g.*, silepin), the deviation from planarity can be expressed by the bow (α) and stern (β) tilt angles (Scheme 5). The X-ray structure of **3a** shows tilt angles α and β of 2.4° and 4.3° respectively (4.6° and 5.5° in the DFT optimized structure), rendering the silepin essentially planar. This structural feature is unique, as other silepins, whose structure was determined by X-ray crystallography, exhibit explicit boat-shaped conformations with bow angles in the range 33.0°−57.3° and stern angles in the range 24.5°−42.4°.[9a,13a,17b,32] The nearly planar geometry of the silepin moiety in **3a** is characteristic of the ring inversion transition state, which connects the two CHT conformers. Previous studies have concluded that CHT is homoaromatic due to delocalization through space.[33] Low temperature ^{1}H NMR measurements showed that the homoaromatic, C_s-symmetrical, boat conformation of CHT is prone to undergo a degenerate ring flip via a planar (α = 0°, β = 0°) antiaromatic C_{2v} transition with a free energy barrier of 5.7 kcal·mol^{-1} in $CBrF_3$ and 6.3 kcal·mol^{-1} in CF_2Cl_2.[35] Our gas phase calculations yield the value $\Delta G^{\ddagger}$ = 7.4 kcal mol^{-1} for CHT. The planar C_{2v} conformation is more easily achievable in parent silepin with $\Delta G^{\ddagger}$ = 3.1 kcal mol^{-1} for the degenerate ring flip. Unlike the C_{2v} conformation of CHT that is predicted to be homoaromatic, previous studies suggested that the planar transition state C_{2v} structure is of an antiaromatic character, due to the pseudo-2π-electron effect of the CH_2 group.[33]

In order to verify the presence of ring currents in **3a** and compare with the parent compounds, the out-of-plane components of nucleus-independent chemical shifts (NICS), *i.e.* NICSzz(1), were calculated.[36] As expected, and in agreement with previous computational results, the homoaromatic C_s-symmetrical CHT exhibits a lower degree of aromaticity than benzene with NICSzz(1) and NICSzz(−1) of −10.6 and −14.6 ppm.[33] Calculations show that the degree of aromaticity is even lower for the parent C_s-symmetrical silepin (NICSzz(1) = −5.9 ppm, NICSzz(−1) = −6.8 ppm). In contrast, the planar C_{2V} CHT exhibits a significant degree of antiaromaticity with NICSzz(1) = 21.1 ppm. To a much lesser extent, the parent C_{2V} silepin is also slightly antiaromatic with NICSzz(1) = 7.2 ppm, whereas **3a** shows NICSzz(1) = 2.3 ppm and NICS(−1) = −1.0 ppm. For comparison, we optimized the structure of an acyclic (*Z*)-hexa-1,3,5-triene in a planar C_{2V} geometry, which corresponds to a second-order saddle point. The calculated NICSzz(1) of this nonaromatic system is 1.3 ppm. Thus, calculations conclude that, in **3a**, the antiaromaticity is negligible and it may be tentatively considered nonaromatic.

The calculated PES of the proposed mechanism of the reaction of imino(silyl)silylene **1** with benzene to form the silepin **3a** is presented in Figure 7 (red). Similar to the intramolecular insertion of the silylene center into the aromatic C−C bond discussed above, the formation of **3a** from **1** proceeds in two steps. The first step involves a formal [2 + 1] cycloaddition across the C−C bond of benzene via **TS(1-Ca)** at 24.5 kcal mol^{-1} to form the bicyclic silanorcaradiene intermediate **Ca**, at 14.5 kcal mol^{-1}. The frontier orbitals of

https://doi.org/10.1021/jacs.2c10467
J. Am. Chem. Soc. 2023, 145, 1011−1021

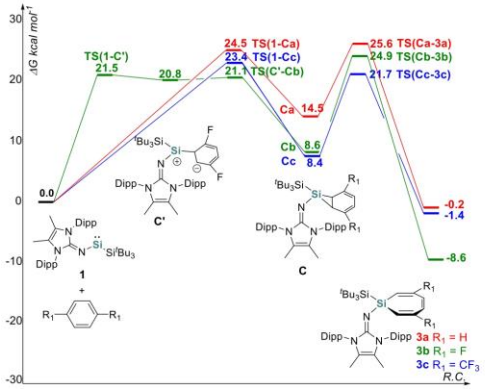

Figure 7. Calculated PES for the proposed mechanisms of the intermolecular insertion of **1** into the C═C bonds of benzene (red), 1,4-difluorobenzene (green), and 1,4-bis(trifluoromethyl)benzene (blue) at the PBE0-D3/def2-TZVP//PBE0-D3/def2-TZVP level of theory.

TS(1-Ca) presented in Figure S56 show that the HOMO mainly corresponds to the interaction of the Si lone pair with the π^*-system of benzene, while the LUMOs correspond to the interaction between the p-orbital of Si with the π^*-system. The second step of the C−C bond cleavage to form **3a** with the transition state at 25.6 kcal mol^{-1} is a rate-determining step (RDS). The overall process is energetically almost neutral with the Gibbs energy difference between the reactants and the product of only −0.2 kcal mol^{-1}. This small energy difference is in line with experiment, where no full conversion of **1** to **3a** could be observed. The calculated barrier for the RDS in this reaction is 2.2 kcal mol^{-1} lower than that of the intramolecular C−H insertion (Figure 2, **TS(B-2)**), which is consistent with the selective intermolecular aromatic C−C bond activation. The overall redox process in the reaction of **1** with benzene can be estimated from the change of the sum of natural charges of the atoms constituting the individual moieties. In comparison with the starting components, it shows that benzene is reduced by one electron, while the oxidation occurs mainly at the silylene Si center (difference in natural charges in **3a** vs **1** + benzene: $\Delta\sum q^{benzene} = -0.89$ el., $\Delta\sum q^{Si} = 0.72$ el., $\Delta\sum q^{SitBu3} = 0.16$ el., $\Delta\sum q^{NHI} = 0.01$ el.). The main reduction step of benzene occurs upon the formation of intermediate **Ca**, when the benzene moiety is reduced by 0.83 el. and the silicon center is oxidized by 0.63 el. (difference in natural charges in **Ca** vs **1** + benzene: $\Delta\sum q^{benzene} = -0.83$ el., $\Delta\sum q^{Si} = 0.63$ el., $\Delta\sum q^{SitBu3} = 0.20$ el., $\Delta\sum q^{NHI} = 0.00$ el.).

Mechanistically, the insertion of the silylene into the aromatic C−C bond of 1,4-bis(trifluoromethyl)benzene to form **3c** is predicted to proceed similarly to the reaction of **1** with benzene (Figure 7, blue). The [2 + 1] cycloaddition of the silylene to the C═C bond of 1,4-bis(trifluoromethyl)-benzene, forming the bicyclic intermediate **Cc**, is followed by the C−C bond cleavage to yield silepin **3c**. The transition state for the first step at 23.4 kcal mol^{-1} (**TS(1-Cc)**, blue) is slightly lower than the respective transition states in the case of benzene (by 1.1 kcal mol^{-1}). This presumably stems from a better energetic compatibility between the π and π^*-orbitals of 1,4-bis(trifluoromethyl)benzene with the frontier orbitals of **1**, in comparison to benzene (the corresponding HOMO−LUMO gaps are 6.70 and 7.12 eV). The higher proclivity of **1** to undergo [2 + 1] cycloaddition with 1,4-bis-(trifluoromethyl)benzene is also reflected in HOMO−LUMO gaps of the transition states with 2.35 eV for 1,4-bis(trifluoromethyl)benzene and 2.86 eV for benzene. The [2 + 1] cycloaddition of **1** with 1,4-difluorobenzene (Figure 7 green) proceeds via a zwitterionic intermediate **C′** (a shallow minimum), which rearranges to the **C** via a low barrier of only 0.3 kcal mol^{-1} (**TS(C′-C)**). The barriers for these steps are lower than those for benzene and 1,4-bis(trifluoromethyl)-benzene, as 1,4-difluorobenzene exhibits the smallest HOMO−LUMO gap in the series of 6.32 eV.

As mentioned above, the formation of the silanorcaradiene intermediate is the step in which most charge transfer from the silylene to the arene takes place. Thus, it is expected that the relative energies of differently substituted intermediates **C** would correlate with the relative ability of the arenes to accept an electron. Calculations show that one-electron reductions of 1,4-difluorobenzene and 1,4-bis(trifluoromethyl)benzene are more favorable than that of benzene by 15.1 and 41.7 kcal mol^{-1}, respectively, making their reduction more benign, which is in line with the calculated Gibbs energies. The fact that bis(CF_3) substituted intermediate **Cc** is lower in energy by only 0.2 kcal mol^{-1} with respect to bis-fluoro substituted intermediate **Cb** is apparently due to the larger steric interaction imposed by the presence of the more bulky CF_3 substituent. According to natural steric analysis, the difference in total steric exchange energy between **1** + arene vs **C** is 30.9 kcal mol^{-1} higher in 1,4-bis(trifluoromethyl)benzene in comparison with 1,4-difluorobenzene.

DFT calculations show that the second transition state, which involves the arene C−C bond cleavage, is the lowest in energy in the case of 1,4-bis(trifluoromethyl)benzene at 21.7 kcal mol^{-1}, compared with **TS(Ca-3a)** (at 25.6 kcal mol^{-1}) and **TS(Cb-3b)** (at 24.9 kcal mol^{-1}). NBO analysis reveals that the weakest bonding interaction of the cleaved C−C bond is present in the bis(CF_3) substituted species, with a WBI of 0.5952, 0.5949, and 0.55 in **TS(Ca-3a)**, **TS(Cb-3b)**, and **TS(Cc-3c)**, respectively. The corresponding σ(C−C) occupancies of 1.71, 1.72, and 1.65 el. denote a higher degree of σ(C−C) delocalization in **TS(Cc-3c)**. The second-order perturbation analysis shows the total donor interactions of σ(C−C) account for 57.7, 65.1, and 70.7 kcal mol^{-1}, while the total acceptor interactions of σ^*(C−C) are 26.5, 21.9, and 25.2 kcal mol^{-1}, respectively.

Unlike the reactions of **1** with benzene and 1,4-difluorobenzene, in which the highest barriers corresponds to the C−C bond cleavage, the rate-determining step for the reaction of **1** with 1,4-bis(trifluoromethyl)benzene is the [2 + 1] cycloaddition. Thus, the overall barrier for formation of **3c** is predicted to be by 2.2 kcal mol^{-1} lower than that of **3a**, which is in line with a shorter time required for this reaction (Scheme 4c). The overall barrier for formation of **3b** is predicted to be 0.7 kcal mol^{-1} lower than that of **3a** and 1.5 kcal mol^{-1} higher than that of **3c**, which is compatible with the intermediate reaction time required for this process (Scheme 4c). The observation of **3c** converted back to **1** is compatible with the calculated small difference in Gibbs energy (−1.4 kcal mol^{-1}) for this reaction, and the barrier of 24.8 kcal mol^{-1} for the reverse reaction (Figure 7, blue). An analogous back reaction of **3b** to form **1** and 1,4-difluorobenzene is essentially irreversible under the experimental conditions due to the large

https://doi.org/10.1021/jacs.2c10467
J. Am. Chem. Soc. 2023, 145, 1011−1021

free energy difference of 8.6 kcal mol^{-1} and a high barrier of 33.5 kcal mol^{-1}.

As mentioned in the introduction, due to the negative inductive effect, pyridine ring opening under mild conditions is a challenging task.[21f,g,i−l] To illustrate the capacity of **1** in *N*-heterocyclic arene dearomatization, we treated **1** with pyridines. The reaction of **1** with pyridine in pentane occurs within seconds, and with 4-*N*,*N*-dimethylaminopyridine (DMAP) in benzene within 12 h, to afford the corresponding

Scheme 6. Activation of Pyridines by Silylene 1

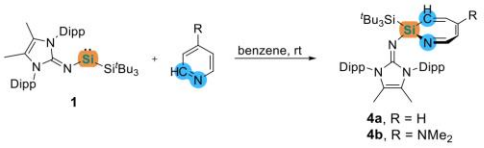

C═N bond insertion products (Scheme 6). A central silicon ^{29}Si{^{1}H} NMR chemical shift was observed at −40.2 (**4a**) and −42.9 (**4b**) ppm, respectively (calculated −44.1 and −48.3 ppm). Similar downfield shifts in NMR spectrum were observed in the known azasilepins **VI** and **VII**.[22,23] SC-XRD analysis of **4a** (Figure 8) revealed the formation of a planar

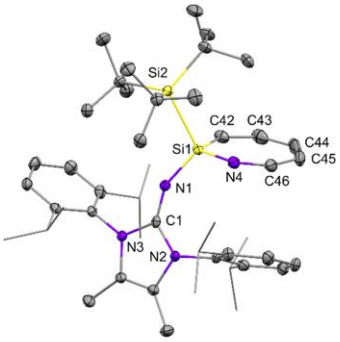

Figure 8. Molecular structure of **4a**. Ellipsoids set at 50% probability. Hydrogen atoms are omitted for clarity. Selected bond lengths [Å] and angles [deg]: Si1−Si2 2.3937(6), Si1−N1 1.6775(12), C1−N1 1.2763(18), Si1−C42 1.8710(16), Si1−N4 1.7416(12), C42−C43 1.345(2), C43−C44 1.456(3), C44−C45 1.339(3), C45−C46 1.459(3), C46−N4 1.2673(19); N1−Si1−Si2 112.51(4), C42−Si1−N4 110.07(7).

SiNC$_5$ ring. The Si1−N4 distance of 1.742(12) Å is similar to previously reported azasilepins 1.750(1) Å.[22,23] And the C46−N4 distance of 1.267(19) Å is also similar to the C1−N1 distance of 1.276(18) Å, indicating a C−N double bond. Both **4a** and **4b** are stable in solid state and solution (benzene, THF, dichloromethane), even when heated to 120 °C for 3 days. According to DFT calculations, both processes are exergonic by 17.2 and 14.3 kcal mol^{-1}, respectively (Figure 9).

Experimentally, a silylene insertion into the C═N bond of DMAP, generating an azasilepin by dearomative ring expansion of DMAP-stabilized bis(silyl)silylene, has been previously reported by our group.[23] This process requires prolonged

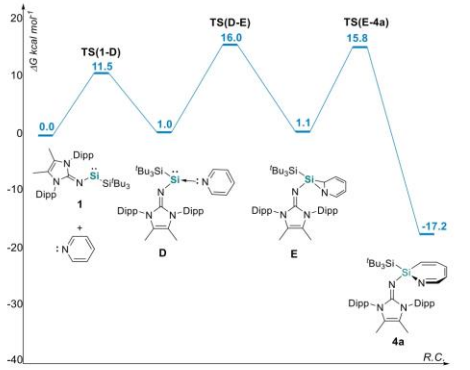

Figure 9. Calculated PES for the proposed mechanisms of the intermolecular insertion of **1** into the C−N bond of pyridine at the PBE0-D3/def2-TZVP//PBE0-D3/def2-TZVP level of theory.

heating of 16 h at 65°C. In the case of **1**, this process proceeds within seconds at room temperature. From a mechanistic point of view, the insertion of the silylene into the C═N bond of pyridine proceeds in three steps (Figure 9). First, a pyridine-stabilized silylene complex **D** at 1.0 kcal mol^{-1} is formed, via a low-lying transition state **TS(1-D)** (11.5 kcal mol^{-1}). NBO analysis shows that this step is nearly redox neutral, as the change of the sum of natural charges at the pyridine moiety ($\Delta\sum q^{pyridine}$) compared to the free pyridine is only +0.06 el. Similarly to the benzene derivatives, the major redox event occurs at the [2 + 1] cycloaddition step, when the bicyclic intermediate **E** at 1.1 kcal mol^{-1} is formed, via **TS(D-E)** at 16.0 kcal mol^{-1}. In **E**, $\Delta\sum q^{pyridine} = -1.03$ el., while the Si center is oxidized by 0.83 el. ($\Delta\sum q^{Si} = 0.83$, $\Delta\sum q^{SitBu3} = 0.18$, $\Delta\sum q^{NHI} = 0.02$). The formation of the final azasilepin product **4a** via **TS(E-4a)** is highly exergonic with $\Delta G_{4a\text{-}E} = -18.3$ kcal mol^{-1}. The overall redox process can be estimated from the change of the sum of charges of the atoms constituting the individual moieties, showing that the pyridine is reduced by one electron while the oxidation occurs mainly at the silylene Si center ($\Delta\sum q^{pyridene} = -1.03$ el., $\Delta\sum q^{Si} = 0.88$ el., $\Delta\sum q^{SitBu3} = 0.15$ el., $\Delta\sum q^{NHI} = 0.01$ el.). The low reaction barriers for the formation of **4a** from **1** and pyridine are in line with the experimentally observed short reaction time. It is also worth mentioning that silepins **3a** and **3c** can be converted to azasilepin **4** in the presence of pyridine and DMAP (Figures S37−S40), once again demonstrating the reversibility of the intermolecular insertion into the aromatic C−C bond.

■ CONCLUSIONS

In conclusion, we successfully synthesized and isolated the acyclic imino(silyl)silylene **1** stabilized by a methylated backbone *N*-heterocyclic imine ligand and a bulky silyl group, which exhibits high σ-donor and π-acceptor abilities and is eminently reactive toward pyridine and DMAP, yielding the corresponding azasilepins. Most remarkably, **1** is capable of forming silepins by oxidative addition into the aromatic C−C bond of benzene and its derivatives. The dearomatization process is reversible in the case of benzene and 1,4-bis(trifluoromethyl)benzene. DFT calculations reveal a Büchner-ring-expansion type mechanism for these transformations

https://doi.org/10.1021/jacs.2c10467
J. Am. Chem. Soc. 2023, 145, 1011−1021

with energy barriers achievable at ambient conditions. Imino(silyl)silylene insertion into an aromatic C−C bond, previously demonstrated by us in an intramolecular fashion, now has been achieved also intermolecularly. **1** exemplifies how seemingly minor structural changes in similar compounds can dramatically alter their reactive capabilities. In this case, the methylation of the NHI backbone prevents the reaction of the silylene center with an aromatic moiety of its substituent, which enables reactivity toward an external aromatic species. The reversibility of this insertion process is accompanied by the interconversion between Si(II) and Si(IV) species in formal oxidative addition/reductive elimination processes, which are key steps in metal-catalyzed reactions. Thus, the presented results are an important milestone on the way to the utilization of low valent silicon species in catalytic transformations. Further studies related to functionalization of silepins and azasilepins formed by the intermolecular insertion of silylenes into aromatic C−C and C−N bonds, as well as development of catalytic transformations, which involve arenes activated by silylenes, are underway.

■ ASSOCIATED CONTENT

Supporting Information

The Supporting Information is available free of charge at https://pubs.acs.org/doi/10.1021/jacs.2c10467.

Experimental details including synthetic, spectroscopic, crystallographic, and computational data (PDF)

Accession Codes

CCDC 2208878−2208883 contain the supplementary crystallographic data for this paper. These data can be obtained free of charge via www.ccdc.cam.ac.uk/data_request/cif, or by emailing data_request@ccdc.cam.ac.uk, or by contacting The Cambridge Crystallographic Data Centre, 12 Union Road, Cambridge CB2 1EZ, UK; fax: +44 1223 336033.

■ AUTHOR INFORMATION

Corresponding Author

Shigeyoshi Inoue − *Department of Chemistry, WACKER-Institute of Silicon Chemistry and Catalysis Research Center, Technische Universität München, 85748 Garching bei München, Germany;* orcid.org/0000-0001-6685-6352; Email: s.inoue@tum.de

Authors

Huaiyuan Zhu − *Department of Chemistry, WACKER-Institute of Silicon Chemistry and Catalysis Research Center, Technische Universität München, 85748 Garching bei München, Germany*

Arseni Kostenko − *Department of Chemistry, WACKER-Institute of Silicon Chemistry and Catalysis Research Center, Technische Universität München, 85748 Garching bei München, Germany*

Daniel Franz − *Department of Chemistry, WACKER-Institute of Silicon Chemistry and Catalysis Research Center, Technische Universität München, 85748 Garching bei München, Germany*

Franziska Hanusch − *Department of Chemistry, WACKER-Institute of Silicon Chemistry and Catalysis Research Center, Technische Universität München, 85748 Garching bei München, Germany;* orcid.org/0000-0002-9509-194X

Complete contact information is available at: https://pubs.acs.org/10.1021/jacs.2c10467

Notes

The authors declare no competing financial interest.

■ ACKNOWLEDGMENTS

H.Z. gratefully acknowledges financial support from the China Scholarship Council. We thank Dr. Shiori Fujimori for the SC-XRD measurements of compounds **3a** and **4a**, and Dr. Amelie Porzelt for the preliminary DFT calculations. We appreciate Mr. Maximilian Muhr (Prof. Roland A. Fischer) for the measurement of LIFDI-MS. We gratefully acknowledge the Leibniz Supercomputing Center for funding this project by providing computing time on its Linux-Cluster.

■ REFERENCES

(1) (a) Buchner, E.; Curtius, T. Ueber die einwirkung von diazoessigäther auf aromatische kohlenwasserstoffe. *Ber. Dtsch. Chem. Ges.* **1885**, *18*, 2377−2379. (b) Buchner, E.; Curtius, T. Synthese von ketonsäureäthern aus aldehyden und diazoessigäther. *Ber. Dtsch. Chem. Ges.* **1885**, *18*, 2371−2377.

(2) (a) Reisman, S. E.; Nani, R. R.; Levin, S. Buchner and beyond: Arene cyclopropanation as applied to natural product total synthesis. *Synlett* **2011**, *2011*, 2437−2442. (b) Ford, A.; Miel, H.; Ring, A.; Slattery, C. N.; Maguire, A. R.; McKervey, M. A. Modern Organic Synthesis with α-Diazocarbonyl Compounds. *Chem. Rev.* **2015**, *115*, 9981−10080.

(3) von E. Doering, W.; Laber, G.; Vonderwahl, R.; Chamberlain, N. F.; Williams, R. B. The structure of the Buchner acids. *J. Am. Chem. Soc.* **1956**, *78*, 5448−5448.

(4) Anciaux, A. J.; Demonceau, A.; Noels, A. F.; Hubert, A. J.; Warin, R.; Teyssie, P. Transition-metal-catalyzed reactions of diazo compounds. 2. Addition to aromatic molecules: Catalysis of Buchner's synthesis of cycloheptatrienes. *J. Org. Chem.* **1981**, *46*, 873−876.

(5) Perera, T. A.; Reinheimer, E. W.; Hudnall, T. W. Photochemically switching diamidocarbene spin states leads to reversible Büchner ring expansions. *J. Am. Chem. Soc.* **2017**, *139*, 14807−14814.

(6) Jutzi, P.; Kanne, D.; Krüger, C. Decamethylsilicocene-synthesis and structure. *Angew. Chem., Int. Ed. Engl.* **1986**, *25*, 164−164.

(7) (a) Kira, M. Reactions of a stable dialkylsilylene and their mechanisms. *J. Chem. Sci.* **2012**, *124*, 1205−1215. (b) Raoufmoghaddam, S.; Zhou, Y.-P.; Wang, Y.; Driess, M. N-heterocyclic silylenes as powerful steering ligands in catalysis. *J. Organomet. Chem.* **2017**, *829*, 2−10. (c) Zhou, Y.-P.; Driess, M. Isolable silylene ligands can boost efficiencies and selectivities in metal-mediated catalysis. *Angew. Chem., Int. Ed.* **2019**, *58*, 3715−3728. (d) Fujimori, S.; Inoue, S. Small molecule activation by two-coordinate acyclic silylenes. *Eur. J. Inorg. Chem.* **2020**, *2020*, 3131−3142. (e) Shan, C.; Yao, S.; Driess, M. Where silylene−silicon centres matter in the activation of small molecules. *Chem. Soc. Rev.* **2020**, *49*, 6733−6754. (f) Reiter, D.; Holzner, R.; Porzelt, A.; Altmann, P. J.; Frisch, P.; Inoue, S. Disilene−silylene interconversion: A synthetically accessible acyclic bis(silyl)-silylene. *J. Am. Chem. Soc.* **2019**, *141*, 13536−13546. (g) Reiter, D.; Holzner, R.; Porzelt, A.; Frisch, P.; Inoue, S. Silylated silicon−carbonyl complexes as mimics of ubiquitous transition-metal carbonyls. *Nat. Chem.* **2020**, *12*, 1131−1135. (h) Wang, L.; Li, Y.; Li, Z.; Kira, M. Isolable silylenes and their diverse reactivity. *Coord. Chem. Rev.* **2022**, *457*, 214413.

(8) (a) Jiang, P.; Gaspar, P. P. Tri-tert-butylsilyl(triisopropylsilyl)-silylene (tBu)3Si−Si−Si(iPr)3 and Chemical Evidence for Its Reactions from a Triplet Electronic State. *J. Am. Chem. Soc.* **2001**, *123*, 8622−8623. (b) Sekiguchi, A.; Tanaka, T.; Ichinohe, M.; Akiyama, K.; Tero-Kubota, S. Bis(tri-tert-butylsilyl)silylene: Triplet Ground State Silylene. *J. Am. Chem. Soc.* **2003**, *125*, 4962−4963. (c) Ashenagar, S.; Kassaee, M. Z. New triplet silylenes M−Si−M′−X along with some unusual cyclic forms (M = Li, Na, and K; M′ = Be, Mg, and Ca; X = F, Cl, and Br). *Turk. J. Chem.* **2018**, *42*, 974−987.

(9) (a) Wendel, D.; Porzelt, A.; Herz, F. A. D.; Sarkar, D.; Jandl, C.; Inoue, S.; Rieger, B. From Si(II) to Si(IV) and back: Reversible

intramolecular carbon−carbon bond activation by an acyclic iminosilylene. *J. Am. Chem. Soc.* **2017**, *139*, 8134−8137. (b) Wendel, D.; Reiter, D.; Porzelt, A.; Altmann, P. J.; Inoue, S.; Rieger, B. Silicon and oxygen's bond of affection: An acyclic three-coordinate silanone and its transformation to an iminosiloxysilylene. *J. Am. Chem. Soc.* **2017**, *139*, 17193−17198.

(10) Eisner, T.; Kostenko, A.; Hanusch, F.; Inoue, S. Room temperature observable interconversion between Si(IV) and Si(II) via reversible intramolecular insertion into an aromatic C-C bond. *Chem.—Eur. J.* **2022**, DOI: 10.1002/chem.202202330.

(11) Reiter, D.; Frisch, P.; Wendel, D.; Hörmann, F. M.; Inoue, S. Oxidation reactions of a versatile, two-coordinate, acyclic iminosiloxysilylene. *Dalton Trans.* **2020**, *49*, 7060−7068.

(12) Suzuki, H.; Tokitoh, N.; Okazaki, R. A novel reactivity of a silylene: The first examples of [1 + 2] cycloaddition with aromatic compounds. *J. Am. Chem. Soc.* **1994**, *116*, 11572−11573.

(13) (a) Kira, M.; Ishida, S.; Iwamoto, T.; Kabuto, C. Excited-state reactions of an isolable silylene with aromatic compounds. *J. Am. Chem. Soc.* **2002**, *124*, 3830−3831. (b) Kira, M.; Ishida, S.; Iwamoto, T.; de Meijere, A.; Fujitsuka, M.; Ito, O. The singlet excited state of a stable dialkylsilylene is responsible for its photoreactions. *Angew. Chem., Int. Ed.* **2004**, *43*, 4510−4512.

(14) Kosai, T.; Ishida, S.; Iwamoto, T. A two-coordinate cyclic (alkyl)(amino)silylene: Balancing thermal stability and reactivity. *Angew. Chem., Int. Ed.* **2016**, *55*, 15554−15558.

(15) Kosai, T.; Ishida, S.; Iwamoto, T. Transformation of azulenes to bicyclic [4]dendralene and heptafulvene derivatives via photochemical cycloaddition of dialkylsilylene. *Chem. Commun.* **2015**, *51*, 10707−10709.

(16) Xu, C.; Ye, Z.; Xiang, L.; Yang, S.; Peng, Q.; Leng, X.; Chen, Y. Insertion of metal-substituted silylene into naphthalene's aromatic ring and subsequent rearrangement for silaspiro-benzocycloheptenyl and cyclobutenosilaindan derivatives. *Angew. Chem., Int. Ed.* **2021**, *60*, 3189−3195.

(17) (a) Liu, L. L.; Zhou, J.; Cao, L. L.; Andrews, R.; Falconer, R. L.; Russell, C. A.; Stephan, D. W. A transient vinylphosphinidene via a phosphirene−phosphinidene rearrangement. *J. Am. Chem. Soc.* **2018**, *140*, 147−150. (b) Hicks, J.; Vasko, P.; Goicoechea, J. M.; Aldridge, S. Reversible, room-temperature C—C Bond Activation of benzene by an isolable metal complex. *J. Am. Chem. Soc.* **2019**, *141*, 11000−11003. (c) Liu, L. L.; Cao, L. L.; Zhou, J.; Stephan, D. W. Facile cleavage of the P = P double bond in vinyl-substituted diphosphenes. *Angew. Chem., Int. Ed.* **2019**, *58*, 273−277. (d) Zhang, X.; Liu, L. L. Modulating the Frontier Orbitals of an Aluminylene for Facile Dearomatization of Inert Arenes. *Angew. Chem., Int. Ed.* **2022**, *61*, e202116658. (e) Zhu, L.; Zhang, J.; Cui, C. Intramolecular cyclopropanation of alkali-metal-substituted silylene with the aryl substituent of an N-heterocyclic framework. *Inorg. Chem.* **2019**, *58*, 12007−12010.

(18) (a) Hu, S.; Shima, T.; Hou, Z. Carbon−carbon bond cleavage and rearrangement of benzene by a trinuclear titanium hydride. *Nature* **2014**, *512*, 413−415. (b) Kang, X.; Luo, G.; Luo, L.; Hu, S.; Luo, Y.; Hou, Z. Mechanistic Insights into Ring Cleavage and Contraction of Benzene over a Titanium Hydride Cluster. *J. Am. Chem. Soc.* **2016**, *138*, 11550−11559. (c) Jakoobi, M.; Sergeev, A. G. Transition-Metal-Mediated Cleavage of C−C Bonds in Aromatic Rings. *Chem.—Asian J.* **2019**, *14*, 2181−2192. (d) Chan, A. P. Y.; Sergeev, A. G. Metal-mediated cleavage of unsaturated C-C bonds. *Coord. Chem. Rev.* **2020**, *413*, 213213.

(19) (a) Joule, J. A.; Mills, K. *Heterocyclic Chemistry*, 5th ed.; Blackwell Publishing, Chichester, 2010. (b) Pal, S. *Pyridine: A Useful Ligand in Transition Metal Complexes*; IntechOpen: Rijeka, 2018; Vol. 5, pp 57−74.

(20) (a) Bull, J. A.; Mousseau, J. J.; Pelletier, G.; Charette, A. B. Synthesis of Pyridine and Dihydropyridine Derivatives by Regio- and Stereoselective Addition to N-Activated Pyridines. *Chem. Rev.* **2012**, *112*, 2642−2713. (b) Murakami, K.; Yamada, S.; Kaneda, T.; Itami, K. C−H Functionalization of Azines. *Chem. Rev.* **2017**, *117*, 9302−9332. (c) Bertuzzi, G.; Bernardi, L.; Fochi, M. Nucleophilic Dearomatization of Activated Pyridines. *Catalysts* **2018**, *8*, 632. (d) Bugaenko, D. I. New methodology for one-pot C−H functionalization of pyridines without the use of transition metal catalysts (microreview). *Chem. Heterocycl. Compd.* **2018**, *54*, 829−831. (e) Wang, D.; Désaubry, L.; Li, G.; Huang, M.; Zheng, S. Recent Advances in the Synthesis of C2-Functionalized Pyridines and Quinolines Using N-Oxide Chemistry. *Adv. Synth. Catal.* **2021**, *363*, 2−39.

(21) (a) Laine, R. M.; Thomas, D. W.; Cary, L. W. Catalytic reactions of pyridine with carbon monoxide and water. Reduction of carbon monoxide to hydrocarbon. Applications of the water-gas shift reaction. *J. Org. Chem.* **1979**, *44*, 4964−4966. (b) Strickler, J. R.; Bruck, M. A.; Wigley, D. E. Synthesis and characterization of a substituted η^2-pyridine complex of tantalum prepared by [2 + 2+2] cycloaddition chemistry. *J. Am. Chem. Soc.* **1990**, *112*, 2814−2816. (c) Gray, S. D.; Smith, D. P.; Bruck, M. A.; Wigley, D. E. Regioselective carbon-nitrogen bond cleavage in an η^2(N,C)-coordinated pyridine and an η^1(N) →η^2(N,C) bonding rearrangment in coordinated quinoline: models for hydrodenitrogenation catalysis. *J. Am. Chem. Soc.* **1992**, *114*, 5462−5463. (d) Gray, S. D.; Weller, K. J.; Bruck, M. A.; Briggs, P. M.; Wigley, D. E. Carbon-Nitrogen Bond Cleavage in an η^2(N,C)-Pyridine Complex Induced by Intramolecular Metal-to-Ligand Alkyl Migration: Models for Hydrodenitrogenation Catalysis. *J. Am. Chem. Soc.* **1995**, *117*, 10678−10693. (e) Kleckley, T. S.; Bennett, J. L.; Wolczanski, P. T.; Lobkovsky, E. B. Pyridine C═N Bond Cleavage Mediated by $(silox)_3Nb$ (silox = $^tBu_3SiO$). *J. Am. Chem. Soc.* **1997**, *119*, 247−248. (f) Bailey, B. C.; Fan, H.; Huffman, J. C.; Baik, M.-H.; Mindiola, D. J. Room Temperature Ring-Opening Metathesis of Pyridines by a Transient Ti⋮C Linkage. *J. Am. Chem. Soc.* **2006**, *128*, 6798−6799. (g) Fout, A. R.; Bailey, B. C.; Tomaszewski, J.; Mindiola, D. J. Cyclic Denitrogenation of N-Heterocycles Applying a Homogeneous Titanium Reagent. *J. Am. Chem. Soc.* **2007**, *129*, 12640−12641. (h) Carver, C. T.; Diaconescu, P. L. Ring-Opening Reactions of Aromatic N-Heterocycles by Scandium and Yttrium Alkyl Complexes. *J. Am. Chem. Soc.* **2008**, *130*, 7558−7559. (i) Fout, A. R.; Bailey, B. C.; Buck, D. M.; Fan, H.; Huffman, J. C.; Baik, M.-H.; Mindiola, D. J. Synthetic and Mechanistic Studies of the Ring Opening and Denitrogenation of Pyridine and Picolines by Ti−C Multiple Bonds. *Organometallics* **2010**, *29*, 5409−5422. (j) Baek, S.-y.; Kurogi, T.; Kang, D.; Kamitani, M.; Kwon, S.; Solowey, D. P.; Chen, C.-H.; Pink, M.; Carroll, P. J.; Mindiola, D. J.; Baik, M.-H. Room-Temperature Ring-Opening of Quinoline, Isoquinoline, and Pyridine with Low-Valent Titanium. *J. Am. Chem. Soc.* **2017**, *139*, 12804−12814. (k) Kurogi, T.; Miehlich, M. E.; Halter, D.; Mindiola, D. J. 1,2-CH Bond Activation of Pyridine across a Transient Titanium Alkylidene Radical and Re-Formation of the Ti═CHtBu Moiety. *Organometallics* **2018**, *37*, 165−167. (l) Breloy, L.; Brezová, V.; Malval, J.-P.; Rios de Anda, A.; Bourgon, J.; Kurogi, T.; Mindiola, D. J.; Versace, D.-L. Well-Defined Titanium Complex for Free-Radical and Cationic Photopolymerizations under Visible Light and Photoinduction of Ti-Based Nanoparticles. *Macromolecules* **2019**, *52*, 3716−3729. (m) Hu, S.; Luo, G.; Shima, T.; Luo, Y.; Hou, Z. Hydrodenitrogenation of pyridines and quinolines at a multinuclear titanium hydride framework. *Nat. Commun.* **2017**, *8*, 1866.

(22) Mizuhata, Y.; Sato, T.; Tokitoh, N. Reactions of an overcrowded silylene with pyridines: Formation of a novel 2*H*-1,2-azasilepine and its further cycloaddition. *Heterocycles* **2012**, *84*, 413−418.

(23) Holzner, R.; Reiter, D.; Frisch, P.; Inoue, S. DMAP-stabilized bis(silyl)silylenes as versatile synthons for organosilicon compounds. *RSC Adv.* **2020**, *10*, 3402−3406.

(24) Driess, M. Breaking the limits with silylenes. *Nat. Chem.* **2012**, *4*, 525−526.

(25) (a) Franz, D.; Irran, E.; Inoue, S. Isolation of a Three-Coordinate Boron Cation with a Boron−Sulfur Double Bond. *Angew. Chem., Int. Ed.* **2014**, *53*, 14264−14268. (b) Franz, D.; Szilvási, T.; Irran, E.; Inoue, S. A monotopic aluminum telluride with an Al = Te double bond stabilized by N-heterocyclic carbenes. *Nat. Commun.* **2015**, *6*, 10037. (c) Ochiai, T.; Franz, D.; Inoue, S. Applications of N-

heterocyclic imines in main group chemistry. *Chem. Soc. Rev.* **2016**, *45*, 6327−6344. (d) Ochiai, T.; Franz, D.; Wu, X.-N.; Irran, E.; Inoue, S. A tin analogue of carbenoid: isolation and reactivity of a lithium bis(imidazolin-2-imino)stannylenoid. *Angew. Chem., Int. Ed.* **2016**, *55*, 6983−6987. (e) Ochiai, T.; Szilvási, T.; Franz, D.; Irran, E.; Inoue, S. Isolation and structure of germylene-germyliumylidenes stabilized by N-heterocyclic imines. *Angew. Chem., Int. Ed.* **2016**, *55*, 11619−11624. (f) Hanusch, F.; Munz, D.; Sutter, J.; Meyer, K.; Inoue, S. A zwitterionic heterobimetallic gold−iron complex supported by bis(N-heterocyclic imine)dilyliumylidene. *Angew. Chem., Int. Ed.* **2021**, *60*, 23274−23280. (g) Zhao, X.-X.; Szilvási, T.; Hanusch, F.; Inoue, S. An Isolable Three-Coordinate Germanone and Its Reactivity. *Chem.—Eur. J.* **2021**, *27*, 15914−15917. (h) Zhao, X.-X.; Szilvási, T.; Hanusch, F.; Kelly, J. A.; Fujimori, S.; Inoue, S. Isolation and Reactivity of Tetrylene-Tetrylone-Iron Complexes Supported by Bis(N-Heterocyclic Imine) Ligands. *Angew. Chem., Int. Ed.* **2022**, *61*, e202208930.

(26) Reiter, D.; Frisch, P.; Szilvási, T.; Inoue, S. Heavier carbonyl olefination: The sila-wittig reaction. *J. Am. Chem. Soc.* **2019**, *141*, 16991−16996.

(27) (a) Wendel, D.; Szilvási, T.; Jandl, C.; Inoue, S.; Rieger, B. Twist of a silicon−silicon double bond: Selective anti-addition of hydrogen to an iminodisilene. *J. Am. Chem. Soc.* **2017**, *139*, 9156−9159. (b) Wendel, D.; Szilvási, T.; Henschel, D.; Altmann, P. J.; Jandl, C.; Inoue, S.; Rieger, B. Precise activation of ammonia and dioxide by an iminodisilene. *Angew. Chem., Int. Ed.* **2018**, *57*, 14575−14579. (c) Holzner, R.; Porzelt, A.; Karaca, U. S.; Kiefer, F.; Frisch, P.; Wendel, D.; Holthausen, M. C.; Inoue, S. Imino(silyl)disilenes: application in versatile bond activation, reversible oxidation and thermal isomerization. *Dalton Trans.* **2021**, *50*, 8785−8793.

(28) (a) Protchenko, A. V.; Birjkumar, K. H.; Dange, D.; Schwarz, A. D.; Vidovic, D.; Jones, C.; Kaltsoyannis, N.; Mountford, P.; Aldridge, S. A stable two-coordinate acyclic silylene. *J. Am. Chem. Soc.* **2012**, *134*, 6500−6503. (b) Rekken, B. D.; Brown, T. M.; Fettinger, J. C.; Tuononen, H. M.; Power, P. P. Isolation of a stable, acyclic, two-coordinate silylene. *J. Am. Chem. Soc.* **2012**, *134*, 6504−6507. (c) Protchenko, A. V.; Schwarz, A. D.; Blake, M. P.; Jones, C.; Kaltsoyannis, N.; Mountford, P.; Aldridge, S. A generic one-pot route to acyclic two-coordinate silylenes from silicon(IV) precursors: Synthesis and structural characterization of a silylsilylene. *Angew. Chem., Int. Ed.* **2013**, *52*, 568−571. (d) Rekken, B. D.; Brown, T. M.; Fettinger, J. C.; Lips, F.; Tuononen, H. M.; Herber, R. H.; Power, P. P. Dispersion sorces and counterintuitive steric effects in main group molecules: Heavier Group 14 (Si−Pb) dichalcogenolate carbene analogues with Sub-90° interligand bond angles. *J. Am. Chem. Soc.* **2013**, *135*, 10134−10148. (e) Hadlington, T. J.; Abdalla, J. A. B.; Tirfoin, R.; Aldridge, S.; Jones, C. Stabilization of a two-coordinate, acyclic diaminosilylene (ADASi): Completion of the series of isolable diaminotetrylenes,:$E(NR_2)_2$ (E = group 14 element). *Chem. Commun.* **2016**, *52*, 1717−1720. (f) Loh, Y. K.; Ying, L.; Fuentes, M. Á.; Do, D. C. H.; Aldridge, S. An N-heterocyclic boryloxy ligand isoelectronic with N-heterocyclic imines: Access to an acyclic dioxysilylene and its heavier congeners. *Angew. Chem., Int. Ed.* **2019**, *58*, 4847−4851. (g) Roy, M. M. D.; Ferguson, M. J.; McDonald, R.; Zhou, Y.; Rivard, E. A vinyl silylsilylene and its activation of strong homo- and heteroatomic bonds. *Chem. Sci.* **2019**, *10*, 6476−6481. (h) Roy, M. M. D.; Baird, S. R.; Dornsiepen, E.; Paul, L. A.; Miao, L.; Ferguson, M. J.; Zhou, Y.; Siewert, I.; Rivard, E. A stable homoleptic divinyl tetrelene series. *Chem.—Eur. J.* **2021**, *27*, 8572−8579.

(29) (a) Inoue, S.; Leszczyńska, K. An Acyclic Imino-Substituted Silylene: Synthesis, Isolation, and its Facile Conversion into a Zwitterionic Silaimine. *Angew. Chem., Int. Ed.* **2012**, *51*, 8589−8593. (b) Du, S.; Jia, H.; Rong, H.; Song, H.; Cui, C.; Mo, Z. Synthesis and Reactivity of N-Heterocyclic Silylene Stabilized Disilicon(0) Complexes. *Angew. Chem., Int. Ed.* **2022**, *61*, e202115570.

(30) (a) Denk, M.; Lennon, R.; Hayashi, R.; West, R.; Belyakov, A. V.; Verne, H. P.; Haaland, A.; Wagner, M.; Metzler, N. Synthesis and Structure of a Stable Silylene. *J. Am. Chem. Soc.* **1994**, *116*, 2691−2692. (b) Kira, M.; Ishida, S.; Iwamoto, T.; Kabuto, C. The First Isolable Dialkylsilylene. *J. Am. Chem. Soc.* **1999**, *121*, 9722−9723. (c) Asay, M.; Inoue, S.; Driess, M. Aromatic Ylide-Stabilized Carbocyclic Silylene. *Angew. Chem., Int. Ed.* **2011**, *50*, 9589−9592.

(31) Benedek, Z.; Szilvási, T. Can low-valent silicon compounds be better transition metal ligands than phosphines and NHCs? *RSC Adv.* **2015**, *5*, 5077−5086.

(32) (a) Nishinaga, T.; Komatsu, K.; Sugita, N. 1,1-Dimethylsila-, -germa-, and -stannacycloheptatrienes fully annelated with bicyclo[2.2.2]octene: Syntheses, structures, and properties. *J. Org. Chem.* **1995**, *60*, 1309−1314. (b) Sohn, H.; Merritt, J.; Powell, D. R.; West, R. A new spirocyclic system: Synthesis of a silaspirotropylidene. *Organometallics* **1997**, *16*, 5133−5134. (c) Nishinaga, T.; Izukawa, Y.; Komatsu, K. The first silatropylium iron stabilized by rigid σ-frameworks: Preparation, properties, and some reactions. *Tetrahedron* **2001**, *57*, 3645−3656.

(33) Chen, Z.; Jiao, H.; Wu, J. I.; Herges, R.; Zhang, S. B.; Schleyer, P. v. R. Homobenzene: Homoaromaticity and Homoantiaromaticity in Cycloheptatrienes. *J. Phys. Chem. A* **2008**, *112*, 10586−10594.

(34) (a) Reed, T. B.; Lipscomb, W. N. The crystallography of cycloheptatriene. *Acta Crystallogr.* **1953**, *6*, 108. (b) Davis, R. E.; Tulinsky, A. The structure of thujic acid: 7,7 dimethylcycloheptatriene-3-carboxylic acid. *Tetrahedron Lett.* **1962**, *3*, 839−846. (c) Butcher, S. S. Microwave Spectrum of 1,3,5-Cycloheptatriene. *J. Chem. Phys.* **1965**, *42*, 1833−1836. (d) Scott, A. P.; Agranat, I.; Biedermann, P. U.; Riggs, N. V.; Radom, L. Fulvalenes, Fulvenes, and Related Molecules: An ab Initio Study. *J. Org. Chem.* **1997**, *62*, 2026−2038. (e) Jarzęcki, A. A.; Gajewski, J.; Davidson, E. R. Thermal Rearrangements of Norcaradiene. *J. Am. Chem. Soc.* **1999**, *121*, 6928−6935. (f) Jansen, H.; Slootweg, J. C.; Lammertsma, K. Valence isomerization of cyclohepta-1,3,5-triene and its heteroelement analogues. *Beilstein J. Org. Chem.* **2011**, *7*, 1713−1721.

(35) (a) Anet, F. A. L. Ring inversion in cycloheptatriene. *J. Am. Chem. Soc.* **1964**, *86*, 458−460. (b) Jensen, F. R.; Smith, L. A. The Structure and interconversion of cycloheptatriene. *J. Am. Chem. Soc.* **1964**, *86*, 956−957.

(36) Schleyer, P. v. R.; Maerker, C.; Dransfeld, A.; Jiao, H.; van Eikema Hommes, N. J. R. Nucleus-Independent Chemical Shifts: A Simple and Efficient Aromaticity Probe. *J. Am. Chem. Soc.* **1996**, *118*, 6317−6318.

https://doi.org/10.1021/jacs.2c10467
J. Am. Chem. Soc. 2023, 145, 1011−1021

6. Facile Bond Activation of Small Molecules by an Acyclic Imino(silyl)silylene

Title: Facile Bond Activation of Small Molecules by an Acyclic Imino(silyl)silylene

Status: Communication; published online: March 15, 2023.

Journal: *Israel Journal of Chemistry* **2023**, *64*, e202300012.

Publisher: Wiley-VCH GmbH

DOI: 10.1002/ijch.202300012

Authors: Huaiyuan Zhu, Franziska Hanusch, Shigeyoshi Inoue*

Reprinted with permission from the Wiley-VCH GmbH. © Wiley-VCH GmbH, Weinheim.

Content: The activation of small molecules by silylenes bearing unique electronic properties has been well established in the past few decades. Herein, we disclose the reactivity study of acyclic imino(silyl)silylene **1** with an *N*-heterocyclic imine ligand (NHI) towards various small molecules. Silylene **1** undergoes facile activation of gaseous molecules like dihydrogen, ethylene, and carbon dioxide. While the cycloaddition of carbonyl compounds to **1** was shown as a straightforward synthetic approach of oxasilacycles, reaction with silane as well as borane led to the corresponding E–H (E = Si, B) insertion products. Moreover, the reaction of **1** with heavier chalcogens allows the isolation of neutral three-coordinate silicon chalcogenides bearing Si=Ch bond (Ch = S, Se, Te).

*H. Zhu and planned and executed all experiments including analysis and wrote the manuscript. F. Hanusch conducted the SC-XRD measurements and processed the corresponding data. All work was performed under the supervision of S. Inoue.

Check for updates

Communication

Israel Journal of Chemistry
www.ijc.wiley-vch.de

doi.org/10.1002/ijch.202300012

Facile Bond Activation of Small Molecules by an Acyclic Imino(silyl)silylene

Huaiyuan Zhu,[a] Franziska Hanusch,[a] and Shigeyoshi Inoue*[a]

Dedicated to Professor Helmut Schwarz on the occasion of his 80th birthday.

Abstract: The activation of small molecules by silylenes bearing unique electronic properties has been well established in the past few decades. Here, we disclose the reactivity study of acyclic imino(silyl)silylene **1** with an *N*-heterocyclic imine ligand (NHI) towards various small molecules. Silylene **1** undergoes facile activation of gaseous molecules like dihydrogen, ethylene, and carbon dioxide. While the cycloaddition of carbonyl compounds to **1** was shown as a straightforward synthetic approach of oxasilacycles, reaction with silane as well as borane led to the corresponding E–H (E=Si, B) insertion products. Moreover, reaction with heavier chalcogens allow the isolation of neutral three-coordinate silicon-heavier chalcogen double bond complexes.

Keywords: silylene · small molecule activation · cycloaddition · oxasilacycle · silicon chalcogenides

Since the isolation of decamethylsilicocene $Cp^*_2Si(II)$ by Jutzi in 1986,[1] silylenes, the silicon analogues of carbenes, have emerged as transition metal mimics since its ambiphilic nature with a lone pair and a vacant p-orbital.[2] With the deep investigations in the past decades, silylenes have been a promising candidate in small molecule activations, especially simple two-coordinate acyclic silylenes, which firstly isolated at ambient temperature until 2012 (*e.g.* **I** and **II**, Chart 1).[3] In contrast to their cyclic counterparts, acyclic silylenes are structurally flexible and possess a smaller HOMO-LUMO gap (~2–4 eV).[2a,4] Both key advantages facilitate rigid σ-bond cleavage or oxidative addition of small molecules. For instance, the direct cleavage of strong σ-bond of dihydrogen was achieved by **I** at room temperature.[3a] while cyclic dialkylsilylene need cooperate with another Lewis acids or bases to form Frustrated Lewis Pairs.[5] And the homologation of carbon monoxide also accomplished by **I** under mild condition.[6] In the following years, the extensions of acyclic silylenes with different substituents, such as aminosilyl **III**,[7] diamino **IV**,[8] and diboryloxy **V**,[9] were achieved by the Aldridge group. Bulky vinyl silylsilylene **VI**[10] and divinylsilylene **VII**[11] were isolated and studied by Rivard *et al.* recently (Chart 1).

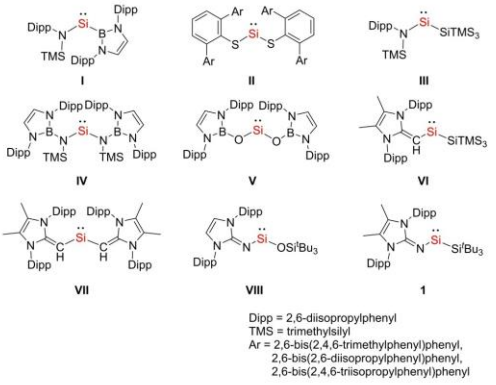

Chart 1. Reported isolable two-coordinate acyclic silylenes

[a] *H. Zhu, Dr. F. Hanusch, Prof. Dr. S. Inoue*
School of Natural Sciences, Department of Chemistry, Catalysis Research Center and Institute of Silicon Chemistry, Technische Universität München
Lichtenbergstraße 4, 85748, Garching bei München, Germany
E-mail: s.inoue@tum.de

Supporting information for this article is available on the WWW under https://doi.org/10.1002/ijch.202300012

© 2023 The Authors. Israel Journal of Chemistry published by Wiley-VCH GmbH. This is an open access article under the terms of the Creative Commons Attribution Non-Commercial License, which permits use, distribution and reproduction in any medium, provided the original work is properly cited and is not used for commercial purposes.

© 2023 The Authors. Israel Journal of Chemistry published by Wiley-VCH GmbH.

18695868, 0, Downloaded from https://onlinelibrary.wiley.com/doi/10.1002/ijch.202300012 by Tu Muenchen Bibliothek, Wiley Online Library on [17/03/2023]. See the Terms and Conditions (https://onlinelibrary.wiley.com/terms-and-conditions) on Wiley Online Library for rules of use; OA articles are governed by the applicable Creative Commons License

18695868, 0, Downloaded from https://onlinelibrary.wiley.com/doi/10.1002/ijch.202300012 by Tu Muenchen Bibliothek, Wiley Online Library on [17/03/2023]. See the Terms and Conditions (https://onlinelibrary.wiley.com/terms-and-conditions) on Wiley Online Library for rules of use; OA articles are governed by the applicable Creative Commons License

Our group has been focusing on the research of low-valent silicon species, especially two-coordinate acyclic silylenes. In 2017, We demonstrated the reversible intramolecular C=C bond activation of its ligand's aromatic framework by a transient acyclic silylene, which can be used as synthetic equivalent of the corresponding silylene in the activation of small molecules.[12] It is worth mentioning that iminosiloxysilylene **VIII** was obtained by oxygen migration from silanone, which formed by the reaction of the silepin and N_2O.[13] We also reported the equilibrium of silepin and silylene, in which both isomers can be observed at ambient conditions.[14] Very recently, we reported the synthesis and isolation of the acyclic imino(silyl)silylene **1** bearing a methylated backbone NHI ligand, which reflects both high σ-donor and π-acceptor abilities.[15] Furthermore, **1** prevents the intramolecular C=C bond activation of its aromatic framework. Instead, it exhibits intermolecular dearomatization of arenes at ambient temperature forming corresponding silepins, which possess almost planar geometry. DFT calculations reveal Büchner-ring-expansion type mechanisms for these transformations with energy barriers achievable at ambient conditions. Besides, we are still interested in the differences in reactivity between the isolated silylene **1**, the masked silylene (silepin),[12,14] and the siloxysilylene.[13,16] Herein, we present the reactivity study of **1** towards small gaseous molecules, alkyne, ketones, silane, borane, and chalcogens.

According to NMR studies, exposure of a freshly prepared solution of **1** to dihydrogen (1 bar) at room temperature led to a color change from blue to pale yellow within 5 minutes (Scheme 1). ^{1}H NMR analysis showed the quantitative formation of a sole product with a new triplet Si–H resonance observed at 4.70 ppm ($^1J_{Si\text{-}H}$ = 178.4 Hz) and its corresponding ^{29}Si{^{1}H} NMR signal to be found at −69.2 ppm. The observed red shift of the Si–H stretching vibration frequencies in the IR spectrum of **2** (2044 cm^{-1}) compared to those known substituted hydrosilanes could be attributed to the stronger electron donating ability of the NHI and silyl ligand.[17] Dihydrosilane **2** also could be obtained by treating silylene **1** with 1,4-cyclohexadiene at ambient temperature. Subsequently, exposure of a freshly prepared solution of **1** to ethylene (1 bar) and carbon dioxide (1 bar) at room temperature, respectively, led to a rapid color change from blue to pale yellow. The cycloaddition products silirane **3** and carbonate silane **4** were isolated finally through the reaction with ethylene (**3**) and CO_2 (**4**) (Scheme 1). The tetracoordinate central silicon nuclei resonate at −110.8 ppm and −45.6 ppm in ^{29}Si{^{1}H} NMR, respectively, about 10 ppm upfield shifted compared with previously reported silepin's results,[12,14] indicating higher π-donor ability of the methylated backbone NHI. However, further or reversible activation of ethylene could not detect even heated to 120 °C.[14,18] Compared with our reversible silepins ("masked silylenes"), the milder condition and faster reaction periods of oxidative reactions, indicate the higher reactivity of **1**. Furthermore, we also investigated the reactivity toward alkynes. Treatment of silylene **1** with an equivalent diphenylacetylene at room temperature resulted the cycloadduct silacyclopropene **5** (Scheme 1). The ^{29}Si{^{1}H} NMR spectrum displayed a signal at −129.3 ppm for the central silicon, which is more upfield shifted than the corresponding cycloadduct using **II** (−72.8 ppm)[19] and **III** (−100.1 ppm).[20]

Over the past decades, oxasilacycles are widely used as cross-linker reagents in polymer chemistry.[21] However, the common methods for the synthesis of oxasilacycles is still limited to intramolecular hydrosilylation, catalyzed by metalloid catalyst,[22] or direct salt metathesis.[23] With the appearance of silylenes, the regio- and stereo-selective oxidation reaction of silylenes with carbonyl compounds, provides a promising approach for the preparation of oxasilacycles.[24] Therefore, the investigation of silylene **1** with carbonyl compounds is presented. Different with the reaction of **1** and carbon dioxide forming silanone intermediate, treatment of **1** with 9,10-phenanthrenequinone in benzene at room temperature, corresponding [1+4] cycloaddition adduct **6** was isolated as the sole product (Scheme 2). The central nucleus was observed in ^{29}Si{^{1}H} NMR at −31.1 ppm. It represents the rare example of rearomatization of phenanthrene, mediated by silylene.[25] When **1** was treated with xanthone in benzene

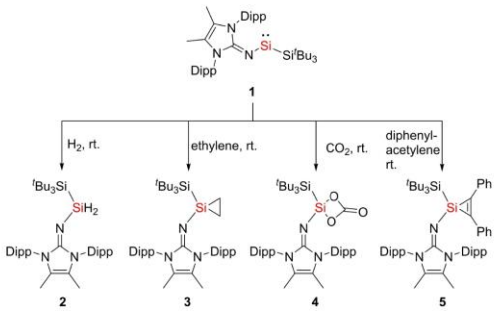

Scheme 1. Small molecule activation of silylene **1** with H_2, ethylene, CO_2, and diphenylacetylene.

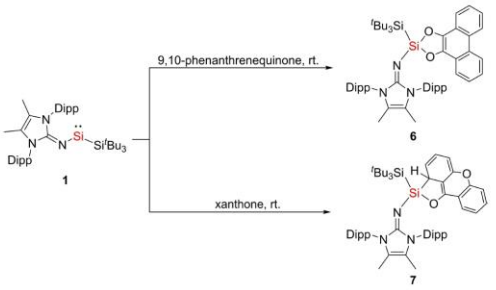

Scheme 2. Reaction of silylene **1** with quinone and xanthone.

© 2023 The Authors. Israel Journal of Chemistry published by Wiley-VCH GmbH.

18695868, 0, Downloaded from https://onlinelibrary.wiley.com/doi/10.1002/ijch.202300012 by Tu Muenchen Bibliothek, Wiley Online Library on [17/03/2023]. See the Terms and Conditions (https://onlinelibrary.wiley.com/terms-and-conditions) on Wiley Online Library for rules of use; OA articles are governed by the applicable Creative Commons License

at room temperature, dearomative cycloaddition adduct **7** was isolated as orange powder in 93% yield (Scheme 2). The ^{29}Si{^{1}H} NMR displayed a resonance at −30.2 ppm for the central silicon. A new singlet signal appeared at 3.55 ppm in ^{1}H NMR, corresponding to the dearomative C–H signal of the benzene ring, is similar with known dearomatization of arylketones by silylenes.[24,26]

While silylene **1** underwent intramolecular C–H bond activation upon heating to 75 °C for 5 days, more reactive

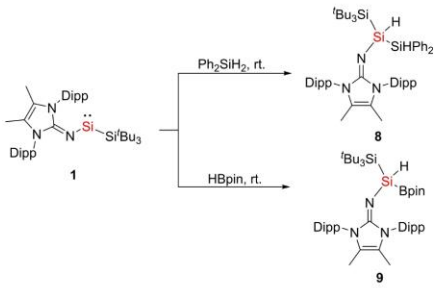

Scheme 3. Reaction of silylene **1** with silane and borane.

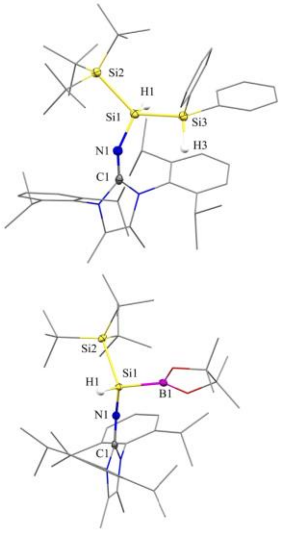

Figure 1. Molecular structures of **8** and **9**. Ellipsoids set at 50% probability. Hydrogen atoms are omitted for clarity, expect for the respective Si–H nuclei of silane. Selected bond lengths [Å] and angles [°]: **8**: Si1–Si2 2.3944(7), Si1–Si3 2.3779(6), Si1–N1 1.7004(14), N1–Si1–Si2 111.04(5), Si2–Si1–Si3 120.65(2); **9**: Si1–Si2 2.4094(11), Si1–B1 2.043(3), Si1–N1 1.702(2), N1–Si1–Si2 110.87(8), Si2–Si1–B1 108.70(8).

Si–H and B–H bonds are worth to investigated as well. When silylene **1** is treated with one equivalent of diphenylsilane (Scheme 3), two triplet Si–H resonances were observed at 4.93 ppm ($^1J_{Si-H}$ = 160.8 Hz) and 5.90 ppm ($^1J_{Si-H}$ = 160.8 Hz) in ^{1}H NMR spectrum, indicating the formation of a new Si–H bond, the signals belong to the central silicon and biphenylsilyl group, respectively. The corresponding ^{29}Si{^{1}H} NMR resonances appeared at −68.6 and −28.0 ppm. Upon treatment of silylene **1** with one equivalent of pinacolborane (Scheme 3), a new triplet Si–H resonance was observed at 4.84 ppm ($^1J_{Si-H}$ = 170.8 Hz) in ^{1}H NMR spectrum, and in ^{11}B{^{1}H} NMR a broad signal was observed at 35.7 ppm, indicating a three-coordinate boron species. However, only one signal was observed at 5.6 ppm in ^{29}Si{^{1}H} NMR, related to the *t*-butylsilyl groups. SC-XRD analysis revealed the Si–H and B–H bonds insertion afforded silane **8** and borylsilane **9** (Figure 1). In **8**, the Si1–Si2 and Si1–Si3 distance of 2.3944(7) and 2.3779(6) Å are almost identical. In **9**, The Si1–B1 distance of 2.043(3) Å is similar to our previously reported silylborane (2.02 Å).[27] Infrared spectroscopy showed Si–H stretching mode of **8** (2058, 2140 cm^{-1}) and **9** (2034 cm^{-1}), respectively. These are red-shifted than related compound.[17f,g] However, further attempt of hydrosilylation and hydroboration of alkenes, alkynes, carbon dioxide or ketones mediated by silylene **1** failed.[28]

With the widespread establishment of neutral three-coordinate silanones in the past five years,[13,29] the research of its heavy congeners is still continuing. Different to oxygen, heavier chalcogens possess smaller electronegativity difference values with silicon, resulting less polarized Si=E bond and more feasible to isolate monomeric R_2Si=E complexes (E=S, Se, and Te).[30] In 1989, Corriu *et al.* demonstrated the isolation of silanethione with a silicon sulfur double bond.[31] Since then, a plethora of donor stabilized terminal silicon-heavy chalcogenides were presented.[6,32] However, among these, only a few neutral three-coordinate silicon-heavy chalcogen double bond compounds **(IX–XI)** were isolated and studied (Scheme 4, a).[6,33] To compare silylene **1** with our previously reported silepin[13] in the formation of silanone and its successful application in Sila-Wittig olefination,[34] a hexane solution of silylene **1** was degassed and exposed to N_2O at −78 °C. However, it just led to an ill-defined mixture, possibly due to the high reactivity of acyclic silylene **1** and its corresponding silanone. Subsequently, treatment of **1** with one equivalent of the weaker oxygen source triethylphosphine oxide at room temperature for 24 h (Scheme 4, b) formed a pale green solution. Colorless crystals were obtained by recrystallization from a saturated pentane solution and fully characterized. The ^{29}Si{^{1}H} NMR spectrum displayed a signal at 59.3 ppm for the central silicon atom, which is almost similar with our previously reported siloxysilylene (58.9 ppm).[13] SC-XRD analysis revealed the structure of iminosiloxysilylene **10** (Figure 2). Similar to the formation of siloxysilylene **VIII**, silylene **1** reacted with triethylphosphine oxide to afford a more polarized silanone intermediate, due to the electronic effect of the methylated backbone NHI, which

© 2023 The Authors. Israel Journal of Chemistry published by Wiley-VCH GmbH.

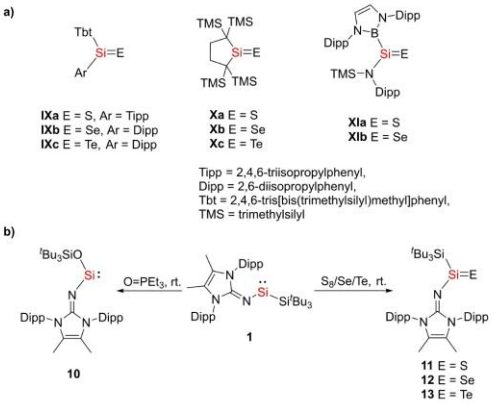

Scheme 4. a) Reported neutral three-coordinate silicon-heavy chalcogenides; b) Reaction of silylene **1** with phosphine oxide and heavy chalcogens.

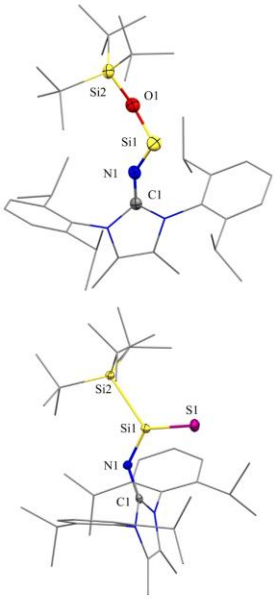

Figure 2. Molecular structures of **10** and **11**. Ellipsoids of **10** set at 30% probability; Ellipsoids of **11** set at 50% probability. Hydrogen atoms are omitted for clarity Selected bond lengths [Å] and angles [°]: **10**: Si1–O1 1.613(3), Si1–N1 1.644(3), N1–Si1–O1 104.33(15); **11**: Si1–Si2 2.3700(6), Si1–S1 1.9838(5), Si1–N1 1.6416(13), N1–Si1–Si2 116.48(5), Si2–Si1–S1 118.21(2), N1–Si1–S1 125.30(5).

more easily undergoes oxygen migration to the silicon-silicon single bond, resulting in siloxysilylene **10**. The Si1–O1 distance of 1.613(3) Å, and N1–Si1–O1 angle of 104.33(15)° are also similar with **VIII**.[13]

Next, 1 : 1 reaction of **1** with S, Se, and Te were conducted, to afford the desired monomeric Si=E compounds **11** (E=S), **12** (E=Se), **13** (E=Te), respectively (Scheme 4, b). The ^{29}Si {^{1}H} NMR spectrums display signals at 105.5, 109.9, and 101.9 ppm for the central silicon atom, respectively. These ^{29}Si {^{1}H} NMR signals are upfield shifted compared to known neutral three-coordinate silicon-chalcogen double bond compounds (133.4–229.5 ppm),[6,33] indicating a more electron dense silicon center donated by the NHI and silyl ligand. SC-XRD analysis confirmed the monomeric form of **11** with a planar silicon center (Figure 2). The Si1–S1 distance of 1.9838(5) Å is slightly longer than known three-coordinate silanethiones (1.948(4) and 1.960(1) Å),[6,33] but still much shorter than some known Si–S single bond lengths (2.093–2.182(11) Å).[18,32t,35]

After the remarkable room temperature intermolecular dearomatization of arenes by imino(silyl)silylene **1**, a variety of small molecule activations of **1** was demonstrated. More facile activation of dihydrogen, ethylene, and carbon dioxide pinpoint the higher reactivity of **1** than the "masked silylene" (silepin) reported by us before could show. Different to carbon dioxide, regioselective rearomatization and dearomatization of carbonyl compounds, provides a promising approach for the preparation of oxasilacycles. Even the activation of a representative hydrosilane and hydroborane were easily achieved by **1**, catalytic hydrosilylation and hydroboration, however, could not be achieved. In addition, the reaction of silylene **1** with heavier chalcogen elements afforded the monomeric $R_2Si{=}E$ (E=S, Se, and Te), which represent rare examples of three-coordinate silicon-heavier chalcogen double bond complexes. Further reactivity studies of **1** towards the activation of various small molecules are currently underway.

Acknowledgements

H.Z. gratefully acknowledges financial support from the China Scholarship Council. Open Access funding enabled and organized by Projekt DEAL.

Data Availability Statement

The data that support the findings of this study are available in the supplementary material of this article.

References

[1] P. Jutzi, D. Kanne, C. Krüger, *Angew. Chem. Int. Ed. Engl.* **1986**, *25*, 164.

© 2023 The Authors. Israel Journal of Chemistry published by Wiley-VCH GmbH.

18695868, 0, Downloaded from https://onlinelibrary.wiley.com/doi/10.1002/ijch.202300012 by Tu Muenchen Bibliothek, Wiley Online Library on [17/03/2023]. See the Terms and Conditions (https://onlinelibrary.wiley.com/terms-and-conditions) on Wiley Online Library for rules of use; OA articles are governed by the applicable Creative Commons License

[2] a) S. Fujimori, S. Inoue, *Eur. J. Inorg. Chem.* **2020**, *2020*, 3131–3142; b) C. Shan, S. Yao, M. Driess, *Chem. Soc. Rev.* **2020**, *49*, 6733–6754; c) L. Wang, Y. Li, Z. Li, M. Kira, *Coord. Chem. Rev.* **2022**, *457*, 214413.
[3] a) A. V. Protchenko, K. H. Birjkumar, D. Dange, A. D. Schwarz, D. Vidovic, C. Jones, N. Kaltsoyannis, P. Mountford, S. Aldridge, *J. Am. Chem. Soc.* **2012**, *134*, 6500–6503; b) B. D. Rekken, T. M. Brown, J. C. Fettinger, H. M. Tuononen, P. P. Power, *J. Am. Chem. Soc.* **2012**, *134*, 6504–6507; c) B. D. Rekken, T. M. Brown, J. C. Fettinger, F. Lips, H. M. Tuononen, R. H. Herber, P. P. Power, *J. Am. Chem. Soc.* **2013**, *135*, 10134–10148.
[4] M. Driess, *Nat. Chem.* **2012**, *4*, 525–526.
[5] Z. Dong, Z. Li, X. Liu, C. Yan, N. Wei, M. Kira, T. Müller, *Chem. Asian J.* **2017**, *12*, 1204–1207.
[6] A. V. Protchenko, P. Vasko, D. C. H. Do, J. Hicks, M. Á. Fuentes, C. Jones, S. Aldridge, *Angew. Chem. Int. Ed.* **2019**, *58*, 1808–1812; *Angew. Chem.* **2019**, *131*, 1822–1826.
[7] A. V. Protchenko, A. D. Schwarz, M. P. Blake, C. Jones, N. Kaltsoyannis, P. Mountford, S. Aldridge, *Angew. Chem. Int. Ed.* **2013**, *52*, 568–571; *Angew. Chem.* **2013**, *125*, 596–599.
[8] T. J. Hadlington, J. A. B. Abdalla, R. Tirfoin, S. Aldridge, C. Jones, *Chem. Commun.* **2016**, *52*, 1717–1720.
[9] Y. K. Loh, L. Ying, M. Á. Fuentes, D. C. H. Do, S. Aldridge, *Angew. Chem. Int. Ed.* **2019**, *58*, 4847–4851; *Angew. Chem.* **2019**, *131*, 4901–4905.
[10] M. M. D. Roy, M. J. Ferguson, R. McDonald, Y. Zhou, E. Rivard, *Chem. Sci.* **2019**, *10*, 6476–6481.
[11] M. M. D. Roy, S. R. Baird, E. Dornsiepen, L. A. Paul, L. Miao, M. J. Ferguson, Y. Zhou, I. Siewert, E. Rivard, *Chem. Eur. J.* **2021**, *27*, 8572–8579.
[12] D. Wendel, A. Porzelt, F. A. D. Herz, D. Sarkar, C. Jandl, S. Inoue, B. Rieger, *J. Am. Chem. Soc.* **2017**, *139*, 8134–8137.
[13] D. Wendel, D. Reiter, A. Porzelt, P. J. Altmann, S. Inoue, B. Rieger, *J. Am. Chem. Soc.* **2017**, *139*, 17193–17198.
[14] T. Eisner, A. Kostenko, F. Hanusch, S. Inoue, *Chem. Eur. J.* **2022**, *28*, e202202330.
[15] H. Zhu, A. Kostenko, D. Franz, F. Hanusch, S. Inoue, *J. Am. Chem. Soc.* **2023**, *145*, 1011–1021.
[16] D. Reiter, P. Frisch, D. Wendel, F. M. Hörmann, S. Inoue, *Dalton Trans.* **2020**, *49*, 7060–7068.
[17] a) J.-M. Denis, Z. Pellerin, P. Guenot, M. Letulle, J.-L. Ripoll, *Chem. Ber.* **1992**, *125*, 1397–1399; b) H. Cui, C. Cui, *Chem. Asian J.* **2011**, *6*, 1138–1141; c) K. Schwedtmann, M. Quest, B. J. Guddorf, J. Keuter, A. Hepp, M. Feldt, J. Droste, M. R. Hansen, F. Lips, *Chem. Eur. J.* **2021**, *27*, 17361–17368; d) Y. Ding, Y. Li, J. Zhang, C. Cui, *Angew. Chem. Int. Ed.* **2022**, *61*, e202205785; e) M. R. Hurst, A. G. Davis, A. K. Cook, *Organometallics* **2022**, *41*, 997–1005; f) T. Kajiwara, N. Takeda, T. Sasamori, N. Tokitoh, *Organometallics* **2004**, *23*, 4723–4734; g) P. T. K. Lee, M. K. Skjel, L. Rosenberg, *Organometallics* **2013**, *32*, 1575–1578.
[18] F. Lips, J. C. Fettinger, A. Mansikkamäki, H. M. Tuononen, P. P. Power, *J. Am. Chem. Soc.* **2014**, *136*, 634–637.
[19] F. Lips, A. Mansikkamäki, J. C. Fettinger, H. M. Tuononen, P. P. Power, *Organometallics* **2014**, *33*, 6253–6258.
[20] A. V. Protchenko, M. P. Blake, A. D. Schwarz, C. Jones, P. Mountford, S. Aldridge, *Organometallics* **2015**, *34*, 2126–2129.
[21] a) C. A. Anger, K. Hindelang, T. Helbich, T. Halbach, J. Stohrer, B. Rieger, *ACS Macro Lett.* **2012**, *1*, 1204–1207; b) C. Anger, F. Deubel, S. Salzinger, J. Stohrer, T. Halbach, R. Jordan, J. G. C. Veinot, B. Rieger, *ACS Macro Lett.* **2013**, *2*, 121–124; c) C. A. Anger, J. Kehrle, K. Hindelang, J. G. C. Veinot, J. Stohrer, B. Rieger, *Macromolecules* **2014**, *47*, 8497–8505.
[22] R. Shchepin, C. Xu, P. Dussault, *Org. Lett.* **2010**, *12*, 4772–4775.
[23] F. S. Tschernuth, T. Thorwart, L. Greb, F. Hanusch, S. Inoue, *Angew. Chem. Int. Ed.* **2021**, *60*, 25799–25803.
[24] K. Uchida, S. Ishida, T. Iwamoto, *Eur. J. Org. Chem.* **2022**, *2022*, e202200522.
[25] T. Kosai, S. Ishida, T. Iwamoto, *Angew. Chem. Int. Ed.* **2016**, *55*, 15554–15558; *Angew. Chem.* **2016**, *128*, 15783–15787.
[26] a) Y. Xiong, S. Yao, M. Driess, *Chem. Eur. J.* **2009**, *15*, 5545–5551; b) S. Ishida, T. Iwamoto, M. Kira, *Organometallics* **2010**, *29*, 5526–5534.
[27] D. Franz, T. Szilvási, A. Pöthig, S. Inoue, *Chem. Eur. J.* **2019**, *25*, 11036–11041.
[28] a) S. Yadav, S. Saha, S. S. Sen, *ChemCatChem* **2016**, *8*, 486–501; b) T. J. Hadlington, M. Driess, C. Jones, *Chem. Soc. Rev.* **2018**, *47*, 4176–4197; c) M. M. D. Roy, A. A. Omaña, A. S. S. Wilson, M. S. Hill, S. Aldridge, E. Rivard, *Chem. Rev.* **2021**, *121*, 12784–12965.
[29] a) I. Alvarado-Beltran, A. Rosas-Sánchez, A. Baceiredo, N. Saffon-Merceron, V. Branchadell, T. Kato, *Angew. Chem. Int. Ed.* **2017**, *56*, 10481–10485; *Angew. Chem.* **2017**, *129*, 10617–10621; b) A. Rosas-Sánchez, I. Alvarado-Beltran, A. Baceiredo, N. Saffon-Merceron, S. Massou, D. Hashizume, V. Branchadell, T. Kato, *Angew. Chem. Int. Ed.* **2017**, *56*, 15916–15920; *Angew. Chem.* **2017**, *129*, 16132–16136; c) R. Kobayashi, S. Ishida, T. Iwamoto, *Angew. Chem. Int. Ed.* **2019**, *58*, 9425–9428; *Angew. Chem.* **2019**, *131*, 9525–9528; d) S. Takahashi, K. Nakaya, M. Frutos, A. Baceiredo, N. Saffon-Merceron, S. Massou, N. Nakata, D. Hashizume, V. Branchadell, T. Kato, *Angew. Chem. Int. Ed.* **2020**, *59*, 15937–15941; *Angew. Chem.* **2020**, *132*, 16071–16075.
[30] A. L. Allred, *J. Inorg. Nucl. Chem.* **1961**, *17*, 215–221.
[31] P. Arya, J. Boyer, F. Carré, R. Corriu, G. Lanneau, J. Lapasset, M. Perrot, C. Priou, *Angew. Chem. Int. Ed. Engl.* **1989**, *28*, 1016–1018.
[32] a) P. P. Power, *Chem. Rev.* **1999**, *99*, 3463–3504; b) R. Okazaki, N. Tokitoh, *Acc. Chem. Res.* **2000**, *33*, 625–630; c) R. C. Fischer, P. P. Power, *Chem. Rev.* **2010**, *110*, 3877–3923; d) S.-H. Zhang, H.-X. Yeong, C.-W. So, *Chem. Eur. J.* **2011**, *17*, 3490–3499; e) F. M. Mück, J. A. Baus, A. Ulmer, C. Burschka, R. Tacke, *Eur. J. Inorg. Chem.* **2016**, *2016*, 1660–1670; f) A. Baceiredo, T. Kato, in *Organosilicon Compounds: Theory and Experiment (Synthesis)* (Ed.: V. Y. Lee), Academic Press, London, **2017**, pp. 533–618; g) A. Burchert, R. Müller, S. Yao, C. Schattenberg, Y. Xiong, M. Kaupp, M. Driess, *Angew. Chem. Int. Ed.* **2017**, *56*, 6298–6301; *Angew. Chem.* **2017**, *129*, 6395–6398; h) H. Wang, J. Zhang, Z. Xie, *J. Organomet. Chem.* **2018**, *865*, 173–177; i) M. K. Bisai, V. S. V. S. N. Swamy, T. Das, K. Vanka, R. G. Gonnade, S. S. Sen, *Inorg. Chem.* **2019**, *58*, 10536–10542; j) T. Muraoka, S. Tanabe, K. Ueno, *Organometallics* **2019**, *38*, 735–738; k) S. Sinhababu, M. M. Siddiqui, S. K. Sarkar, A. Münch, R. Herbst-Irmer, A. George, P. Parameswaran, D. Stalke, H. W. Roesky, *Chem. Eur. J.* **2019**, *25*, 11422–11426; l) M. L. Bin Ismail, M. X.-Y. Ong, C.-W. So, *Eur. J. Inorg. Chem.* **2020**, *2020*, 3703–3707; m) M. Ghosh, P. Panwaria, S. Tothadi, A. Das, S. Khan, *Inorg. Chem.* **2020**, *59*, 17811–17821; n) M.-P. Luecke, E. Pens, S. Yao, M. Driess, *Chem. Eur. J.* **2020**, *26*, 4500–4504; o) F. Hanusch, D. Munz, J. Sutter, K. Meyer, S. Inoue, *Angew. Chem. Int. Ed.* **2021**, *60*, 23274–23280; p) X. Sun, C. Röder, P. W. Roesky, *Inorg. Chem.* **2021**, *60*, 13861–13868; q) S. Takahashi, A. Ishii, N. Nakata, *Chem. Commun.* **2021**, *57*, 3203–3206; r) N. Tiessen, N. Schwarze, H.-G. Stammler, B. Neumann, B. Hoge, *Inorg. Chem.* **2021**, *60*, 15112–15117; s) M. Chen, B. Lei, X. Wang, H. Rong, H. Song, Z. Mo, *Angew. Chem. Int. Ed.* **2022**, *61*, e202204495; t) M.-P. Luecke, L. Giarrana, A. Kostenko, T. Gensch, S. Yao, M. Driess, *Angew. Chem. Int. Ed.* **2022**, *61*, e202110398.

© 2023 The Authors. Israel Journal of Chemistry published by Wiley-VCH GmbH.

18695868, 0, Downloaded from https://onlinelibrary.wiley.com/doi/10.1002/ijch.202300012 by Tu Muenchen Bibliothek, Wiley Online Library on [17/03/2023]. See the Terms and Conditions (https://onlinelibrary.wiley.com/terms-and-conditions) on Wiley Online Library for rules of use; OA articles are governed by the applicable Creative Commons License

[33] a) H. Suzuki, N. Tokitoh, R. Okazaki, S. Nagase, M. Goto, *J. Am. Chem. Soc.* **1998**, *120*, 11096–11105; b) T. Norihiro, S. Tomonori, H. Ken, S. Takayo, T. Nobuhiro, O. Renji, *Chem. Lett.* **2002**, *31*, 34–35; c) T. Iwamoto, K. Sato, S. Ishida, C. Kabuto, M. Kira, *J. Am. Chem. Soc.* **2006**, *128*, 16914–16920; d) H. Suzuki, N. Tokitoh, S. Nagase, R. Okazaki, *J. Am. Chem. Soc.* **1994**, *116*, 11578–11579.
[34] D. Reiter, P. Frisch, T. Szilvási, S. Inoue, *J. Am. Chem. Soc.* **2019**, *141*, 16991–16996.
[35] a) W. Ando, Y. Hamada, A. Sekiguchi, K. Ueno, *Tetrahedron Lett.* **1983**, *24*, 4033–4036; b) K. Kabeta, D. R. Powell, J. Hanson, R. West, *Organometallics* **1991**, *10*, 827–828; c) J. Keuter, K. Schwedtmann, A. Hepp, K. Bergander, O. Janka, C. Doerenkamp, H. Eckert, C. Mück-Lichtenfeld, F. Lips, *Angew. Chem. Int. Ed.* **2017**, *56*, 13866–13871; *Angew. Chem.* **2017**, *129*, 14054–14059.

Manuscript received: January 23, 2023
Revised manuscript received: February 20, 2023
Version of record online: ■■, ■■

© 2023 The Authors. Israel Journal of Chemistry published by Wiley-VCH GmbH.

18695868, 0, Downloaded from https://onlinelibrary.wiley.com/doi/10.1002/ijch.202300012 by Tu Muenchen Bibliothek, Wiley Online Library on [17/03/2023]. See the Terms and Conditions (https://onlinelibrary.wiley.com/terms-and-conditions) on Wiley Online Library for rules of use; OA articles are governed by the applicable Creative Commons License

18695868, 0, Downloaded from https://onlinelibrary.wiley.com/doi/10.1002/ijch.202300012 by Tu Muenchen Bibliothek, Wiley Online Library on [17/03/2023]. See the Terms and Conditions (https://onlinelibrary.wiley.com/terms-and-conditions) on Wiley Online Library for rules of use; OA articles are governed by the applicable Creative Commons License

COMMUNICATION

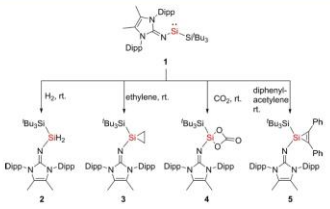

*H. Zhu, Dr. F. Hanusch, Prof. Dr. S. Inoue**

7. Substituent Exchange between an Imino(silyl)silylene and Aryl Isocyanides

Title: Substituent Exchange between an Imino(silyl)silylene and Aryl Isocyanides

Status: Article;

Journal: *Chem* **2024**, accepted.

Publisher: Cell Press

DOI:

Authors: Huaiyuan Zhu, Arseni Kostenko, John A. Kelly, Shigeyoshi Inoue*

Reprinted with permission from the Cell Press. © 2023 Cell Press.

Content: Isocyanides, being isoelectronic and isolobal to carbon monoxide, are an important class of compounds in organic synthesis and coordination chemistry. From reactivity point of view, the R–NC bond cleavage has gained particular interest since the cleaved moieties can be used as a CN/R source in cross-coupling reactions. Herein, we demonstrate that the challenging Ar–NC bond activation and cleavage can be achieved by a stable and isolable imino(silyl)silylene **1**, which transforms aryl isocyanides to a silylcyanide and diaryldiiminodisilenes. The process is enabled by a formal Si(II) → Si(IV) → Si(II) interconversion. This involves the initial migratory insertion of an isocyanide into the Si–Si bond of the silylene and the consecutive intramolecular oxidative addition of the silylene into the Ar–NC bond, followed by the reductive elimination of the cyanide at the silicon center. Oxidative addition/reductive elimination processes are key steps in metal-catalyzed reactions, and the striking transition-metal-like behavior of the silicon center in this case allows for an unprecedented metathetic substituent exchange between the silylene and aryl.

---

*H. Zhu and planned and executed all experiments including analysis and wrote the manuscript. A. Kostenko designed and performed the theoretical analysis. J. A. Kelly conducted the SC-XRD measurements and processed the corresponding data. All work was performed under the supervision of S. Inoue.

Chem

CellPress

Article

Substituent Exchange between an Imino(silyl)silylene and Aryl Isocyanides

Huaiyuan Zhu,[1] Arseni Kostenko,[1] John A. Kelly,[1] and Shigeyoshi Inoue[1,*]

[1]TUM School of Natural Sciences, Department of Chemisrty

Catalysis Research Center and Institute of Silicon Chemistry, Technische Universität München (TUM)

Lichtenbergstrasse 4, 85748, Garching bei München, Germany

*Correspondence: s.inoue@tum.de

SUMMARY

Isocyanides, being isoelectronic and isolobal to carbon monoxide, are an important class of compounds in organic synthesis and coordination chemistry. From reactivity point of view, the R–NC bond cleavage has gained particular interest since the cleaved moieties can be used as a CN/R source in cross-coupling reactions. Herein, we disclose the Ar–NC bond cleavage, and transformation of aryl isocyanides to silylcyanide and diaryldiiminodisilenes, utilizing the ambiphilic acyclic imino(silyl)silylene **1**. A proposed reaction mechanism for the aryl and silyl group exchange, based on experimental evidence and supported by quantum chemical calculations, involves an initial insertion of aryl isocyanide into the Si–Si bond of **1** and a subsequent aryl transfer to the silylene center *via* aryl C–N bond cleavage.

THE BIGGER PICTURE

Herein, we demonstrate that the challenging Ar–NC bond activation and cleavage can be achieved by a stable and isolable imino(silyl)silylene, which transforms aryl isocyanides to a silylcyanide and diaryldiiminodisilenes. The process is enabled by a formal Si(II)→Si(IV)→Si(II) interconversion. This involves the initial migratory insertion of an isocyanide into the Si–Si bond of the silylene and the consecutive intramolecular oxidative addition of the silylene into the Ar–NC bond, followed by the reductive elimination of the cyanide at the silicon center. Oxidative addition/reductive elimination processes are key steps in metal-catalyzed reactions, and the striking transition-metal-like behavior of the silicon center in this case allows for an unprecedented metathetic substituent exchange between the silylene and aryl isocyanides.

INTRODUCTION

Isocyanides (R–NC), isoelectronic to carbon monoxide, exhibit ambiphilic reactivity due to their carbenic electronic structure,[1] which allows isocyanides to act as electrophiles, nucleophiles, and radical acceptors in organic synthesis and coordination chemistry.[2-11] In the past few decades, a plethora of functionalization on the terminal carbon or the C–N triple bond was achieved by transition metal complexes.[5-7,10-11] However, related reaction pathways of isocyanide complexation or activation by heavier main group compounds, especially by silylenes (R_2Si:) – the silicon analogs of carbenes, are rare.[12] Owing to the bonding characteristics, the so far reported genuine silylene-isocyanide complexes can be divided into three resonance forms:[13-16] silylene-isocyanide donor-acceptor adduct **I**,[17-18] zwitterionic adducts **II**,[19-20] and allenic silaketenimines **III** (Figure 1A).[13,15,21-22] While **Ia** and **IIa** easily undergo intramolecular C–C bond activation of substituent of isocyanides, followed by 1,2-silyl migration,[18,20] the Si=C moiety of **IIIa** was demonstrated to exhibit cycloaddition reactivity with unsaturated compound (Figure 1B).[15] In addition, a few homocoupling reactions of isocyanides by silylenes have also been reported.[23-28]

The cleavage of the isocyanides R–NC single bond is also attractive since the R and the NC (cyano/isocyano) moieties can be used in substituent transfer reactions for the efficient synthesis of useful molecules.[20,22-23,28-40] For instance, the Okazaki and Rivard group independently described the cyanation of silylenes by ^{t}BuNC with the elimination of isobutylene (Figure 1C).[29,38] However, due to the high bond dissociation energy of C–N bond (85–104 kcal mol^{-1}), especially C(sp^2)–N bond (104 kcal mol^{-1}),[41] the progress in achieving C–N bond cleavage and further transformations is lagging.[34,42-43] Although several examples of alkyl isocyanides R–NC single bond cleavage reactions are known,[20,22-23,29-40] to the best of our knowledge, the cleavage of C(sp^2)–N bond of aryl isocyanides, which are better π-acceptors in comparison with alkyl isocyanides,[2,44] was only reported by the Weidenbruch group in 1990 by treating

transient bis(*t*-butyl)silylene (generated *in situ* from a hexa(*t*-butyl)cyclotrisilane) with 2,4,6-tri(*t*-butyl)phenylisocyanide forming trialkylsilylcyanide.[28]

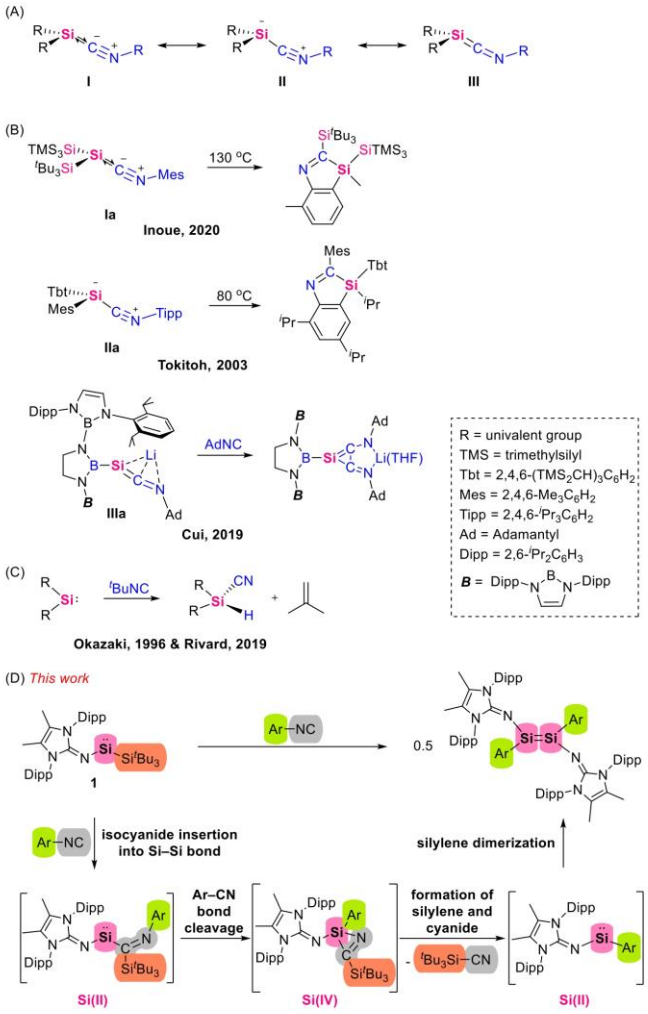

Figure 1. Reactions related the study

(A) Possible bonding descriptions for silylene-isocyanide adducts.
(B) Selected reactivity of silylene-isocyanide complex.
(C) Selected C–N bond cleavage of isocyanide by silylenes.
(D) Present work.

Chem

CellPress

Earlier this year, we reported the synthesis and isolation of an ambiphilic acyclic imino(silyl)silylene **1**[45-47], which intermolecularly dearomatizes arenes *via* a Büchner-ring-expansion type reaction. Building upon our recent investigations into the remarkable reactive properties of **1**, herein we report the C(sp^2)–N bond activation and cleavage with consecutive transformation of aryl isocyanides to silylcyanide and diaryldiimniodisilenes by **1** (Figure 1D). We show that **1** undergoes a metathesis type process with aryl isocyanides, which involves the exchange of the silyl ligand of **1** with the aryl substituent of the isocyanides. We present experimental and computational evidence that such reactivity is enabled by an initial migratory insertion of the isocyanides into the Si–Si bond of **1**, which is the key step of the functionalization of carbon monoxide and isocyanides as C1 building blocks.[34,48-54] Subsequent reductive elimination at the silicon center of the metathetic exchange products form the silylcyanide and a silylene, which dimerizes to the respective disilene.

RESULTS AND DISCUSSION

The reaction of silylene 1 with ^{t}BuNC and mechanism study

We began the reactivity studies of silylene **1** towards isocyanides with ^{t}BuNC in C_6D_6 at room temperature (Figure 2A). This led to rapid decolorization of the reaction mixture from intense blue to pale yellow, quantitatively forming the cyanosilane **2** and isobutylene (^{1}H NMR: 1.60 and 4.74 ppm, Figure S4) in 1:1, in an outcome similar to Okazaki's and Rivard's reports.[29,38] The ^{1}H NMR was observed at 5.10 ppm and the corresponding ^{29}Si{^{1}H} NMR spectrum displayed a signal at –78.8 ppm for the central silicon, is similar to the previously reported cyanosilane formed by reaction of silylenes and ^{t}BuNC.[38] Despite only the signal of Si–*C*≡N was observed at 124.5 ppm in ^{13}C{^{1}H} NMR spectrum, the infrared (ATR-IR) spectrum of **4** in the solid state shows two sharp but relatively weak signals at 2230 cm^{-1} and 2079 cm^{-1} for the Si–C≡N and Si–N≡C stretching vibrations, respectively (Figure S5). This type of isomerization is also known in other main group elements substituted cyanides.[55-57]

In the original report by Tokitoh, in which the corresponding cyanosilane was obtained by the reaction of an *in situ* generated silylene (MesTbtSi:, Tbt = 2,4,6-(TMS_2CH)$_3C_6H_2$) with ^{t}BuNC, it was proposed that formation of cyanosilane proceeds by initial formation of silaylide, followed by the proton-migration from the ^{t}Bu group accompanied with elimination of isobutylene.[20] In this case, the authors did not provide a theoretical support this proposed mechanism. Our quantum chemical calculations suggest that in the case of **1**, the proposed scenario is indeed plausible. The initial complexation of the isocyanide with **1** results in the allenic silaketenimine intermediate **A^{tBu}** (Figure 2B). The process is exergonic by 1.6 kcal·mol^{-1} and proceeds without a barrier. The silicon center of **A^{tBu}** can in one step abstract a proton from the ^{t}Bu substituent, *via* a six-membered transition state **TS(A^{tBu}-2)** at 16.2 kcal·mol^{-1}, to form **2** and isobutylene. The reaction is highly exergonic, with ΔG = –46.5 kcal·mol^{-1}. Similar mechanism was proposed by Power for the reaction of a diarylgermylene with ^{t}BuNC.[31]

Chem

CellPress

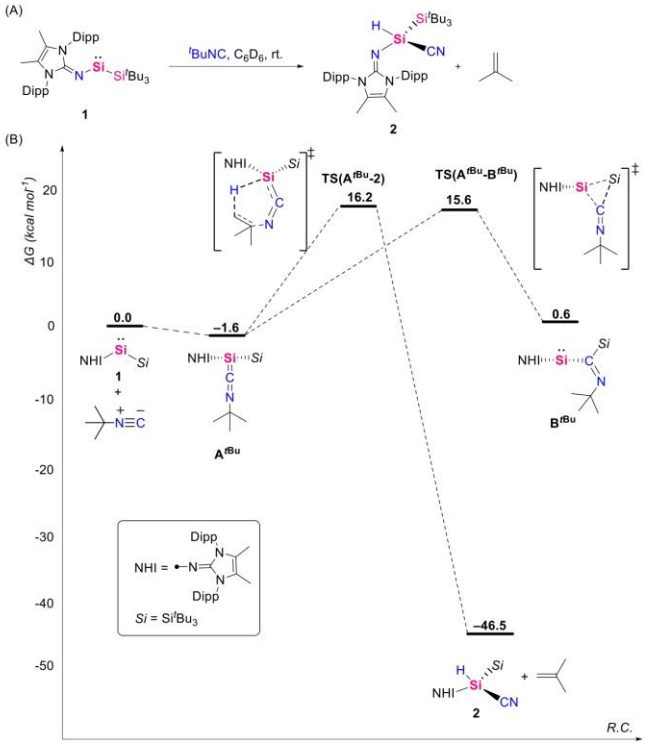

Figure 2. Reaction of 1 with ^{t}BuNC and proposed mechanism of formation of 2

(A) Reaction of **1** with ^{t}BuNC.

(B) Calculated reaction pathways for the proposed mechanisms of the formation of compound **2** and hypothetical reactive intermediate B^{tBu} at the DLPNO-CCSD(T)-(SMD=Benzene)/def2-TZVP//r^{2}SCAN-3c level of theory.

Interestingly, in the course of the computational mechanistic investigation of the silaketenimine **A^{tBu}**, it came to our attention that isocyanide moiety could quite easily undergo an intramolecular insertion into the Si–Si bond. This would result in **B^{tBu}**, which can be described as a silylene substituted by an *N*-heterocyclic imino (NHI) and an η^1-iminoacyl substituents. This process is reminiscent of isocyanide insertion into M–C bonds, which is a well-known occurrence in transition metal chemistry,[34,49,53] but only scarcely reported in the realm of group 14 chemistry.[58-60] The calculated barrier for formation of **B^{tBu}**, *i.e.* **TS(A^{tBu}-B^{tBu})** (at ΔG = 15.6 kcal·mol^{-1}), is only 16.2 kcal·mol^{-1}, and by 0.6 kcal·mol^{-1} lower than the transition state for the formation of **2**. Thus, [**1** + ^{t}BuNC], **A^{tBu}** and **B^{tBu}** are expected to be in thermodynamic equilibrium in ambient conditions. However, the barriers for further possible transformations of the reactive intermediate **B^{tBu}** are much higher than **TS(A^{tBu}-2)** (Figure S32). Thus **2** is expected to be, and in fact is, the only outcome of the reaction.

The reaction of silylene 1 with aryl isocyanides

To explore further reactivity pathways of **1** toward isocyanides, which would preferentially involve the isocyanide migratory insertion into the Si–Si bond, we turned our attention to aryl isocyanides, in which the pathway of hydride abstraction by the Si

Chem

CellPress

center is unavailable. Hence, when treating **1** with 2,6-dimethylphenylisocyanide (XylNC) or 2,4,6-trimethylphenylisocyanide (MesNC), a swift color change from blue to a deep green occurred in both cases. Subsequently, within 1 hour, the reaction mixtures transitioned to an orange hue, from which red crystals formed (Figure 3).

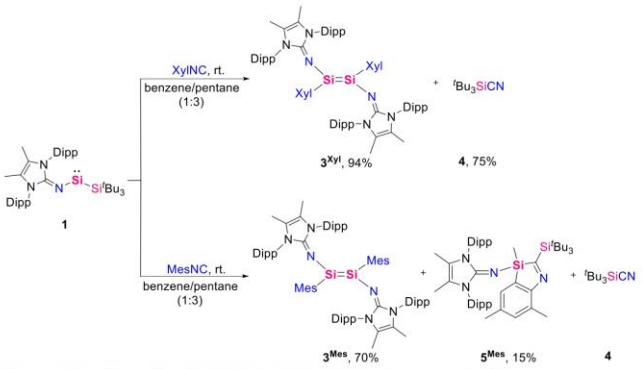

Figure 3. Reactions of 1 with XylNC and MesNC forming 3, 4, and 5^{Mes}

Single crystal X-ray diffraction (SC-XRD) analysis revealed disilenes **3^{Xyl}** and **3^{Mes}** with *trans*-bent geometries (Figure 3A-B), having bent angles θ(Si) of 41.08° and 40.01°, respectively. The Si–Si distances (**3^{Xyl}**: 2.2292(9) Å; **3^{Mes}**: 2.241(10) Å) are in the range of known disilenes (2.118(1)–2.623(1) Å).[61-66] Since disilenes **3^{Xyl}** and **3^{Mes}** are poorly soluble in common organic solvents (pentane, benzene, THF, fluorobenzene), solid state ^{29}Si{^{1}H} cross-polarization magic angle spinning(CP-MAS) NMR spectroscopy was carried out. In both cases only one signal was observed (52.5 (**3^{Xyl}**) and 50.3 (**3^{Mes}**) ppm), implying the absence of other rotational isomers. These ^{29}Si chemical shift values are similar to our previously reported iminodisilenes (67.4–72.5 ppm)[64,66] and within the established range for three-coordinate disilenes.[67] Both disilene **3^{Xyl}** and **3^{Mes}** are stable in solid state under argon atmosphere at room temperature, but slowly degrade to ill-defined mixture within 3 days in solution, similarly to our previously reported disilyldiiminodisilene.[64] Different with the isocyanides activation by disilenes reported by West, Scheschkewitz and Baines,[68-70] the combination of isolable disilene **3^{Xyl}** and **3^{Mes}** with isocyanide only led to the ill-defined mixture. In addition, silylcyanide **4** was isolated in 75% yield as pale yellow solid from the filtrate of the reaction of **1** with XylNC. The ^{13}C{^{1}H} NMR spectrum of **4** displayed a signal at 124.1 ppm. And the subsequent infrared spectroscopy of **4** in the solid state shows stretching mode of Si–C≡N (2172 cm^{-1}) and Si–N≡C (2097 cm^{-1}), respectively, which is similar to **2** (Figure S11). To the best of our knowledge, this reaction represents the first example of a metathetic exchange between a silylene and an isocyanide. Interestingly, the 3*H*-1,3-benzazasilole derivative **5^{Mes}** was isolated as minor product (15% yield) from the filtrate of the reaction of **1** with MesNC, in which both **5^{Mes}** and **4** were observed in a ratio of 1:3 (Figure S15). Such compound was observed in the similar reaction between a transient diarylsilylene and MesNC.[20,29] The molecular structure of **5^{Mes}** was determined by XRD (Figure 4C), revealing the intramolecular insertion of transient silylene **6^{Mes}** (see below) into the C(sp^2)–C(sp^3) bond of methyl substituent of the Mes moiety. The ^{29}Si{^{1}H} NMR spectrum of **5^{Mes}** displayed two signals at 0.8 and –24.3 ppm, corresponding to the trialkylsilyl group and central silicon atom.

Chem

CellPress

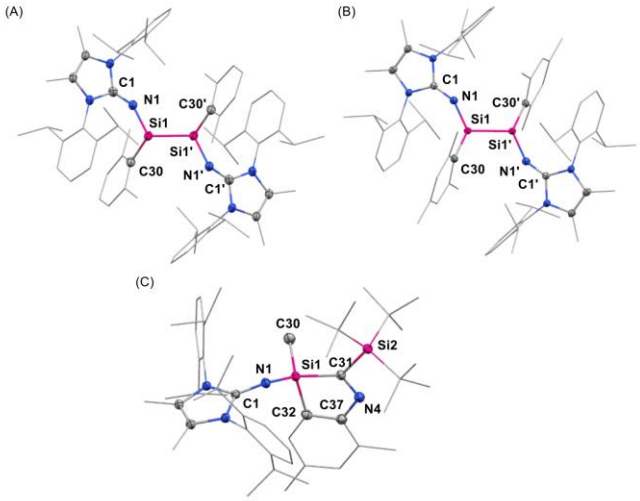

Figure 4. X-ray characterization

Molecular structures of $\mathbf{3}^{Xyl}$ (A), $\mathbf{3}^{Mes}$ (B) and $\mathbf{5}^{Mes}$ (C).

Thermal ellipsoids are set at the 50% probability level. For clarity, hydrogen atoms are omitted and parts of molecules are represented as wireframes.

In an attempt to identify the reactive intermediate responsible for the deep green color observed in the reactions with XylNC and MesNC, **1** was reacted with the bulkier 2,6-diisopropylphenylisocyanide (DippNC) in C_6D_6, resulting in a deep green solution immediately (Figure 5A). However, the solution color turned yellow within 10 minutes (instead of orange hug, like in the case of XylNC or MesNC) and in the $^{29}Si\{^1H\}$ NMR spectrum, two signals at –1.0 and –19.9 ppm were observed. Subsequent SC-XRD analysis revealed the molecular structure of the 3*H*-1,3-benzazasilole derivative $\mathbf{5}^{Dipp}$ (Figure 5B), analogous to the minor product $\mathbf{5}^{Mes}$ in the reaction of **1** with MesNC (Figure 3 and 4C).

Chem

CellPress

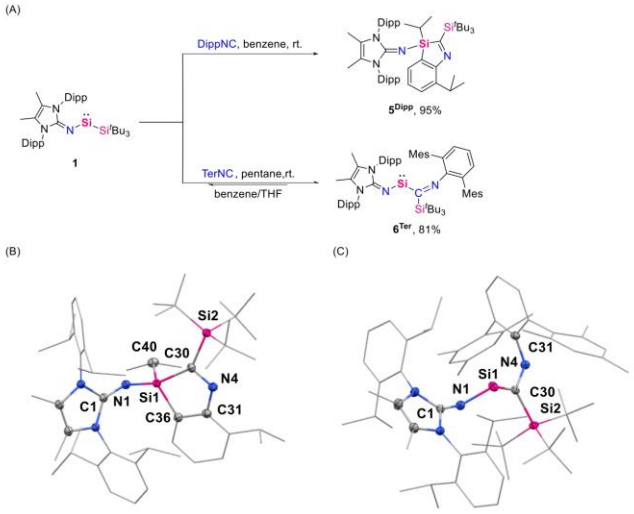

Figure 5. Synthesis and X-ray characterization

(A) Reaction of **1** with DippNC and TerNC forming $\mathbf{5^{Dipp}}$ and $\mathbf{6^{Ter}}$.
(B and C) Molecular structures of $\mathbf{5^{Dipp}}$ (B)and $\mathbf{6^{Ter}}$ (C).
Thermal ellipsoids are set at the 50% probability level. For clarity, hydrogen atoms are omitted and parts of molecules are represented as wireframes.

Since no formation of the corresponding disilene in the reaction of **1** with DippNC was observed, we considered that further increasing steric bulk of the isocyanide could prevent the Ar–NC bond cleavage and enable the isolation of additional reactive intermediates. Thus, **1** was reacted with an even bulkier isocyanide, *i.e.* TerNC (Ter = 2,6-(2,4,6-trimethylphenyl)phenyl) (Figure 5A). Similarly in this instance, the reaction mixture turned deep green and green crystals formed overnight. SC-XRD analysis revealed the molecular structure of (imino-κ^1N)(η^1-iminoacyl-κ^1C)silylene $\mathbf{6^{Ter}}$ (Figure 5C), formed by the insertion of TerNC into the Si–Si bond of **1**. The Si1–C30 distance (1.9941(11) Å) is longer than the bond distance for Si2–C30 (1.9439(11) Å) and vinylsilylenes (1.7620(14)–1.798(2)).[38,71] The N1–Si1–C30 angle of 111.83(5)° is more obtuse than **1** at silylene center (106.15(9)°). The ^{29}Si{^{1}H} NMR spectrum displayed a signal at 229.1 ppm for the central silicon, which is upfield shifted in comparison to **1** (454.0 ppm).[47] In ^{13}C{^{1}H} NMR spectrum a downfield shifted signal, corresponding to newly formed iminoacyl carbon,[31,58-60,72-75] appeared at 218.4 ppm. Remarkably, when $\mathbf{6^{Ter}}$ was redissolved in C_6D_6 or THF-d_8, silylene **1** was observed by ^{1}H NMR spectroscopy, illustrating the **1** + TerNC ⇌ $\mathbf{6^{Ter}}$ equilibrium. This represents the first example of a reversible migratory insertion of an isocyanide into an E–E bond (E = main group element).[12] Additionally, $\mathbf{6^{Ter}}$ is first example of a silylene with an iminoacyl substituent, and the described process provides a new approach for the synthesis of novel acyclic silylenes bearing iminoacyl substituents.[76]

In order to understand the origin of the intense green color, we carried out UV-vis spectroscopy of $\mathbf{6^{Ter}}$, showing an absorption curve extending from the UV to the visible region and a peak around 650 nm (Figure S31).[47] Considering the **1** + TerNC ⇌ $\mathbf{6^{Ter}}$ equilibrium we carried out TD-DFT calculations to rationalize the UV-vis spectroscopy result. The calculations show that **1** and $\mathbf{6^{Ter}}$ are expected to have similarly looking absorption spectra, with transitions at the regions of 600 to 400 nm, which in combination would result in a broad low frequency peak and unresolved peaks at the high frequency region (Figure S36–37). Thus, we turned our attention to the reaction

of **1** with DippNC, where two resolved maximum absorption peaks were observed at 423 and 589 nm, which disappeared after 8 min since the further transfered to $\mathbf{6}^{\mathbf{Dipp}}$ (Figure S31). TD-DFT calculations of (imino)(η^1-iminoacyl)silylene $\mathbf{6}^{\mathbf{Dipp}}$ reproduce well the experimental spectrum, with calculated transitions at 423 and 582 nm, corresponding to the n→ p and n→ π* transitions (Figures S33–35). Similar results were obtained for (imino)(iminoacyl)silylenes $\mathbf{6}^{\mathbf{Xyl}}$ and $\mathbf{6}^{\mathbf{Mes}}$ (Figure S38).

Calculated mechanism for the formation of 3, 4, 5, 6

Based on the UV-Vis spectroscopy, TD-DFT calculations, NMR and the X-ray structure of $\mathbf{6}^{\mathbf{Ter}}$, we suggest that an (imino)(iminoacyl)silylene intermediate forms in all the reactions of **1** with the various aryl isocyanides, and propose a mechanism for the formation of disilenes **3** and benzazasilole **5** (Figure 6). The first step is a barrierless complexation of isocyanide, forming the allenic silaketenimine intermediate $\mathbf{A}^{\mathbf{Xyl}}$ (ΔG = –4.2 kcal·mol^{-1}). $\mathbf{A}^{\mathbf{Xyl}}$ rearranges to the (imino-κ^1N)(iminoacyl-κ^1C)silylene $\mathbf{6}^{\mathbf{Xyl}}$, which is a product of the isocyanide insertion into the Si–Si bond of **1**, akin to the isolated $\mathbf{6}^{\mathbf{Ter}}$. The formation of $\mathbf{6}^{\mathbf{Mes}}$ in the reaction of **1** with MesNC was observed using low-temperature NMR spectroscopy (Figures S39, S40). Upon the formation of $\mathbf{6}^{\mathbf{Xyl}}$, the reaction can follow two pathways. The first (Figure 6, yellow) leads to the production of $\mathbf{5}^{\mathbf{Xyl}}$. This outcome explains the isolated products $\mathbf{5}^{\mathbf{Mes}}$ and $\mathbf{5}^{\mathbf{Dipp}}$ in the reactions of **1** with MesNC and DippNC. The pathway involves the initial formation of a Meisenheimer-type complex $\mathbf{C}^{\mathbf{Xyl}}$ at 4.0 kcal·mol^{-1}, followed by a methyl shift to the silicon center, accompanied by the emergence of the Si(IV) five-membered heterocycle and rearomatization of the aryl group. Calculations show that this process is highly exergonic (ΔG = –48.0 kcal·mol^{-1}) and irreversible. Alternatively, $\mathbf{6}^{\mathbf{Xyl}}$ can rearrange to the Si(IV) intermediate $\mathbf{D}^{\mathbf{Xyl}}$, by an intramolecular oxidative addition *via* $\mathbf{TS(6^{Xyl}\text{-}D^{Xyl})}$, which will ultimately lead to the disilene product (Figure 6, purple). For MesNC, this process in only by 1.9 kcal·mol^{-1} kinetically preferred over the formation $\mathbf{5}^{\mathbf{Xyl}}$. But overall it can be said that the barriers $\mathbf{TS(6^{Xyl}\text{-}D^{Xyl})}$ and $\mathbf{TS(C^{Xyl}\text{-}5^{Xyl})}$, which determine the outcome of the reaction, are energetically very similar. This can result in competing reactions that lead to the two different outcomes as we observed when **1** was reacted with XylNC, MesNC and DippNC. The small energy differences of the transition states leading to **5** and **D** can explain the isolation of the respective products $\mathbf{3}^{\mathbf{Xyl}}$, $\mathbf{3}^{\mathbf{Mes}}$, $\mathbf{5}^{\mathbf{Mes}}$ and $\mathbf{5}^{\mathbf{Dipp}}$. The evidence for the formation of *2H*-azasilirene intermediate **D**, could be obtained using low-temperature NMR spectroscopy (Figures S39, S40).

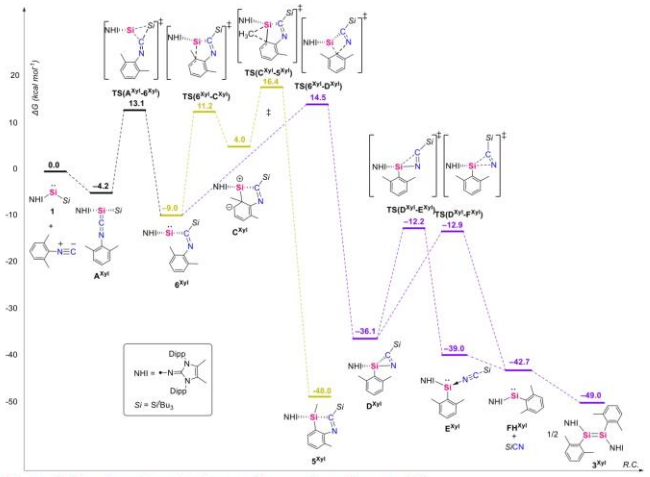

Figure 6. Proposed mechanisms of formation of 3, 5 and 6

SMD(Benzene)-DLPNO-CCSD(T)/def2-TZVP//r²SCAN-3c calculated reaction coordinate diagram for the formation of **5** (yellow path) and **3** (purple path) *via* **6**.

Chem

CellPress

The Si(IV) intermediate $\mathbf{D}^{\mathbf{Xyl}}$, which contains a strained three-membered SiNC ring can reductively eliminate the cyanide *via* a [2 + 1] cycloreversion, resulting in the direct formation of the aryl-substituted iminosilylene $\mathbf{F}^{\mathbf{Xyl}}$ at –42.7 kcal·mol^{-1} (Figure 6, purple). Alternatively, $\mathbf{D}^{\mathbf{Xyl}}$ can first undergoes a rearrangement to form the cyanide-coordinated imino(aryl)silylene $\mathbf{E}^{\mathbf{Xyl}}$, at –39.0 kcal·mol^{-1}, which then releases the cyanide without a barrier. The barriers for both paths **TS($\mathbf{D}^{\mathbf{Xyl}}$-$\mathbf{E}^{\mathbf{Xyl}}$)** and **TS($\mathbf{D}^{\mathbf{Xyl}}$-$\mathbf{F}^{\mathbf{Xyl}}$)** are very similar (–12.2 and –12.9 kcal mol^{-1}). Thus generated silylene $\mathbf{F}^{\mathbf{Xyl}}$ dimerizes to the disilene $\mathbf{3}^{\mathbf{Xyl}}$ with a total energy gain of 49.0 kcal·mol^{-1}.

Conclusions

In summary, we presented metathetic substituent exchange reactions between an imino(silyl)silylene **1** and aryl isocyanides. Experiments and theory suggest that the process is enabled by a formal Si(II)→ Si(IV)→ Si(II) interconversion, whereby the initial insertion of an isocyanide into the Si–Si bond of **1** and the consecutive intramolecular oxidative addition of the silylene into the Ar–NC bond allows for the reductive elimination of the cyanide at the silicon center. After the striking reversible insertion of (imino)silylenes into aromatic C–C bonds,[47,77-78] here we again exemplify the ability of a silicon center to undergo oxidative addition/reductive elimination processes, which are key steps in metal-catalyzed reactions. Further studies in this area, as well as the reactivity studies of the newly formed (imino)(η^1-iminoacyl)silylene and 1,2-diaryl-1,2-diiminodisilenes are underway.

EXPERIMENTAL PROCEDURES

Resource availability

Lead contact

Further information and requests for resources should be directed to and will be fulfilled by the lead contact, Shigeyoshi Inoue (s.inoue@tum.de).

Materials availability

All materials generated in this study are available from the lead contact without restriction.

Data and code availability

Deposition numbers 2287658 (for $\mathbf{3}^{\mathbf{Xyl}}$), 2287660 (for $\mathbf{3}^{\mathbf{Mes}}$), 2287661 (for $\mathbf{5}^{\mathbf{Mes}}$), 2287659 (for $\mathbf{5}^{\mathbf{Dipp}}$), and 2287662 (for $\mathbf{6}^{\mathbf{Ter}}$) contain the supplementary crystallographic data for this paper. These data are provided free of charge by the joint Cambridge Crystallographic Data Centre.

SUPPLEMENTAL INFORMATION

Supplemental information can be found online

ACKNOWLEDGMENTS

This work is dedicated to Professor Mitsuo Kira on the occasion of his 80th birthday. H.Z. gratefully acknowledges financial support from the China Scholarship Council. The authors gratefully acknowledge the computational and data resources provided by the Leibniz Supercomputing Centre.

AUTHOR CONTRIBUTIONS

H.Z. and S.I. devised the project. H.Z. preformed the experimental work. A.K. performed the computational work. J.K. performed the X-ray crystallographic analysis. S.I. supervised the project. H.Z., A.K. and S.I. wrote the paper with input from all authors. All authors discussed the results in detail and commented on the manuscript.

DECLARATION OF INTERESTS

The authors declare no competing interests.

REFERENCES*

1. Ramozzi, R., Chéron, N., Braïda, B., Hiberty, P.C. and Fleurat-Lessard, P. (2012). A valence bond view of isocyanides' electronic structure. New J. Chem. *36*, 1137-1140. https://doi.org/10.1039/C2NJ40050B.

2. Pruchnik, F.P. and Duraj, S.A. (1990). Isocyanide Complexes. In *Organometallic Chemistry of the Transition Elements*; Pruchnik, F.P. andDuraj, S.A., Eds.; Springer US: Boston, MA; Vol., 617-645.

3. Dömling, A. and Ugi, I. (2000). Multicomponent Reactions with Isocyanides. Angew. Chem. Int. Ed. *39*, 3168-3210. https://doi.org/https://doi.org/10.1002/1521-3773(20000915)39:18<3168::AID-ANIE3168>3.0.CO;2-U.

4. Dömling, A. (2006). Recent Developments in Isocyanide Based Multicomponent Reactions in Applied Chemistry. Chem. Rev. *106*, 17-89. https://doi.org/10.1021/cr0505728.

5. Qiu, G., Ding, Q. and Wu, J. (2013). Recent advances in isocyanide insertion chemistry. Chem. Soc. Rev. *42*, 5257-5269. https://doi.org/10.1039/C3CS35507A.

6. Giustiniano, M., Basso, A., Mercalli, V., Massarotti, A., Novellino, E., Tron, G.C. and Zhu, J. (2017). To each his own: isonitriles for all flavors. Functionalized isocyanides as valuable tools in organic synthesis. Chem. Soc. Rev. *46*, 1295-1357. https://doi.org/10.1039/C6CS00444J.

7. Song, B. and Xu, B. (2017). Metal-catalyzed C–H functionalization involving isocyanides. Chem. Soc. Rev. *46*, 1103-1123. https://doi.org/10.1039/C6CS00384B.

8. Gomes, G.d.P., Loginova, Y., Vatsadze, S.Z. and Alabugin, I.V. (2018). Isonitriles as Stereoelectronic Chameleons: The Donor–Acceptor Dichotomy in Radical Additions. J. Am. Chem. Soc. *140*, 14272-14288. https://doi.org/10.1021/jacs.8b08513.

9. Knorn, M., Lutsker, E. and Reiser, O. (2020). Isonitriles as supporting and non-innocent ligands in metal catalysis. Chem. Soc. Rev. *49*, 7730-7752. https://doi.org/10.1039/D0CS00223B.

10. Massarotti, A., Brunelli, F., Aprile, S., Giustiniano, M. and Tron, G.C. (2021). Medicinal Chemistry of Isocyanides. Chem. Rev. *121*, 10742-10788. https://doi.org/10.1021/acs.chemrev.1c00143.

11. Wang, W., Liu, T., Ding, C.-H. and Xu, B. (2021). C(sp^3)–H functionalization with isocyanides. Org. Chem. Front. *8*, 3525-3542. https://doi.org/10.1039/D1QO00153A.

12. Mukhopadhyay, S., Patro, A.G., Vadavi, R.S. and Nembenna, S. (2022). Coordination Chemistry of Main Group Metals with Organic Isocyanides. Eur. J. Inorg. Chem. *2022*, e202200469. https://doi.org/https://doi.org/10.1002/ejic.202200469.

13. Abe, T., Iwamoto, T., Kabuto, C. and Kira, M. (2006). Synthesis, Structure, and Bonding of Stable Dialkylsilaketenimines. J. Am. Chem. Soc. *128*, 4228-4229. https://doi.org/10.1021/ja057917o.

14. Mansikkamäki, A., Power, P.P. and Tuononen, H.M. (2013). Computational Analysis of n→π* Back-Bonding in Metallylene–Isocyanide Complexes R2MCNR′ (M = Si, Ge, Sn; R = *t*Bu, Ph; R′ = Me, *t*Bu, Ph). Organometallics *32*, 6690-6700. https://doi.org/10.1021/om400558e.

15. Zhu, L., Zhang, J., Yang, H. and Cui, C. (2019). Synthesis of Silaketenimine Anion and Its Coupling with Isocyanide. J. Am. Chem. Soc. *141*, 19600-19604. https://doi.org/10.1021/jacs.9b11913.

16. Karwasara, S., Maurer, L.R., Peerless, B., Schnakenburg, G., Das, U. and Filippou, A.C. (2021). (NHC)Si=C=N–R: A Two-Coordinated Si0-Isocyanide Compound as Si(NHC) Transfer Reagent. J. Am. Chem. Soc. *143*, 14780-14794. https://doi.org/10.1021/jacs.1c06628.

17. Ganesamoorthy, C., Schoening, J., Wölper, C., Song, L., Schreiner, P.R. and Schulz, S. (2020). A silicon–carbonyl complex stable at room temperature. Nat. Chem. *12*, 608-614. https://doi.org/10.1038/s41557-020-0456-x.

18. Reiter, D., Holzner, R., Porzelt, A., Frisch, P. and Inoue, S. (2020). Silylated silicon–carbonyl complexes as mimics of ubiquitous transition-metal carbonyls. Nat. Chem. *12*, 1131-1135. https://doi.org/10.1038/s41557-020-00555-4.

19. Takeda, N., Suzuki, H., Tokitoh, N., Okazaki, R. and Nagase, S. (1997). Reaction of a Sterically Hindered Silylene with Isocyanides: The First Stable Silylene−Lewis Base Complexes. J. Am. Chem. Soc. *119*, 1456-1457. https://doi.org/10.1021/ja963092u.

20. Takeda, N., Kajiwara, T., Suzuki, H., Okazaki, R. and Tokitoh, N. (2003). Synthesis and Properties of the First Stable Silylene–Isocyanide Complexes. Chem. Eur. J. *9*, 3530-3543. https://doi.org/https://doi.org/10.1002/chem.200204643.

21. Takeuchi, K., Ichinohe, M. and Sekiguchi, A. (2008). Reactivity of the Disilyne RSi≡SiR (R = SiⁱPr[$CH(SiMe_3)_2$]$_2$) toward Silylcyanide: Two Pathways To Form the Bis-Adduct [RSiSiR($CNSiMe_3$)$_2$] with Some Silaketenimine Character and a 1,4-Diaza-2,3-disilabenzene Analogue. J. Am. Chem. Soc. *130*, 16848-16849. https://doi.org/10.1021/ja807974a.

22. Takeuchi, K., Ichinohe, M. and Sekiguchi, A. (2012). A New Disilene with π-Accepting Groups

from the Reaction of Disilyne RSi≡SiR (R = Si*i*Pr[CH(SiMe$_3$)$_2$]$_2$) with Isocyanides. J. Am. Chem. Soc. *134*, 2954-2957. https://doi.org/10.1021/ja212065a.

23. Xiong, Y., Yao, S. and Driess, M. (2009). Striking Reactivity of a Stable, Zwitterionic Silylene Towards Substituted Diazomethanes, Azides, and Isocyanides. Chem. Eur. J. *15*, 8542-8547. https://doi.org/https://doi.org/10.1002/chem.200901337.

24. Xiong, Y., Yao, S. and Driess, M. (2010). Synthesis and Rearrangement of Stable NHC→Silylene Adducts and Their Unique Reactivity towards Cyclohexylisocyanide. Chem. Asian J. *5*, 322-327. https://doi.org/https://doi.org/10.1002/asia.200900434.

25. Wang, Y., Kostenko, A., Hadlington, T.J., Luecke, M.-P., Yao, S. and Driess, M. (2019). Silicon-Mediated Selective Homo- and Heterocoupling of Carbon Monoxide. J. Am. Chem. Soc. *141*, 626-634. https://doi.org/10.1021/jacs.8b11899.

26. Xiong, Y., Yao, S., Szilvási, T., Ruzicka, A. and Driess, M. (2020). Homocoupling of CO and isocyanide mediated by a C,C′-bis(silylenyl)-substituted ortho-carborane. Chem. Commun. *56*, 747-750. https://doi.org/10.1039/C9CC08680C.

27. Zhao, Y., Chen, Y., Zhang, L., Li, J., Peng, Y., Chen, Z., Jiang, L. and Zhu, H. (2022). Homocoupling of Isocyanide at the Si(II) Center of Borylaminoamidinatosilylene. Inorg. Chem. *61*, 5215-5223. https://doi.org/10.1021/acs.inorgchem.1c03349.

28. Weidenbruch, M., Brand-Roth, B., Pohl, S. and Saak, W. (1990). A Cyclodimeric Silaketenimine. Angew. Chem. Int. Ed. Engl. *29*, 90-92. https://doi.org/https://doi.org/10.1002/anie.199000901.

29. Okazaki, R. (1996). New aspects of low-coordinated organosilicon compounds: Thermal dissociation of disilenes into silylenes. Pure & Appl. Chem. *68*, 895-900. https://doi.org/doi:10.1351/pac199668040895.

30. Gehrhus, B., Hitchcock, P.B. and Lappert, M.F. (2001). The Thermally Stable Silylene Si[(NCH$_2$Bu^t)$_2$C$_6$H$_4$-1,2]: Reactions with Bu^{t}CN, AdCN, Bu^{t}NC, AdN$_3$, and Me$_3$SiN$_3$ (Ad = 1-Adamantyl). Z. Anorg. Allg. Chem. *627*, 1048-1054. https://doi.org/https://doi.org/10.1002/1521-3749(200105)627:5<1048::AID-ZAAC1048>3.0.CO;2-D.

31. Brown, Z.D., Vasko, P., Fettinger, J.C., Tuononen, H.M. and Power, P.P. (2012). A Germanium Isocyanide Complex Featuring (n → π*) Back-Bonding and Its Conversion to a Hydride/Cyanide Product via C–H Bond Activation under Mild Conditions. J. Am. Chem. Soc. *134*, 4045-4048. https://doi.org/10.1021/ja211874u.

32. Peng, J., Zhao, J., Hu, Z., Liang, D., Huang, J. and Zhu, Q. (2012). Palladium-Catalyzed C(sp^2)–H Cyanation Using Tertiary Amine Derived Isocyanide as a Cyano Source. Org. Lett. *14*, 4966-4969. https://doi.org/10.1021/ol302372p.

33. Xu, S., Huang, X., Hong, X. and Xu, B. (2012). Palladium-Assisted Regioselective C–H Cyanation of Heteroarenes Using Isonitrile as Cyanide Source. Org. Lett. *14*, 4614-4617. https://doi.org/10.1021/ol302070t.

34. Boyarskiy, V.P., Bokach, N.A., Luzyanin, K.V. and Kukushkin, V.Y. (2015). Metal-Mediated and Metal-Catalyzed Reactions of Isocyanides. Chem. Rev. *115*, 2698-2779. https://doi.org/10.1021/cr500380d.

35. Garner, M.E., Hohloch, S., Maron, L. and Arnold, J. (2016). Carbon–Nitrogen Bond Cleavage by a Thorium-NHC-bpy Complex. Angew. Chem. Int. Ed. *55*, 13789-13792. https://doi.org/https://doi.org/10.1002/anie.201607899.

36. Lu, W., Hu, H., Li, Y., Ganguly, R. and Kinjo, R. (2016). Isolation of 1,2,4,3-Triazaborol-3-yl-metal (Li, Mg, Al, Au, Zn, Sb, Bi) Derivatives and Reactivity toward CO and Isonitriles. J. Am. Chem. Soc. *138*, 6650-6661. https://doi.org/10.1021/jacs.6b03432.

37. Tashkandi, N.Y., Cook, E.E., Bourque, J.L. and Baines, K.M. (2016). Addition of Isocyanides to Tetramesityldigermene: A Comparison of the Reactivity between Surface and Molecular Digermenes. Chem. Eur. J. *22*, 14006-14012. https://doi.org/https://doi.org/10.1002/chem.201602222.

38. Roy, M.M.D., Ferguson, M.J., McDonald, R., Zhou, Y. and Rivard, E. (2019). A vinyl silylsilylene and its activation of strong homo- and heteroatomic bonds. Chem. Sci. *10*, 6476-6481. https://doi.org/10.1039/C9SC01192G.

39. Böserle, J., Jambor, R., Růžička, A., Erben, M. and Dostál, L. (2020). Reactivity of boraguanidinato germylenes toward carbonyl compounds and isocyanides: C–O, C–F and C–N bond activation. Dalton Trans. *49*, 4869-4877. https://doi.org/10.1039/C9DT04839A.

40. Zhang, Y., Zhang, Z., Hu, Y., Liu, Y., Jin, H. and Zhou, B. (2022). Nickel-catalyzed cyanation reaction of aryl/alkenyl halides with alkyl isocyanides. Org. Biomol. Chem. *20*, 8049-8053. https://doi.org/10.1039/D2OB01240E.

41. Blanksby, S.J. and Ellison, G.B. (2003). Bond Dissociation Energies of Organic Molecules. Acc. Chem. Res. *36*, 255-263. https://doi.org/10.1021/ar020230d.

42. Ouyang, K., Hao, W., Zhang, W.-X. and Xi, Z. (2015). Transition-Metal-Catalyzed Cleavage of C–N Single Bonds. Chem. Rev. *115*,

12045-12090. https://doi.org/10.1021/acs.chemrev.5b00386.

43. Liu, J., Yang, Y., Ouyang, K. and Zhang, W.-X. (2021). Transition-metal-catalyzed transformations of C–N single bonds: Advances in the last five years, challenges and prospects. Green Synth. Catal. *2*, 87-122. https://doi.org/https://doi.org/10.1016/j.gresc.2021.04.005.

44. Barybin, M.V. (2010). Nonbenzenoid aromatic isocyanides: New coordination building blocks for organometallic and surface chemistry. Coord. Chem. Rev. *254*, 1240-1252. https://doi.org/https://doi.org/10.1016/j.ccr.2009.11.002.

45. Zhu, H., Fujimori, S., Kostenko, A. and Inoue, S. (2023). Dearomatization of C_6 Aromatic Hydrocarbons by Main Group Complexes. Chem. Eur. J. e202301973. https://doi.org/https://doi.org/10.1002/chem.202301973.

46. Zhu, H., Hanusch, F. and Inoue, S. (2023). Facile Bond Activation of Small Molecules by an Acyclic Imino(silyl)silylene. Isr. J. Chem. e202300012. https://doi.org/https://doi.org/10.1002/ijch.202300012.

47. Zhu, H., Kostenko, A., Franz, D., Hanusch, F. and Inoue, S. (2023). Room Temperature Intermolecular Dearomatization of Arenes by an Acyclic Iminosilylene. J. Am. Chem. Soc. *145*, 1011-1021. https://doi.org/10.1021/jacs.2c10467.

48. Kuhlmann, E.J. and Alexander, J.J. (1980). Carbon monoxide insertion into transition metal-carbon sigma-bonds. Coord. Chem. Rev. *33*, 195-225. https://doi.org/https://doi.org/10.1016/S0010-8545(00)80454-3.

49. Durfee, L.D. and Rothwell, I.P. (1988). Chemistry of η^2-acyl, η^2-iminoacyl and related functional groups. Chem. Rev. *88*, 1059-1079. https://doi.org/10.1021/cr00089a005.

50. Cavell, K.J. (1996). Recent fundamental studies on migratory insertion into metal-carbon bonds. Coord. Chem. Rev. *155*, 209-243. https://doi.org/https://doi.org/10.1016/S0010-8545(96)90182-4.

51. Sunley, G.J. and Watson, D.J. (2000). High productivity methanol carbonylation catalysis using iridium: The Cativa™ process for the manufacture of acetic acid. Catal. Today *58*, 293-307. https://doi.org/https://doi.org/10.1016/S0920-5861(00)00263-7.

52. Brennführer, A., Neumann, H. and Beller, M. (2009). Palladium-Catalyzed Carbonylation Reactions of Aryl Halides and Related Compounds. Angew. Chem. Int. Ed. *48*, 4114-4133. https://doi.org/https://doi.org/10.1002/anie.200900013.

53. Vlaar, T., Ruijter, E., Maes, B.U.W. and Orru, R.V.A. (2013). Palladium-Catalyzed Migratory Insertion of Isocyanides: An Emerging Platform in Cross-Coupling Chemistry. Angew. Chem. Int. Ed. *52*, 7084-7097. https://doi.org/https://doi.org/10.1002/anie.201300942.

54. Wu, X.-F., Fang, X., Wu, L., Jackstell, R., Neumann, H. and Beller, M. (2014). Transition-Metal-Catalyzed Carbonylation Reactions of Olefins and Alkynes: A Personal Account. Acc. Chem. Res. *47*, 1041-1053. https://doi.org/10.1021/ar400222k.

55. Booth, M.R. and Frankiss, S.G. (1968). Trimethylsilyl isocyanide. Chem. Commun. 1347-1348. https://doi.org/10.1039/C19680001347.

56. Ballmann, G., Elsen, H. and Harder, S. (2019). Magnesium Cyanide or Isocyanide? Angew. Chem. Int. Ed. *58*, 15736-15741. https://doi.org/https://doi.org/10.1002/anie.201909511.

57. Evans, M.J., Anker, M.D., McMullin, C.L. and Coles, M.P. (2023). Controlled reductive C–C coupling of isocyanides promoted by an aluminyl anion. Chem. Sci. *14*, 6278-6288. https://doi.org/10.1039/D3SC01387A.

58. Brown, Z.D., Vasko, P., Erickson, J.D., Fettinger, J.C., Tuononen, H.M. and Power, P.P. (2013). Mechanistic Study of Stepwise Methylisocyanide Coupling and C–H Activation Mediated by a Low-Valent Main Group Molecule. J. Am. Chem. Soc. *135*, 6257-6261. https://doi.org/10.1021/ja4003553.

59. Ohmori, Y., Ichinohe, M., Sekiguchi, A., Cowley, M.J., Huch, V. and Scheschkewitz, D. (2013). Functionalized Cyclic Disilenes via Ring Expansion of Cyclotrisilenes with Isocyanides. Organometallics *32*, 1591-1594. https://doi.org/10.1021/om400054u.

60. Nieder, D., Huch, V., Yildiz, C.B. and Scheschkewitz, D. (2016). Regiodiscriminating Reactivity of Isolable NHC-Coordinated Disilenyl Germylene and Its Cyclic Isomer. J. Am. Chem. Soc. *138*, 13996-14005. https://doi.org/10.1021/jacs.6b07815.

61. Abersfelder, K. and Scheschkewitz, D. (2008). Syntheses of Trisila Analogues of Allyl Chlorides and Their Transformations to Chlorocyclotrisilanes, Cyclotrisilanides, and a Trisilaindane. J. Am. Chem. Soc. *130*, 4114-4121. https://doi.org/10.1021/ja711169w.

62. Sasamori, T., Hironaka, K., Sugiyama, Y., Takagi, N., Nagase, S., Hosoi, Y., Furukawa, Y. and Tokitoh, N. (2008). Synthesis and Reactions of a Stable 1,2-Diaryl-1,2-dibromodisilene: A Precursor for Substituted Disilenes and a 1,2-Diaryldisilyne. J. Am. Chem. Soc. *130*, 13856-13857. https://doi.org/10.1021/ja8061002.

63. Leszczyńska, K., Abersfelder, K., Mix, A., Neumann, B., Stammler, H.-G., Cowley, M.J., Jutzi, P. and Scheschkewitz, D. (2012). Reversible Base Coordination to a Disilene. Angew. Chem. Int. Ed. *51*, 6785-6788. https://doi.org/https://doi.org/10.1002/anie.201202277.

64. Wendel, D., Szilvási, T., Jandl, C., Inoue, S. and Rieger, B. (2017). Twist of a silicon–silicon double bond: Selective anti-addition of hydrogen to an iminodisilene. J. Am. Chem. Soc. *139*, 9156-9159. https://doi.org/10.1021/jacs.7b05335.

65. Kostenko, A. and Driess, M. (2018). Geometrically Compelled Disilene with λ^4-Coordinate Si^{II} Atoms. J. Am. Chem. Soc. *140*, 16962-16966. https://doi.org/10.1021/jacs.8b11393.

66. Holzner, R., Porzelt, A., Karaca, U.S., Kiefer, F., Frisch, P., Wendel, D., Holthausen, M.C. and Inoue, S. (2021). Imino(silyl)disilenes: application in versatile bond activation, reversible oxidation and thermal isomerization. Dalton Trans. *50*, 8785-8793. https://doi.org/10.1039/D1DT01629F.

67. Fujimori, S. and Inoue, S. (2022). 10.01 - Low-Valent Silicon Compounds. In *Comprehensive Organometallic Chemistry IV*; Parkin, G., Meyer, K. andO'hare, D., Eds.; Elsevier: Oxford; Vol., 1-51. https://doi.org/https://doi.org/10.1016/B978-0-12-820206-7.00174-8.

68. Yokelson, H.B., Millevolte, A.J., Haller, K.J. and West, R. (1987). The synthesis and molecular structure of a disilacyclopropanimine. J. Chem. Soc., Chem. Commun. 1605-1606. https://doi.org/10.1039/C39870001605.

69. Majumdar, M., Huch, V., Bejan, I., Meltzer, A. and Scheschkewitz, D. (2013). Reversible, Complete Cleavage of Si=Si Double Bonds by Isocyanide Insertion. Angew. Chem. Int. Ed. *52*, 3516-3520. https://doi.org/https://doi.org/10.1002/anie.201209281.

70. Tashkandi, N.Y., McOnie, S.L., Bourque, J.L., Reinhold, C.R.W. and Baines, K.M. (2019). The Diverse Reactivity of Disilenes Toward Isocyanides. Angew. Chem. Int. Ed. *58*, 3167-3172. https://doi.org/https://doi.org/10.1002/anie.201808490.

71. Roy, M.M.D., Baird, S.R., Dornsiepen, E., Paul, L.A., Miao, L., Ferguson, M.J., Zhou, Y., Siewert, I. and Rivard, E. (2021). A stable homoleptic divinyl tetrelene series. Chem. Eur. J. *27*, 8572-8579. https://doi.org/https://doi.org/10.1002/chem.202100969.

72. Uhl, W., Hahn, I., Schütz, U., Pohl, S., Saak, W., Martens, J. and Manikowski, J. (1996). Twofold Insertion of Isocyanides into the Ga–Ga Bond of Tetrakis[bis(trimethylsilyl)methyl]digallane(4). Chem. Ber. *129*, 897-901. https://doi.org/https://doi.org/10.1002/cber.19961290804.

73. Bertani, R., Crociani, L., D'Arcangelo, G., Rossetto, G., Traldi, P. and Zanella, P. (2001). Reactions of $InMe_3$ with isocyanides in the presence of amines: chemical and mass spectrometric evidence of unprecedented insertion into In–N bonds. J. Organomet. Chem. *626*, 11-15. https://doi.org/https://doi.org/10.1016/S0022-328X(01)00649-0.

74. Li, J., Hermann, M., Frenking, G. and Jones, C. (2012). The Facile Reduction of Carbon Dioxide to Carbon Monoxide with an Amido-Digermyne. Angew. Chem. Int. Ed. *51*, 8611-8614. https://doi.org/https://doi.org/10.1002/anie.201203607.

75. Chen, W., Zhao, Y., Xu, W., Su, J.-H., Shen, L., Liu, L., Wu, B. and Yang, X.-J. (2019). Reductive linear- and cyclo-trimerization of isocyanides using an Al–Al-bonded compound. Chem. Commun. *55*, 9452-9455. https://doi.org/10.1039/C9CC04344F.

76. Fujimori, S. and Inoue, S. (2020). Small molecule activation by two-coordinate acyclic silylenes. Eur. J. Inorg. Chem. *2020*, 3131-3142. https://doi.org/https://doi.org/10.1002/ejic.202000479.

77. Wendel, D., Porzelt, A., Herz, F.A.D., Sarkar, D., Jandl, C., Inoue, S. and Rieger, B. (2017). From Si(II) to Si(IV) and back: Reversible intramolecular carbon–carbon bond activation by an acyclic iminosilylene. J. Am. Chem. Soc. *139*, 8134-8137. https://doi.org/10.1021/jacs.7b05136.

78. Eisner, T., Kostenko, A., Hanusch, F. and Inoue, S. (2022). Room-Temperature-Observable Interconversion Between Si(IV) and Si(II) via Reversible Intramolecular Insertion Into an Aromatic C–C Bond. Chem. Eur. J. *28*, e202202330. https://doi.org/https://doi.org/10.1002/chem.202202330.

8. Summary and Outlook

Within the versatile class of low-coordinate organosilicon compounds, genuine silylenes represent one of the most suitable candidates to substitute transition metal complexes in catalysis. The isolation and structural characterization of first monomeric Si(II) compound, *i.e.* decamethylsiliconcene (**L1**) by Jutzi in 1986 is most important milestones in modern main group chemistry. A breakthrough was achieved by the group of Aldridge, Jones and Power with the isolation of genuine acyclic silylenes (**L9** and **L10**) in 2012, respectively. Driven by these extraordinary discoveries, this thesis is dedicated to expand the class of acyclic, genuine silylenes and explore their reactivity towards strong small molecules for estimating the potential silicon-based catalysis.

Initially, a novel non-transient acyclic iminosilylene (**1**), bearing a bulky super silyl group (-Si^{t}Bu$_3$) and *N*-heterocyclic imine ligand with a methylated backbone, was prepared and isolated via reductive debromination of corresponding tribromosilane with sodium silanide (Figure 23). The methylated backbone is the feature of **1** that distinguishes it from the previously reported non-isolable iminosilylenes, as it prevents the intramolecular silylene center insertion into an aromatic C–C bond of an aryl substituent. DFT calculations revealed an ambiphilic nature of **1** (high σ-donor and π-acceptor abilities) with the HOMO−LUMO gap of 3.22 eV and the ΔE_{ST} = 14.1 kcal mol^{-1}. Since the intramolecular aromatic C–C bond activation product was not observed, the optimized structure of the intramolecular aromatic C–C bond activation product shows a higher steric repulsion between the NHI methyl groups and the closest isopropyl substituent of Dipp. Furthermore, the second Dipp substituent is oriented in a way that leads to additional steric repulsion associated with the $^{i\text{Pr}}$Dipp$\cdots$^{t}Bu$_3$Si interaction. Instead, **1** underwent an intramolecular C–H bond of an aryl substituent at elevated temperature forming **2** with hetero seven-membered cycle ring, in which mechanism was also illustrated by DFT calculations (Figure). Remarkably, the dearomative capacity of **1** is reserved, which allowed extraordinary reactivity of intermolecular dearomatization of arenes at ambient temperatures. The silylene **1** is capable of dearomatization of benzene and its derivatives, giving the corresponding silepins **3a-c**, featuring seven-membered SiC$_6$ rings with nearly planar geometry (Figure 23), in which the nearly planar geometry of the silepin moiety is characteristic of the ring inversion transition state. DFT calculations reveal a Büchner-ring-expansion type mechanism for these transformations with energy barriers achievable at ambient conditions.

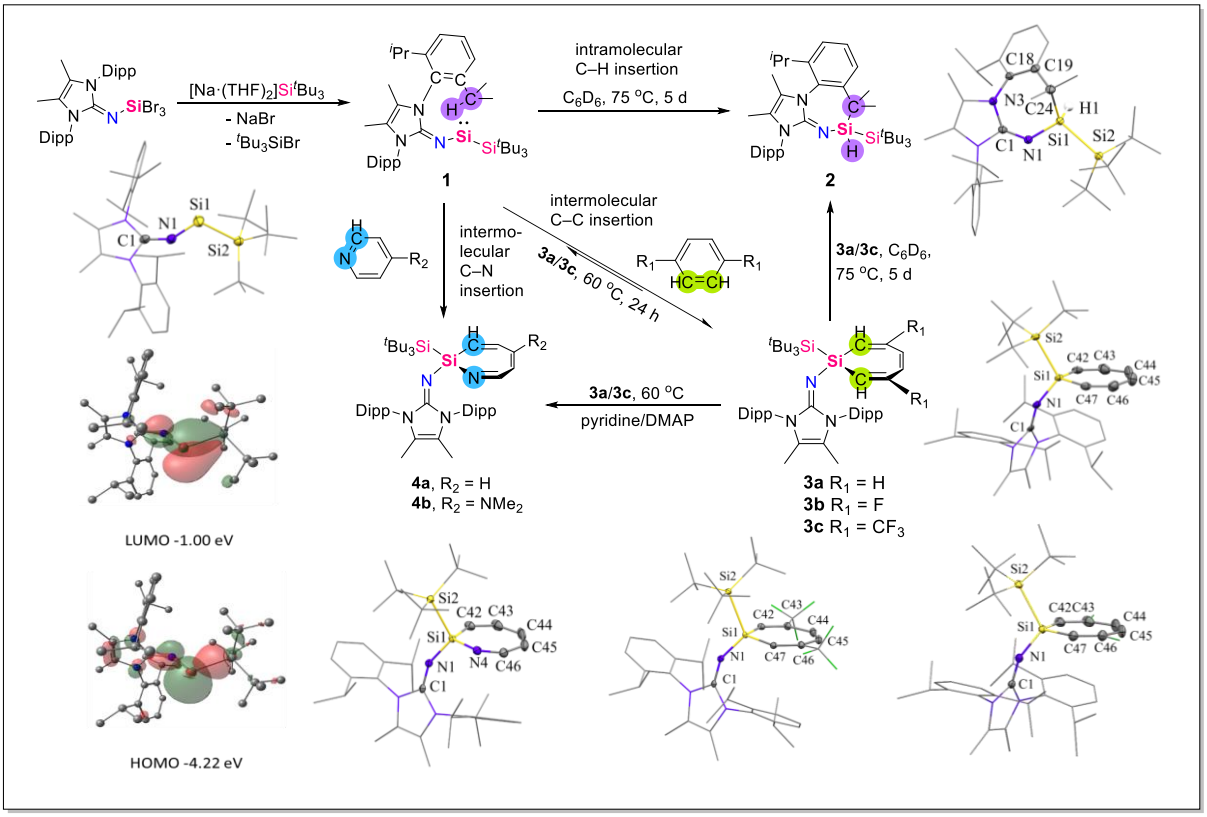

Figure 23. General overview of structural and electronic property of acyclic imino(silyl)silylene **1** and its reactivity toward arenes.

Similar reactions of **1** with *N*-heteroarenes (pyridine and DMAP) proceed more rapidly and irreversibly forming the corresponding azasilepins **4a-b**, also with nearly planar seven-membered $SiNC_5$ rings. DFT calculations revealed an initial coordination from pyridine to silylene and subsequent Büchner-ring-expansion type mechanism for these transformations. Notably, the ring expansion reactions of **1** with benzene and 1,4-bis(trifluoromethyl)benzene are reversible.

After the remarkable room temperature intermolecular dearomatization of arenes by imino(silyl)silylene **1**, a variety of small molecule activations by **1** was conducted (Figure 24). More facile activation of dihydrogen, ethylene, and carbon dioxide forming corresponding oxidative addition products **5-8** pinpoint the higher reactivity of **1** than the "masked silylene" (silepin) reported by us before could show. And different to carbon dioxide, regioselective rearomatization and dearomatization of carbonyl compounds, *i.e.* quinone and xanthone forming oxasilacycle **9** and **10**, respectively, provides a promising approach for the preparation of oxasilacycles. Even the activation of a representative hydrosilane and hydroborane were easily achieved by **1** affording **11** and **12**, catalytic hydrosilylation and hydroboration, however, could not be achieved.

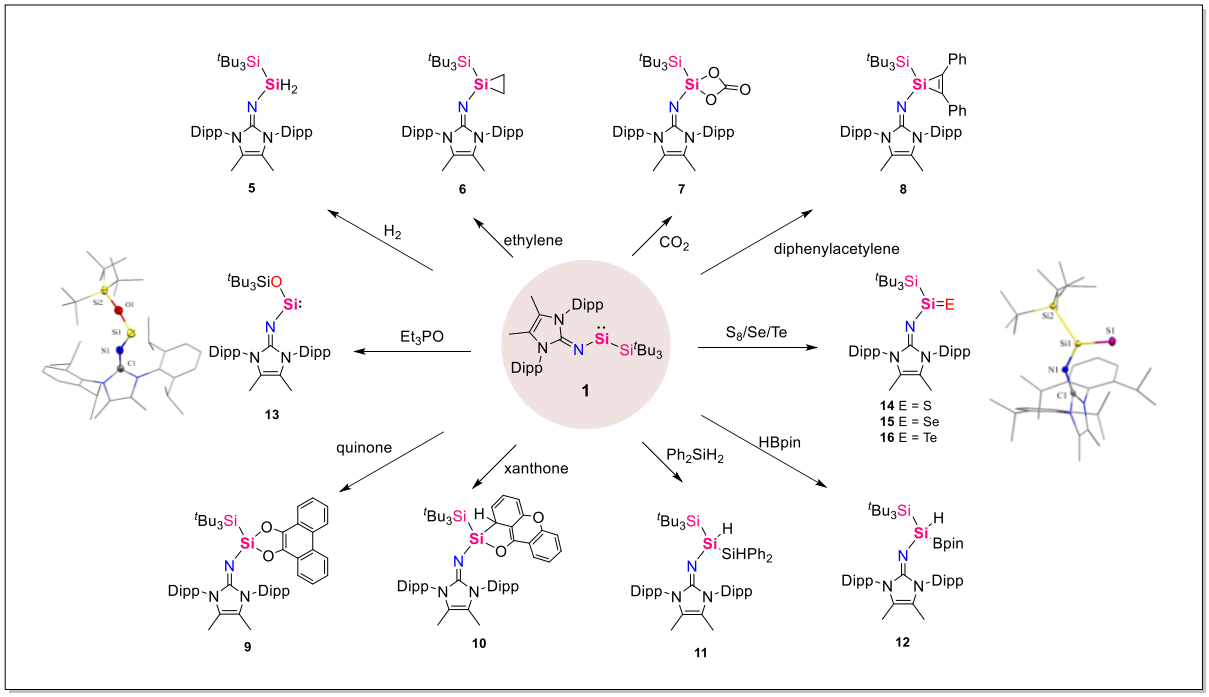

Figure 24. The reactivities of acyclic imino(silyl)silylene **1** toward small molecules.

Whereas treatment of **1** with weaker oxygen source (triethylphosphine oxide) led to the formation of iminosiloxysilylene **13**, the reaction of **1** with heavier chalcogen elements afforded the monomeric $R_2Si{=}E$ compounds **14** (E = S), **15** (E = Se), **16** (E = Te), which represent rare examples of three-coordinate silicon-heavier chalcogen double bond complexes.

Since the first isolation of silicon carbonyls by the reaction of transient silylenes with carbon monoxide promote us to examine whether the stable silylene can be complexation with carbon monoxide. With imino(silyl)silylene **1** in hand, exposure **1** to carbon monoxide at room temperature, the rapid color change from blue to deep green was observed. Unfortunately, the isolation was failed since deep green stuff was easily converted back to **1**. Therefore, we turned our attention to isocyanides, which is the isoelectronic species of carbon monoxide. And silylene isocyanide complexes were known more than 20 years in contrast to silicon carbonyls. Initial reaction of **1** with ^{t}BuNC resulted in the formation of the cyanosilane **17** and isobutylene quantitatively (Figure 25). DFT calculation revealed the formation of cyanosilane proceeds by initial formation of silaylide, followed by the proton-migration from the ^{t}Bu group accompanied with elimination of isobutylene. Interestingly, during the computational mechanistic investigation of the silaketenimine intermediate, it came to our attention that isocyanide moiety could quite easily undergo an intramolecular insertion into the Si–Si bond, which provide another potential pathway for the formation of **17**. To explore further reactivity pathways of **1** toward isocyanides, which would preferentially involve the isocyanide migratory insertion into

the Si–Si bond, we turned our attention to aryl isocyanides, in which the pathway of hydride abstraction by the Si center is unavailable.

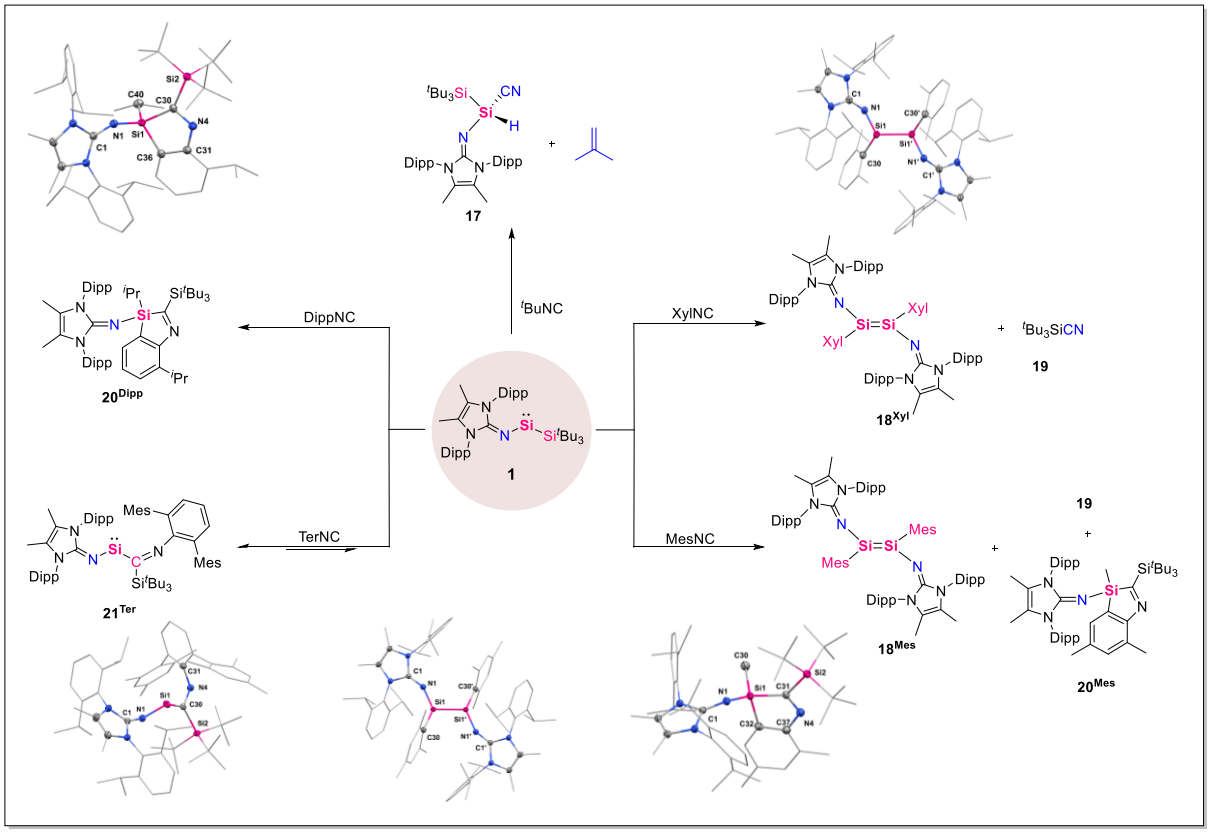

Figure 25. The reactivities of acyclic imino(silyl)silylene **1** toward isocyanides.

Thus, the reaction of **1** with Xyl/MesNC, led to the Ar–NC bond cleavage, and transformation of aryl isocyanides to diaryldiiminodisilenes **18** and silylcyanide **19**. Notably, the 3*H*-1,3-benzazasilole derivative **20^{Mes}** was isolated as minor product from the filtrate of the reaction of **1** with MesNC, in which the quantitative formation of **20^{Dipp}** in the reaction of **1** with DipNC. Thus, the effect of the steric hindrance to prevent the cleavage Ar–NC bond and isolate intermediate is promising. Therefore, the reaction of **1** with bulkier TerNC afforded (imino)(iminoacyl)silylene **21Ter** reversibly *via* the migratory insertion of isocyanide to Si–Si bond of **1**. A proposed reaction mechanism for the aryl and silyl group exchange, based on experimental evidence and supported by quantum chemical calculations, involves an initial insertion of aryl isocyanide into the Si–Si bond of imino(silyl)silylene and a subsequent aryl transfer to the silylene center *via* aryl C–N bond cleavage.

In summary, this doctoral thesis reveals new aspects and a deeper understanding of silylenes at the interface between the versatile chemistry of carbon and transition metals. Accordingly, novel two-coordinate acyclic silylene **1** was successfully isolated and reactivity studies toward various challenging small molecules were outlined. Remarkably, the reaction of **1** with benzene,

1,4-bis(trifluoromethyl)benzene are reversible. The reversibility of this insertion process is accompanied by the interconversion between Si(II) and Si(IV) species in formal oxidative addition/reductive elimination processes, which are key steps in metal-catalyzed reactions. Moreover, the challenging transformation of aryl isocyanides to a silylcyanide and diaryldiiminodisilenes *via* Ar–NC bond cleavage. The process is enabled by a formal Si(II)→ Si(IV)→Si(II) interconversion, once again illustrated the particularity of imino(silyl)silylene **1** Thus, new avenues and opportunities to achieve the ultimate goal of a diverse silicon-based catalysis are disclosed.

9. Licenses for Copyrighted Content

9.1 License for Chapter 5

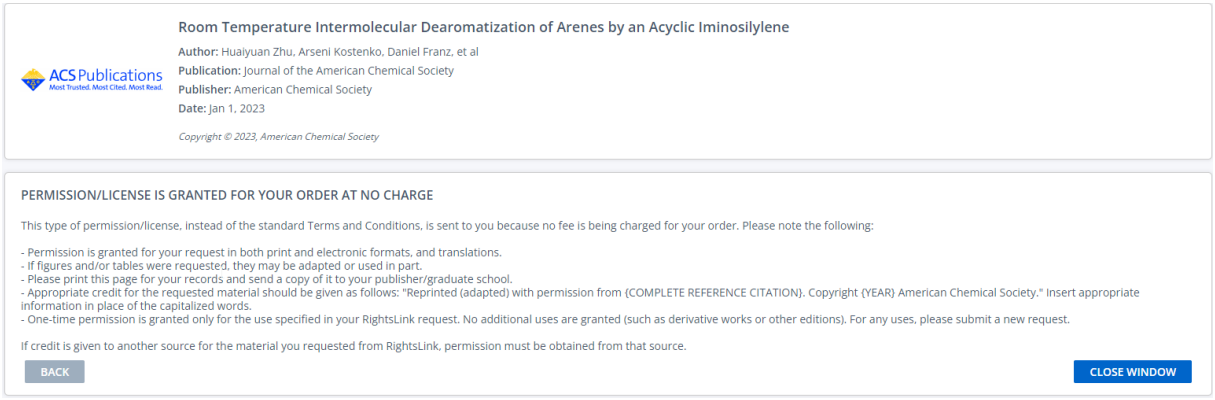

Room Temperature Intermolecular Dearomatization of Arenes by an Acyclic Iminosilylene

Author: Huaiyuan Zhu, Arseni Kostenko, Daniel Franz, et al
Publication: Journal of the American Chemical Society
Publisher: American Chemical Society
Date: Jan 1, 2023

Copyright © 2023, American Chemical Society

PERMISSION/LICENSE IS GRANTED FOR YOUR ORDER AT NO CHARGE

This type of permission/license, instead of the standard Terms and Conditions, is sent to you because no fee is being charged for your order. Please note the following:

- Permission is granted for your request in both print and electronic formats, and translations.
- If figures and/or tables were requested, they may be adapted or used in part.
- Please print this page for your records and send a copy of it to your publisher/graduate school.
- Appropriate credit for the requested material should be given as follows: "Reprinted (adapted) with permission from {COMPLETE REFERENCE CITATION}. Copyright {YEAR} American Chemical Society." Insert appropriate information in place of the capitalized words.
- One-time permission is granted only for the use specified in your RightsLink request. No additional uses are granted (such as derivative works or other editions). For any uses, please submit a new request.

If credit is given to another source for the material you requested from RightsLink, permission must be obtained from that source.

BACK CLOSE WINDOW

9.2 License for Chapter 6

JOHN WILEY AND SONS LICENSE
TERMS AND CONDITIONS

Dec 19, 2023

This Agreement between Technical University of Munich -- Huaiyuan Zhu ("You") and John Wiley and Sons ("John Wiley and Sons") consists of your license details and the terms and conditions provided by John Wiley and Sons and Copyright Clearance Center.

License Number	5692520388033
License date	Dec 19, 2023
Licensed Content Publisher	John Wiley and Sons
Licensed Content Publication	Israel Journal of Chemistry
Licensed Content Title	Facile Bond Activation of Small Molecules by an Acyclic Imino(silyl)silylene
Licensed Content Author	Shigeyoshi Inoue, Franziska Hanusch, Huaiyuan Zhu
Licensed Content Date	Mar 15, 2023
Licensed Content Volume	63
Licensed Content Issue	7-8
Licensed Content Pages	6
Type of use	Dissertation/Thesis
Requestor type	Author of this Wiley article

Format	Electronic
Portion	Full article
Will you be translating?	No
Title of new work	Doctoral thesis
Institution name	Technical University of Munich
Expected presentation date	Feb 2024
Order reference number	0901
Requestor Location	Technical University of Munich Connollytraße 5a, Room 404 München, 80809 Germany Attn: Technical University of Munich
Publisher Tax ID	EU826007151
Total	0.00 EUR

Terms and Conditions

TERMS AND CONDITIONS

This copyrighted material is owned by or exclusively licensed to John Wiley & Sons, Inc. or one of its group companies (each a"Wiley Company") or handled on behalf of a society with which a Wiley Company has exclusive publishing rights in relation to a particular work (collectively "WILEY"). By clicking "accept" in connection with completing this licensing transaction, you agree that the following terms and conditions apply to this transaction (along with the billing and payment terms and conditions established by the Copyright Clearance Center Inc., ("CCC's Billing and Payment terms and conditions"), at the time that you opened your RightsLink account (these are available at any time at http://myaccount.copyright.com).

Terms and Conditions

- The materials you have requested permission to reproduce or reuse (the "Wiley Materials") are protected by copyright.

- You are hereby granted a personal, non-exclusive, non-sub licensable (on a stand-alone basis), non-transferable, worldwide, limited license to reproduce the Wiley Materials for the purpose specified in the licensing process. This license, **and any CONTENT (PDF or image file) purchased as part of your order,** is for a one-time use only and limited to any maximum distribution number specified in the license. The first instance of republication or reuse granted by this license must be completed within two years of the date of the grant of this license (although copies prepared before the end date may be distributed thereafter). The Wiley Materials shall not be used in any other manner or for any other purpose, beyond what is granted in the license. Permission is granted subject to an appropriate acknowledgement given to the author, title of the material/book/journal and the publisher. You shall also duplicate the copyright notice that appears in the Wiley publication in your use of the Wiley Material. Permission is also granted on the understanding that nowhere in the text is a previously published source acknowledged for all or part of this Wiley Material. Any third party content is expressly excluded from this permission.

- With respect to the Wiley Materials, all rights are reserved. Except as expressly granted by the terms of the license, no part of the Wiley Materials may be copied, modified, adapted (except for minor reformatting required by the new Publication), translated, reproduced, transferred or distributed, in any form or by any means, and no derivative works may be made based on the Wiley Materials without the prior permission of the respective copyright owner.**For STM Signatory Publishers clearing permission under the terms of the STM Permissions Guidelines only, the terms of the license are extended to include subsequent editions and for editions in other languages, provided such editions are for the work as a whole in situ and does not involve the separate exploitation of the permitted figures or extracts,** You may not alter, remove or suppress in any manner any copyright, trademark or other notices displayed by the Wiley Materials. You may not license, rent, sell, loan, lease, pledge, offer as security, transfer or assign the Wiley Materials on a stand-alone basis, or any of the rights granted to you hereunder to any other person.

- The Wiley Materials and all of the intellectual property rights therein shall at all times remain the exclusive property of John Wiley & Sons Inc, the Wiley Companies, or their respective licensors, and your interest therein is only that of having possession of and the right to reproduce the Wiley Materials pursuant to Section 2 herein during the continuance of this Agreement. You agree that you own no right, title or interest in or to the Wiley Materials or any of the intellectual property rights therein. You shall have no rights hereunder other than the license as provided for above in Section 2. No right, license or interest to any trademark, trade name, service mark or other branding ("Marks") of WILEY or its licensors is granted hereunder, and you agree that you shall not assert any such right, license or interest with respect thereto

- NEITHER WILEY NOR ITS LICENSORS MAKES ANY WARRANTY OR REPRESENTATION OF ANY KIND TO YOU OR ANY THIRD PARTY, EXPRESS, IMPLIED OR STATUTORY, WITH RESPECT TO THE MATERIALS OR THE ACCURACY OF ANY INFORMATION CONTAINED IN THE MATERIALS, INCLUDING, WITHOUT LIMITATION, ANY IMPLIED WARRANTY OF MERCHANTABILITY, ACCURACY, SATISFACTORY

QUALITY, FITNESS FOR A PARTICULAR PURPOSE, USABILITY, INTEGRATION OR NON-INFRINGEMENT AND ALL SUCH WARRANTIES ARE HEREBY EXCLUDED BY WILEY AND ITS LICENSORS AND WAIVED BY YOU.

- WILEY shall have the right to terminate this Agreement immediately upon breach of this Agreement by you.
- You shall indemnify, defend and hold harmless WILEY, its Licensors and their respective directors, officers, agents and employees, from and against any actual or threatened claims, demands, causes of action or proceedings arising from any breach of this Agreement by you.
- IN NO EVENT SHALL WILEY OR ITS LICENSORS BE LIABLE TO YOU OR ANY OTHER PARTY OR ANY OTHER PERSON OR ENTITY FOR ANY SPECIAL, CONSEQUENTIAL, INCIDENTAL, INDIRECT, EXEMPLARY OR PUNITIVE DAMAGES, HOWEVER CAUSED, ARISING OUT OF OR IN CONNECTION WITH THE DOWNLOADING, PROVISIONING, VIEWING OR USE OF THE MATERIALS REGARDLESS OF THE FORM OF ACTION, WHETHER FOR BREACH OF CONTRACT, BREACH OF WARRANTY, TORT, NEGLIGENCE, INFRINGEMENT OR OTHERWISE (INCLUDING, WITHOUT LIMITATION, DAMAGES BASED ON LOSS OF PROFITS, DATA, FILES, USE, BUSINESS OPPORTUNITY OR CLAIMS OF THIRD PARTIES), AND WHETHER OR NOT THE PARTY HAS BEEN ADVISED OF THE POSSIBILITY OF SUCH DAMAGES. THIS LIMITATION SHALL APPLY NOTWITHSTANDING ANY FAILURE OF ESSENTIAL PURPOSE OF ANY LIMITED REMEDY PROVIDED HEREIN.
- Should any provision of this Agreement be held by a court of competent jurisdiction to be illegal, invalid, or unenforceable, that provision shall be deemed amended to achieve as nearly as possible the same economic effect as the original provision, and the legality, validity and enforceability of the remaining provisions of this Agreement shall not be affected or impaired thereby.
- The failure of either party to enforce any term or condition of this Agreement shall not constitute a waiver of either party's right to enforce each and every term and condition of this Agreement. No breach under this agreement shall be deemed waived or excused by either party unless such waiver or consent is in writing signed by the party granting such waiver or consent. The waiver by or consent of a party to a breach of any provision of this Agreement shall not operate or be construed as a waiver of or consent to any other or subsequent breach by such other party.
- This Agreement may not be assigned (including by operation of law or otherwise) by you without WILEY's prior written consent.
- Any fee required for this permission shall be non-refundable after thirty (30) days from receipt by the CCC.
- These terms and conditions together with CCC's Billing and Payment terms and conditions (which are incorporated herein) form the entire agreement between you and WILEY concerning this licensing transaction and (in the absence of fraud) supersedes all prior agreements and representations of the parties, oral or written. This Agreement may not be amended except in writing signed by both parties. This Agreement shall be binding upon and inure to the benefit of the parties' successors,

legal representatives, and authorized assigns.

- In the event of any conflict between your obligations established by these terms and conditions and those established by CCC's Billing and Payment terms and conditions, these terms and conditions shall prevail.
- WILEY expressly reserves all rights not specifically granted in the combination of (i) the license details provided by you and accepted in the course of this licensing transaction, (ii) these terms and conditions and (iii) CCC's Billing and Payment terms and conditions.
- This Agreement will be void if the Type of Use, Format, Circulation, or Requestor Type was misrepresented during the licensing process.
- This Agreement shall be governed by and construed in accordance with the laws of the State of New York, USA, without regards to such state's conflict of law rules. Any legal action, suit or proceeding arising out of or relating to these Terms and Conditions or the breach thereof shall be instituted in a court of competent jurisdiction in New York County in the State of New York in the United States of America and each party hereby consents and submits to the personal jurisdiction of such court, waives any objection to venue in such court and consents to service of process by registered or certified mail, return receipt requested, at the last known address of such party.

WILEY OPEN ACCESS TERMS AND CONDITIONS

Wiley Publishes Open Access Articles in fully Open Access Journals and in Subscription journals offering Online Open. Although most of the fully Open Access journals publish open access articles under the terms of the Creative Commons Attribution (CC BY) License only, the subscription journals and a few of the Open Access Journals offer a choice of Creative Commons Licenses. The license type is clearly identified on the article.

The Creative Commons Attribution License

The Creative Commons Attribution License (CC-BY) allows users to copy, distribute and transmit an article, adapt the article and make commercial use of the article. The CC-BY license permits commercial and non-

Creative Commons Attribution Non-Commercial License

The Creative Commons Attribution Non-Commercial (CC-BY-NC)License permits use, distribution and reproduction in any medium, provided the original work is properly cited and is not used for commercial purposes.(see below)

Creative Commons Attribution-Non-Commercial-NoDerivs License

The Creative Commons Attribution Non-Commercial-NoDerivs License (CC-BY-NC-ND) permits use, distribution and reproduction in any medium, provided the original work is properly cited, is not used for commercial purposes and no modifications or adaptations are made. (see below)

Use by commercial "for-profit" organizations

Use of Wiley Open Access articles for commercial, promotional, or marketing purposes requires further explicit permission from Wiley and will be subject to a fee.

Further details can be found on Wiley Online Library
http://olabout.wiley.com/WileyCDA/Section/id-410895.html

Other Terms and Conditions:

v1.10 Last updated September 2015

Questions? customercare@copyright.com.

10. Appendix

10.1 Supporting Information for Chapter 5

Supporting Information

Room Temperature Intermolecular Dearomatization of Arenes by an Acyclic Iminosilylene

*Huaiyuan Zhu, Arseni Kostenko, Daniel Franz, Franziska Hanusch and Shigeyoshi Inoue**

Department of Chemistry, WACKER-Institute of Silicon Chemistry and Catalysis Research Center, Technische Universität München, Lichtenbergstraße 4, 85748 Garching bei München, Germany

Contents

1. Experimental Procedures

1.1 General Methods and Instrumentation

All experiments and manipulations were carried out under argon atmosphere using standard Schlenk or glovebox techniques. The glassware was heat-dried under vacuum prior to use. All glass junctions were coated with PTFE-based grease Merkel Triboflon III. For stirring, PTFE-coated magnetic stirrer bars were used or glass-coated ones if stated. Liquid phases were transferred using standard PE/PP syringes equipped with stainless steel cannula or directly canted from vessel to vessel if not stated otherwise. Solvents were dried by standard methods (withdrawal from MBraun Solvent Purification System and storage over molecular sieves (3 Å), or distilled from sodium/benzophenone or CaH_2 under argon atmosphere and degassed via freeze-pump-thaw cycling). All chemicals were purchased from commercial suppliers and used as received if not stated otherwise. Deuterated benzene (C_6D_6), CD_2Cl_2 and THF-D_8 were obtained from Deutero Deutschland GmbH and were dried over 3 Å molecular sieves. All NMR samples were prepared under argon in J. Young Sealed tubes with PTFE caps. NMR spectra were monitored on a Bruker AV400US, DRX400, AVHD300 or AV500cr at ambient temperature (300 K) if not stated otherwise. ^{1}H and ^{13}C NMR spectra were calibrated against the residual proton and natural abundance carbon resonances of the respective deuterated solvent as internal standard. The following abbreviations are used to describe signal multiplicities: s = singlet, d = doublet, t = triplet, sept = septet, m = multiplet, br = broad and combinations thereof. Some NMR spectra include resonances for silicone grease (C_6D_6: (^{1}H) = 0.29 ppm, (^{13}C) = 1.4 ppm and (^{29}Si) = –21.8 ppm) derived from *B. Braun Melsungen AG Sterican*® cannulas. Quantitative elemental analyses (EA) were carried out using a EURO EA (HEKA tech) instrument equipped with a CHNS combustion analyzer at the Laboratory for Microanalysis at the TUM Catalysis Research Center. Elemental analyses provided partially and reproducibly low carbon percentages (~1% deviation), presumably due to the formation of incombustible silicon carbide compounds. Liquid Injection Field Desorption Ionization Mass Spectrometry (LIFDI-MS) was measured directly from an inert atmosphere glovebox with a Thermo Fisher Scientific Exactive Plus Orbitrap equipped with an ion source from Linden CMS. The UV-vis spectra were taken on a *Agilent Cary 50* spectrophotometer with a *Schlenk* quartz cuvette at the Central Analytic Department at the TUM Catalysis Research Center. Melting points (Tm) were

recorded using a Büchi M-565 at the TUM Catalysis Research Center which were prepared in sealed glass capillaries under inert argon atmosphere. ^{Me}IPrNSiBr$_3$ and NaSi^{t}Bu$_3$·(THF)$_2$ were synthesized according to procedures described in literature.[S1-2]

1.2 Synthesis and Characterization

1.2.1 Synthesis of iminosilylene (1)

A solution of NaSi^{t}Bu$_3$·(THF)$_2$ (2.44 g, 6.67 mmol, 2.0 eq) in toluene (30 mL) was added to ^{Me}IPrNSiBr$_3$ (2.32 g, 3.33 mmol, 1.0 eq) in toluene (30 mL) at room temperature. The color changed to deep green rapidly. The resulting mixture was stirred for 30 minutes, all volatiles were removed *in vacuum*. The obtained residue was extracted with pentane (3 × 20 mL). Pentane was removed from the filtrate *in vacuum*, the resulting deep green solid was washed with cold hexamethyldisiloxane (3 × 10 mL). The remaining solid was dried *in vacuum* to yield silylene **1** as blue powder (1.31 g, 60%). Crystal suitable for single crystal X-ray diffraction analysis was obtained by storing saturated pentane solution at -30 °C for 2 days.

^{1}H NMR (400.1 MHz, C$_6$D$_6$): δ [ppm] 7.19-7.22 (m, 2H, *p*-C*H*-Dipp), 7.11-7.13 (m, 4H, *m*-C*H*-Dipp), 3.22 (sept, *J* = 6.8 Hz, 4H, C*H*(CH$_3$)$_2$), 1.61 (s, 6H, CC*H*$_3$), 1.38 (d, *J* = 6.8 Hz, 12H, CH(C*H*$_3$)$_2$), 1.22 (s, 27H, C(C*H*$_3$)$_3$), 1.13 (d, *J* = 6.8 Hz, 12H, CH(C*H*$_3$)$_2$).

^{13}C{^{1}H} NMR (100.6 MHz, C$_6$D$_6$): δ [ppm] 157.9 (N*C*N), 147.7 (Ar*C*), 131.4 (Ar*C*), 129.4 (Ar*C*), 123.7 (Ar*C*), 118.5 (N*C*-CH$_3$), 32.3 (C(*C*H$_3$)$_3$), 28.6 (*C*H(CH$_3$)$_2$), 25.1 (CH(*C*H$_3$)$_2$), 23.9 (CH(*C*H$_3$)$_2$), 23.9 (*C*(CH$_3$)$_3$), 9.5 (NC-*C*H$_3$).

^{29}Si{^{1}H} NMR (79.5 MHz, C$_6$D$_6$): δ [ppm] -16.1 (*Si*^{t}Bu$_3$), 454.0 (*central Si*).

Elemental Analysis (%): Calcd: C 74.82, H 10.26, N 6.38; Found: C 74.17, H 10.35, N 6.31.

LIFDI-MS: Calcd: 657.4874; Found: 657.4879.

m.p.: 184.8 °C (color changed from blue to green-yellow)

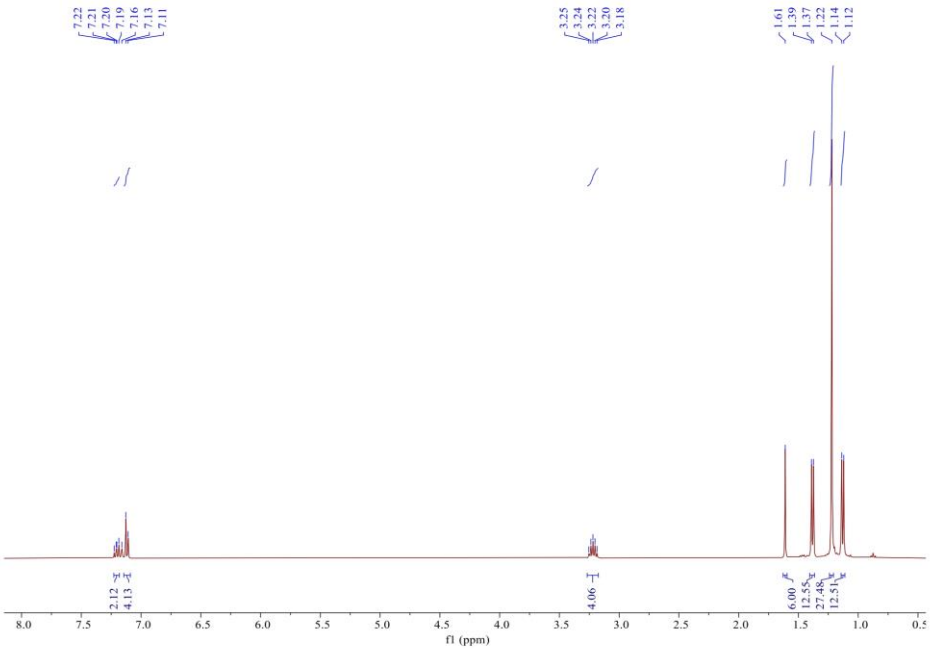

Figure S1. ^{1}H NMR spectrum of silylene **1** in C_6D_6 at 300 K.

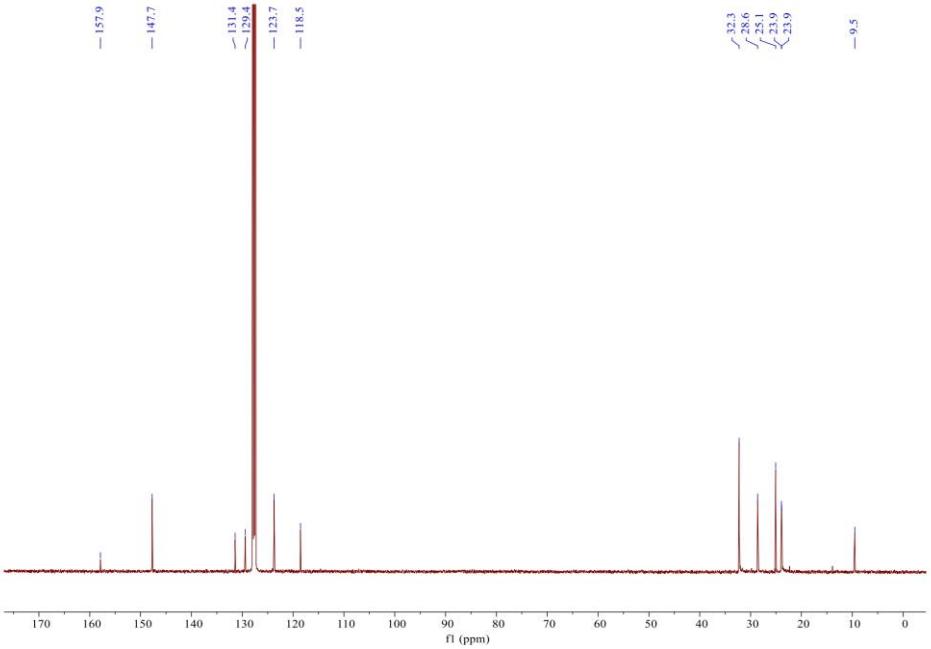

Figure S2. $^{13}C\{^{1}H\}$ NMR spectrum of silylene **1** in C_6D_6 at 300 K.

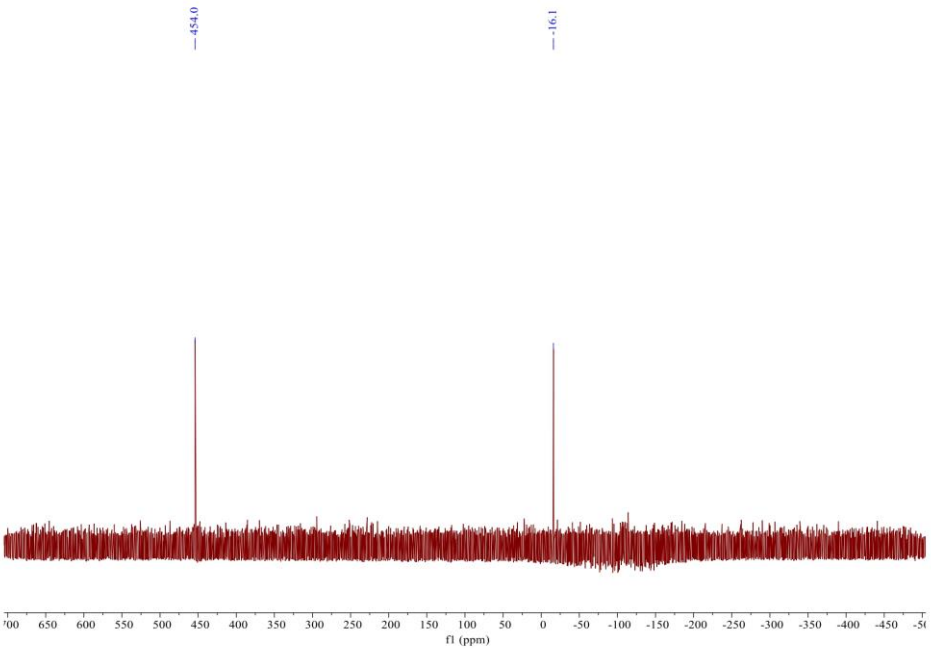

Figure S3. $^{29}Si\{^{1}H\}$ NMR spectrum of silylene **1** in C_6D_6 at 300 K

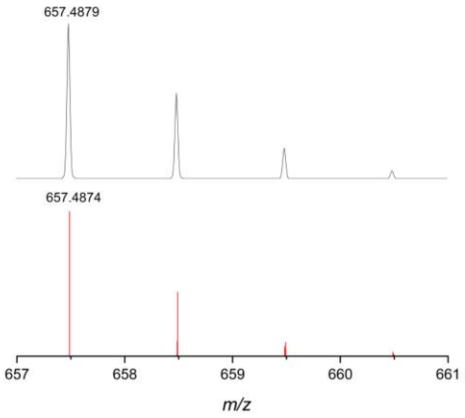

Figure S4. LIFDI-MS spectrometry of silylene **1**. Measured (top) and simulated (bottom) mass spectrum.

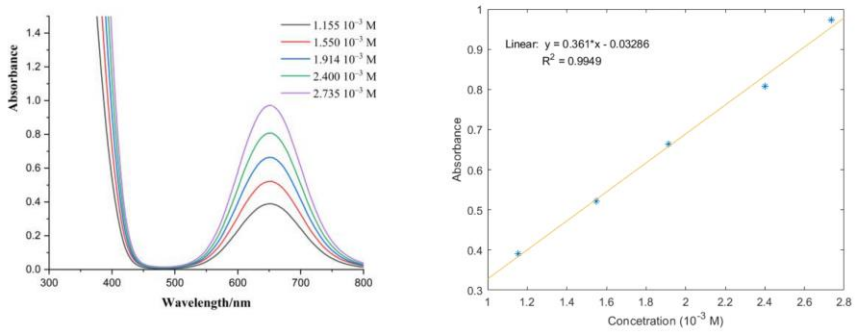

Figure S5. UV-vis spectrum of silylene **1**, λ_{max} (r.t., toluene) = 651 nm (left). Polt of the extinction coefficient in different molar concentrations(right), ε = 361 M^{-1} cm^{-1} at 651 nm. This coefficient is close to Iwamoto's cyclic silylene[S3], and also lies in the range of reported silylenes.[S3-6]

1.2.2 Thermal decomposition of 1 - Synthesis of hydrosilane (2)

A solution of silylene **1** (100 mg, 0.15 mmol) in toluene (5 mL) was heated to 75 °C for 5 days. The color of mixture changed to pale green from blue. After work-up, all volatiles were removed *in vacuum* and washed with cold pentane (3 × 3 mL), the residue was dried *in vacuum* to yield cyclic hydrosilane **2** (75.8 mg, 76%) as off-white power. Crystal suitable for single crystal X-ray diffraction analysis was obtained by slow diffusion of pentane into a saturated toluene solution at -30 °C for several days.

^{1}H NMR (400.1 MHz, C_6D_6): δ [ppm] 7.21-7.29 (m, 4H, C*H*-Dipp), 7.15-7.17 (m, 1H, C*H*-Dipp, overlapping with C_6D_6), 7.06-7.08 (m, 1H, C*H*-Dipp), 4.93 (s, *J* = 177.2 Hz, 1H, Si-*H*), 3.29 (sept, *J* = 6.8 Hz, 1H, C*H*$(CH_3)_2$), 3.18 (sept, *J* = 6.8 Hz, 1H, C*H*$(CH_3)_2$), 3.04 (sept, *J* = 6.8 Hz, 1H, C*H*$(CH_3)_2$), 1.82 (s, 3H, CC*H*$_3$), 1.74 (s, 3H, CC*H*$_3$), 1.56 (s, 3H, NCC*H*$_3$), 1.55 (s, 3H, NCC*H*$_3$), 1.40 (d, *J* = 6.8 Hz, 3H, CH(C*H*$_3)_2$), 1.32 (d, *J* = 7.2 Hz, 3H, CH(C*H*$_3)_2$), 1.28 (d, *J* = 6.8 Hz, 3H, CH(C*H*$_3)_2$), 1.22 (s, 27H, C(C*H*$_3)_3$), 1.17 (d, *J* = 6.8 Hz, 3H, CH(C*H*$_3)_2$), 1.09 (d, *J* = 7.2 Hz, 3H, CH(C*H*$_3)_2$), 1.05 (d, *J* = 6.8 Hz, 3H, CH(C*H*$_3)_2$)

^{13}C{^{1}H} NMR (100.6 MHz, C_6D_6,): δ [ppm] 151.1 (N*C*N), 148.0 (Ar*C*), 147.2 (Ar*C*), 146.8 (Ar*C*), 145.7 (Ar*C*), 132.7 (Ar*C*), 132.4 (Ar*C*), 128.7 (Ar*C*), 128.4 (Ar*C*), 123.6 (Ar*C*), 123.4 (Ar*C*), 122.1 (Ar*C*), 121.4 (Ar*C*), 117.7 (N*C*-CH_3), 115.5 (N*C*-CH_3), 33.1 (*C*$(CH_3)_2$), 31.8 (C(*C*$H_3)_3$), 28.7 (*C*H$(CH_3)_2$), 28.4 (C(*C*$H_3)_2$), 28.3 (C(*C*$H_3)_2$), 27.1 (*C*H$(CH_3)_2$), 26.9 (*C*H$(CH_3)_2$), 25.9 (CH(*C*$H_3)_2$), 24.2 (CH(*C*$H_3)_2$), 23.5 (C(*C*$H_3)_3$), 23.3

($CH(CH_3)_2$), 23.1 ($CH(CH_3)_2$), 22.3 ($CH(CH_3)_2$), 20.6 ($CH(CH_3)_2$), 9.7 (NC-CH_3), 9.3 (NC-CH_3).

$^{29}Si\{^1H\}$ NMR (79.5 MHz, C_6D_6): δ [ppm] 6.7 (*Si*^{t}Bu$_3$), -19.0 (*central Si*)

Elemental Analysis (%): Calcd: C 74.82, H 10.26, N 6.38; Found: C 73.47, H 10.22, N 6.52.

LIFDI-MS: Calcd: 657.4874; Found: 657.4865.

m.p.: 191.6 °C (off-white substance)

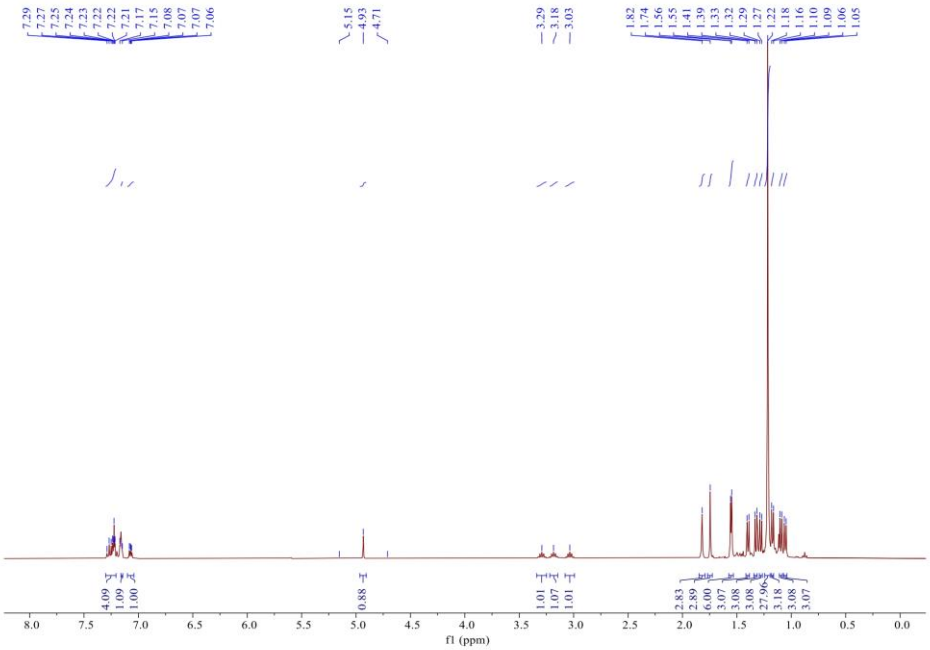

Figure S6. ^1H NMR spectrum of hydrosilane **2** in C_6D_6 at 300 K.

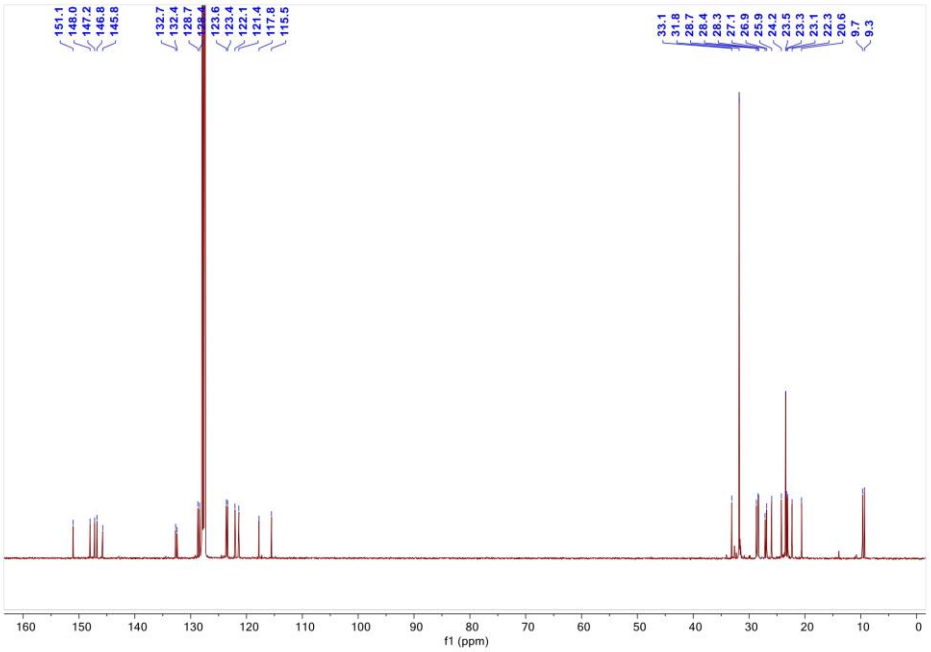

Figure S7. $^{13}C\{^{1}H\}$ NMR spectrum of hydrosilane **2** in C_6D_6 at 300 K.

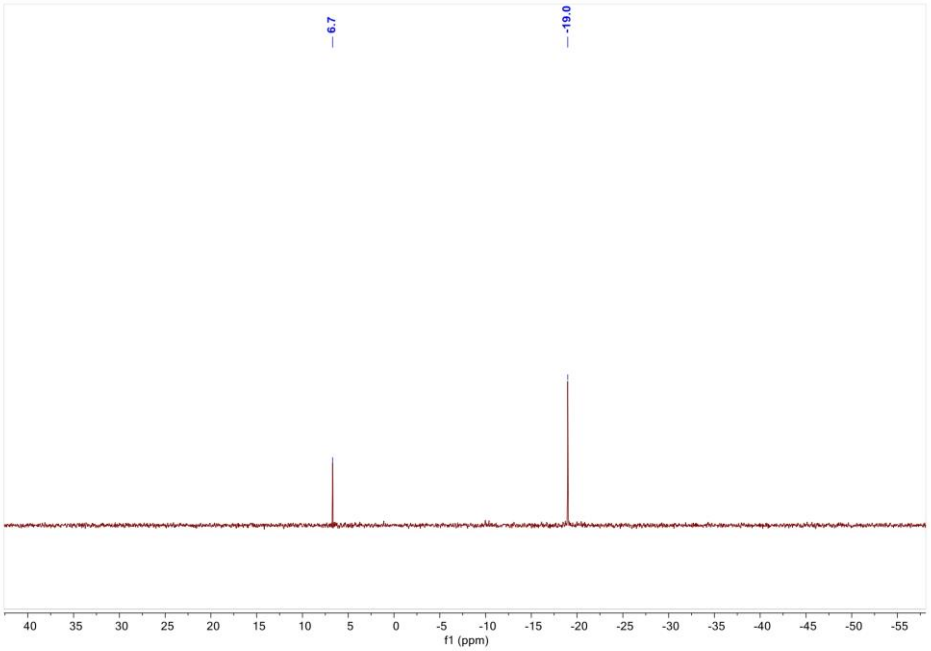

Figure S8. $^{29}Si\{^{1}H\}$ NMR spectrum of hydrosilane **2** in C_6D_6 at 300 K.

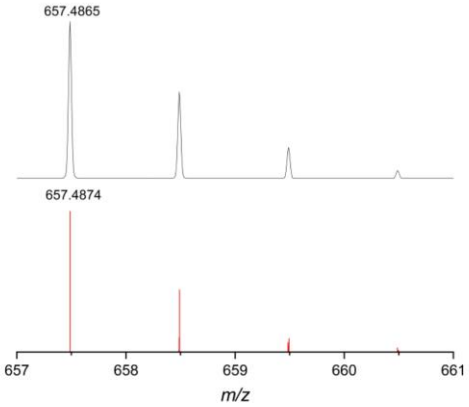

Figure S9. LIFDI-MS spectrometry of hydrosilane **2**. Measured (top) and simulated (bottom) mass spectrum.

1.2.3 Synthesis of silepin (3a)

A solution of silylene **1** (400 mg, 0.61 mmol) in benzene (10 mL) was heated to 40 °C for 1 week. The color of mixture changed to green from blue. After work-up, all volatiles were removed *in vacuum* and washed with cold pentane (3 × 3 mL), the residue was dried *in vacuum* to yield silepin **3a** (180 mg, 40%) as yellow flocculent power. Crystal suitable for single crystal X-ray diffraction analysis was obtained by slow evaporation of benzene solution at room temperature for several days.

^{1}H NMR (400.1 MHz, C_6D_6): δ [ppm] 7.22-7.26 (m, 2H, *p*-C*H*-Dipp), 7.13-7.15 (m, 4H, *m*-C*H*-Dipp), 5.98-6.02 (m, 2H, SiCHCHC*H*), 5.98-6.02 (m, 2H, SiCHC*H*), 5.98-6.02 (d, *J* = 14.8 Hz, 2H, SiC*H*), 3.18 (sept, *J* = 6.8 Hz, 4H, C*H*(CH_3)$_2$), 1.46 (s, 6H, CCH_3), 1.38 (d, *J* = 6.8 Hz, 12H, CH(CH_3)$_2$), 1.22 (s, 27H, C(CH_3)$_3$), 1.14 (d, *J* = 6.8 Hz, 12H, CH(CH_3)$_2$).

^{13}C{^{1}H} NMR (100.6 MHz, C_6D_6): δ [ppm] 147.2 (NCN), 143.3 (Ar*C*), 136.9 (SiCHCH*C*H), 134.2 (SiCH*C*H), 134.2 (Ar*C*), 131.2 (Si*C*H), 128.8 (Ar*C*), 124.1 (Ar*C*), 116.6 (N*C*-CH_3), 32.0 (*C*(CH_3)$_3$), 28.4 (*C*H(CH_3)$_2$), 23.7 (CH(*C*H_3)$_2$), 23.6 (CH(*C*H_3)$_2$), 23.2 (*C*(CH_3)$_3$), 10.2 (NC-*C*H_3).

^{29}Si{^{1}H} NMR (79.5 MHz, C_6D_6): δ [ppm] -1.4 (*Si*^{t}Bu$_3$), -38.8 (*central Si*).

Elemental Analysis (%): Calcd: C 76.67, H 9.99, N 5.71; Found: C 75.12, H 10.01, N 5.85.

LIFDI-MS: Calcd: 735.5343; Found: 735.5346.

m.p.: 174.3 °C (color changed from yellow to green)

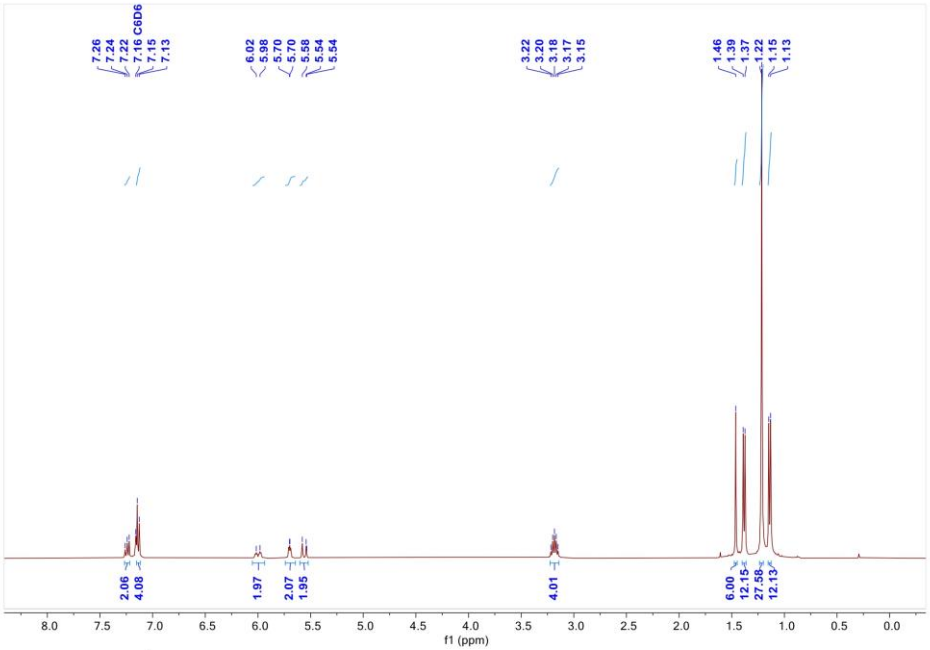

Figure S10. ^{1}H NMR spectrum of silepin **3a** in C_6D_6 at 300 K.

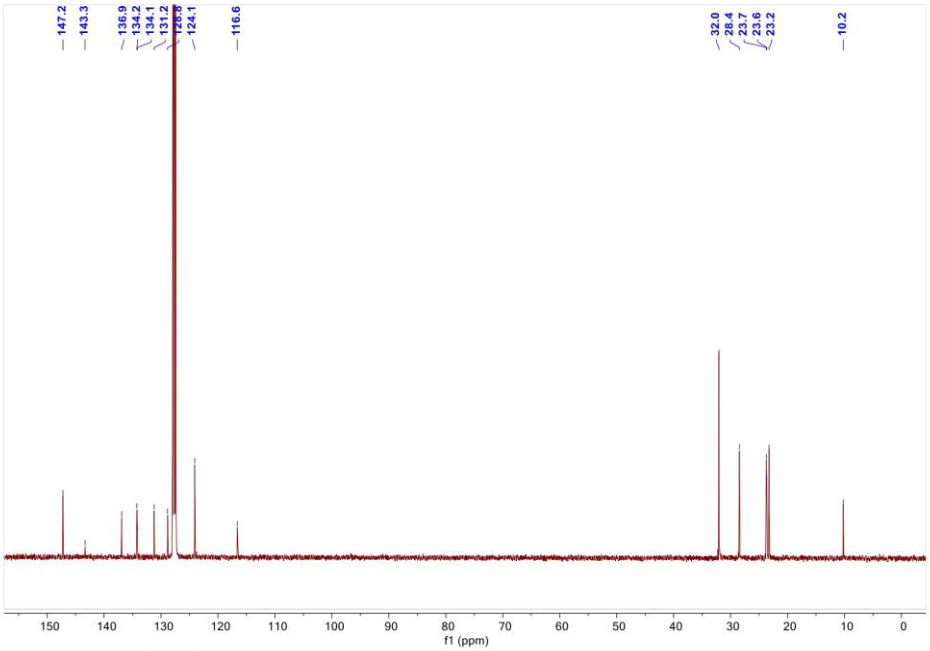

Figure S11. $^{13}C\{^{1}H\}$ NMR spectrum of silepin **3a** in C_6D_6 at 300 K.

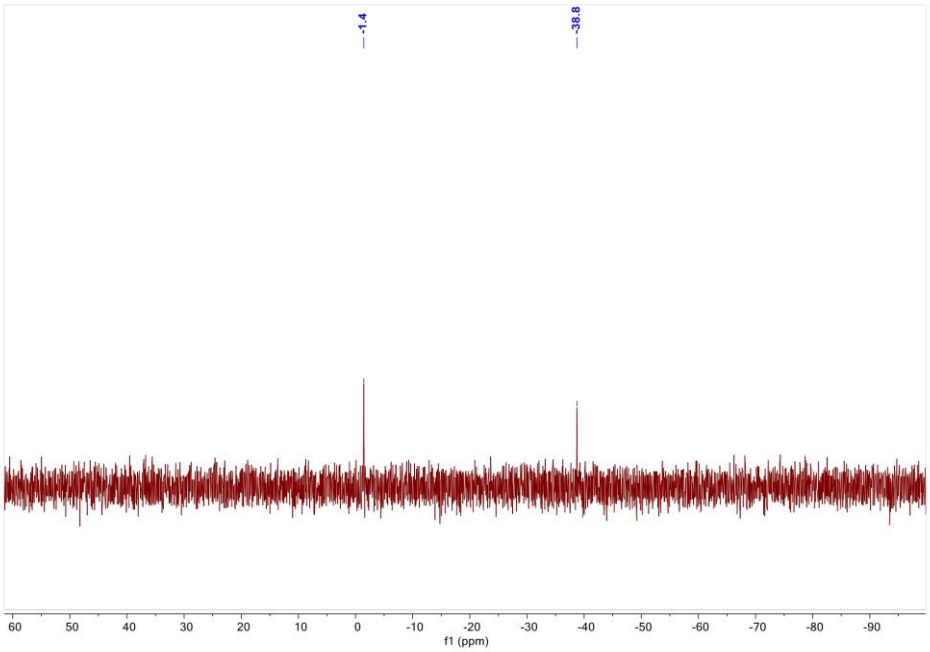

Figure S12. $^{29}Si\{^{1}H\}$ NMR spectrum of silepin **3a** in C_6D_6 at 300 K.

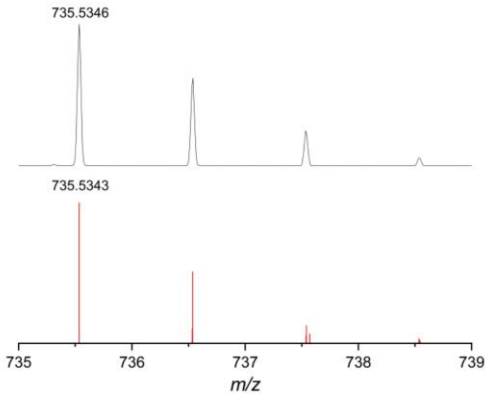

Figure S13. LIFDI-MS spectrometry of silepin **3a**. Measured (top) and simulated (bottom) mass spectrum.

1.2.4 Synthesis of silepin (3b)

1,4-difluorobenzene (1 mL) was added to silylene **1** (200 mg, 0.30 mmol) in benzene (5 mL), the blue solution was heated to 40 °C for 1 day. The color of mixture changed

to yellow with the formation of yellow crystals. After work-up, all volatiles were removed *in vacuum* and washed with cold pentane (3 × 1 mL), the residue was dried *in vacuum* to yield silepin **3b** (210 mg, 94%) as yellow power. Crystal suitable for single crystal X-ray diffraction analysis was obtained by slow evaporation of benzene solution at room temperature for several days.

^{1}H NMR (400.1 MHz, THF-D$_8$): δ [ppm] 7.31-7.35 (m, 2H, *p*-C*H*-Dipp), 7.24-7.26 (m, 4H, *m*-C*H*-Dipp), 5.56-5.61 (m, 2H, SiCHCFC*H*), 5.03 (s, 1H, SiC*H*), 4.93 (s, 1H, SiC*H*), 3.08 (sept, *J* = 6.8 Hz, 4H, C*H*(CH$_3$)$_2$), 1.72 (s, 6H, CC*H*$_3$, overlapping with THF-D$_8$), 1.32 (d, *J* = 6.8 Hz, 12H, CH(C*H*$_3$)$_2$), 1.16 (d, *J* = 6.8 Hz, 12H, CH(C*H*$_3$)$_2$), 0.92 (s, 27H, C(C*H*$_3$)$_3$).

^{13}C{^{1}H} NMR (100.6 MHz, THF-D$_8$): δ [ppm] 158.3 (d, $^{1}J_{C\text{-}F}$ = 250.0 Hz ,*C*F), 146.7 (N*C*N), 143.6 (Ar*C*), 133.6 (Ar*C*), 129.4 (Ar*C*), 125.5 (d, $^{2}J_{C\text{-}F}$ = 15.3 Hz , SiCHCF*C*H), 125.0 (d, $^{2}J_{C\text{-}F}$ = 15.3 Hz , SiCHCF*C*H), 124.1 (Ar*C*), 117.3 (N*C*-CH$_3$), 109.9 (d, $^{2}J_{C\text{-}F}$ = 1.9 Hz ,Si*C*HCF), 31.3 (C(*C*H$_3$)$_3$), 28.4 (*C*H(CH$_3$)$_2$), 23.2 (CH(*C*H$_3$)$_2$), 23.1 (CH(*C*H$_3$)$_2$), 22.7 (*C*(CH$_3$)$_3$), 9.6 (NC-*C*H$_3$).

^{19}F{^{1}H} NMR (376.5 MHz, THF-D$_8$): δ [ppm] -66.96--66.81(m, 2F, C*F*)

^{29}Si{^{1}H} NMR (79.5 MHz, THF-D$_8$): δ [ppm] -2.5 (t, $^{4}J_{Si\text{-}F}$ = 3.9 Hz, *Si*^{t}Bu$_3$), -49.6 (t, $^{3}J_{Si\text{-}F}$ = 17.6 Hz, *central Si*).

Elemental Analysis (%): Calcd: C 73.10, H 9.27, N 5.44; Found: C 69.98, H 9.10, N 5.66.

LIFDI-MS: Calcd: 771.5155; Found: 771.5112.

m.p.: 237.7 °C (color changed from yellow to orange)

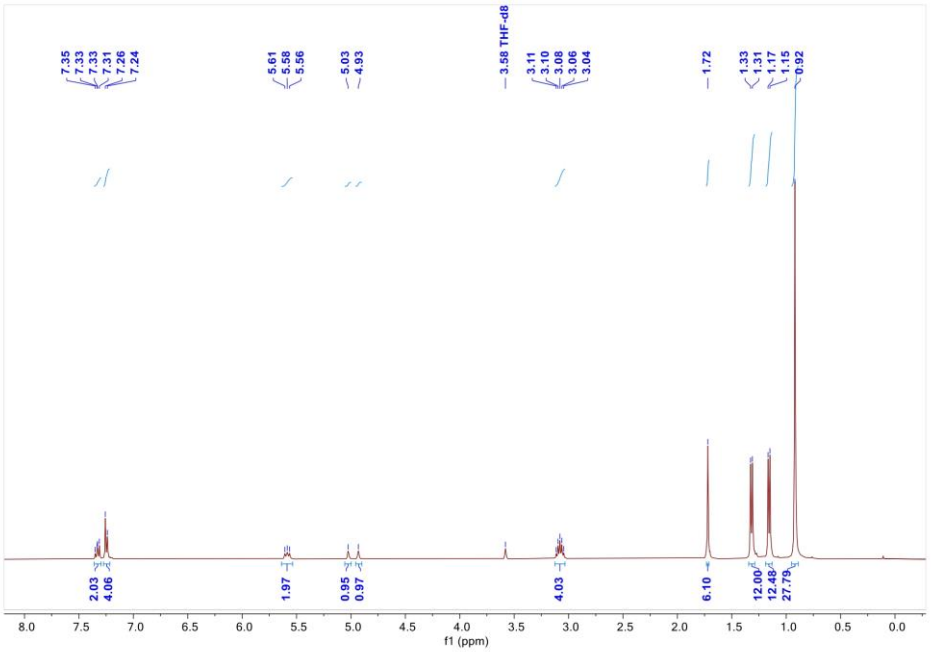

Figure S14. ^{1}H NMR spectrum of silepin **3b** in THF-D_8 at 300 K.

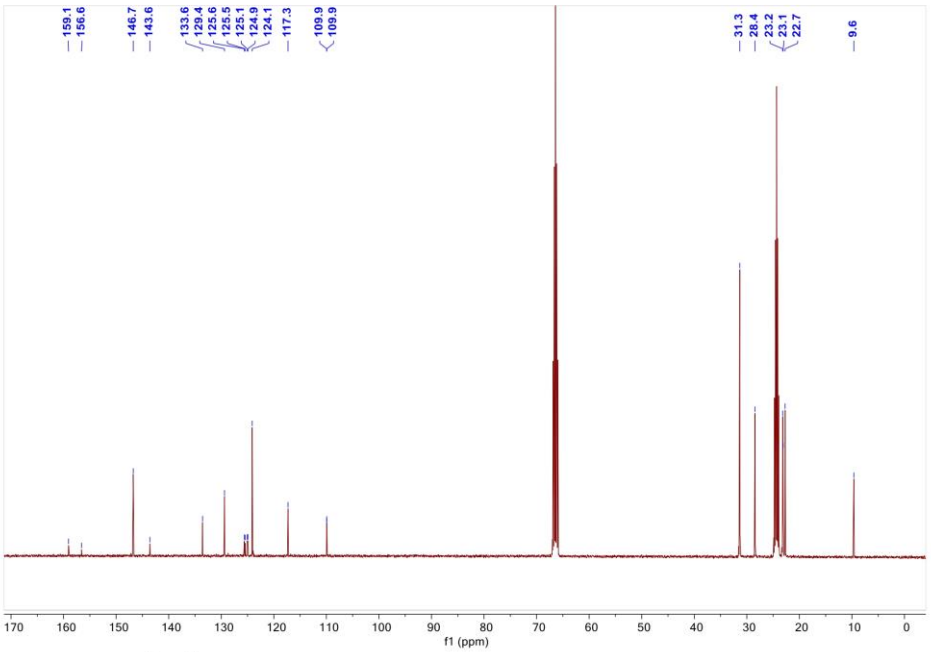

Figure S15. $^{13}C\{^{1}H\}$ NMR spectrum of silepin **3b** in THF-d_8 at 300 K.

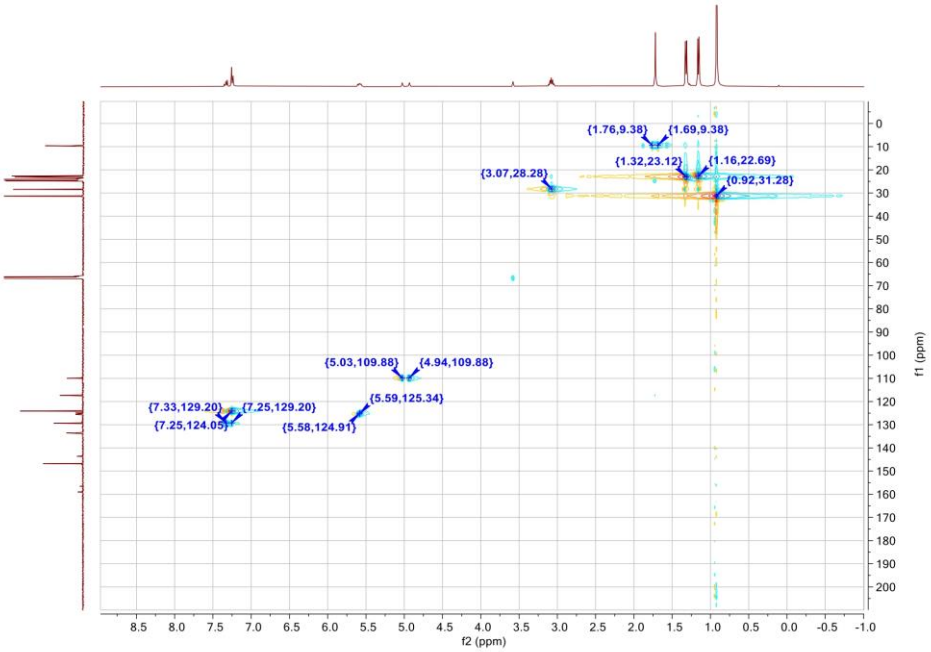

Figure S16. $^{1}H/^{13}C$ HSQC of silepin **3b** in THF-d_8 at 300 K.

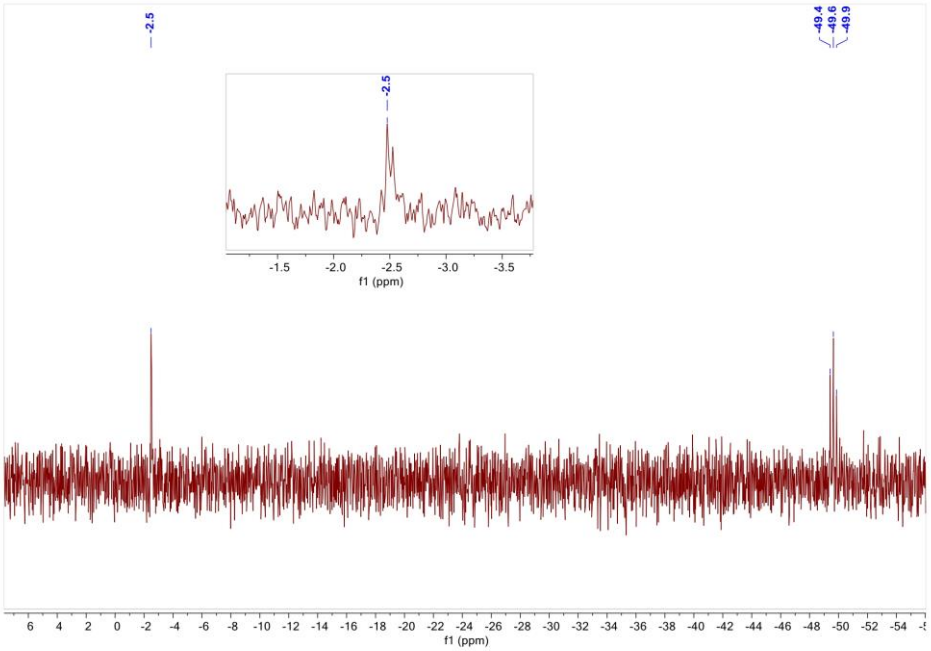

Figure S17. $^{29}Si\{^{1}H\}$ NMR spectrum of silepin **3b** in THF-d_8 at 300 K.

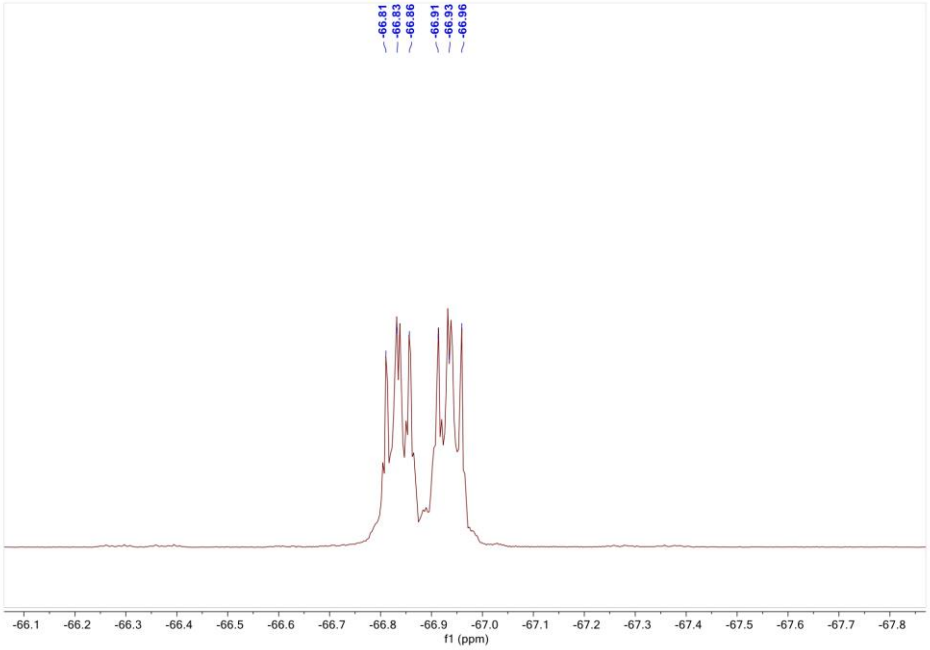

Figure S18. $^{19}F\{^{1}H\}$ NMR spectrum of silepin **3b** in THF-d_8 at 300 K.

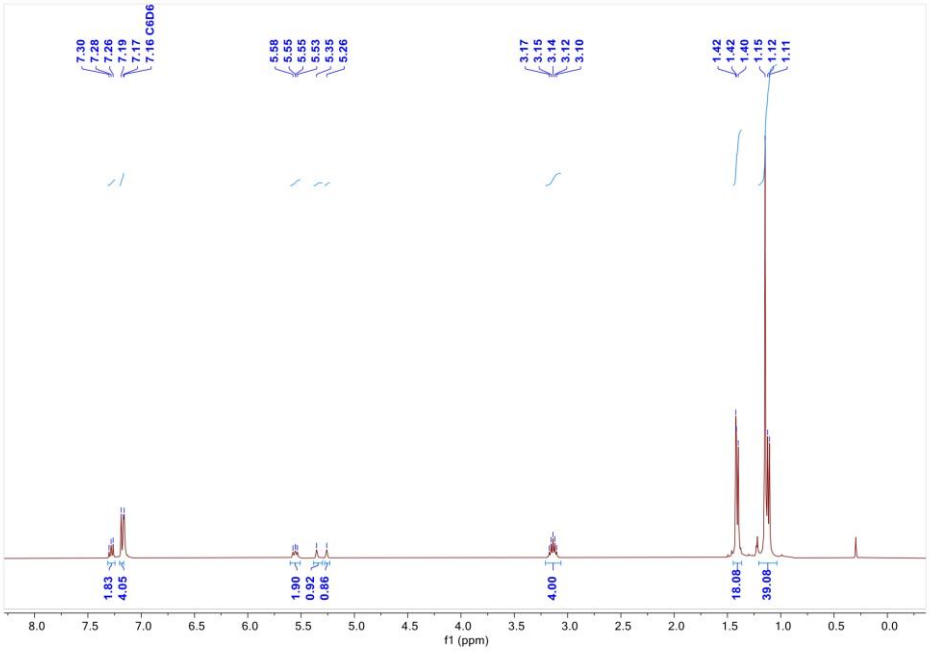

Figure S19. ^{1}H NMR spectrum of silepin **3b** in C_6D_6 at 300 K

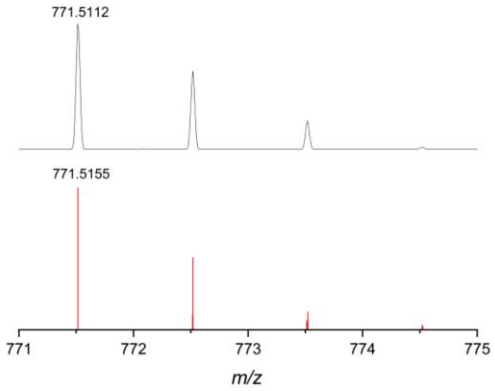

Figure S20. LIFDI-MS spectrometry of silepin **3b**. Measured (top) and simulated (bottom) mass spectrum.

1.2.5 Synthesis of silepin (3c)

1,4-bis(trifluoromethyl)benzene (2 mL) was added to silylene **1** (200 mg, 0.30 mmol) in benzene (2 mL), the color of mixture changed to deep blue rapidly. The resulting solution was stirred for 2 days at room temperature gave to yellow-green solution. After work-up, all volatiles were removed *in vacuum* and washed with cold pentane (3 × 1 mL), the residue was dried *in vacuum* to yield silepin **3c** (115 mg, 52%) as orange power. Crystal suitable for single crystal X-ray diffraction analysis was obtained by slow evaporation of pentane, THF and toluene solution at -30 °C for several days.

^{1}H NMR (400.1 MHz, C_6D_6): δ [ppm] 7.25-29 (m, 2H, *p*-C*H*-Dipp), 7.13-7.15 (m, 4H, *m*-C*H*-Dipp, overlapping with C_6D_6), 6.37 (s, 2H, SiCHCF$_3$C*H*), 5.90 (s, 2H, SiC*H*), 3.06 (sept, *J* = 6.8 Hz, 4H, C*H*(CH$_3$)$_2$), 1.37 (d, *J* = 7.2 Hz, 12H, CH(C*H*$_3$)$_2$), 1.34 (s, 6H, CC*H*$_3$), 1.09 (s, 27H, C(C*H*$_3$)$_3$), 1.07 (d, *J* = 7.2 Hz, 12H, CH(C*H*$_3$)$_2$).

^{13}C{^{1}H} NMR (100.6 MHz, C_6D_6): δ [ppm] 146.7 (N*C*N), 143.7 (Ar*C*), 137.1 (d, $^{3}J_{C\text{-}F}$ = 2.9 Hz ,SiCHC(CF$_3$)*C*H), 133.2 (Ar*C*), 133.1 (d, $^{2}J_{C\text{-}F}$ = 81.0 Hz ,SiCH*C*(CF$_3$)CH), 133.1 (d, $^{3}J_{C\text{-}F}$ = 27.2 Hz ,Si*C*HC(CF$_3$)CH), 129.7 (Ar*C*), 124.3 (Ar*C*), 123.9 (d, $^{1}J_{C\text{-}F}$ = 276.9 Hz ,*C*F$_3$), 117.3 (N*C*-CH$_3$), 109.9 (d, $^{2}J_{C\text{-}F}$ = 1.9 Hz ,SiCHCF*C*H), 31.7 (C(*C*H$_3$)$_3$), 28.5 (*C*H(CH$_3$)$_2$), 23.5 (CH(*C*H$_3$)$_2$), 23.5 (CH(*C*H$_3$)$_2$), 23.1 (*C*(CH$_3$)$_3$), 10.0 (NC-*C*H$_3$).

^{19}F{^{1}H} NMR (376.5 MHz, C_6D_6): δ [ppm] -67.68(s, 6F, C*F*$_3$)

^{29}Si{^{1}H} NMR (79.5 MHz, C_6D_6): δ [ppm] 1.7 (*Si*^{t}Bu$_3$), -43.9 (*central Si*).

Elemental Analysis (%): Calcd: C 67.47, H 8.20, N 4.82; Found: C 66.63, H 8.29, N 5.02.

LIFDI-MS: Calcd: 871.5091; Found: 871.5038.

m.p.: 176.4 °C (color changed from yellow to brown)

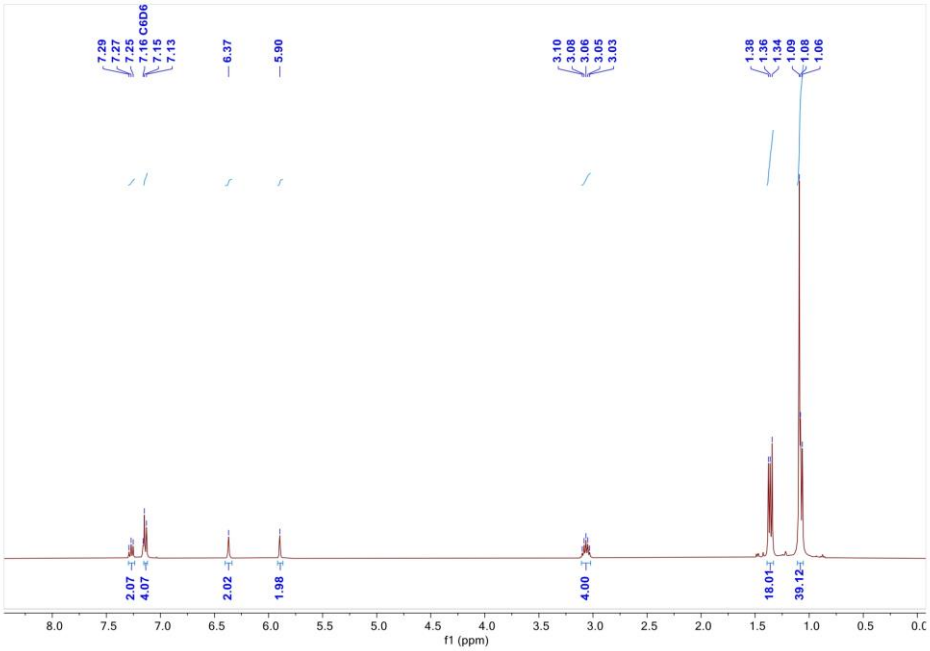

Figure S21. ^{1}H NMR spectrum of silepin **3c** in C_6D_6 at 300 K.

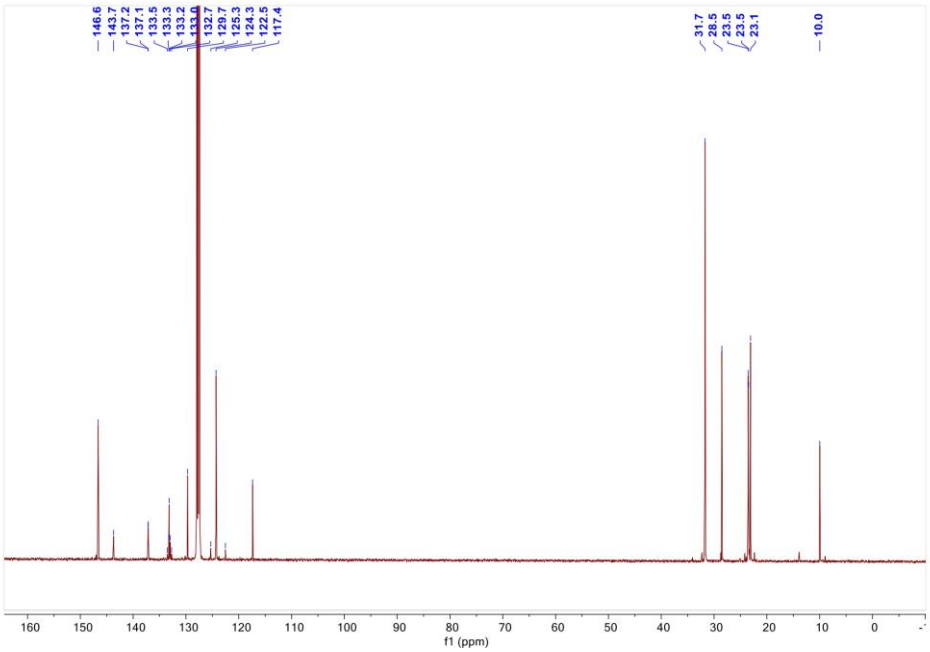

18

Figure S22. $^{13}C\{^{1}H\}$ NMR spectrum of silepin **3c** in C_6D_6 at 300 K.

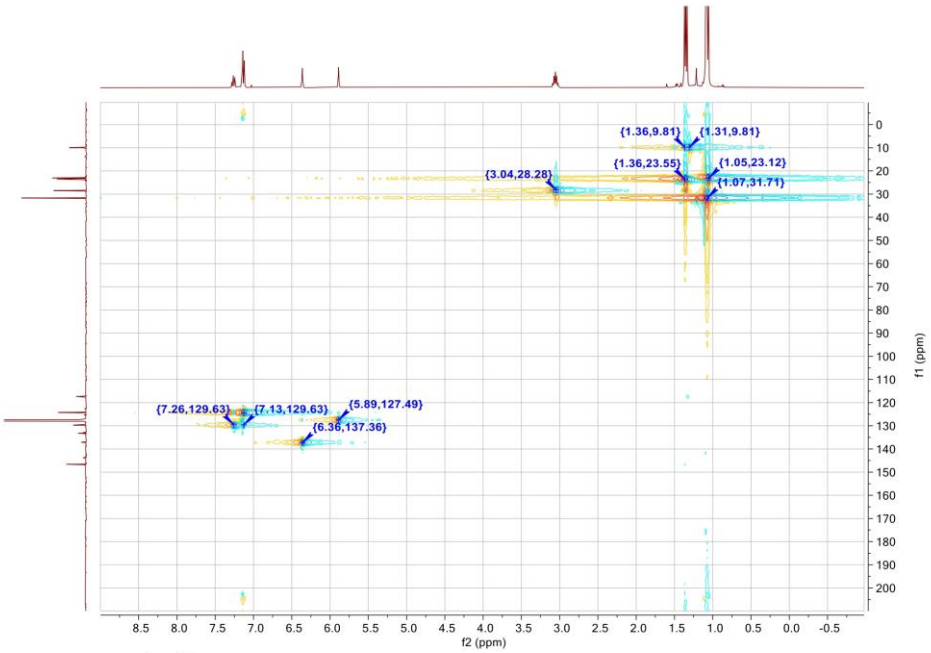

Figure S23. $^{1}H/^{13}C$ HSQC of silepin **3c** in C_6D_6 at 300 K.

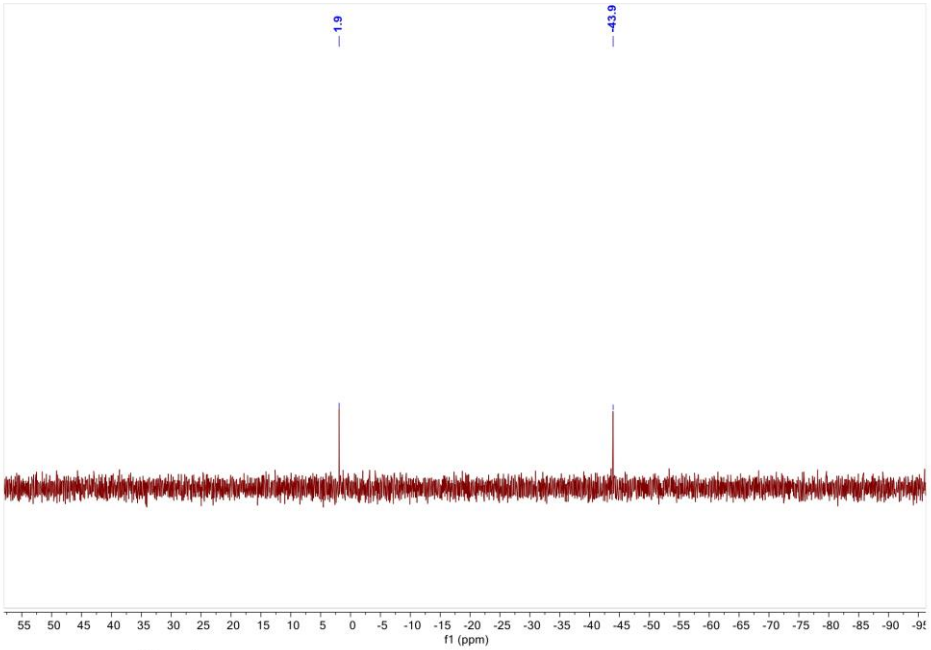

Figure S24. $^{29}Si\{^{1}H\}$ NMR spectrum of silepin **3c** in C_6D_6 at 300 K.

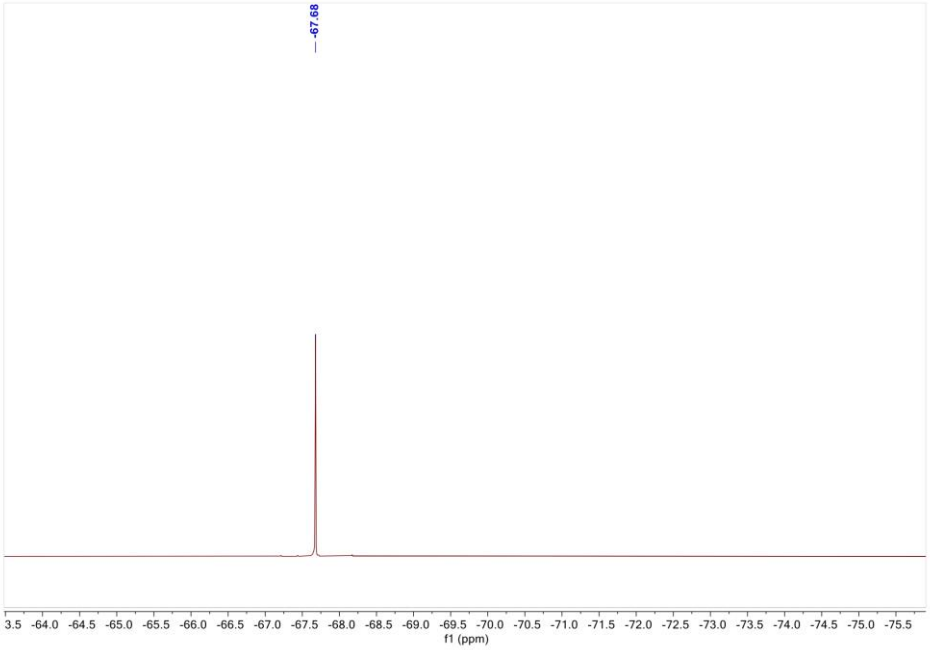

Figure S25. $^{19}F\{^{1}H\}$ NMR spectrum of silepin **3c** in C_6D_6 at 300 K.

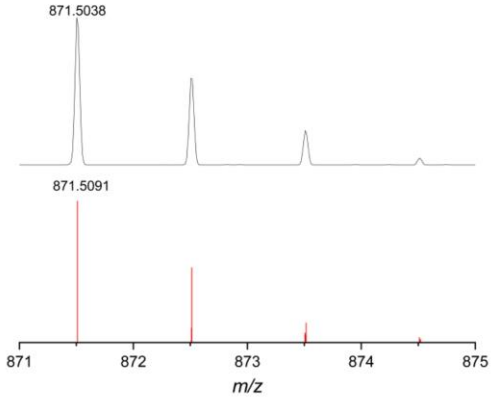

Figure S26. LIFDI-MS spectrometry of silepin **3c**. Measured (top) and simulated (bottom) mass spectrum.

1.2.6 Synthesis of azasilepin (4a)

Pyridine (0.1 mL) was added dropwise to silylene **1** (200 mg, 0.30 mmol) in benzene (5 mL), the color of solution turned to green rapidly, and some orange precipitate

formed within few seconds. After filtration, the residue was washed with pentane (3 × 5 mL), then dried *in vacuum* to yield azasilepin **4a** (205 mg, 91%) as orange power. Crystal suitable for single crystal X-ray diffraction analysis was obtained by slow evaporation of saturated benzene solution at room temperature for several days.

^{1}H NMR (400.1 MHz, CD_2Cl_2): δ [ppm] 7.36 (d, *J* = 1.6 Hz, 1H, NC*H*), 7.29-7.33 (m, 2H, *p*-C*H*-Dipp), 7.14-7.18 (m, 4H, *m*-C*H*-Dipp), 5.94-5.99 (dd, *J* = 7.6 Hz, 1H, SiCHC*H*), 5.63-5.67 (d, *J* = 15.2 Hz, 1H, SiC*H*), 5.52-5.57 (dd, *J* = 4.8 Hz, 1H, SiCHCHC*H*), 5.38-5.42 (dd, *J* = 10.8 Hz, 1H, NCHC*H*), 3.22 (sept, *J* = 6.8 Hz, 2H, C*H*(CH_3)$_2$), 2.87 (sept, *J* = 6.8 Hz, 2H, C*H*(CH_3)$_2$), 1.67 (s, 6H, CC*H*$_3$), 1.30 (d, *J* = 6.8 Hz, 6H, CH(C*H*$_3$)$_2$), 1.19 (d, *J* = 7.2 Hz, 6H, CH(C*H*$_3$)$_2$), 1.17 (d, *J* = 8.0 Hz, 6H, CH(C*H*$_3$)$_2$), 1.05 (d, *J* = 6.8 Hz, 6H, CH(C*H*$_3$)$_2$), 0.88 (s, 27H, C(C*H*$_3$)$_3$).

^{13}C{^{1}H} NMR (100.6 MHz, CD_2Cl_2): δ [ppm] 156.0 (SiN*C*H), 148.2 (N*C*N), 147.0 (Ar*C*), 139.4 (N*C*HCH), 134.5 (Ar*C*), 134.4 (Ar*C*), 133.8 (Ar*C*), 132.0 (N*C*HCH), 130.1 (SiCHCH*C*H), 128.5 (Ar*C*), 124.1 (Ar*C*), 123.5 (SiCH*C*H),116.7 (N*C*-CH$_3$), 31.4 (C(*C*H$_3$)$_3$), 28.4 (*C*H(CH$_3$)$_2$), 28.3 (*C*H(CH$_3$)$_2$), 24.6 (CH(*C*H$_3$)$_2$), 23.5 (CH(*C*H$_3$)$_2$), 23.1 (*C*(CH$_3$)$_3$), 22.9 (CH(*C*H$_3$)$_2$), 22.3 (CH(*C*H$_3$)$_2$), 10.2 (NC-*C*H$_3$).

^{29}Si{^{1}H} NMR (79.5 MHz, CD_2Cl_2): δ [ppm] -2.9 (*Si*^{t}Bu$_3$), -40.2 (*central Si*).

Elemental Analysis (%): Calcd: C 74.84, H 9.84, N 7.60; Found: C 73.32, H 9.84, N 7.64.

LIFDI-MS: Calcd: 736.5296; Found: 736.5274.

m.p.: 262.4 °C (color changed from yellow to brown)

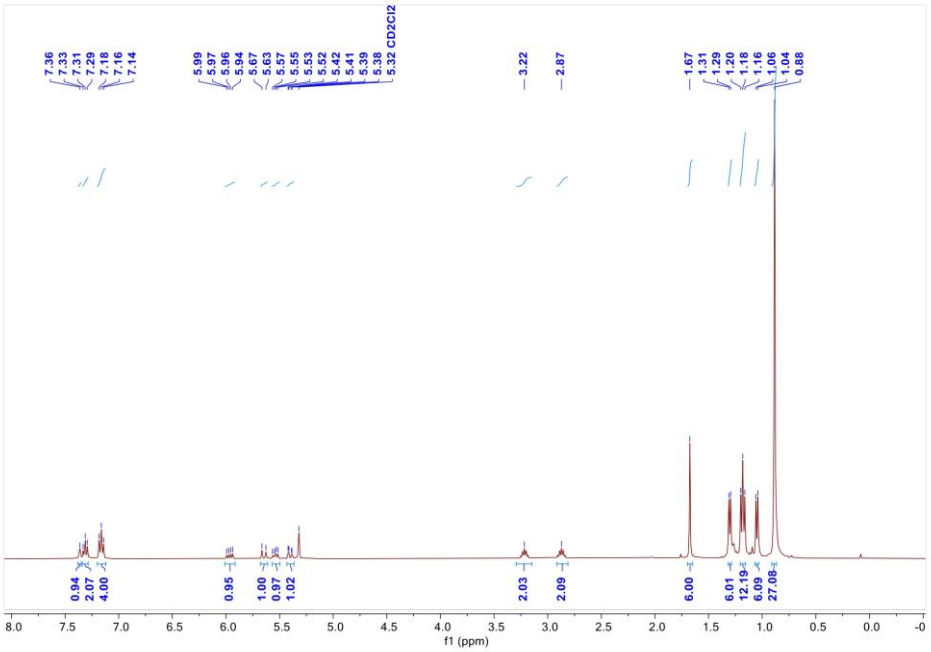

Figure S27. ^{1}H NMR spectrum of azasilepin **4a** in CD_2Cl_2 at 300 K.

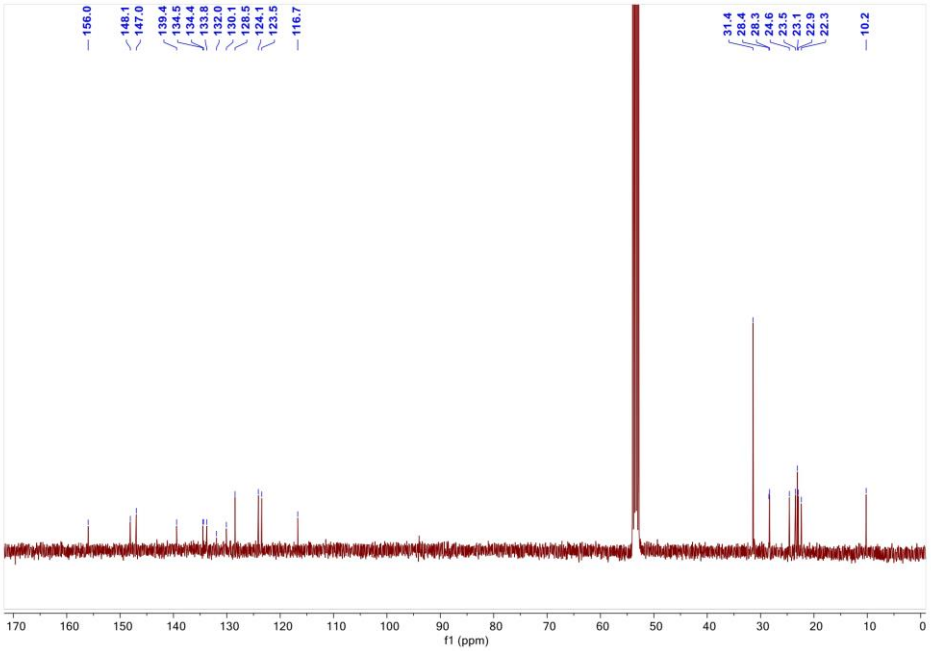

Figure S28. $^{13}C\{^{1}H\}$ NMR spectrum of azasilepin **4a** in CD_2Cl_2 at 300 K.

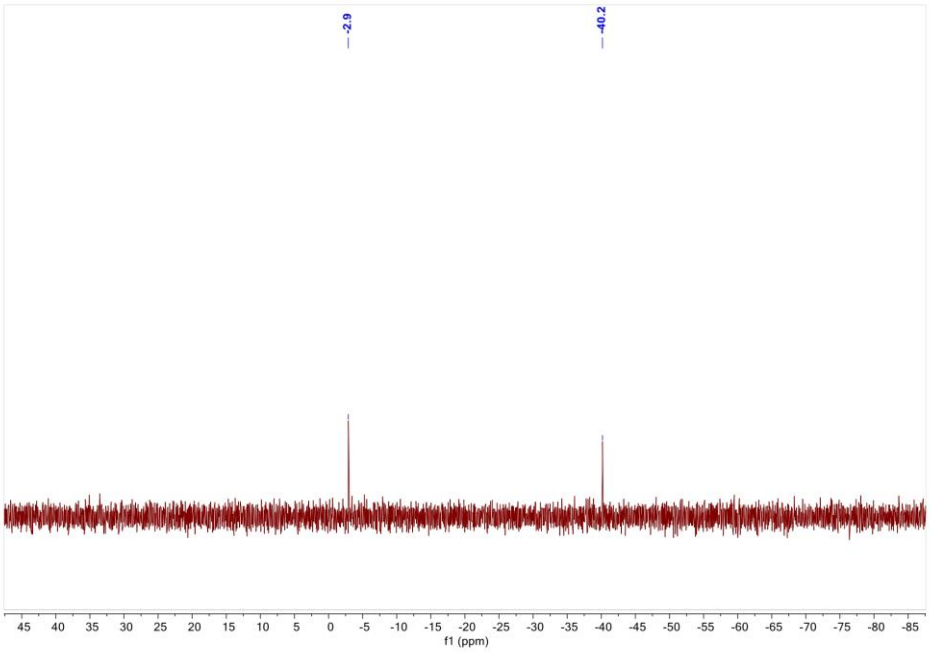

Figure S29. $^{29}Si\{^{1}H\}$ NMR spectrum of azasilepin **4a** in CD_2Cl_2 at 300 K.

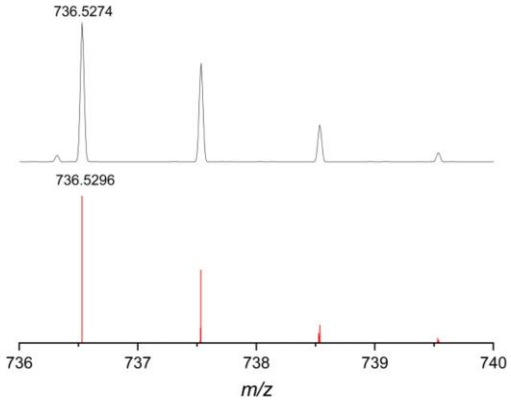

Figure S30. LIFDI-MS spectrometry of azasilepin **4a**. Measured (top) and simulated (bottom) mass spectrum.

1.2.7 Synthesis of azasilepin (4b)

DMAP (36 mg, 0.30 mmol) was added to silylene **1** (200 mg, 0.30 mmol) in benzene (5 mL), the color of mixture turned to green rapidly. The resulting solution was stirred for 1 day at room temperature to furnish yellow solution. After work-up, all volatiles

were removed *in vacuum* and washed with cold pentane (3 × 1 mL), the residue was dried *in vacuum* to yield silepin **4b** (200 mg, 84%) as yellow power.

^{1}H NMR (400.1 MHz, C_6D_6): δ [ppm] 7.68 (d, *J* = 4.8 Hz, 1H, NC*H*), 7.26-7.30 (m, 2H, *p*-C*H*-Dipp), 7.18-7.22 (m, 4H, *m*-C*H*-Dipp), 6.14-6.19 (dd, *J* = 13.6 Hz, 1H, SiCHC*H*), 5.70-5.74 (d, *J* = 16.0 Hz, 1H, SiC*H*), 4.69-4.71 (dd, *J* = 2.4 Hz, 1H, NCHC*H*), 3.41 (sept, *J* = 6.8 Hz, 2H, C*H*(CH_3)$_2$), 3.16 (sept, *J* = 6.8 Hz, 2H, C*H*(CH_3)$_2$), 2.28 (s, 6H, N(CH_3)$_2$, 1.54 (d, *J* = 6.8 Hz, 6H, CH(CH_3)$_2$), 1.50 (s, 6H, CCH_3), 1.41 (d, *J* = 6.8 Hz, 6H, CH(CH_3)$_2$), 1.27 (s, 27H, C(CH_3)$_3$), 1.19 (d, *J* = 6.8 Hz, 6H, CH(CH_3)$_2$), 1.18 (d, *J* = 6.8 Hz, 6H, CH(CH_3)$_2$).

^{13}C{^{1}H} NMR (100.6 MHz, C_6D_6): δ [ppm] 156.3 (SiN*C*H), 155.8 (*C*NMe_2), 148.2 (N*C*N), 147.1 (Ar*C*), 143.3 (Ar*C*), 137.6 (N*C*H*C*H), 134.6 (Ar*C*), 134.2 (Ar*C*), 128.7 (Ar*C*), 123.9 (Ar*C*), 123.7 (Si*C*H), 116.5 (N*C*-CH_3), 107.8 (SiCH*C*H), 40.6 (N*C*H_3), 32.0 (C(*C*H_3)$_3$), 28.6 (*C*H(CH_3)$_2$), 28.4 (*C*H(CH_3)$_2$), 24.4 (CH(*C*H_3)$_2$), 23.6 (CH(*C*H_3)$_2$), 23.4 (CH(*C*H_3)$_2$), 23.2 (CH(*C*H_3)$_2$), 23.1 (*C*(CH_3)$_3$), 10.2 (NC-*C*H_3).

^{29}Si{^{1}H} NMR (79.5 MHz, C_6D_6): δ [ppm] -2.0 (*Si*^{t}Bu$_3$), -42.9 (*central Si*).

Elemental Analysis (%): Calcd: C 73.88, H 9.95, N 8.97; Found: C 72.54, H 9.95, N 8.87.

LIFDI-MS: Calcd: 764.5483; Found: 765.5420 (lost one methyl group).

m.p.: 166.9 °C (color changed from yellow to black)

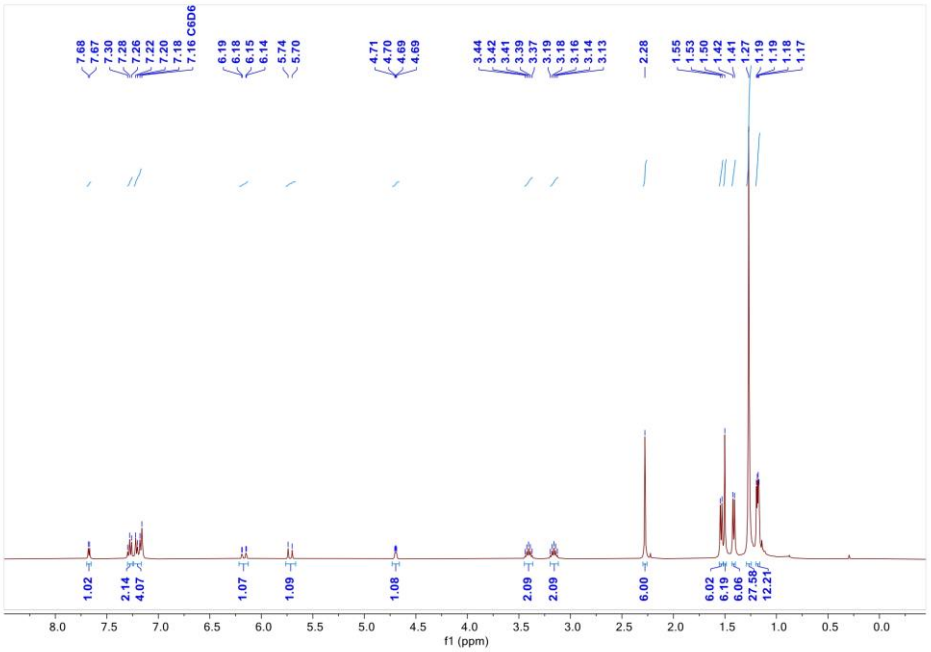

Figure S31. ^{1}H NMR spectrum of silepin **4b** in C_6D_6 at 300 K.

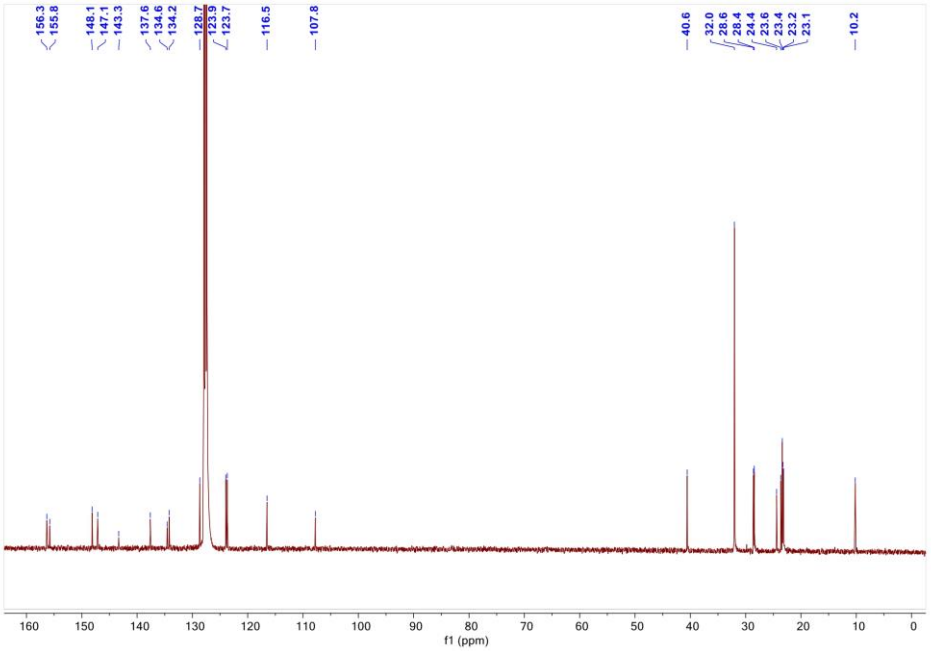

Figure S32. $^{13}C\{^{1}H\}$ NMR spectrum of silepin **4b** in C_6D_6 at 300 K.

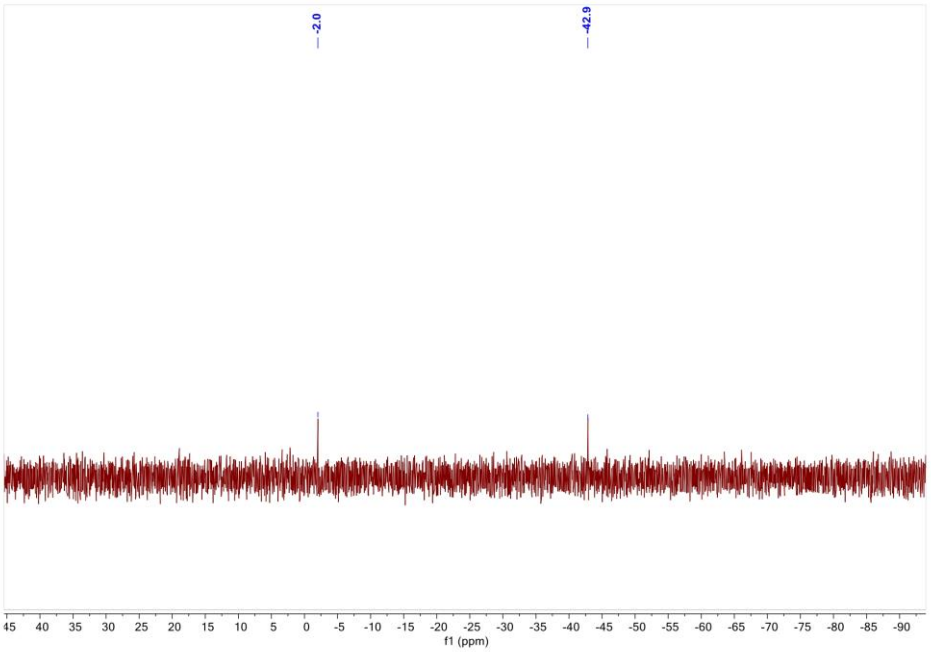

Figure S33. $^{29}Si\{^{1}H\}$ NMR spectrum of silepin **4b** in C_6D_6 at 300 K

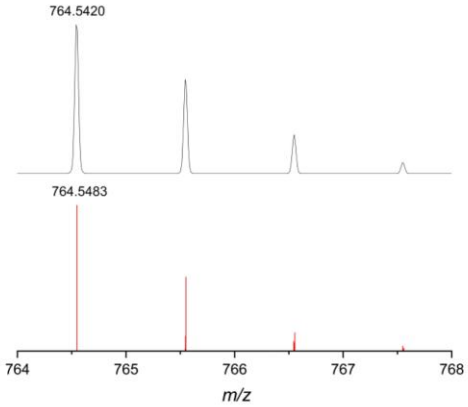

Figure S34. LIFDI-MS spectrometry of azasilepin **4b**. Measured (top) and simulated (bottom) mass spectrum.

1.3 Ligand exchanged reaction

1.3.1 Reversibility of silepin 3a

To test the reversibility of **3a**, the solution of **3a** in C_6D_6 was heated to 60°C in a J. Young NMR tube and monitored by ^{1}H NMR.

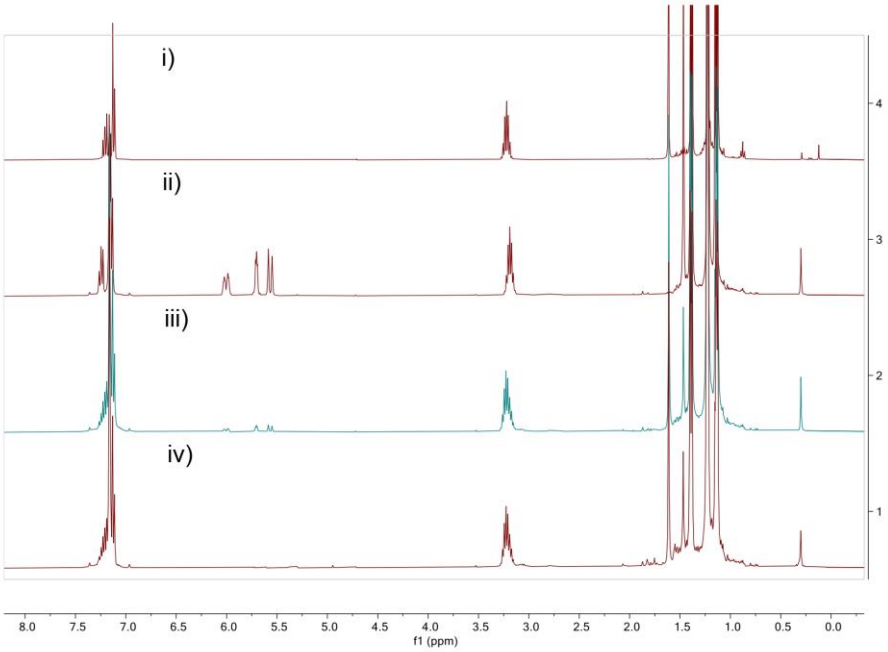

Figure S35. Stacked ^{1}H NMR spectra showing reversibility of silepin **3a**. i) silylene **1**; ii) silepin **3a**; iii) 60°C for 16 hours; iv) 60°C for 20 hours.

1.3.2 Reversibility of silepin 3c

To test the reversibility of **3c**, the solution of **3c** in C_6D_6 was left at room temperature or heated to 60°C in a J. Young NMR tube and monitored by ^{1}H NMR.

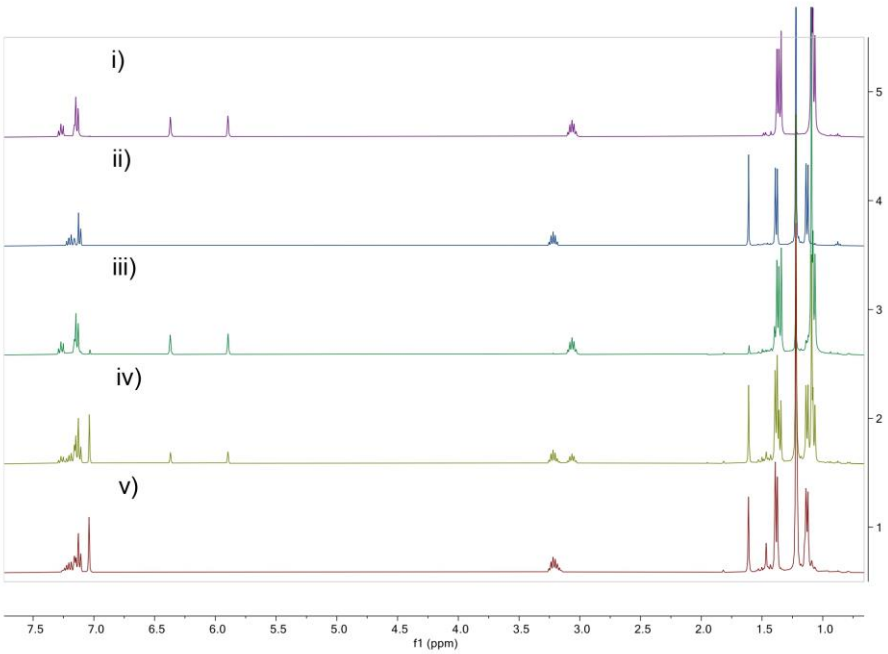

Figure S36. Stacked ^{1}H NMR spectra showing reversibility of silepin **3c**. i) silepin **3c**; ii) silylene **1**; iii) RT for 16 hours; iv) RT for 2 weeks; v) 60°C for 12 hours.

1.3.3 Reaction of silepin 3a with pyridine

To test the reaction of **3a** with pyridine, **3a** and pyridine were combined in C_6D_6 and left at room temperature or heated to 60°C in a J. Young NMR tube monitored by ^{1}H NMR.

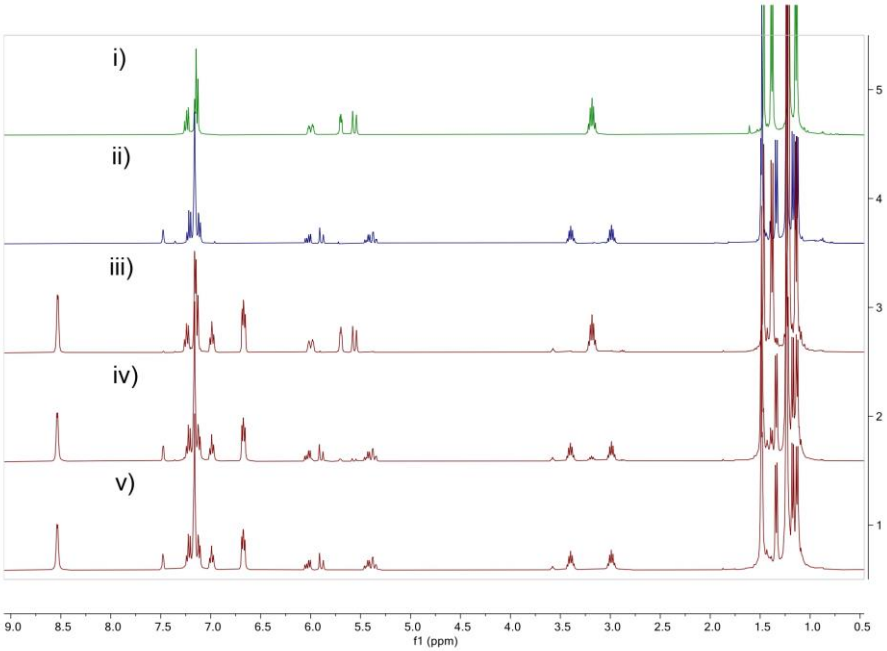

Figure S37. Stacked ^{1}H NMR spectra showing formation of silepin **4a** from silepin **3a**. i) silepin **3a**; ii) silepin **4a**; iii) RT for 2 days; iv) 60°C for 16 hours; v) 60°C for 20 hours.

1.3.4 Reaction of silepin 3a with DMAP

To test the reaction of **3a** with DMAP, **3a** and DMAP were combined in C_6D_6 and left at room temperature or heated to 60°C in a J. Young NMR tube, monitored by ^{1}H NMR.

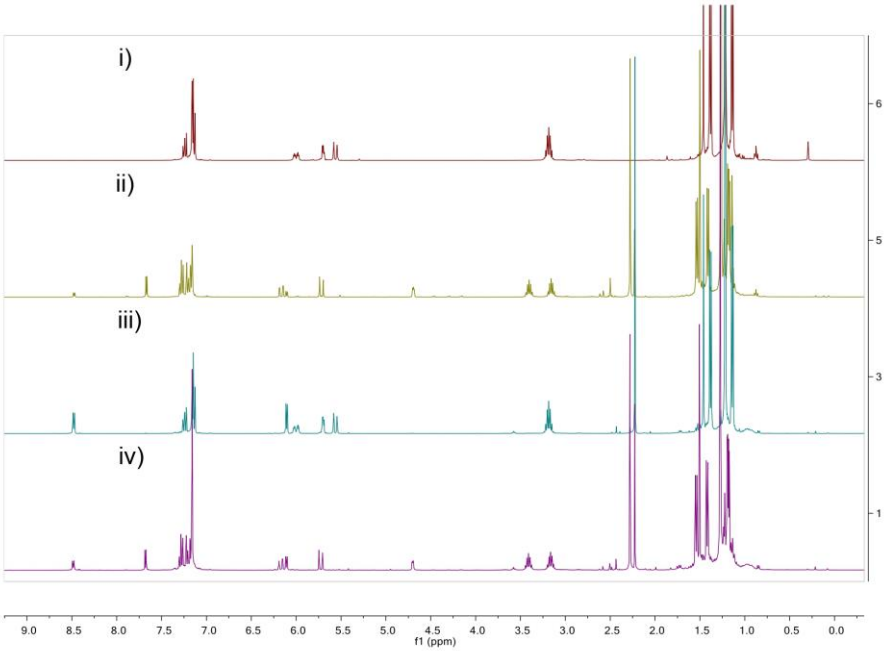

Figure S38. Stacked ^{1}H NMR spectra showing formation of azasilepin **4b** from silepin **3a**. i) silepin **3a**; ii) azasilepin **4b**; iii) RT for 2 days; iv) 60°C for 20 hours.

1.3.5 Reaction of silepin 3c with pyridine

To test the reaction of **3c** with pyridine, **3c** and pyridine were combined in C_6D_6 and left at room temperature or heated to 60°C in a J. Young NMR tube, monitored by ^{1}H NMR.

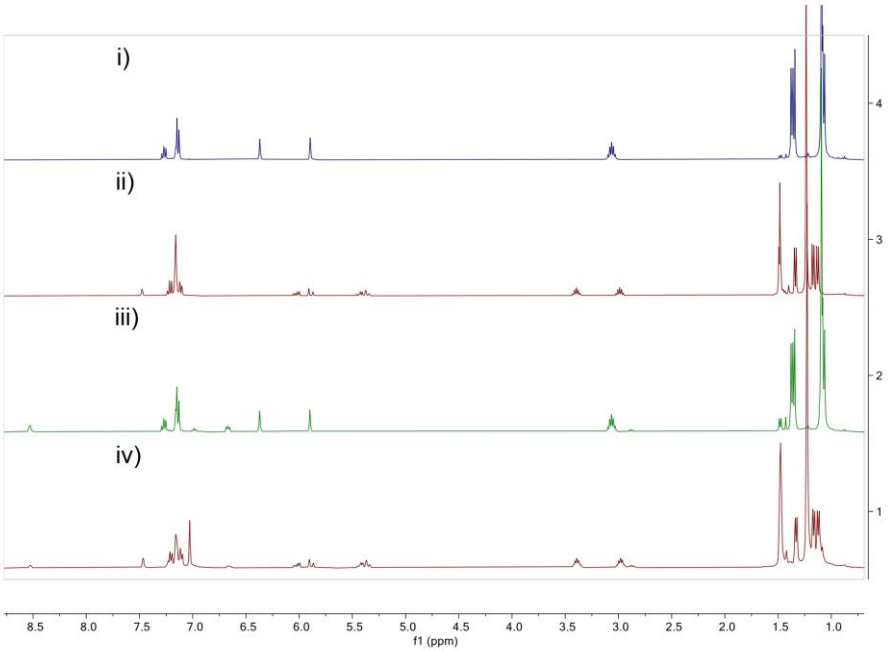

Figure S39. Stacked ^{1}H NMR spectra showing formation of azasilepin **4a** from silepin **3c**. i) silepin **3c**; ii) azasilepin **4a**; iii) RT for 2 hours; iv) 60°C for 16 hours.

1.3.6 Reaction of silepin 3c with DMAP

To test the reaction of **3c** with DMAP, **3c** and DMAP were combined in C_6D_6 and left at room temperature or heated to 60°C in a J. Young NMR tube, monitored by ^{1}H NMR.

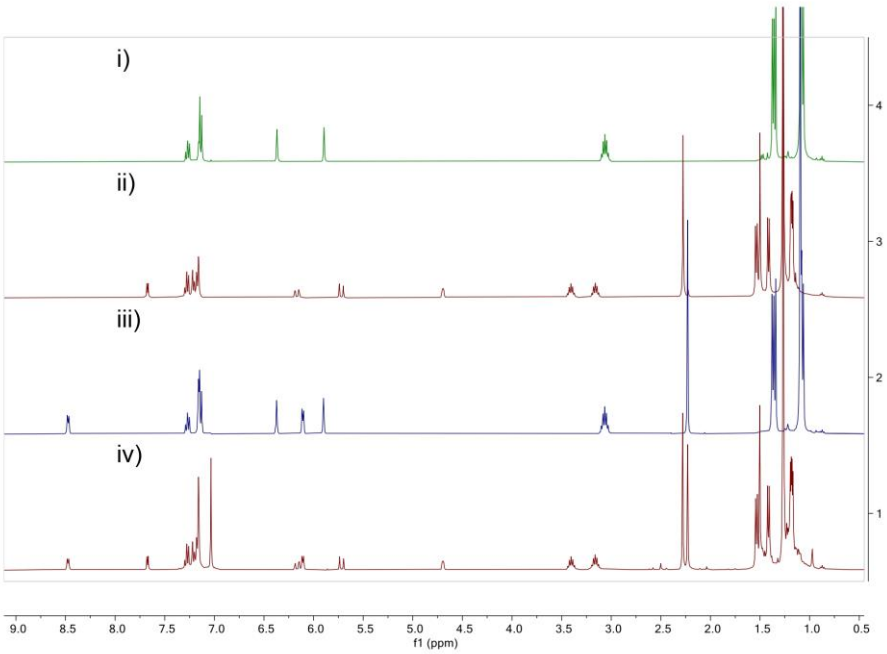

Figure S40. Stacked ^{1}H NMR spectra showing formation of azasilepin **4b** from silepin **3c**. i) silepin **4b**; ii) azasilepin **4b**; iii) RT for 2 hours; iv) 60°C for 16 hours.

1.4 Reaction of silylene 1 with fluorobenzene.

Fluorobenzene (0.1 mL) was added to silylene **1** (33 mg, 0.05 mmol) in benzene (1 mL), the blue solution was heated to 60 °C for 2 days. The color of mixture changed to yellow with the formation of yellow crystals. After work-up, all volatiles were removed in *vacuum* and washed with cold pentane (3 × 1 mL), the residue was dried in *vacuum*. Due to the similar regioselectivity of fluorobenzene, and based the integral of ^{i}Pr moiety, it should be two C-C double insertion products were formed. Due to the poor solubility of yellow crystal, no signal was observed in ^{29}Si NMR.

a)

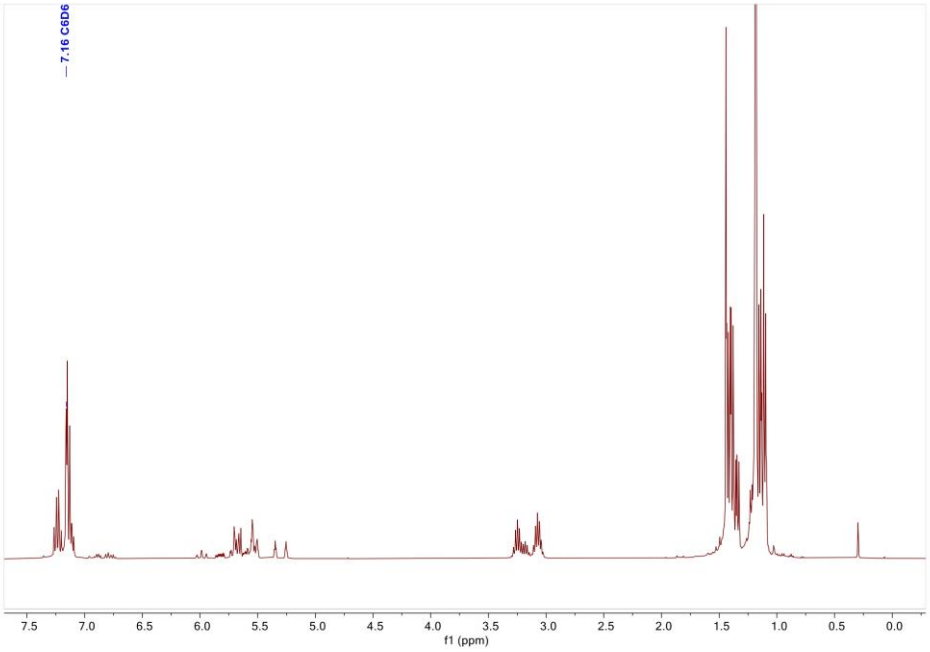
7.16 C6D6
7.5 7.0 6.5 6.0 5.5 5.0 4.5 4.0 3.5 3.0 2.5 2.0 1.5 1.0 0.5 0.0
f1 (ppm)

b)

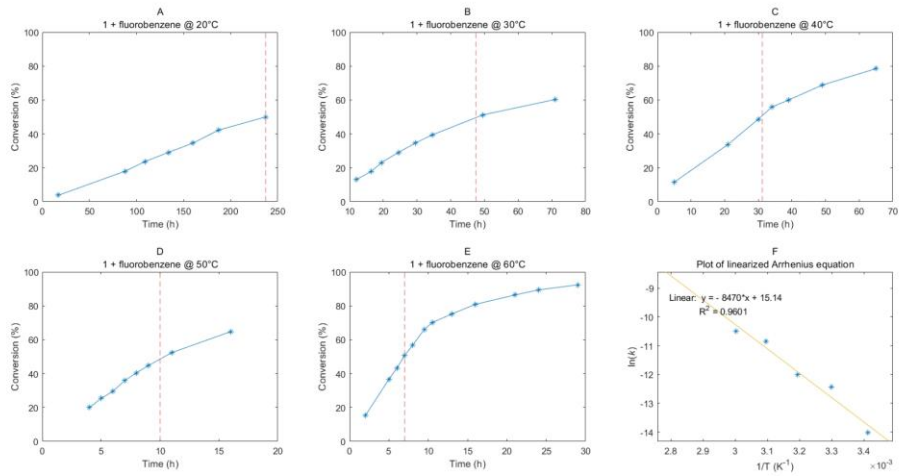
A
1 + fluorobenzene @ 20°C
B
1 + fluorobenzene @ 30°C
C
1 + fluorobenzene @ 40°C
D
1 + fluorobenzene @ 50°C
E
1 + fluorobenzene @ 60°C
F
Plot of linearized Arrhenius equation
Linear: y = -8470*x + 15.14
R² = 0.9601
Conversion (%)
Time (h)
ln(k)
1/T (K⁻¹)

c)

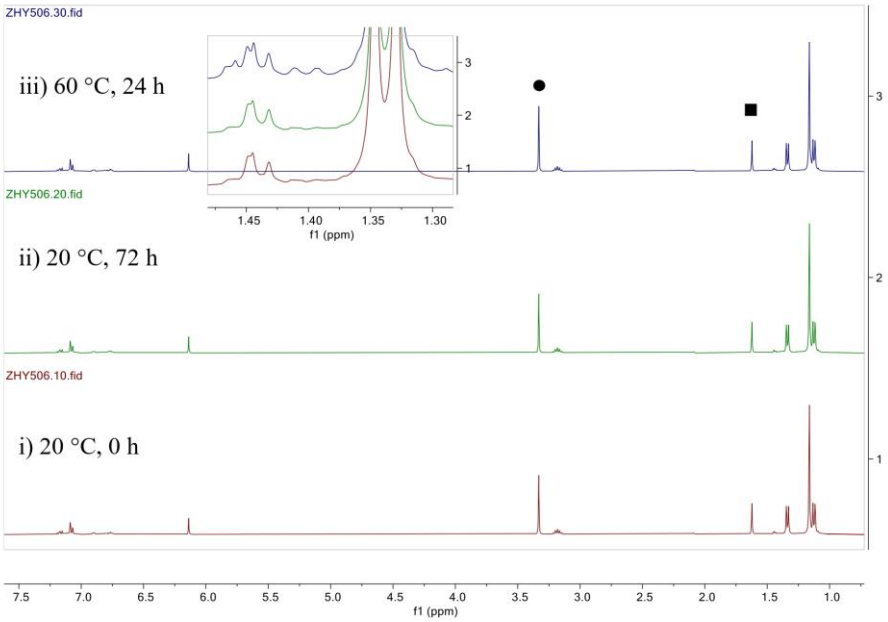

Figure S41. a) ^{1}H NMR spectrum of product of silylene with fluorobenzene in C_6D_6 at 300K; b) Kinetic of the reaction of **1** with fluorobenzene in benzene (C_6H_5F:C_6D_6 = 1:1); c) Stacked ^{1}H NMR of silylene with fluorobenzene (1:1) in toluene-d_8. ● is trimethoxzbenzene; ■ is methylated backbone of NHI. i) 20 °C for 0 h; ii) 20 °C for 72 h; iii) 60 °C for 24 h.

1.5 Photolysis of 1

To test the photochemical reaction of **1**, **1** was dissolved in C_6D_6 in a J. Young NMR tube, irradiated and monitored by ^{1}H NMR. From the NMR spectrum, **1** was slowly decomposed at 300 nm, and completely decomposed at 250 nm for 24 hours. And only some signal of isopropyl moiety was observed, and it's not 2,6-isopropylaniline.

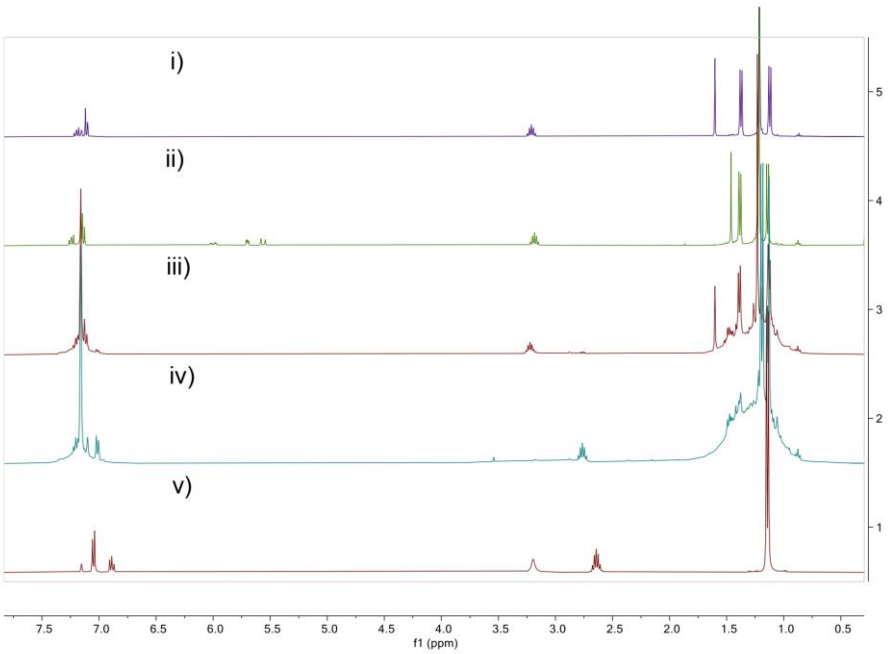

Figure S42. Stacked ^{1}H NMR spectra showing photolysis of silylene **1**. i) silylene **1**; ii) silepin **3a**; iii) 300nm for 2 days; iv) 250 nm for 24 hours; v) 2,6-isopropylaniline.

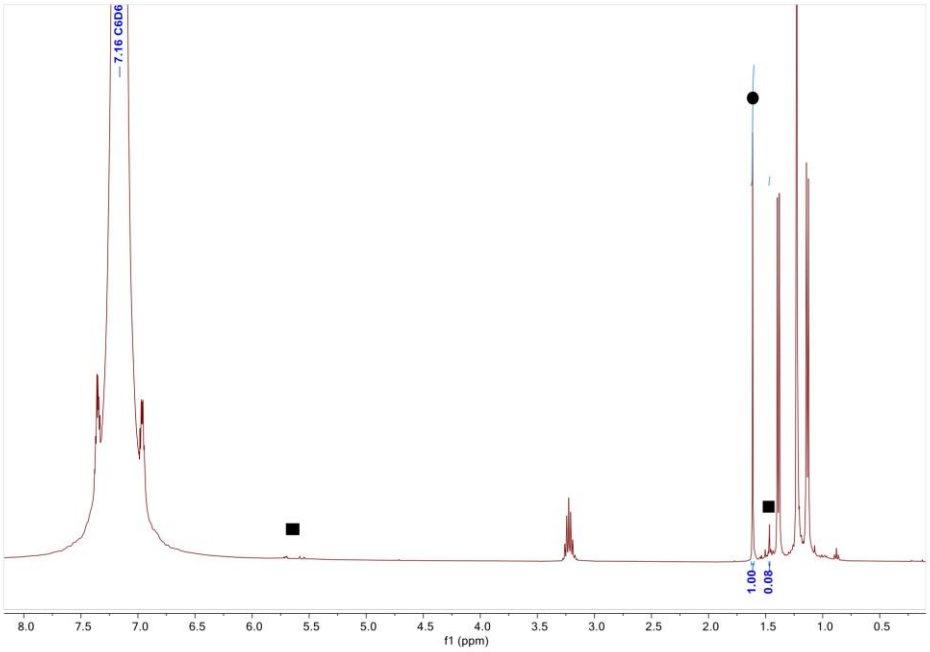

35

Figure S43. Irradiation of **1** at 360 nm. After 10 days, only 7.4 % transformation of silylene **1** to silepin **3a** (1.61 ppm is **1**, 1.47 ppm is **3a**).

2. Single Crystal X-Ray Structure Determination

Single crystal diffraction data were recorded on a Bruker Photon D8 Venture DUO IMS system equipped with a Helios optic monochromator and a Mo IMS microsource (λ = 0.71073 Å) and an Atlas SuperNova system equipped with a mirror monochromator and a Cu micro-focus sealed X-ray tube (λ = 1.54178 Å). The data collection was performed, using the APEX IV software package[S7] and CrysAlisPro[S8] on single crystals coated with Fomblin®Y as perfluorinated ether. The single crystal was picked on a micro sampler, transferred to the diffractometer, and measured frozen under a stream of cold nitrogen or at room temperature. A matrix scan was used to determine the initial lattice parameters. Reflections were merged and corrected for Lorenz and polarization effects, scan speed, and background using SAINT.[S9] Absorption corrections, including odd and even ordered spherical harmonics were performed using SADABS.[S9] Space group assignments were based upon systematic absences, E statistics, and successful refinement of the structures. Structures were solved by direct methods with the aid of successive difference Fourier maps and were refined against all data using the APEX IV software in conjunction with SHELXL-2014[S10] and SHELXLE.[S11] H atoms were placed in calculated positions and refined using a riding model, with methylene and aromatic C–H distances of 0.99 and 0.95 Å, respectively, and Uiso(H) = 1.2·Ueq(C). Non-hydrogen atoms were refined with anisotropic displacement parameters. Full-matrix least-squares refinements were carried out by minimizing $\Sigma w(Fo^2-Fc^2)^2$ with the SHELXL weighting scheme.[S12] Neutral atom scattering factors for all atoms and anomalous dispersion corrections for the non-hydrogen atoms were taken from International Tables for Crystallography.[S13] The images of the crystal structures were generated by Mercury.[S14] The CCDC numbers 2208878 to 2208883 contain the supplementary crystallographic data for the structures **1** to **4a**. These data can be obtained free of charge from the Cambridge Crystallographic Data Centre via https://www.ccdc.cam.ac.uk/structures/.

Table S1. Crystallographic details

	compound_1[a]	compound_2	compound_3a
CCDC-Number	2208878	2208879	2208880
Crystal data			
Chemical formula	$C_{41}H_{67}N_3Si_2$	$C_{41}H_{67}N_3Si_2$	$C_{47}H_{73}N_3Si_2$
M_r	658.16	658.16	736.26
Crystal system, space group	Triclinic, P^-1	Triclinic, P^-1	Triclinic, P^-1
Temperature (K)	293	123	100
a (Å), α(°) *b* (Å), β(°) *c* (Å), γ(°)	10.3915(7), 87.145(5) 11.7618(7), 86.414(5) 17.911(1), 73.584(6)	10.7948(6), 99.601(2) 12.6971(7), 92.999(3) 15.9973(9), 110.590(2)	10.352(3), 88.708(10) 11.958(4), 87.132(10) 18.803(6), 71.970(9)
V (Å^3)	2094.6 (2)	2009.1 (2)	2210.5 (12)
Z	2	2	2
F(000)	724	724	808
D_x (Mg m^{-3})	1.043	1.088	1.106
Radiation type	Cu *K*α	Mo *K*α	Mo *K*α
No. refl. for cell meas.	3649	9750	9172
θ range (°) for cell meas.	3.9–73.4	2.4–25.4	2.2–25.1
μ (mm^{-1})	0.97	0.12	0.11
Crystal shape, Color	Blue fragment	Colorless fragment	Yellow fragment
Crystal size (mm)	0.21 × 0.16 × 0.15	0.18 × 0.13 × 0.12	0.25 × 0.19 × 0.12
Data collection			
Diffractometer	SuperNova, Single source Atlas	Bruker Photon CMOS	Bruker Photon CMOS
Radiation source	micro-focus Source	IMS microsource	IMS microsource
Monochromator	Mirror	Helios optic	Helios optic
Detector res. (pix. mm^{-1})	10.5435	16	16
Absorption correction	Multi-scan	Multi-scan	Multi-scan
T_{min}, T_{max}	0.269, 1.000	0.711, 0.745	0.589, 0.745
No. of meas., indep. & obs. [$I > 2\sigma(I)$] refl.	15229, 8209, 5737	74620, 7351, 6439	71581, 8196, 6545
R_{int}	0.045	0.047	0.147
θ values (°)	θ_{max} = 73.9, θ_{min} = 2.5	θ_{max} = 25.4, θ_{min} = 2.0	θ_{max} = 25.5, θ_{min} = 2.1
$(\sin\theta/\lambda)_{max}$ (Å^{-1})	0.623	0.602	0.606
Range of *h*, *k*, *l*	*h* = -12→12, *k* = -14→10, *l* = -22→21	*h* = -13→13, *k* = -15→15, *l* = -19→19	*h* = -12→12, *k* = -14→14, *l* = -22→22
Refinement			
$R[F^2 > 2\sigma(F^2)]$, $wR(F^2)$, *S*	0.072, 0.232, 1.00	0.036, 0.094, 1.03	0.083, 0.202, 1.13
No. of refl., para., res.	8209, 554, 306	7351, 438, 0	8196, 489, 0
H-atom treatment	constrained	mixed	constrained
Weighting scheme	W = 1/[$\Sigma^2(FO^2)$ + **Y**] WHERE $P = (FO^2 + 2FC^2)/3$		
	$(0.1312P)^2 + 0.7524P$	$(0.0417P)^2 + 1.0961P$	$(0.0872P)^2 + 2.7498P$
$\Delta\rho_{max}$, $\Delta\rho_{min}$ (e Å^{-3})	1.21, -0.54	0.34, -0.28	0.53, -0.48

	compound_3b	compound_3c	compound_4a
CCDC-Number	2208881	2208882	2208883
Crystal data			
Chemical formula	$C_{47}H_{71}F_2N_3Si_2$	$C_{49}H_{71}F_6N_3Si_2$	$C_{46}H_{72}N_4Si_2$
M_r	772.25	872.27	737.26
Crystal system, space group	Triclinic, $P\bar{1}$	Monoclinic, $P2_1/n$	Triclinic, $P\bar{1}$
Temperature (K)	100	100	100
a (Å), α(°) *b* (Å), β(°) *c* (Å), γ(°)	10.6200(5), 87.029(2) 11.7453(4), 85.189(2) 18.5793(8), 73.950(6)	12.1897(8), 90 19.1781(10), 93.618(2) 20.4965(13), 90	10.4150(7), 87.581(3) 11.6756(8), 85.060(3) 18.6865(11), 74.013(3)
V (Å^3)	2218.32 (17)	4782.0 (5)	2175.9 (2)
Z	2	4	2
F(000)	840	1872	808
D_x (Mg m^{-3})	1.156	1.212	1.125
Radiation type	Mo *K*α	Mo *K*α	Mo *K*α
No. of refl. for cell meas.	9704	9796	9224
θ range (°) for cell meas.	2.6–25.7	2.7–25.3	2.2–25.7
μ (mm^{-1})	0.12	0.13	0.12
Crystal shape	Yellow fragment	Orange fragment	Orange fragment
Crystal size (mm)	0.93 × 0.62 × 0.28	0.28 × 0.14 × 0.11	0.34 × 0.29 × 0.24
Data collection			
Diffractometer	Bruker Photon CMOS	Bruker Photon CMOS	Bruker Photon CMOS
Radiation source	IMS microsource	TXS rotating anode	IMS microsource
Monochromator	Helios optic	Helios optic	Helios optic
Detector res. (pix. mm^{-1})	16	16	16
Absorption correction	Multi-scan	Multi-scan	Multi-scan
T_{min}, T_{max}	0.695, 0.745	0.454, 0.745	0.722, 0.745
No. of meas., indep. & obs. [$I > 2\sigma(I)$] refl.	43763, 8400, 7860	140251, 8751, 7846	86489, 8305, 7499
R_{int}	0.025	0.079	0.046
θ values (°)	θ_{max} = 25.7, θ_{min} = 2.0	θ_{max} = 25.4, θ_{min} = 2.4	θ_{max} = 25.7, θ_{min} = 2.0
$(\sin\theta/\lambda)_{max}$ (Å^{-1})	0.610	0.602	0.610
Range of *h*, *k*, *l*	*h* = -12→12, *k* = -14→13, *l* = -22→22	*h* = -14→14, *k* = -23→22, *l* = -24→24	*h* = -12→12, *k* = -14→14, *l* = -22→22
Refinement			
$R[F^2 > 2\sigma(F^2)]$, $wR(F^2)$, *S*	0.038, 0.102, 1.02	0.034, 0.104, 1.04	0.037, 0.094, 1.00
No. of refl., para., res.	8400, 566, 132	8751, 560, 56	8305, 548, 149
H-atom treatment	constrained	constrained	constrained
Weighting scheme	$W = 1/[\Sigma^2(FO^2) + \mathbf{Y}]$ WHERE $P = (FO^2 + 2FC^2)/3$		
Y	$(0.0488P)^2 + 1.4349P$	$(0.0651P)^2 + 1.6532P$	$(0.0416P)^2 + 1.4167P$
$\Delta\rho_{max}$, $\Delta\rho_{min}$ (e Å^{-3})	0.37, -0.40	0.31, -0.33	0.31, -0.30

a. Measurement at elevated temperature (185 K) caused bigger than usual ellipsoids. Further rotational disorder of the Si^{t}Bu$_3$ group was treated *via* a 2-part disorder modeling procedure. The structural identity and quality of the structure model was not affected.

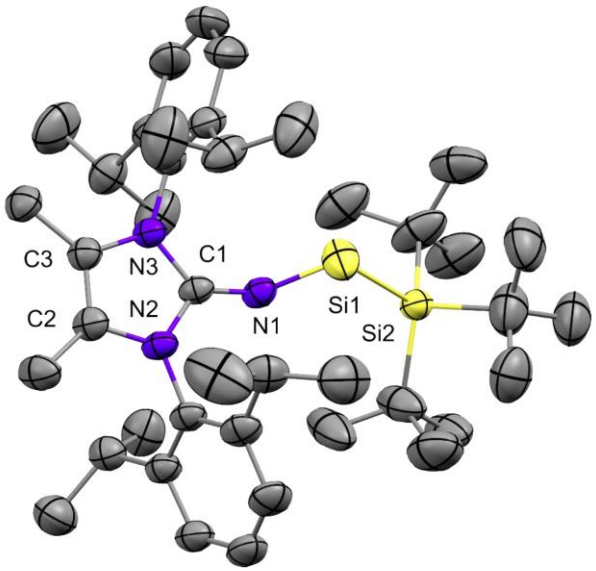

Figure S44. Molecular structure of **1**. Ellipsoids set at 50% probability to compensate for advanced thermal motion at measurement temperature 185K. Hydrogen atoms are omitted for clarity. Selected bond lengths [Å] and angles [°]: Si1–Si2 2.4438(13), Si1–N1 1.665(2), C1–N1 1.297(3); N1–Si1–Si2 106.15(9), C1–N1–Si1 138.4(2). Rotational disorder of all *t*Bu groups were treated as a two-part disorder und the minor occupied part (25%) is omitted for clarity.

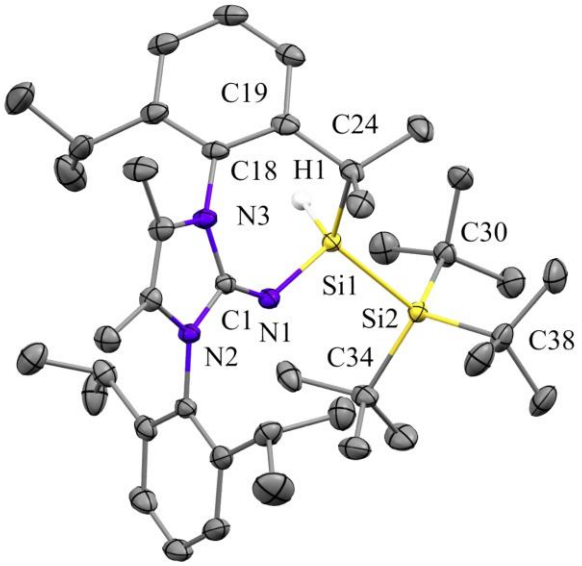

40

Figure S45. Molecular structure of **2**. Ellipsoids set at 50% probability. Hydrogen atoms are omitted for clarity, except for the respective Si–H nuclei of silane (H1). Selected bond lengths [Å] and angles [°]: Si1–Si2 2.4168(6), Si1–N1 1.7135(13), Si1–C24 1.9623(17), C1–N1 1.2841(19), C1–N3 1.385(2); N1–Si1–Si2 108.44(5), C1–N1–Si1 126.03(11), N1–Si1–C24 106.03(7). Hydrogen atom H1 could be located in the difference Fourier maps and was allowed to refine freely. Other hydrogens were calculated in ideal positions (riding model).

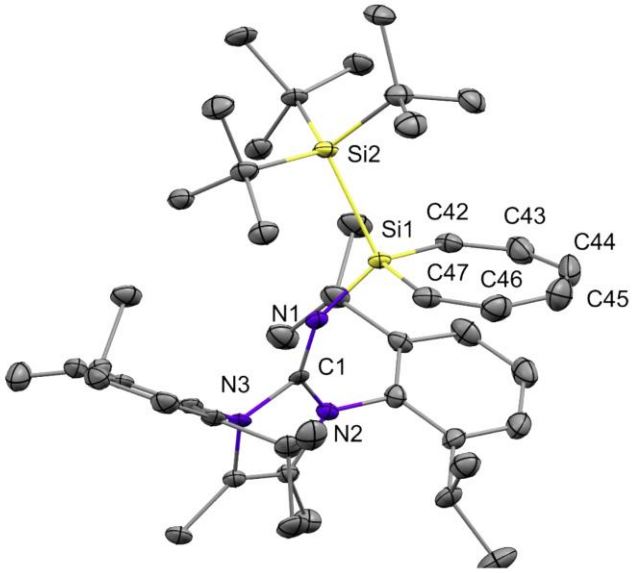

Figure S46. Molecular structure of **3a**. Ellipsoids set at 50% probability. Hydrogen atoms are omitted for clarity. Selected bond lengths [Å] and angles [°]: Si1–Si2 2.3967(15), Si1–N1 1.689(3), Si1–C42 1.875(4), Si1–C47 1.877(4), C42–C43 1.336(5), C43–C44 1.452(7), C44–C45 1.359(7), C45–C46 1.432(5), C46–C47 1.338(6); N1–Si1–Si2 111.14(11), C42–Si1–C47 107.28(18). For refinement the structure was treated as a merohedral twin using appropriate twin law.

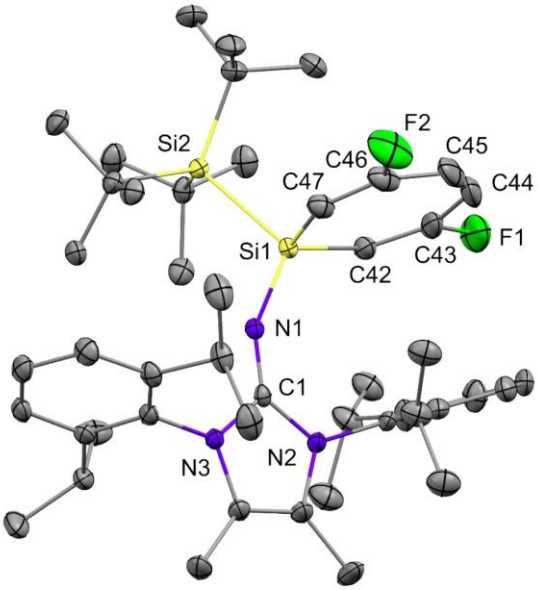

Figure S47. Molecular structures of **3b**. Ellipsoids set at 50% probability. Hydrogen atoms are omitted for clarity. Selected bond lengths [Å] and angles [°]: Si1–Si2 2.4051(5), Si1–N1 1.6837(12), Si1–C42 1.8660(15), Si1–C47 1.8674(16), C42–C43 1.333(2), C43–C44 1.437(3), C44–C45 1.335(3), C45–C46 1.442(3), C46–C47 1.327(2); N1–Si1–Si2 111.96(4), C42–Si1–C47 106.93(7). Rotational disorder of two Dipp-groups were treated as a two-part disorder und the minor occupied part (44%) are omitted for clarity.

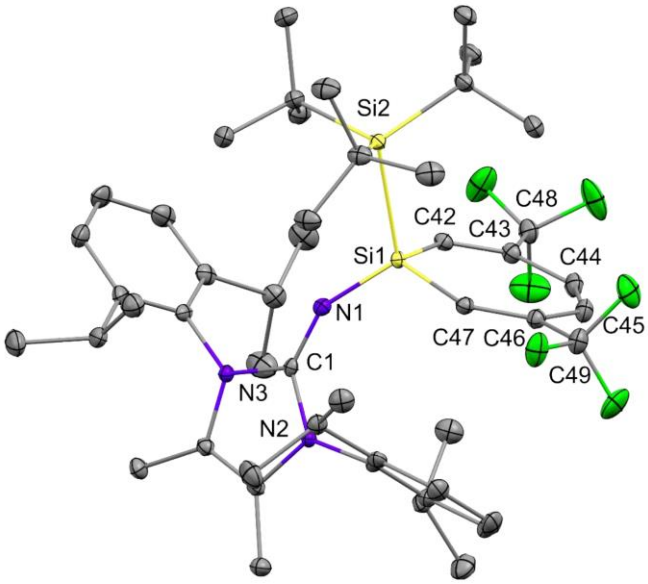

Figure S48. Molecular structures of **3c**. Ellipsoids set at 50% probability. Hydrogen atoms are omitted for clarity. Selected bond lengths [Å] and angles [°]: Si1–Si2 2.4143(6), Si1–N1 1.6769(11), Si1–C42 1.8752(13), Si1–C47 1.8670(14), C42–C43 1.3423(18), C43–C44 1.4609(19), C44–C45 1.345(2), C45–C46 1.4647(19), C46–C47 1.3442(19); N1–Si1–Si2 114.18(4), C42–Si1–C47 108.08(6).

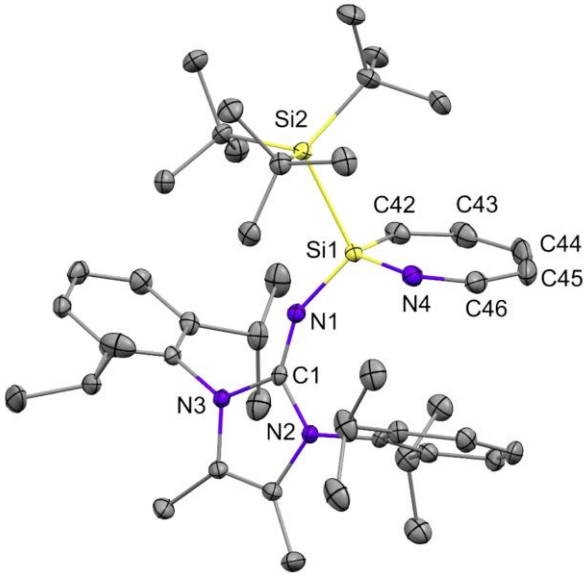

43

Figure S49. Molecular structure of **4a**. Ellipsoids set at 50% probability. Hydrogen atoms are omitted for clarity. Selected bond lengths [Å] and angles [°]: Si1–Si2 2.3937(6), Si1–N1 1.6775(12), C1–N1 1.2763(18), Si1–C42 1.8710(16), Si1–N4 1.7416(12), C42–C43 1.345(2), C43–C44 1.456(3), C44–C45 1.339(3), C45–C46 1.459(3), C46–N4 1.2673(19); N1–Si1–Si2 112.51(4), C42–Si1–N4 110.07(7). Rotational disorder of two Dipp-groups were treated as a two-part disorder und the minor occupied part (40%) are omitted for clarity.

3. Computational Details

Calculations were carried out using ORCA 5.0.2 and ORCA 5.0.3 software.[S15] The geometries of all compounds were optimized at the PBE0[S16] level of theory with the atom-pairwise dispersion correction with the Becke-Johnson damping scheme (D3BJ)[S17] and def2-TZVP basis set[S18] for all atoms. The method is denoted as PBE0-D3/def2-TZVP. The optimized geometries were verified as minima or transition states by analytical frequency calculations. The transition states were verified by the corresponding IRC calculations. The calculations were accelerated by resolution-of-identity (RI) approximation with def2/J auxiliary basis set.[S19] The reported energies (Table S2) and properties are at the PBE0-D3/def2-TZVP//PBE0-D3/def2-TZVP level of theory. For TD-DTF calculation the solvent effect of benzene was taken into account by the Conductor-like Polarizable Continuum Model (CPCM), the method is denoted as PBE0-D3/def2-TZVP//PBE0-D3(CPCM=Benzene). NMR and NICS calculation were carried out using Gaussian 16, Revision C.01 software.[S20] ^{29}Si NMR chemical shifts were calculated at the HCTH407[S21]/6-311+G(2d)[S22]//PBE0-D3/def2-TZVP level of theory. NICS calculations were performed at the B3LYP[S23]/6-31+g*[S24]//PBE0-D3/def2-TZVP level of theory NBO 7 software was used for NBO analysis.

Table S2. Energies (E_h) (E – electronic energy; H – total enthalpy; G – Gibbs energy) and imaginary frequencies (im. freq.) (cm^{-1}) of the calculated compounds.

Compound	E	H	G	im. freq.
1	-2344.408738	-2343.349096	-2343.482567	-
TS(1-A)	-2344.385872	-2343.328253	-2343.458989	-164.03
A	-2344.397615	-2343.338713	-2343.470038	-
TS(A-1')	-2344.378956	-2343.321887	-2343.452648	-188.32
1'	-2344.399272	-2343.339906	-2343.470390	-
TS(1-B)	-2344.358751	-2343.306300	-2343.438731	-469.69
B	-2344.392583	-2343.336269	-2343.468055	-
TS(B-2)	-2344.359856	-2343.306193	-2343.438259	-306.15
2	-2344.399272	-2343.339906	-2343.470390	-
TS(1-Ca)	-2576.449557	-2575.283047	-2575.423744	-249.05
Ca	-2576.465961	-2575.298168	-2575.439720	-
TS(Ca-3a)	-2576.447234	-2575.281454	-2575.422009	-403.64
3a	-2576.489433	-2575.321674	-2575.463158	-
TS(1-C')	-2774.840348	-2773.688160	-2773.832557	-146.99
C'	-2774.841110	-2773.688098	-2773.833742	-
TS(C'-Cb)	-2774.841163	-2773.689143	-2773.833277	-101.46
Cb	-2774.861650	-2773.707900	-2773.853091	-
TS(Cb-3b)	-2774.834455	-2773.682984	-2773.827178	-419.67
3b	-2774.889339	-2773.736040	-2773.880553	-
TS(1-Cc)	-3250.221604	-3249.037328	-3249.192198	-112.71
Cc	-3250.247069	-3249.061675	-3249.216165	-
TS(Cc-3c)	-3250.223676	-3249.040444	-3249.195012	-324.15
3c	-3250.262134	-3249.076930	-3249.231753	-
TS(1-D)	-2592.500008	-2591.344471	-2591.487070	-36.84
D	-2592.519411	-2591.362661	-2591.503742	-
TS(D-E)	-2592.493955	-2591.339304	-2591.479799	-313.17
E	-2592.518058	-2591.362201	-2591.503577	-
TS(E-4a)	-2592.493035	-2591.339419	-2591.480211	-494.68
4a	-2592.547410	-2591.391591	-2591.532699	-
4b	-2726.416186	-2725.182975	-2725.332265	-
benzene	-232.054820	-231.948779	-231.980275	-
1,4-(diflouro)benzene	-430.440100	-430.348645	-430.384268	-
1,4-bis(trifluoromethyl)benzene	-905.819135	-905.695991	-905.747001	-
pyridine	-248.084495	-247.990150	-248.022753	-
DMAP	-381.955906	-381.784035	-381.826891	-
cyclohepta-1,3,5-triene Cs	-271.284610	-271.149585	-271.185327	-
cyclohepta-1,3,5-triene C2v	-271.273630	-271.139190	-271.173488	-117.21
silepin Cs	-522.589138	-522.464566	-522.502966	-
silepin C2V	-522.585735	-522.461686	-522.497958	-76.23
(Z)-hexa-1,3,5-triene C2V	-233.172870	-233.047556	-233.081845	-192.32, -150.99

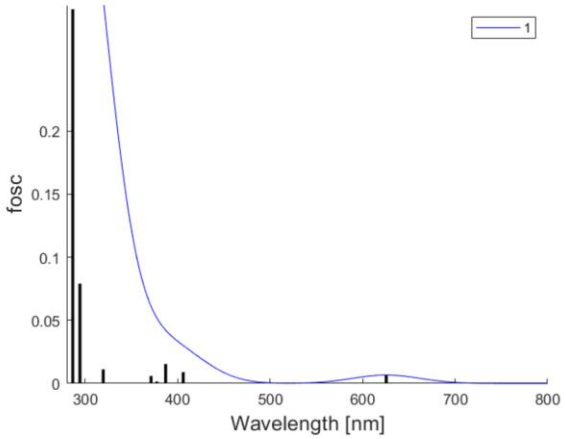

Figure S50. Simulated UV-Vis absorption spectrum of **1**, derived from TD-DFT calculation at the PBE0-D3/def3-TZVP (CPCM = benzene)//PBE0-D3/def3-TZVP level of theory (Table S3). The calculated oscillator strengths are shown as black vertical lines.

Table S3. Calculated transitions (S_1 – S_{10}) of **1** at the PBE0-D3/def2-TZVP (CPCM=benzene)//PBE0-D3/def2-TZVP level of theory.

STATE	Transitions	fosc	E (cm^{-1})	λ (nm)
S_1	179a → 181a : 0.018878 (c= 0.13739865) 180a → 181a : 0.956235 (c= 0.97787290)	0.004518951	15987.1	625.5
S_2	180a → 182a : 0.973720 (c= 0.98677238)	0.001692986	24630.0	406.0
S_3	180a → 183a : 0.897150 (c= 0.94718021) 180a → 184a : 0.013836 (c= 0.11762611) 180a → 185a : 0.026728 (c= -0.16348689) 180a → 187a : 0.037633 (c= -0.19399335)	0.003399316	25839.7	387.0
S_4	180a → 183a : 0.021923 (c= -0.14806309) 180a → 184a : 0.886589 (c= 0.94158865) 180a → 185a : 0.048779 (c= -0.22086025) 180a → 189a : 0.010945 (c= -0.10462004)	0.001662851	26492.7	377.5
S_5	180a -> 183a : 0.024838 (c= -0.15760222) 180a -> 184a : 0.057377 (c= -0.23953438) 180a -> 185a : 0.901714 (c= -0.94958627)	0.002580171	26941.9	371.2
S_6	180a -> 183a : 0.019653 (c= -0.14018845) 180a -> 184a : 0.023331 (c= 0.15274544) 180a -> 186a : 0.224971 (c= -0.47431137) 180a -> 187a : 0.194151 (c= -0.44062590) 180a -> 189a : 0.326541 (c= 0.57143804) 180a -> 190a : 0.122486 (c= -0.34998046)	0.003768778	31300.7	319.5

S_7	172a -> 181a : 0.019918 (c= -0.14113033) 179a -> 181a : 0.885012 (c= 0.94075056) 180a -> 181a : 0.017409 (c= -0.13194212) 180a -> 187a : 0.011280 (c= 0.10620798)	0.060714468	33983.0	294.3
S_8	172a -> 181a : 0.035682 (c= 0.18889775) 179a -> 181a : 0.021524 (c= -0.14671116) 179a -> 187a : 0.013385 (c= -0.11569159) 179a -> 188a : 0.015278 (c= 0.12360551) 180a -> 183a : 0.018405 (c= 0.13566584) 180a -> 186a : 0.165813 (c= -0.40720132) 180a -> 187a : 0.525529 (c= 0.72493372) 180a -> 190a : 0.031478 (c= -0.17742168) 180a -> 191a : 0.067800 (c= 0.26038367)	0.107172838	34892.7	286.6
S_9	179a -> 182a : 0.023244 (c= 0.15246039) 179a -> 186a : 0.020839 (c= -0.14435653) 179a -> 188a : 0.254898 (c= -0.50487435) 180a -> 187a : 0.027284 (c= 0.16517726) 180a -> 188a : 0.553307 (c= 0.74384608) 180a -> 189a : 0.022597 (c= 0.15032411)	0.008859883	37022.8	270.1
S_{10}	173a -> 182a : 0.033685 (c= 0.18353367) 173a -> 183a : 0.086408 (c= -0.29395292) 174a -> 182a : 0.272995 (c= 0.52248950) 174a -> 183a : 0.056781 (c= -0.23828816) 175a -> 184a : 0.157303 (c= 0.39661465) 175a -> 185a : 0.197985 (c= 0.44495535) 176a -> 184a : 0.074195 (c= 0.27238744) 179a -> 182a : 0.022619 (c= -0.15039540)	0.012745838	37529.0	266.5

The weakly allowed transition (S1) that is essentially composed of a single natural transition orbital (NTO) pair, *i.e.*, 180a → 181a (n=0.99676036). The NTOs are presented in Figure 48. It is evident that the S1 state donor orbital (180a) similarly to HOMO mainly corresponds to the Si lone pair. The acceptor orbital (181a), similarly to LUMO, mainly corresponds to the non-bonding 3p orbital of Si.

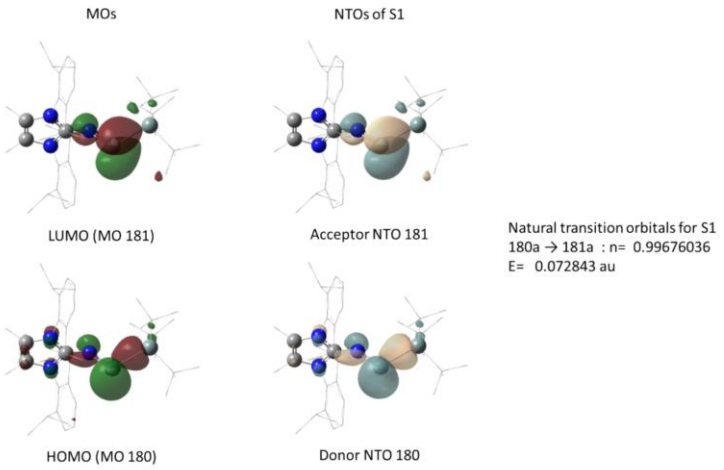

Figure S51. Frontier molecular orbitals and the natural transition orbitals for **1** in S1.

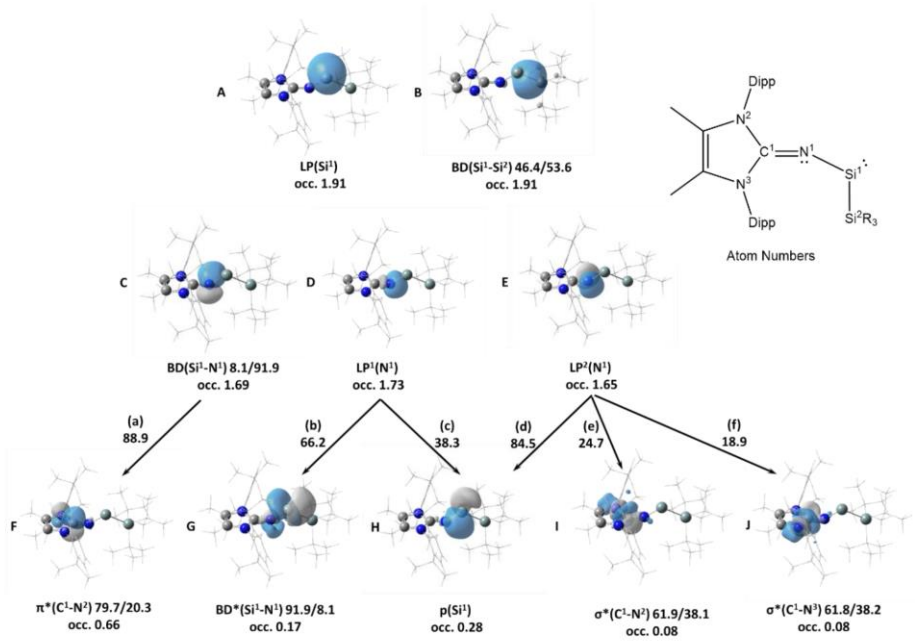

Figure S52. Selected NBOs of **1**.

NBO analysis (Figure S52) shows a lone pair on the central Si atom (A) and a single σ-bond between Si^1 and Si^2 (B) with WBI(Si^1–Si^2) = 0.94. Additional bonding interaction exists between Si^1 and N^1 in the form of a single extremely polarized Si–N bond with 92% of the electron density located on the nitrogen atom (C) WBI(Si^1–N^1) = 0.88. This NBO shows a strong donor acceptor interaction (a) of 88.9 kcal mol^{-1} with the π*-orbital of the C^1–N^2 bond (F) which contributes to the increased double bond nature of N^1–C^1 with Wiberg bond index of 1.47. Additional factors that contribute to the N^1–C^1 double bond character are donor-acceptor interactions between the π-type lone pair of N^1 (E) and the σ*-orbitals of C^1–N^2 and C^1–N^3 bonds (I and J) of 24.7 and 18.9 kcal mol^{-1}. The π-type lone pair (E) and the σ-type lone pair (D) also strongly interact with the p-orbital of the central Si (H). Additionally, there is a strong interaction (66.2 kcal mol^{-1}) between the σ-type lone pair of N^1 (D) and the antibonding Si^1–N^1 interaction (G), which weakens the Si^1–N^1 bond.

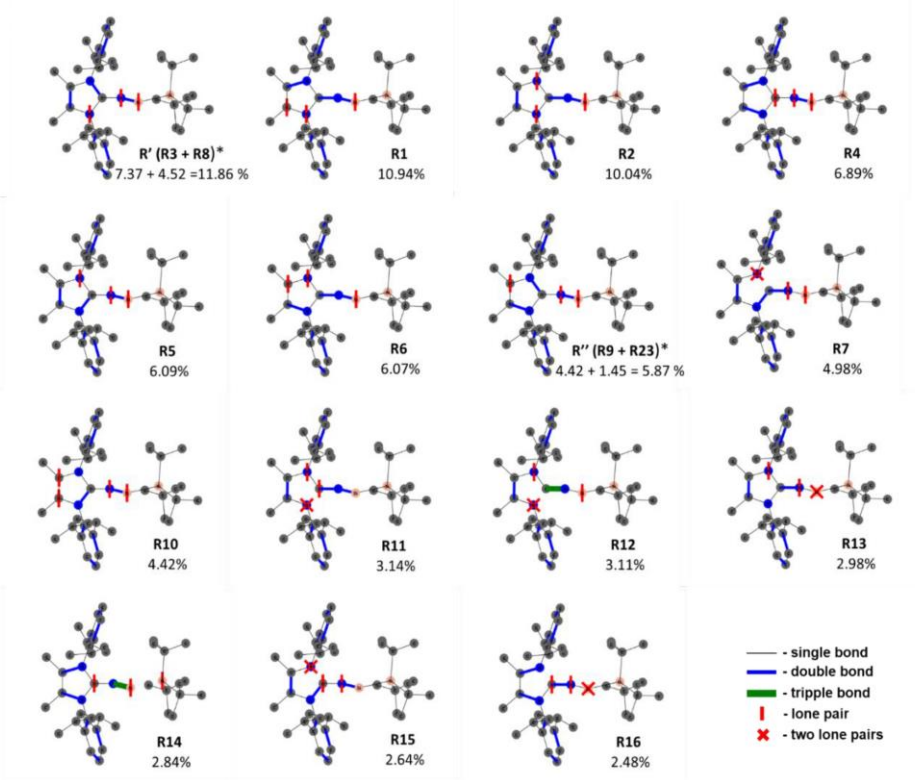

Figure S53. NRT analysis of **1**. Hydrogens are omitted for clarity. * In **R'** resonance structure **R3** and **R8** are equivalent; in **R''** resonance structures **R9** and **R23** are equivalent.

Natural Resonance theory (NRT) analysis were carried out on the local subset of atoms Si^1, Si^2, N^1, N^2, N^3, C^1, C^2 and C^3. The resonance structures with dominance of > 2%, representing 84.38% of all resonance structures (32 in total) are presented in Figure S50. Resonance structures **R', R1-R6**, **R''**, **R10-R11** (65.32%) show Si^1–N^1 double bond, and **R12**, **R14** (5.95%) show Si^1–N^1 triple bond. Out of all structures, 78.20% show a multiple bond between Si^1 and N^1. The resonance natural bond orbital (RNBO) analysis of resonance-averaged NLMOs for 24 leading structures (using 1.0% weight threshold) shows a double bonding interaction between Si^1 and N^1. The first bonding interaction contains 12.6% of electron density on the p-orbital of silicon (s (15.33%); p (83.30%)) and 85.8% of electron density of the sp-orbital of nitrogen (s (57.51%); p (42.15%)). The second bonding interaction contains 11.3% of electron density mainly on the p-orbital of silicon (s (0.10%), p (97.42%)) and 82.5% of electron density mainly of the sp-orbital of nitrogen (s (0.14%); p (99.66%)).

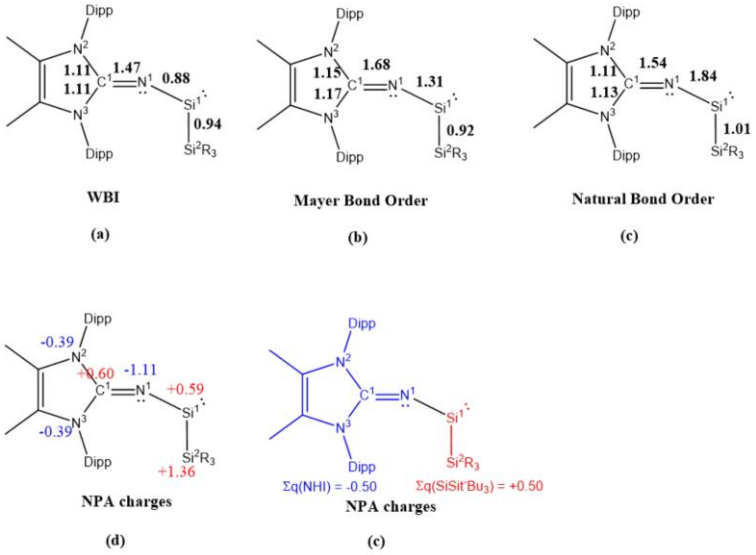

Figure S54. Bond indexes and NPA charges of **1**.

Wiberg bond indexes (WBI) show a high double bond character between C1 and N1 (1.47), while WBI for Si^1–N^1 is 0.88 (Figure S54(a)). Mayer bond order shows double bond character for both C^1–N^1 and Si^1–N^1 with the respective values of 1.68 and 1.31 (Figure S54(b)). The Natural Bond Orders for C^1–N^1 and Si^1–N^1 are 1.54 and 1.84 (Figure S54(c)). The NPA charges reflect the nature of the polarized Si^1–N^1 interaction with the difference of charges of 1.70 el. between the two atom (-1.11 el. on N^1, +0.59 el. on Si^1) (Figure S54(d)). The sum of charges of the atoms constituting the NHI and the $SiSiR_3$ moieties are -0.50 el. and +0.50 el. respectively (Figure S54(e)).

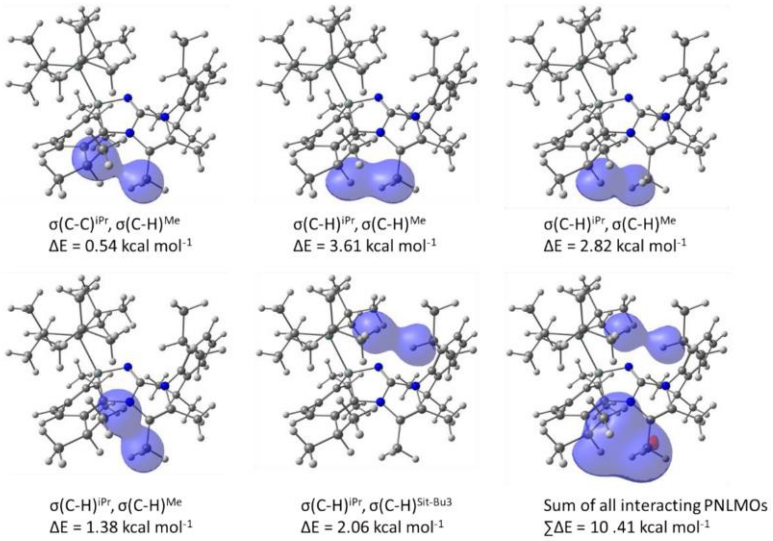

Figure S55. PNLMO overlaps and the pairwise steric exchange energies for disjoint interactions present in **1'** and absent in **IIb**.

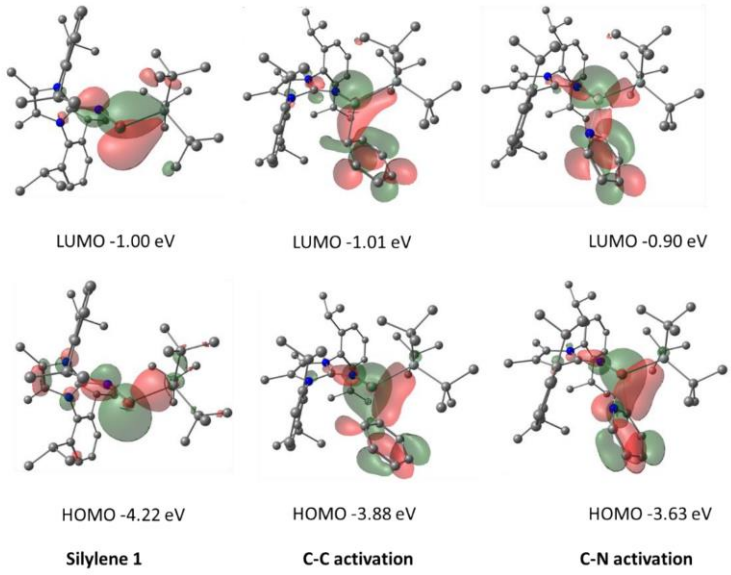

Figure S56. Frontier molecular orbitals of the silylene, and the transition states corresponding to C–C and C–N bond activation of benzene and pyridine.

The frontier orbitals (HOMOs and LUMOs) of the transition states **TS(1-Ca)** and **TS(D-E)** corresponding to the C–C and C–N activation of benzene in pyridine are shown in Figure S56. The respective orbitals present essentially very similar picture, showing that the HOMOs correspond to the interaction of the lone pair of silylene with the π* system of benzene and pyridine, while the LUMOs correspond to the interaction between the p-orbital of Si with the π* system. The HOMO–2 orbitals show the interaction between the arene π systems and the silylene. In the benzene case, according to the NBO analysis, the two newly forming silicon carbon bonds with Si–C distances of 2.018, 2.367 Å, WBIs of 0.60, 0.41 and occupancies of 1.80, 1.63 el., are polarized to toward the carbons with Si(34.9%)/C(65.1%), Si(38.0%)/C(62.0%) respectively. The composition of the first orbital is Si($sp^{1.33}$) and C($sp^{7.29}$), corresponding to the lone pair interaction with the π* system of benzene, while the composition the second orbital is practically Si(p) and C(p) (Si($sp^{28.81}$), C($sp^{33.00}$)) corresponding to the Si p interaction with the π system of benzene. And in the pyridine case is very similar with the respective Si–N and C–N bond distances, WBIs, occupancies, polarization and NBO compositions: r = 1.775, 2.261Å; WBI = 0.58, 0.49; occ. = 1.80, 1.70 el.; Si(19.0%)/N(81.0%), Si(34.8%)/C(65.2%); (Si($sp^{2.02}$), N($sp^{14.47}$), (Si($sp^{99.99}$), C($sp^{13.55}$). However, it is apparent that the Si–N bond in more polarized toward the nitrogen and the corresponding atomic hybrid contributions of silicon exhibits more explicit sp^2 and p character than in the case of benzene. In both cases, the ambiphilic nature of the silylene allows the C–C and C–N bond activation to take place.

4. Appendix A: Cartesian coordinates of the optimized geometries (Å)

1

H	2.115375	7.310650	5.482096
Si	-0.334728	5.733856	2.809631
Si	-0.766916	3.772917	4.179331
N	0.072111	6.970722	3.868853
N	-0.497256	9.262631	4.154274
N	1.534300	8.832465	3.506875
C	0.342728	8.227315	3.825709
C	0.173034	10.486990	4.062715
C	1.430958	10.221574	3.653983
C	-2.800689	8.833741	3.510227
C	-4.122876	8.659700	3.901951
H	-4.878278	8.451802	3.155439
C	-4.488118	8.733354	5.235428
H	-5.525208	8.591633	5.517462
C	-3.537662	8.976918	6.209649
H	-3.837143	9.021274	7.249361
C	-2.200658	9.151045	5.869714
C	-1.858874	9.083869	4.516476
C	-2.392637	8.757193	2.054199
H	-1.435825	8.227556	2.015049
C	-3.360547	7.959866	1.193225
H	-4.315335	8.477581	1.065794
H	-3.555425	6.971703	1.612753
H	-2.929272	7.819172	0.200268
C	-2.182601	10.146301	1.453702
H	-1.914832	10.060687	0.397479
H	-1.381140	10.690240	1.954162
H	-3.097903	10.740687	1.522530
C	-1.140132	9.341401	6.930906
H	-0.303348	9.876008	6.474676
C	-0.604098	7.985157	7.381310
H	-0.238827	7.408080	6.531091
H	-1.391083	7.401867	7.866750
H	0.215884	8.111310	8.093342
C	-1.617084	10.166958	8.117430
H	-2.044823	11.121347	7.800838
H	-0.779798	10.373837	8.787680
H	-2.373239	9.637931	8.702478
C	-0.491013	11.767227	4.394283
H	0.172166	12.601422	4.169145
H	-0.760572	11.823747	5.452606
H	-1.412839	11.900031	3.822555
C	2.563989	11.125255	3.357396
H	2.778461	11.165295	2.286517
H	3.479372	10.798767	3.855952
H	2.333871	12.135634	3.693328
C	2.666907	8.138706	3.000512
C	3.499967	7.462904	3.902777
C	4.599873	6.793635	3.382601
H	5.260283	6.250631	4.045959
C	4.861059	6.798391	2.021376
H	5.724052	6.266381	1.637416
C	4.020722	7.466250	1.152691
H	4.224982	7.448480	0.088518
C	2.902168	8.148007	1.623320
C	3.195296	7.456752	5.385685
C	3.874926	6.319251	6.132548
H	3.673974	5.351443	5.671037
H	3.503316	6.282511	7.158264
H	4.958192	6.460095	6.183456
C	3.543829	8.787831	6.050584
H	4.602287	9.024851	5.911615
H	3.351000	8.728967	7.124764
H	2.950478	9.612087	5.655664
C	1.971141	8.832945	0.648296
H	1.250926	9.418844	1.224704
C	2.714077	9.789464	-0.280386
H	3.378825	9.248262	-0.958147
H	3.323209	10.508636	0.271629
H	2.002312	10.345054	-0.895462
C	1.183681	7.808212	-0.164334
H	0.488668	8.315381	-0.839203
H	0.611215	7.134770	0.479994
H	1.856533	7.196844	-0.771921
C	-0.653477	2.373002	2.826486
C	-0.704981	0.951794	3.384459
H	-1.618706	0.763016	3.951943
H	0.142611	0.732554	4.036080
H	-0.674873	0.227368	2.559874
C	-1.781210	2.526335	1.803418
H	-1.794726	3.525247	1.357912
H	-2.765341	2.324607	2.228444
H	-1.626656	1.808752	0.987182
C	0.652281	2.548319	2.042777
H	0.694834	1.810150	1.231292
H	1.542062	2.412117	2.655513
H	0.712073	3.537934	1.575895
C	-2.606150	4.041884	4.777684
C	-3.376854	4.808897	3.698499

55

H	-3.415376	4.293738	2.739840
H	-2.941008	5.799868	3.533920
H	-4.409985	4.974971	4.031462
C	-3.348708	2.743103	5.088089
H	-4.359499	2.972151	5.451383
H	-2.848622	2.155304	5.860149
H	-3.458499	2.108544	4.207128
C	-2.646180	4.935098	6.018719
H	-2.104828	5.870447	5.859054
H	-2.241458	4.444836	6.905428
H	-3.689096	5.196886	6.239688
C	0.423048	3.406192	5.672017
C	-0.111784	2.337162	6.625891
H	-1.041307	2.647110	7.106137
H	0.620514	2.157370	7.424258
H	-0.294499	1.383119	6.128132
C	1.794824	2.957065	5.167049
H	1.770732	1.972603	4.698172
H	2.486850	2.893637	6.016649
H	2.220641	3.664987	4.450205
C	0.653096	4.692002	6.465158
H	1.017349	5.493053	5.821096
H	1.400866	4.510459	7.248153
H	-0.250191	5.049370	6.954896

TS(1-A)

Si	-1.014804	-0.088890	0.821249
Si	-2.520078	-1.667356	-0.127492
N	0.548313	-0.372817	0.217799
N	2.679948	0.688584	-0.043137
N	0.908362	1.967257	0.158490
C	1.324003	0.655034	0.129560
C	2.025818	2.809819	0.053807
C	3.111277	2.014234	-0.087045
C	-0.456511	2.248637	0.375610
C	-1.156155	3.124770	-0.501711
C	-2.431601	3.505278	-0.179523
C	-3.038335	3.020879	1.012605
C	-2.408714	2.177087	1.853853
C	-1.034585	1.681881	1.641215
C	-0.517712	3.566570	-1.804676
C	-1.225262	4.736645	-2.470454
C	-0.396140	2.401624	-2.781868
C	-0.136586	1.757618	2.892887
C	-0.639159	0.871968	4.017843
C	0.016836	3.200948	3.351641
C	3.500756	-0.466672	-0.137957
C	3.515771	-1.187089	-1.337656
C	4.362292	-2.286666	-1.415393
C	5.154884	-2.653399	-0.340746
C	5.090643	-1.949982	0.848558
C	4.247964	-0.851485	0.978376
C	2.620915	-0.786430	-2.490189
C	3.185435	0.407912	-3.257217
C	2.322744	-1.933025	-3.444530
C	4.057480	-0.159756	2.308351
C	2.898889	-0.821068	3.057099
C	5.313103	-0.128295	3.167573
C	-4.717634	-0.226880	1.042176
C	-5.273433	-2.484354	0.205672
C	-3.957568	-2.180698	2.294329
C	-1.438706	-0.991548	-2.684594
C	-3.653381	-0.058063	-2.164417
C	-3.426700	-2.464234	-2.767838
C	-0.402674	-3.505727	-0.849805
C	-2.442790	-4.539078	0.084885
C	-0.845388	-3.316414	1.553028
H	-3.001062	4.142946	-0.839721
H	-4.048857	3.338182	1.249818
H	-2.911281	1.851130	2.757639
H	0.499294	3.897575	-1.592465
H	-1.335972	5.585069	-1.792062
H	-2.218902	4.455848	-2.828834
H	-0.649445	5.066855	-3.338046
H	0.187421	1.584258	-2.358664
H	0.099042	2.727770	-3.700464
H	-1.382501	2.013837	-3.044679
H	0.851067	1.384694	2.603084
H	-0.794806	-0.152331	3.663523
H	-1.583918	1.237122	4.430152
H	0.084038	0.839860	4.835873
H	0.712650	3.273040	4.191306
H	-0.945769	3.608391	3.671599
H	0.388943	3.834926	2.545254
H	4.399291	-2.870819	-2.325916
H	5.814396	-3.509644	-0.425871
H	5.692103	-2.268734	1.690873
H	1.666871	-0.485817	-2.048862
H	4.163830	0.167107	-3.682254
H	3.295609	1.284329	-2.617664
H	2.516503	0.680261	-4.077484
H	3.204661	-2.224895	-4.021353
H	1.556226	-1.624027	-4.158284
H	1.954199	-2.812710	-2.913012
H	3.766817	0.875451	2.110632
H	3.145187	-1.859452	3.295037

H	1.988572	-0.824595	2.454528
H	2.695724	-0.295880	3.994279
H	5.592090	-1.125957	3.514951
H	5.141010	0.483882	4.055582
H	6.164524	0.289970	2.625510
H	-4.025669	0.398683	1.602940
H	-5.661455	-0.264713	1.600760
H	-4.913770	0.277686	0.097841
H	-4.970873	-3.514616	0.013774
H	-5.595751	-2.045605	-0.740321
H	-6.152862	-2.516223	0.860603
H	-3.689749	-3.236667	2.318076
H	-4.886181	-2.066939	2.866688
H	-3.179468	-1.619720	2.819692
H	-0.881949	-0.230161	-2.140475
H	-1.625555	-0.614066	-3.697532
H	-0.800264	-1.867363	-2.772558
H	-3.259996	0.793790	-1.600338
H	-4.682196	-0.233705	-1.847388
H	-3.686305	0.233806	-3.221390
H	-2.797877	-3.356768	-2.763770
H	-3.572833	-2.178212	-3.817056
H	-4.402737	-2.739123	-2.366688
H	0.275208	-2.650926	-0.870755
H	-0.788425	-3.686186	-1.854395
H	0.183829	-4.389353	-0.568395
H	-2.964659	-4.598162	-0.872690
H	-3.191098	-4.563630	0.877516
H	-1.837850	-5.448855	0.182829
H	-0.375242	-4.293963	1.718978
H	-1.535152	-3.139656	2.377259
H	-0.053176	-2.565599	1.601971
C	1.964457	4.284783	0.225852
H	2.198305	4.828128	-0.693479
H	0.964243	4.586247	0.537983
H	2.668720	4.613827	0.993206
C	4.539654	2.373307	-0.224541
H	4.972583	1.961063	-1.140456
H	4.645621	3.457298	-0.257590
H	5.138612	1.995902	0.609222
C	-2.776730	-1.302713	-2.013284
C	-4.180565	-1.648140	0.876528
C	-1.521919	-3.317915	0.177020

A

Si	-1.116987	-0.004000	0.403570
Si	-2.679757	-1.659043	-0.253073
N	0.497704	-0.533404	0.088085
N	2.582206	0.656576	-0.144639
N	0.736656	1.808081	0.075721
C	1.232919	0.528942	0.001464
C	1.791939	2.726810	0.074672
C	2.930172	2.012920	-0.086407
C	-0.677652	1.891890	0.305383
C	-1.421886	2.978895	-0.346518
C	-2.563451	3.416259	0.216146
C	-3.036355	2.892791	1.478490
C	-2.370412	1.952982	2.163540
C	-1.100353	1.352781	1.729201
C	-0.925048	3.469527	-1.686936
C	-1.725764	4.631847	-2.249026
C	-0.854746	2.330175	-2.702676
C	-0.040125	1.297108	2.832177
C	-0.442757	0.337761	3.941966
C	0.265272	2.678056	3.398155
C	3.476258	-0.429814	-0.329699
C	3.546752	-1.035247	-1.589622
C	4.469675	-2.060232	-1.758726
C	5.282871	-2.466527	-0.713535
C	5.162986	-1.881708	0.533982
C	4.243760	-0.861279	0.754032
C	2.628749	-0.594235	-2.708934
C	3.116070	0.696201	-3.365973
C	2.407295	-1.671146	-3.760639
C	3.994500	-0.315204	2.140239
C	2.947166	-1.186340	2.835762
C	5.253611	-0.190828	2.985941
C	-4.849735	0.177213	0.107693
C	-5.506903	-2.203701	-0.053008
C	-4.386228	-1.332439	1.991896
C	-1.258096	-1.578627	-2.734561
C	-3.539382	-0.667099	-2.798241
C	-3.215587	-3.115074	-2.682823
C	-0.664169	-3.731992	-0.228194
C	-2.881306	-4.386176	0.671816
C	-1.357554	-2.915903	1.970192
H	-3.164679	4.165009	-0.282135
H	-3.961585	3.287909	1.883839
H	-2.749754	1.640946	3.131653
H	0.100924	3.823271	-1.557395
H	-1.755048	5.476213	-1.556980
H	-2.755242	4.336993	-2.469342
H	-1.275608	4.975569	-3.182876
H	-0.232894	1.510727	-2.341704
H	-0.428297	2.688543	-3.642895
H	-1.851286	1.935867	-2.912949

H	0.879297	0.904127	2.389425
H	-0.648565	-0.657899	3.547421
H	-1.335049	0.685151	4.469589
H	0.356197	0.251779	4.682387
H	1.068410	2.625014	4.138344
H	-0.616339	3.101956	3.886479
H	0.573697	3.372504	2.616730
H	4.551753	-2.554162	-2.718454
H	6.002351	-3.262352	-0.869646
H	5.780570	-2.233910	1.351198
H	1.655494	-0.396101	-2.251595
H	4.108766	0.555352	-3.802538
H	3.167566	1.519200	-2.652353
H	2.433530	0.994214	-4.166120
H	3.306707	-1.852268	-4.355569
H	1.621096	-1.354860	-4.449389
H	2.098964	-2.615850	-3.308379
H	3.565051	0.684839	2.035883
H	3.331027	-2.200168	2.979330
H	2.035174	-1.254941	2.238940
H	2.695304	-0.775956	3.817102
H	5.675753	-1.168042	3.232406
H	5.020045	0.305141	3.930741
H	6.026625	0.391170	2.478430
H	-4.112612	0.916546	0.419745
H	-5.783902	0.411700	0.633555
H	-5.035687	0.310336	-0.955797
H	-5.288714	-3.251196	0.157756
H	-5.658855	-2.102562	-1.129291
H	-6.461707	-1.962867	0.430323
H	-4.215345	-2.347460	2.352034
H	-5.349861	-0.999872	2.395918
H	-3.612539	-0.685024	2.413188
H	-0.860560	-0.595943	-2.477643
H	-1.283133	-1.652784	-3.829032
H	-0.552239	-2.319104	-2.364920
H	-3.276506	0.322451	-2.418289
H	-4.603534	-0.828402	-2.620883
H	-3.389997	-0.655313	-3.884646
H	-2.586150	-3.954419	-2.385915
H	-3.249323	-3.108025	-3.779292
H	-4.228533	-3.313132	-2.327176
H	0.095017	-2.954559	-0.333449
H	-0.931510	-4.106324	-1.216716
H	-0.210873	-4.568201	0.318588
H	-3.306819	-4.664118	-0.294580
H	-3.704968	-4.160321	1.350848
H	-2.369302	-5.270997	1.069667
H	-0.977138	-3.836622	2.429760
H	-2.120562	-2.508433	2.632688
H	-0.523684	-2.211060	1.927106
C	1.627892	4.188719	0.291829
H	1.786502	4.770325	-0.620520
H	0.623887	4.413255	0.652640
H	2.337867	4.547338	1.039622
C	4.336514	2.462513	-0.173331
H	4.809992	2.126599	-1.100308
H	4.379095	3.551091	-0.146202
H	4.942102	2.075828	0.651738
C	-2.674850	-1.770529	-2.187974
C	-4.426708	-1.250035	0.464019
C	-1.876654	-3.236202	0.565258

TS(A_1')

Si	-1.006845	0.122462	0.504162
Si	-2.570722	-1.511900	-0.225775
N	0.601153	-0.487025	0.227788
N	2.678976	0.660913	-0.164163
N	0.824051	1.835707	-0.135444
C	1.329586	0.545391	-0.025600
C	1.890777	2.749242	-0.155707
C	3.027471	2.019559	-0.211278
C	-0.569270	1.884517	0.059425
C	-1.422040	2.931604	-0.396727
C	-2.594869	3.198292	0.263308
C	-2.913911	2.796045	1.579888
C	-2.122035	2.030027	2.392740
C	-1.038113	1.202044	2.025636
C	-1.047599	3.669676	-1.674556
C	-2.047209	4.737488	-2.089815
C	-0.817846	2.698866	-2.832903
C	0.104705	1.060330	3.014896
C	-0.348042	0.245386	4.225397
C	0.697401	2.396781	3.441641
C	3.572596	-0.440238	-0.223077
C	3.671781	-1.149856	-1.426703
C	4.585013	-2.194152	-1.486436
C	5.362662	-2.523651	-0.387677
C	5.215079	-1.836336	0.801903
C	4.305060	-0.789381	0.912423
C	2.798406	-0.787631	-2.608099
C	3.359706	0.410706	-3.371578
C	2.556150	-1.953925	-3.554665
C	4.046617	-0.136898	2.249648
C	3.187889	-1.069847	3.103552
C	5.322036	0.254821	2.985375

C	-4.806401	0.236818	0.219401
C	-5.380611	-2.148326	-0.071331
C	-4.297195	-1.343985	2.025566
C	-1.123696	-1.226834	-2.665201
C	-3.425326	-0.367143	-2.709010
C	-3.043450	-2.810582	-2.756113
C	-0.530601	-3.571719	-0.305722
C	-2.733033	-4.289281	0.568792
C	-1.231777	-2.845882	1.925678
H	-3.277197	3.906534	-0.188421
H	-3.773904	3.278694	2.033450
H	-2.291987	2.135511	3.464142
H	-0.100873	4.183863	-1.503751
H	-2.190160	5.491116	-1.312957
H	-3.022036	4.302820	-2.326886
H	-1.688192	5.243273	-2.988985
H	-0.050040	1.961779	-2.594127
H	-0.498132	3.239461	-3.727570
H	-1.738091	2.162365	-3.073714
H	0.894897	0.484713	2.526286
H	-0.734633	-0.729940	3.925403
H	-1.133726	0.763346	4.781312
H	0.489626	0.083373	4.908804
H	1.538933	2.243735	4.123905
H	-0.044002	3.015625	3.953065
H	1.060255	2.957037	2.577961
H	4.686818	-2.766025	-2.399934
H	6.074251	-3.338625	-0.456218
H	5.800582	-2.128834	1.665626
H	1.823681	-0.502421	-2.203953
H	4.355278	0.185709	-3.763977
H	3.433983	1.294756	-2.737262
H	2.711521	0.661316	-4.215185
H	3.461761	-2.232844	-4.099937
H	1.804983	-1.673512	-4.295914
H	2.192464	-2.834414	-3.020958
H	3.467258	0.773313	2.075191
H	3.735835	-1.986069	3.339764
H	2.275132	-1.351176	2.574984
H	2.913081	-0.587261	4.044984
H	5.912214	-0.621990	3.262566
H	5.076569	0.785642	3.908129
H	5.957134	0.904069	2.378436
H	-4.099479	0.986105	0.573622
H	-5.752115	0.407123	0.749248
H	-4.991141	0.419847	-0.836975
H	-5.134657	-3.198932	0.084650
H	-5.528055	-1.992810	-1.142009
H	-6.344961	-1.959573	0.416101
H	-4.089745	-2.366386	2.343376
H	-5.276473	-1.068944	2.435317
H	-3.556173	-0.681773	2.481936
H	-0.765562	-0.244152	-2.350466
H	-1.121538	-1.241655	-3.762586
H	-0.402480	-1.963680	-2.317895
H	-3.197363	0.599505	-2.253451
H	-4.487888	-0.568123	-2.566019
H	-3.255413	-0.272950	-3.788647
H	-2.403128	-3.654978	-2.499460
H	-3.053997	-2.733334	-3.850532
H	-4.059297	-3.050885	-2.436320
H	0.227955	-2.789380	-0.361027
H	-0.792888	-3.890982	-1.314971
H	-0.079929	-4.437359	0.196031
H	-3.147128	-4.538852	-0.410698
H	-3.564920	-4.102619	1.249182
H	-2.208221	-5.179267	0.937554
H	-0.828012	-3.774847	2.347410
H	-2.004605	-2.486437	2.604578
H	-0.412752	-2.122237	1.913608
C	1.745850	4.217742	0.002435
H	1.701545	4.754564	-0.948818
H	0.838698	4.452974	0.562221
H	2.594486	4.613074	0.562329
C	4.439211	2.453831	-0.273144
H	4.955418	2.013318	-1.130791
H	4.492326	3.537693	-0.368341
H	4.997533	2.159509	0.620016
C	-2.544488	-1.491267	-2.161996
C	-4.333113	-1.190406	0.502539
C	-1.747311	-3.120475	0.508091

1'

Si	-1.021390	0.289521	0.718457
Si	-2.529070	-1.330379	-0.232296
N	0.584919	-0.370538	0.531641
N	2.600251	0.519673	-0.408669
N	0.773723	1.768434	-0.487255
C	1.275835	0.516644	-0.078661
C	1.865066	2.575621	-0.883557
C	2.966464	1.794126	-0.853671
C	-0.579024	1.914104	-0.167442
C	-1.473517	2.901260	-0.478980
C	-2.673721	3.005208	0.302792
C	-2.955946	2.633115	1.585015
C	-2.216175	1.918717	2.587692

C	-1.340688	0.898128	2.448516
C	-1.292141	3.898493	-1.622396
C	-2.516679	4.752371	-1.931751
C	-0.863083	3.190118	-2.907260
C	-0.589238	0.350311	3.644516
C	-1.528267	-0.286737	4.665570
C	0.270331	1.429870	4.295306
C	3.483756	-0.582485	-0.255432
C	3.528902	-1.551981	-1.264846
C	4.442549	-2.589128	-1.125917
C	5.275602	-2.661846	-0.022001
C	5.193137	-1.708996	0.975556
C	4.290493	-0.654616	0.881833
C	2.609324	-1.469054	-2.461593
C	3.172746	-0.553768	-3.546785
C	2.270090	-2.831706	-3.048941
C	4.136760	0.323313	2.021860
C	3.283718	-0.315089	3.116337
C	5.469244	0.813574	2.574820
C	-4.909626	0.157793	0.487761
C	-5.302715	-2.132026	-0.337235
C	-4.372248	-1.728671	1.933284
C	-1.090467	-0.668368	-2.602740
C	-3.406829	0.139344	-2.525878
C	-2.952504	-2.262470	-2.954107
C	-0.424694	-3.294022	-0.574302
C	-2.611243	-4.219786	0.083525
C	-1.215267	-2.966739	1.719955
H	-3.461605	3.598597	-0.143536
H	-3.906839	3.016259	1.949922
H	-2.458028	2.240812	3.603098
H	-0.509896	4.603152	-1.336262
H	-2.812767	5.382398	-1.091335
H	-3.375031	4.140889	-2.223860
H	-2.285821	5.410048	-2.773005
H	0.008754	2.550764	-2.769430
H	-0.627085	3.920092	-3.686468
H	-1.675617	2.559860	-3.275747
H	0.084693	-0.432557	3.283256
H	-2.102199	-1.102682	4.223138
H	-2.235864	0.445981	5.061783
H	-0.958166	-0.692378	5.505602
H	0.856632	1.015181	5.119901
H	-0.352846	2.234223	4.694625
H	0.958181	1.871180	3.571046
H	4.499947	-3.356318	-1.887591
H	5.983756	-3.477937	0.066168
H	5.830484	-1.790446	1.847967
H	1.675624	-1.024108	-2.111183
H	4.138622	-0.923624	-3.901997
H	3.307022	0.466747	-3.187020
H	2.489897	-0.516685	-4.399420
H	3.127997	-3.278824	-3.558242
H	1.474656	-2.726663	-3.790277
H	1.927274	-3.526057	-2.280475
H	3.591368	1.193951	1.648856
H	3.782019	-1.198938	3.524201
H	2.318156	-0.624175	2.712550
H	3.114550	0.388953	3.934110
H	6.029172	0.007249	3.054411
H	5.301058	1.584778	3.330000
H	6.101699	1.236484	1.790641
H	-4.347346	0.804273	1.157212
H	-5.944474	0.119940	0.851457
H	-4.923834	0.630771	-0.492592
H	-4.977293	-3.168114	-0.429245
H	-5.457826	-1.736721	-1.342542
H	-6.281986	-2.138492	0.157816
H	-4.102691	-2.777404	2.054683
H	-5.390851	-1.608314	2.322521
H	-3.712323	-1.125971	2.561690
H	-0.751259	0.261033	-2.142504
H	-1.083638	-0.511529	-3.689206
H	-0.364424	-1.444822	-2.373392
H	-3.183889	1.029205	-1.931475
H	-4.465841	-0.093958	-2.409420
H	-3.246397	0.396043	-3.580896
H	-2.278417	-3.110195	-2.823666
H	-2.955729	-2.013715	-4.023089
H	-3.958990	-2.592936	-2.693455
H	0.299476	-2.483501	-0.485753
H	-0.651346	-3.465631	-1.627467
H	0.051499	-4.207628	-0.195566
H	-2.987233	-4.309026	-0.937974
H	-3.468119	-4.195106	0.757164
H	-2.053215	-5.137870	0.306069
H	-0.813111	-3.947585	2.003571
H	-2.015399	-2.728256	2.419414
H	-0.407375	-2.243773	1.850197
C	1.833348	4.037047	-1.117874
H	1.365678	4.316262	-2.063038
H	1.307967	4.552030	-0.310085
H	2.855808	4.412889	-1.131860
C	4.382604	2.114002	-1.138795
H	4.820295	1.389526	-1.830131
H	4.470587	3.102228	-1.586193

60

H	4.991170	2.090485	-0.229903
C	-2.505190	-1.038288	-2.152932
C	-4.341064	-1.260282	0.476738
C	-1.678472	-3.019175	0.259151

TS(1-B)

H	0.776639	1.925840	1.366760
Si	1.044022	1.072046	0.058585
Si	3.207883	0.148681	-0.337079
N	-0.067465	-0.200828	-0.007398
N	-2.206965	-1.129479	0.325681
N	-2.095679	1.039225	0.447857
C	-1.334194	-0.080884	0.243874
C	-3.491431	-0.673562	0.613345
C	-3.424915	0.675810	0.674931
C	-1.688392	-2.917201	-1.235577
C	-1.314798	-4.239279	-1.437488
H	-1.188380	-4.611064	-2.445876
C	-1.084697	-5.090154	-0.368035
H	-0.790970	-6.117448	-0.551428
C	-1.212376	-4.630391	0.927548
H	-1.009442	-5.297728	1.756810
C	-1.580279	-3.312468	1.182416
C	-1.825441	-2.480638	0.090260
C	-1.920702	-1.976641	-2.399479
H	-1.449948	-1.026876	-2.131539
C	-1.275182	-2.442845	-3.696003
H	-1.778643	-3.322892	-4.105964
H	-0.219088	-2.679162	-3.563562
H	-1.350647	-1.650160	-4.443511
C	-3.407376	-1.714440	-2.638638
H	-3.537370	-1.066795	-3.509442
H	-3.880568	-1.221323	-1.790124
H	-3.936733	-2.650787	-2.835626
C	-1.629988	-2.800280	2.601922
H	-2.109083	-1.818832	2.591325
C	-0.210509	-2.607063	3.130309
H	0.356753	-1.943351	2.476936
H	0.317868	-3.562954	3.180834
H	-0.226625	-2.172486	4.132844
C	-2.441667	-3.702491	3.524146
H	-3.449659	-3.871486	3.138432
H	-2.526316	-3.249320	4.514565
H	-1.968048	-4.678768	3.651614
C	-4.616993	-1.605106	0.844693
H	-5.551997	-1.052656	0.926828
H	-4.479544	-2.179964	1.764793
H	-4.714665	-2.323681	0.027472
C	-4.457411	1.685993	0.987786
H	-4.656522	2.342726	0.137047
H	-4.135180	2.326320	1.813711
H	-5.389675	1.198027	1.269315
C	-1.661607	2.390364	0.320941
C	-1.025383	3.054408	1.417265
C	-0.781148	4.439082	1.213908
H	-0.282077	4.998248	1.993085
C	-1.208113	5.104047	0.097440
H	-1.028438	6.170157	0.011496
C	-1.875379	4.431754	-0.930838
H	-2.177332	4.972957	-1.817957
C	-2.102091	3.076370	-0.834797
C	-0.450704	2.392445	2.529277
C	0.407846	3.170819	3.485160
H	1.120033	3.823316	2.974658
H	0.987403	2.481859	4.103214
H	-0.179332	3.798525	4.171288
C	-0.970334	1.090975	3.079521
H	-0.695297	1.002797	4.132712
H	-0.559460	0.207884	2.576439
H	-2.058596	1.012794	3.022850
C	-2.693022	2.314129	-2.002982
H	-3.203403	1.427811	-1.617801
C	-3.718323	3.110780	-2.797396
H	-3.256933	3.939151	-3.340098
H	-4.497546	3.524939	-2.153533
H	-4.195129	2.465536	-3.539041
C	-1.570476	1.827891	-2.920927
H	-1.976142	1.239477	-3.748670
H	-0.850469	1.211464	-2.379670
H	-1.029048	2.679846	-3.340797
C	4.114572	1.412081	-1.501299
C	5.636783	1.268315	-1.471085
H	5.967088	0.262942	-1.740422
H	6.051935	1.503142	-0.489651
H	6.087915	1.965976	-2.188108
C	3.644290	1.238770	-2.947044
H	2.556231	1.311735	-3.035076
H	3.958726	0.289419	-3.381804
H	4.075405	2.037597	-3.563135
C	3.748299	2.846584	-1.105624
H	4.241825	3.547586	-1.790543
H	4.056414	3.106320	-0.094139
H	2.670776	3.024173	-1.177254
C	3.066598	-1.621863	-1.119126
C	2.030298	-1.616664	-2.246790
H	2.296233	-0.961570	-3.074825

61

H	1.049626	-1.324298	-1.868151
H	1.945640	-2.634964	-2.648012
C	4.396793	-2.130024	-1.677148
H	4.260179	-3.144889	-2.072278
H	5.180420	-2.178795	-0.918601
H	4.764774	-1.512882	-2.498788
C	2.551978	-2.629693	-0.087469
H	1.593988	-2.315659	0.331621
H	3.259418	-2.802748	0.724875
H	2.388431	-3.594085	-0.584715
C	3.990066	0.112669	1.448419
C	5.255699	-0.743262	1.509369
H	5.051430	-1.794603	1.300913
H	5.688265	-0.690796	2.516995
H	6.020373	-0.405004	0.807262
C	4.338628	1.521802	1.931001
H	5.139420	1.981310	1.350626
H	4.683937	1.465706	2.971140
H	3.473867	2.190488	1.912022
C	2.972697	-0.443451	2.449586
H	2.078363	0.184388	2.509354
H	3.420846	-0.461670	3.451294
H	2.651636	-1.455952	2.213702

b

H	1.310423	0.972947	1.806439
Si	0.950770	0.631509	0.394007
Si	3.134568	0.439390	-0.583383
N	0.039290	-0.835689	0.303713
N	-2.323151	-1.289598	0.506882
N	-1.670643	0.785183	0.427399
C	-1.209953	-0.507051	0.406156
C	-3.466896	-0.477764	0.601696
C	-3.057588	0.809951	0.553854
C	-2.460298	-3.375566	-0.724071
C	-2.494342	-4.765813	-0.710673
H	-2.594826	-5.304946	-1.645735
C	-2.392606	-5.467805	0.476032
H	-2.419528	-6.551549	0.468238
C	-2.249770	-4.789263	1.673663
H	-2.161426	-5.348462	2.597443
C	-2.214075	-3.400533	1.709291
C	-2.325772	-2.710850	0.497227
C	-2.521459	-2.631790	-2.036125
H	-2.555891	-1.563155	-1.813477
C	-1.253440	-2.895140	-2.843058
H	-1.179097	-3.950017	-3.120474
H	-0.367983	-2.635300	-2.262217
H	-1.248384	-2.304747	-3.762604
C	-3.770466	-2.978189	-2.839006
H	-3.812369	-2.378183	-3.751365
H	-4.681029	-2.789112	-2.266131
H	-3.776717	-4.029991	-3.135679
C	-2.000910	-2.670372	3.012138
H	-2.293288	-1.630014	2.856801
C	-0.516048	-2.682686	3.374961
H	0.084842	-2.268150	2.563251
H	-0.176811	-3.705534	3.561899
H	-0.337054	-2.095281	4.279268
C	-2.852866	-3.217887	4.150204
H	-3.912319	-3.240758	3.884293
H	-2.737953	-2.590301	5.037070
H	-2.555913	-4.231333	4.430840
C	-4.811119	-1.070112	0.767414
H	-5.564154	-0.284337	0.813949
H	-4.879338	-1.661647	1.685583
H	-5.063489	-1.737534	-0.061354
C	-3.818140	2.073669	0.673261
H	-3.589225	2.758521	-0.147335
H	-3.567592	2.599387	1.599127
H	-4.889047	1.873268	0.664807
C	-0.707252	1.862431	0.285452
C	-0.619243	2.753567	1.518380
C	-0.110531	4.090752	1.267274
H	0.243058	4.673219	2.105992
C	-0.049037	4.621852	0.037410
H	0.354541	5.617682	-0.105933
C	-0.579249	3.909381	-1.094089
H	-0.707947	4.448803	-2.023390
C	-0.960234	2.625887	-1.001159
C	-0.875699	2.357784	2.790786
C	-0.786273	3.299565	3.956114
H	0.128105	3.119273	4.535016
H	-1.621847	3.110151	4.637213
H	-0.820059	4.353058	3.689179
C	-1.241109	0.966984	3.217944
H	-1.056619	0.855342	4.288777
H	-0.656957	0.200451	2.710208
H	-2.301247	0.744410	3.051852
C	-1.672335	1.935019	-2.141080
H	-2.575941	1.480031	-1.718990
C	-2.129232	2.880128	-3.241435
H	-1.281228	3.316009	-3.776822
H	-2.741432	3.696266	-2.852116
H	-2.724417	2.327904	-3.972117
C	-0.858708	0.799199	-2.741669

62

H	-1.444888	0.261981	-3.491397
H	-0.546589	0.079968	-1.986365
H	0.035558	1.187216	-3.232013
C	3.661669	2.151646	-1.317703
C	5.175201	2.306857	-1.473510
H	5.614277	1.540595	-2.114697
H	5.692281	2.276680	-0.513317
H	5.395011	3.280952	-1.928121
C	3.009187	2.371186	-2.683518
H	1.921288	2.277263	-2.630641
H	3.381046	1.685468	-3.445729
H	3.229815	3.389963	-3.025446
C	3.145995	3.271324	-0.413452
H	3.409190	4.242653	-0.851796
H	3.561821	3.242133	0.592209
H	2.059141	3.250109	-0.325140
C	3.218144	-0.995442	-1.889010
C	2.066216	-0.891858	-2.884484
H	2.050686	0.049069	-3.431563
H	1.110906	-1.010300	-2.377387
H	2.151001	-1.701227	-3.620582
C	4.531814	-0.978143	-2.674708
H	4.555584	-1.842513	-3.350114
H	5.412784	-1.039764	-2.034359
H	4.628691	-0.085112	-3.295059
C	3.063913	-2.362617	-1.217381
H	2.148055	-2.420697	-0.623789
H	3.910869	-2.620429	-0.581521
H	3.003115	-3.131843	-1.997456
C	4.174898	-0.020627	1.007769
C	5.567114	-0.543035	0.641269
H	5.528588	-1.498505	0.116897
H	6.142792	-0.704591	1.561343
H	6.131731	0.157242	0.023106
C	4.363278	1.191022	1.923368
H	4.984747	1.965052	1.471343
H	4.869537	0.864809	2.840346
H	3.412441	1.639643	2.218146
C	3.471721	-1.096204	1.845148
H	2.512257	-0.753122	2.235942
H	4.102479	-1.338605	2.709811
H	3.295782	-2.019961	1.298568

TS(B-2)

H	-1.917609	1.775925	-0.728605
Si	-1.414552	0.517956	-0.143438
Si	-2.805336	-1.364565	-0.365010
N	0.198703	0.100896	-0.081947
N	2.556583	0.312263	0.056855
N	1.402346	2.140774	0.311980
C	1.276736	0.804081	0.064735
C	3.465864	1.345077	0.279650
C	2.748895	2.479518	0.447594
C	2.770864	-1.893922	1.054275
C	3.139454	-3.225565	0.915913
H	3.048290	-3.895766	1.760342
C	3.610492	-3.717598	-0.290584
H	3.889104	-4.761811	-0.375106
C	3.714120	-2.884797	-1.386188
H	4.070183	-3.281143	-2.329971
C	3.357072	-1.541948	-1.300006
C	2.895614	-1.065119	-0.071550
C	2.237169	-1.361779	2.367526
H	1.388092	-0.718304	2.119889
C	1.721647	-2.455141	3.291587
H	2.540032	-3.051296	3.704833
H	1.031087	-3.125308	2.779701
H	1.190540	-2.003974	4.132210
C	3.267610	-0.514554	3.112826
H	2.846587	-0.163965	4.058409
H	3.572167	0.363695	2.544562
H	4.159154	-1.105443	3.340671
C	3.435920	-0.668978	-2.530139
H	3.236127	0.360630	-2.226486
C	2.358795	-1.069758	-3.534928
H	1.368004	-1.040897	-3.082390
H	2.529876	-2.085148	-3.902592
H	2.364606	-0.393353	-4.393133
C	4.815523	-0.709976	-3.180680
H	5.608707	-0.468297	-2.470211
H	4.865444	0.005597	-4.004728
H	5.032969	-1.698590	-3.592119
C	4.927691	1.119532	0.261954
H	5.446892	2.012399	0.607702
H	5.288394	0.884480	-0.742701
H	5.210838	0.286505	0.909797
C	3.178095	3.883220	0.625256
H	2.877719	4.286671	1.595172
H	2.723515	4.521038	-0.137817
H	4.261690	3.959657	0.543181
C	0.321662	3.044724	0.454924
C	-0.402173	3.480308	-0.709605
C	-1.443817	4.422544	-0.421020
H	-2.060595	4.777659	-1.234705
C	-1.645970	4.936984	0.825871
H	-2.426158	5.676822	0.971420

C	-0.872377	4.529448	1.922037
H	-1.085037	4.921356	2.907605
C	0.097643	3.565420	1.746848
C	-0.233191	3.007773	-2.013423
C	-1.199413	3.419185	-3.085973
H	-2.241155	3.394299	-2.756685
H	-1.117262	2.745147	-3.941291
H	-1.008476	4.435087	-3.465095
C	0.969033	2.264241	-2.505269
H	1.054109	2.374460	-3.588923
H	0.923718	1.183385	-2.306792
H	1.905275	2.622700	-2.071556
C	0.799150	2.963178	2.948113
H	1.771829	2.577556	2.634038
C	1.051196	3.961673	4.069255
H	0.120643	4.281136	4.543749
H	1.562983	4.855271	3.704954
H	1.669459	3.504689	4.845733
C	-0.003839	1.769494	3.466403
H	0.506065	1.295939	4.310359
H	-0.148902	1.018625	2.687008
H	-0.992489	2.093751	3.802374
C	-4.576453	-0.794502	0.183479
C	-5.671041	-1.746494	-0.302575
H	-5.521934	-2.768263	0.052699
H	-5.742026	-1.779095	-1.390824
H	-6.644039	-1.407180	0.074015
C	-4.678007	-0.691558	1.706244
H	-3.903980	-0.042130	2.124650
H	-4.617218	-1.661891	2.200778
H	-5.648561	-0.253772	1.969707
C	-4.864634	0.610309	-0.356871
H	-5.870088	0.916800	-0.042732
H	-4.829775	0.669715	-1.443398
H	-4.162948	1.348676	0.039428
C	-2.077436	-2.761373	0.760284
C	-1.703228	-2.183439	2.128032
H	-2.548042	-1.744608	2.655548
H	-0.925220	-1.421612	2.038884
H	-1.307994	-2.987923	2.759657
C	-3.070767	-3.905492	0.972396
H	-2.601593	-4.686154	1.584175
H	-3.380959	-4.369382	0.034028
H	-3.969560	-3.580507	1.499387
C	-0.790452	-3.336247	0.164444
H	-0.042690	-2.560557	-0.015299
H	-0.963436	-3.876541	-0.767483
H	-0.360619	-4.055661	0.872814
C	-2.727882	-1.805619	-2.259414
C	-3.245327	-3.216929	-2.541623
H	-2.625969	-3.984676	-2.075498
H	-3.232074	-3.402693	-3.623046
H	-4.271996	-3.360708	-2.198599
C	-3.539388	-0.815681	-3.096359
H	-4.611099	-0.873067	-2.904204
H	-3.387399	-1.041209	-4.159099
H	-3.214280	0.215785	-2.934123
C	-1.284564	-1.693107	-2.756871
H	-0.921632	-0.663913	-2.682034
H	-1.242779	-1.978848	-3.815512
H	-0.586533	-2.326223	-2.211730

2

Si	-1.021390	0.289521	0.718457
Si	-2.529070	-1.330379	-0.232296
N	0.584919	-0.370538	0.531641
N	2.600251	0.519673	-0.408669
N	0.773723	1.768434	-0.487255
C	1.275835	0.516644	-0.078661
C	1.865066	2.575621	-0.883557
C	2.966464	1.794126	-0.853671
C	-0.579024	1.914104	-0.167442
C	-1.473517	2.901260	-0.478980
C	-2.673721	3.005208	0.302792
C	-2.955946	2.633115	1.585015
C	-2.216175	1.918717	2.587692
C	-1.340688	0.898128	2.448516
C	-1.292141	3.898493	-1.622396
C	-2.516679	4.752371	-1.931751
C	-0.863083	3.190118	-2.907260
C	-0.589238	0.350311	3.644516
C	-1.528267	-0.286737	4.665570
C	0.270331	1.429870	4.295306
C	3.483756	-0.582485	-0.255432
C	3.528902	-1.551981	-1.264846
C	4.442549	-2.589128	-1.125917
C	5.275602	-2.661846	-0.022001
C	5.193137	-1.708996	0.975556
C	4.290493	-0.654616	0.881833
C	2.609324	-1.469054	-2.461593
C	3.172746	-0.553768	-3.546785
C	2.270090	-2.831706	-3.048941
C	4.136760	0.323313	2.021860
C	3.283718	-0.315089	3.116337
C	5.469244	0.813574	2.574820
C	-4.909626	0.157793	0.487761

64

C	-5.302715	-2.132026	-0.337235
C	-4.372248	-1.728671	1.933284
C	-1.090467	-0.668368	-2.602740
C	-3.406829	0.139344	-2.525878
C	-2.952504	-2.262470	-2.954107
C	-0.424694	-3.294022	-0.574302
C	-2.611243	-4.219786	0.083525
C	-1.215267	-2.966739	1.719955
H	-3.461605	3.598597	-0.143536
H	-3.906839	3.016259	1.949922
H	-2.458028	2.240812	3.603098
H	-0.509896	4.603152	-1.336262
H	-2.812767	5.382398	-1.091335
H	-3.375031	4.140889	-2.223860
H	-2.285821	5.410048	-2.773005
H	0.008754	2.550764	-2.769430
H	-0.627085	3.920092	-3.686468
H	-1.675617	2.559860	-3.275747
H	0.084693	-0.432557	3.283256
H	-2.102199	-1.102682	4.223138
H	-2.235864	0.445981	5.061783
H	-0.958166	-0.692378	5.505602
H	0.856632	1.015181	5.119901
H	-0.352846	2.234223	4.694625
H	0.958181	1.871180	3.571046
H	4.499947	-3.356318	-1.887591
H	5.983756	-3.477937	0.066168
H	5.830484	-1.790446	1.847967
H	1.675624	-1.024108	-2.111183
H	4.138622	-0.923624	-3.901997
H	3.307022	0.466747	-3.187020
H	2.489897	-0.516685	-4.399420
H	3.127997	-3.278824	-3.558242
H	1.474656	-2.726663	-3.790277
H	1.927274	-3.526057	-2.280475
H	3.591368	1.193951	1.648856
H	3.782019	-1.198938	3.524201
H	2.318156	-0.624175	2.712550
H	3.114550	0.388953	3.934110
H	6.029172	0.007249	3.054411
H	5.301058	1.584778	3.330000
H	6.101699	1.236484	1.790641
H	-4.347346	0.804273	1.157212
H	-5.944474	0.119940	0.851457
H	-4.923834	0.630771	-0.492592
H	-4.977293	-3.168114	-0.429245
H	-5.457826	-1.736721	-1.342542
H	-6.281986	-2.138492	0.157816
H	-4.102691	-2.777404	2.054683
H	-5.390851	-1.608314	2.322521
H	-3.712323	-1.125971	2.561690
H	-0.751259	0.261033	-2.142504
H	-1.083638	-0.511529	-3.689206
H	-0.364424	-1.444822	-2.373392
H	-3.183889	1.029205	-1.931475
H	-4.465841	-0.093958	-2.409420
H	-3.246397	0.396043	-3.580896
H	-2.278417	-3.110195	-2.823666
H	-2.955729	-2.013715	-4.023089
H	-3.958990	-2.592936	-2.693455
H	0.299476	-2.483501	-0.485753
H	-0.651346	-3.465631	-1.627467
H	0.051499	-4.207628	-0.195566
H	-2.987233	-4.309026	-0.937974
H	-3.468119	-4.195106	0.757164
H	-2.053215	-5.137870	0.306069
H	-0.813111	-3.947585	2.003571
H	-2.015399	-2.728256	2.419414
H	-0.407375	-2.243773	1.850197
C	1.833348	4.037047	-1.117874
H	1.365678	4.316262	-2.063038
H	1.307967	4.552030	-0.310085
H	2.855808	4.412889	-1.131860
C	4.382604	2.114002	-1.138795
H	4.820295	1.389526	-1.830131
H	4.470587	3.102228	-1.586193
H	4.991170	2.090485	-0.229903
C	-2.505190	-1.038288	-2.152932
C	-4.341064	-1.260282	0.476738
C	-1.678472	-3.019175	0.259151

TS(1-Ca)

Si	-0.211680	1.123821	0.924132
Si	-1.228339	2.828572	-0.460223
N	0.082988	-0.281825	-0.022541
N	0.446073	-2.391644	-1.021190
N	0.398298	-2.399132	1.154850
C	0.499380	-2.004964	2.515578
C	0.287668	-1.541040	0.063806
C	-0.757614	2.572882	-2.327525
C	0.626997	-3.713968	-0.610845
C	-0.594402	-2.315841	-3.208386
C	-0.516207	-1.954777	-4.548916
H	-1.330600	-2.199343	-5.218712
C	-3.520851	2.850097	1.273347
H	-2.861388	2.408910	2.026102

H	-4.538385	2.492981	1.476303
H	-3.523281	3.930687	1.412905
C	-1.821858	-3.007232	-2.653404
H	-1.498151	-3.681991	-1.857930
C	0.481843	-1.980463	-2.379622
C	-3.117581	2.430176	-0.140708
C	-1.368907	1.283511	-2.874820
H	-1.116185	0.425472	-2.252129
H	-0.963200	1.092082	-3.875306
H	-2.454010	1.345637	-2.973720
C	1.755562	-2.044905	3.137793
C	0.584924	-1.276104	-5.037923
H	0.623859	-0.994379	-6.084018
C	0.589263	-3.720677	0.735323
C	1.636308	-0.952012	-4.198170
H	2.489265	-0.417329	-4.595517
C	1.614316	-1.307501	-2.855360
C	0.757994	2.407744	-2.440114
H	1.310850	3.281842	-2.096339
H	1.025603	2.230185	-3.489700
H	1.085974	1.543096	-1.861469
C	-0.659589	-1.609648	3.195920
C	1.384326	1.284640	2.148572
H	1.454311	0.220843	2.354552
C	-3.378314	0.928487	-0.227131
H	-3.224228	0.536864	-1.227814
H	-4.418953	0.723694	0.055823
H	-2.738549	0.364761	0.456571
C	2.781651	-1.007107	-1.939871
H	2.348983	-0.664291	-0.996482
C	-0.531072	-1.230523	4.526884
H	-1.404638	-0.904604	5.075821
C	0.882523	-4.816387	-1.565878
H	0.044336	-4.994581	-2.243308
H	1.078827	-5.738628	-1.020320
H	1.753874	-4.600502	-2.189947
C	-1.210369	3.723576	-3.228596
H	-2.290386	3.878585	-3.193637
H	-0.949489	3.487481	-4.268363
H	-0.730057	4.671305	-2.984257
C	3.024284	-2.431626	2.405238
H	2.744575	-2.905508	1.462171
C	0.699232	-1.258471	5.160874
H	0.778147	-0.955416	6.198768
C	2.063834	1.776057	0.955376
H	2.271610	1.096803	0.140201
C	2.722390	3.020570	0.985176
C	1.827655	-1.665742	4.474921
H	2.786419	-1.673212	4.979219
C	-4.053956	3.110488	-1.141446
H	-3.951313	4.195522	-1.153284
H	-5.094626	2.882113	-0.877412
H	-3.894536	2.746456	-2.157812
C	0.480878	5.141238	-0.431097
H	1.307786	4.468874	-0.217068
H	0.719341	6.109202	0.027258
H	0.430971	5.297197	-1.508825
C	1.499265	2.115464	3.335115
C	-2.752218	-1.993145	-1.999426
H	-2.232343	-1.434914	-1.220928
H	-3.613730	-2.493104	-1.548997
H	-3.119446	-1.274324	-2.735936
C	-0.695310	4.642175	1.672718
H	-1.612956	4.359618	2.187053
H	-0.427951	5.653470	2.006243
H	0.094719	3.974282	2.011470
C	3.605284	-2.262153	-1.652322
H	3.016908	-3.033143	-1.155021
H	4.449174	-2.017248	-1.002699
H	4.005159	-2.679681	-2.580522
C	-0.837889	4.630688	0.149853
C	3.864693	-1.204231	2.059342
H	3.344190	-0.529595	1.380656
H	4.797795	-1.512812	1.581212
H	4.117093	-0.635202	2.957804
C	2.153630	3.298480	3.310709
H	2.234232	3.883049	4.220907
C	-1.918256	5.640216	-0.246854
H	-2.087142	5.669051	-1.325320
H	-1.595254	6.642921	0.060558
H	-2.874786	5.449876	0.239684
C	-2.564360	-3.845335	-3.683699
H	-3.042236	-3.223396	-4.444532
H	-3.355100	-4.418154	-3.194527
H	-1.898797	-4.547677	-4.191308
C	3.696965	0.096375	-2.449255
H	4.266980	-0.223620	-3.325871
H	4.419605	0.355912	-1.672124
H	3.143896	0.999177	-2.711011
C	2.772580	3.781309	2.117977
H	3.295509	4.729150	2.124672
C	0.706828	-4.843004	1.693151
H	1.654181	-4.826956	2.236223
H	0.638652	-5.791963	1.162553
H	-0.090145	-4.813913	2.439689
C	-3.011127	-0.678661	3.138105

66

H	-3.323588	-1.010374	4.131983
H	-3.907142	-0.623070	2.517416
H	-2.594782	0.327467	3.219634
C	-2.007680	-1.632896	2.511011
H	-1.848147	-1.306135	1.480241
C	3.866330	-3.427618	3.197926
H	4.311503	-2.961571	4.080217
H	4.686667	-3.797668	2.578775
H	3.281276	-4.284481	3.538201
C	-2.578146	-3.049272	2.458060
H	-1.932341	-3.723062	1.894168
H	-3.556171	-3.041304	1.970453
H	-2.704964	-3.455088	3.465491
H	3.242960	3.346392	0.090409
H	1.077645	1.736506	4.258602

Ca

Si	0.233278	1.284656	0.613499
Si	-1.198495	2.864212	-0.477114
N	0.066589	-0.284220	-0.003786
N	0.482944	-2.364938	-1.039062
N	0.470041	-2.399060	1.139020
C	0.500546	-2.036765	2.513203
C	0.326887	-1.529994	0.057581
C	-0.840090	2.579532	-2.366385
C	0.685569	-3.689665	-0.648338
C	-0.621603	-2.302946	-3.192090
C	-0.590178	-1.942303	-4.534624
H	-1.418357	-2.205035	-5.180348
C	-3.328285	2.869251	1.425735
H	-2.583366	2.488329	2.130157
H	-4.305238	2.473336	1.729402
H	-3.371230	3.953066	1.532869
C	-1.818982	-3.017656	-2.601996
H	-1.462613	-3.669862	-1.801722
C	0.471067	-1.944440	-2.394442
C	-3.033943	2.434595	-0.010364
C	-1.488623	1.287051	-2.862259
H	-1.193944	0.431388	-2.254491
H	-1.152831	1.090158	-3.886975
H	-2.577998	1.349113	-2.885250
C	1.719427	-2.079044	3.204423
C	0.482474	-1.242406	-5.055570
H	0.486937	-0.962690	-6.102967
C	0.666729	-3.713709	0.697249
C	1.548629	-0.892021	-4.245347
H	2.376752	-0.338121	-4.667738
C	1.572868	-1.243083	-2.901121
C	0.665173	2.409174	-2.582296
H	1.248245	3.274259	-2.268324
H	0.859279	2.238790	-3.648721
H	1.036690	1.537995	-2.040205
C	-0.696694	-1.664661	3.141957
C	1.175846	1.318687	2.248160
H	1.209922	0.293008	2.602422
C	-3.261009	0.927316	-0.069976
H	-3.193125	0.539111	-1.081622
H	-4.264942	0.695708	0.307480
H	-2.539831	0.384725	0.541074
C	2.749765	-0.893851	-2.014343
H	2.325835	-0.508043	-1.083613
C	-0.638271	-1.287081	4.477036
H	-1.540895	-0.972986	4.983985
C	0.950055	-4.774397	-1.620700
H	0.119616	-4.937454	-2.311244
H	1.138974	-5.706933	-1.090202
H	1.829682	-4.548819	-2.230159
C	-1.342256	3.722557	-3.250681
H	-2.414563	3.896121	-3.138792
H	-1.162017	3.464460	-4.301904
H	-0.827751	4.664530	-3.058411
C	3.031289	-2.463483	2.554309
H	2.818049	-2.850491	1.555591
C	0.558469	-1.303481	5.173677
H	0.582207	-0.998931	6.213726
C	2.052174	1.606621	0.983866
H	2.641795	0.771912	0.603673
C	2.809868	2.856582	1.017362
C	1.719699	-1.706159	4.545485
H	2.651912	-1.713026	5.097509
C	-4.056574	3.091181	-0.940163
H	-3.978538	4.178148	-0.960612
H	-5.069078	2.841197	-0.598300
H	-3.966657	2.728529	-1.965738
C	0.568431	5.113957	-0.559427
H	1.383027	4.441012	-0.290698
H	0.827870	6.106312	-0.170469
H	0.523200	5.193970	-1.645610
C	1.294877	2.278279	3.345313
C	-2.764893	-2.019159	-1.945070
H	-2.244954	-1.435288	-1.185838
H	-3.601078	-2.537652	-1.468541
H	-3.169342	-1.322447	-2.683734
C	-0.614117	4.785202	1.572024
H	-1.556796	4.649237	2.099225
H	-0.240525	5.785504	1.825555

H	0.098368	4.068129	1.973474
C	3.593382	-2.123260	-1.675900
H	3.021244	-2.883771	-1.144893
H	4.433150	-1.835137	-1.038286
H	4.000955	-2.572073	-2.586046
C	-0.763637	4.677701	0.054534
C	3.946128	-1.252583	2.394223
H	3.473731	-0.460118	1.817064
H	4.871364	-1.543071	1.889812
H	4.211538	-0.832619	3.367702
C	2.027761	3.396953	3.258417
H	2.093475	4.071696	4.104285
C	-1.831256	5.684703	-0.382347
H	-2.031074	5.659381	-1.454706
H	-1.483999	6.696095	-0.136861
H	-2.776456	5.537490	0.142423
C	-2.557288	-3.893141	-3.604076
H	-3.066933	-3.298469	-4.366098
H	-3.321786	-4.479937	-3.090311
H	-1.881875	-4.585029	-4.113051
C	3.648661	0.192945	-2.586042
H	4.202727	-0.160254	-3.460252
H	4.384312	0.486453	-1.833976
H	3.087525	1.083369	-2.871591
C	2.783508	3.704284	2.055923
H	3.368068	4.616664	2.023870
C	0.786747	-4.856122	1.631054
H	1.760038	-4.894396	2.122920
H	0.648267	-5.791276	1.089350
H	0.029276	-4.804722	2.416372
C	-3.090016	-0.839316	3.035691
H	-3.419621	-1.257021	3.990927
H	-3.962630	-0.796377	2.382254
H	-2.750973	0.184219	3.207381
C	-2.009225	-1.692618	2.391338
H	-1.813449	-1.283448	1.397425
C	3.765218	-3.548732	3.340502
H	4.135283	-3.161597	4.292884
H	4.631012	-3.899945	2.774417
H	3.129176	-4.407203	3.562500
C	-2.514678	-3.122984	2.206402
H	-1.818427	-3.726826	1.624243
H	-3.470365	-3.116392	1.676138
H	-2.668901	-3.608109	3.174266
H	3.452305	3.067515	0.166831
H	0.798424	2.024479	4.276853

TS(Ca_3a)

Si	0.328257	1.313009	0.610729
Si	-1.128699	2.913178	-0.453248
N	0.048915	-0.250995	0.018740
N	0.571582	-2.295128	-1.054069
N	0.615258	-2.347245	1.122282
C	0.469922	-2.042202	2.504351
C	0.394665	-1.479768	0.052708
C	-0.882415	2.554026	-2.347392
C	0.855167	-3.609514	-0.681004
C	-0.719813	-2.295704	-3.100667
C	-0.814602	-1.968461	-4.448833
H	-1.693847	-2.257850	-5.010426
C	-3.172177	3.050254	1.554443
H	-2.394479	2.720723	2.249412
H	-4.131387	2.665453	1.923178
H	-3.226920	4.138121	1.596373
C	-1.845788	-3.022448	-2.396683
H	-1.411076	-3.604707	-1.581077
C	0.432293	-1.899520	-2.411622
C	-2.939082	2.531787	0.134479
C	-1.595650	1.268271	-2.764098
H	-1.286167	0.424108	-2.148524
H	-1.328469	1.030867	-3.800637
H	-2.682265	1.358910	-2.722806
C	1.608040	-1.962423	3.317497
C	0.198621	-1.272752	-5.081774
H	0.106217	-1.020391	-6.132039
C	0.879494	-3.644485	0.663239
C	1.329747	-0.893051	-4.380204
H	2.110830	-0.344815	-4.890261
C	1.476027	-1.202975	-3.033364
C	0.604711	2.320760	-2.618636
H	1.234727	3.164494	-2.339860
H	0.749404	2.127565	-3.688895
H	0.961409	1.440898	-2.080717
C	-0.824329	-1.866243	3.022350
C	0.866242	1.318661	2.380134
H	0.749293	0.330920	2.821027
C	-3.169849	1.024821	0.179903
H	-3.085579	0.559929	-0.798086
H	-4.178650	0.822482	0.561090
H	-2.459436	0.528459	0.842385
C	2.719980	-0.813458	-2.263178
H	2.372733	-0.407364	-1.309345
C	-0.947503	-1.564346	4.372125
H	-1.929615	-1.402974	4.795698
C	1.101664	-4.678798	-1.674772
H	0.222332	-4.880326	-2.291472

H	1.380067	-5.600772	-1.166024
H	1.912553	-4.408904	-2.356055
C	-1.376719	3.679840	-3.256319
H	-2.434619	3.905437	-3.105105
H	-1.254175	3.371587	-4.302302
H	-0.812882	4.604129	-3.125346
C	3.018505	-2.140171	2.800235
H	2.959919	-2.402930	1.740962
C	0.166490	-1.465148	5.189306
H	0.046453	-1.224868	6.239483
C	2.158097	1.492312	0.766793
H	2.671003	0.587134	0.431976
C	3.012512	2.584611	1.020916
C	1.426480	-1.671981	4.666962
H	2.293830	-1.587188	5.310927
C	-3.998359	3.144804	-0.784324
H	-3.907331	4.227980	-0.871195
H	-4.995732	2.930561	-0.379395
H	-3.963616	2.725376	-1.791017
C	0.720768	5.077483	-0.656581
H	1.503271	4.383817	-0.342185
H	1.025824	6.079841	-0.331398
H	0.684698	5.089661	-1.746247
C	1.239610	2.305224	3.316358
C	-2.802496	-2.024819	-1.753615
H	-2.273146	-1.381022	-1.051668
H	-3.596804	-2.546330	-1.213267
H	-3.265623	-1.386394	-2.510570
C	-0.488994	4.955579	1.480218
H	-1.439459	4.895550	2.006197
H	-0.081927	5.958968	1.658699
H	0.194003	4.246291	1.940768
C	3.613182	-2.017008	-1.960865
H	3.115505	-2.756116	-1.333954
H	4.512298	-1.687632	-1.433755
H	3.929168	-2.504324	-2.887486
C	-0.632814	4.740337	-0.026272
C	3.823411	-0.847420	2.922802
H	3.319502	-0.003918	2.455046
H	4.805275	-0.970834	2.458457
H	3.984657	-0.591277	3.973188
C	2.007861	3.415417	3.090171
H	2.146157	4.115072	3.908037
C	-1.666773	5.753143	-0.527255
H	-1.870045	5.676920	-1.595458
H	-1.290893	6.766012	-0.335513
H	-2.615179	5.661223	0.005031
C	-2.594794	-3.993589	-3.298119
H	-3.183505	-3.473649	-4.057820
H	-3.291975	-4.587670	-2.703019
H	-1.915014	-4.678681	-3.810317
C	3.548979	0.266309	-2.943530
H	4.031256	-0.110307	-3.849979
H	4.342096	0.594663	-2.268345
H	2.953211	1.140055	-3.207805
C	2.850020	3.561715	1.967070
H	3.570407	4.372743	1.987172
C	1.099064	-4.787904	1.576595
H	2.108276	-4.799672	1.991235
H	0.947731	-5.724137	1.040008
H	0.401068	-4.761950	2.416153
C	-3.295665	-1.372109	2.739257
H	-3.650268	-1.923964	3.614150
H	-4.098694	-1.382608	2.000289
H	-3.126051	-0.334365	3.032299
C	-2.049261	-2.009693	2.144068
H	-1.829720	-1.490181	1.207789
C	3.753888	-3.257302	3.540248
H	3.949080	-2.970319	4.576450
H	4.719877	-3.450764	3.067784
H	3.189408	-4.190102	3.563139
C	-2.335138	-3.474065	1.811443
H	-1.521447	-3.935343	1.251969
H	-3.239608	-3.548803	1.202638
H	-2.496391	-4.052325	2.725513
H	3.956651	2.582673	0.478539
H	0.975958	2.092470	4.350879

3a

Si	3.218785	-0.080721	0.296747
Si	1.085937	-0.930212	-0.413121
N	-2.020697	1.611674	-0.216826
N	-2.495563	-0.421709	0.386412
N	-0.175234	0.149966	-0.069347
C	-3.695014	0.302318	0.370585
C	-1.423687	0.383130	0.019282
C	-3.398889	1.561605	-0.003863
C	-1.149518	3.769634	0.441314
C	-2.459684	-1.811421	0.675536
C	-0.502815	4.948722	0.087691
C	-2.035572	-2.231307	1.942553
C	-0.853918	2.968523	-1.859995
C	-1.317202	2.796883	-0.550470
C	-0.206228	4.160430	-2.161280
C	-1.621304	3.529894	1.860533
C	-4.273201	2.736446	-0.220183

C	0.783218	-2.613893	0.326155
C	-0.035269	5.141390	-1.199494
C	3.362438	-0.324751	2.222971
C	1.179825	-1.134614	-2.267197
C	2.465763	2.651987	0.734415
C	-2.929910	-2.707036	-0.290351
C	-2.075143	-3.591931	2.219539
C	-1.550231	-1.228766	2.967495
C	3.324710	1.796171	-0.194697
C	-3.389686	-2.235844	-1.652426
C	3.563984	-1.798789	2.582754
C	-1.057592	1.887812	-2.901160
C	2.723960	1.978526	-1.590217
C	4.583844	-1.116952	-0.633003
C	-0.561551	2.787654	2.670037
C	2.050682	0.105085	2.880154
C	0.719142	-3.841917	-0.216572
C	4.209396	-2.602327	-0.646475
C	-2.942514	-4.059594	0.031377
C	4.747109	2.355126	-0.184811
C	-4.991921	-0.316506	0.726219
C	4.497539	0.479169	2.858556
C	-2.049939	4.803810	2.575551
C	-2.504309	1.832724	-3.389939
C	-0.687808	-1.849548	4.056431
C	1.200561	-2.223826	-3.056077
C	-2.237405	-2.273992	-2.648367
C	-2.519849	-4.498279	1.272046
C	-0.120123	2.008912	-4.093618
C	4.722024	-0.701075	-2.099724
C	-2.706824	-0.463182	3.608389
C	5.960371	-0.972925	0.020746
C	0.941446	-4.289310	-1.570964
C	-4.589168	-3.015087	-2.177752
C	1.146793	-3.629167	-2.731837
H	-0.355195	5.723208	0.829788
H	0.176725	4.324593	-3.160078
H	-2.492585	2.872547	1.815728
H	-4.043752	3.556929	0.464663
H	-5.315332	2.454745	-0.074661
H	-4.165483	3.130057	-1.234303
H	0.571435	-2.594763	1.394115
H	0.472743	6.064082	-1.456195
H	1.231912	-0.191555	-2.809369
H	2.437601	3.680736	0.354255
H	2.854336	2.693045	1.753012
H	1.438204	2.289280	0.761763
H	-1.748052	-3.952887	3.185961
H	-0.933195	-0.504634	2.426971
H	-3.694667	-1.190629	-1.562041
H	4.536355	-2.180524	2.270212
H	2.795788	-2.439775	2.144497
H	3.506411	-1.911448	3.673080
H	-0.835700	0.936870	-2.408364
H	2.794971	3.033877	-1.882258
H	1.663317	1.720550	-1.579387
H	3.221736	1.385725	-2.356736
H	0.347254	3.387929	2.760795
H	-0.292241	1.842806	2.196692
H	-0.931810	2.576105	3.676668
H	1.847781	1.167410	2.763399
H	2.092857	-0.109422	3.955668
H	1.197700	-0.437281	2.469217
H	0.482359	-4.662287	0.459621
H	3.306777	-2.788252	-1.229412
H	4.051723	-3.016329	0.347868
H	5.021094	-3.172014	-1.117405
H	-3.290141	-4.779552	-0.699028
H	4.716407	3.424936	-0.428483
H	5.391383	1.875121	-0.922261
H	5.227437	2.256799	0.790762
H	-5.767020	0.447785	0.770227
H	-4.946050	-0.810612	1.699735
H	-5.301251	-1.072184	-0.000292
H	4.360542	1.554487	2.734806
H	5.475568	0.218554	2.451756
H	4.527200	0.278835	3.937544
H	-1.199688	5.457317	2.785767
H	-2.507254	4.554198	3.535520
H	-2.775546	5.374107	1.990502
H	-2.797995	2.786071	-3.838273
H	-3.199347	1.602505	-2.582753
H	-2.611887	1.055105	-4.150469
H	-0.257920	-1.061560	4.677017
H	0.137971	-2.434725	3.646363
H	-1.273112	-2.499640	4.712423
H	1.279357	-2.048223	-4.128997
H	-2.562855	-1.908737	-3.626343
H	-1.857917	-3.291239	-2.768939
H	-1.404733	-1.657005	-2.314200
H	-2.538036	-5.556879	1.505537
H	-0.363254	2.876498	-4.713518
H	-0.217229	1.122868	-4.724844
H	0.924084	2.093078	-3.787182
H	5.102757	0.313559	-2.221271
H	3.775679	-0.783086	-2.636824

70

H	5.435090	-1.374892	-2.591737
H	-2.325351	0.229839	4.362412
H	-3.397055	-1.152300	4.103001
H	-3.265693	0.120246	2.877281
H	6.701964	-1.520357	-0.575152
H	5.988216	-1.391173	1.027569
H	6.290473	0.065706	0.080325
H	0.933889	-5.372122	-1.667682
H	-4.963324	-2.547405	-3.091249
H	-5.405322	-3.045823	-1.451744
H	-4.326136	-4.045267	-2.429364
H	1.277640	-4.272818	-3.597909

TS(1-C')

Si	-0.386982	1.060195	1.009236
Si	-1.272422	2.802596	-0.479649
N	0.039611	-0.268972	-0.000096
F	1.195935	1.778909	4.374141
F	3.455980	3.396908	-0.266967
N	0.447190	-2.370339	-1.001267
N	0.369334	-2.392021	1.170037
C	0.470436	-2.003727	2.534646
C	0.263531	-1.532006	0.085021
C	-0.822604	2.564708	-2.352584
C	0.631153	-3.693256	-0.599437
C	-0.564843	-2.281017	-3.202621
C	-0.466984	-1.909068	-4.538910
H	-1.271387	-2.148578	-5.222350
C	-3.563235	2.870827	1.270534
H	-2.916874	2.413562	2.025057
H	-4.590093	2.539602	1.472120
H	-3.538983	3.950931	1.410894
C	-1.796247	-2.986218	-2.673895
H	-1.480350	-3.659535	-1.874019
C	0.498975	-1.949349	-2.357335
C	-3.170304	2.441707	-0.144411
C	-1.451940	1.284581	-2.898897
H	-1.198663	0.424042	-2.279744
H	-1.057655	1.091020	-3.903767
H	-2.537761	1.354709	-2.985907
C	1.728737	-2.043257	3.153522
C	0.640696	-1.226038	-5.006677
H	0.693916	-0.935563	-6.049693
C	0.572490	-3.709028	0.747001
C	1.680743	-0.909237	-4.150465
H	2.538909	-0.370674	-4.530983
C	1.638808	-1.274246	-2.810883
C	0.690212	2.370672	-2.460807
H	1.263424	3.230763	-2.116110
H	0.960542	2.185818	-3.508579
H	0.994728	1.496234	-1.882857
C	-0.693669	-1.642377	3.225778
C	1.619404	1.340758	2.103352
H	1.529923	0.282282	2.309726
C	-3.445172	0.940786	-0.218668
H	-3.274760	0.532466	-1.210382
H	-4.491858	0.746543	0.050023
H	-2.826146	0.377492	0.487546
C	2.795316	-0.984576	-1.878119
H	2.352233	-0.682408	-0.925891
C	-0.567370	-1.288781	4.562760
H	-1.443457	-0.983795	5.119212
C	0.902038	-4.789383	-1.557487
H	0.067795	-4.973930	-2.238003
H	1.106171	-5.711215	-1.014120
H	1.772897	-4.562357	-2.177896
C	-1.255073	3.723629	-3.251162
H	-2.333437	3.891671	-3.219954
H	-0.991549	3.491473	-4.291485
H	-0.764686	4.664136	-2.998475
C	2.998049	-2.449161	2.428830
H	2.718331	-2.913700	1.481110
C	0.665503	-1.304686	5.191123
H	0.743767	-1.011325	6.231381
C	2.240166	1.784047	0.906400
H	2.303366	1.140200	0.041887
C	2.867910	3.019123	0.879869
C	1.797500	-1.682751	4.496036
H	2.756581	-1.688442	4.999871
C	-4.103731	3.128229	-1.141910
H	-3.986313	4.212060	-1.155494
H	-5.146756	2.913713	-0.873580
H	-3.952128	2.761991	-2.158711
C	0.473550	5.089686	-0.444732
H	1.287790	4.392500	-0.268266
H	0.745024	6.040080	0.032071
H	0.414788	5.271873	-1.517808
C	1.727075	2.200963	3.222444
C	-2.755843	-1.988621	-2.036144
H	-2.264258	-1.429036	-1.240251
H	-3.620464	-2.505346	-1.611485
H	-3.115681	-1.269919	-2.776207
C	-0.687891	4.584515	1.661972
H	-1.600215	4.301828	2.185444
H	-0.402899	5.586059	2.010532
H	0.098535	3.898303	1.975525

C	3.634093	-2.237027	-1.625328
H	3.052778	-3.028837	-1.152711
H	4.473411	-2.001843	-0.966272
H	4.041289	-2.622188	-2.564102
C	-0.849725	4.598433	0.140698
C	3.880805	-1.249331	2.093329
H	3.403588	-0.576261	1.382852
H	4.821179	-1.590081	1.653005
H	4.117746	-0.671495	2.990341
C	2.349393	3.411959	3.173630
H	2.386705	4.026437	4.064299
C	-1.911461	5.635684	-0.231384
H	-2.083996	5.683100	-1.308688
H	-1.570953	6.628806	0.089431
H	-2.869659	5.453989	0.254974
C	-2.505281	-3.830863	-3.722631
H	-2.975589	-3.212585	-4.491027
H	-3.298250	-4.416153	-3.252345
H	-1.819567	-4.521802	-4.218951
C	3.694971	0.150027	-2.345448
H	4.275202	-0.132006	-3.228202
H	4.409556	0.398477	-1.557441
H	3.129517	1.052438	-2.580233
C	2.942138	3.843995	1.973859
H	3.440073	4.801214	1.903215
C	0.682384	-4.838313	1.697876
H	-0.104580	-4.798392	2.453886
H	1.636606	-4.842542	2.228450
H	0.590466	-5.783118	1.163320
C	-3.058088	-0.742499	3.185950
H	-3.364555	-1.092645	4.175298
H	-3.955845	-0.691523	2.566944
H	-2.652780	0.266938	3.280144
C	-2.043669	-1.675598	2.544477
H	-1.891174	-1.332287	1.517473
C	3.807552	-3.467712	3.228597
H	4.265994	-3.009352	4.108071
H	4.616316	-3.867326	2.612596
H	3.195801	-4.302642	3.575662
C	-2.597891	-3.097714	2.473395
H	-1.950220	-3.756362	1.894008
H	-3.579888	-3.092818	1.993805
H	-2.712773	-3.520439	3.475218

C'

Si	-0.266958	1.097515	0.959929
Si	-1.258040	2.821481	-0.460617
N	0.046563	-0.289305	0.007245
F	0.977813	1.827809	4.334831
F	3.477067	3.345683	-0.230702
N	0.435206	-2.389294	-1.006631
N	0.378975	-2.408620	1.166853
C	0.487663	-2.013891	2.528406
C	0.267094	-1.550871	0.081821
C	-0.793963	2.568339	-2.328089
C	0.620009	-3.712983	-0.603732
C	-0.575010	-2.286290	-3.208619
C	-0.476854	-1.905700	-4.542465
H	-1.282340	-2.138339	-5.227049
C	-3.545093	2.856282	1.284265
H	-2.888469	2.417306	2.040898
H	-4.564195	2.505112	1.489582
H	-3.543010	3.937731	1.416849
C	-1.809469	-2.989251	-2.684260
H	-1.497004	-3.667195	-1.887072
C	0.490159	-1.964074	-2.361191
C	-3.145605	2.427700	-0.128370
C	-1.419072	1.286115	-2.875355
H	-1.166511	0.424896	-2.256936
H	-1.020896	1.094945	-3.878818
H	-2.504538	1.354240	-2.966592
C	1.748166	-2.053182	3.141926
C	0.632617	-1.222759	-5.006103
H	0.686259	-0.925300	-6.047155
C	0.573997	-3.727078	0.742935
C	1.674213	-0.915464	-4.148255
H	2.534265	-0.377738	-4.525610
C	1.632414	-1.290075	-2.811231
C	0.719248	2.386210	-2.444009
H	1.289197	3.243141	-2.086724
H	0.984221	2.219492	-3.495953
H	1.033737	1.506461	-1.880764
C	-0.670499	-1.636494	3.220261
C	1.459973	1.330969	2.080392
H	1.539361	0.280883	2.354134
C	-3.409839	0.925786	-0.206592
H	-3.247599	0.525314	-1.202638
H	-4.453197	0.725543	0.069413
H	-2.779448	0.363444	0.487857
C	2.792508	-1.012960	-1.879083
H	2.355279	-0.710816	-0.924244
C	-0.536927	-1.273964	4.554420
H	-1.408345	-0.956884	5.111521
C	0.878614	-4.810654	-1.563367
H	0.037201	-4.993528	-2.235477
H	1.085443	-5.732542	-1.021156

H	1.744150	-4.586721	-2.192357
C	-1.236815	3.726311	-3.224550
H	-2.315168	3.892809	-3.186996
H	-0.980272	3.490525	-4.265405
H	-0.745136	4.667737	-2.978449
C	3.014124	-2.444957	2.405803
H	2.731253	-2.904233	1.456345
C	0.697288	-1.298068	5.179715
H	0.781036	-0.998926	6.217851
C	2.169503	1.772707	0.893560
H	2.324960	1.098731	0.064823
C	2.833202	2.996149	0.897779
C	1.824203	-1.688212	4.482693
H	2.785572	-1.694817	4.982196
C	-4.082077	3.107672	-1.129102
H	-3.975074	4.192412	-1.142760
H	-5.123040	2.883691	-0.862348
H	-3.925762	2.741962	-2.145239
C	0.475993	5.107416	-0.417867
H	1.291278	4.419669	-0.210686
H	0.731593	6.068742	0.044716
H	0.433434	5.267922	-1.495064
C	1.573732	2.227661	3.203418
C	-2.764125	-1.989400	-2.043028
H	-2.270671	-1.439751	-1.241372
H	-3.634447	-2.502147	-1.625199
H	-3.115540	-1.262678	-2.779432
C	-0.719021	4.633420	1.679326
H	-1.639037	4.357695	2.192516
H	-0.446785	5.644183	2.010206
H	0.067844	3.963288	2.022648
C	3.621016	-2.273576	-1.632874
H	3.033763	-3.062840	-1.163347
H	4.462446	-2.047869	-0.973245
H	4.024586	-2.657636	-2.573660
C	-0.853446	4.617960	0.155954
C	3.876918	-1.228723	2.076504
H	3.375255	-0.541220	1.396699
H	4.809166	-1.548265	1.604141
H	4.131817	-0.671481	2.981664
C	2.243698	3.399251	3.173514
H	2.273533	4.012634	4.065571
C	-1.920820	5.638543	-0.247767
H	-2.086705	5.665180	-1.326594
H	-1.588371	6.638963	0.056947
H	-2.880670	5.459629	0.236947
C	-2.521696	-3.825808	-3.737303
H	-2.989439	-3.201941	-4.502778
H	-3.317129	-4.410262	-3.270110
H	-1.838597	-4.516962	-4.236847
C	3.701687	0.115340	-2.343210
H	4.280042	-0.169548	-3.226346
H	4.417190	0.356296	-1.553862
H	3.144704	1.023535	-2.575617
C	2.898774	3.819545	1.984560
H	3.427438	4.760668	1.933242
C	0.689109	-4.854429	1.695174
H	-0.095097	-4.814209	2.454187
H	1.645534	-4.855448	2.221939
H	0.596691	-5.800554	1.163058
C	-3.022380	-0.704490	3.174941
H	-3.331712	-1.037982	4.169047
H	-3.920652	-0.646811	2.557485
H	-2.604184	0.300638	3.259425
C	-2.022637	-1.659921	2.542703
H	-1.869945	-1.334457	1.510225
C	3.840766	-3.461498	3.189509
H	4.294631	-3.008507	4.074121
H	4.653762	-3.840964	2.566342
H	3.242314	-4.310253	3.526185
C	-2.595025	-3.075680	2.494215
H	-1.953968	-3.751378	1.927014
H	-3.576431	-3.067346	2.013406
H	-2.715250	-3.480170	3.502914

TS(C'-Cb)

Si	-0.232052	1.112705	0.936032
Si	-1.255237	2.827561	-0.458131
N	0.052864	-0.289697	0.003699
F	0.912121	1.848769	4.342235
F	3.484512	3.327477	-0.200468
N	0.435654	-2.390117	-1.011150
N	0.386376	-2.408310	1.162824
C	0.493557	-2.015169	2.524916
C	0.272384	-1.551102	0.077596
C	-0.783938	2.567378	-2.322752
C	0.620497	-3.713994	-0.607915
C	-0.581689	-2.292469	-3.209709
C	-0.488412	-1.915682	-4.544944
H	-1.295733	-2.151449	-5.226280
C	-3.543365	2.855445	1.282952
H	-2.884854	2.422888	2.041610
H	-4.560352	2.498484	1.488279
H	-3.548230	3.937327	1.412122
C	-1.814035	-2.994222	-2.678823
H	-1.498429	-3.672571	-1.883233

C	0.485981	-1.966866	-2.366554
C	-3.140041	2.425676	-0.128053
C	-1.408002	1.284567	-2.870249
H	-1.157788	0.423592	-2.250617
H	-1.006766	1.092565	-3.872245
H	-2.493118	1.353105	-2.965120
C	1.752704	-2.057672	3.140700
C	0.618730	-1.232779	-5.014186
H	0.668706	-0.938410	-6.056297
C	0.579333	-3.727178	0.738778
C	1.662538	-0.921486	-4.160505
H	2.520757	-0.383875	-4.542117
C	1.625907	-1.292565	-2.822312
C	0.729581	2.387193	-2.437300
H	1.298408	3.244291	-2.078748
H	0.994361	2.221842	-3.489446
H	1.045981	1.508031	-1.874426
C	-0.664719	-1.634756	3.214746
C	1.420599	1.328709	2.097068
H	1.525241	0.284885	2.389958
C	-3.400237	0.923275	-0.206113
H	-3.237858	0.523750	-1.202456
H	-4.443081	0.720882	0.069982
H	-2.767879	0.362638	0.487274
C	2.788498	-1.010421	-1.894708
H	2.352695	-0.698635	-0.942334
C	-0.532651	-1.272759	4.549160
H	-1.403960	-0.952815	5.104744
C	0.877499	-4.811503	-1.568204
H	0.032662	-4.999348	-2.234661
H	1.092413	-5.731926	-1.026685
H	1.737789	-4.583606	-2.202916
C	-1.226747	3.724477	-3.220822
H	-2.305063	3.891394	-3.184024
H	-0.970026	3.486424	-4.260993
H	-0.734515	4.666010	-2.976352
C	3.019800	-2.443474	2.404128
H	2.738820	-2.902692	1.454065
C	0.700112	-1.301308	5.177115
H	0.782654	-1.002519	6.215429
C	2.149884	1.766885	0.909956
H	2.345415	1.077473	0.102527
C	2.822722	2.989167	0.921626
C	1.827140	-1.694567	4.482059
H	2.787661	-1.703414	4.983109
C	-4.075918	3.102434	-1.131897
H	-3.972321	4.187458	-1.146187
H	-5.116644	2.875452	-0.867270
H	-3.916135	2.736151	-2.147250
C	0.479646	5.109927	-0.410679
H	1.293759	4.424387	-0.191316
H	0.730618	6.074788	0.046814
H	0.444773	5.262505	-1.489272
C	1.526432	2.239866	3.216168
C	-2.763513	-1.992791	-2.032510
H	-2.264087	-1.442505	-1.235016
H	-3.631522	-2.503941	-1.607968
H	-3.119136	-1.266648	-2.767499
C	-0.730078	4.647615	1.681159
H	-1.654943	4.379461	2.189448
H	-0.456351	5.659575	2.006838
H	0.051910	3.977564	2.035229
C	3.615161	-2.270445	-1.639250
H	3.027571	-3.056257	-1.164491
H	4.456753	-2.040803	-0.981228
H	4.018601	-2.661273	-2.577337
C	-0.853591	4.623551	0.157108
C	3.873491	-1.220288	2.077137
H	3.362412	-0.530709	1.406459
H	4.804385	-1.530578	1.596030
H	4.131123	-0.668002	2.984571
C	2.205741	3.402680	3.188595
H	2.229159	4.020080	4.078152
C	-1.920147	5.640525	-0.258447
H	-2.081378	5.661214	-1.338048
H	-1.589703	6.642661	0.042325
H	-2.881901	5.463398	0.223295
C	-2.533286	-3.830038	-3.727589
H	-3.003870	-3.205859	-4.491065
H	-3.327257	-4.412791	-3.255808
H	-1.854024	-4.522835	-4.230061
C	3.699954	0.111486	-2.369730
H	4.274640	-0.182101	-3.252435
H	4.418506	0.355532	-1.584147
H	3.145725	1.020095	-2.606664
C	2.880039	3.815910	2.002849
H	3.413919	4.754109	1.954719
C	0.694989	-4.853641	1.691747
H	1.644020	-4.843202	2.231540
H	0.621154	-5.800249	1.157742
H	-0.099595	-4.823470	2.440538
C	-3.013414	-0.695190	3.166830
H	-3.325115	-1.030226	4.159645
H	-3.910623	-0.633462	2.548281
H	-2.593111	0.308752	3.255170
C	-2.015193	-1.651668	2.533766

74

H	-1.858645	-1.323084	1.502912
C	3.852845	-3.456548	3.185161
H	4.302378	-3.003768	4.072067
H	4.669367	-3.827738	2.561649
H	3.260349	-4.311166	3.517699
C	-2.592022	-3.065297	2.478366
H	-1.951110	-3.740866	1.910858
H	-3.571750	-3.052264	1.994238
H	-2.716815	-3.472982	3.485222

Cb

Si	0.210830	1.274763	0.607710
Si	-1.207493	2.870001	-0.484733
N	0.067003	-0.290796	0.004091
F	0.492206	2.007945	4.430799
F	3.519715	3.108004	0.011662
N	0.483174	-2.366315	-1.041155
N	0.461900	-2.409519	1.135065
C	0.515791	-2.045854	2.509098
C	0.325627	-1.539762	0.057919
C	-0.840035	2.568836	-2.367596
C	0.682568	-3.693311	-0.655796
C	-0.611543	-2.293504	-3.198504
C	-0.572011	-1.929228	-4.539728
H	-1.396575	-2.189304	-5.191030
C	-3.341122	2.894917	1.417652
H	-2.600304	2.525673	2.132424
H	-4.318410	2.500298	1.721288
H	-3.388540	3.979906	1.509976
C	-1.812270	-3.010156	-2.616823
H	-1.458689	-3.674010	-1.824881
C	0.478101	-1.938738	-2.394926
C	-3.039596	2.441769	-0.011313
C	-1.490688	1.275026	-2.856770
H	-1.197620	0.422328	-2.244356
H	-1.153102	1.071932	-3.879506
H	-2.579980	1.337716	-2.881755
C	1.745494	-2.095262	3.180025
C	0.504794	-1.229446	-5.052683
H	0.515668	-0.947614	-6.099451
C	0.656938	-3.722751	0.689907
C	1.566547	-0.881773	-4.235798
H	2.397619	-0.327119	-4.651268
C	1.583226	-1.236104	-2.892193
C	0.665757	2.393254	-2.575332
H	1.253508	3.254073	-2.259653
H	0.863475	2.220909	-3.640584
H	1.033079	1.520163	-2.033463
C	-0.669485	-1.669538	3.157624
C	1.118289	1.324920	2.268236
H	1.185879	0.313928	2.661114
C	-3.262023	0.933006	-0.051176
H	-3.177279	0.527797	-1.054938
H	-4.270680	0.704993	0.315364
H	-2.550201	0.401727	0.580905
C	2.756648	-0.888847	-1.999322
H	2.329555	-0.511165	-1.066623
C	-0.588155	-1.296185	4.492019
H	-1.479017	-0.971665	5.012288
C	0.950969	-4.774145	-1.631272
H	0.125324	-4.932239	-2.328544
H	1.133812	-5.709262	-1.103215
H	1.835722	-4.548189	-2.233052
C	-1.334337	3.707541	-3.262036
H	-2.406211	3.887412	-3.155732
H	-1.151300	3.439541	-4.310094
H	-0.814861	4.647968	-3.075894
C	3.044310	-2.496854	2.513278
H	2.814467	-2.888192	1.519968
C	0.619582	-1.315729	5.168253
H	0.662386	-1.003360	6.204880
C	2.019857	1.608945	1.028377
H	2.656075	0.790674	0.693485
C	2.753026	2.862231	1.093677
C	1.768652	-1.721867	4.520958
H	2.709675	-1.732063	5.057859
C	-4.059028	3.084875	-0.954298
H	-3.982216	4.171699	-0.987480
H	-5.072397	2.837966	-0.613364
H	-3.964249	2.710357	-1.975035
C	0.574955	5.110999	-0.568247
H	1.388721	4.440610	-0.294620
H	0.833233	6.105863	-0.185777
H	0.539011	5.182122	-1.655235
C	1.209755	2.311153	3.333826
C	-2.756220	-2.018270	-1.946835
H	-2.236649	-1.445084	-1.179075
H	-3.593118	-2.542140	-1.477622
H	-3.159886	-1.311729	-2.676412
C	-0.631330	4.811030	1.555122
H	-1.578036	4.678918	2.075309
H	-0.263167	5.815701	1.798529
H	0.081088	4.103491	1.972625
C	3.601298	-2.119445	-1.667677
H	3.028688	-2.886582	-1.146506
H	4.437677	-1.834972	-1.024214

H	4.013842	-2.558763	-2.580136
C	-0.763497	4.683260	0.037991
C	3.972268	-1.299670	2.331429
H	3.509300	-0.516892	1.733875
H	4.895349	-1.608484	1.834402
H	4.239499	-0.860861	3.295917
C	1.959026	3.413860	3.304312
H	1.960831	4.091586	4.147793
C	-1.825744	5.686765	-0.421486
H	-2.015235	5.649897	-1.495180
H	-1.478872	6.700045	-0.184068
H	-2.775964	5.546835	0.095934
C	-2.554430	-3.870079	-3.629466
H	-3.061110	-3.263485	-4.384005
H	-3.321753	-4.459224	-3.122759
H	-1.882383	-4.559023	-4.146714
C	3.654234	0.204481	-2.560585
H	4.218593	-0.144970	-3.429753
H	4.378334	0.505795	-1.801056
H	3.091357	1.092446	-2.848961
C	2.747317	3.714793	2.118755
H	3.322175	4.629939	2.063344
C	0.770525	-4.868101	1.620866
H	1.744041	-4.913910	2.111483
H	0.625183	-5.801079	1.077226
H	0.014303	-4.813284	2.407002
C	-3.050866	-0.809642	3.082585
H	-3.374723	-1.219593	4.042987
H	-3.931395	-0.753303	2.440724
H	-2.690551	0.207458	3.249292
C	-1.993248	-1.683385	2.426601
H	-1.807893	-1.283384	1.426806
C	3.776843	-3.585422	3.296649
H	4.169004	-3.195294	4.238835
H	4.627227	-3.954459	2.718722
H	3.132072	-4.432005	3.537934
C	-2.521189	-3.107542	2.258266
H	-1.841129	-3.724745	1.670741
H	-3.484293	-3.091981	1.741814
H	-2.667495	-3.583933	3.231622

TS(Cb_3b)

Si	0.320833	1.307300	0.603269
Si	-1.134719	2.911502	-0.456762
N	0.046551	-0.253852	0.022176
F	0.830155	2.085675	4.576972
F	4.152302	2.582656	0.300349
N	0.569815	-2.296722	-1.053852
N	0.608466	-2.350020	1.120916
C	0.465595	-2.038131	2.502146
C	0.392256	-1.485352	0.052796
C	-0.892069	2.548778	-2.349219
C	0.853672	-3.611435	-0.681254
C	-0.715343	-2.292893	-3.104796
C	-0.804336	-1.963720	-4.452883
H	-1.681867	-2.251030	-5.018224
C	-3.168580	3.055041	1.561060
H	-2.393345	2.719933	2.256124
H	-4.129576	2.676750	1.931372
H	-3.216112	4.143265	1.603360
C	-1.843870	-3.020936	-2.406036
H	-1.411626	-3.604587	-1.590095
C	0.435194	-1.899089	-2.411893
C	-2.941462	2.534375	0.140955
C	-1.609570	1.264329	-2.762323
H	-1.299228	0.419852	-2.147728
H	-1.346454	1.025762	-3.799541
H	-2.695800	1.356758	-2.717023
C	1.605806	-1.950949	3.311314
C	0.213004	-1.269685	-5.081471
H	0.125036	-1.016804	-6.131998
C	0.874535	-3.647008	0.663302
C	1.342565	-0.893034	-4.375699
H	2.127455	-0.346166	-4.881508
C	1.482780	-1.204069	-3.028477
C	0.593929	2.310527	-2.622629
H	1.228753	3.151392	-2.346351
H	0.736664	2.116260	-3.692736
H	0.947997	1.427809	-2.087339
C	-0.828117	-1.864106	3.022029
C	0.835459	1.321529	2.383922
H	0.702577	0.357420	2.873016
C	-3.174382	1.027478	0.188602
H	-3.092611	0.560709	-0.788830
H	-4.182663	0.827488	0.571954
H	-2.464359	0.530004	0.850814
C	2.723814	-0.816957	-2.252694
H	2.371591	-0.425718	-1.294845
C	-0.948231	-1.555743	4.370588
H	-1.929204	-1.392626	4.795902
C	1.101997	-4.679877	-1.675386
H	0.222308	-4.884157	-2.290651
H	1.383839	-5.600891	-1.166828
H	1.911103	-4.407472	-2.357636
C	-1.385996	3.675049	-3.257874
H	-2.443447	3.901866	-3.105287

H	-1.265360	3.365940	-4.303680
H	-0.820962	4.598787	-3.128581
C	3.015170	-2.128920	2.790875
H	2.955110	-2.396049	1.732685
C	0.167620	-1.446423	5.183445
H	0.050627	-1.191196	6.229994
C	2.152934	1.491821	0.744381
H	2.703296	0.616352	0.392273
C	2.998908	2.578864	1.024585
C	1.426603	-1.652929	4.659372
H	2.294954	-1.557224	5.300236
C	-4.002729	3.148731	-0.774878
H	-3.910407	4.231770	-0.862295
H	-4.998818	2.936171	-0.366298
H	-3.972182	2.728908	-1.781501
C	0.723843	5.071839	-0.671876
H	1.509510	4.377922	-0.366175
H	1.032839	6.073306	-0.348237
H	0.680276	5.084540	-1.761006
C	1.228619	2.316702	3.296628
C	-2.804647	-2.026322	-1.763999
H	-2.279773	-1.383649	-1.057582
H	-3.600153	-2.550995	-1.228540
H	-3.266069	-1.386705	-2.520968
C	-0.466659	4.948982	1.474523
H	-1.407708	4.868125	2.014145
H	-0.076079	5.959090	1.651219
H	0.236323	4.251481	1.922460
C	3.621743	-2.019762	-1.961812
H	3.126968	-2.767575	-1.342680
H	4.519132	-1.691140	-1.431583
H	3.939778	-2.496280	-2.893247
C	-0.624660	4.735051	-0.030570
C	3.818802	-0.834858	2.906834
H	3.309520	0.004957	2.438322
H	4.798386	-0.954894	2.437512
H	3.983299	-0.574819	3.955602
C	2.049237	3.388178	3.113001
H	2.183133	4.061268	3.951357
C	-1.661246	5.749848	-0.522423
H	-1.874309	5.672341	-1.588628
H	-1.281763	6.762170	-0.335660
H	-2.604854	5.660102	0.018520
C	-2.588674	-3.991092	-3.312098
H	-3.175050	-3.470325	-4.073023
H	-3.287506	-4.586995	-2.720796
H	-1.906323	-4.674496	-3.823061
C	3.549231	0.275797	-2.916692
H	4.046837	-0.092114	-3.818393
H	4.326728	0.613561	-2.228623
H	2.946839	1.143313	-3.186093
C	2.897186	3.526523	1.997505
H	3.649230	4.306257	2.011107
C	1.095366	-4.788935	1.578168
H	2.106079	-4.800483	1.989179
H	0.941130	-5.726175	1.044195
H	0.400476	-4.759860	2.420068
C	-3.301496	-1.378216	2.742228
H	-3.653053	-1.926862	3.620247
H	-4.106144	-1.393556	2.005023
H	-3.133241	-0.339199	3.031351
C	-2.055077	-2.016485	2.147573
H	-1.840035	-1.503244	1.206779
C	3.753525	-3.242406	3.533208
H	3.947724	-2.952695	4.568760
H	4.719778	-3.434908	3.060962
H	3.190714	-4.176151	3.558079
C	-2.338795	-3.483650	1.825424
H	-1.525522	-3.947161	1.267255
H	-3.244486	-3.564415	1.219150
H	-2.496781	-4.056009	2.743700

3b

Si	5.428078	5.678665	14.451056
Si	4.021893	7.258916	13.310775
N	5.327493	4.129965	13.786366
F	5.152621	6.107419	18.542571
F	9.280724	7.136871	14.635153
N	5.805226	2.054001	12.768688
N	5.680030	2.021882	14.936859
C	5.596466	2.374782	16.309881
C	5.586010	2.882715	13.855337
C	4.211730	6.950672	11.402064
C	6.022610	0.734605	13.170406
C	4.599944	2.089315	10.671300
C	4.563603	2.441186	9.326689
H	3.704981	2.171845	8.724533
C	1.972967	7.527252	15.318258
H	2.690401	7.111993	16.029166
H	0.969380	7.244077	15.660381
H	2.036944	8.614043	15.376335
C	3.438003	1.370015	11.323562
H	3.835125	0.764781	12.141456
C	5.729365	2.459051	11.410566
C	2.184372	6.996929	13.898187
C	3.455844	5.689988	10.985763

H	3.764245	4.832573	11.583678
H	3.690084	5.456753	9.939752
H	2.373159	5.802367	11.058207
C	6.777892	2.432192	17.055507
C	5.608604	3.138864	8.748772
H	5.561807	3.409457	7.700021
C	5.943311	0.712957	14.514923
C	6.710678	3.501768	9.503823
H	7.512384	4.060191	9.038346
C	6.797785	3.168147	10.850176
C	5.681605	6.671722	11.081949
H	6.346727	7.491783	11.350149
H	5.791170	6.490189	10.005504
H	6.013921	5.765473	11.592088
C	4.335116	2.581361	16.883072
C	5.033306	5.732887	16.270811
H	4.047511	5.366167	16.546393
C	1.878863	5.500122	13.942736
H	1.931120	5.028985	12.963945
H	0.866111	5.342806	14.335102
H	2.570441	4.967139	14.597062
C	7.999691	3.550690	11.688389
H	7.608104	3.902245	12.647451
C	4.284375	2.869502	18.240855
H	3.329827	3.052576	18.715835
C	6.313421	-0.346803	12.202813
H	5.480393	-0.526899	11.518692
H	6.521324	-1.274507	12.734481
H	7.183756	-0.104945	11.587143
C	3.723775	8.110956	10.534589
H	2.674311	8.352596	10.713988
H	3.820100	7.834424	9.476770
H	4.305938	9.021464	10.682467
C	8.129724	2.193504	16.418880
H	7.975450	1.582328	15.526759
C	5.441565	2.948614	18.996004
H	5.379823	3.191467	20.050234
C	7.176637	6.289692	14.237179
H	7.552351	6.269805	13.216652
C	8.062691	6.758631	15.115244
C	6.673737	2.733107	18.409667
H	7.569985	2.797349	19.014207
C	1.153736	7.665684	12.986748
H	1.300190	8.743917	12.907641
H	0.147890	7.500309	13.394052
H	1.163362	7.251765	11.977385
C	5.956038	9.392413	13.060441
H	6.748574	8.668367	13.257296
H	6.311240	10.366750	13.419328
H	5.825455	9.475470	11.981334
C	5.743510	6.156088	17.316106
C	2.471128	2.367059	11.956008
H	2.985029	3.010452	12.671004
H	1.668854	1.840837	12.479810
H	2.019247	3.006675	11.193640
C	4.979152	9.118492	15.287413
H	4.128007	8.882147	15.924326
H	5.300618	10.139518	15.529741
H	5.795576	8.450333	15.562202
C	8.905430	2.351369	11.966149
H	8.393673	1.573601	12.532844
H	9.774320	2.668094	12.548442
H	9.267257	1.916127	11.030481
C	4.659536	9.038276	13.791701
C	8.746117	3.505291	15.949865
H	8.089806	4.020772	15.249816
H	9.702739	3.324841	15.452484
H	8.920243	4.177253	16.793523
C	7.062226	6.721026	17.446194
H	7.299314	6.983669	18.471692
C	3.631657	10.123752	13.462557
H	3.354481	10.133131	12.406920
H	4.057364	11.107215	13.699122
H	2.717325	10.021430	14.048018
C	2.705792	0.427062	10.379186
H	2.157412	0.969098	9.604865
H	1.974673	-0.162333	10.937004
H	3.392442	-0.263410	9.883641
C	8.822449	4.683889	11.091235
H	9.355958	4.365056	10.191521
H	9.572252	5.011100	11.814639
H	8.206060	5.546343	10.831871
C	8.019474	6.976187	16.538042
H	8.934105	7.416737	16.920102
C	6.077150	-0.407523	15.473202
H	6.969201	-0.312672	16.097586
H	6.139185	-1.351945	14.933885
H	5.219195	-0.455837	16.148018
C	1.879068	3.181798	16.686813
H	1.535634	2.638490	17.571117
H	1.049560	3.210584	15.978264
H	2.096895	4.209389	16.985086
C	3.076812	2.497156	16.044544
H	3.292887	3.014035	15.104260
C	9.089710	1.438233	17.329398
H	9.406421	2.046554	18.179985

78

H	9.991313	1.167533	16.775358
H	8.642814	0.521885	17.722600
C	2.708991	1.053718	15.701785
H	3.474979	0.566010	15.099442
H	1.776642	1.031937	15.132031
H	2.559804	0.467844	16.612966

TS(1-Cc)

Si	1.302075	0.001519	-0.299969
Si	2.436574	0.936968	1.655059
F	1.144445	-4.081906	2.302407
F	2.123718	-5.721340	1.312110
F	3.725056	-0.175414	-2.898103
F	4.182866	-1.992903	-3.950144
N	-2.285644	1.101496	-1.144081
F	2.165394	-1.221683	-3.941426
N	-2.394383	-1.053850	-0.884417
F	3.270660	-4.346992	2.506207
N	-0.365480	0.050119	-0.198140
C	-0.982621	2.947861	-2.035818
C	-2.311359	-2.051252	1.802461
H	-1.772627	-1.111395	1.648093
C	4.858982	1.349525	0.157958
H	4.286791	1.116274	-0.743258
H	5.894054	1.036326	-0.025501
H	4.869944	2.431683	0.289815
C	-1.544299	0.022374	-0.704746
C	-3.626475	-0.635291	-1.401197
C	-2.049265	-2.417986	-0.695267
C	-1.995852	-2.929437	0.609036
C	-4.749607	-1.575337	-1.625053
H	-4.579325	-2.246746	-2.469857
H	-5.665270	-1.017571	-1.817969
H	-4.914435	-2.202764	-0.746417
C	1.521802	-2.708626	-0.039337
H	0.555765	-2.682549	0.443935
C	-3.552807	0.698385	-1.574772
C	1.721469	-1.930592	-1.236295
H	0.842148	-1.798328	-1.855061
C	-2.133934	4.624636	-0.109170
H	-2.566888	5.288148	0.628384
C	-1.992999	-2.678655	-3.237966
H	-2.670901	-1.825478	-3.191756
C	2.253410	-4.422775	1.633886
C	0.915193	2.561515	-3.682605
H	1.369864	1.787832	-4.303820
H	1.640649	2.838688	-2.916446
H	0.735959	3.431947	-4.319881
C	-1.645116	-4.265072	0.760003
H	-1.570277	-4.691467	1.750721
C	-1.455625	-4.536726	-1.617302
H	-1.250399	-5.174688	-2.467720
C	-1.822002	-3.210641	-1.827057
C	-4.531688	1.650879	-2.147121
H	-4.824624	2.427350	-1.436808
H	-5.428348	1.116341	-2.457855
H	-4.120234	2.160049	-3.022674
C	-4.418202	3.720457	1.459891
H	-5.160063	3.218680	2.084802
H	-4.944955	4.238738	0.655128
H	-3.929944	4.473259	2.083737
C	-3.423828	2.700666	0.923480
H	-4.001655	1.913796	0.433095
C	2.385738	-1.096478	3.656540
H	2.160213	-1.784168	2.840478
H	1.922025	-1.501883	4.564073
H	3.464281	-1.097355	3.815846
C	-3.800311	-1.718803	1.898118
H	-4.152272	-1.138439	1.046066
H	-3.987109	-1.126445	2.797016
H	-4.397263	-2.632317	1.969110
C	-1.885204	2.461687	-1.083706
C	5.176248	1.000567	2.595012
H	5.060313	2.049222	2.872572
H	6.235219	0.839121	2.357184
H	4.951269	0.392966	3.473000
C	4.556272	-0.878679	1.105697
H	4.240400	-1.528930	1.918859
H	5.624865	-1.059824	0.934097
H	4.032167	-1.191052	0.204684
C	2.055811	2.831931	1.411166
C	2.072662	3.191898	-0.074595
H	3.022236	2.983054	-0.563599
H	1.859952	4.261694	-0.193041
H	1.287819	2.657514	-0.616006
C	3.256943	-1.411345	-3.176840
C	-0.677208	4.303496	-1.992814
H	0.024522	4.716214	-2.705830
C	-2.623855	-3.709596	-4.168133
H	-1.931677	-4.522334	-4.399866
H	-2.893194	-3.236573	-5.115071
H	-3.524869	-4.151216	-3.736073
C	-1.842973	-2.636342	3.125692
H	-2.408880	-3.533762	3.390911
H	-2.000917	-1.906126	3.921142
H	-0.783489	-2.890747	3.112861

C	-1.372481	1.702027	-4.189602
H	-1.711801	2.615973	-4.684751
H	-2.245807	1.169345	-3.811932
H	-0.896798	1.068267	-4.941722
C	-2.678452	2.028360	2.072961
H	-2.116210	2.763520	2.653092
H	-1.974299	1.277847	1.712084
H	-3.386950	1.536646	2.744299
C	-2.469601	3.275756	-0.104916
C	3.892180	-3.065056	-1.458726
H	4.809614	-3.216736	-2.014247
C	-0.376047	2.030274	-3.078163
H	-0.123662	1.094511	-2.569234
C	0.652603	3.170668	1.906431
H	-0.099362	2.552328	1.417020
H	0.424338	4.214679	1.660071
H	0.547535	3.059330	2.986290
C	4.328725	0.603063	1.384353
C	1.829721	0.299620	3.384409
C	3.049502	3.736324	2.142079
H	3.097991	3.528021	3.212328
H	2.733888	4.781005	2.025280
H	4.059857	3.660498	1.739473
C	0.307813	0.169247	3.377502
H	-0.200325	1.124745	3.263590
H	-0.022115	-0.272585	4.325763
H	-0.026284	-0.482027	2.569253
C	-1.248925	5.132339	-1.043911
H	-0.997252	6.186715	-1.029671
C	3.683733	-3.776975	-0.271795
H	4.427544	-4.472209	0.091821
C	-0.694217	-2.153751	-3.834497
H	-0.342816	-1.269351	-3.302991
H	-0.847167	-1.864979	-4.877284
H	0.094698	-2.907668	-3.805540
C	-1.356834	-5.054988	-0.340162
H	-1.057367	-6.086650	-0.197165
C	2.959383	-2.190603	-1.943526
C	2.236228	1.213808	4.541646
H	3.316935	1.344352	4.614880
H	1.896257	0.770663	5.486431
H	1.782718	2.203503	4.470541
C	2.498089	-3.574857	0.418494

Cc

Si	1.197217	-0.496054	0.137297
Si	2.505710	0.789165	1.691511
F	1.469816	-3.905579	2.016944
F	1.114044	-5.234292	0.361541
F	3.338213	0.707401	-2.944559
F	4.536093	-0.844326	-3.831234
N	-2.300128	1.056718	-1.034015
F	2.420937	-0.748081	-4.238598
N	-2.334981	-1.098742	-0.789061
F	3.060867	-5.154748	1.275847
N	-0.359854	0.110107	-0.060516
C	-1.049097	2.919273	-1.976116
C	-2.414934	-2.107516	1.894638
H	-1.821722	-1.207680	1.707203
C	4.992507	0.880686	0.274947
H	4.467504	0.471103	-0.589522
H	6.037417	0.554131	0.207522
H	4.989337	1.967543	0.192496
C	-1.523335	0.004619	-0.581947
C	-3.575700	-0.720063	-1.319843
C	-2.043632	-2.473795	-0.582292
C	-2.204785	-3.012013	0.698753
C	-4.676257	-1.690990	-1.522319
H	-5.496329	-1.216964	-2.060789
H	-5.064215	-2.053583	-0.566314
H	-4.357794	-2.569230	-2.083955
C	1.371772	-2.318518	-0.349267
H	0.385300	-2.766189	-0.434120
C	-3.546870	0.615704	-1.483157
C	1.736348	-1.292183	-1.481557
H	0.955280	-1.139249	-2.223751
C	-2.241596	4.607805	-0.082359
H	-2.694300	5.274601	0.640248
C	-1.334320	-2.649618	-3.028817
H	-1.064810	-1.607603	-2.834770
C	2.023604	-4.400952	0.895705
C	0.763730	2.623095	-3.730591
H	1.239915	1.872532	-4.362701
H	1.518988	3.001294	-3.041552
H	0.444900	3.443118	-4.380447
C	-2.132458	-4.393049	0.829728
H	-2.241567	-4.845888	1.806506
C	-1.679675	-4.639082	-1.514921
H	-1.438088	-5.280462	-2.353551
C	-1.718986	-3.260275	-1.694772
C	-4.550330	1.536472	-2.064692
H	-4.936053	2.254759	-1.337100
H	-5.391755	0.965027	-2.454428
H	-4.120731	2.114433	-2.886954
C	-4.493800	3.674751	1.517079
H	-5.212785	3.164510	2.161670

H	-5.045151	4.155687	0.705581
H	-4.024278	4.458158	2.117243
C	-3.472843	2.674925	0.994244
H	-4.028215	1.855412	0.532341
C	2.323145	-0.934214	3.988672
H	2.176533	-1.755884	3.283878
H	1.777962	-1.189818	4.905697
H	3.380805	-0.886143	4.249251
C	-3.870616	-1.673992	2.056046
H	-4.211084	-1.066693	1.216913
H	-3.981566	-1.074075	2.962697
H	-4.527196	-2.543891	2.145572
C	-1.936047	2.428930	-1.010600
C	5.174065	1.041903	2.745233
H	5.036186	2.121846	2.796994
H	6.245361	0.854403	2.601456
H	4.905304	0.619496	3.714746
C	4.674213	-1.115335	1.663410
H	4.379911	-1.562601	2.610164
H	5.750778	-1.286929	1.538677
H	4.167467	-1.657231	0.870285
C	2.154368	2.618371	1.141254
C	2.230483	2.714974	-0.383274
H	3.202061	2.436796	-0.787388
H	2.021342	3.748095	-0.686108
H	1.476005	2.082818	-0.854698
C	3.349507	-0.596302	-3.271370
C	-0.771250	4.281724	-1.953015
H	-0.081794	4.698908	-2.674649
C	-2.463369	-2.638745	-4.057131
H	-2.871885	-3.643297	-4.197306
H	-2.080550	-2.295436	-5.021185
H	-3.274078	-1.970794	-3.769180
C	-1.904112	-2.722616	3.189899
H	-2.527984	-3.558844	3.516731
H	-1.925030	-1.973390	3.983508
H	-0.877792	-3.080611	3.089531
C	-1.428128	1.500841	-4.039605
H	-1.858160	2.341773	-4.590883
H	-2.242173	0.928328	-3.596095
H	-0.923424	0.853339	-4.761066
C	-2.680505	2.062210	2.144359
H	-2.096612	2.827098	2.662428
H	-1.988622	1.300899	1.783861
H	-3.354882	1.597582	2.868192
C	-2.543889	3.251455	-0.054193
C	3.943840	-2.382667	-1.686690
H	4.907112	-2.458596	-2.172865
C	-0.419019	1.999595	-3.004034
H	-0.046154	1.130468	-2.451296
C	0.740194	3.048978	1.528106
H	-0.006969	2.367089	1.124488
H	0.541165	4.039308	1.102653
H	0.601918	3.126108	2.607512
C	4.401593	0.385373	1.596118
C	1.789777	0.394775	3.452255
C	3.133725	3.627489	1.743605
H	3.143755	3.603542	2.835245
H	2.829451	4.637496	1.442339
H	4.156166	3.482951	1.392649
C	0.271426	0.250037	3.378240
H	-0.222083	1.147186	3.013942
H	-0.120944	0.030719	4.379197
H	-0.016575	-0.577264	2.726724
C	-1.362613	5.116618	-1.021171
H	-1.132976	6.176140	-1.026233
C	3.607129	-3.333656	-0.648327
H	4.330538	-4.092500	-0.382121
C	-0.111532	-3.344474	-3.624506
H	0.689703	-3.460740	-2.893808
H	0.274929	-2.760304	-4.462214
H	-0.365971	-4.335570	-4.007945
C	-1.909124	-5.200231	-0.272708
H	-1.863687	-6.276075	-0.150822
C	3.052981	-1.467213	-2.092183
C	2.122938	1.487732	4.470832
H	3.196867	1.641099	4.586337
H	1.726832	1.197470	5.451954
H	1.674320	2.448116	4.214369
C	2.402810	-3.313395	-0.059867

TS(Cc_3c)

Si	1.214951	-0.511630	0.119945
Si	2.476335	0.776995	1.738777
F	1.159212	-4.729743	1.296774
F	1.459677	-5.363483	-0.736838
F	3.659239	0.602966	-3.441547
F	4.355438	-1.314977	-4.115073
N	-2.263112	1.056611	-1.051586
F	2.277478	-0.792205	-4.326269
N	-2.340046	-1.089388	-0.743993
F	3.103238	-5.394355	0.656865
N	-0.350776	0.089263	-0.023705
C	-1.001602	2.912807	-1.999540
C	-2.515274	-2.047164	1.956693
H	-1.980849	-1.116804	1.746373

C	5.008171	0.770299	0.424110
H	4.508831	0.331016	-0.441154
H	6.051351	0.432539	0.405395
H	5.017724	1.853008	0.298245
C	-1.510699	0.003392	-0.560821
C	-3.562948	-0.708775	-1.310273
C	-2.055210	-2.459702	-0.500554
C	-2.248906	-2.970248	0.787173
C	-4.668856	-1.671261	-1.523982
H	-4.329800	-2.586280	-2.009512
H	-5.442900	-1.219630	-2.143832
H	-5.126767	-1.970201	-0.577131
C	1.321253	-2.355416	-0.116342
H	0.333506	-2.811868	-0.162567
C	-3.509824	0.621169	-1.509781
C	1.785629	-0.914454	-1.594928
H	1.016593	-0.704219	-2.338346
C	-2.217223	4.620405	-0.140149
H	-2.680705	5.294526	0.568723
C	-1.282103	-2.684888	-2.923583
H	-1.068429	-1.624802	-2.761364
C	2.032216	-4.685385	0.277786
C	0.835135	2.592403	-3.726536
H	1.314946	1.833635	-4.345999
H	1.583078	2.971855	-3.030123
H	0.532741	3.408976	-4.388268
C	-2.152446	-4.346007	0.955186
H	-2.285156	-4.776471	1.939219
C	-1.618402	-4.639177	-1.366097
H	-1.330442	-5.294538	-2.178509
C	-1.683942	-3.267076	-1.582937
C	-4.493125	1.540847	-2.126170
H	-4.894600	2.267423	-1.415233
H	-5.327324	0.968899	-2.530584
H	-4.041140	2.109411	-2.942681
C	-4.506240	3.703206	1.420633
H	-5.232588	3.199831	2.062382
H	-5.046689	4.161492	0.588937
H	-4.055584	4.503691	2.012622
C	-3.466617	2.702391	0.938314
H	-4.005314	1.867713	0.483732
C	2.143751	-0.913562	4.038321
H	2.018885	-1.732542	3.324389
H	1.542871	-1.155241	4.923699
H	3.186174	-0.893530	4.356251
C	-3.995141	-1.701394	2.106819
H	-4.372120	-1.146953	1.247000
H	-4.145141	-1.078951	2.992531
H	-4.596805	-2.606737	2.225306
C	-1.898253	2.430229	-1.039148
C	5.115968	1.035316	2.888876
H	4.996987	2.118416	2.891289
H	6.187618	0.823295	2.787845
H	4.809061	0.657183	3.865414
C	4.615791	-1.160185	1.906184
H	4.377073	-1.520191	2.904522
H	5.678919	-1.366791	1.731131
H	4.051695	-1.756300	1.194609
C	2.187121	2.600168	1.132114
C	2.303943	2.646616	-0.393021
H	3.269865	2.311302	-0.768554
H	2.149653	3.678298	-0.731582
H	1.529293	2.038178	-0.863100
C	3.336375	-0.704770	-3.500585
C	-0.721722	4.274851	-1.986164
H	-0.023143	4.683684	-2.703824
C	-2.379093	-2.774848	-3.982138
H	-2.721577	-3.806757	-4.098164
H	-1.988972	-2.441411	-4.946751
H	-3.239377	-2.150717	-3.742853
C	-1.970190	-2.598347	3.267186
H	-2.549396	-3.456523	3.617520
H	-2.026576	-1.830514	4.040908
H	-0.927279	-2.907610	3.172238
C	-1.359218	1.479189	-4.057480
H	-1.782128	2.316185	-4.619958
H	-2.178373	0.909316	-3.619993
H	-0.845144	0.826677	-4.767635
C	-2.686832	2.123464	2.113167
H	-2.123037	2.906773	2.626261
H	-1.976743	1.367783	1.777501
H	-3.364867	1.661306	2.835302
C	-2.521254	3.264656	-0.102642
C	3.969295	-2.101968	-1.571181
H	4.938648	-2.182225	-2.046267
C	-0.363275	1.984502	-3.012765
H	-0.005581	1.119771	-2.445732
C	0.774999	3.078168	1.468111
H	0.019975	2.400260	1.072655
H	0.608455	4.056928	1.003477
H	0.615856	3.198086	2.540844
C	4.367931	0.339717	1.746497
C	1.680957	0.431597	3.475254
C	3.173578	3.605514	1.728329
H	3.153066	3.615116	2.820260
H	2.900411	4.611980	1.387983

82

H	4.201286	3.427148	1.410256
C	0.161696	0.356866	3.358965
H	-0.275145	1.288575	3.012031
H	-0.266524	0.129979	4.343375
H	-0.153199	-0.430528	2.672679
C	-1.323815	5.119531	-1.070361
H	-1.092460	6.178597	-1.082120
C	3.650025	-3.078968	-0.622992
H	4.392465	-3.846422	-0.444239
C	-0.008936	-3.339903	-3.454436
H	0.778454	-3.365580	-2.701656
H	0.361921	-2.780961	-4.315637
H	-0.196207	-4.364244	-3.784981
C	-1.871064	-5.174835	-0.117001
H	-1.800863	-6.245544	0.034120
C	3.035299	-1.260982	-2.133742
C	2.025102	1.521232	4.494480
H	3.099047	1.634558	4.645938
H	1.583417	1.259201	5.464192
H	1.623794	2.495526	4.211852
C	2.381629	-3.276328	-0.122854

3c

Si	5.731076	4.382084	12.440975
Si	6.995242	5.692469	14.022211
F	5.641512	0.441011	14.677255
F	6.069413	-0.814811	12.982700
F	7.989973	5.174347	8.602702
F	9.442642	3.639294	9.006794
N	2.262143	5.949804	11.160302
F	7.682477	3.180129	7.854374
N	2.223576	3.797879	11.444069
F	7.677800	0.120123	14.063098
N	4.204396	5.016565	12.128364
C	3.527414	7.823168	10.265321
C	2.169539	2.867415	14.159591
H	2.735105	3.791464	14.000762
C	9.499584	5.825275	12.569721
H	8.962342	5.549349	11.661018
H	10.523863	5.446938	12.463938
H	9.561936	6.912733	12.614082
C	3.035129	4.902692	11.626775
C	0.995031	4.165745	10.880887
C	2.568406	2.442192	11.690604
C	2.506566	1.951721	13.001233
C	-0.066270	3.174406	10.595292
H	0.236778	2.452782	9.832823
H	-0.963004	3.682702	10.242953
H	-0.327822	2.602593	11.489145
C	5.743196	2.625869	13.082933
H	5.184566	2.504432	14.007304
C	1.021225	5.500990	10.704241
C	6.705878	4.421548	10.844593
H	6.713241	5.403833	10.379216
C	2.346521	9.480269	12.190322
H	1.900889	10.135015	12.928352
C	2.921357	2.177959	9.186556
H	2.265810	3.051175	9.144445
C	6.427558	0.321896	13.604113
C	5.403067	7.495979	8.584456
H	5.872597	6.743438	7.948773
H	6.136287	7.811168	9.328475
H	5.170644	8.356315	7.950712
C	2.766947	0.601207	13.194195
H	2.741665	0.186215	14.192711
C	3.135678	0.284484	10.843473
H	3.381269	-0.374480	10.020269
C	2.870596	1.626578	10.595014
C	0.015784	6.418428	10.120962
H	-0.360080	7.141199	10.849643
H	-0.830938	5.847535	9.742241
H	0.437251	6.992491	9.291913
C	0.046898	8.522930	13.723632
H	-0.674207	8.004811	14.359545
H	-0.498749	8.991995	12.901437
H	0.495140	9.316117	14.327035
C	1.091524	7.537247	13.220219
H	0.556527	6.707991	12.751451
C	6.858670	3.909087	16.294013
H	6.615310	3.101500	15.601491
H	6.380208	3.671272	17.252280
H	7.935752	3.891687	16.458981
C	0.686737	3.236089	14.197129
H	0.372041	3.778050	13.305800
H	0.485684	3.875329	15.060225
H	0.069757	2.338363	14.293238
C	2.627468	7.320839	11.211736
C	9.708506	5.670709	15.023451
H	9.643041	6.746861	15.192989
H	10.763477	5.431773	14.839191
H	9.424815	5.167712	15.948263
C	9.034257	3.694660	13.680671
H	8.604635	3.130955	14.507380
H	10.102657	3.449022	13.635967
H	8.585426	3.328272	12.757358
C	6.711309	7.561012	13.575547

C	6.757538	7.725478	12.054910
H	7.701560	7.408161	11.613250
H	6.606647	8.781737	11.799907
H	5.943760	7.168246	11.586629
C	8.123908	3.882992	8.913778
C	3.820567	9.181098	10.318056
H	4.520963	9.605529	9.610865
C	2.424875	1.187879	8.140399
H	3.114604	0.349942	8.015039
H	2.343940	1.684587	7.171032
H	1.444399	0.780033	8.397808
C	2.579671	2.303523	15.512535
H	1.961018	1.447165	15.794253
H	2.449303	3.066654	16.281840
H	3.622890	1.983413	15.532838
C	3.154504	6.533540	8.128178
H	2.784096	7.425747	7.615759
H	2.300766	5.981169	8.520218
H	3.645459	5.899728	7.385661
C	1.875827	6.942259	14.385988
H	2.425775	7.721474	14.919635
H	2.598545	6.201888	14.041006
H	1.198196	6.457839	15.093723
C	2.026973	8.127280	12.185481
C	7.615149	2.084861	10.492207
H	8.230760	1.572815	9.759553
C	4.149702	6.916004	9.223624
H	4.439745	5.998301	9.744737
C	5.316342	8.017673	13.997914
H	4.546058	7.378181	13.566873
H	5.141105	9.033257	13.623009
H	5.189045	8.045196	15.081045
C	8.874576	5.210563	13.824468
C	6.354385	5.271809	15.812684
C	7.737368	8.502164	14.207157
H	7.750285	8.435559	15.296504
H	7.484331	9.537469	13.945485
H	8.751055	8.318771	13.849630
C	4.827534	5.193452	15.799920
H	4.358376	6.135781	15.526311
H	4.465916	4.917019	16.798493
H	4.466155	4.435599	15.102622
C	3.234991	10.000869	11.266921
H	3.477693	11.057243	11.288418
C	7.214628	1.296702	11.506455
H	7.576781	0.276429	11.430727
C	4.323363	2.666464	8.846237
H	4.651956	3.435669	9.543868
H	4.351078	3.086131	7.837455
H	5.046170	1.848539	8.894598
C	3.080994	-0.223192	12.127667
H	3.295172	-1.270434	12.303557
C	7.403026	3.485472	10.185123
C	6.769380	6.316022	16.851457
H	7.852371	6.426109	16.924267
H	6.403647	6.009444	17.839763
H	6.346052	7.299317	16.642682
C	6.402191	1.527084	12.686054

TS(1-D)

Si	4.035201	6.974221	13.639186
Si	5.294374	5.232741	14.880442
N	5.119214	3.889682	13.836941
N	5.653038	1.788577	12.885758
N	8.050189	6.422458	14.488087
N	5.369517	1.791432	15.038689
C	3.720236	5.689285	11.100183
H	4.078460	5.562481	10.070321
H	2.636210	5.807704	11.051071
H	3.952635	4.772757	11.644939
C	4.407077	6.902356	11.728052
C	5.369738	2.629636	13.940083
C	5.646641	2.173681	11.517707
C	4.538343	1.818255	10.741231
C	4.556787	2.153119	9.392246
H	3.714119	1.894149	8.763704
C	5.634667	2.823992	8.846132
H	5.632579	3.083312	7.793551
C	3.979271	8.148592	10.954098
H	4.497160	9.048755	11.288410
H	2.906409	8.335413	11.032149
H	4.211605	8.017901	9.888356
C	5.910571	6.690452	11.533620
H	6.124050	6.555619	10.464589
H	6.248097	5.792519	12.055892
H	6.502445	7.534585	11.885881
C	8.198521	6.762439	15.763873
H	7.499815	6.289604	16.450660
C	9.150287	7.670458	16.201422
H	9.220197	7.919519	17.253208
C	9.993449	8.248390	15.267273
H	10.746095	8.967484	15.569950
C	9.850462	7.893389	13.935746
H	10.482228	8.320915	13.166865
C	8.865328	6.978872	13.598019
H	8.712776	6.693011	12.563656

C	5.823169	0.474552	13.322287
C	5.649059	0.476175	14.660657
C	5.261306	2.216618	16.390818
C	6.430298	2.333848	17.147862
C	6.304921	2.754005	18.466985
H	7.192203	2.868585	19.078172
C	5.064821	3.041382	19.004793
H	4.986636	3.378395	20.032152
C	3.918852	2.895968	18.240288
H	2.956213	3.122259	18.679475
C	3.990013	2.472775	16.919936
C	2.746892	2.303620	16.073483
H	2.982266	2.704712	15.083965
C	1.548435	3.074348	16.605673
H	1.170452	2.640483	17.535631
H	0.737473	3.039977	15.876153
H	1.787024	4.123080	16.788445
C	2.373081	0.833354	15.887286
H	2.212077	0.347766	16.853704
H	3.141952	0.282427	15.346245
H	1.446699	0.755191	15.312579
C	7.794976	2.064128	16.553989
H	7.654563	1.483350	15.639465
C	8.475745	3.369123	16.157170
H	7.852785	3.951756	15.476425
H	9.434764	3.170639	15.671146
H	8.663720	3.987629	17.038869
C	8.687637	1.247098	17.481204
H	9.610973	0.974024	16.964971
H	8.197774	0.328922	17.813974
H	8.970551	1.813537	18.371624
C	5.751461	-0.620722	15.649128
H	4.888437	-0.640040	16.317639
H	6.640226	-0.517135	16.277348
H	5.807952	-1.580421	15.136786
C	6.158068	-0.626560	12.392896
H	6.290066	-1.554736	12.947626
H	7.083463	-0.419586	11.848955
H	5.377334	-0.784817	11.644456
C	6.713309	3.176876	9.638533
H	7.539874	3.714388	9.193749
C	6.747815	2.857929	10.991372
C	7.924567	3.242782	11.864476
H	7.508988	3.714972	12.761385
C	8.850941	4.252878	11.205047
H	9.380681	3.816126	10.353560
H	9.604991	4.576590	11.924702
H	8.309827	5.133451	10.854085
C	8.746862	2.029837	12.300990
H	8.171128	1.331651	12.907231
H	9.600937	2.358109	12.898482
H	9.133005	1.493643	11.429306
C	3.331507	1.149081	11.361491
H	3.674961	0.553084	12.210562
C	2.606777	0.205296	10.412320
H	2.109406	0.744347	9.602380
H	1.833296	-0.343597	10.954096
H	3.288412	-0.521479	9.963665
C	2.381369	2.205204	11.919188
H	2.897913	2.866077	12.614846
H	1.543609	1.735895	12.441916
H	1.978771	2.824103	11.112869
C	4.575044	8.700963	14.396188
C	3.562250	9.823367	14.165066
H	2.614148	9.641372	14.672444
H	3.350479	9.981217	13.105312
H	3.964448	10.764872	14.562742
C	4.791878	8.550682	15.905789
H	5.567961	7.816483	16.132775
H	3.892299	8.245652	16.439542
H	5.113703	9.513341	16.325226
C	5.911703	9.172974	13.822304
H	6.234990	10.072398	14.362417
H	5.848032	9.437617	12.766139
H	6.693396	8.423946	13.938887
C	2.136736	6.676173	14.004257
C	1.786388	5.209469	13.759272
H	0.759713	5.017462	14.097691
H	2.450457	4.539315	14.306070
H	1.842730	4.934116	12.709010
C	1.845988	6.943689	15.482303
H	0.819823	6.628836	15.713242
H	1.927763	7.998026	15.747260
H	2.517186	6.381582	16.139050
C	1.189610	7.523479	13.155150
H	1.272357	7.278615	12.094407
H	1.361454	8.594329	13.265075
H	0.150672	7.323518	13.451604

D

Si	3.978226	7.058046	13.556794
Si	4.913268	5.252071	14.959533
N	5.422869	4.020676	13.805639
N	5.785569	1.890465	12.859102
N	6.700714	6.039414	15.280898
N	5.646592	1.905836	15.031266

85

C	3.626564	5.675625	11.060722
H	3.973879	5.506181	10.033532
H	2.546300	5.819421	11.017355
H	3.842683	4.770052	11.628008
C	4.363460	6.879304	11.647829
C	5.588872	2.757431	13.928153
C	5.702314	2.273831	11.495993
C	4.553838	1.930118	10.774648
C	4.503050	2.281068	9.429847
H	3.627311	2.031975	8.843656
C	5.551209	2.957097	8.833240
H	5.490513	3.230988	7.786092
C	4.011230	8.108856	10.811809
H	4.614888	8.979429	11.072861
H	2.960789	8.391106	10.904519
H	4.200671	7.892435	9.751589
C	5.848010	6.563031	11.464434
H	6.076714	6.489040	10.392734
H	6.066437	5.591919	11.913713
H	6.508822	7.319244	11.890823
C	6.955244	6.475864	16.522265
H	6.145264	6.332611	17.229075
C	8.165901	7.037100	16.871694
H	8.314594	7.390846	17.883577
C	9.175833	7.106453	15.924744
H	10.143199	7.524040	16.175497
C	8.925055	6.606661	14.653745
H	9.678808	6.631184	13.877289
C	7.681662	6.088142	14.368961
H	7.423965	5.708424	13.391477
C	5.947071	0.572183	13.288602
C	5.861466	0.579729	14.632726
C	5.627311	2.282837	16.401083
C	6.841744	2.308192	17.098644
C	6.806943	2.635868	18.449851
H	7.727965	2.668584	19.018220
C	5.607163	2.909365	19.081170
H	5.597590	3.160996	20.135851
C	4.417151	2.853676	18.376447
H	3.488896	3.076647	18.885302
C	4.399970	2.538826	17.023870
C	3.104907	2.478929	16.244609
H	3.313315	2.923758	15.266840
C	1.994062	3.299270	16.879077
H	1.654827	2.865303	17.823825
H	1.132520	3.332055	16.209594
H	2.324501	4.324638	17.057314
C	2.638384	1.043584	16.008151
H	2.502154	0.514004	16.955218
H	3.344654	0.482817	15.395503
H	1.678744	1.047129	15.484856
C	8.154044	2.014248	16.402488
H	7.960449	1.270090	15.626092
C	8.674267	3.255591	15.689484
H	7.949383	3.606393	14.956718
H	9.611337	3.040590	15.169075
H	8.855541	4.063591	16.402793
C	9.216256	1.438632	17.328486
H	10.079130	1.112457	16.743542
H	8.841964	0.580326	17.891131
H	9.575706	2.181274	18.045513
C	5.947947	-0.530972	15.608793
H	5.084539	-0.540630	16.278295
H	6.836654	-0.462530	16.242240
H	5.979989	-1.484311	15.082484
C	6.188805	-0.542118	12.344517
H	6.347034	-1.468498	12.895522
H	7.072902	-0.357858	11.728224
H	5.351325	-0.693761	11.658840
C	6.675515	3.292713	9.568661
H	7.482014	3.831463	9.088186
C	6.777603	2.952703	10.911602
C	8.005374	3.290217	11.728619
H	7.634146	3.635494	12.697732
C	8.846383	4.409312	11.131840
H	9.337910	4.097578	10.206366
H	9.636253	4.686416	11.834727
H	8.249991	5.297756	10.916870
C	8.878854	2.060899	11.974013
H	8.352456	1.297943	12.547135
H	9.772820	2.340114	12.537886
H	9.202460	1.621103	11.026580
C	3.381063	1.251860	11.449223
H	3.768239	0.655411	12.278180
C	2.617630	0.308366	10.530561
H	2.078938	0.847486	9.747429
H	1.874510	-0.248404	11.105877
H	3.282309	-0.411362	10.046549
C	2.451117	2.292603	12.063607
H	2.991986	2.938102	12.755952
H	1.636626	1.808838	12.609184
H	2.013930	2.927081	11.288220
C	4.514778	8.836636	14.186884
C	3.578785	9.957368	13.728804
H	2.582507	9.862566	14.162559
H	3.469510	10.002033	12.644742

86

H	3.981735	10.924679	14.058851
C	4.570105	8.888919	15.715735
H	5.228096	8.126921	16.129757
H	3.594905	8.762763	16.181547
H	4.961872	9.865589	16.030586
C	5.921704	9.177293	13.690596
H	6.231149	10.141442	14.114883
H	5.975191	9.271142	12.605615
H	6.659875	8.435459	14.000462
C	2.063053	6.810253	13.878197
C	1.719283	5.323753	13.783591
H	0.667457	5.172527	14.060655
H	2.324751	4.733431	14.476691
H	1.858564	4.921466	12.783589
C	1.702543	7.239029	15.301613
H	0.673993	6.924873	15.522244
H	1.743062	8.321047	15.433425
H	2.357348	6.771781	16.042584
C	1.153218	7.564692	12.908345
H	1.269513	7.219781	11.879837
H	1.324028	8.641897	12.919954
H	0.104211	7.396281	13.186873

TS(D-E)

Si	-1.124313	2.886471	-0.413626
Si	-0.090823	1.123147	0.786318
N	0.036055	-0.310059	-0.099711
N	0.448565	-2.433432	-1.033716
N	1.325122	1.264804	1.847440
N	0.485845	-2.352714	1.140359
C	-1.445905	1.431233	-2.877264
H	-1.092195	1.261895	-3.901471
H	-2.530150	1.545548	-2.924918
H	-1.207712	0.536888	-2.299645
C	-0.753439	2.671299	-2.309627
C	0.303991	-1.554317	0.023140
C	0.372966	-2.064477	-2.402511
C	-0.774892	-2.409366	-3.122585
C	-0.817425	-2.079375	-4.472815
H	-1.691884	-2.331577	-5.059550
C	0.239858	-1.421667	-5.073654
H	0.188092	-1.165350	-6.125728
C	-1.198292	3.880952	-3.134907
H	-0.669192	4.795440	-2.864874
H	-2.268492	4.075812	-3.045001
H	-0.990549	3.688596	-4.195356
C	0.746242	2.451587	-2.508711
H	0.952518	2.330342	-3.580012
H	1.067082	1.541793	-1.999964
H	1.354170	3.278241	-2.141894
C	1.511227	1.623955	3.148126
H	0.903441	1.086117	3.866091
C	2.391610	2.588891	3.495272
H	2.561206	2.813152	4.539652
C	3.059093	3.335771	2.461233
H	3.708831	4.160122	2.729323
C	2.870939	3.003799	1.161393
H	3.397928	3.532015	0.374656
C	2.033443	1.898223	0.816477
H	2.341963	1.251920	-0.003894
C	0.672702	-3.734210	-0.580587
C	0.691176	-3.688454	0.766037
C	0.514692	-1.921089	2.493142
C	1.742512	-1.925536	3.167923
C	1.739150	-1.589963	4.517104
H	2.671035	-1.583256	5.067951
C	0.563389	-1.254352	5.164609
H	0.581918	-0.992765	6.216561
C	-0.634477	-1.238399	4.472663
H	-1.543735	-0.963883	4.991155
C	-0.688649	-1.580878	3.124629
C	-2.006974	-1.647830	2.383282
H	-1.828282	-1.261601	1.376511
C	-3.092949	-0.789177	3.012018
H	-3.419812	-1.187861	3.976236
H	-3.966544	-0.764158	2.358356
H	-2.755744	0.238867	3.158200
C	-2.494115	-3.089551	2.240893
H	-2.630397	-3.552252	3.222316
H	-1.796359	-3.698277	1.665362
H	-3.455909	-3.108882	1.722103
C	3.042759	-2.251980	2.463306
H	2.813945	-2.898464	1.613474
C	3.688268	-0.994394	1.888883
H	3.041031	-0.521472	1.152836
H	4.636299	-1.246174	1.406401
H	3.885878	-0.257969	2.671985
C	4.028134	-2.999593	3.353258
H	4.875069	-3.346148	2.757095
H	3.569767	-3.868066	3.832704
H	4.431837	-2.357049	4.139418
C	0.845428	-4.771654	1.763379
H	0.028264	-4.761066	2.488979
H	1.775868	-4.687351	2.330080
H	0.841281	-5.738315	1.261177
C	0.872022	-4.867433	-1.511244

H	1.065021	-5.780742	-0.949926
H	1.722830	-4.689073	-2.174404
H	0.000973	-5.036421	-2.148835
C	1.362737	-1.082311	-4.337709
H	2.176253	-0.558682	-4.822510
C	1.458124	-1.400743	-2.988600
C	2.687684	-1.053597	-2.176548
H	2.324169	-0.650811	-1.226089
C	3.562105	0.014264	-2.817291
H	4.064359	-0.361640	-3.713056
H	4.340162	0.316919	-2.112920
H	2.990952	0.902116	-3.090750
C	3.536490	-2.287015	-1.868688
H	2.995748	-3.021588	-1.272614
H	4.426418	-1.995355	-1.305483
H	3.866544	-2.767275	-2.794099
C	-1.955113	-3.064716	-2.439815
H	-1.575055	-3.647763	-1.597835
C	-2.724348	-4.018738	-3.342264
H	-3.253715	-3.489887	-4.138569
H	-3.475877	-4.555991	-2.759415
H	-2.064973	-4.754758	-3.808613
C	-2.874100	-1.999264	-1.851192
H	-2.325902	-1.348234	-1.170217
H	-3.699228	-2.459930	-1.301462
H	-3.297461	-1.374523	-2.642286
C	-0.592012	4.627637	0.261434
C	-1.639097	5.710961	-0.013349
H	-2.578181	5.536447	0.511110
H	-1.859686	5.817671	-1.077700
H	-1.249370	6.675085	0.336761
C	-0.361521	4.547582	1.772996
H	0.424662	3.839245	2.030435
H	-1.259278	4.266061	2.322130
H	-0.041541	5.530289	2.142831
C	0.713838	5.104520	-0.372825
H	1.033484	6.028134	0.125041
H	0.605251	5.329466	-1.434200
H	1.510021	4.374374	-0.254894
C	-3.013411	2.570862	-0.025636
C	-3.356200	1.088933	-0.168955
H	-4.395317	0.926000	0.144533
H	-2.721509	0.467809	0.467222
H	-3.258849	0.730802	-1.189922
C	-3.322193	2.936863	1.426540
H	-4.342936	2.616338	1.669849
H	-3.263945	4.007620	1.620252
H	-2.642548	2.428260	2.116631
C	-3.955776	3.349685	-0.945806
H	-3.877836	3.015107	-1.981958
H	-3.780920	4.425451	-0.926300
H	-4.993327	3.179512	-0.631272

E

Si	4.078298	7.165780	13.428953
Si	5.559527	5.514534	14.284065
N	5.151946	3.967566	13.801003
N	5.697566	1.888182	12.833350
N	6.446701	5.653761	15.765143
N	5.729296	1.943098	15.009532
C	3.478821	5.687769	11.029576
H	3.709326	5.516209	9.971126
H	2.395532	5.793126	11.110369
H	3.790242	4.797751	11.578462
C	4.223712	6.936809	11.503215
C	5.515100	2.741463	13.898157
C	5.589404	2.268325	11.468752
C	4.443423	1.888827	10.763337
C	4.368145	2.229243	9.416984
H	3.493917	1.951598	8.841487
C	5.392849	2.927505	8.806097
H	5.316620	3.190195	7.757079
C	3.679258	8.133246	10.720749
H	4.242586	9.049347	10.901565
H	2.630563	8.334654	10.949343
H	3.744609	7.919816	9.646397
C	5.692216	6.721543	11.130314
H	5.776808	6.606122	10.042267
H	6.077589	5.805398	11.583296
H	6.340218	7.543760	11.431409
C	6.712161	6.218571	16.972126
H	6.073775	5.913180	17.796010
C	7.706361	7.121473	17.117547
H	7.927258	7.538413	18.090274
C	8.376103	7.619257	15.931455
H	9.002599	8.500396	16.025568
C	8.189899	7.062302	14.724102
H	8.678479	7.465079	13.842396
C	7.378551	5.832517	14.614406
H	7.992892	4.936500	14.432036
C	5.977148	0.593744	13.269071
C	5.995020	0.623949	14.615462
C	5.590105	2.360215	16.366158
C	6.729794	2.508752	17.164024
C	6.552270	2.910856	18.484759
H	7.421962	3.044107	19.117200

88

C	5.293800	3.154267	18.994647
H	5.177258	3.476547	20.023175
C	4.176878	2.980529	18.194460
H	3.194573	3.162687	18.609505
C	4.297497	2.568781	16.873406
C	3.069419	2.312466	16.026364
H	3.270798	2.727044	15.035970
C	1.814818	2.987414	16.560133
H	1.472882	2.521811	17.488501
H	1.008523	2.888624	15.831018
H	1.968388	4.051626	16.745339
C	2.807211	0.815107	15.860522
H	2.653219	0.341130	16.833765
H	3.629449	0.307224	15.357047
H	1.905833	0.658274	15.262444
C	8.133390	2.226540	16.676710
H	8.074635	1.924528	15.627800
C	9.033082	3.455426	16.762781
H	8.625875	4.300549	16.214884
H	10.022355	3.221973	16.360660
H	9.163569	3.774207	17.799840
C	8.769762	1.087506	17.475284
H	9.727190	0.803680	17.031438
H	8.134227	0.203199	17.522072
H	8.965433	1.403525	18.503037
C	6.224517	-0.479693	15.577750
H	5.730369	-0.275775	16.528704
H	7.286064	-0.633072	15.782905
H	5.823649	-1.413939	15.182883
C	6.223225	-0.525142	12.333216
H	6.412834	-1.439808	12.894066
H	7.090797	-0.332237	11.696023
H	5.372360	-0.699809	11.670164
C	6.513401	3.301448	9.528622
H	7.299449	3.858939	9.036608
C	6.640441	2.978077	10.874116
C	7.861339	3.380607	11.674383
H	7.490794	3.789815	12.618453
C	8.694944	4.467982	11.011696
H	9.202584	4.096481	10.117016
H	9.466857	4.805990	11.706288
H	8.095265	5.334727	10.731284
C	8.757042	2.185216	12.000088
H	8.247505	1.440443	12.610829
H	9.636685	2.521681	12.554590
H	9.103376	1.701982	11.082215
C	3.295473	1.187174	11.455112
H	3.703828	0.627943	12.300051
C	2.566908	0.194084	10.560955
H	2.013107	0.694594	9.762992
H	1.841033	-0.372024	11.149025
H	3.256321	-0.515364	10.096913
C	2.329666	2.216169	12.035833
H	2.849980	2.898143	12.708200
H	1.527849	1.723502	12.592301
H	1.876602	2.812933	11.239569
C	4.670789	8.927133	13.988865
C	3.598786	9.994164	13.749535
H	2.723372	9.846973	14.383934
H	3.261930	10.037569	12.712123
H	4.014643	10.977562	14.001409
C	5.024516	8.941531	15.478027
H	5.835692	8.256983	15.716380
H	4.179481	8.696637	16.119407
H	5.361441	9.949257	15.752324
C	5.933370	9.349847	13.236615
H	6.278733	10.311506	13.635805
H	5.765279	9.484640	12.168032
H	6.746876	8.636778	13.376324
C	2.290375	6.782273	14.082241
C	1.988082	5.290388	13.958397
H	1.018545	5.078932	14.425336
H	2.743035	4.680874	14.454800
H	1.932490	4.961079	12.924262
C	2.181283	7.130094	15.568008
H	1.216224	6.774983	15.950607
H	2.225279	8.203790	15.751527
H	2.966466	6.652929	16.162346
C	1.199121	7.538211	13.321534
H	1.163735	7.252455	12.268636
H	1.314324	8.620909	13.371355
H	0.221337	7.291966	13.754768

TS(E-4a)

Si	-1.058192	2.915978	-0.408601
Si	0.403556	1.266947	0.550443
N	0.034488	-0.248214	-0.079296
N	0.540423	-2.330882	-1.061824
N	0.978216	1.222243	2.154887
N	0.607070	-2.293233	1.114863
C	-1.602324	1.366279	-2.776298
H	-1.356765	1.166617	-3.826319
H	-2.686029	1.477147	-2.713834
H	-1.299236	0.491956	-2.199924
C	-0.856721	2.621521	-2.321919
C	0.380524	-1.479651	0.013291

C	0.380090	-1.963650	-2.424949
C	-0.794115	-2.347708	-3.080636
C	-0.919881	-2.026676	-4.428115
H	-1.817798	-2.307047	-4.964441
C	0.084187	-1.345729	-5.090295
H	-0.032475	-1.097382	-6.139094
C	-1.354393	3.795335	-3.167128
H	-0.774127	4.705321	-3.009664
H	-2.404445	4.029214	-2.979042
H	-1.262861	3.533429	-4.228804
C	0.618827	2.374004	-2.642195
H	0.732250	2.225409	-3.723576
H	0.971689	1.464237	-2.153330
H	1.271779	3.193944	-2.345313
C	1.323167	1.926957	3.229941
H	1.038890	1.493600	4.192069
C	2.124470	3.036420	3.236745
H	2.325107	3.522236	4.184743
C	2.929437	3.377090	2.121926
H	3.652093	4.175826	2.251225
C	3.053145	2.590414	1.011221
H	3.963912	2.706441	0.425490
C	2.233662	1.495379	0.647389
H	2.795675	0.602511	0.345587
C	0.817372	-3.631043	-0.640687
C	0.857726	-3.610759	0.704548
C	0.451795	-1.927100	2.485396
C	1.583338	-1.786792	3.295654
C	1.389808	-1.464997	4.635431
H	2.252809	-1.341464	5.279335
C	0.122733	-1.285185	5.150968
H	-0.007616	-1.024981	6.195355
C	-0.984571	-1.438273	4.334155
H	-1.972863	-1.298279	4.751423
C	-0.847119	-1.773311	2.993327
C	-2.066205	-1.984958	2.120357
H	-1.854749	-1.513097	1.157613
C	-3.326958	-1.341510	2.678831
H	-3.681353	-1.863850	3.571635
H	-4.123239	-1.392674	1.933929
H	-3.174402	-0.291255	2.933100
C	-2.327940	-3.469195	1.862969
H	-2.481892	-4.002223	2.805275
H	-1.505540	-3.944826	1.329185
H	-3.229545	-3.590053	1.256895
C	2.998441	-1.972202	2.794798
H	2.949758	-2.228648	1.733052
C	3.824159	-0.695596	2.936643
H	3.341296	0.156826	2.466083
H	4.810804	-0.835334	2.486931
H	3.975503	-0.447210	3.990232
C	3.708462	-3.104097	3.538472
H	4.679033	-3.309203	3.079934
H	3.129588	-4.027618	3.548956
H	3.890386	-2.823197	4.578872
C	1.090341	-4.721502	1.655687
H	0.490250	-4.597249	2.558729
H	2.135742	-4.789137	1.962222
H	0.815834	-5.669791	1.193515
C	1.033387	-4.743363	-1.592319
H	1.244237	-5.661859	-1.045890
H	1.877180	-4.543822	-2.258324
H	0.159860	-4.914587	-2.226123
C	1.237099	-0.973967	-4.419681
H	2.009411	-0.434717	-4.952147
C	1.413927	-1.278530	-3.075597
C	2.674505	-0.886992	-2.334026
H	2.345926	-0.463890	-1.380629
C	3.498209	0.176384	-3.045607
H	3.963623	-0.217733	-3.953497
H	4.304697	0.511200	-2.389443
H	2.903014	1.048959	-3.315636
C	3.564384	-2.091946	-2.027870
H	3.072480	-2.814961	-1.378178
H	4.476056	-1.761308	-1.523598
H	3.858451	-2.598032	-2.951582
C	-1.917706	-3.039743	-2.340212
H	-1.482622	-3.582825	-1.498092
C	-2.671739	-4.049751	-3.193599
H	-3.254066	-3.564069	-3.980283
H	-3.374860	-4.608160	-2.571537
H	-1.995796	-4.764562	-3.669013
C	-2.867441	-2.004121	-1.747474
H	-2.329384	-1.321513	-1.090255
H	-3.658780	-2.489600	-1.170302
H	-3.335024	-1.410021	-2.537285
C	-0.503363	4.708456	0.087126
C	-1.535821	5.768167	-0.307335
H	-2.462676	5.664424	0.259288
H	-1.785347	5.754987	-1.368869
H	-1.130226	6.761327	-0.077026
C	-0.281740	4.826293	1.595465
H	0.428278	4.093506	1.971340
H	-1.201913	4.722776	2.167087
H	0.129924	5.818880	1.818613
C	0.825760	5.060338	-0.585154

90

H	1.157587	6.042488	-0.225971
H	0.744795	5.124126	-1.670491
H	1.611092	4.344114	-0.336396
C	-2.867495	2.558794	0.196076
C	-3.144883	1.059227	0.166913
H	-4.146469	0.867016	0.571214
H	-2.428574	0.503576	0.772233
H	-3.110488	0.650127	-0.838629
C	-3.054725	3.010767	1.645546
H	-4.023445	2.648272	2.011754
H	-3.059486	4.096144	1.746152
H	-2.281899	2.610740	2.308395
C	-3.927388	3.247282	-0.666797
H	-3.922232	2.878466	-1.693902
H	-3.811166	4.330925	-0.699534
H	-4.921613	3.035813	-0.252943

4a

Si	3.996741	7.111476	13.396944
Si	5.377008	5.519583	14.532612
N	5.339988	3.977477	13.856385
N	5.749766	1.874896	12.873510
N	4.851643	5.516793	16.184000
N	5.644666	1.883449	15.045678
C	3.488154	5.583543	11.032395
H	3.746404	5.370506	9.987777
H	2.404276	5.696830	11.082496
H	3.780910	4.713426	11.620883
C	4.234531	6.836486	11.489267
C	5.560985	2.727178	13.948543
C	5.663327	2.267793	11.512883
C	4.519338	1.910836	10.790314
C	4.466957	2.262192	9.445938
H	3.596036	2.002516	8.857289
C	5.508909	2.951049	8.852799
H	5.448543	3.223461	7.805215
C	3.767371	8.012028	10.631148
H	4.344836	8.920406	10.809294
H	2.713878	8.249926	10.791785
H	3.887486	7.755976	9.570489
C	5.712381	6.561185	11.202480
H	5.849445	6.393826	10.126595
H	6.033467	5.649389	11.710572
H	6.370104	7.377884	11.498586
C	5.377930	5.832785	17.288636
H	4.774647	5.685272	18.196892
C	6.688649	6.394607	17.596991
H	6.820718	6.607410	18.654916
C	7.739005	6.696045	16.805990
H	8.589823	7.119435	17.335126
C	7.969151	6.563808	15.383309
H	8.970238	6.879689	15.091499
C	7.150149	6.125259	14.412144
H	7.587455	6.131152	13.413678
C	5.934110	0.557218	13.296468
C	5.866770	0.560718	14.641958
C	5.639743	2.267877	16.413309
C	6.858868	2.296081	17.099998
C	6.832080	2.617152	18.452855
H	7.758298	2.657115	19.012314
C	5.635915	2.875204	19.096387
H	5.633147	3.117688	20.153234
C	4.441616	2.827510	18.398163
H	3.516128	3.043760	18.915392
C	4.417380	2.531689	17.041432
C	3.120857	2.491620	16.263911
H	3.331313	2.940633	15.289833
C	2.016047	3.311118	16.910933
H	1.678979	2.867747	17.852032
H	1.151949	3.352822	16.245576
H	2.346706	4.334012	17.099911
C	2.644738	1.059949	16.022883
H	2.499284	0.533207	16.970232
H	3.351654	0.492445	15.416818
H	1.688648	1.068488	15.493295
C	8.170426	2.001717	16.404360
H	7.958168	1.365229	15.542299
C	8.794702	3.279616	15.859295
H	8.124183	3.783942	15.165243
H	9.728348	3.056972	15.335559
H	9.013431	3.982188	16.667408
C	9.158913	1.253649	17.290012
H	10.022492	0.939951	16.699240
H	8.711556	0.363877	17.739587
H	9.535793	1.883494	18.099509
C	5.983739	-0.547341	15.616820
H	5.138495	-0.557126	16.309022
H	6.890358	-0.471092	16.222816
H	6.005307	-1.502006	15.092540
C	6.188383	-0.548240	12.345838
H	6.360001	-1.475161	12.891713
H	7.069925	-0.347527	11.730920
H	5.352379	-0.707315	11.660312
C	6.625177	3.304056	9.591810
H	7.424403	3.855801	9.114323
C	6.729566	2.967744	10.936057

C	7.947966	3.335683	11.756244
H	7.572810	3.702902	12.716005
C	8.783318	4.448985	11.140194
H	9.290872	4.117441	10.230096
H	9.556842	4.757541	11.847124
H	8.180856	5.324962	10.894400
C	8.834205	2.121357	12.030937
H	8.311985	1.355086	12.603501
H	9.713761	2.422437	12.605620
H	9.180149	1.676490	11.093746
C	3.354058	1.216044	11.462011
H	3.748158	0.618587	12.286900
C	2.601106	0.269641	10.537741
H	2.054959	0.807641	9.759044
H	1.865600	-0.300172	11.109979
H	3.273916	-0.438448	10.047975
C	2.409617	2.239718	12.084782
H	2.939396	2.884719	12.786327
H	1.600987	1.738066	12.622747
H	1.964843	2.875877	11.315170
C	4.627173	8.878535	13.931170
C	3.610652	9.976517	13.610293
H	2.684700	9.861657	14.174940
H	3.354657	10.013981	12.549732
H	4.034636	10.952238	13.880647
C	4.916278	8.915609	15.434996
H	5.722782	8.234982	15.708753
H	4.049688	8.667467	16.045864
H	5.239703	9.927177	15.713106
C	5.939638	9.245023	13.236002
H	6.289251	10.211306	13.621980
H	5.832494	9.348988	12.156071
H	6.725681	8.514732	13.436337
C	2.151983	6.835869	13.944451
C	1.846607	5.338567	13.943373
H	0.826310	5.174253	14.313585
H	2.527438	4.798507	14.602503
H	1.912942	4.894414	12.953362
C	1.929395	7.315731	15.380510
H	0.914180	7.040463	15.694418
H	2.014309	8.398033	15.482491
H	2.629323	6.842807	16.073123
C	1.138418	7.534111	13.037241
H	1.164626	7.149771	12.016089
H	1.286517	8.614204	12.992207
H	0.125724	7.357751	13.422539

4b

Si	4.063162	7.094415	13.458759
Si	5.403197	5.456823	14.580219
N	5.359994	3.938296	13.839841
N	5.720500	1.837662	12.835933
N	4.911709	5.400273	16.229581
N	5.652551	1.826770	15.009950
C	3.535373	5.607865	11.072077
H	3.794940	5.402243	10.026303
H	2.453755	5.742710	11.117969
H	3.807993	4.725439	11.651844
C	4.305042	6.839203	11.548322
C	5.560854	2.684018	13.922339
C	5.628331	2.246515	11.481009
C	4.470996	1.920266	10.765482
C	4.411835	2.289399	9.426085
H	3.530067	2.053871	8.843352
C	5.460587	2.966046	8.830879
H	5.394622	3.253229	7.787558
C	3.867703	8.034654	10.702204
H	4.466984	8.926885	10.889987
H	2.820066	8.296950	10.863892
H	3.983248	7.786792	9.639027
C	5.778208	6.534974	11.265734
H	5.919036	6.388539	10.187140
H	6.071471	5.604588	11.756119
H	6.454311	7.327609	11.584900
C	5.471203	5.748526	17.313968
H	4.906949	5.555992	18.239631
C	6.716619	6.422338	17.611788
H	6.765349	6.717162	18.652852
C	7.785979	6.776986	16.841529
N	8.877840	7.409515	17.434496
C	8.014342	6.486561	15.424532
H	9.049957	6.654418	15.138763
C	7.194118	6.007137	14.481501
H	7.673997	5.864590	13.512796
C	5.893369	0.513504	13.242753
C	5.849670	0.505222	14.588885
C	5.662391	2.187381	16.384618
C	6.885261	2.183885	17.064602
C	6.870780	2.472741	18.424927
H	7.800927	2.486372	18.979087
C	5.682499	2.732992	19.081431
H	5.689061	2.951687	20.143478
C	4.484097	2.719461	18.389099
H	3.564817	2.938723	18.916027
C	4.448151	2.454928	17.026246
C	3.146890	2.450425	16.256012

92

H	3.360328	2.912892	15.288963
C	2.061277	3.278934	16.923395
H	1.722111	2.826422	17.859435
H	1.193681	3.347141	16.264600
H	2.415106	4.291431	17.125855
C	2.645132	1.031417	15.993674
H	2.493632	0.492146	16.933043
H	3.340589	0.461332	15.376625
H	1.687631	1.064592	15.467450
C	8.190319	1.894610	16.355059
H	7.969175	1.276002	15.481973
C	8.815308	3.181344	15.831452
H	8.144400	3.691855	15.142921
H	9.751352	2.968896	15.307447
H	9.028604	3.875224	16.648943
C	9.181415	1.125440	17.219545
H	10.039024	0.817550	16.617070
H	8.732456	0.230383	17.656852
H	9.567332	1.739178	18.037077
C	5.964681	-0.614500	15.550559
H	5.127717	-0.620762	16.252886
H	6.879181	-0.555586	16.146573
H	5.968340	-1.563845	15.016196
C	6.111716	-0.586338	12.276527
H	6.279394	-1.521248	12.809876
H	6.983707	-0.393314	11.645723
H	5.259397	-0.725160	11.606874
C	6.591222	3.287712	9.562550
H	7.396421	3.829471	9.083554
C	6.702359	2.932153	10.901197
C	7.936162	3.263175	11.713781
H	7.577271	3.619972	12.683742
C	8.786293	4.370904	11.108118
H	9.276390	4.046396	10.185990
H	9.574465	4.650461	11.811135
H	8.198370	5.262911	10.886440
C	8.801311	2.027284	11.958064
H	8.269287	1.262006	12.522767
H	9.692850	2.299990	12.528617
H	9.128569	1.592078	11.009661
C	3.299980	1.238417	11.440440
H	3.690962	0.628907	12.258029
C	2.526086	0.310586	10.514403
H	1.984026	0.862521	9.742623
H	1.785091	-0.251338	11.087391
H	3.184602	-0.404716	10.015773
C	2.376140	2.271138	12.078445
H	2.920093	2.898573	12.785097
H	1.561360	1.777577	12.614641
H	1.938871	2.923848	11.318372
C	4.721891	8.846498	14.011096
C	3.735317	9.969622	13.685774
H	2.799201	9.869745	14.236557
H	3.495097	10.023730	12.622385
H	4.176880	10.933160	13.972071
C	4.991875	8.868969	15.517769
H	5.749682	8.141463	15.807407
H	4.103655	8.673850	16.116542
H	5.369539	9.860912	15.800060
C	6.051291	9.186253	13.333853
H	6.418620	10.142008	13.730532
H	5.959197	9.300566	12.253602
H	6.816640	8.434894	13.536871
C	2.211542	6.847563	13.995177
C	1.879727	5.356070	13.975076
H	0.855764	5.204877	14.340866
H	2.549264	4.795629	14.629034
H	1.940881	4.923666	12.979552
C	1.997524	7.313461	15.437005
H	0.981240	7.043309	15.751932
H	2.091035	8.394239	15.548548
H	2.696157	6.828169	16.122796
C	1.212494	7.574762	13.094990
H	1.234523	7.202199	12.069300
H	1.380364	8.652461	13.062797
H	0.195729	7.412252	13.475778
C	9.415314	8.591098	16.789825
C	8.949902	7.496378	18.867588
H	8.779711	6.516553	19.315122
H	8.225715	8.206917	19.296477
H	9.950849	7.834949	19.141858
H	9.317112	8.530456	15.709094
H	10.472736	8.704533	17.039744
H	8.883260	9.496114	17.118543

Benzene

C	1.840638	7.380693	0.000055
C	3.228162	7.380626	0.000497
C	3.921873	8.582279	-0.000052
C	3.228274	9.784013	-0.001040
C	1.840763	9.784081	-0.001482
C	1.147046	8.582416	-0.000934
H	1.298551	6.441958	0.000483
H	3.770148	6.441832	0.001273
H	5.005879	8.582251	0.000294
H	3.770406	10.722722	-0.001468

93

H	1.298731	10.722848	-0.002258
H	0.063040	8.582493	-0.001279

1,4-(diflouro)benzene

C	2.200615	1.021989	0.000064
C	3.587455	1.021914	0.000514
C	4.256462	2.230322	-0.000046
C	3.587575	3.438786	-0.001033
C	2.200732	3.438862	-0.001483
C	1.531725	2.230459	-0.000924
H	1.638826	0.096670	0.000478
H	4.149150	0.096539	0.001287
H	4.149400	4.364084	-0.001442
H	1.639003	4.364216	-0.002256
F	5.596099	2.230258	0.000379
F	0.192090	2.230526	-0.001344

1,4-bis(trifluoromethyl)benzene

C	-0.691975	1.205219	-0.048175
C	0.691891	1.205277	-0.048158
C	1.380578	0.001231	-0.046979
C	0.691848	-1.203058	-0.047894
C	-0.691764	-1.203116	-0.047895
C	-1.380578	0.001121	-0.046996
H	-1.236591	2.140619	-0.057347
H	1.236438	2.140713	-0.057311
H	1.236492	-2.138491	-0.056885
H	-1.236339	-2.138585	-0.056882
C	2.882158	0.000016	0.005710
C	-2.882157	-0.000036	0.005706
F	3.404299	1.084498	-0.576777
F	3.402435	-1.072142	-0.601106
F	3.322563	-0.014802	1.273302
F	-3.404263	1.083519	-0.578555
F	-3.402488	-1.073154	-0.599341
F	-3.322545	-0.012736	1.273328

Pyridine

N	1.847700	7.393087	0.000049
C	3.175964	7.424081	0.000452
C	3.917552	8.596660	-0.000063
C	3.240559	9.805240	-0.001051
C	1.855425	9.787560	-0.001480
C	1.210795	8.559014	-0.000899
H	3.677539	6.460131	0.001232
H	5.000158	8.558898	0.000309
H	3.782624	10.744050	-0.001479
H	1.281450	10.706248	-0.002252
H	0.125194	8.511287	-0.001213

DMAP

N	3.691460	6.207635	1.380425
N	2.122402	6.076601	5.271489
C	2.636985	6.128053	4.010418
C	3.836278	5.481842	3.668437
C	4.297105	5.554849	2.368381
C	2.561664	6.826673	1.710960
C	1.999526	6.827675	2.972682
C	0.949835	6.845160	5.597500
C	2.880243	5.458800	6.327976
H	4.407217	4.927372	4.399393
H	5.224121	5.049560	2.109358
H	2.062416	7.368712	0.911947
H	1.079405	7.369599	3.138862
H	0.107660	6.575431	4.953270
H	1.117033	7.925839	5.502541
H	0.659400	6.635401	6.625077
H	3.837445	5.965077	6.506330
H	2.302731	5.493847	7.249573
H	3.089574	4.407875	6.106080

cyclohepta-1,3,5-triene Cs

C	-0.254407	0.960209	1.201303
C	-0.254406	0.960209	-1.201303
C	-0.257326	-0.346209	1.512941
C	-0.257327	-0.346209	-1.512941
C	0.266253	-1.391664	0.678733
C	0.266253	-1.391664	-0.678733
H	-0.779655	1.666623	1.836405
H	-0.779654	1.666623	-1.836406
H	-0.706045	-0.654862	2.453256
H	-0.706046	-0.654861	-2.453255
H	0.556032	-2.313587	1.175023
H	0.556032	-2.313587	-1.175023
C	0.476241	1.469332	-0.000000
H	0.533027	2.557577	0.000000
H	1.498306	1.070441	0.000000

cyclohepta-1,3,5-triene C2v

C	1.297818	0.000000	0.944962
C	-1.297818	0.000000	0.944962
C	1.567924	0.000000	-0.362645
C	-1.567924	0.000000	-0.362645
C	0.670025	-0.000000	-1.502814
C	-0.670025	-0.000000	-1.502814
H	2.162336	-0.000000	1.605745

H	-2.162336	0.000000	1.605745
H	2.622540	0.000000	-0.624134
H	-2.622540	0.000000	-0.624134
H	1.160613	-0.000000	-2.471329
H	-1.160613	-0.000000	-2.471329
C	-0.000000	-0.000000	1.692070
H	0.000000	0.862605	2.375937
H	-0.000000	-0.862605	2.375937

silepin Cs

Si	-1.007741	-1.173662	-0.000000
C	0.023651	-0.729344	1.473726
C	0.023651	-0.729344	-1.473726
C	0.582992	0.485421	1.608389
C	0.582992	0.485421	-1.608389
C	0.557847	1.589656	0.676432
C	0.557846	1.589656	-0.676432
H	0.196531	-1.448081	2.271165
H	0.196531	-1.448081	-2.271165
H	1.112169	0.708534	2.534890
H	1.112169	0.708534	-2.534890
H	0.662840	2.567088	1.140814
H	0.662840	2.567088	-1.140814
H	-1.325264	-2.626700	-0.000000
H	-2.288730	-0.410740	0.000000

silepin C2v

Si	-0.000000	0.000000	1.645976
C	0.000000	1.530357	0.606615
C	0.000000	-1.530357	0.606615
C	-0.000000	1.663716	-0.730072
C	0.000000	-1.663716	-0.730072
C	-0.000000	0.674810	-1.786346
C	-0.000000	-0.674810	-1.786346
H	0.000001	2.468275	1.161722
H	0.000001	-2.468275	1.161722
H	0.000001	2.682047	-1.116232
H	0.000001	-2.682047	-1.116232
H	-0.000001	1.119424	-2.777839
H	-0.000000	-1.119424	-2.777839
H	1.185892	-0.000000	2.553183
H	-1.185894	0.000000	2.553182

(Z)-hexa-1,3,5-triene C2V

C	0.000000	1.736418	-0.137469
C	0.000000	-1.736418	-0.137469
C	0.000000	0.676253	-1.128074
C	-0.000000	-0.676253	-1.128074
H	0.000000	2.721529	-0.599083
H	-0.000000	-2.721529	-0.599083
H	0.000000	1.086636	-2.134785
H	-0.000000	-1.086635	-2.134785
C	0.000000	-1.733698	1.197916
H	0.000000	-2.675243	1.734072
H	0.000001	-0.843320	1.803665
C	-0.000000	1.733698	1.197916
H	-0.000001	0.843320	1.803664
H	-0.000000	2.675243	1.734072

5. References

(S1) Lui, M. W.; Merten, C.; Ferguson, M. J.; McDonald, R.; Xu, Y.; Rivard, E., *Inorg. Chem.* **2015**, *54*, 2040-2049.

(S2) Wiberg, N.; Amelunxen, K.; Lerner, H.-W.; Schuster, H.; Nöth, H.; Krossing, I.; Schmidt-Amelunxen, M.; Seifert, T. *J. Organomet. Chem.* **1997**, *542*, 1-8.

(S3) Kosai, T.; Ishida, S.; Iwamoto, T. A Two-Coordinate Cyclic (Alkyl)(Amino)Silylene: Balancing Thermal Stability and Reactivity. *Angew. Chem. Int. Ed.* **2016**, *55*, 15554-15558.

(S4) Kira, M.; Ishida, S.; Iwamoto, T.; Kabuto, C. *J. Am. Chem. Soc.* **1999**, *121*, 9722-9723.

(S5) Rekken, B. D.; Brown, T. M.; Fettinger, J. C.; Tuononen, H. M.; Power, P. P. Isolation of a Stable, Acyclic, Two-Coordinate Silylene. *J. Am. Chem. Soc.* **2012**, *134*, 6504-6507.

(S6) Roy, M. M. D.; Ferguson, M. J.; McDonald, R.; Zhou, Y.; Rivard, E. A Vinyl Silylsilylene and Its Activation of Strong Homo- and Heteroatomic Bonds. *Chem. Sci.* **2019**, *10*, 6476-6481.

(S7) *APEX suite of crystallographic software*, APEX 4 version 2021.10-0; Bruker AXS Inc.: Madison, Wisconsin, USA, 2021.

(S8) *CrysAlisPRO*, Oxford Diffraction /Agilent Technologies UK Ltd, Yarnton, England.

(S9) *SAINT, Version 7.56a and SADABS Version 2008/1*; Bruker AXS Inc.: Madison, Wisconsin, USA, 2008.

(S10) Sheldrick, G. M. *SHELXL-2014*, University of Göttingen, Göttingen, Germany, 2014.

(S11) Hübschle, C. B.; Sheldrick, G. M.; Dittrich, B. *J. Appl. Cryst.* **2011**, *44*, 1281-1284.

(S12) Sheldrick, G. M. *SHELXL-97*, University of Göttingen, Göttingen, Germany, 1998.

(S13) Wilson, A. J. C. International Tables for Crystallography, Vol. C, Tables 6.1.1.4 (pp. 500-502), 4.2.6.8 (pp. 219-222), and 4.2.4.2 (pp. 193-199); Kluwer Academic Publishers: Dordrecht, The Netherlands, 1992.

(S14) Macrae, C. F.; Bruno, I. J.; Chisholm, J. A.; Edgington, P. R.; McCabe, P.; Pidcock, E.; Rodriguez-Monge, L.; Taylor, R.; van de Streek, J.; Wood, P. A. *J. Appl. Cryst.* **2008**, *41*, 466-470.

(S15) Neese, F.; Wennmohs, F.; Becker, U.; Riplinger, C. *J. Chem. Phys.* **2020**, *152*, 224108.

(S16) Adamo, C.; Barone, V. *J. Chem. Phys.* **1999**, 110, 6158-6169.

(S17) (a) Grimme, S.; Ehrlich, S.; Goerigk, L. *J. Comput. Chem.* **2011**, *32*, 1456-1465; (b) Grimme, S.; Antony, J.; Ehrlich, S.; Krieg, H. *J. Chem. Phys.*, **2010** ,*132*, 154104.

(S18) Weigend, F.; Ahlrichs, R. *Phys. Chem. Chem. Phys*. **2005**, *7*, 3297-3305.

(S19) Weigend, F. *Phys. Chem. Chem. Phys*. **2006**, *8*, 1057-1065.

(S20) Frisch, M. J.; Trucks, G. W.; Schlegel, H. B.; Scuseria, G. E.; Robb, M. A.; Cheeseman, J. R.; Scalmani, G.; Barone, V.; Petersson, G. A.; Nakatsuji, H.; Li, X.; Caricato, M.; Marenich, A. V.; Bloino, J.; Janesko, B. G.; Gomperts, R.; Mennucci, B.; Hratchian, H. P.; Ortiz, J. V.; Izmaylov, A. F.; Sonnenberg, J. L.; Williams-Young, D.; Ding, F.; Lipparini, F.; Egidi, F.; Goings, J.; Peng, B.; Petrone, A.; Henderson, T.; Ranasinghe, D.; Zakrzewski, V. G.; Gao, J.; Rega, N.; Zheng, G.; Liang, W.; Hada, M.; Ehara, M.; Toyota, K.; Fukuda, R.; Hasegawa, J.; Ishida, M.; Nakajima, T.; Honda, Y.; Kitao, O.; Nakai, H.; Vreven, T.; Throssell, K.; Montgomery, Jr., J. A.; Peralta, J. E.; Ogliaro, F.; Bearpark, M. J.; Heyd, J. J.; Brothers, E. N.; Kudin, K. N.; Staroverov, V. N.; Keith, T. A.; Kobayashi, R.; Normand, J.; Raghavachari, K.; Rendell, A. P.; Burant, J. C.; Iyengar, S. S.; Tomasi, J.; Cossi, M.; Millam, J. M.; Klene, M.; Adamo, C.; Cammi, R.; Ochterski, J. W.; Martin, R. L.; Morokuma, K.; Farkas, O.; Foresman, J. B.; Fox, D. J. Gaussian, Inc., Wallingford CT, **2019**.

(S21) Boese, A. D.; Handy, N. C. *J. Chem. Phys*. **2001**, *114*, 5497-5503.

(S22) (a) Krishnan, R.; S. Binkley, J.; Seeger, R.; Pople, J. A. *J. Chem. Phys.* **1980**, *72*, 650; (b) McLean, A. D.; Chandler, G. S. *J. Chem. Phys*. **1980**, *72*, 5639-5648.

(S23) (a) Becke, A. D. *J. Chem. Phys*. **1993**, *98*, 5648-5652; (b) Lee, C.; Yang, W.; Parr, R.G. *Phys. Rev. B* **1988**, *37*, 785-789; (c) Vosko, S.H.; Wilk, L.; Nusair, M. *Can. J. Phys*. **1980**, *58*, 1200-1211; (d) Stephens, P. J.; Devlin, F.J.; Chabalowski, C. F.; Frisch, M. J. *J. Phys. Chem*. **1994**, *98*, 11623-11627.

(S24) Glendening, E. D.; Badenhoop, J. K.; Reed, A. E.; Carpenter, J. E.; Bohmann, J. A.; Morales, C. M.; Karafiloglou, P.; Landis, C. R.; Weinhold, F. NBO 7.0, Theoretical Chemistry Institute, University of Winsconsin: Madison, **2018**.

10.2 Supporting Information for Chapter 6

Israel Journal of Chemistry

Supporting Information

Facile Bond Activation of Small Molecules by an Acyclic Imino(silyl)silylene

Huaiyuan Zhu, Franziska Hanusch, and Shigeyoshi Inoue*© 2023 The Authors. Israel Journal of Chemistry published by Wiley-VCH GmbH. This is an open access article under the terms of the Creative Commons Attribution Non-Commercial License, which permits use, distribution and reproduction in any medium, provided the original work is properly cited and is not used for commercial purposes.

Supporting Information
©Wiley-VCH 2021
69451 Weinheim, Germany

Facile Bond Activation of Small Molecules by an Acyclic Imino(silyl)silylene

Huaiyuan Zhu, Franziska Hanusch, and Shigeyoshi Inoue*

Abstract: The activation of small molecules was accomplished by low-valent main group elements in the past few decades. Especially silylenes stand out due to their unique electronic properties and reactivity. Here, we present the small molecule activation by isolable acyclic iminosilylsilylene **1**, bearing an N-heteroimine ligand (NHI) with methylated backbone. **1** undergoes facile activation of small gaseous molecules like dihydrogen, ethylene, and carbon dioxide. Additionally, the cycloaddition of carbonyl compounds to **1**, is a promising candidate for the synthetic approach of oxasilacycles. More reactive silane and borane activation led to the corresponding Si–H and B–H cleavage products, but further attempts for hydrosilylation and hydroboration catalysed by **1** remained unsuccessful. Further reactivity studies towards heavier chalcogens elements allow the isolation of neutral three-coordinate silicon-heavier chalcogen double bond complexes.

DOI: 10.1002/ijch.200

Contents

1. Experimental Procedures

1.1 General Methods and Instrumentation

All experiments and manipulations were carried out under argon atmosphere using standard Schlenk or glovebox techniques. The glassware was heat-dried under vacuum prior to use. All glass junctions were coated with PTFE-based grease Merkel Triboflon III. For stirring, PTFE-coated magnetic stirrer bars were used or glass-coated ones if stated. Liquid phases were transferred using standard PE/PP syringes equipped with stainless steel cannula or directly canted from vessel to vessel if not stated otherwise. Solvents were dried by standard methods (withdrawal from MBraun Solvent Purification System and storage over molecular sieves (3 Å), or distilled from sodium/ benzophenone or CaH_2 under argon atmosphere and degassed via freeze-pump-thaw cycling). All chemicals were purchased from commercial suppliers and used as received if not stated otherwise. Deuterated benzene (C_6D_6) were obtained from Deutero Deutschland GmbH and were dried over 3 Å molecular sieves. All NMR samples were prepared under argon in J. Young PTFE tubes. Carbon dioxide (5.0), hydrogen (5.0) and ethylene (3.5) were purchased from Westfalen AG and used as received. NMR spectra were recorded on a Bruker AV400US, DRX400, AVHD300 or AV500cr at ambient temperature (300 K) if not stated otherwise. ^{1}H and ^{13}C NMR spectra were calibrated against the residual proton and natural abundance carbon resonances of the respective deuterated solvent as internal standard. Elemental analyses (EA) were conducted with a EURO EA (HEKA tech) instrument equipped with a CHNS combustion analyzer. Infrared (IR) spectra were recorded on a Perkin Elmer FT-IR spectrometer (diamond ATR, Spectrum Two) in a range of 400–4000 cm^{-1} at room temperature inside an argon-filled glovebox. The intensities of the IR bands are abbreviated as following: s = strong, m = medium, w = weak. **1** was synthesized according to procedures described in literature.[S1]

1.2 Synthesis and Characterization

1.2.1 Synthesis of 2.

A solution of silylene **1** (65.8 mg, 0.1 mmol) in pentane (5 mL) was degassed and subsequently exposed to dihydrogen (1 bar) under vigorous stirring at room temperature. The characteristic blue color vanished within 5 min, resulting in a clear pale yellow solution. The pentane solution was concentrated and cooled to –30 °C to yield iminosilane **2** (57.5 mg, 87%) as colorless crystals.

^{1}H NMR (400 MHz, C_6D_6): δ [ppm] 7.27-7.29 (m, 2H, *p*-C*H*-Dipp), 7.16-7.18 (m, 4H, *m*-C*H*-Dipp, overlapping with C_6D_6), 4.70 (t, *J* = 178.4 Hz, 2H, Si*H*) 3.12 (sept, *J* = 6.8 Hz, 4H, C*H*$(CH_3)_2$), 1.53 (s, 6H, CC*H*$_3$), 1.46 (d, *J* = 6.8 Hz, 12H, CH(C*H*$_3)_2$), 1.16 (d, *J* = 6.8 Hz, 12H, CH(C*H*$_3)_2$), 1.12 (s, 27H, C(C*H*$_3)_3$).

^{13}C{^{1}H} NMR (101 MHz, C_6D_6): δ [ppm] 147.9 (N*C*N), 145.9 (Ar*C*), 132.9 (Ar*C*), 129.2 (Ar*C*), 123.6 (Ar*C*), 115.9 (N*C*-CH$_3$), 31.3 (C(*C*H$_3)_3$), 28.6 (*C*H$(CH_3)_2$), 23.7 (CH(*C*H$_3)_2$), 23.5 (CH(*C*H$_3)_2$), 23.1 (*C*(CH$_3)_3$), 9.4 (NC-*C*H$_3$).

^{29}Si{^{1}H} NMR (80 MHz, C_6D_6): δ [ppm] 0.3 (*Si*^{t}Bu$_3$), –69.2 (*central Si*).

Elemental Analysis (%): Calcd: C 74.59, H 10.54, N 6.36; Found: C 71.98, H 10.29, N 6.02.

IR (Si–H, cm^{-1}): 2044(m).

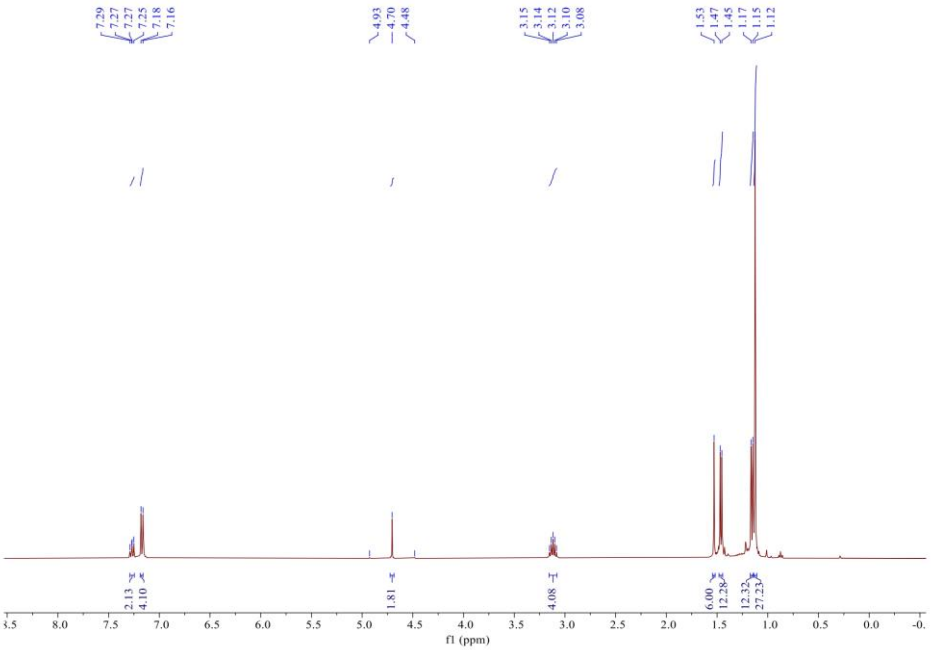

Figure S1. ^{1}H NMR spectrum of **2** in C_6D_6 at 300K.

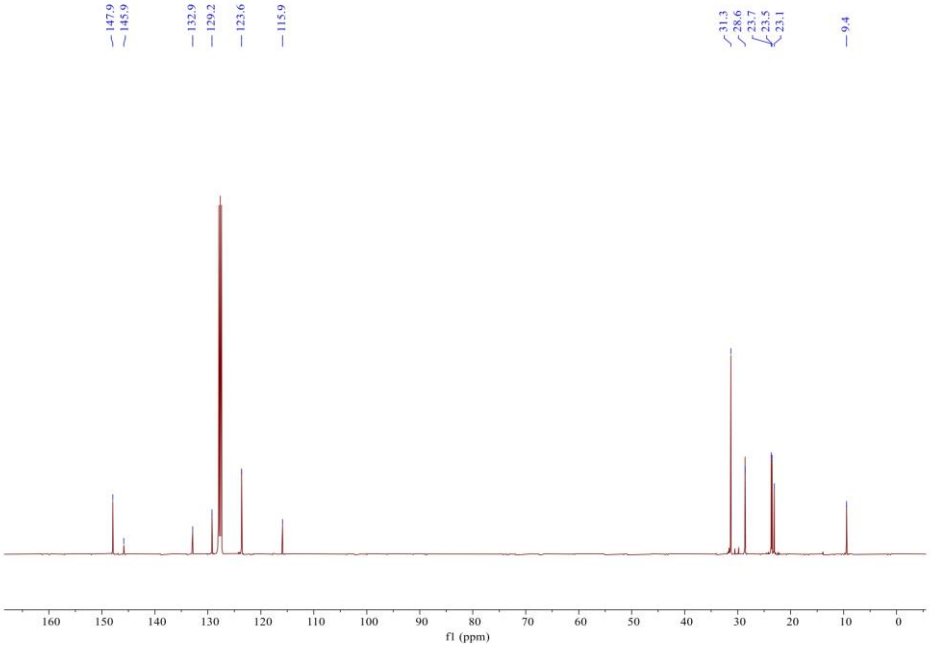

Figure S2. $^{13}C\{^{1}H\}$ NMR spectrum of **2** in C_6D_6 at 300K.

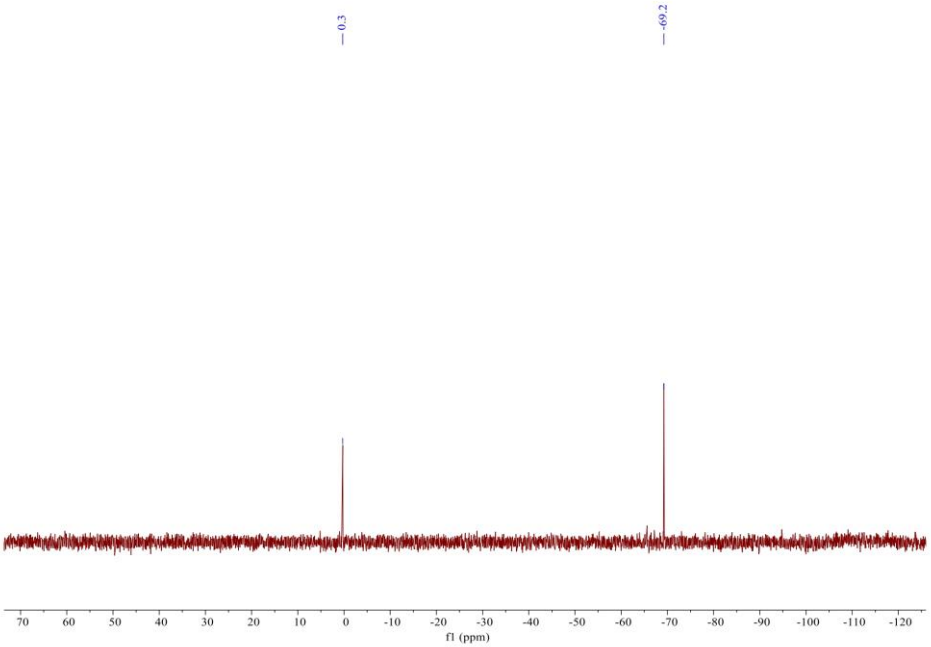

Figure S3. $^{29}Si\{^{1}H\}$ NMR spectrum of **2** in C_6D_6 at 300K.

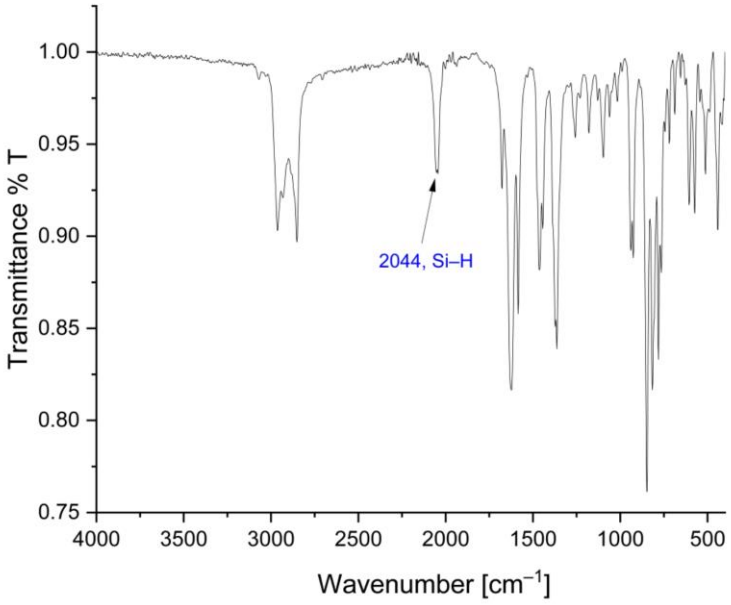

Figure S4. Solid-state FT-IR spectrum of **2**.

1.2.2 Synthesis of 3.

A solution of silylene **1** (32.9 mg, 0.05 mmol) in C_6D_6 in J-Young PTFE tube was degassed and subsequently exposed to ethylene (1 bar) at room temperature. The color changed to colorless rapidly. With ethylene, monitoring ^{1}H NMR spectrum at room temperature showed silirane **3** as sole product . All volatiles were removed *in vacuum* to give to silirane **3** (32.5 mg, 95%) as colorless powder.

^{1}H NMR (400 MHz, C_6D_6): δ [ppm] 7.27-7.30 (m, 2H, *p*-C*H*-Dipp), 7.18-7.19 (m, 4H, *m*-C*H*-Dipp), 3.11 (sept, *J* = 6.8 Hz, 4H, C*H*(CH$_3$)$_2$), 1.45 (d, *J* = 6.8 Hz, 12H, CH(C*H*$_3$)$_2$),1.44 (s, 6H, CC*H*$_3$), 1.16 (s, 27H, C(C*H*$_3$)$_3$), 1.12 (d, *J* = 6.8 Hz, 12H, CH(C*H*$_3$)$_2$), 0.08-0.12 (m, 2H, C*H*$_2$CH$_2$), –0.10—0.06 (m, 2H, CH$_2$C*H*$_2$).

^{13}C{^{1}H} NMR (101 MHz, C_6D_6): δ [ppm] 147.5 (N*C*N), 141.4 (Ar*C*), 133.9 (Ar*C*), 129.2 (Ar*C*), 122.6(Ar*C*), 116.3(N*C*-CH$_3$), 31.8 (C(*C*H$_3$)$_3$), 28.5 (*C*H(CH$_3$)$_2$), 23.9(CH(*C*H$_3$)$_2$), 23.4 (CH(*C*H$_3$)$_2$), 23.1 (*C*(CH$_3$)$_3$), 9.9 (NC-*C*H$_3$), 2.0 (*C*H$_2$CH$_2$).

^{29}Si{^{1}H} NMR (80 MHz, C_6D_6): δ [ppm] 9.2 (*Si*^{t}Bu$_3$), –110.8 (*central Si*).

Elemental Analysis (%): Calcd: C 75.26, H 10.43, N 6.12; Found: C 72.32, H 10.02, N 6.00.

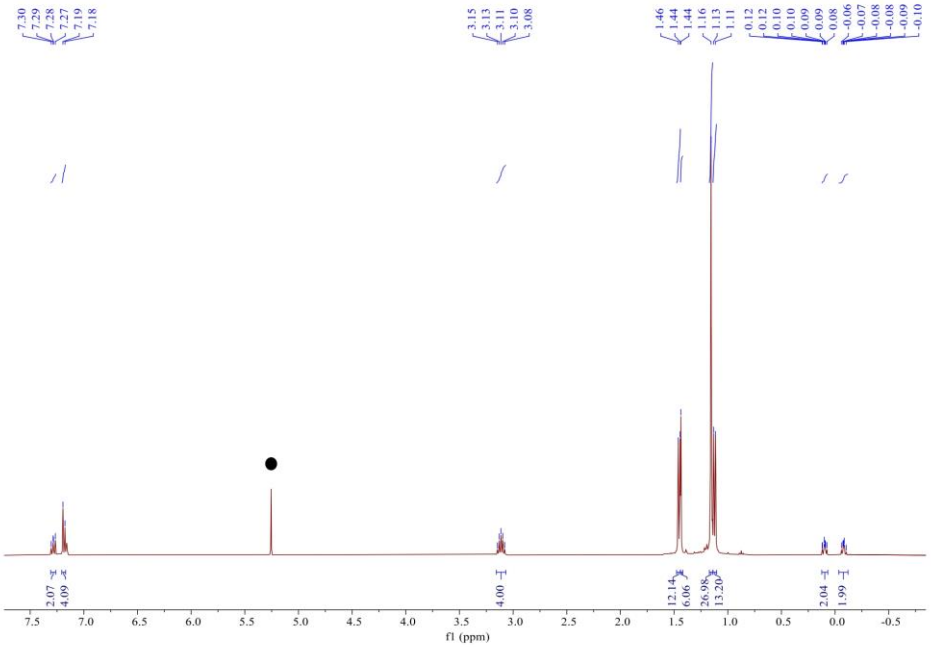

Figure S5. ^{1}H NMR spectrum of **3** in C_6D_6 at 300K. ● is ethylene.

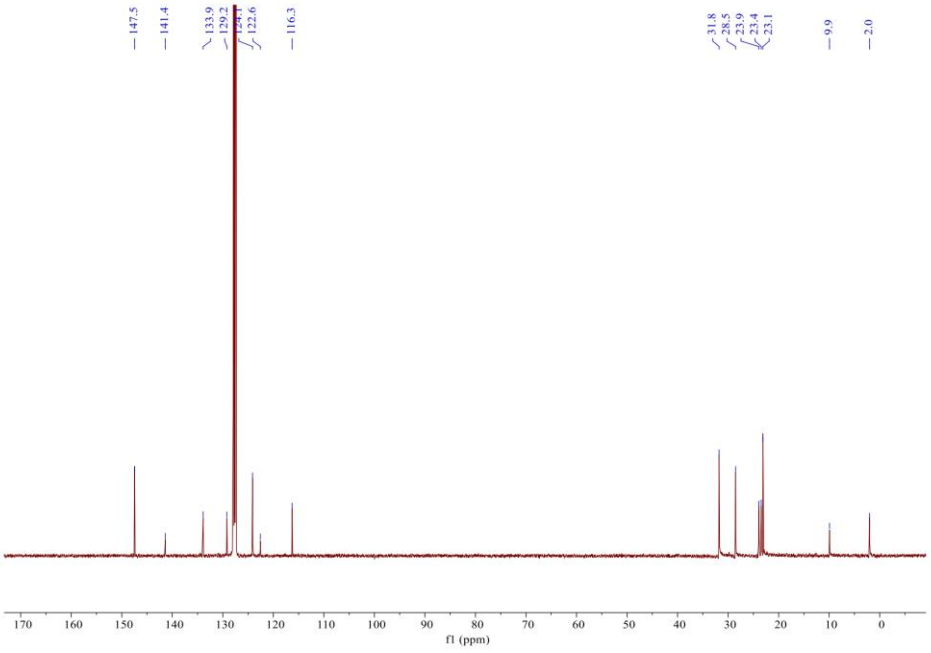

Figure S6. $^{13}C\{^{1}H\}$ NMR spectrum of **3** in C_6D_6 at 300K.

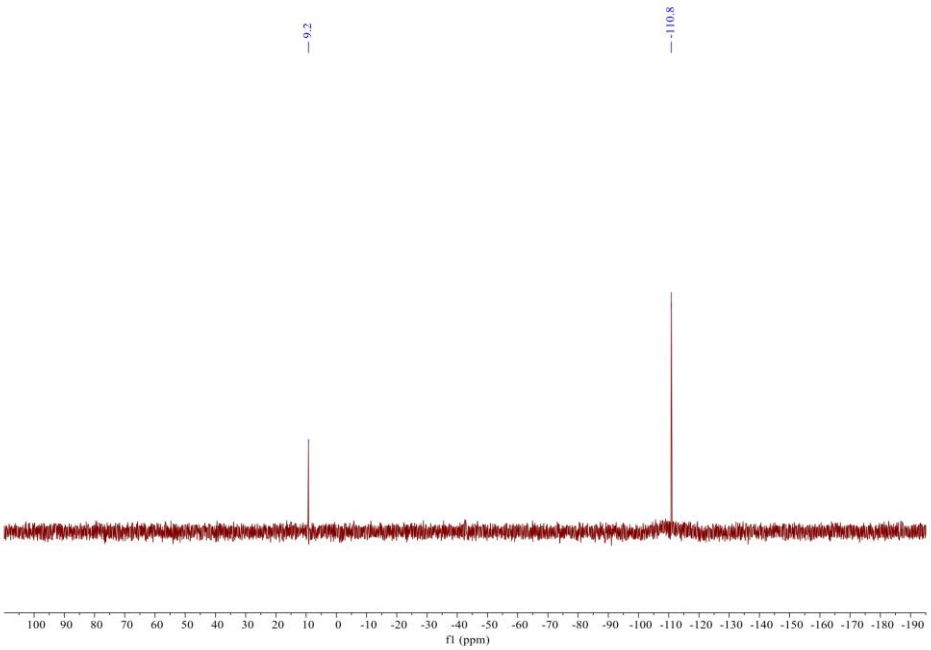

Figure S7. $^{29}Si\{^{1}H\}$ NMR spectrum of **3** in C_6D_6 at 300K.

1.2.3 Synthesis of 4.

A solution of silylene **1** (65.8 mg, 0.1 mmol) in pentane (5 mL) was degassed and subsequently exposed to carbon dioxide (1 bar) under vigorous stirring at –78 °C. A white precipitate formed rapidly. The suspension was allowed to warm to room temperature. After filtration, the residue was washed with cold pentane (3 × 1 mL) and dried *in vacuum* to give to pure carbonato silane **4** (60.3 mg, 84%).

^{1}H NMR (400 MHz, C_6D_6): δ [ppm] 7.35 (t, *J* = 6.8 Hz, 2H, *p*-C*H*-Dipp), 7.22 (d, *J* = 7.6 Hz, 4H, *m*-C*H*-Dipp), 2.92 (sept, *J* = 6.8 Hz, 4H, C*H*$(CH_3)_2$), 1.46 (d, *J* = 6.8 Hz, 12H, CH(C*H*$_3)_2$), 1.41 (s, 6H, CC*H*$_3$), 1.08 (s, 27H, C(C*H*$_3)_3$), 1.07 (d, *J* = 7.2 Hz, 12H, CH(C*H*$_3)_2$, overlapping with $^{t}Bu_3$).

^{13}C{^{1}H} NMR (101 MHz, C_6D_6): δ [ppm] 150.2 (O_2C=O), 146.4 (N*C*N), 144.4 (Ar*C*), 131.4 (Ar*C*), 130.2 (Ar*C*), 124.7 (Ar*C*), 118.0 (N*C*-CH_3), 31.2 (C(*C*$H_3)_3$), 28.7 (*C*H$(CH_3)_2$), 23.5 (CH(*C*$H_3)_2$), 22.3 (C(*C*$H_3)_3$), 9.5 (NC-*C*H_3).

^{29}Si{^{1}H} NMR (80 MHz, C_6D_6): δ [ppm] 7.0 (*Si*$^{t}Bu_3$), –45.6 (*central Si*).

Elemental Analysis (%): Calcd: C 70.24, H 9.40, N 5.85; Found: C 69.80, H 9.65, N 5.77.

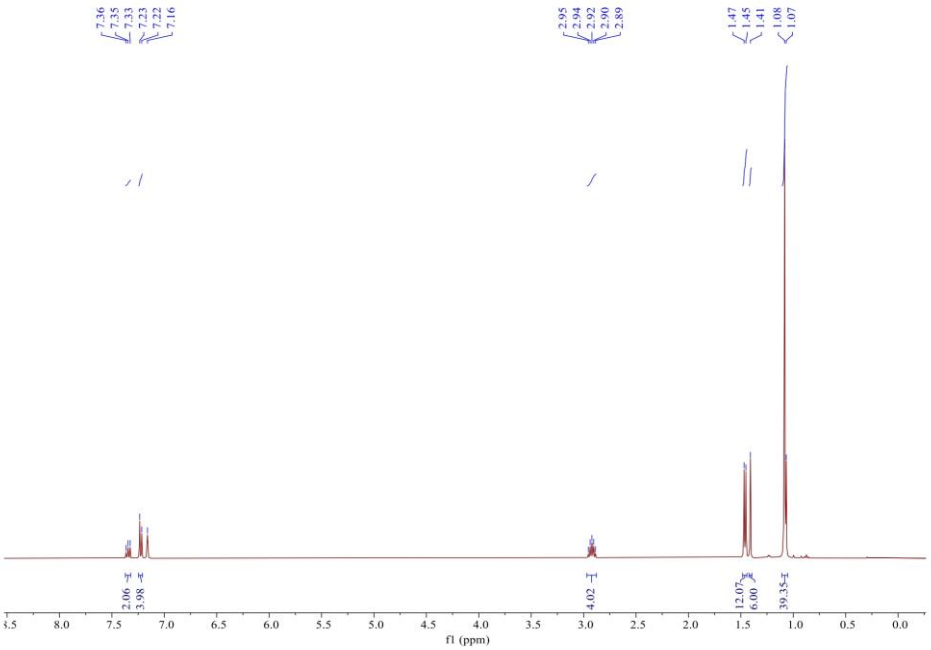

Figure S8. ^{1}H NMR spectrum of **4** in C_6D_6 at 300K.

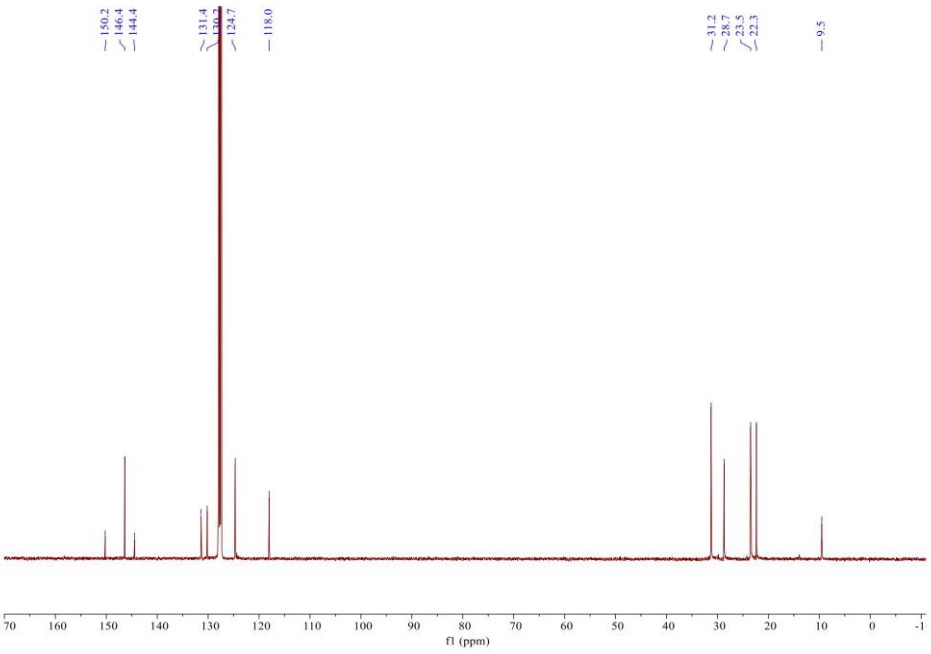

Figure S9. $^{13}C\{^{1}H\}$ NMR spectrum of **4** in C_6D_6 at 300K.

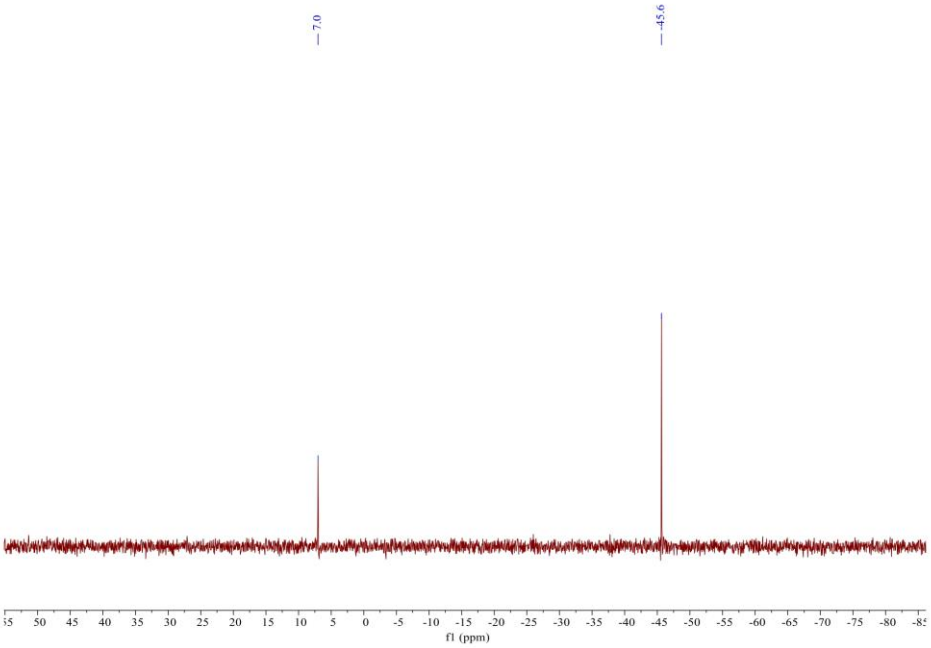

Figure S10. $^{29}Si\{^{1}H\}$ NMR spectrum of **4** in C_6D_6 at 300K.

1.2.4 Synthesis of 5.

Silylene **1** (65.8 mg, 0.1 mmol) and diphenylacetylene (17.8 mg, 0.1 mmol) were combined in pentane (5 mL) under vigorous stirring at room temperature. The color changed to yellow rapidly. After stirring for 1 hour, all volatiles were removed *in vacuo*, the residue was washed with cold pentane (3 × 0.5 mL) and dried *in vacuum* to give to **5** (76.7 mg, 92%) as yellow powder.

^{1}H NMR (400 MHz, C_6D_6): δ [ppm] 7.53-7.55 (m, 4H, *o*-C*H*-Ar PhCCPh), 7.19 (t, *J* = 7.6 Hz, 4H, *m*-C*H*-Ar PhCCPh), 7.05 (t, *J* = 7.2 Hz, 2H, *p*-C*H*-Ar PhCCPh), 6.97 (d, *J* = 7.6 Hz, 4H, *m*-C*H*-Ar Dipp), 6.86 (t, *J* = 7.2 Hz, 2H, *p*-C*H*-Ar Dipp), 3.22 (sept, *J* = 6.8 Hz, 4H, C*H*$(CH_3)_2$), 1.46 (d, *J* = 6.8 Hz, 12H, CH(C*H*$_3)_2$), 1.35 (s, 6H, CC*H*$_3$), 1.15 (s, 27H, C(C*H*$_3)_3$), 1.11 (d, *J* = 6.8 Hz, 12H, CH(C*H*$_3)_2$).

^{13}C{^{1}H} NMR (101 MHz, C_6D_6): δ [ppm] 164.7 (Ph*C*CPh), 146.1 (N*C*N), 140.5 (Ar*C*), 136.7 (Ar*C*), 133.3 (Ar*C*), 131.6 (Ar*C*), 129.0 (Ar*C*), 128.6 (Ar*C*), 126.4 (Ar*C*), 123.9 (Ar*C*), 116.6 (N*C*-CH_3), 31.8 (C(*C*$H_3)_3$), 28.5 (*C*H$(CH_3)_2$), 24.1 (CH(*C*$H_3)_2$), 23.0 (CH(*C*$H_3)_2$), 22.8 (*C*$(CH_3)_3$), 9.9 (NC-*C*H_3).

^{29}Si{^{1}H} NMR (80 MHz, C_6D_6): δ [ppm] 8.9 (*Si*^{t}Bu$_3$), –129.3 (*central Si*).

Elemental Analysis (%): Calcd: C 78.98, H 9.28, N 5.02; Found: C 77.71, H 9.38, N 4.96.

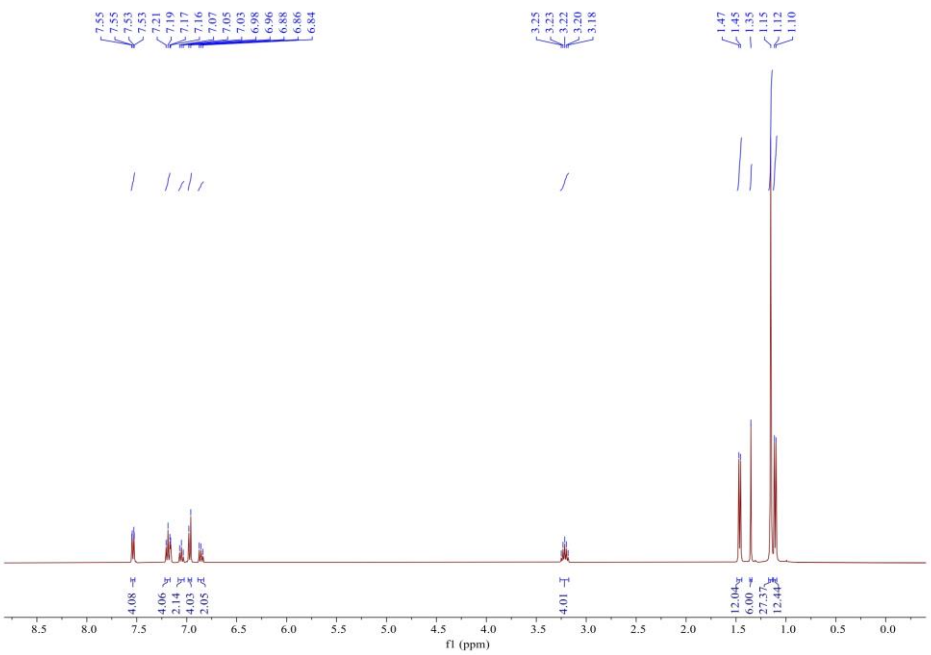

Figure S11. ^{1}H NMR spectrum of **5** in C_6D_6 at 300K.

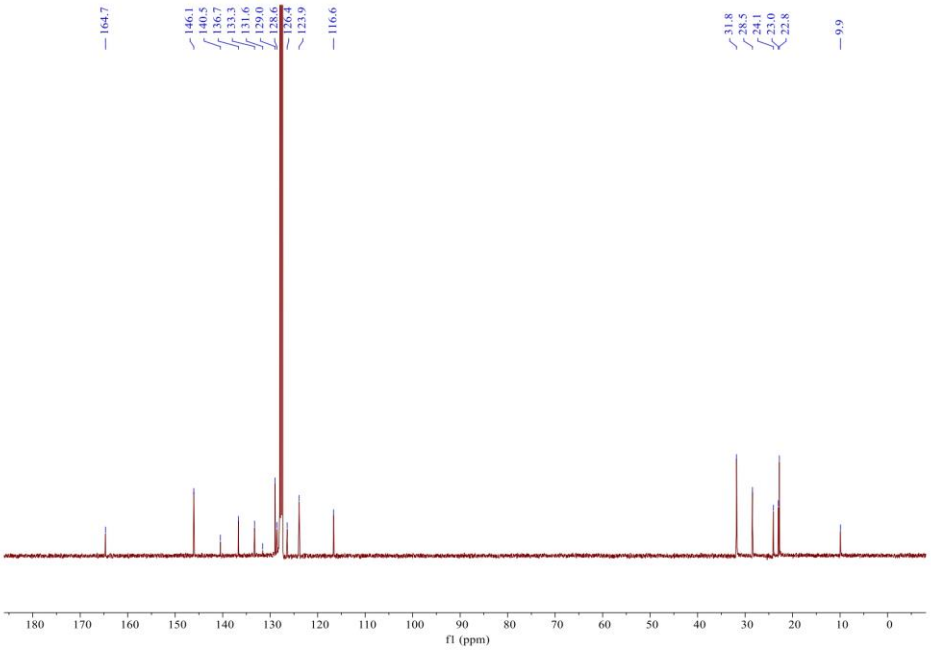

Figure S12. $^{13}C\{^{1}H\}$ NMR spectrum of **5** in C_6D_6 at 300K.

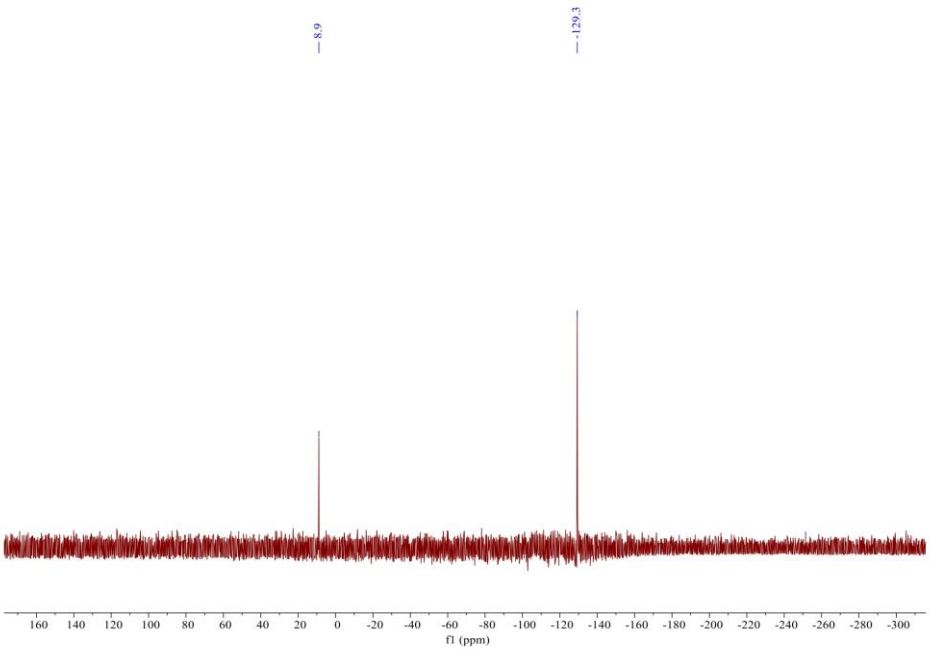

Figure S13. $^{29}Si\{^{1}H\}$ NMR spectrum of **5** in C_6D_6 at 300K.

1.2.5 Synthesis of 6.

Silylene **1** (65.8 mg, 0.1 mmol) and 9,10-phenanthrenequinone (20.8 mg, 0.1 mmol) were combined in benzene (3 mL) under vigorous stirring at room temperature. The color changed to pale yellow gradually with the formation of some colorless crystals. After stirring overnight, all volatiles were removed *in vacuum*, the residue was washed with cold pentane (3 × 0.5 mL) and dried *in vacuum* to give to **6** (80.5 mg, 93%) as off-white powder.

^{1}H NMR (400 MHz, C_6D_6): δ [ppm] 8.54 (d, *J* = 8.4 Hz, 2H, ArC*H*), 8.12 (d, *J* = 8.0 Hz, 2H, ArC*H*), 7.50-7.54 (m, 2H, ArC*H*), 7.35-7.40 (m, 2H, ArC*H*), 6.85-6.88 (m, 4H, *m*-C*H*-Dipp), 6.77-6.81 (m, 2H, *p*-C*H*-Dipp), 3.04 (sept, *J* = 6.8 Hz, 4H, C*H*$(CH_3)_2$), 1.41 (d, *J* = 6.8 Hz, 12H, CH(C*H*$_3)_2$), 1.37 (s, 6H, CC*H*$_3$), 1.13 (s, 27H, C(C*H*$_3)_3$), 1.01 (d, *J* = 6.4 Hz, 12H, CH(C*H*$_3)_2$).

$^{13}C\{^{1}H\}$ NMR (101 MHz, C_6D_6): δ [ppm] 146.5 (N*C*N), 143.3 (Ar*C*), 140.1 (Ar*C*), 132.0 (Ar*C*), 129.4 (Ar*C*), 126.1 (Ar*C*), 125.7 (Ar*C*), 125.4 (Ar*C*), 124.0 (Ar*C*), 123.1 (Ar*C*), 122.7 (Ar*C*), 121.7 (Ar*C*), 117.1 (N*C*-CH_3), 31.5 (C(*C*$H_3)_3$), 28.6 (*C*H$(CH_3)_2$), 23.5 (CH(*C*$H_3)_2$), 23.4 (CH(*C*$H_3)_2$), 22.4 (*C*$(CH_3)_3$), 9.6 (NC-*C*H_3).

$^{29}Si\{^{1}H\}$ NMR (80 MHz, C_6D_6): δ [ppm] 3.5 (*Si*^{t}Bu$_3$), –31.1 (*central Si*).

Elemental Analysis (%): Calcd: C 76.25, H 8.73, N 4.85; Found: C 75.71, H 9.12, N 4.79.

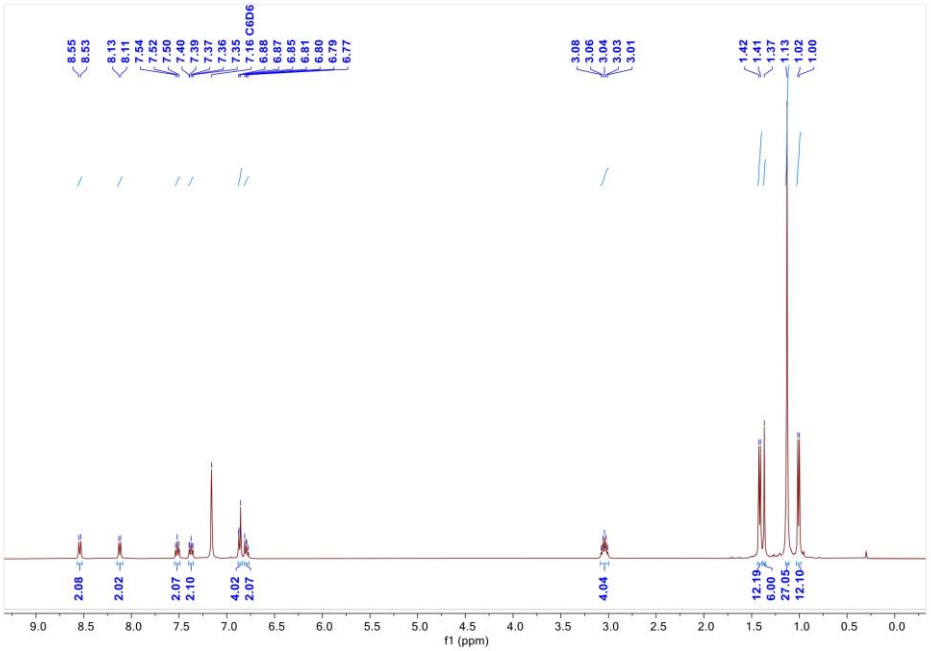

Figure S14. ^{1}H NMR spectrum of **6** in C_6D_6 at 300K.

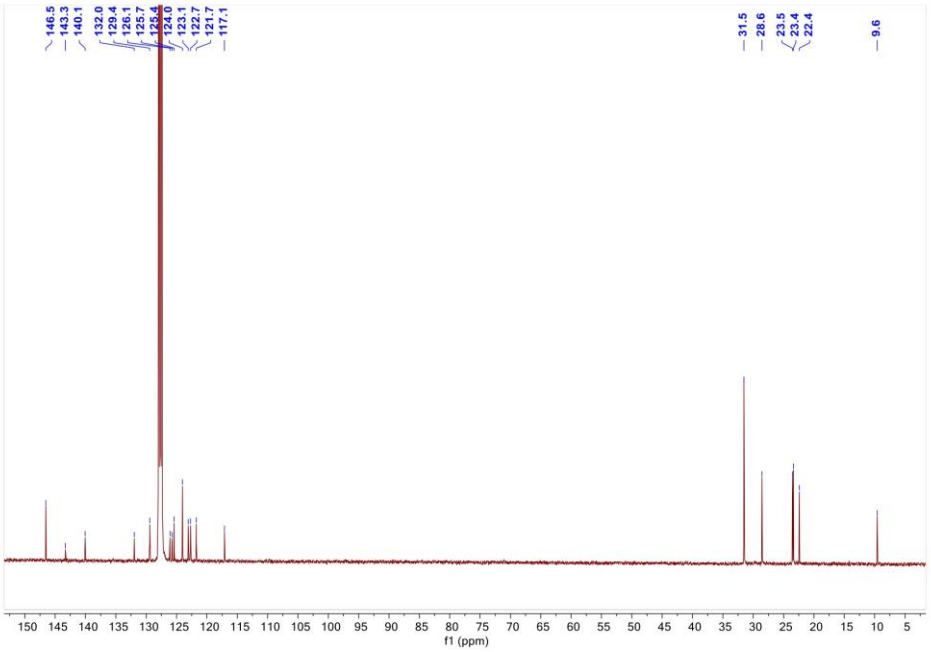

13

Figure S15. $^{13}C\{^{1}H\}$ NMR spectrum of **6** in C_6D_6 at 300K.

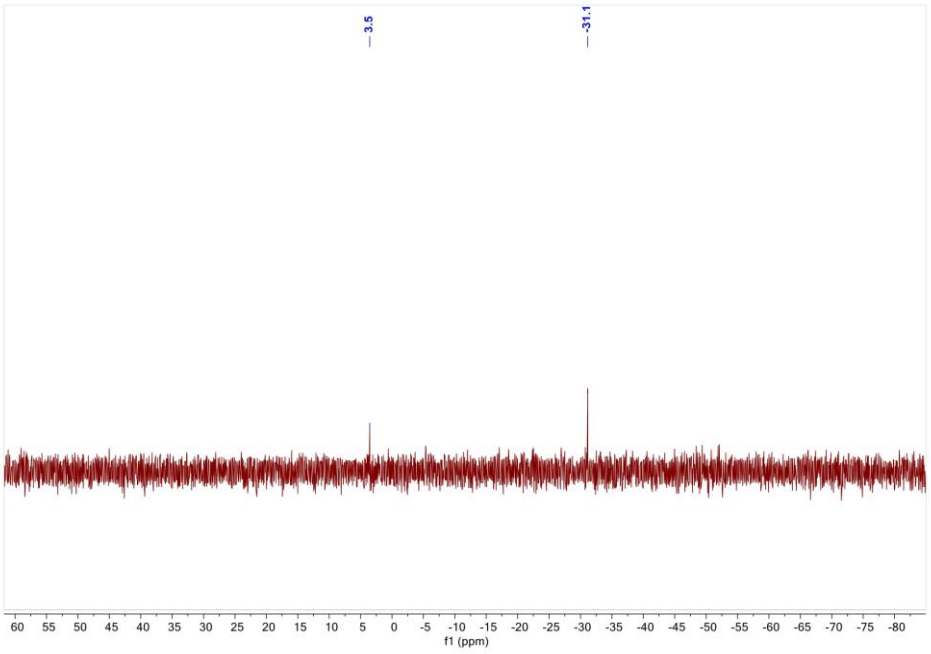

Figure S16. $^{29}Si\{^{1}H\}$ NMR spectrum of **6** in C_6D_6 at 300K.

1.2.6 Synthesis of 7.

Silylene **1** (65.8 mg, 0.1 mmol) and xanthone (19.6 mg, 0.1 mmol) were combined in benzene (3 mL) under vigorous stirring at room temperature. The color changed to orange rapidly. After stirring for 1 h, all volatiles were removed *in vacuum* to give to pure **7** (80.3 mg, 94%) as orange powder.

^{1}H NMR (400 MHz, C_6D_6): δ [ppm] 7.09-7.11 (m, 3H, *p*-C*H*-Dipp and ArC*H*), 7.03-7.05 (m, 2H, *m*-C*H*-Dipp), 6.87-6.91 (m, 2H, *p*-C*H*-Dipp), 6.81-6.84 (m, 2H, Ar*H*), 6.74-6.78 (m, 1H, ArC*H*), 5.88-5.93 (m, 1H, SiCHC*H*), 5.59-5.62 (m, 1H, SiCHCH=C*H*), 5.15-5.17 (m, 1H, SiCHCH=CHC*H*), 3.55 (s, 1H, SiC*H*), 3.43 (sept, *J* = 6.8 Hz, 2H, C*H*(CH_3)$_2$), 2.84 (sept, *J* = 6.8 Hz, 2H, C*H*(CH_3)$_2$), 1.55 (d, *J* = 6.8 Hz, 6H, CH(C*H*$_3$)$_2$), 1.40 (d, *J* = 6.8 Hz, 6H, CH(C*H*$_3$)$_2$), 1.38 (s, 6H, CC*H*$_3$), 1.15 (d, *J* = 6.8 Hz, 12H, CH(C*H*$_3$)$_2$), 1.11 (s, 27H, C(C*H*$_3$)$_3$), 1.04 (d, *J* = 6.8 Hz, 6H, CH(C*H*$_3$)$_2$).

$^{13}C\{^{1}H\}$ NMR (101 MHz, C_6D_6): δ [ppm] 154.7 (N*C*N), 154.7(SiO*C*), 146.9 (SiOC=*C*), 146.8 (Ar*C*), 146.5 (Ar*C*), 142.5 (Ar*C*), 132.7 (Ar*C*), 129.2 (Ar*C*), 125.6 (SiCH*C*H), 124.2 (Ar*C*), 124.2 (Ar*C*), 121.7 (Ar*C*), 121.3 (Ar*C*), 117.5 (N*C*-CH$_3$), 115.2 (SiCHCH=*C*H), 114.6 (Ar*C*), 110.0 (SiOC=C*C*), 92.7 (SiCHCH=CH*C*H), 39.6 (Si*C*H), 31.5 (C(*C*H$_3$)$_3$), 28.7 (*C*H(CH$_3$)$_2$), 28.3

($CH(CH_3)_2$), 25.8 ($CH(CH_3)_2$), 23.5 ($CH(CH_3)_2$), 22.8 ($C(CH_3)_3$), 22.7 ($CH(CH_3)_2$), 22.7 ($CH(CH_3)_2$), 10.1 (NC-CH_3).

$^{29}Si\{^1H\}$ NMR (80 MHz, C_6D_6): δ [ppm] 3.5 (Si^tBu_3), –30.5 (*central Si*).

Elemental Analysis (%): Calcd: C 75.91, H 8.85, N 4.92; Found: C 74.32, H 9.72, N 4.79.

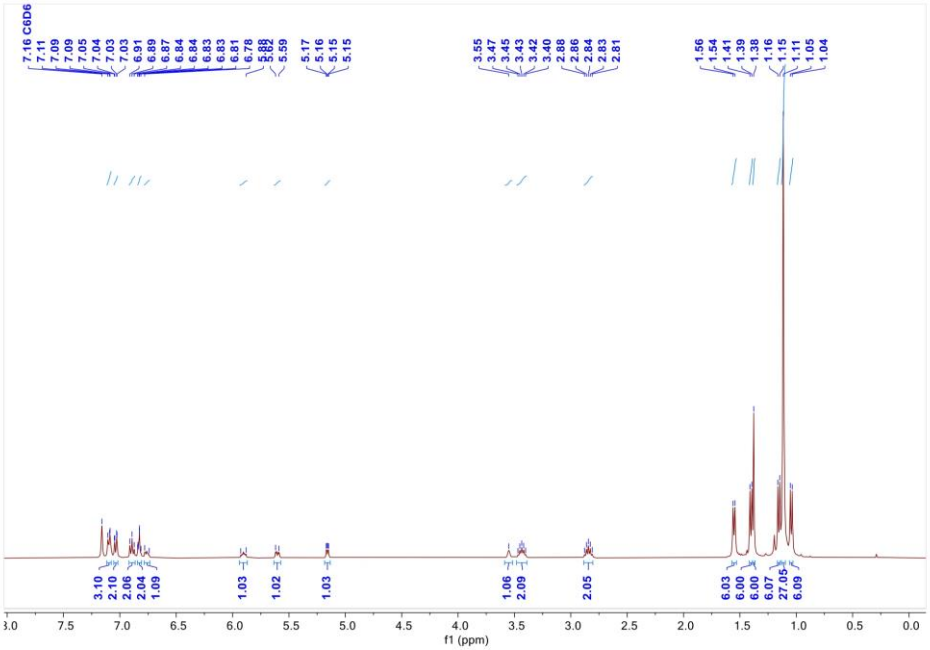

Figure S17. ^1H NMR spectrum of **7** in C_6D_6 at 300K.

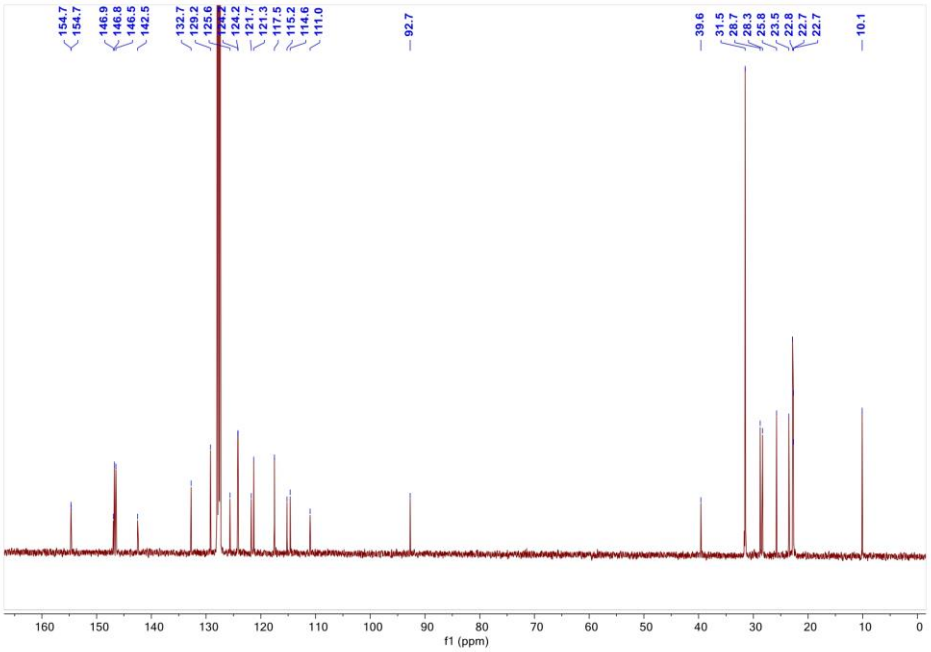

Figure S18. $^{13}C\{^{1}H\}$ NMR spectrum of **7** in C_6D_6 at 300K.

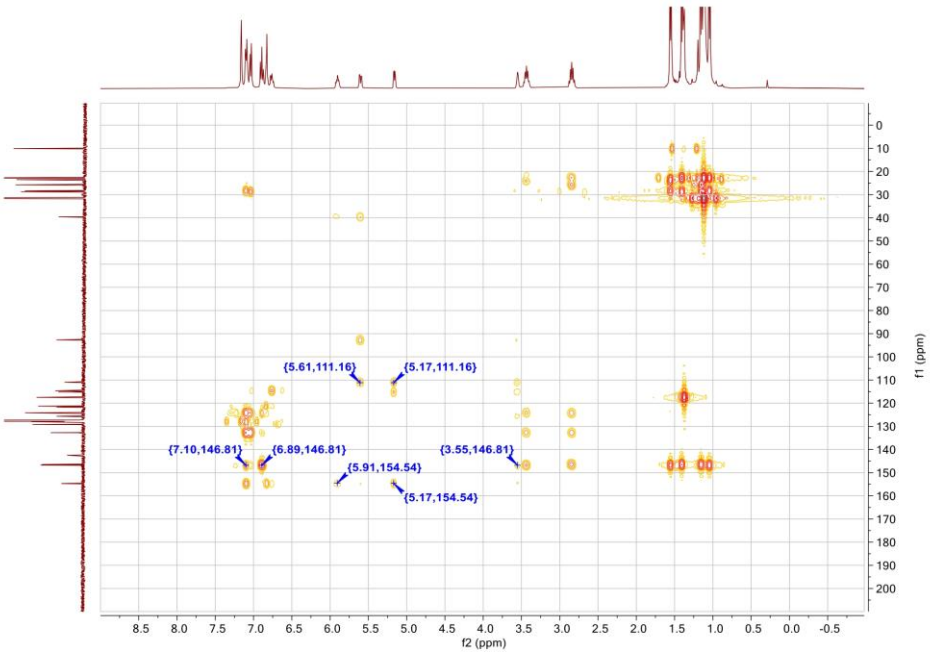

Figure S19. $^{1}H/^{13}C$ HMBC NMR spectrum of **7** in C_6D_6 at 300K.

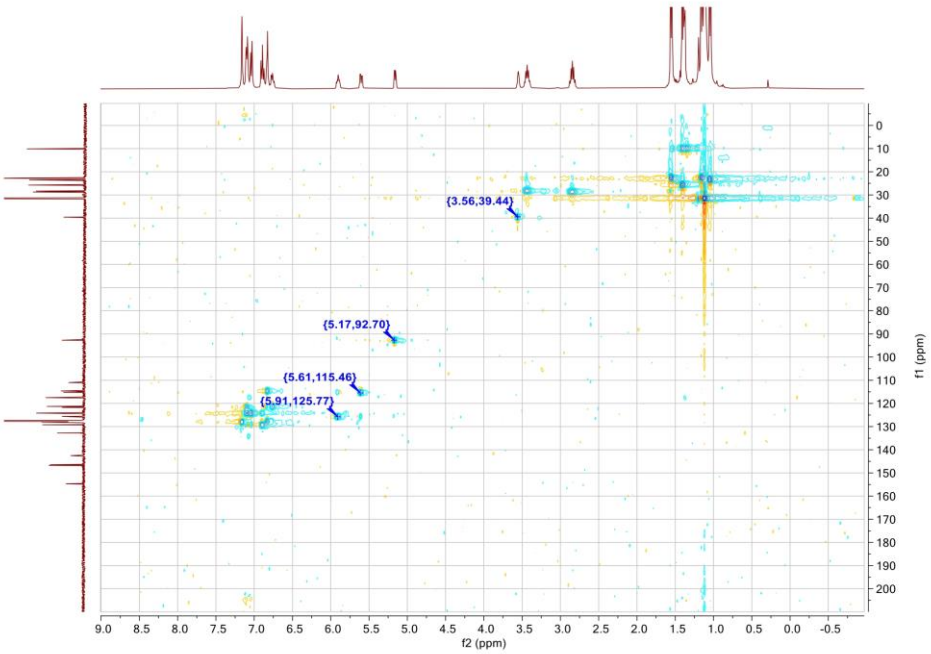

Figure S20. $^{1}H/^{13}C$ HSQC NMR spectrum of **7** in C_6D_6 at 300K.

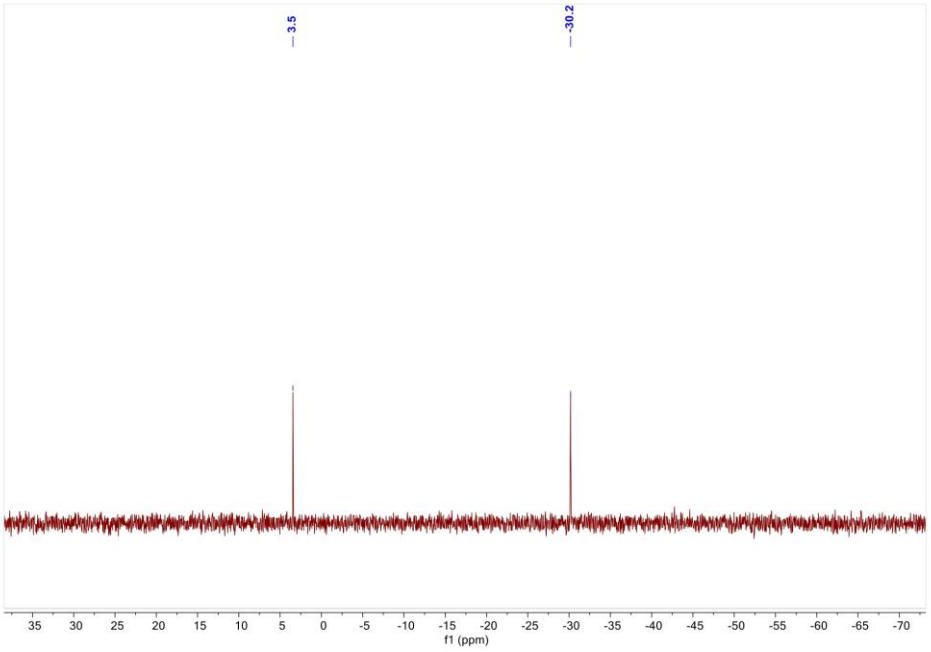

Figure S21. $^{29}Si\{^{1}H\}$ NMR spectrum of **7** in C_6D_6 at 300K.

1.2.7 Synthesis of 8.

Diphenylsilane (9.2 mg, 0.05 mmol) was added dropwise to silylene **1** (32.9 mg, 0.1 mmol) under vigorous stirring by micro syringe at room temperature. The color changed to colorless rapidly. After stirring for 1 h, all volatiles were removed *in vacuum* to give to **8** (39.8 mg, 94%) as colorless powder. Crystals suitable for single crystal X-ray diffraction analysis was obtained by slow evaporation of pentane solution at –30 °C for several days.

^{1}H NMR (400 MHz, C_6D_6): δ [ppm] 7.68-7.70 (m, 2H, *o*-C*H*-Si*Ph*$_2$), δ = 7.50-7.52 (m, 2H, *o*-C*H*-Si*Ph*$_2$), 7.23-7.25 (m, 2H, *p*-C*H*-Dipp), 7.14-7.18 (m, 8H, *m*-C*H*-*Dipp* and *m*-C*H*-Si*Ph*$_2$, overlapping with C_6D_6), 6.99-7.01 (m, 2H, *p*-C*H*-Si*Ph*$_2$), 5.90 (s, *J* = 160.8 Hz, 1H, Ph_2Si-*H*), 4.93 (s, *J* = 180.2 Hz, 1H, Si-*H*), 3.58 (sept, *J* = 6.8 Hz, 2H, C*H*(CH_3)$_2$), 3.01 (sept, *J* = 6.8 Hz, 2H, C*H*(CH_3)$_2$), 1.57 (d, *J* = 6.8 Hz, 6H, CH(C*H*$_3$)$_2$), 1.50 (s, 6H, CC*H*$_3$), 1.27 (d, *J* = 7.2 Hz, 6H, CH(C*H*$_3$)$_2$), 1.14 (d, *J* = 6.8 Hz, 6H, CH(C*H*$_3$)$_2$), 1.11 (d, *J* = 6.8 Hz, 6H, CH(C*H*$_3$)$_2$), 1.03 (s, 27H, C(C*H*$_3$)$_3$).

^{13}C{^{1}H} NMR (101 MHz, C_6D_6): δ [ppm] 147.8 (N*C*N), 147.2 (Ar*C*), 143.3 (Ar*C*), 137.5 (Ar*C*), 137.3 (Ar*C*), 136.8 (Ar*C*), 136.2 (Ar*C*), 133.9 (Ar*C*), 129.0 (Ar*C*), 128.5 (Ar*C*), 127.3 (Ar*C*), 124.6 (Ar*C*), 123.5 (Ar*C*), 117.2 (N*C*-CH_3), 31.6 (C(*C*H_3)$_3$), 28.8 (*C*H(CH_3)$_2$), 28.5 (*C*H(CH_3)$_2$), 25.3 (CH(*C*H_3)$_2$), 23.8 (CH(*C*H_3)$_2$), 23.6 (CH(*C*H_3)$_2$), 23.2 (CH(*C*H_3)$_2$), 22.9 (*C*(CH_3)$_3$), 10.1 (NC-*C*H_3).

^{29}Si{^{1}H} NMR (80 MHz, C_6D_6): δ [ppm] 8.5 (*Si*^{t}Bu$_3$), –28.0 (Ph_2*Si*), –68.6 (*central Si*).

Elemental Analysis (%): Calcd: C 75.56, H 9.45, N 4.99; Found: C 75.06, H 9.95, N 4.96.

IR (Si–H, cm^{-1}): 2058(m), 2140(w).

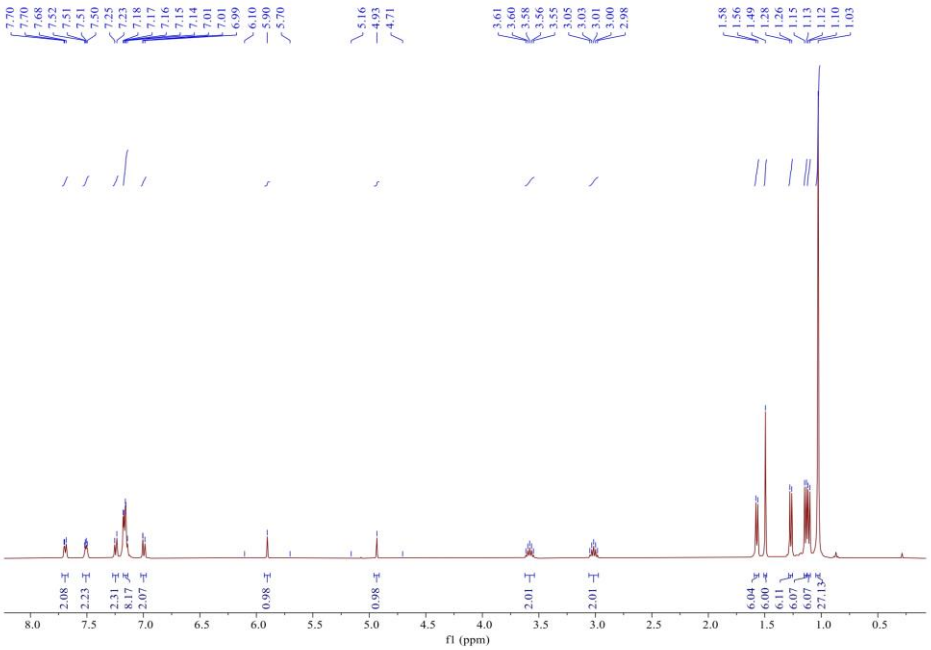

Figure S22. ^{1}H NMR spectrum of **8** in C_6D_6 at 300K.

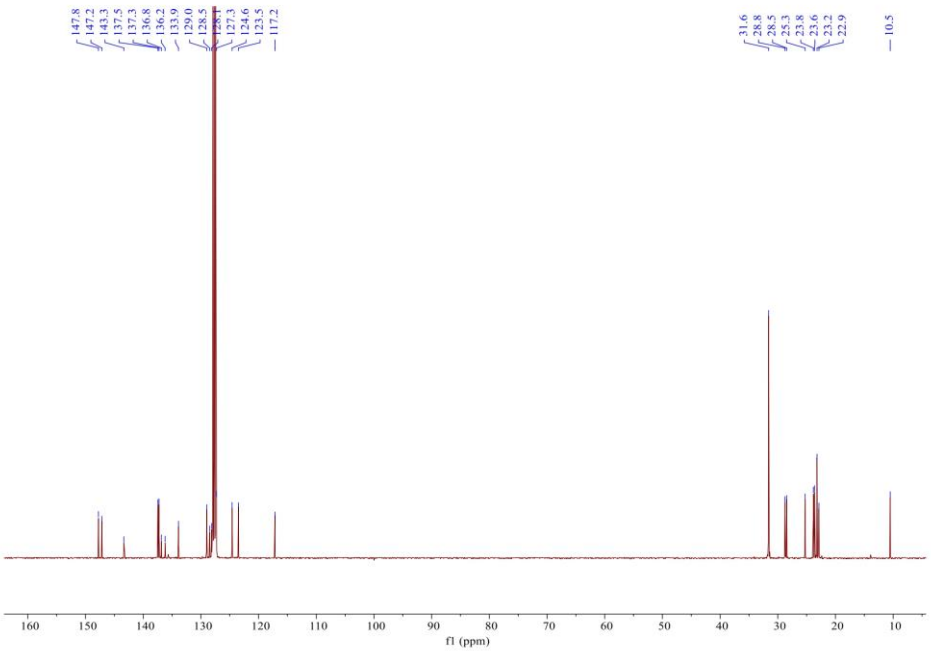

Figure S23. $^{13}C\{^{1}H\}$ NMR spectrum of **8** in C_6D_6 at 300K.

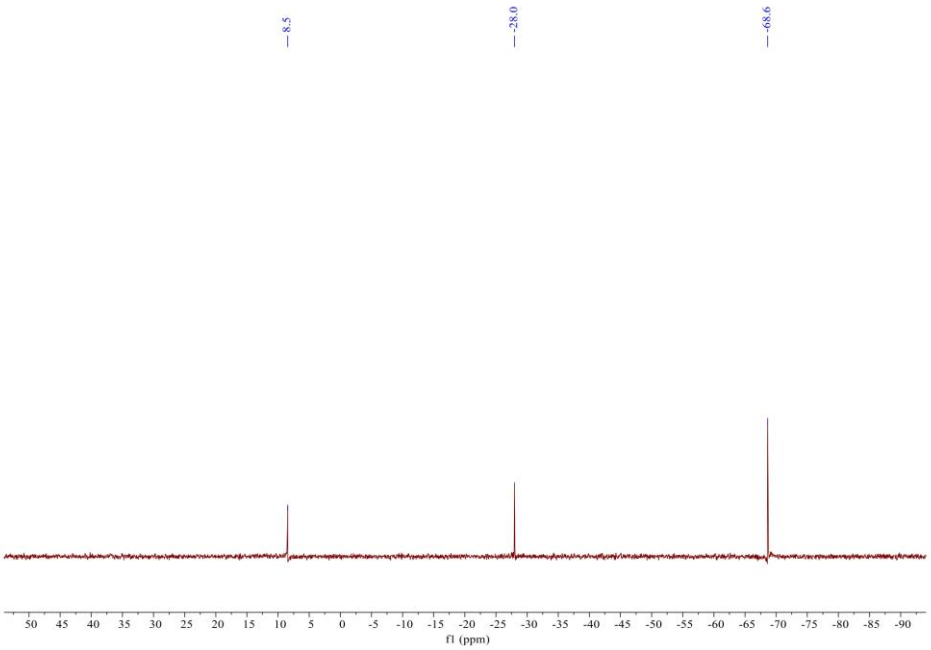

Figure S24. $^{29}Si\{^{1}H\}$ NMR spectrum of **8** in C_6D_6 at 300K.

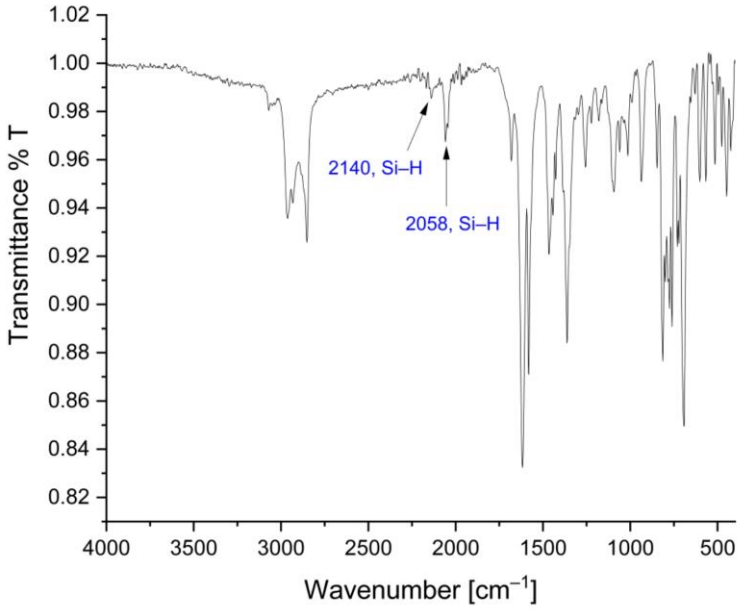

Figure S25. Solid-state FT-IR spectrum of **8**.

1.2.8 Synthesis of 9.

Pinacolborane (8.6 mg, 0.075 mmol) was added dropwise to silylene **1** (44.0 mg, 0.075 mmol) under vigorous stirring by micro syringe at room temperature. The color changed to colorless rapidly. After stirring for 1 h, all volatiles were removed *in vacuum*, the residue was washed with cold pentane (3 × 0.5 mL) and dried *in vacuum* to give to **9** (42.8 mg, 81%) as colorless powder. Crystals suitable for single crystal X-ray diffraction analysis was obtained by slow diffusion of pentane into a saturated toluene solution at –30 °C for several days.

^{1}H NMR (400 MHz, C_6D_6): δ [ppm] 7.25-7.26 (m, 4H, *m*-C*H*-Dipp), 7.15-7.17 (m, 2H, *p*-C*H*-Dipp, overlapping with C_6D_6), 4.84 (s, *J* = 170.8 Hz, 1H, Si-*H*), 3.60 (sept, *J* = 6.8 Hz, 2H, C*H*$(CH_3)_2$), 2.98 (sept, *J* = 6.8 Hz, 2H, C*H*$(CH_3)_2$), 1.57 (d, *J* = 6.8 Hz, 6H, CH(C*H*$_3)_2$), 1.55 (s, 6H, CC*H*$_3$), 1.40 (d, *J* = 6.8 Hz, 6H, CH(C*H*$_3)_2$), 1.22 (d, *J* = 6.8 Hz, 6H, CH(C*H*$_3)_2$), 1.21 (s, 27H, C(C*H*$_3)_3$), 1.21 (s, 27H, C(C*H*$_3)_3$), 1.15 (d, *J* = 6.8 Hz, 6H, CH(C*H*$_3)_2$), 1.13 (s, 6H, CC*H*$_3$), 1.11 (s, 6H, CC*H*$_3$).

^{13}C{^{1}H} NMR (101 MHz, C_6D_6): δ [ppm] 148.3 (N*C*N), 147.2 (Ar*C*), 143.3 (Ar*C*), 133.8 (Ar*C*), 128.9 (Ar*C*), 123.8 (Ar*C*), 123.5 (Ar*C*), 116.4 (N*C*-CH$_3$), 82.5 (BO*C*), 31.8 (C(*C*H$_3)_3$), 28.4

(*C*H(CH$_3$)$_2$), 28.3 (*C*H(CH$_3$)$_2$), 26.2 (CH(*C*H$_3$)$_2$), 25.0 (CH(*C*H$_3$)$_2$), 24.3 (CH(*C*H$_3$)$_2$), 23.8 (CH(*C*H$_3$)$_2$), 23.5 (*C*(CH$_3$)$_3$), 23.2 (C*C*H$_3$), 23.0 (C*C*H$_3$), 10.1 (NC-*C*H$_3$).

^{29}Si{^{1}H} NMR (80 MHz, C_6D_6): δ [ppm] 5.6 (*Si*^{t}Bu$_3$).

^{11}B{^{1}H} NMR (128 MHz, C_6D_6,): δ [ppm] 35.7 (broad).

Elemental Analysis (%): Calcd: C 70.38, H 10.05, N 5.24; Found: C 71.13, H 10.14, N 5.17.

IR (Si–H, cm^{-1}): 2034(m).

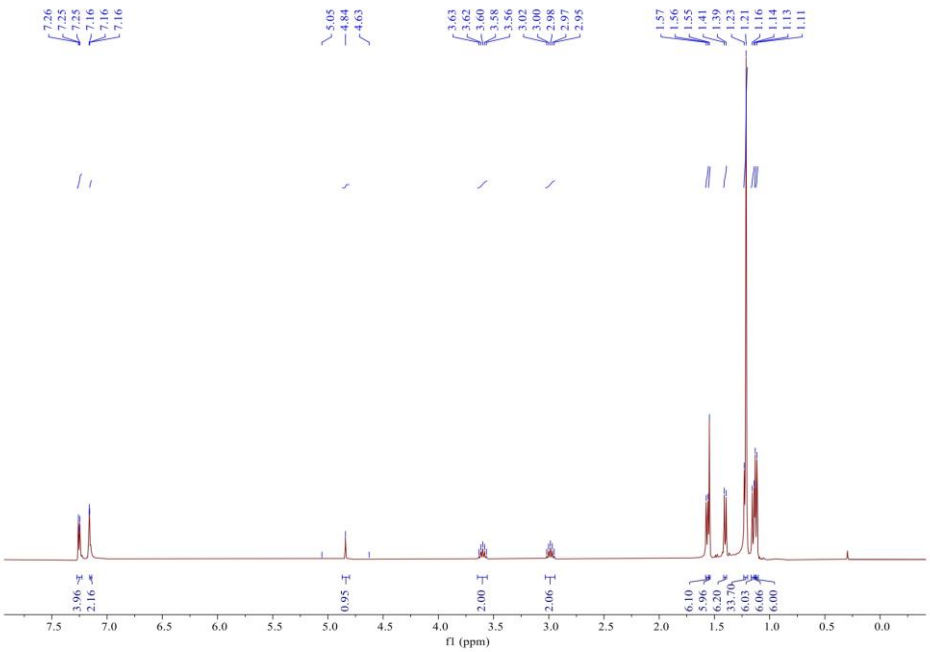

Figure S26. ^{1}H NMR spectrum of **9** in C_6D_6 at 300K.

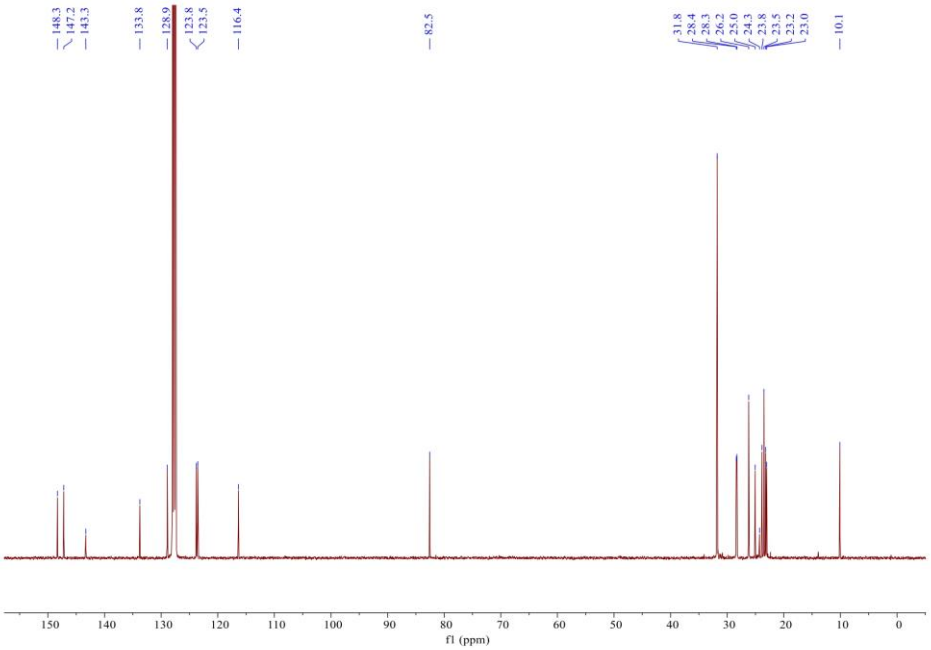

Figure S27. $^{13}C\{^{1}H\}$ NMR spectrum of **9** in C_6D_6 at 300K.

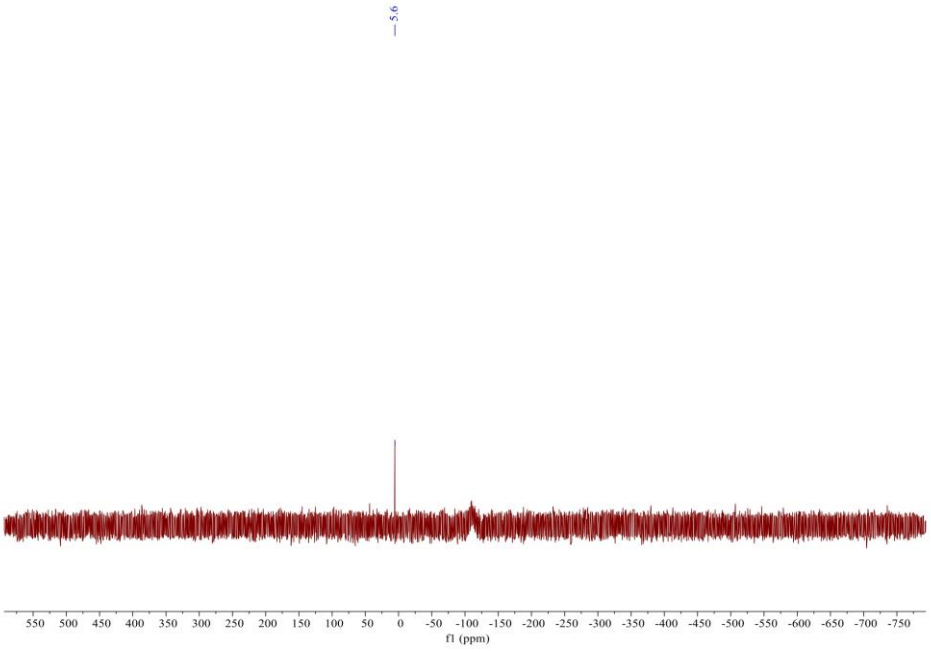

Figure S28. $^{29}Si\{^{1}H\}$ NMR spectrum of **9** in C_6D_6 at 300K.

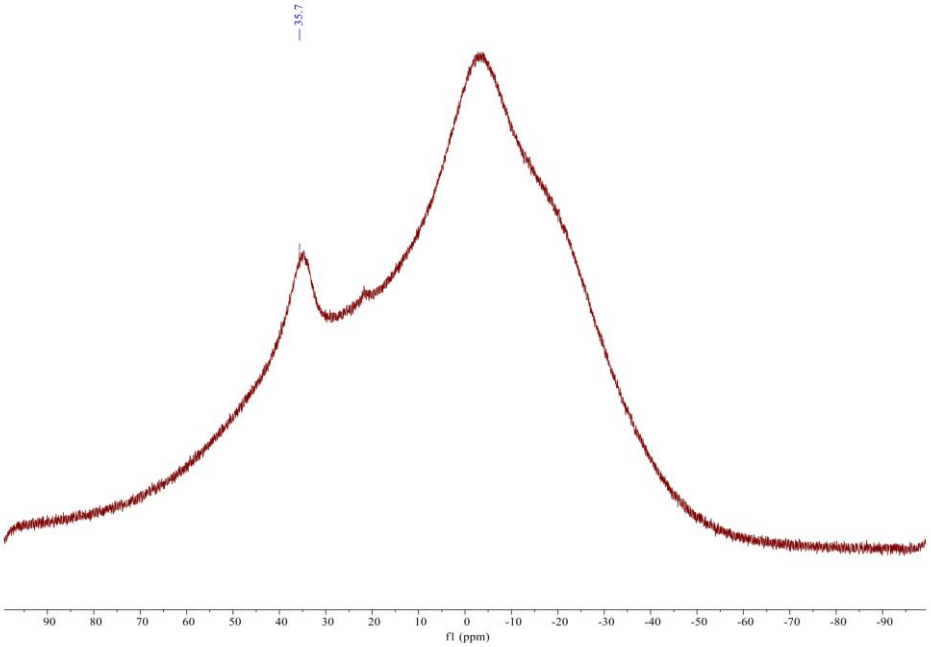

Figure S29. $^{11}B\{^{1}H\}$ NMR spectrum of **9** in C_6D_6 at 300K.

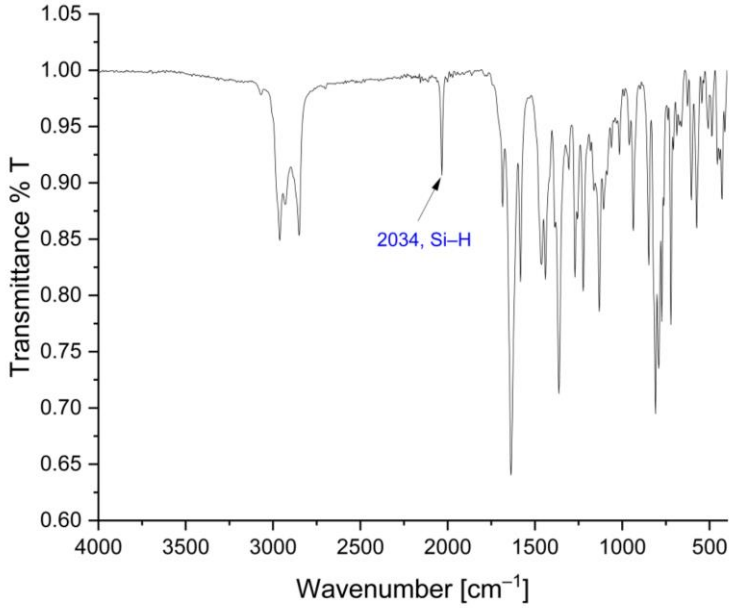

Figure S30. Solid-state FT-IR spectrum of **9**.

1.2.9 Synthesis of 10.

Silylene **1** (100 mg, 0.15 mmol) and triethylphosphine oxide (20.4 mg, 0.15 mmol) were combined in pentane (5 mL) under vigorous stirring at room temperature for 24 h. The pentane solution was concentrated and cooled to –30 °C to yield iminosiloxysilylene **10** (80.3 mg, 78%) as colorless crystals.

^{1}H NMR (400 MHz, C_6D_6): δ [ppm] 7.22-7.26 (m, 2H, *p*-C*H*-Dipp), 7.13-7.15 (m, 4H, *m*-C*H*-Dipp, overlapping with C_6D_6), 3.03 (sept, *J* = 6.8 Hz, 4H, C*H*$(CH_3)_2$), 1.55 (s, 6H, CCH_3), 1.49 (d, *J* = 6.8 Hz, 12H, CH(CH_3)$_2$), 1.16 (s, 27H, C(CH_3)$_3$), 1.07 (d, *J* = 6.8 Hz, 12H, CH(CH_3)$_2$).

^{13}C{^{1}H} NMR (101 MHz, C_6D_6): δ [ppm] 147.7 (N*C*N), 145.3 (Ar*C*), 131.4 (Ar*C*), 129.5 (Ar*C*), 123.7 (Ar*C*), 116.4 (N*C*-CH_3), 30.8 (C(*C*H_3)$_3$), 28.7 (*C*H$(CH_3)_2$), 24.5 (CH(*C*H_3)$_2$), 23.5 (CH(*C*H_3)$_2$), 22.4 (*C*$(CH_3)_3$), 9.3 (NC-*C*H_3).

^{29}Si{^{1}H} NMR (80 MHz, C_6D_6): δ [ppm] 4.2 (*Si*^{t}Bu$_3$), 59.3 (*central Si*).

Elemental Analysis (%): Calcd: C 73.04, H 10.02, N 6.23; Found: C 69.51, H 10.55, N 5.78.

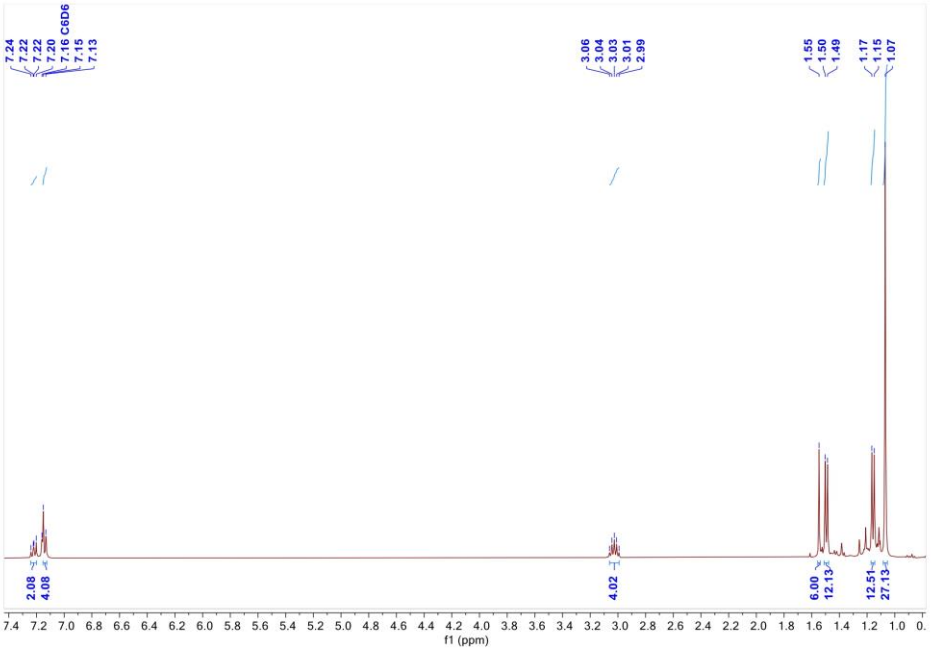

Figure S31. ^{1}H NMR spectrum of **10** in C_6D_6 at 300K.

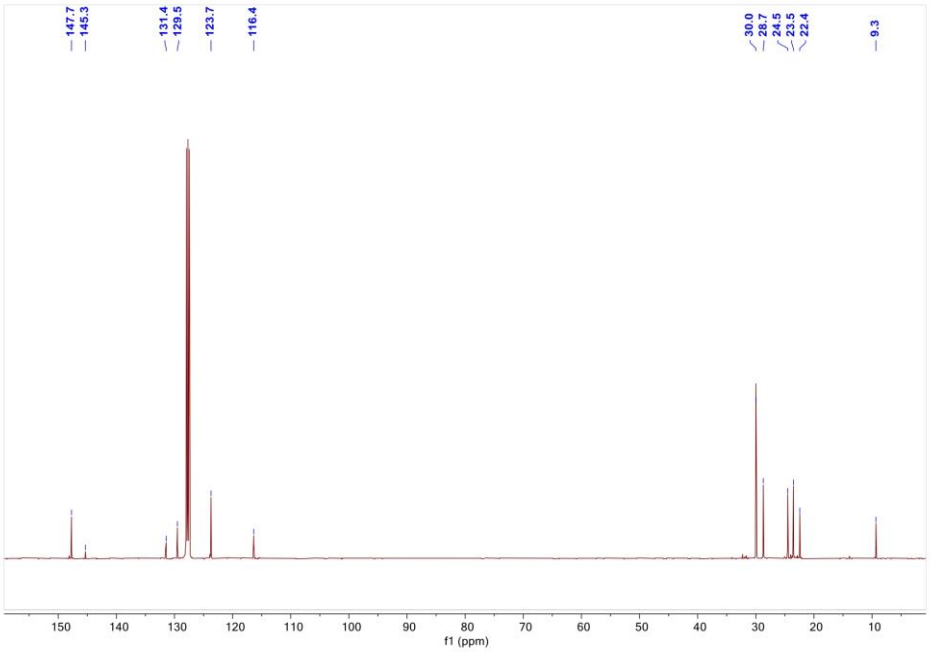

Figure S32. $^{13}C\{^{1}H\}$ NMR spectrum of **10** in C_6D_6 at 300K.

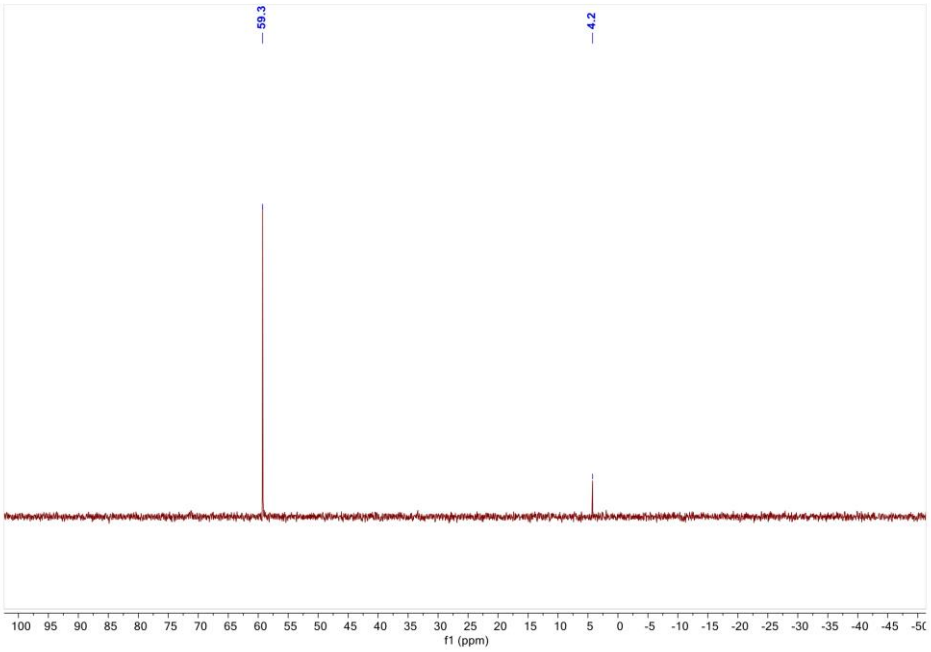

Figure S33. $^{29}Si\{^{1}H\}$ NMR spectrum of **10** in C_6D_6 at 300K.

1.2.10 Synthesis of 11.

Silylene **1** (65.8 mg, 0.1 mmol) and sulfur (3.2 mg, 0.0125 mmol) were combined in THF (2 mL) under vigorous stirring at room temperature. The color changed to pale yellow gradually. After stirring overnight, all volatiles were removed *in vacuum*, the residue was washed with cold pentane (3 × 0.5 mL) and dried *in vacuum* to give to **11** (57.6 mg, 84%) as pale yellow powder. Crystals suitable for single crystal X-ray diffraction analysis was obtained by slow evaporation of benzene solution at room temperature for several days.

^{1}H NMR (400 MHz, C_6D_6): δ [ppm] 7.22-7.26 (m, 2H, *p*-C*H*-Dipp), 7.15-7.17 (m, 4H, *m*-C*H*-Dipp, overlapping with C_6D_6), 3.36 (sept, *J* = 6.8 Hz, 4H, C*H*(CH_3)$_2$), 1.54 (s, 6H, CCH_3), 1.49 (d, *J* = 6.8 Hz, 12H, CH(CH_3)$_2$), 1.19 (s, 27H, C(CH_3)$_3$), 1.07 (d, *J* = 6.8 Hz, 12H, CH(CH_3)$_2$).

^{13}C{^{1}H} NMR (101 MHz, C_6D_6): δ [ppm] 149.8 (N*C*N), 147.7 (Ar*C*), 131.4 (Ar*C*), 129.7 (Ar*C*), 124.4 (Ar*C*), 119.0 (N*C*-CH_3), 31.8 (C(*C*H_3)$_3$), 28.4 (*C*H(CH_3)$_2$), 24.9 (CH(*C*H_3)$_2$), 24.4 (CH(*C*H_3)$_2$), 23.4 (*C*(CH_3)$_3$), 9.8 (NC-*C*H_3).

^{29}Si{^{1}H} NMR (80 MHz, C_6D_6): δ [ppm] 10.6 (*Si*^{i}Bu$_3$), 105.5 (*central Si*).

Elemental Analysis (%): Calcd: C 71.35, H 9.78, N 6.09; S 4.64, Found: C 69.46, H 10.78, N 6.01, S 3.48.

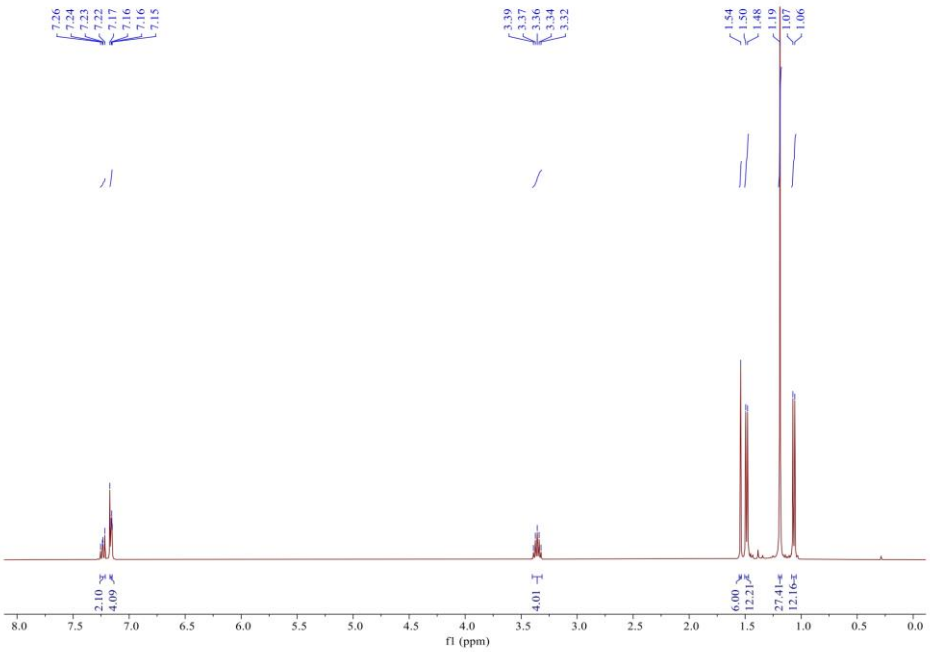

Figure S34. ^{1}H NMR spectrum of **11** in C_6D_6 at 300K.

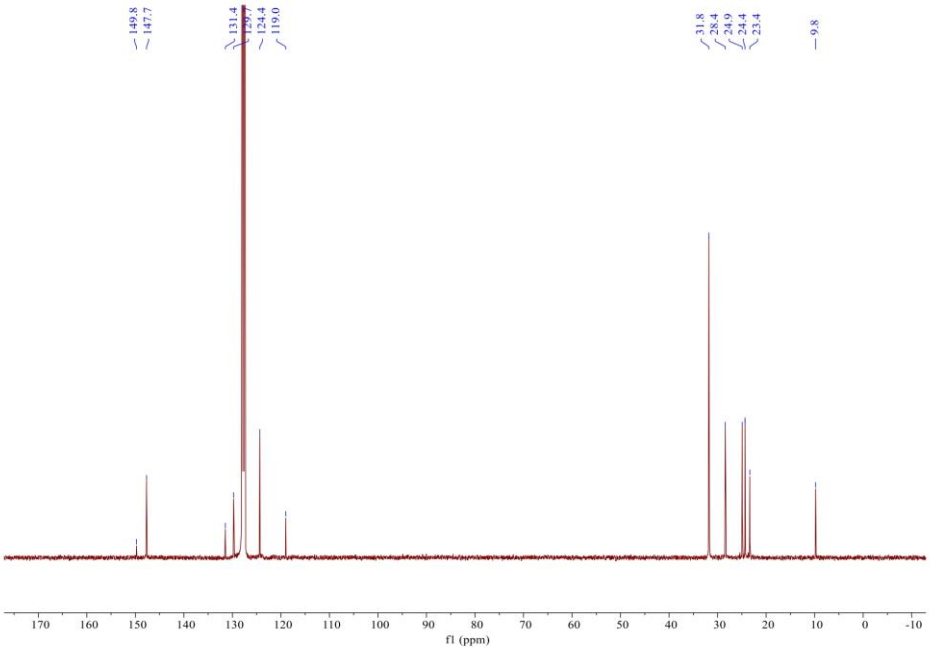

Figure S35. $^{13}C\{^{1}H\}$ NMR spectrum of **11** in C_6D_6 at 300K.

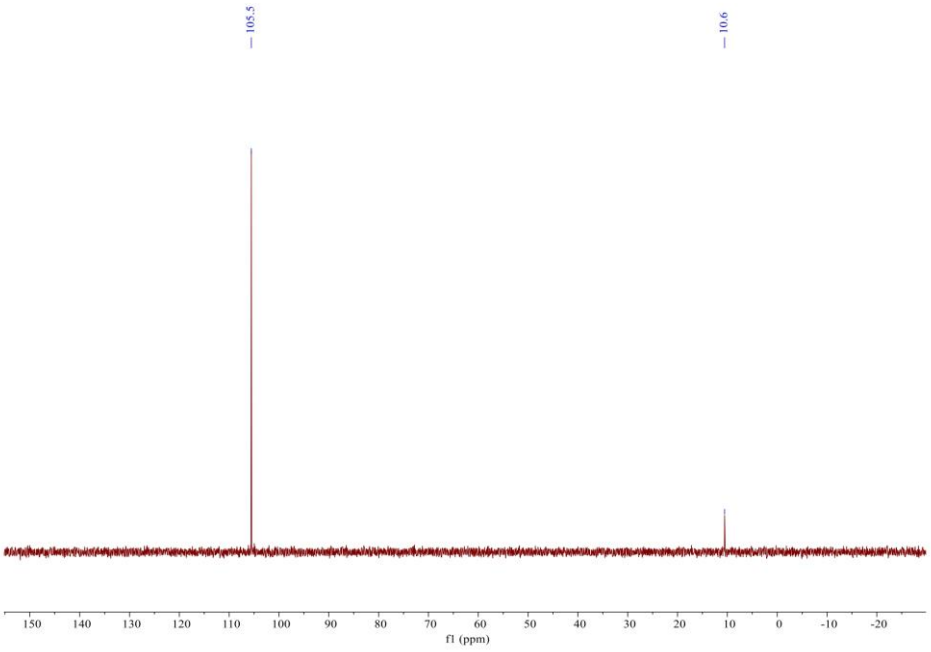

Figure S36. $^{29}Si\{^{1}H\}$ NMR spectrum of **11** in C_6D_6 at 300K.

1.2.11 Synthesis of 12.

Silylene **1** (65.8 mg, 0.1 mmol) and selenium (8.0 mg, 0.1 mmol) were combined in THF (2 mL) under vigorous stirring at room temperature. The color changed to yellow rapidly. After stirring for 1 h, all volatiles were removed *in vacuo*, the residue was washed with cold pentane (3 × 0.5 mL) and dried *in vacuum* to give to **12** (61.5 mg, 83%) as yellow powder.

^{1}H NMR (400 MHz, C_6D_6): δ [ppm] 7.20-7.24 (m, 2H, *p*-C*H*-Dipp), 7.14-7.16 (m, 4H, *m*-C*H*-Dipp, overlapping with C_6D_6), 3.40 (sept, *J* = 6.8 Hz, 4H, C*H*$(CH_3)_2$), 1.53 (s, 6H, CC*H*$_3$), 1.47 (d, *J* = 6.8 Hz, 12H, CH(C*H*$_3)_2$), 1.19 (s, 27H, C(C*H*$_3)_3$), 1.05 (d, *J* = 6.8 Hz, 12H, CH(C*H*$_3)_2$).

^{13}C{^{1}H} NMR (101 MHz, C_6D_6): δ [ppm] 150.5 (N*C*N), 147.6 (Ar*C*), 131.5 (Ar*C*), 129.8 (Ar*C*), 124.4 (Ar*C*), 119.3 (N*C*-CH$_3$), 31.9 (C(*C*H$_3)_3$), 28.4 (*C*H$(CH_3)_2$), 25.2 (CH(*C*H$_3)_2$), 24.4 (CH(*C*H$_3)_2$), 23.6 (*C*(CH$_3)_3$), 9.9 (NC-*C*H$_3$).

^{29}Si{^{1}H} NMR (80 MHz, C_6D_6): δ [ppm] 11.1 (*Si*^{t}Bu$_3$), 109.9 (*central Si*).

Elemental Analysis (%): Calcd: C 66.80, H 9.16, N 5.70; Found: C 65.88, H 9.69, N 5.51.

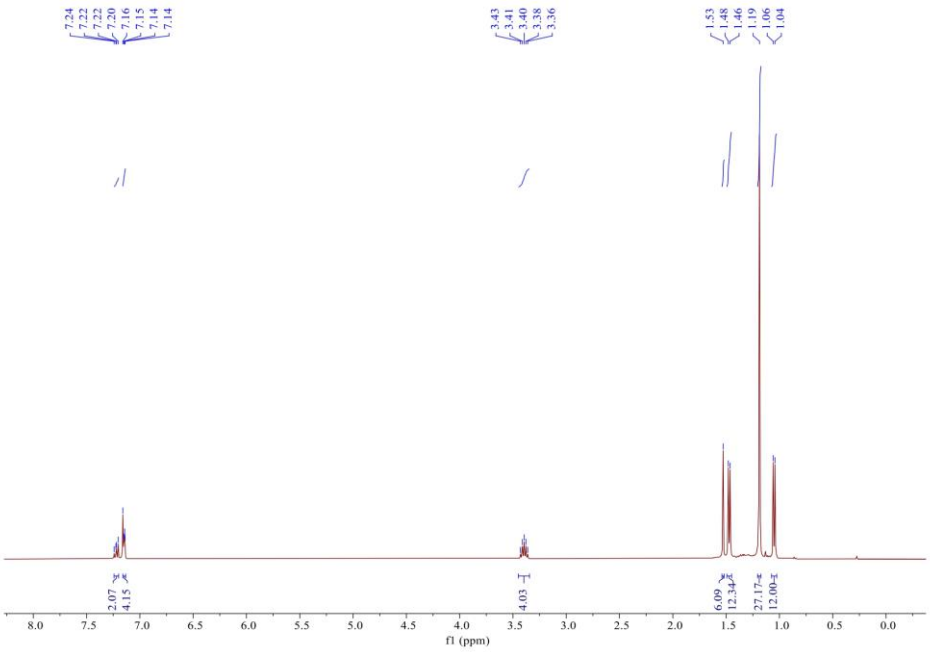

Figure S37. ^{1}H NMR spectrum of **12** in C_6D_6 at 300K.

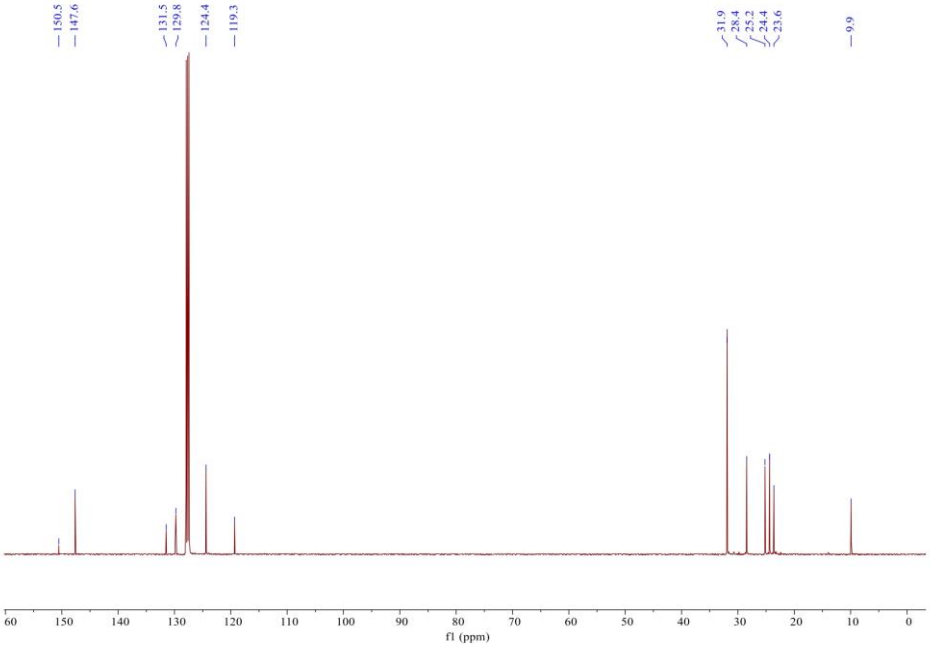

Figure S38. $^{13}C\{^{1}H\}$ NMR spectrum of **12** in C_6D_6 at 300K.

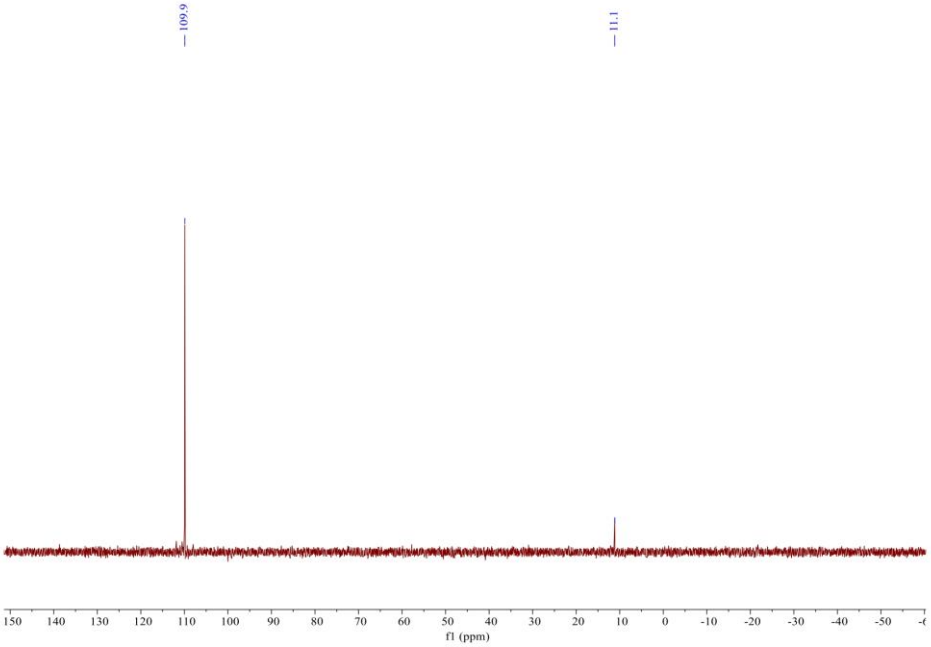

Figure S39. $^{29}Si\{^{1}H\}$ NMR spectrum of **12** in C_6D_6 at 300K.

1.2.12 Synthesis of 13.

Silylene **1** (65.8 mg, 0.1 mmol) and tellurium (12.8 mg, 0.1 mmol) were combined in THF (2 mL) under vigorous stirring at room temperature. The color changed to reddish brown gradually. After stirring overnight, all volatiles were removed *in vacuum*, the residue was washed with cold pentane (3 × 0.5 mL) and dried *in vacuum* to give to **13** (68.3 mg, 87%) as brown powder.

^{1}H NMR (400 MHz, C_6D_6): δ [ppm] 7.22-7.25 (m, 2H, *p*-C*H*-Dipp), 7.16-7.18 (m, 4H, *m*-C*H*-Dipp, overlapping with C_6D_6), 3.49 (sept, *J* = 6.8 Hz, 4H, C*H*$(CH_3)_2$), 1.54 (s, 6H, CCH_3), 1.48 (d, *J* = 6.8 Hz, 12H, CH(CH_3)$_2$), 1.22 (s, 27H, C(CH_3)$_3$), 1.06 (d, *J* = 6.8 Hz, 12H, CH(CH_3)$_2$).

^{13}C{^{1}H} NMR (101 MHz, C_6D_6): δ [ppm] 152.0 (N*C*N), 147.6 (Ar*C*), 131.7 (Ar*C*), 129.8 (Ar*C*), 124.5 (Ar*C*), 119.9 (N*C*-CH_3), 32.2 (C(*C*H_3)$_3$), 28.6 (*C*H$(CH_3)_2$), 25.8 (CH(*C*H_3)$_2$), 24.4 (CH(*C*H_3)$_2$), 24.1 (*C*$(CH_3)_3$), 10.1 (NC-*C*H_3).

^{29}Si{^{1}H} NMR (80 MHz, C_6D_6): δ [ppm] 11.0 (*Si*^{t}Bu$_3$), 101.9 (*central Si*).

Elemental Analysis (%): Calcd: C 62.67, H 8.59, N 5.35; Found: C 61.27, H 9.36, N 5.27.

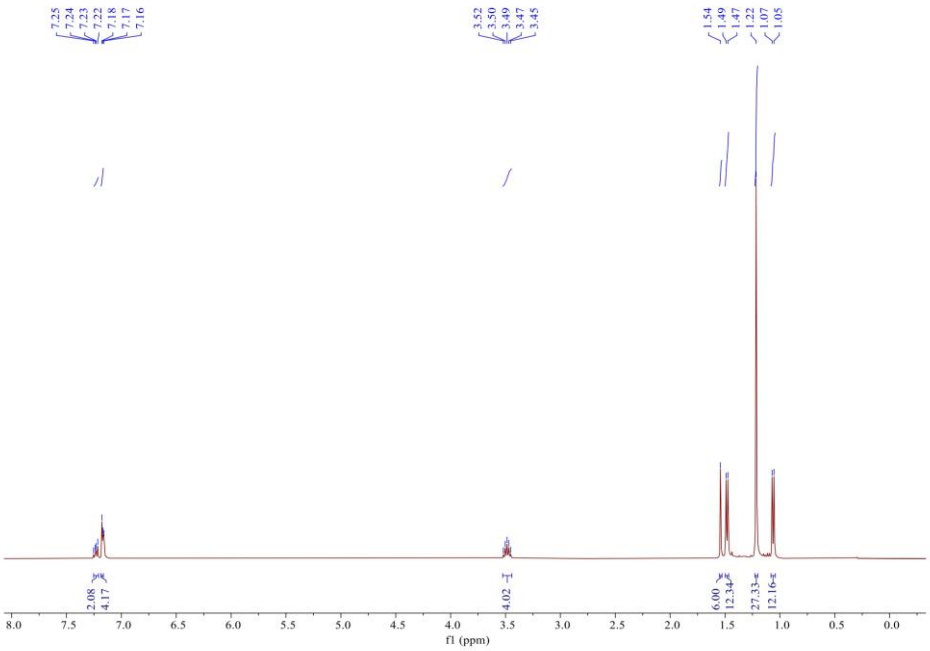

Figure S40. ^{1}H NMR spectrum of **13** in C_6D_6 at 300K.

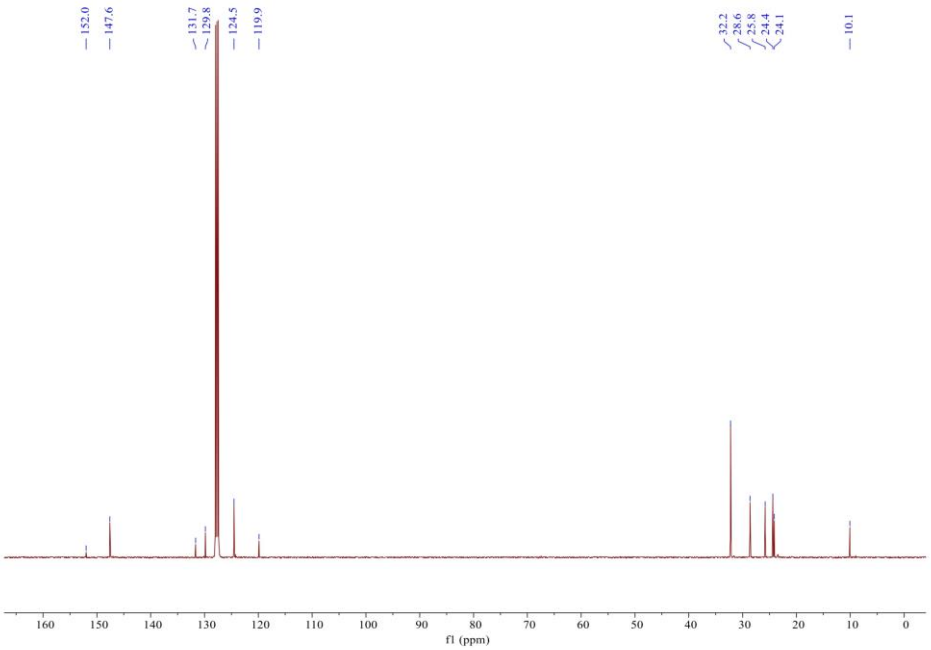

Figure S41. $^{13}C\{^{1}H\}$ NMR spectrum of **13** in C_6D_6 at 300K.

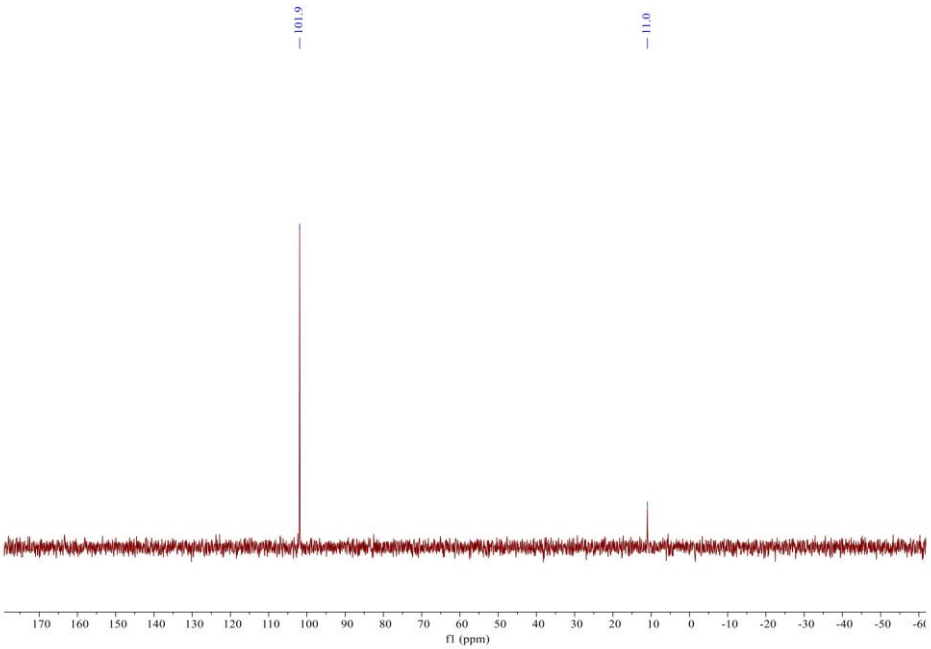

Figure S42. $^{29}Si\{^{1}H\}$ NMR spectrum of **13** in C_6D_6 at 300K.

2. Single Crystal X-Ray Structure Determination

Single crystal diffraction data were recorded on a Bruker Photon D8 Venture DUO IMS system equipped with a Helios optic monochromator and a Mo IMS microsource (λ = 0.71073 Å) The data collection was performed, using the APEX III & IV software package[S2] on single crystals coated with Fomblin®Y as perfluorinated ether. The single crystals were picked on a micro sampler, transferred to the diffractometer, and measured frozen under a stream of cold nitrogen (100 K). A matrix scan was used to determine the initial lattice parameters. Reflections were merged and corrected for Lorenz and polarization effects, scan speed, and background using SAINT.[S3] Absorption corrections, including odd and even ordered spherical harmonics were performed using SADABS.[S3] Space group assignments were based upon systematic absences, E statistics, and successful refinement of the structures. Structures were solved by direct methods with the aid of successive difference Fourier maps and were refined against all data using the APEX IV software in conjunction with SHELXL-2014[S4] and SHELXLE.[S5] H atoms were placed in calculated positions and refined using a riding model, with methylene and aromatic C–H distances of 0.99 and 0.95 Å, respectively, and Uiso(H) = 1.2·Ueq(C). Non-hydrogen atoms were refined with anisotropic displacement parameters. Full-matrix least-squares refinements were carried out by minimizing Σw(Fo2-Fc2)2 with the SHELXL weighting scheme.5 Neutral atom scattering factors for all atoms and anomalous dispersion corrections for the non-hydrogen atoms were taken from International Tables for Crystallography.[S6] The images of the crystal structures were generated by Mercury.[S7] The CCDC numbers XXXX to XXXX contain the supplementary crystallographic data for the structures **8** to **11**. These data can be obtained free of charge from the Cambridge Crystallographic Data Centre via https://www.ccdc.cam.ac.uk/structures/.

	Compound **8**	Compound **9**	Compound **10**	Compound **11**
CCDC	2237043	2237044	2237045	2237046
Crystal data				
Chemical formula	$C_{53}H_{79}N_3Si_3$	$C_{47}H_{80}BN_3O_2Si_2$	$C_{41}H_{67}N_3OSi_2$	$C_{41}H_{67}N_3SSi_2$
M_r	842.46	786.13	674.16	690.22
Crystal system, space group	Monoclinic, $P2_1/n$	Orthorhombic, $P2_12_12_1$	Triclinic, $P\bar{1}$	Monoclinic, $P2_1/n$
Temperature (K)	100	100	150	100
a, b, c (Å)	15.2552 (13), 20.4843 (16), 16.2530 (13)	11.8821 (7), 15.6734 (9), 25.2215 (13)	13.6704 (17), 17.545 (2), 17.765 (2)	13.6229 (16), 18.327 (2), 16.8266 (19)
α, β, γ (°)	90, 95.035 (3), 90	90, 90, 90	85.418 (5), 87.968 (4), 85.162 (3)	90, 96.999 (4), 90
V (Å^3)	5059.3 (7)	4697.1 (5)	4230.4 (9)	4169.7 (8)
Z	4	4	4	4
F(000)	1840	1728	1480	1512
D_x (Mg m^{-3})	1.106	1.112	1.059	1.099
Radiation type	Mo $K\alpha$	Mo $K\alpha$	Mo $K\alpha$	Mo $K\alpha$
No. of refl. for cell meas.	9960	9616	9927	9847
θ range (°) for cell meas.	2.5–25.4	2.3–25.6	2.3–25.5	2.3–25.3
μ (mm^{-1})	0.13	0.11	0.12	0.17
Crystal shape	Fragment	Fragment	Fragment	Fragment
Colour	Clear colourless	Clear colourless	Clear colourless	Clear colourless
Crystal size (mm)	0.39 × 0.25 × 0.21	0.27 × 0.23 × 0.09	0.35 × 0.27 × 0.21	0.39 × 0.27 × 0.12
Data collection				
Radiation source	IMS microsource	IMS microsource	IMS microsource	IMS microsource
Detector resolution (pixels mm^{-1})	16	16	16	16
T_{min}, T_{max}	0.716, 0.745	0.714, 0.745	0.661, 0.745	0.713, 0.745
No. of meas., indep. and obs. [$I > 2\sigma(I)$] refl.	83075, 9269, 7926	150143, 8601, 8326	173649, 16247, 12008	156245, 7644, 6827
R_{int}	0.052	0.065	0.097	0.050
θ values (°)	θ_{max} = 25.4, θ_{min} = 2.0	θ_{max} = 25.4, θ_{min} = 1.9	θ_{max} = 25.9, θ_{min} = 1.9	θ_{max} = 25.4, θ_{min} = 2.1
$(\sin\theta/\lambda)_{max}$ (Å^{-1})	0.602	0.602	0.614	0.602
Range of h, k, l	h = –18→18, k = –24→24, l = –19→19	h = –14→14, k = –18→18, l = –30→30	h = –16→16, k = –21→21, l = –21→21	h = –16→16, k = –22→22, l = –20→20
Refinement				
Refinement on	F^2	F^2	F^2	F^2
$R[F^2 > 2\sigma(F^2)]$, $wR(F^2)$, S	0.039, 0.090, 1.05	0.036, 0.076, 1.16	0.083, 0.263, 1.06	0.039, 0.113, 1.04
No. of refl. / para. / restr.	9269 / 559 / 0	8601 / 553 / 69	16247 / 918 / 78	7644 / 443 / 0
Weighting scheme	W = 1/[S^2(FO^2) + (**X** P)^2 + **Y** P] WHERE P = (FO^2 + 2FC^2)/3			
X / **Y**	0.029 / 3.7596	0.0222 / 2.1537	0.1334 / 6.3764	0.0586 / 2.6009
$\Delta\rho_{max}$, $\Delta\rho_{min}$ (e Å^{-3})	0.33, –0.29	0.22, –0.19	0.98, –0.53	0.63, –0.28

Compound **9**

Positional disorder at one isopropyl group (of a Dipp wingtip) was treated via a 2-part disorder modelling procedure.

Compound **10**

The asymmetric unit contains two identical molecules out of which one is shown. Positional disorder at one isopropyl group (of a Dipp wingtip) was treated via a 2-part disorder modelling procedure and a merohedral twin law (-1 0 0.055 0 -1 0.158 0 0 1) was used for further refinement. Residual electron density (0.77 – 1.00) near Si1 and Si3 is found. The density was tried to refine freely and restrained as hydrogen atoms, which was not plausible due to the respective bond symmetry, further there is no hint for Si–H bonding in the spectroscopic analysis.

3. References

(S1) Zhu, H.; Kostenko, A.; Franz, D.; Hanusch, F.; Inoue, S. *J. Am. Chem. Soc.* **2023**, *145*, 1011-1021.

(S2) APEX suite of crystallographic software, APEX 4 version 2021.10-0; Bruker AXS Inc.: Madison, Wisconsin, USA, 2021.

(S3) SAINT, Version 7.56a and SADABS Version 2008/1; Bruker AXS Inc.: Madison, Wisconsin, USA, 2008.

(S4) Sheldrick, G. M. SHELXL-2014, University of Göttingen, Göttingen, Germany, 2014.

(S5) Hübschle, C. B.; Sheldrick, G. M.; Dittrich, B. J. Appl. Cryst. 2011, 44, 1281-1284.

(S6) Sheldrick, G. M. SHELXL-97, University of Göttingen, Göttingen, Germany, 1998.

(S7) Wilson, A. J. C. International Tables for Crystallography, Vol. C, Tables 6.1.1.4 (pp. 500-502), 4.2.6.8 (pp. 219-222), and 4.2.4.2 (pp. 193-199); Kluwer Academic Publishers: Dordrecht, The Netherlands, 1992.

(S8) Macrae, C. F.; Bruno, I. J.; Chisholm, J. A.; Edgington, P. R.; McCabe, P.; Pidcock, E.; Rodriguez-Monge, L.; Taylor, R.; van de Streek, J.; Wood, P. A. J. Appl. Cryst. 2008, 41, 466-470.

10.3 Supporting Information for Chapter 7

Supplemental Experimental Procedures

1. Experimental Procedures

1.1 General Methods and Instrumentation

All experiments and manipulations were carried out under argon atmosphere using standard Schlenk or glovebox techniques. The glassware was heat-dried under vacuum prior to use. All glass junctions were coated with PTFE-based grease Merkel Triboflon III. For stirring, PTFE-coated magnetic stirrer bars were used or glass-coated ones if stated. Liquid phases were transferred using standard PE/PP syringes equipped with stainless steel cannula or directly canted from vessel to vessel if not stated otherwise. Solvents were dried by standard methods (withdrawal from MBraun Solvent Purification System and storage over molecular sieves (3 Å), or distilled from sodium/ benzophenone or CaH_2 under argon atmosphere and degassed via freeze-pump-thaw cycling). All chemicals were purchased from commercial suppliers and used as received if not stated otherwise. Deuterated benzene (C_6D_6) and THF-D_8 were obtained from Deutero Deutschland GmbH and were dried over 3 Å molecular sieves. All NMR samples were prepared under argon in J. Young PTFE tubes. NMR spectra were recorded on a Bruker AV400US, DRX400, AVHD300, AV500cr or CP MAS NMR (for solid state ^{29}Si NMR) at ambient temperature (300 K) if not stated otherwise. ^{1}H and ^{13}C NMR spectra were calibrated against the residual proton and natural abundance carbon resonances of the respective deuterated solvent as internal standard. ATRFT-IR spectra were recorded on a Bruker Alpha FT-IR spectrometer (diamond ATR, located inside an argon-filled glovebox) in a range of 500–4000 cm^{-1}. Elemental analyses (EA) were conducted with a EURO EA (HEKA tech) instrument equipped with a CHNS combustion analyzer at the Laboratory for Microanalysis at the TUM Catalysis Research Center. Elemental analysis provided partially and reproducibly low carbon percentages (~2% deviation), presumably due to the formation of incombustible silicon carbide compounds. Liquid Injection Field Desorption Ionization Mass Spectrometry (LIFDI-MS) was measured directly from an inert atmosphere glovebox with a Thermo Fisher Scientific Exactive Plus Orbitrap equipped with an ion source from Linden CMS. Melting points (m.p.) were recorded using a Büchi M-565 at the TUM Catalysis Research Center which were prepared in sealed glass capillaries under inert argon atmosphere. **1** was synthesized according to procedures described in literature.[S1] MesNC[S2], DippNC[S3] and TerNC[S4] were synthesized according to procedures described in literature.

1.2 Synthesis and Characterization

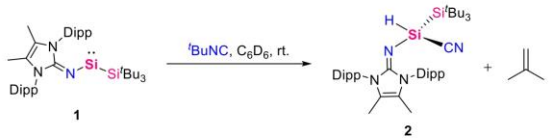

Figure S1. Synthesis of **2**.

^{t}BuNC (8.4 mg, 0.1 mmol) was added dropwise to silylene **1** (66 mg, 0.1 mmol) in C_6D_6 (0.5 mL) without stirring at room temperature. The color of mixture turned to pale yellow rapidly. All volatiles were removed from yellow solution after stirring overnight at room temperature, the residue was washed with cold pentane (–30 °C, 3 × 0.5 mL) and dried *in vacuum* to yield **2** (60.1 mg, 88%) as an off-white powder.
^{1}H NMR (400 MHz, C_6D_6): δ [ppm] 7.28-7.32 (m, 2H, *p*-C*H*-Dipp), 7.18-7.21 (m, 4H, *m*-C*H*-Dipp), 5.10 (s, *J* = 198.8 Hz, 1H, Si*H*), 3.14 (sept, *J* = 6.8 Hz, 2H, C*H*(CH$_3$)$_2$), 3.03 (sept, *J* = 6.8 Hz, 2H, C*H*(CH$_3$)$_2$), 1.49 (d, *J* = 3.6 Hz, 6H, CH(C*H*$_3$)$_2$), 1.47 (d, *J* = 3.6 Hz, 6H, CH(C*H*$_3$)$_2$), 1.46 (s, 6H, CC*H*$_3$), 1.47 (d, *J* = 6.0 Hz, 6H, CH(C*H*$_3$)$_2$, overlapping with ^{t}Bu group), 1.14 (s, 27H, C(C*H*$_3$)$_3$), 1.10 (d, *J* = 6.8 Hz, 6H, CH(C*H*$_3$)$_2$).
^{13}C{^{1}H} NMR (101 MHz, C_6D_6): δ [ppm] 147.3 (N*C*N), 147.2 (Ar*C*), 146.5 (Ar*C*), 132.3 (Ar*C*), 129.0 (Ar*C*), 124.5 (Si*C*N), 124.0 (Ar*C*), 117.2 (N*C*-CH$_3$), 31.3 (C(*C*H$_3$)$_3$), 28.6 (*C*H(CH$_3$)$_2$), 28.6 (*C*H(CH$_3$)$_2$), 24.4 (CH(*C*H$_3$)$_2$), 23.7 (CH(*C*H$_3$)$_2$), 23.5 (CH(*C*H$_3$)$_2$), 22.4 (CH(*C*H$_3$)$_2$), 22.4 (*C*(CH$_3$)$_3$), 9.6 (NC-*C*H$_3$).
^{29}Si{^{1}H} NMR (80 MHz, C_6D_6): δ [ppm] 0.6 (*Si*^{t}Bu$_3$), –78.8 (*central Si*).
IR (cm^{-1}): 2962-2855(m), 2230(w), 2079(w), 1675(m), 1627(s), 1584(s), 1460(m), 1442(m), 1365(s), 1254(w), 1183(w), 1136(w), 1099(m), 1060(w), 1015(w), 991(w), 950(m), 939(m), 820(s), 787(m), 765(s), 744(w), 687(m), 610(m), 573(m), 520(m), 506(w).
Elemental Analysis (%): Calcd: C 73.62, H 10.00, N 8.18; Found: C 71.48, H 9.65, N 8.00.
m.p.: 264.6 °C.

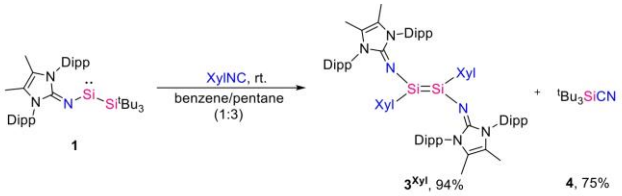

Figure S2. Synthesis of **3^{Xyl}** and **4**.

Silylene **1** (100 mg, 0.15 mmol) and XylNC (19.8 mg, 0.15 mmol) were combined in benzene/pentane (1:3, 3 mL) without stirring at room temperature. The color of mixture changed to deep green rapidly, then turned to orange within the formation of red crystals in 1 h. After filtration, the red crystals were washed with pentane (3 × 1 mL) and dried *in vacuum* to yield disilene **3^{Xyl}** (75.8 mg, 94%) as an orange powder. The volatiles were removed from combined filtrate, and the residue was extracted with dried methanol (3 × 4 mL). The methanol solution was concentrated and cooled to –30 °C to yield silylcyanide **4** (25.4 mg, 75%) as pale yellow crystals.
3^{Xyl}:
^{29}Si{^{1}H} CP-MAS NMR: δ [ppm] 52.5 (*Si*=*Si*).
IR (cm^{-1}): 2964-2862(m), 1679(w), 1613(s), 1579(s), 1444(m), 1403(m), 1358(s), 1258(m), 1226(w), 1161(w), 1091(w), 1061(w), 989(w), 936(m), 779(s), 779(s), 760(s), 736(w), 703(w), 624(m), 581(w, *Si*=*Si*), 512(w).
Elemental Analysis (%): Calcd: C 78.81, H 8.76, N 7.45; Found: C 77.78, H 8.94, N 7.29.
m.p.: 312.5 °C (color changed from orange to yellow)
4:
^{1}H NMR (400 MHz, C_6D_6): δ [ppm] 1.02 (s, 27H, C(C*H*$_3$)$_3$).
^{13}C{^{1}H} NMR (101 MHz, C_6D_6): δ [ppm] 124.4 (Si*C*N), 31.8 (C(*C*H$_3$)$_3$), 23.1 (*C*(CH$_3$)$_3$).
^{29}Si{^{1}H} NMR (80 MHz, C_6D_6): δ [ppm] 4.5 (*Si*^{t}Bu$_3$).
IR (cm^{-1}): 2976-2857(m), 2172(w), 2097(w), 1461(m), 1383(m), 1366(s), 1257(w), 1232(w), 1181(w), 1136(w), 1108(m), 1060(w), 1015(w), 973(w), 934(m), 818(s), 612(s), 569(m), 524(m), 504(m).
Elemental Analysis (%): Calcd: C 78.97, H 8.90, N 7.27; Found: C 78.49, H 8.92, N 7.35.

m.p.: 72.6 °C.

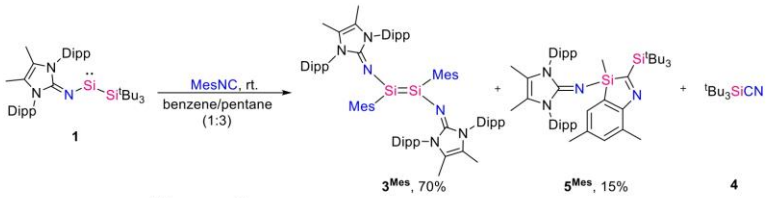

Figure S3. Synthesis of **3^{Mes}** and **5^{Mes}**.

Silylene **1** (100 mg, 0.15 mmol) and MesNC (22.5 mg, 0.15 mmol) were combined in benzene/pentane (1:3, 3 mL) without stirring at room temperature. The color of mixture changed to deep green rapidly, then turned to orange within the formation of red crystals in 1 h. After filtration, the red crystals were washed with pentane (3 × 1 mL) and dried to yield disilene **3^{Mes}** (61 mg, 70%) as an orange powder. The combined pentane solution was concentrated and cooled to –30 °C to give to some yellow crystals. The yellow crystals was washed with cold pentane (–30 °C) and dried *in vacuum* to yield 3*H*-1,3-benzazasilole **5^{Mes}** (18.1 mg, 15%) as a yellow powder.

3^{Mes}:

^{1}H NMR (400 MHz, C$_6$D$_6$): δ [ppm] 7.23-7.27 (m, 2H, *p*-C*H*-Dipp), 7.04-7.05 (d, *J* = 7.7 Hz, 4H, *m*-C*H*-Dipp), 6.62 (s, 2H, *m*-C*H*-Mes), 2.92 (sept, *J* = 6.8 Hz, 4H, C*H*(CH$_3$)$_2$), 2.37 (s, 3H, *p*-C*H*$_3$-Mes), 2.14 (s, 6H, *o*-C*H*$_3$-Mes), 1.34 (s, 6H, CC*H*$_3$), 1.04 (d, *J* = 6.8 Hz, 12H, CH(C*H*$_3$)$_2$), 0.98 (d, *J* = 6.8 Hz, 12H, CH(C*H*$_3$)$_2$).

^{29}Si{^{1}H} CP-MAS NMR: δ [ppm] 50.3 (*Si*=*Si*).

IR (cm^{-1}): 2960-2866(m), 1680(w), 1613(s), 1581(s), 1456(m), 1442(m), 1403(w), 1363(s), 1257(m), 1226(w), 1179(w), 1091(w), 1060(w), 1026(w), 989(w), 936(m), 840(w), 777(s), 738(w), 701(w), 604(m), 545(w, *Si*=*Si*), 509(w).

Elemental Analysis (%): Calcd: C 78.97, H 8.90, N 7.27; Found: C 78.49, H 8.92, N 7.35.

m.p.: 295.0 °C (color changed from orange to yellow).

5^{Mes}:

^{1}H NMR (400 MHz, C$_6$D$_6$): δ [ppm] 7.21-7.25 (m, 2H, *p*-C*H*-Dipp), 7.16 (m, 2H, *m*-C*H*-Dipp, overlapping with C$_6$D$_6$), 7.02-7.03 (m, 2H, *m*-C*H*-Dipp, overlapping with C$_6$D$_6$), 6.90 (s, 1H, C*H*-Mes), 6.03 (s, 1H, C*H*-Mes), 3.15 (sept, *J* = 6.8 Hz, 2H, C*H*(CH$_3$)$_2$), 2.97 (sept, *J* = 6.8 Hz, 2H, C*H*(CH$_3$)$_2$), 2.74 (s, 3H, C*H*$_3$-Mes), 2.21 (s, 3H, C*H*$_3$-Mes), 1.35 (s, 6H, CC*H*$_3$), 1.28 (s, 27H, C(C*H*$_3$)$_3$), 1.26 (6 6H, CH(C*H*$_3$)$_2$, overlapping with Si^{t}Bu3), 1.15 (d, *J* = 8.0 Hz, 6H, CH(C*H*$_3$)$_2$), 1.13 (d, *J* = 7.2 Hz, 6H, CH(C*H*$_3$)$_2$), 1.05 (d, *J* = 6.8 Hz, 6H, CH(C*H*$_3$)$_2$), 0.24 (s, 3H, SiC*H*$_3$).

^{13}C{^{1}H} NMR (101 MHz, C$_6$D$_6$): δ [ppm] 208.4 (Si*C*N), 154.5 (Ar*C*), 147.7 (N*C*N), 147.0 (Ar*C*), 146.0 (Ar*C*), 143.0 (Ar*C*), 135.6 (Ar*C*), 133.2 (Ar*C*), 132.4 (Ar*C*), 131.7 (Ar*C*), 129.3 (Ar*C*), 128.8 (Ar*C*), 124.3 (Ar*C*), 123.9 (Ar*C*), 116.5 (NC-CH$_3$), 31.6 (C(*C*H$_3$)$_3$), 28.6 (*C*H(CH$_3$)$_2$), 28.3 (*C*H(CH$_3$)$_2$), 24.6 (CH(*C*H$_3$)$_2$), 23.4 (CH(*C*H$_3$)$_2$), 22.9 (CH(*C*H$_3$)$_2$), 22.5 (CH(*C*H$_3$)$_2$), 22.4 (*C*(CH$_3$)$_3$), 21.4 (CH(*C*H$_3$)$_2$), 18.2 (Ar*C*H$_3$), 9.7 (NC-*C*H$_3$), 1.5 (Si*C*H$_3$).

^{29}Si{^{1}H} NMR (80 MHz, C$_6$D$_6$): δ [ppm] 0.8 (*Si*^{t}Bu$_3$), –24.3 (*central Si*).

IR (cm^{-1}): 2962-2854(m), 1676(m), 1630(s), 1587(s), 1458(m), 1442(m), 1403(m), 1383(m), 1365(s), 1234(w), 1181(w), 1108(m), 1091(w), 1059(w), 1016(w), 971(w), 946(m), 934(m), 848(m), 818(s), 795(s), 763(m), 687(s), 612(m), 567(m), 522(m), 506(m).

Elemental Analysis (%): Calcd: C 76.25, H 9.79, N 6.97; Found: C 74.24, H 9.55, N 6.53.

LIFDI-MS: Calcd: 802.5765; Found: 802.5762.

m.p.: 199.8 °C.

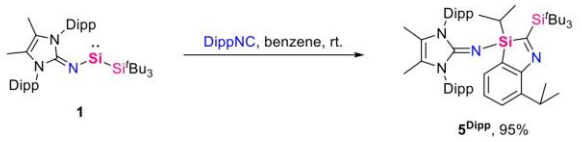

Figure S4. Synthesis of **5^{Dipp}**.

Silylene **1** (66.0 mg, 0.1 mmol) and DippNC (19.0 mg, 0.1 mmol) were combined in benzene (3 mL) under vigorous stirring at room temperature. The color of mixture changed to deep green rapidly. All volatiles were removed from yellow solution after stirring at room temperature for 10 minutes, the residue was washed with cold pentane (–30 °C, 3 × 0.5 mL) and dried *in vacuum* to yield **5^{Dipp}** (80.6 mg, 95%) as a yellow powder. Crystal suitable for single crystal X-ray diffraction analysis was obtained by slow evaporation of benzene/pentane (1:1) solution at room temperature for 2 days.
^{1}H NMR (400 MHz, C_6D_6): δ [ppm] 7.29 (d, *J* = 7.6 Hz, 2H, *m*-C*H*-Dipp), 7.23 (t, *J* = 7.6 Hz, 2H, *p*-C*H*-Dipp), 7.15-7.16 (m, 3H, *m*/*p*-C*H*-Dipp, overlapping with C_6D_6), 7.00 (d, *J* = 7.2 Hz, 2H, *m*-C*H* Dipp), 6.94 (t, *J* = 7.2 Hz, 1H, *p*-C*H*-Dipp), 6.21 (d, *J* = 6.4 Hz, 2H, *m*-C*H*-Dipp), 4.48 (sept, *J* = 6.8 Hz, 1H, C*H*(CH_3)$_2$), 3.22 (sept, *J* = 6.4 Hz, 2H, C*H*(CH_3)$_2$), 2.97 (sept, *J* = 6.4 Hz, 2H, C*H*(CH_3)$_2$), 1.44 (d, *J* = 6.8 Hz, 3H, SiCH(C*H*$_3$)$_2$), 1.39 (d, *J* = 6.8 Hz, 3H, SiCH(C*H*$_3$)$_2$), 1.34 (s, 6H, CC*H*$_3$), 1.30 (s, 27H, C(C*H*$_3$)$_3$), 1.24 (d, *J* = 6.8 Hz, 6H, CH(C*H*$_3$)$_2$), 1.06-1.13 (m, 16H, C*H*(CH_3)$_2$, CH(C*H*$_3$)$_2$), 1.02 (d, *J* = 6.8 Hz, 6H, CH(C*H*$_3$)$_2$). 0.68 (d, *J* = 7.2 Hz, 3H, CH(C*H*$_3$)$_2$).
^{13}C{^{1}H} NMR (101 MHz, C_6D_6): δ [ppm] 210.1 (Si*C*N), 155.0 (Ar*C*), 147.7 (N*C*N), 147.0 (Ar*C*), 143.1 (Ar*C*), 142.4 (Ar*C*), 133.6 (Ar*C*), 129.4 (Ar*C*), 129.0 (Ar*C*), 126.1 (Ar*C*), 125.4 (Ar*C*), 124.5 (Ar*C*), 124.2 (Ar*C*), 117.0 (N*C*-CH$_3$), 31.7 (C(*C*H$_3$)$_3$), 28.5 (*C*H(CH_3)$_2$), 28.3 (*C*H(CH_3)$_2$), 27.2 (*C*H(CH_3)$_2$), 24.9 (CH(*C*H$_3$)$_2$), 24.8 (CH(*C*H$_3$)$_2$), 23.7 (CH(*C*H$_3$)$_2$), 23.1 (CH(*C*H$_3$)$_2$), 23.1 (CH(*C*H$_3$)$_2$), 22.7 (*C*(CH_3)$_3$), 22.5 (CH(*C*H$_3$)$_2$), 18.1 (SiCH(*C*H$_3$)$_2$), 17.5 (CH(*C*H$_3$)$_2$), 15.4 (CH(*C*H$_3$)$_2$), 10.1 (NC-*C*H$_3$).
^{29}Si{^{1}H} NMR (80 MHz, C_6D_6): δ [ppm] –1.0 (*Si*^{t}Bu$_3$), –19.9 (*central Si*).
IR (cm^{-1}): 2960-2860(m), 1689(w), 1634(s), 1585(m), 1458(m), 1438(m), 1383(m), 1363(s), 1260(w), 1183(w), 1132(w), 1099(m), 1063(w), 1016(w), 995(w), 932(m), 877(w), 820(m), 791(m), 779(s), 765(m), 744(w), 705(w), 689(w), 667(m), 630(s), 561(m), 522(m), 503(m).
Elemental Analysis (%): Calcd: C 76.71, H 10.01, N 6.63; Found: C 74.92, H 9.80, N 6.53.
m.p.: 235.1 °C.

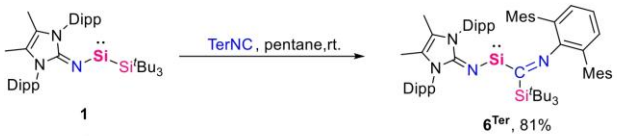

Figure S5. Synthesis of **6Ter**.

Silylene **1** (100 mg, 0.15 mmol) and TerNC (34.0 mg, 0.1 mmol) were combined in pentane (5 mL) without stirring at room temperature. The color of mixture turned to deep green rapidly. Deep green crystals were formed on standing overnight. After filtration, the residue was washed with pentane (3 × 1 mL) and dried *in vacuum* to yield **6Ter** (80.5 mg, 81%) as a green powder.
^{1}H NMR (400 MHz, C_6D_6): δ [ppm] 7.16-7.19 (m, 2H, *p*-C*H*-Dipp, overlapping with C_6D_6), 7.08-7.10 (m, 4H, *m*-C*H*-Dipp), 6.98-7.01 (m, 3H, *m*/*p*-C*H*-Ter), 6.88 (s, 2H, *p*-C*H*-Mes), 6.83 (s, 2H, *p*-C*H*-Mes), 3.10 (sept, *J* = 6.8 Hz, 4H, C*H*(CH_3)$_2$), 2.32 (s, 6H, C*H*$_3$-Mes), 2.23 (s, 6H, C*H*$_3$-Mes), 2.05 (s, 6H, C*H*$_3$-Mes), 1.31 (d, *J* = 6.8 Hz, 12H, CH(C*H*$_3$)$_2$), 1.28 (s, 6H, CC*H*$_3$), 1.05 (d, *J* = 6.8 Hz, 12H, CH(C*H*$_3$)$_2$), 0.91 (s, 27H, C(C*H*$_3$)$_3$).
^{1}H NMR (400 MHz, THF-D_8): δ [ppm] 7.37-7.39 (m, 2H, *p*-C*H*-Dipp), 7.26-7.28 (m, 4H, *m*-C*H*-Dipp), 6.83-6.87 (m, 1H, *m*-C*H*-Ter), 6.73-6.75 (m, 2H, *p*-C*H*-Ter), 6.59 (s, 2H, *p*-C*H*-Mes), 6.55 (s, 2H, *p*-C*H*-Mes), 3.05 (sept, *J* = 6.8 Hz, 4H, C*H*(CH_3)$_2$), 2.11 (s, 6H, C*H*$_3$-Mes), 1.94 (s, 6H, CC*H*$_3$), 1.76 (s, 6H, C*H*$_3$-Mes), 1.61 (s, 6H, C*H*$_3$-Mes), 1.20 (d, *J* = 6.8 Hz, 12H, CH(C*H*$_3$)$_2$), 1.15 (d, *J* = 6.8 Hz, 12H, CH(C*H*$_3$)$_2$), 0.58 (s, 27H, C(C*H*$_3$)$_3$).
^{13}C{^{1}H} NMR (101 MHz, THF-D_8): δ [ppm] 230.2 (Si*C*N), 155.4 (N*C*N), 148.6(Ar*C*), 139.2 (Ar*C*), 137.5 (Ar*C*), 137.3 (Ar*C*), 136.0 (Ar*C*), 133.9 (Ar*C*), 131.0 (Ar*C*), 129.9 (Ar*C*), 129.4 (Ar*C*), 129.1 (Ar*C*), 128.7 (Ar*C*), 125.5 (Ar*C*), 122.5 (Ar*C*), 120.7 (N*C*-CH$_3$), 32.2 (C(*C*H$_3$)$_3$), 29.5 (*C*H(CH_3)$_2$), 24.5 (CH(*C*H$_3$)$_2$), 22.8 (Mes-*C*H$_3$), 22.6 (*C*(CH_3)$_3$), 22.4 (Mes-*C*H$_3$), 21.2 (Mes-*C*H$_3$), 10.5 (NC-*C*H$_3$).
^{29}Si{^{1}H} NMR (80 MHz, THF-D_8): δ [ppm] 0.6 (*Si*^{t}Bu$_3$), 218.1 (*central Si*).
IR (cm^{-1}): 2957-2855(m), 1677(w), 1632(s), 1587(m), 1540(s), 1460(s), 1442(s), 1363(s), 1257(w), 1232(w), 1181(w), 1101(m), 1060(w), 1015(w), 934(m), 847(m), 818(s), 793(s), 763(m), 742(s), 714(w), 687(m), 653(w), 616(s), 569(w), 524(m), 504(m).
Elemental Analysis (%): Calcd: C 79.46, H 9.30, N 5.62; Found: C 77.07, H 9.29, N 5.72.
m.p.: 324.1 °C (color changed from dark green to yellow).

1.3 UV-vis measurement

Since the deep green color of $\mathbf{6}^{Ter}$, we did the measurement of UV-vis for $\mathbf{6}^{Ter}$ in THF (Figure S6, top). However, we only can observed the maximum absorption peak of **1** at 650 nm[S1]. Due to the poor solubility of $\mathbf{6}^{Ter}$, the concentration could not be increased anymore. TD-DFT calculations to understand the UV-vis spectroscopy result. The calculations show that **1** and $\mathbf{6}^{Ter}$ are expected to have similarly looking absorption spectra, with transitions at the regions of 600 the 400 nm, which in combination would result in a broad low frequency absorption peak and unresolved peaks at the high frequency region (Figure S41–42).Therefore, we turned our attention to the measurement of the reaction of **1** with DippNC. The UV-vis measurement was carried out at 1.0×10^{-3} M in toluene every 2 minutes (Figure S6, bottom). Two maximum absorption peaks were observed at 423 and 589 nm for the green intermediate $\mathbf{6}^{Dipp}$. After 8 minutes, only a maximum absorption peak was observed at 430 nm for $\mathbf{5}^{Dipp}$.

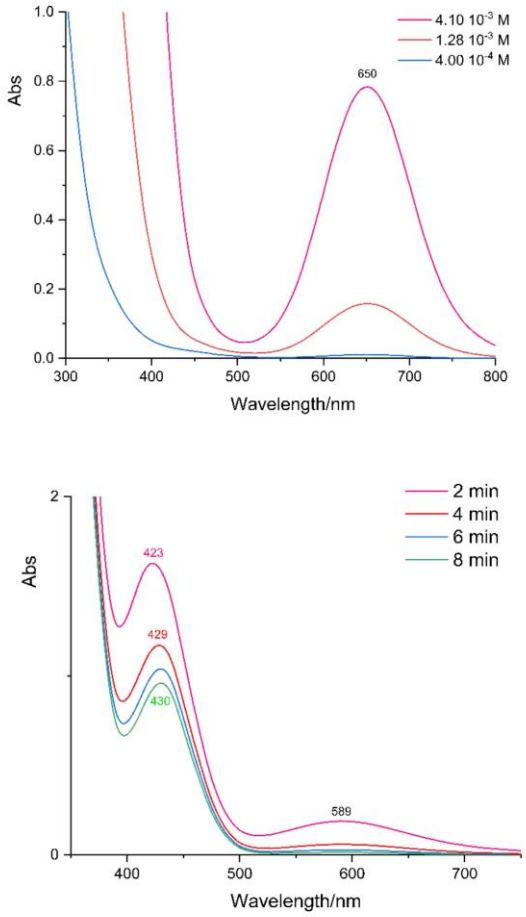

Figure S6. UV-vis measurement of $\mathbf{6}^{Ter}$ in THF(top), the reaction of **1** and DippNC in toluene (bottom).

2. NMR and IR Spectra

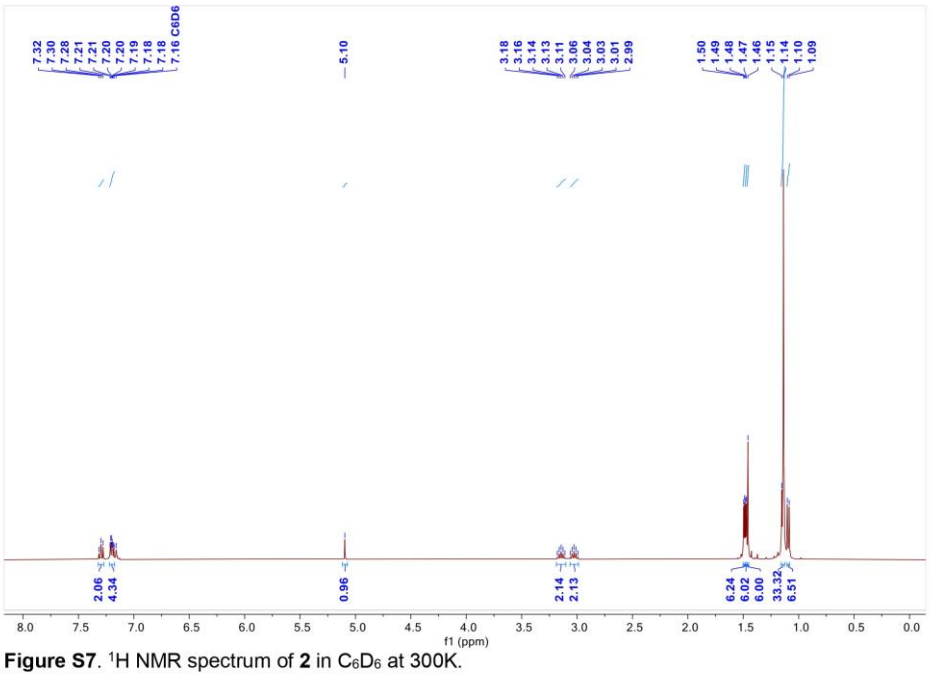

Figure S7. ^{1}H NMR spectrum of **2** in C_6D_6 at 300K.

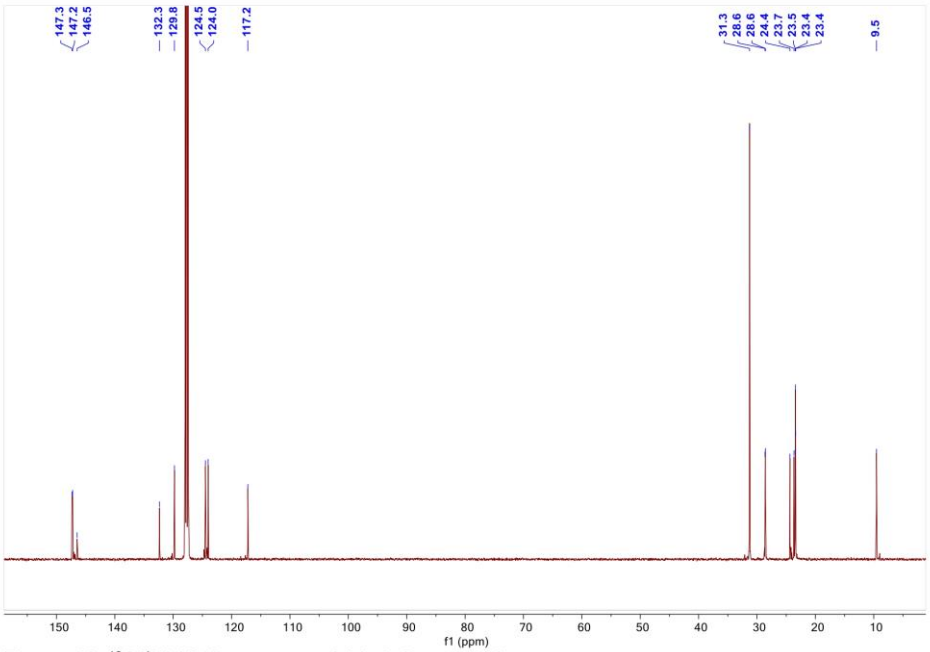

Figure S8. $^{13}C\{^{1}H\}$ NMR spectrum of **2** in C_6D_6 at 300K.

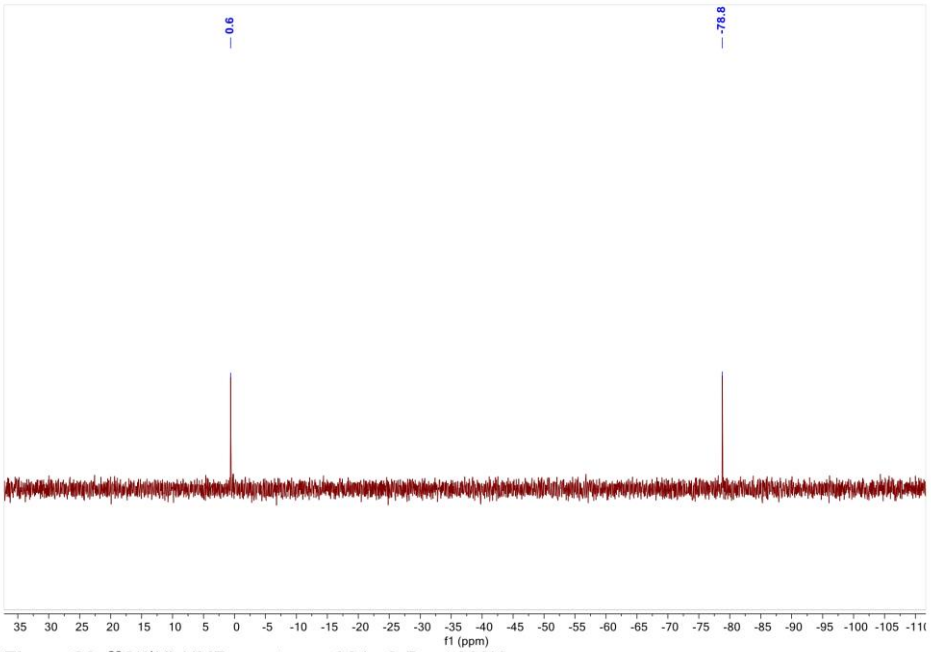

Figure S9. $^{29}Si\{^{1}H\}$ NMR spectrum of **2** in C_6D_6 at 300K.

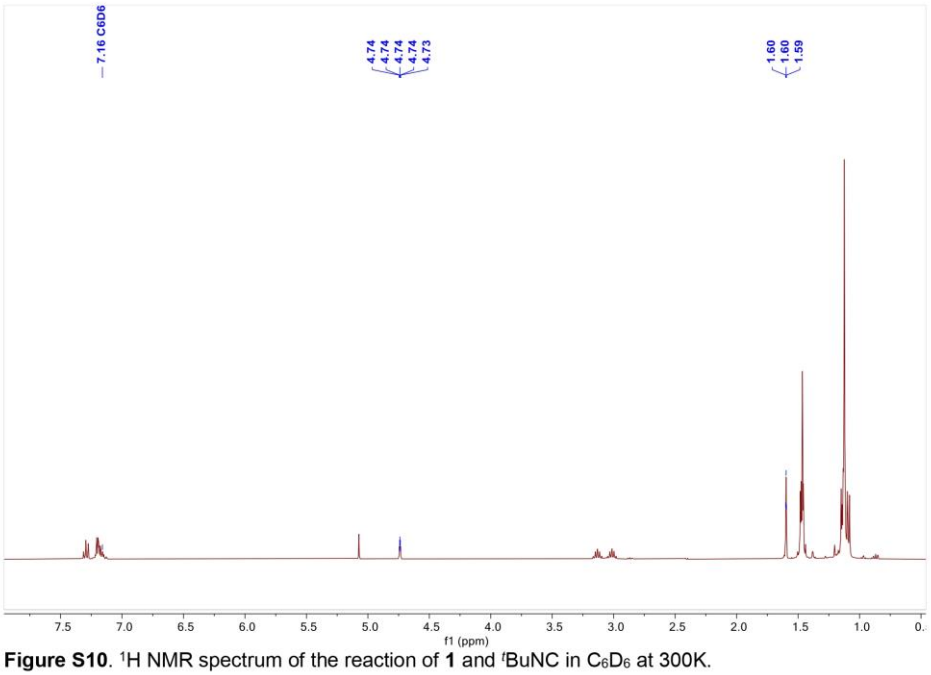

Figure S10. ^{1}H NMR spectrum of the reaction of **1** and $^{t}BuNC$ in C_6D_6 at 300K.

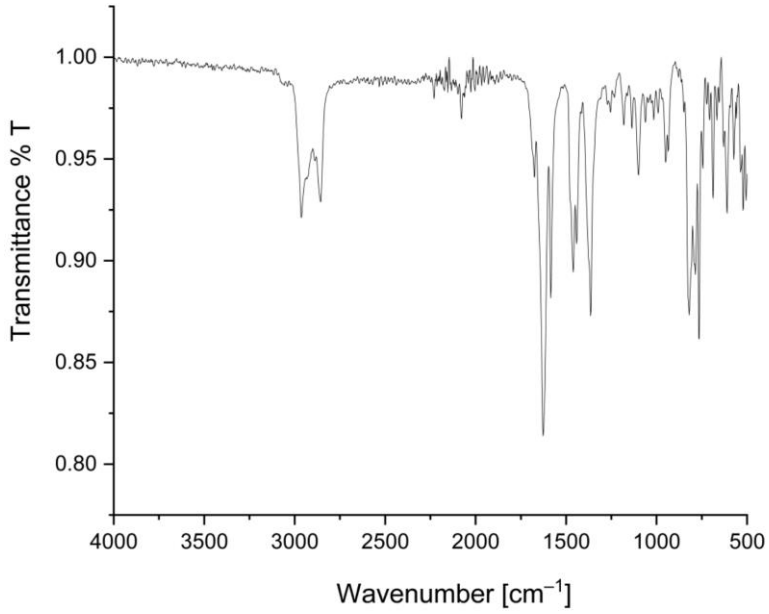

Figure S11. IR spectrum of **2** in the solid state.

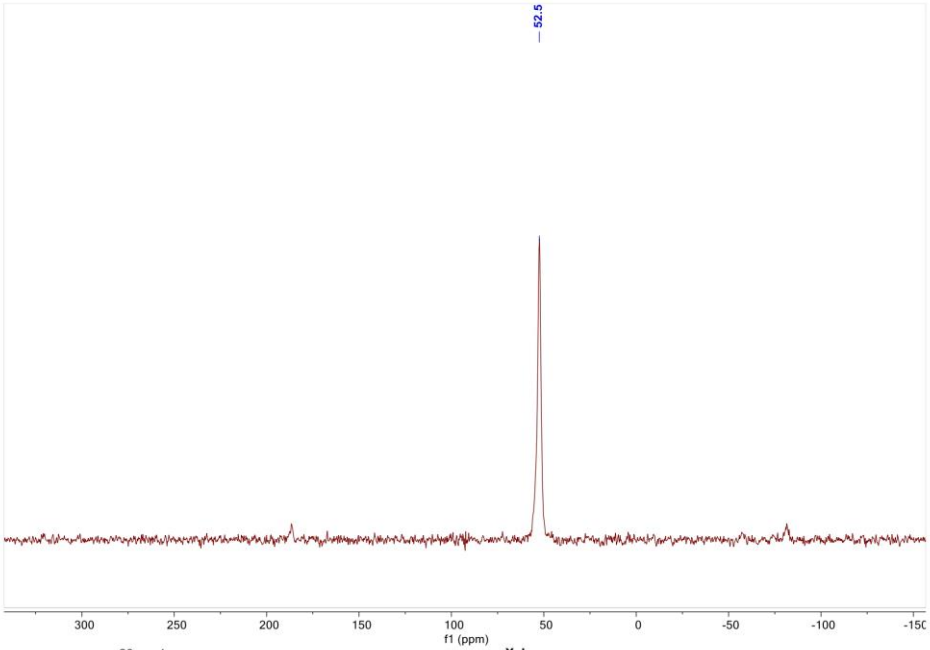

Figure S12. $^{29}Si\{^{1}H\}$ CP-MAS NMR NMR spectrum of $\mathbf{3^{Xyl}}$ at 300K.

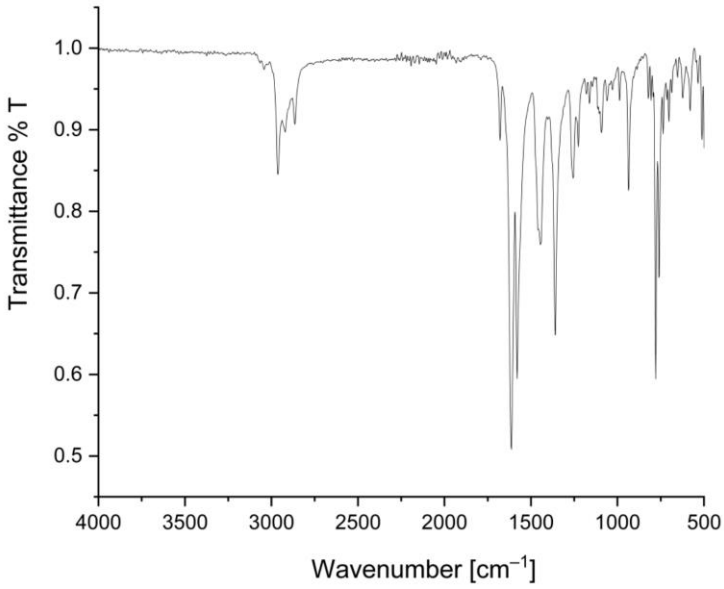

Figure S13. IR spectrum of **3^{Xyl}** in the solid state.

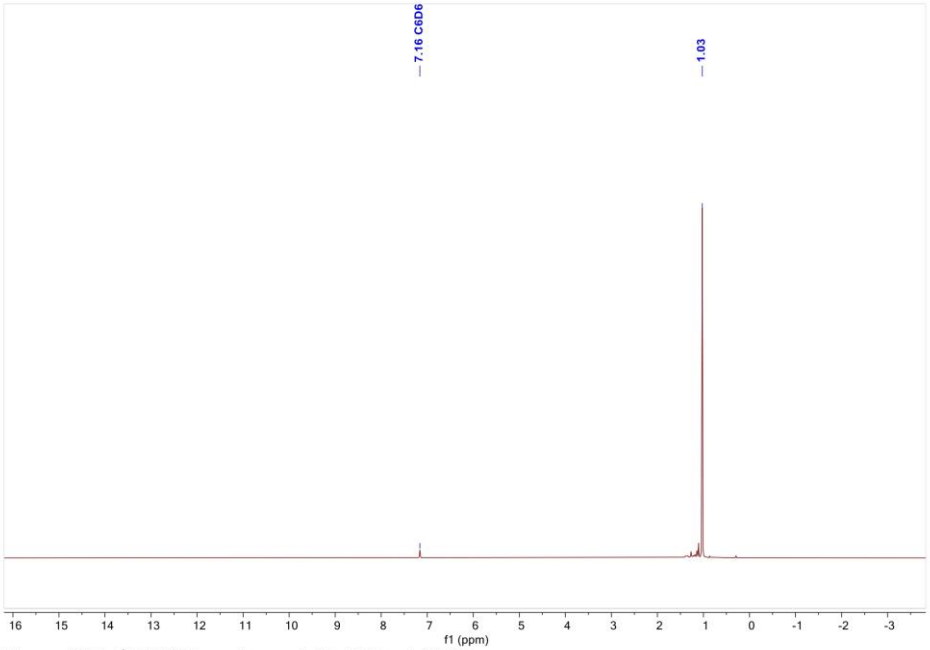

Figure S14. ^{1}H NMR spectrum of **4** in C_6D_6 at 300K.

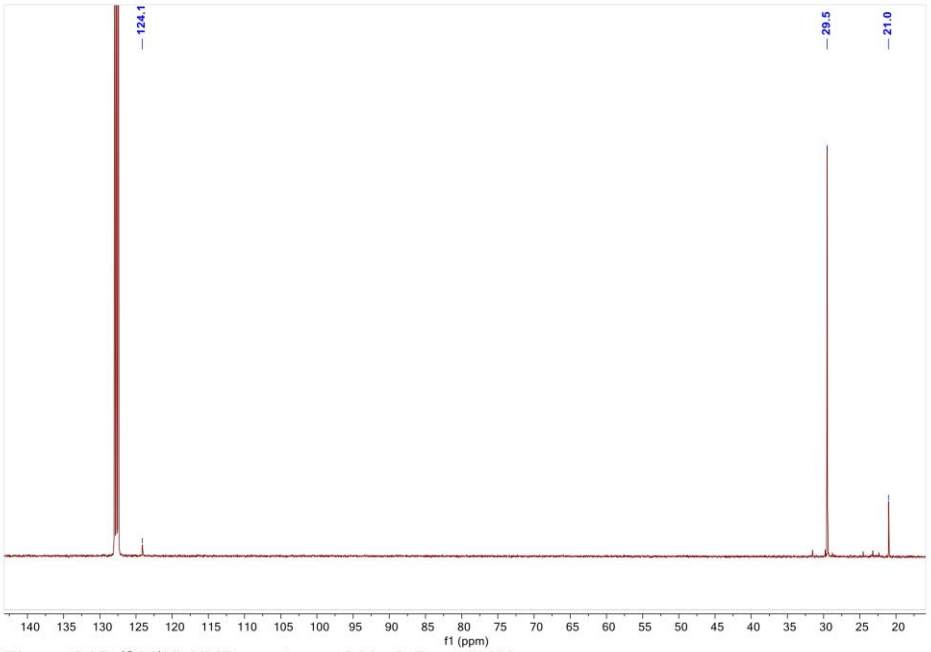

Figure S15. $^{13}C\{^{1}H\}$ NMR spectrum of **4** in C_6D_6 at 300K.

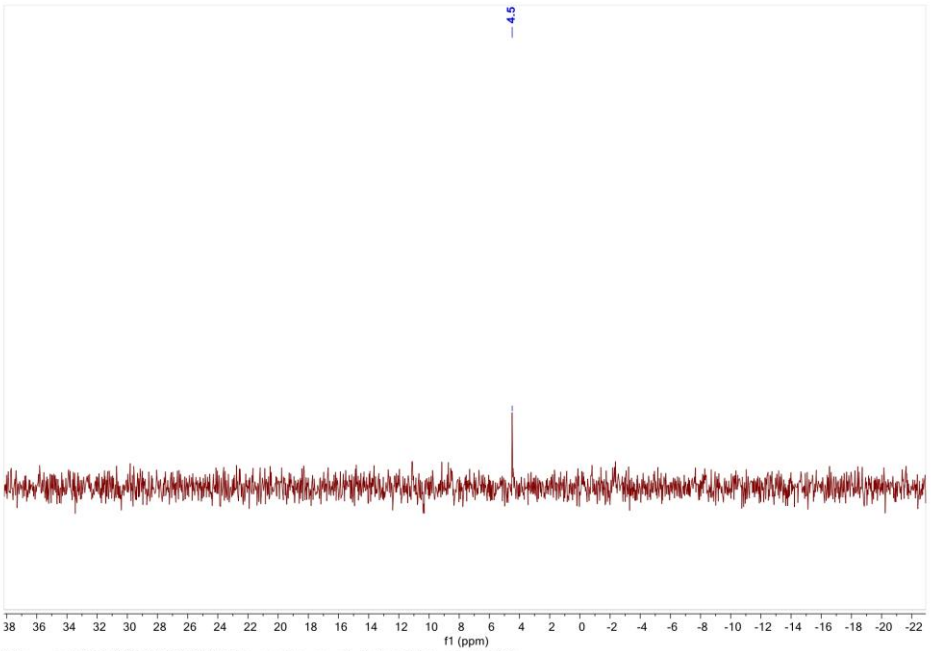

Figure S16. $^{29}Si\{^{1}H\}$ NMR spectrum of **4** in C_6D_6 at 300K.

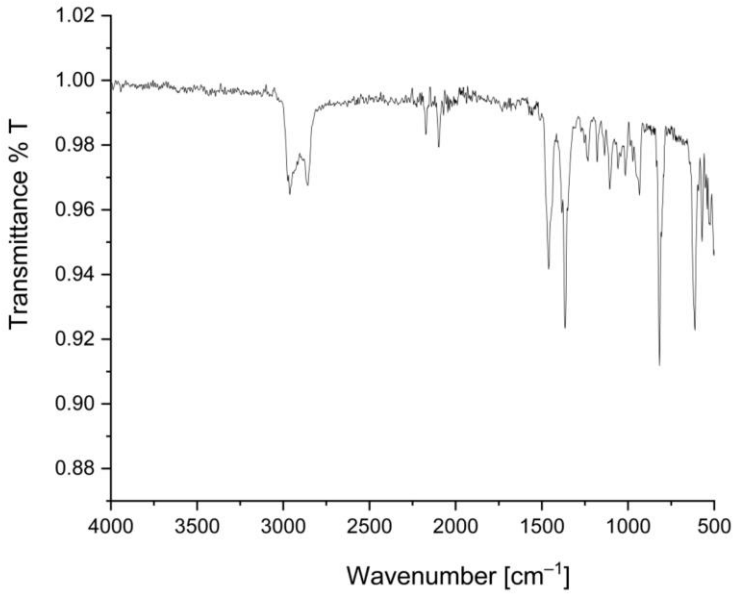

Figure S17. IR spectrum of **4** in the solid state.

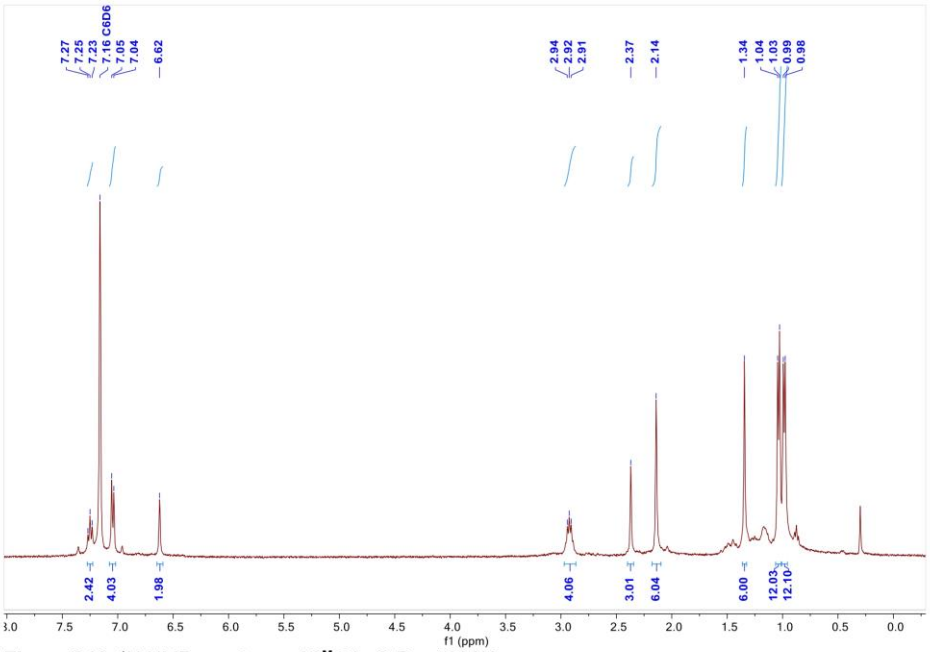

Figure S18. ^{1}H NMR spectrum of $\mathbf{3^{Mes}}$ in C_6D_6 at 300K.

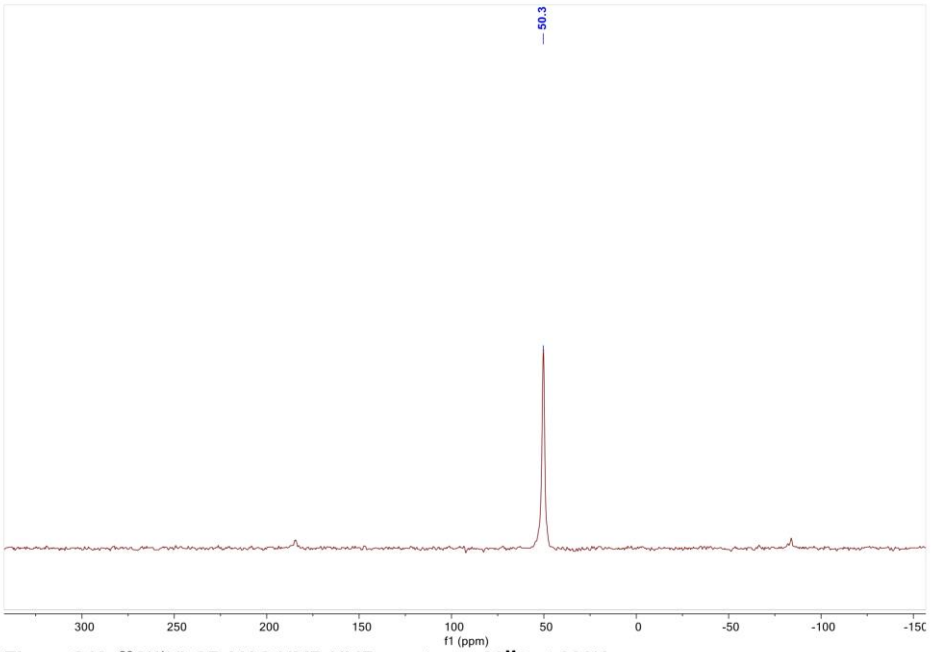

Figure S19. $^{29}Si\{^{1}H\}$ CP-MAS NMR NMR spectrum of **3^{Mes}** at 300K.

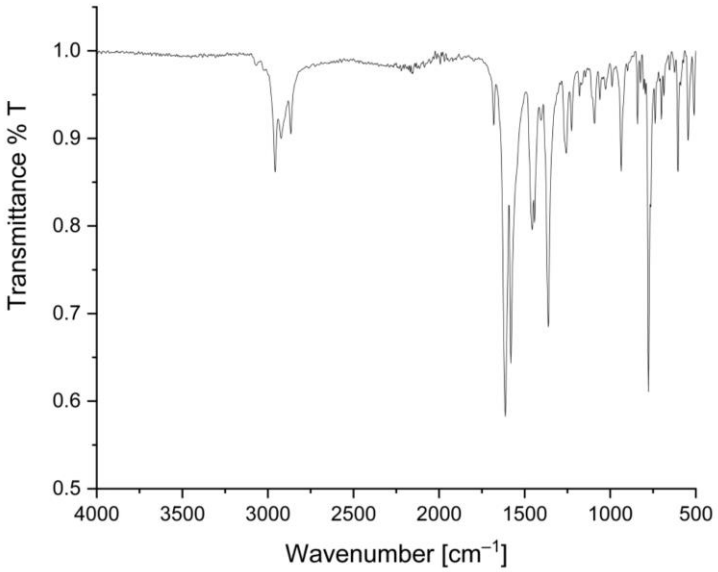

Figure S20. IR spectrum of **3^{Mes}** in the solid state.

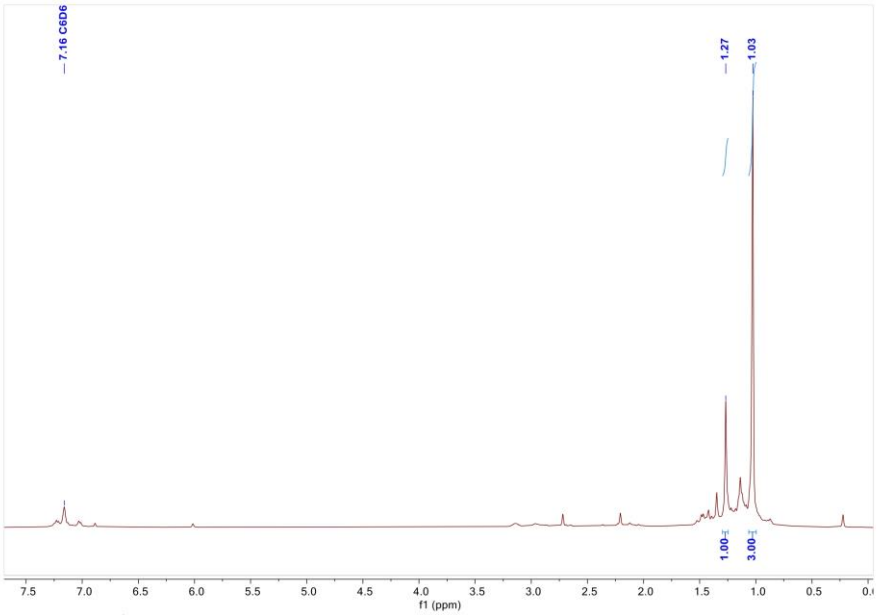

Figure S21. ^{1}H NMR spectrum of the filtrate of the reaction of **1** and MesNC in C_6D_6 at 300K.

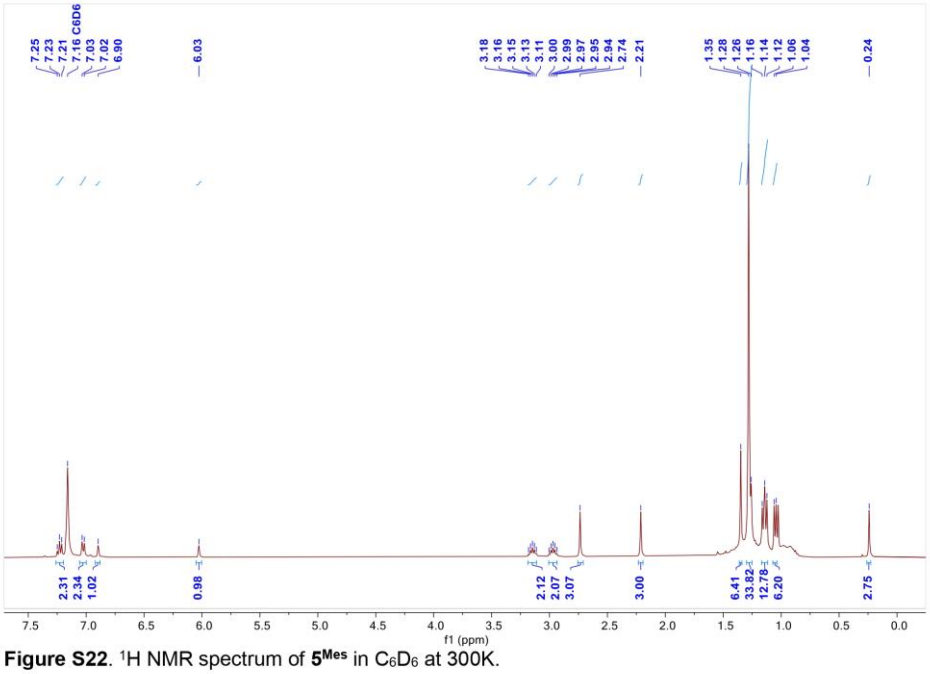

Figure S22. ^{1}H NMR spectrum of $\mathbf{5^{Mes}}$ in C_6D_6 at 300K.

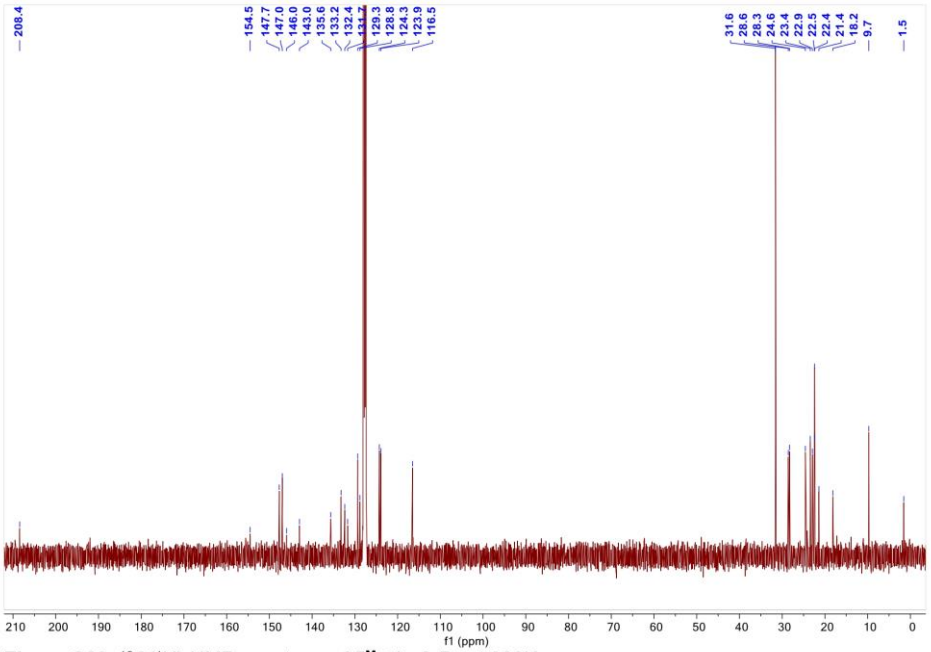

Figure S23. $^{13}C\{^{1}H\}$ NMR spectrum of **5^{Mes}** in C_6D_6 at 300K.

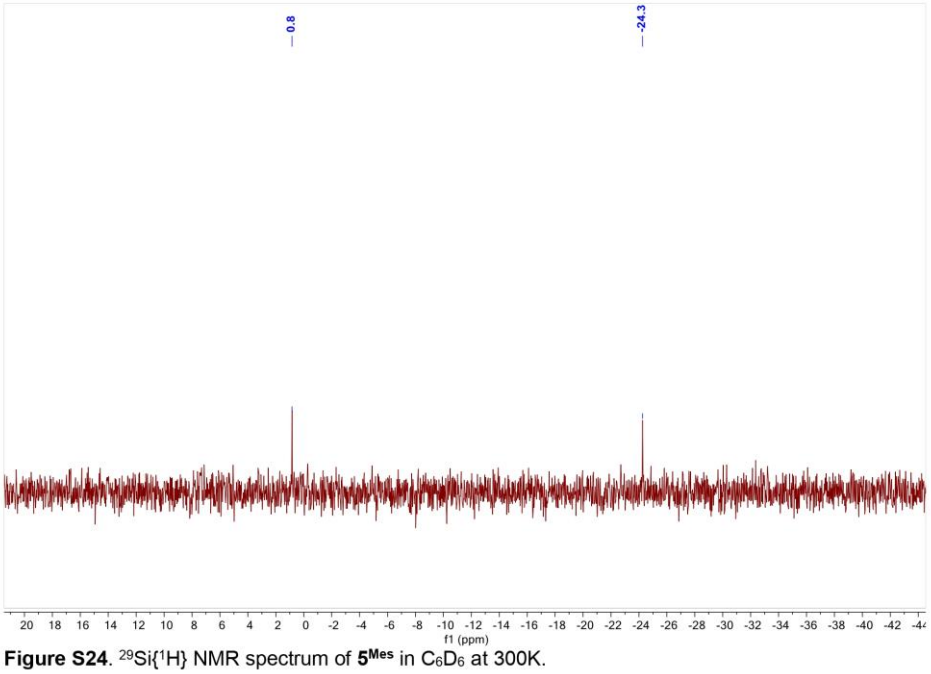

Figure S24. $^{29}Si\{^{1}H\}$ NMR spectrum of **5^{Mes}** in C_6D_6 at 300K.

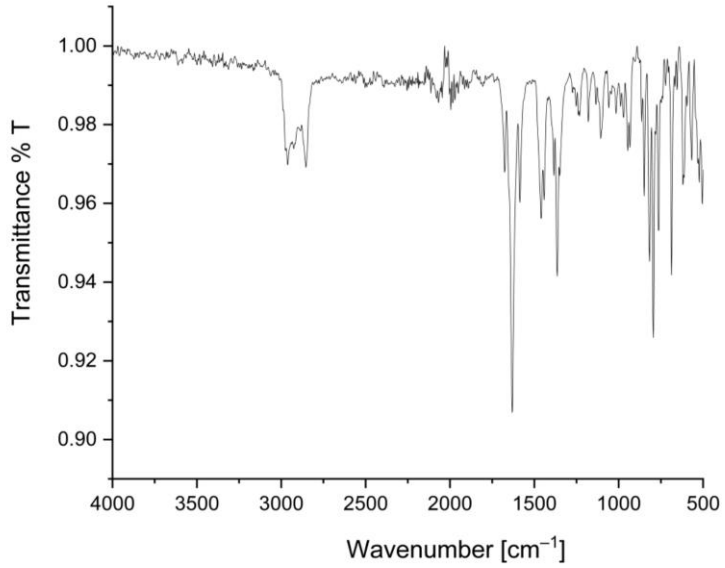

Figure S25. IR spectrum of **5^{Mes}** in the solid state.

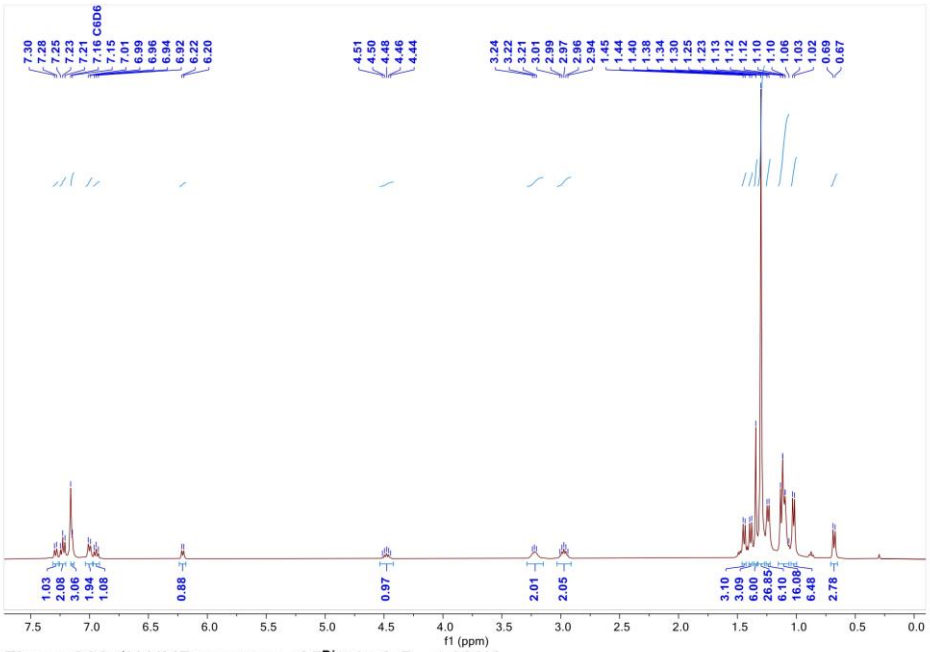

Figure S26. ^{1}H NMR spectrum of **5^{Dipp}** in C_6D_6 at 300K.

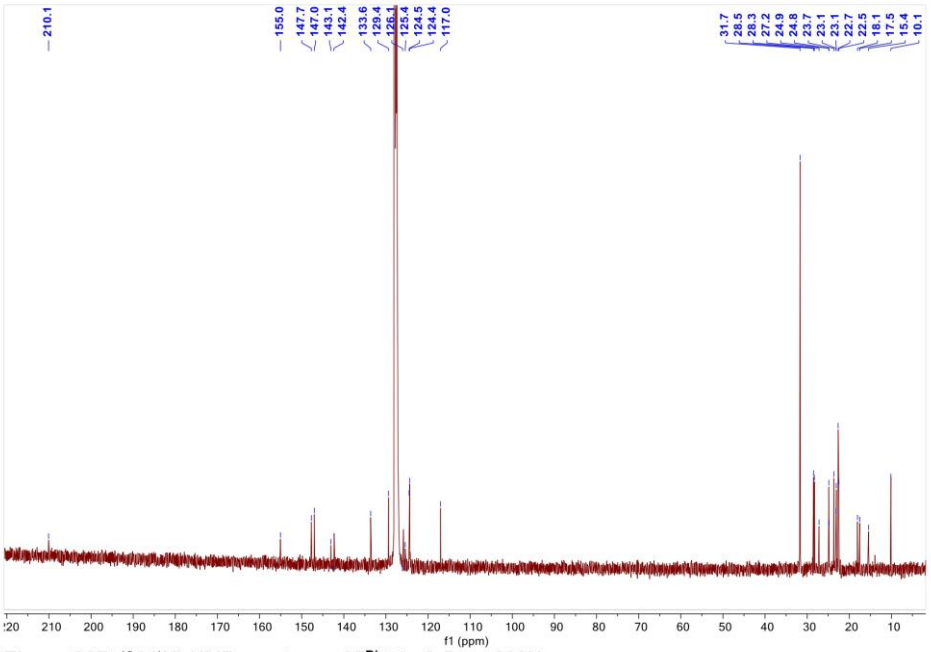

Figure S27. $^{13}C\{^{1}H\}$ NMR spectrum of $\mathbf{5^{Dipp}}$ in C_6D_6 at 300K.

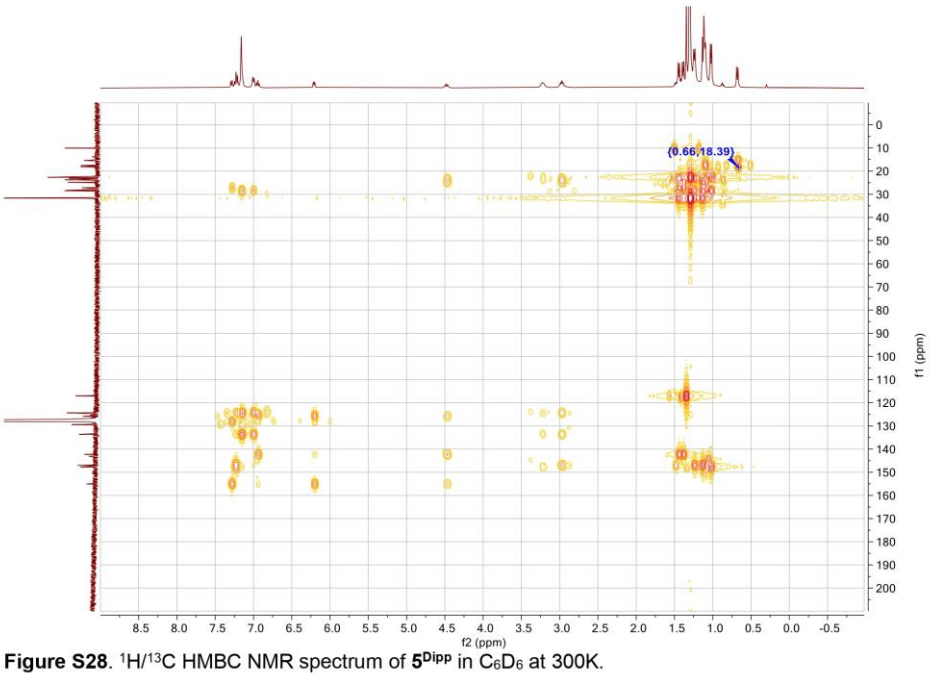

Figure S28. $^{1}H/^{13}C$ HMBC NMR spectrum of $\mathbf{5^{Dipp}}$ in C_6D_6 at 300K.

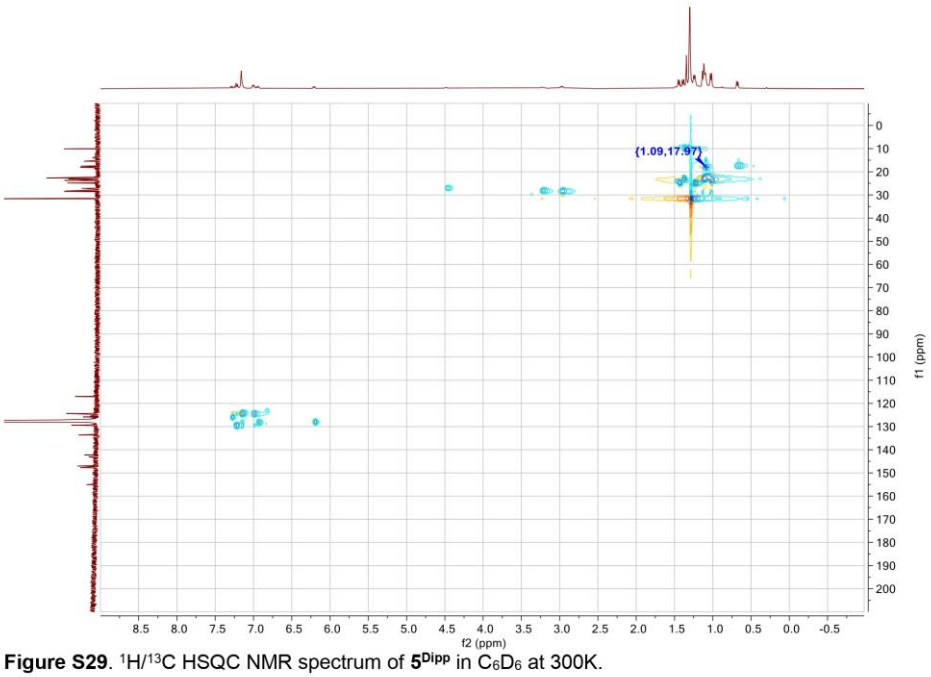

Figure S29. $^{1}H/^{13}C$ HSQC NMR spectrum of $\mathbf{5^{Dipp}}$ in C_6D_6 at 300K.

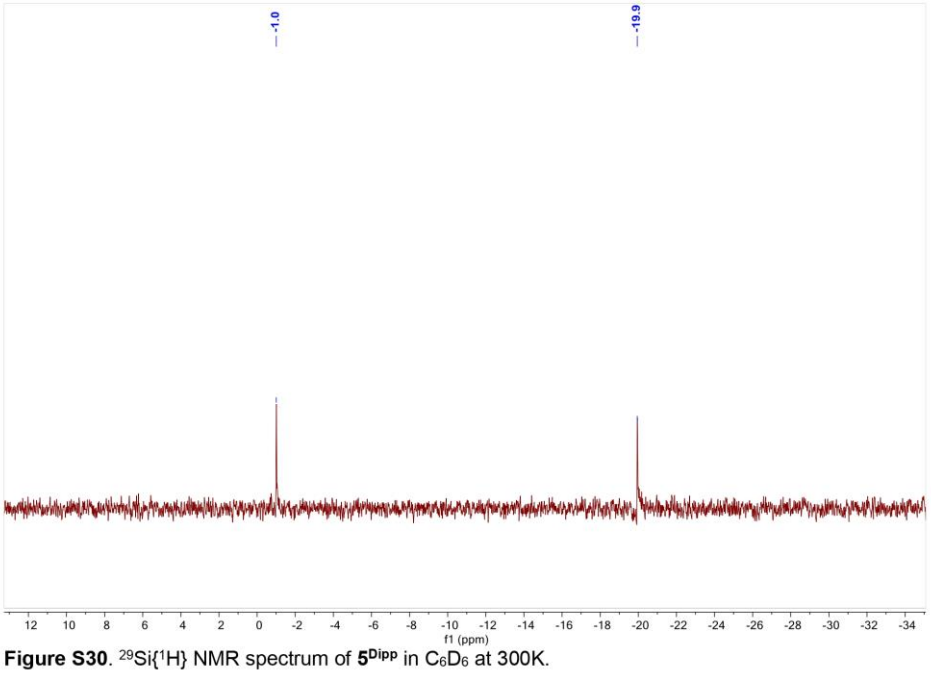

Figure S30. $^{29}Si\{^{1}H\}$ NMR spectrum of $\mathbf{5^{Dipp}}$ in C_6D_6 at 300K.

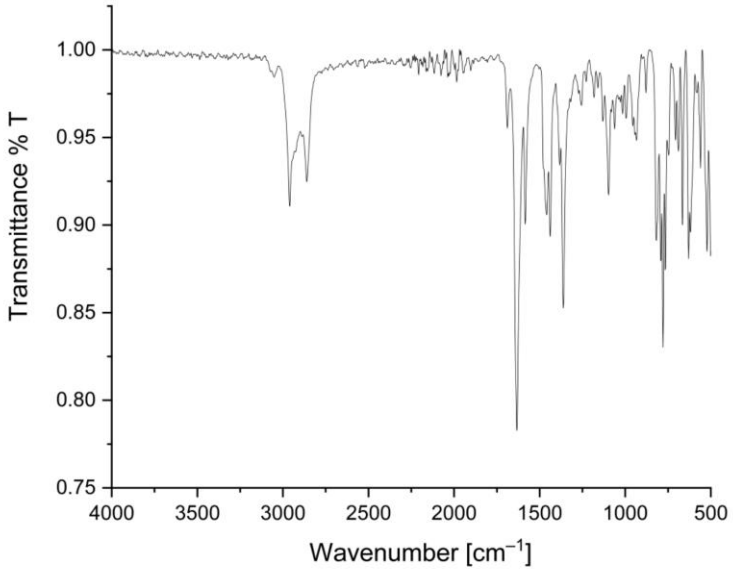

Figure S31. IR spectrum of **5^{Dipp}** in the solid state.

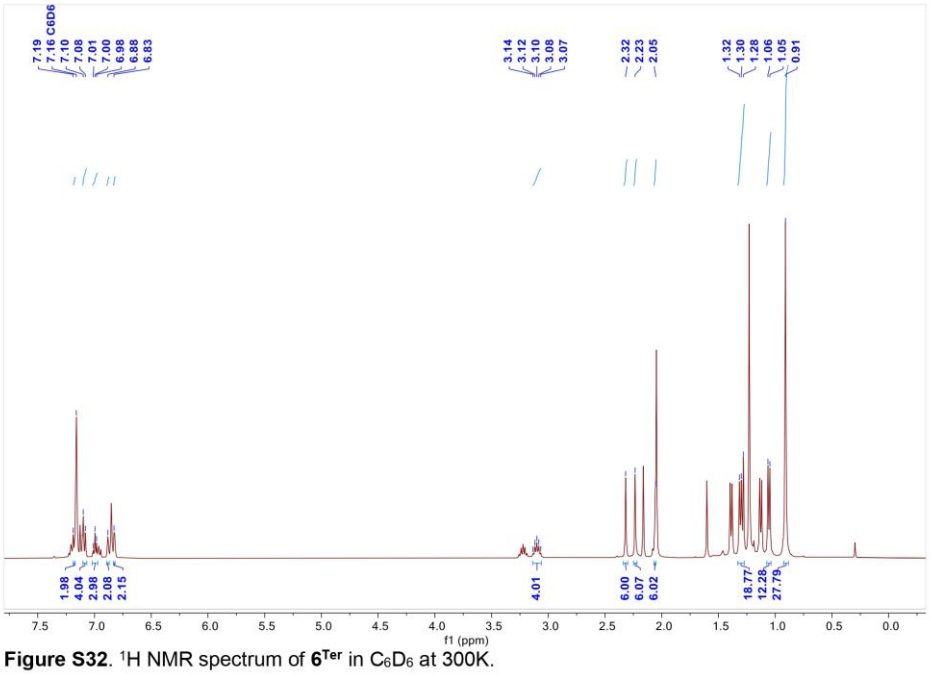

Figure S32. ^{1}H NMR spectrum of **6Ter** in C_6D_6 at 300K.

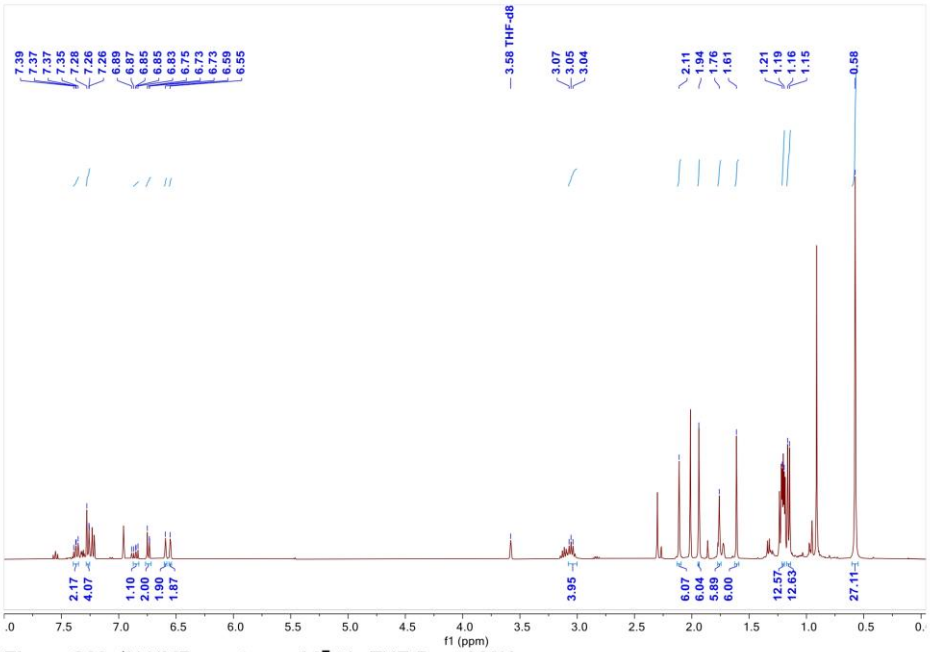

Figure S33. ^{1}H NMR spectrum of $\mathbf{6^{Ter}}$ in THF-D_8 at 300K.

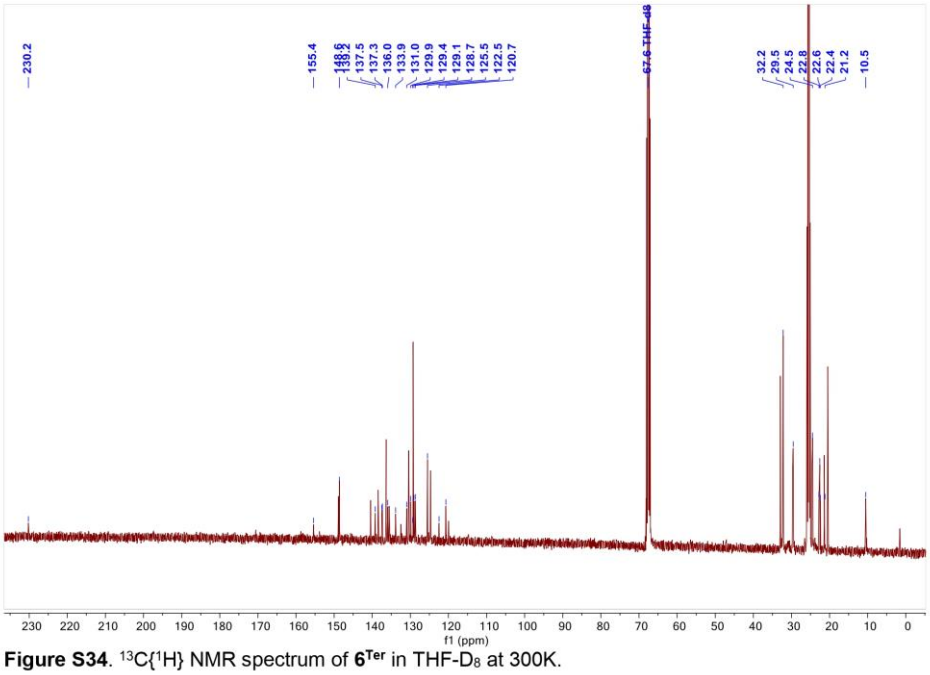

Figure S34. $^{13}C\{^{1}H\}$ NMR spectrum of $\mathbf{6^{Ter}}$ in THF-D_8 at 300K.

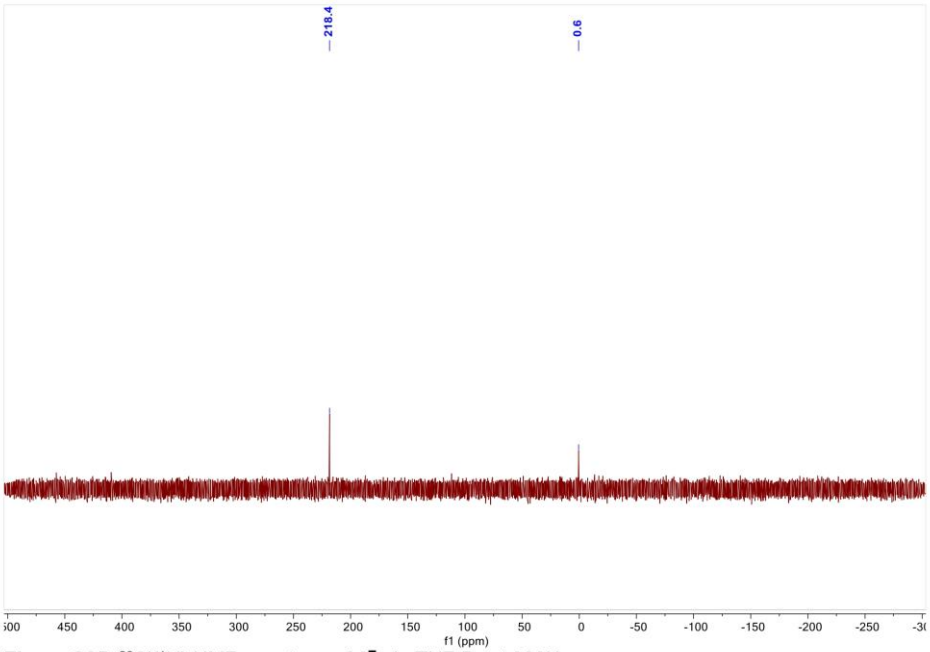

Figure S35. $^{29}Si\{^{1}H\}$ NMR spectrum of **6Ter** in THF-D_8 at 300K.

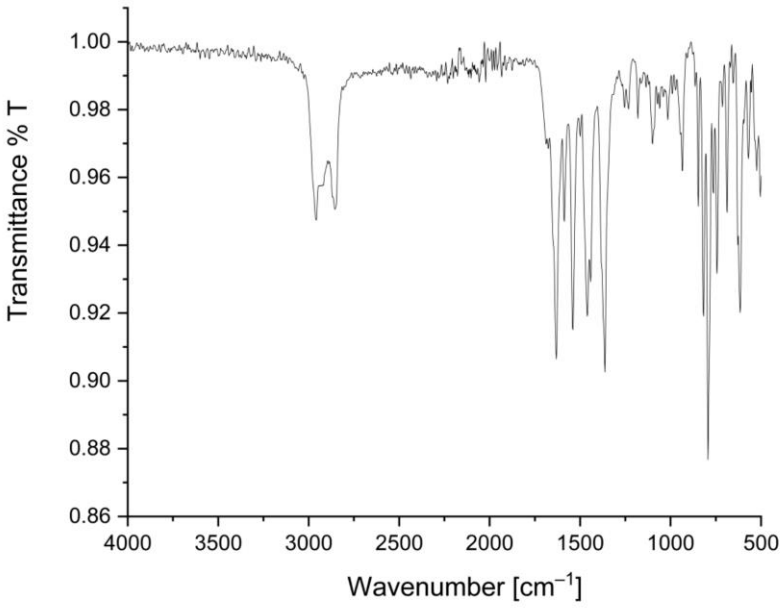

Figure S36. IR spectrum of **6Ter** in the solid state.

3. Single Crystal X-Ray Structure Determination

Single crystal diffraction data were recorded on a Bruker Photon D8 Venture DUO IMS system equipped with a Helios optic monochromator and a Mo IMS microsource (λ = 0.71073 Å) The data collection was performed, using the APEX III & IV software package[S5] on single crystals coated with Fomblin®Y as perfluorinated ether. The single crystals were picked on a micro sampler, transferred to the diffractometer, and measured frozen under a stream of cold nitrogen (100 K). A matrix scan was used to determine the initial lattice parameters. Reflections were merged and corrected for Lorenz and polarization effects, scan speed, and background using SAINT.[S6] Absorption corrections, including odd and even ordered spherical harmonics were performed using SADABS.[S6] Space group assignments were based upon systematic absences, E statistics, and successful refinement of the structures. Structures were solved by direct methods with the aid of successive difference Fourier maps and were refined against all data using the APEX IV software in conjunction with SHELXL-2014[S7] and SHELXLE.[S8] H atoms were placed in calculated positions and refined using a riding model, with methylene and aromatic C–H distances of 0.99 and 0.95 Å, respectively, and Uiso(H) = 1.2·Ueq(C). Non-hydrogen atoms were refined with anisotropic displacement parameters. Full-matrix least-squares refinements were carried out by minimizing Σw(Fo2-Fc2)2 with the SHELXL weighting scheme.[S9] Neutral atom scattering factors for all atoms and anomalous dispersion corrections for the non-hydrogen atoms were taken from International Tables for Crystallography.[S10] The images of the crystal structures were generated by Mercury.[S11] The CCDC numbers 2287658 to 2287662 contain the supplementary crystallographic data for the structures 3^{Mes} to 6^{Ter}. These data can be obtained free of charge from the Cambridge Crystallographic Data Centre *via* https://www.ccdc.cam.ac.uk/structures/.

Table S1. Crystallographic details

	compound_3^{Xyl}	compound_3^{Mes}	compound_5^{Mes}
CCDC-Number	2287658	2287660	2287661
Chemical formula	$C_{74}H_{98}N_6Si_2$	$C_{76}H_{102}N_6Si_2$	$C_{51}H_{78}N_4Si_2$
M_r	1127.76	1155.81	803.35
Crystal system, space group	Monoclinic, $P2_1/n$	Triclinic, $P\bar{1}$	Triclinic, $P\bar{1}$
Temperature (K)	100	100	100
a (Å), α(°) *b* (Å), β(°) *c* (Å), γ(°)	10.5433(4), 90 15.6783(7), 97.576(1) 19.6532(9), 90	10.7679(7), 71.516(2) 15.4889(10), 83.775(2) 22.5891(16), 73.243(2)	12.8491(5), 85.769(2) 13.0479(5), 83.213(2) 16.6152(7), 62.4790(10)
V (Å^3)	3220.3(2)	3420.8(4)	2452.49(17)
Z	2	2	2
F(000)	1224	1256	880
D_x (g/cm^3)	1.163	1.122	1.088
Radiation type	Mo $K\alpha$	Mo $K\alpha$	Mo $K\alpha$
μ (mm^{-1})	0.102	0.098	0.109
θ range (°) for cell meas.	4.18–50.7	3.802–50.79	4.16–66.446
Crystal size (mm)	0.35 × 0.317 × 0.138	0.1 × 0.07 × 0.04	0.07 × 0.05 × 0.04
Diffractometer	Bruker Photon CMOS	Bruker Photon CMOS	Bruker Photon CMOS
Radiation source	IMS microsource	IMS microsource	IMS microsource
Monochromator	Helios optic	Helios optic	Helios optic
Absorption correction	Multi-scan	Multi-scan	Multi-scan
T_{min}, T_{max}	0.664, 0.745	0.667, 0.745	0.685, 0.747
θ_{max} (°)	25.350	25.395	33.233
Range of *h*, *k*, *l*	*h* = -12→12, *k* = -18→18, *l* = -23→23	*h* = -12→12, *k* = -18→18, *l* = -27→27	*h* = -19→19, *k* = -20→20, *l* = -25→25
Refinement method	Full-matrix least-squares on F^2	Full-matrix least-squares on F^2	Full-matrix least-squares on F^2
Data/restraints/parameters	5902/167/415	12560/0/771	18793/0/536
Goodness-of-fit on F^2	1.08	1.066	1.072
Final *R* indices (I>2σ(I))	R_1(all) = 0.0923, wR_2(all) = 0.1692 R_1 = 0.0693, wR_2 = 0.1561	R_1(all) = 0.0648, wR_2(all) = 0.1300 R_1 = 0.0549, wR_2 = 0.1361	R_1(all) = 0.0470, wR_2(all) = 0.1254 R_1 = 0.0411, wR_2 = 0.1191
$\Delta\rho_{max}$, $\Delta\rho_{min}$ (e Å^{-3})	0.58, -0.28	0.69, -0.39	0.79, -0.35

	compound_**5**^{Dipp}	compound_**6**^{Ter}
CCDC-Number	2287659	2287662
Chemical formula	$C_{57}H_{87}N_4Si_2$	$C_{66}H_{92}N_4Si_2$
M_r	884.48	997.61
Crystal system, space group	Triclinic, $P\bar{1}$	Monoclinic, $P2_1/n$
Temperature (K)	100	100
a (Å), α(°) *b* (Å), β(°) *c* (Å), γ(°)	12.4845(7), 78.880(2) 13.5411(8), 77.647(2) 17.1607(10), 72.709(2)	12.7861(12), 90 21.446(2), 100.052(4) 22.311(2), 90
V (Å^3)	2679.7(3)	6024.0(10)
Z	2	4
F(000)	970	2176
D_x (g/cm^3)	1.096	1.1
Radiation type	Mo *K*α	Mo *K*α
μ (mm^{-1})	0.105	0.101
θ range (°) for cell meas.	4.03–50.904	4.226–70.566
Crystal size (mm)	0.12 × 0.08 × 0.05	0.05 × 0.04 × 0.04
Diffractometer	Bruker Photon CMOS	Bruker Photon CMOS
Radiation source	IMS microsource	IMS microsource
Monochromator	Helios optic	Helios optic
Absorption correction	Multi-scan	Multi-scan
T_{min}, T_{max}	0.676, 0.745	0.574, 0.747
θ_{max} (°)	25.452	35.283
Range of *h*, *k*, *l*	*h* = -15→15, *k* = -16→16, *l* = -20→20	*h* = -20→20, *k* = -33→33, *l* = -35→34
Refinement method	Full-matrix least-squares on F^2	Full-matrix least-squares on F^2
Data/restraints/parameters	9868/0/591	26045/0/674
Goodness-of-fit on F^2	1.025	1.026
Final *R* indices (I>2σ(I))	R_1(all) = 0.0399, wR_2(all) = 0.0972 R_1 = 0.0372, wR_2 = 0.0950	R_1(all) = 0.1153, wR_2(all) = 0.1476 R_1 = 0.0628, wR_2 = 0.1244
$\Delta\rho_{max}$, $\Delta\rho_{min}$ (e Å^{-3})	0.87, -0.41	0.72, -0.36

4. Computational Details

4.1 Computational Methods

Calculations were carried out using ORCA 5.0.4.[S12] Geometry optimizations for the mechanistic investigations were carried using the r^{2}SCAN-3c composite method,[S13] utilizing the regularized and restored SCAN functional,[S14-15] geometrical counterpoise correction gCP,[S16] the atom-pairwise dispersion correction based on tight binding partial charges (D4),[S17-19] the def2-mTZVPP basis set and def2-mTZVPP/J auxiliary basis set.[S13] The optimized geometries were verified as minima or transition states by analytical frequency calculations. The transition states were additionally verified by IRC calculations. Single point calculations of the optimized geometries were carried at the r^{2}SCAN-3c level using the SMD solvation module[S20] and benzene as a solvent to obtain electrostatic contribution and the cavity term in order to account for the solvent effects. Single point calculations of the optimized geometries were also carried out at the DLPNO-CCSD(T) level of theory, with the def2-TZVP[S21] basis set and the def2-TZVP/C[S22] auxiliary basis set for all atoms, to get more accurate electronic energies. The results are presented in Table . The TD-DFT calculations were carried out at the PBE0/def2-TZVP//r^{2}SCAN-3c level of theory. Cartesian coordinates of the optimized geometries are given in individual Data S1. Cartesian coordinates of computationally optimized structures.

4.2 Reactivity of 1 toward ^{t}BuNC

In addition to the experimentally observed reaction pathway in the reaction of **1** with ^{t}BuNC, which yield the silane **2** and isobutylene, we explored additional reaction pathways for this reaction (Figure S37). As described in the main text, the product of the isocyanide migratory insertion into the Si–Si bond, *i.e.* the (imino)(iminoacyl)silylene B^{tBu}, is predicted to be a viable process, as the transition state **TS(A^{tBu}-B^{tBu})** that leads to it, is slightly lower in energy than the transition state TS(**A^{tBu}-2**) that leads to the formation of the final products. Our calculations show that the reason for the formation of **2** and isobutylene as sole products is due to **TS(A^{tBu}-2)** being lower in energy than the transition states associated with further reactivity of **B^{tBu}**. That is in contrast to what we observed in reactions of **1** with MesNC, XylNC, DippNC where the (imono)(iminoacyl)silylenes (**6**) were a key intermediate for further reactivity. To convert **B^{tBu}** to **D^{tBu}**, in a process similar to aryl migration to form the bicyclic reactive intermediates **D** in the reactions of **1** with aryl isocyanides, would require to overcome a barrier of **TS(B^{tBu}-D^{tBu})** at 37.2 kcal mol^{-1}, that is 21 kcal mol^{-1} higher than **TS(A^{tBu}-2)**. The rearrangement of B^{tBu} to the cylic silane **G^{tBu}**, in a process that maybe reminiscent of the alkyl migration to the silicon center to form the benzazasilole derivative **5**, is predicted to be exergonic by 41.7 kcal mol^{-1}. However, the transition state **TS(B^{tBu}-G^{tBu})** is by 11.7 kcal mol^{-1} higher than **TS(A^{tBu}-2)**. The transition state that leads to the fragmentation of **B^{tBu}** to the silylene H^{tBu}, isobutylene and the silylcyanide is also higher in energy than **TS(A^{tBu}-2)**, by 28.8 kcal mol^{-1}.

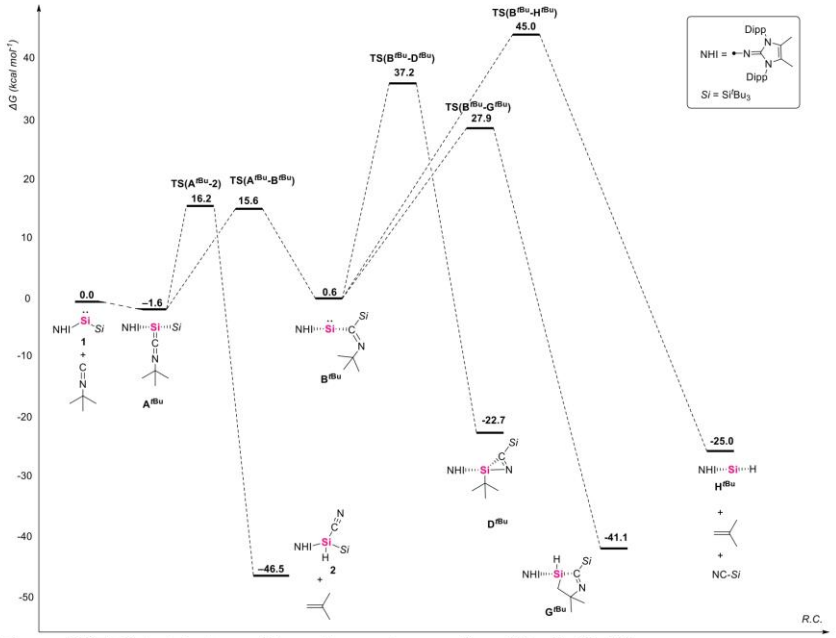

Figure S37. Calculated possible pathways for reaction of **1** with ᵗBuNC.

4.3 Thermochemistry

Table S2. Calculated energies (Eh). $E_{DLPO\text{-}CCSD(T)}$ - electronic energy at the DLPNO-CCSD(T)/def2-TZVP//r^{2}SCAN-3c level; G-E_{el} - Gibbs energy minus the electronic energy at the r^{2}SCAN-3c// r^{2}SCAN-3c level; G_{cds} (cavity term) and G_{enp} (electrostatic contribution) at r^{2}SCAN-3c(SMD=Benzene)// r^{2}SCAN-3c level; G_{conc} - concentration-induced free-energy shift (G_{conc} = RTln(24.5)); G – free energy, G = [$E_{DLPO\text{-}CCSD(T)}$] + [G-E_{el}] + G_{cds} + G_{enp} + G_{conc}. Thermochemistry at 298.15 K.

MET_000	$E_{DLPO\text{-}CCSD(T)}$	G-E_{el}	G_{cds}	G_{enp}	G_{conc}	G
1	-2341.73633	0.91937	-0.01362	-0.01994	0.00302	-2340.84749
XylCN	-402.33327	0.11843	-0.00670	-0.00520	0.00302	-402.22372
A^{Xyl}	-2744.11055	1.06752	-0.01538	-0.02253	0.00302	-2743.07793
TS(A^{Xyl}-6^{Xyl})	-2744.08099	1.06658	-0.01611	-0.02276	0.00302	-2743.05026
6^{Xyl}	-2744.11605	1.06660	-0.01728	-0.02187	0.00302	-2743.08557
TS(6^{Xyl}-C^{Xyl})	-2744.08607	1.06960	-0.01638	-0.02351	0.00302	-2743.05333
C^{Xyl}	-2744.09672	1.06913	-0.01827	-0.02195	0.00302	-2743.06479
TS(C^{Xyl}-5^{Xyl})	-2744.07585	1.06770	-0.01845	-0.02145	0.00302	-2743.04503
5^{Xy}	-2744.18184	1.06875	-0.01570	-0.02196	0.00302	-2743.14773
TS(6^{Xyl}-D^{Xyl})	-2744.07847	1.06539	-0.01703	-0.02103	0.00302	-2743.04812
D^{Xyl}	-2744.15921	1.06713	-0.01797	-0.02168	0.00302	-2743.12872
TS(D^{Xyl}-E^{Xyl})	-2744.11629	1.06339	-0.01847	-0.02236	0.00302	-2743.09071
E^{Xyl}	-2744.14287	1.06349	-0.03787	-0.01912	0.00302	-2743.13335
TS(D^{Xyl}-F^{Xyl})	-2744.11686	1.06256	-0.01864	-0.02178	0.00302	-2743.09171
F^{Xyl}	-1889.74824	0.70438	-0.01540	-0.01973	0.00302	-1889.07598
4 (tBu_3SiCN)	-854.38556	0.33043	-0.00785	-0.00330	0.00302	-854.06327
3^{Xy}	-3779.56210	1.44505	-0.02621	-0.03254	0.00302	-3778.17279
A^{tBu}	-2591.97018	1.04650	-0.01468	-0.01925	0.00302	-2590.95459

TS(A^{tBu}-2)	-2591.93631	1.04169	-0.01630	-0.01829	0.00302	-2590.92619
2	-2435.10528	0.93703	-0.01633	-0.01684	0.00302	-2434.19840
Isobutylene	-156.90654	0.08056	-0.00244	-0.00246	0.00302	-156.82786
TS(A^{tBu}-B^{tBu})	-2591.94175	1.04657	-0.01413	-0.02098	0.00302	-2590.92726
B^{tBu}	-2591.96409	1.04586	-0.01526	-0.02068	0.00302	-2590.95115
TS(B^{tBu}-D^{tBu})	-2591.90534	1.04498	-0.01513	-0.02037	0.00302	-2590.89283
D^{tBu}	-2592.00239	1.04608	-0.01496	-0.02002	0.00302	-2590.98826
TS(B^{tBu}-G^{tBu})	-2591.91835	1.04268	-0.01435	-0.02058	0.00302	-2590.90757
G^{tBu}	-2592.03201	1.04567	-0.01395	-0.02030	0.00302	-2591.01757
TS(B^{tBu}-H^{tBu})	-2591.88188	1.03539	-0.01609	-0.02076	0.00302	-2590.88032
H^{tBu}	-1580.64911	0.57469	-0.01282	-0.01656	0.00302	-1580.10077

4.4 TD-DFT calculations

TD-DFT calculations at the PBE0/def2-TZVP//r^{2}SCAN-3c level of theory of the first 10 excitations for **5**^{Dipp} and **6**^{Dipp} were carried out. The simulated UV-vis spectra are presented in Figure S38. In the 350-750 nm range **5**^{Dipp} exhibits only one excitation at 445 nm with a very low oscillator strength, corresponding to the HOMO-LUMO transition. **6**^{Dipp} exhibits six transitions in 350-750 nm region, two of which are the visible region, at 582 and 423 nm. They are in the very good agreement with the experimentally observed peaks at 589 and 423 nm (Figure S6), and correspond to the n→p and n→π* transitions (Figure S40).

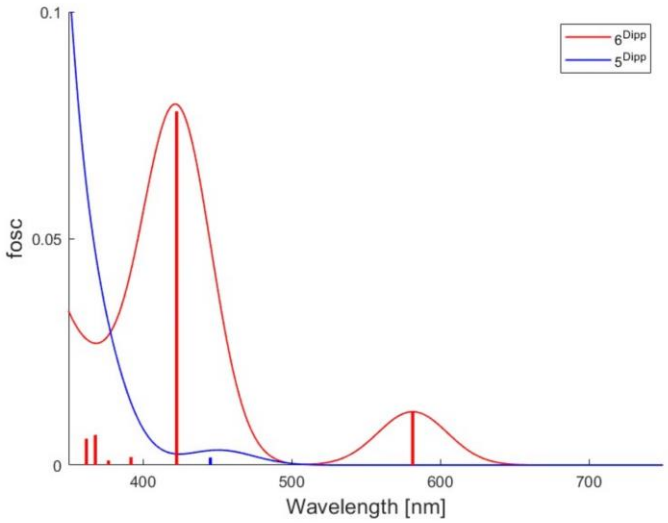

Figure S38. Simulated UV-Vis spectra in the 350-700 nm range of **5**^{Dipp} (blue) and **6**^{Dipp} (red). The corresponding excitations are shown as vertical lines.

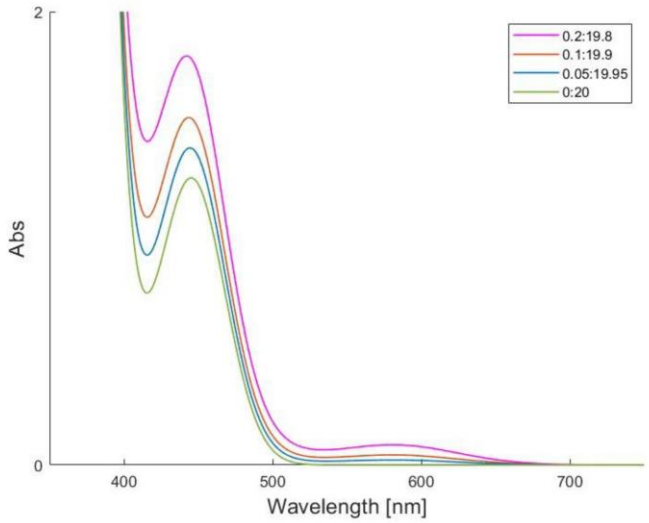

Figure S39. Simulated UV-Vis of a mixture of $\mathbf{5^{Dipp}}$ and $\mathbf{6^{Dipp}}$ in different ratios, simulating the spectrum of the reaction between **1** and DippNC (Figure S6).

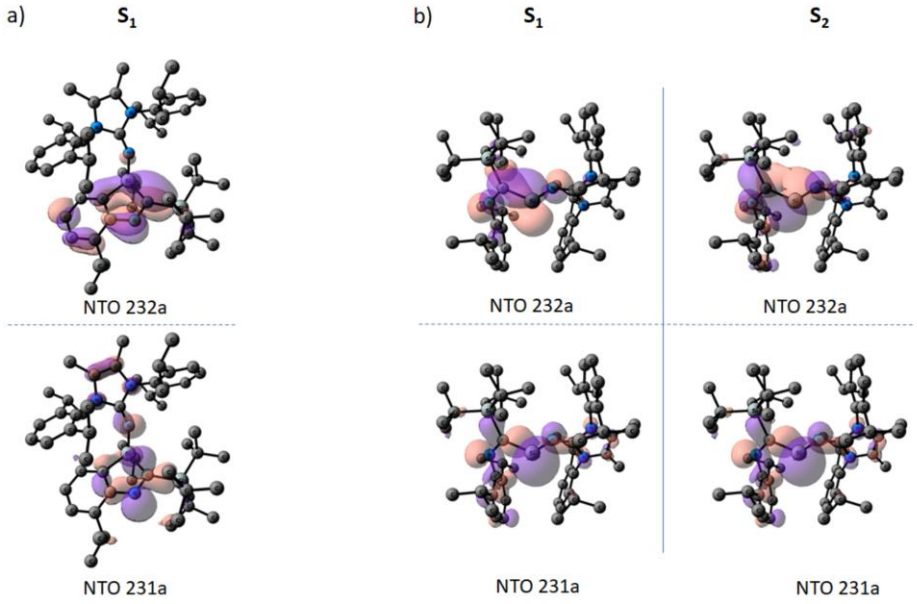

Figure S40. Natural Transition Orbitals (NTOs, (donors – bottom, acceptors - top) for $\mathbf{5^{Dipp}}$ (a) in the S_1 state and for $\mathbf{6^{Dipp}}$ (b) in the S_1 and S_2 states. Hydrogens are omitted for clarity.

Table S3. TD-DFT calculated excites states (S_1-S_{10}) of $\mathbf{5^{Dipp}}$ and the corresponding Natural Transition Orbitals (NTOs) for S_1.

STATE	Transitions	f_{osc}	E (cm^{-1})	λ (nm)	NTOs
S_1	230a → 232a : 0.290645 (c= 0.53911544) 231a → 232a : 0.685481 (c= 0.82793774)	0.001686004	22450.0	445.4	231a → 232a : n= 0.99547404 230a → 233a : n= 0.00202779
S_2	230a → 232a : 0.676741 (c= 0.82264280) 231a → 232a : 0.300754 (c= -0.54841047)	0.025070328	28668.5	348.8	
S_3	229a → 232a : 0.024716 (c= 0.15721378) 230a → 233a : 0.022542 (c= 0.15013858) 231a → 233a : 0.936531 (c= -0.96774506)	0.027846752	31613.5	316.3	
S_4	227a → 232a : 0.021663 (c= -0.14718404) 228a → 232a : 0.022278 (c= 0.14925853) 229a → 232a : 0.486419 (c= 0.69743772) 231a → 233a : 0.021252 (c= 0.14578114) 231a → 234a : 0.397624 (c= -0.63057445)	0.119201897	32609.7	306.7	
S_5	227a → 232a : 0.017149 (c= 0.13095294) 228a → 232a : 0.067328 (c= -0.25947552) 229a → 232a : 0.304937 (c= -0.55221120) 230a → 234a : 0.015622 (c= 0.12498814) 231a → 234a : 0.551870 (c= -0.74287958)	0.062332298	32856.8	304.4	
S_6	227a → 232a : 0.028856 (c= -0.16986914) 228a → 232a : 0.684085 (c= 0.82709433) 229a → 232a : 0.068931 (c= -0.26254627) 229a → 237a : 0.045947 (c= 0.21435255) 231a → 235a : 0.090634 (c= 0.30105547) 231a → 236a : 0.025458 (c= -0.15955580)	0.038722613	34058.7	293.6	
S_7	228a → 232a : 0.078776 (c= -0.28067104) 230a → 235a : 0.018640 (c= -0.13652835) 231a → 235a : 0.876431 (c= 0.93617895)	0.010459293	34206.8	292.3	
S_8	228a → 232a : 0.021086 (c= -0.14521134) 230a → 236a : 0.015902 (c= 0.12610352) 231a → 236a : 0.943898 (c= -0.97154436)	0.006349253	34506.5	289.8	

S_9	226a → 232a : 0.010352 (c= -0.10174620) 227a → 232a : 0.591626 (c= 0.76917204) 228a → 232a : 0.018820 (c= 0.13718647) 229a → 232a : 0.036161 (c= 0.19016137) 229a → 237a : 0.041674 (c= 0.20414261) 230a → 237a : 0.033664 (c= -0.18347854) 231a → 237a : 0.235084 (c= -0.48485411)		0.045718214	35763.7	279.6	
S_{10}	227a → 232a : 0.238100 (c= -0.48795509) 229a → 237a : 0.021796 (c= -0.14763523) 230a → 237a : 0.086112 (c= -0.29344922) 231a → 237a : 0.619158 (c= -0.78686609)		0.005830532	36104.1	277.0	

Table S4. TD-DFT calculated excites states (S_1-S_{10}) of $\mathbf{6^{Dipp}}$ and the corresponding Natural Transition Orbitals (NTOs) for S_1 and S_2.

STATE	Transitions		f_{osc}	E (cm^{-1})	λ (nm)	NTOs
S_1	231a → 232a : (c= -0.97039791) 231a → 236a : (c= -0.11865730)	0.941672 0.014080	0.011789793	17197.9	581.5	231a → 232a : n= 0.99151774 230a → 233a : n= 0.00461266
$2S_2$	230a → 232a : (c= 0.13378064) 231a → 232a : (c= 0.18494386) 231a → 233a : (c= -0.33158100) 231a → 234a : (c= 0.39613449) 231a → 235a : (c= 0.26110754) 231a → 236a : (c= -0.70768766) 231a → 237a : (c= 0.22984054) 231a → 239a : (c= 0.14373963)	0.017897 0.034204 0.109946 0.156923 0.068177 0.500822 0.052827 0.020661	0.078058565	23660.1	422.7	231a → 232a : n= 0.96652719 230a → 233a : n= 0.02652604 229a → 234a : n= 0.00119446
S_3	231a → 233a : (c= -0.88707370) 231a → 234a : (c= -0.39075466) 231a → 236a : (c= 0.18439709)	0.786900 0.152689 0.034002	0.001766012	25513.3	392.0	
S_4	231a → 233a : (c= 0.28105134) 231a → 234a : (c= -0.57675446) 231a → 235a : (c= 0.73641012)	0.078990 0.332646 0.542300	0.001030964	26534.6	376.9	

	231a → 236a : 0.031798 (c= -0.17832085)				
S_5	231a → 234a : 0.331989 (c= 0.57618452) 231a → 235a : 0.346515 (c= 0.58865518) 231a → 236a : 0.237120 (c= 0.48694949) 231a → 237a : 0.067254 (c= -0.25933330)	0.006660529	27172.1	368.0	
S_6	231a → 235a : 0.014753 (c= 0.12146369) 231a → 236a : 0.117149 (c= 0.34227036) 231a → 237a : 0.860208 (c= 0.92747411)	0.005851074	27622.7	362.0	
S_7	230a → 232a : 0.922747 (c= -0.96059704) 231a → 236a : 0.017443 (c= -0.13207110) 231a → 238a : 0.014177 (c= 0.11906840)	0.009970031	29428.8	339.8	
S_8	230a → 232a : 0.016115 (c= -0.12694647) 231a → 238a : 0.939321 (c= -0.96918567)	0.006563592	31075.8	321.8	
S_9	228a → 232a : 0.011875 (c= -0.10897459) 229a → 232a : 0.010133 (c= 0.10066453) 231a → 236a : 0.018115 (c= -0.13459106) 231a → 239a : 0.895532 (c= -0.94632578)	0.047785012	32523.4	307.5	
S_{10}	227a → 232a : 0.013267 (c= 0.11518304) 228a → 232a : 0.340287 (c= -0.58334127) 229a → 232a : 0.222324 (c= 0.47151206) 230a → 233a : 0.068869 (c= 0.26242981) 230a → 234a : 0.066563 (c= -0.25799808) 230a → 235a : 0.017565 (c= -0.13253373) 230a → 236a : 0.170247 (c= 0.41261018) 231a → 240a : 0.023753 (c= -0.15412108)	0.030228824	34481.6	290.0	

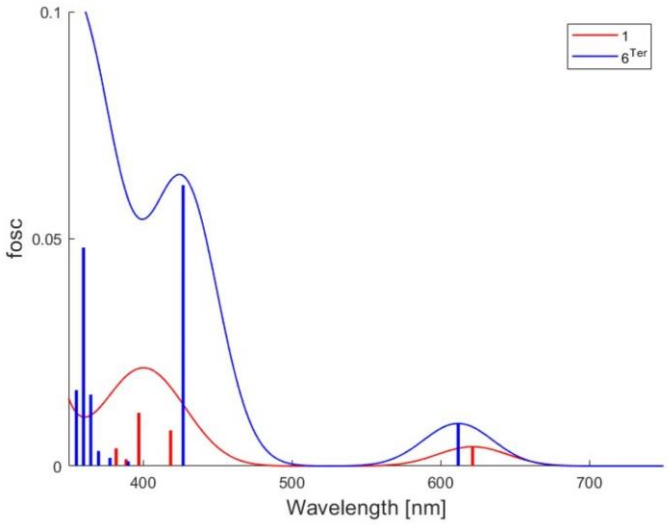

Figure S41. Simulated UV-Vis spectra in the 350-700 nm range of **1** (red) and **6Ter**(blue). The corresponding excitations are shown as vertical lines.

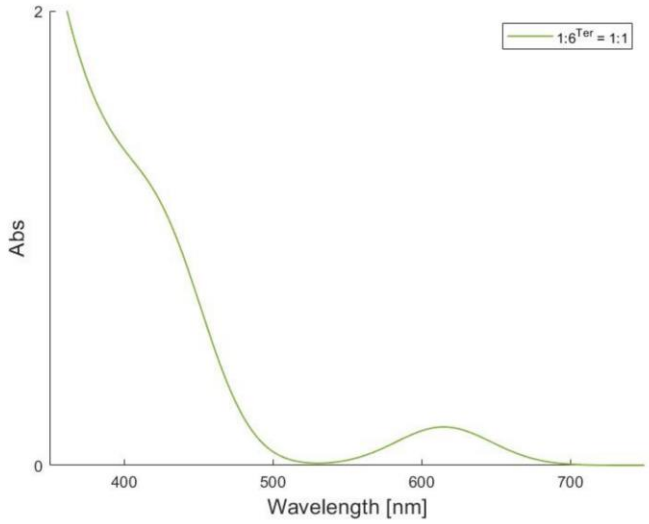

Figure S42. Simulated UV-Vis of a mixture of **1** and **6Ter** in 1:1 ratio.

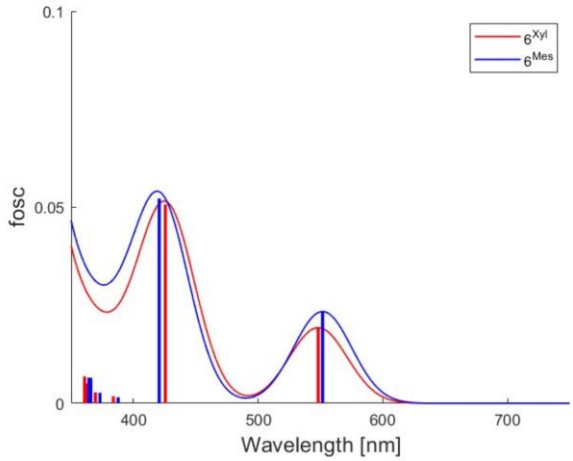

Figure S43. Simulated UV-Vis spectra in the 350-700 nm range of $\mathbf{6^{Xyl}}$ (red) and $\mathbf{6^{Mes}}$ (blue). The corresponding excitations are shown as vertical lines.

4.5 Experimental evidence for the formation of intermediate D

Our proposed mechanism of formation of disilenes $\mathbf{3^{Xyl}}$ or $\mathbf{3^{Mes}}$ along with tBu_3SiCN in the reaction of **1** with XylNC and MesNC, involved the formation of a *2H*-azasilirene reactive intermediate **D**. Such species, were reported and isolated by the Tokitoh and Iwamoto group in 2002 and 2019 (Figure S44).[S23-24] In ^{29}Si NMR spectroscopy, the central silicon atoms of these compounds displayed signals at –107.4 and –51.4 ppm. Since in our case **D** is proposed to form as a transient species, we attempted to observe this reactive intermediate, using low temperature ^{29}Si NMR spectroscopy, that is in order to provide an experimental evidence for its existence. The initial attempt was the reaction of **1** with XylNC. However, we could not observe any signals in the ^{29}Si NMR spectrum since the rapidly generated $\mathbf{3^{Xyl}}$ was stuck on the side of the J-Young NMR tube. Therefore, we monitored the reaction of **1** with MesNC at –60°C. The obtained ^{29}Si NMR spectrum is presented in the Figure S45, showing characteristic low and high field signals at 205.4, –77.2 and –125.7 ppm. The peaks around the region of 0 ppm correspond to the Si^tBu_3 substitutes of species found in the reaction mixture (Figure S44). In order to identify the intermediates responsible for the observed signals we carried out GIAO NMR calculations at the M06L/6-311G(2d,p)//r^{2}SCAN-3c level of theory. The calculations suggest that the peak at 205.4 ppm corresponds to the intermediate that is formed upon the isocyanide insertion into the Si–Si bond of **1**, *i.e.* $\mathbf{6^{Mes}}$, for which the calculated shift is 206.4 ppm. The signal at –77.2 ppm corresponds to $\mathbf{A^{Mes}}$, for which the calculated shift of the central silicon is –84.5 ppm. The peak at the high field, at –125.7 ppm, is characteristic of a tetracoordinate silicon bound to an isocyanate, similarly to *2H*-azasilirenes reported by Tokitoh and Iwamoto. For Tokitoh and Iwamoto *2H*-azasilirenes the GIAO NMR calculations yield a fairly good agreement with the experiment, with the respective calculated chemical shift at –62.2 and –116.9 ppm, that are slightly higher field shifted than the experimental values (–51.4 to –107.4 ppm). Similarity, the calculated chemical shift of the central Si atom in $\mathbf{D^{Mes}}$ is –139.9 ppm, also at a slightly higher field than the especially observed shift at –125.7 ppm. Thus, it is reasonable to suggest that the peak observed at –125.7 ppm may belongs to the reactive intermediate $\mathbf{D^{Mes}}$.

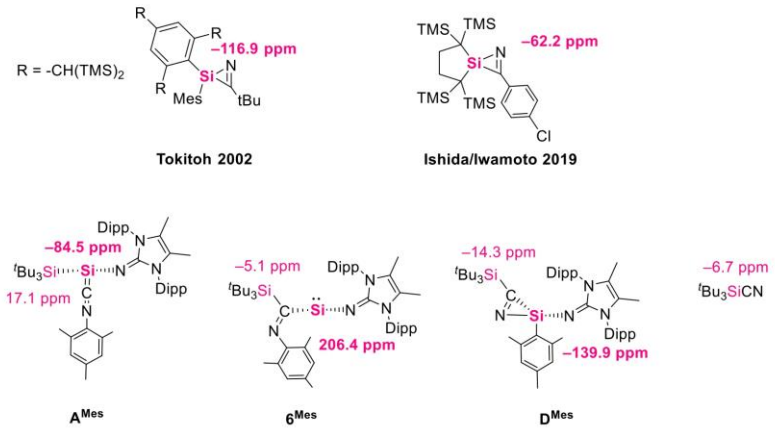

Figure S44. Calculated ^{29}Si NMR chemical shifts (ppm) of known azasilirenes and the reactive intermediates in reaction of **1** with MesNC of $\mathbf{A}^{\mathbf{Mes}}$, $\mathbf{6}^{\mathbf{Mes}}$, $\mathbf{D}^{\mathbf{Mes}}$ and ^{t}Bu$_3$SiCN at the r^{2}SCAN-3c//M06L/6-311G(2d,p) level of theory.

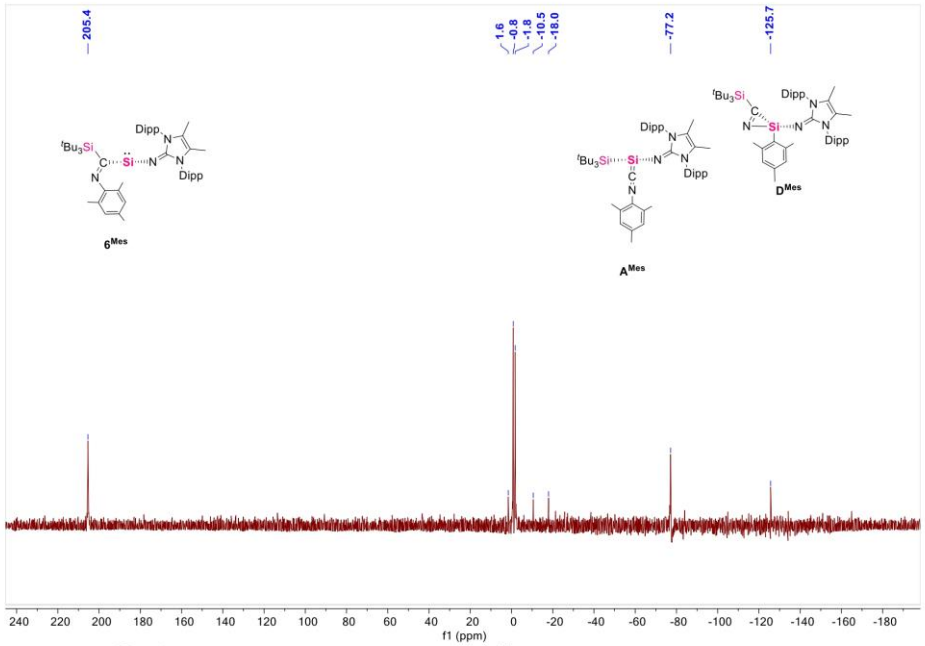

Figure S45. ^{29}Si{^{1}H} NMR of intermediate azasilirene $\mathbf{D}^{\mathbf{Mes}}$ in Tol-d$_8$ at 213 K.

5. References

[S1] Zhu, H., Kostenko, A., Franz, D., Hanusch, F., and Inoue, S. (2023). Room temperature intermolecular dearomatization of arenes by an acyclic iminosilylene. J. Am. Chem. Soc. 145, 1011-1021. 10.1021/jacs.2c10467.
[S2] Singh, C., Prakasham, A. P., Gangwar, M. K., Butcher, R. J., and Ghosh, P. (2018). One-pot tandem hiyama alkynylation/cyclizations by palladium(II) acyclic diaminocarbene (ADC) complexes yielding biologically relevant benzofuran scaffolds. ACS Omega 3, 1740−1756. 10.1021/acsomega.7b01974.
[S3] Dietl, M. C., Vethacke, V., Keshavarzi, A, Mulks, F. F., Rominger,F., Mkhalid, I. A. I., and Hashmi, S. K. (2022). Synthesis of heterobimetallic gold(I) palladium(II) bis(acyclic diaminocarbene) complexes via the isonitrile route. Organometallics 41, 802-810. 10.1021/acs.organomet.2c00021.
[S4] Carpenter, A. E., Mokhtarzadeh, C. C., Ripatti, D. S., Havrylyuk, I., Kamezawa, R., Moore, C. E., Rheingold, A. L., and Figueroa, J. S. (2015). Comparative measure of the electronic influence of highly substituted aryl isocyanides. Inorg. Chem. 54, 2936-2944. 10.1021/ic5030845.
[S5] APEX suite of crystallographic software, APEX 4 version 2021.10-0; Bruker AXS Inc.: Madison, Wisconsin, USA, 2021.
[S6] SAINT, Version 7.56a and SADABS Version 2008/1; Bruker AXS Inc.: Madison, Wisconsin, USA, 2008.
[S7] Sheldrick, G. M. SHELXL-2014, University of Göttingen, Göttingen, Germany, 2014.
[S8] Hübschle, C. B., Sheldrick, G. M., and Dittrich, B. (2011). ShelXle: a Qt graphical user interface for SHELXL. J. Appl. Cryst. 44, 1281-1284. 10.1107/S0021889811043202.
[S9] Sheldrick, G. M. SHELXL-97, University of Göttingen, Göttingen, Germany, 1998.
[S10] Wilson, A. J. C. (1992). International Tables for Crystallography. (Kluwer Academic Publishers).
[S11] Macrae, C. F., Bruno, I. J., Chisholm, J. A., Edgington, P. R., McCabe, P., Pidcock, E., Rodriguez-Monge, L.,Taylor, R., van de Streek, J., and Wood, P. A. (2008). J. Appl. Cryst. 41, 466-470. 10.1107/S0021889807067908.
[S12] Neese, F. (2022). Software update: The ORCA program system—Version 5.0. WIREs Comput Mol Sci. 12, e1606. 10.1002/wcms.1606.
[S13] Grimme, S., Hansen, A., Ehlert, S., and Mewes, J.-M. (2021). r^{2}SCAN-3c: A “Swiss army knife” composite electronic-structure method. J. Chem. Phys. 154, 064103. 10.1063/5.0040021.
[S14] Furness, J. W., Kaplan, A. D., Ning, J., Perdew, J. P., and Sun, J. (2020). Accurate and numerically efficient r^{2}SCAN meta-generalized gradient approximation. J. Phys. Chem. Lett. 11, 8208-8215. 10.1021/acs.jpclett.0c02405.
[S15] Furness, J. W., Kaplan, A. D., Ning, J., Perdew, J. P., and Sun, J. (2020). Correction to “Accurate and numerically efficient r^{2}SCAN meta-generalized gradient approximation”. J. Phys. Chem. Lett. 11, 9248.10.1021/acs.jpclett.0c03077.
[S16] Kruse, H., and Grimme, S. (2012). A geometrical correction for the inter- and intra-molecular basis set superposition error in Hartree-Fock and density functional theory calculations for large systems. J. Chem. Phys. *136*, 154101. 10.1063/1.3700154.
[S17] Caldeweyher, E., Mewes, J.-M., Ehlert, S., and Grimme, S. (2020). Extension and evaluation of the D4 London-dispersion model for periodic systems. Phys. Chem. Chem. Phys. 22, 8499-8512. 10.1039/D0CP00502A.
[S18] Caldeweyher, E., Ehlert, S., Hansen, A., Neugebauer, H., Spicher, S., Bannwarth, C., and Grimme, S. (2019). A generally applicable atomic-charge dependent London dispersion correction. J. Chem. Phys. 150, 154122. 10.1063/1.5090222.
[S19] Caldeweyher, E., Bannwarth, C., and Grimme, S. (2017). Extension of the D3 dispersion coefficient model. J. Chem. Phys. 147, 034112. 10.1063/1.4993215.
[S20] Marenich, A. V., Cramer, C. J., and Truhlar, D. G. (2009). Universal solvation model based on solute electron density and on a continuum model of the solvent defined by the bulk dielectric constant and atomic surface tensions. J. Phys. Chem. B 113, 6378-6396. 10.1021/jp810292n.
[S21] Weigend, F., and Ahlrichs, R.(2005). Balanced basis sets of split valence, triple zeta valence and quadruple zeta valence quality for H to Rn: Design and assessment of accuracy. Phys. Chem. Chem. Phys. 7, 3297-3305. 10.1039/B508541A.
[S22] Hellweg, A., Hättig, C., Höfener, S., and Klopper, W. (2007). Optimized accurate auxiliary basis sets for RI-MP2 and RI-CC2 calculations for the atoms Rb to Rn. Theor. Chem. Acc. 117, 587-597. 10.1007/s00214-007-0250-5.
[S23] Tokitoh, N., Suzuki, H., Takeda, N., Kajiwara, T., Sasamori, T., and Okazaki, R. (2002). Stable 2*H*-azasilirene and 2*H*-phosphasilirene: Addition reaction of an overcrowded silylene to a nitrile and a phosphaalkyne. Silicon Chem. 1, 313-319. 10.1023/B:SILC.0000025574.54359.7a.

[S24] Ishida, S., Uchida, K., Mori, M., and Iwamoto, T. (2019). Structures and properties of phenylene-bridged 1,3-diaza-2-silole and related 2*H*-azasilirenes bbtained by the reactions of a dialkylsilylene with arylnitriles. Eur. J. Inorg. Chem. 3366–3372. 10.1002/ejic.201900590.

11. References

[1] G. T. Carroll, D. L. Kirschman, Catalytic Surgical Smoke Filtration Unit Reduces Formaldehyde Levels in a Simulated Operating Room Environment, *ACS Chem. Health Saf.* **2023**, *30*, 21-28.

[2] C. Weetman, S. Inoue, The Road Travelled: After Main-Group Elements as Transition Metals, *ChemCatChem* **2018**, *10*, 4213-4228.

[3] L. C. Wilkins, R. L. Melen, Enantioselective Main Group Catalysis: Modern Catalysts for Organic Transformations, *Coord. Chem. Rev.* **2016**, *324*, 123-139.

[4] G. H. Spikes, J. C. Fettinger, P. P. Power, Facile Activation of Dihydrogen by an Unsaturated Heavier Main Group Compound, *J. Am. Chem. Soc.* **2005**, *127*, 12232-12233.

[5] Y. Peng, B. D. Ellis, X. Wang, J. C. Fettinger, P. P. Power, Reversible Reactions of Ethylene with Distannynes Under Ambient Conditions, *Science* **2009**, *325*, 1668-1670.

[6] G. C. Welch, R. R. S. Juan, J. D. Masuda, D. W. Stephan, Reversible, Metal-Free Hydrogen Activation, *Science* **2006**, *314*, 1124-1126.

[7] D. W. Stephan, Frustrated Lewis Pairs: From Concept to Catalysis, *Acc. Chem. Res.* **2015**, *48*, 306-316.

[8] D. W. Stephan, G. Erker, Frustrated Lewis Pair Chemistry: Development and Perspectives, *Angew. Chem. Int. Ed.* **2015**, *54*, 6400-6441.

[9] D. W. Stephan, Catalysis, FLPs, and Beyond, *Chem* **2020**, *6*, 1520-1526.

[10] D. W. Stephan, Frustrated Lewis pair chemistry of CO, *Chem. Soc. Rev.* **2023**, *52*, 4632-4643.

[11] H. F. T. Klare, L. Albers, L. Süsse, S. Keess, T. Müller, M. Oestreich, Silylium Ions: From Elusive Reactive Intermediates to Potent Catalysts, *Chem. Rev.* **2021**, *121*, 5889-5985.

[12] L. Greb, p-Block Element Catecholates: Lewis Superacidic, Constitutionally Dynamic, and Redox Active, *Synlett* **2023**.

[13] E. Fritz-Langhals, Silicon(II) Cation Cp*Si:+ X–: A New Class of Efficient Catalysts in Organosilicon Chemistry, *Org. Process Res. Dev.* **2019**, *23*, 2369-2377.

[14] B.-X. Leong, J. Lee, Y. Li, M.-C. Yang, C.-K. Siu, M.-D. Su, C.-W. So, A Versatile NHC-Parent Silyliumylidene Cation for Catalytic Chemo- and Regioselective Hydroboration, *J. Am. Chem. Soc.* **2019**, *141*, 17629-17636.

[15] B.-X. Leong, Y.-C. Teo, C. Condamines, M.-C. Yang, M.-D. Su, C.-W. So, A NHC-Silyliumylidene Cation for Catalytic N-Formylation of Amines Using Carbon Dioxide, *ACS Catal.* **2020**, *10*, 14824-14833.

[16] M. M. D. Roy, A. A. Omaña, A. S. S. Wilson, M. S. Hill, S. Aldridge, E. Rivard, Molecular Main Group Metal Hydrides, *Chem. Rev.* **2021**, *121*, 12784-12965.

[17] J. Lee, J. Fan, A.-P. Koh, W.-J. Joslyn Cheang, M.-C. Yang, M.-D. Su, C.-W. So, Amidinato Isopropylmethylamidosilylene-Catalyzed Hydroboration of Carbonyl Compounds, *Eur. J. Inorg. Chem.* **2022**, *2022*, e202200129.

[18] R. Nougué, S. Takahashi, A. Dajnak, E. Maerten, A. Baceiredo, N. Saffon-Merceron, V. Branchadell, T. Kato, Labile Base-Stabilized Silyliumylidene Ions. Non-Metallic Species Capable of Activating Multiple Small Molecules, *Chem. Eur. J.* **2022**, *28*, e202202037.

[19] Y.-C. Teo, D. Loh, B.-X. Leong, Z.-F. Zhang, M.-D. Su, C.-W. So, NHC-Silyliumylidene Cation-Catalyzed Hydroboration of Isocyanates with Pinacolborane, *Inorg. Chem.* **2023**, *62*, 16867-16873.

[20] S. R. Taylor, Abundance of chemical elements in the continental crust: a new table, *Geochimica et Cosmochimica Acta* **1964**, *28*, 1273-1285.
[21] A. F. Holleman, E. Wiberg, N. Wiberg, *Lehrbuch der Anorganischen Chemie. de Gruyter*, Berlin, **2007**.
[22] L. Rösch, P. John, R. Reitmeier, Silicon Compounds, Organic. in *Ullmann's Encyclopedia of Industrial Chemistry*. Wiley-VCH Verlag GmbH & Co. KGaA, Weinheim, **2012**.
[23] J. E. Mark, D. W. Schaefer, G. Lin, The Polysiloxanes. Oxford University Press, New York, **2015**.
[24] C. Friedel, J. M. Crafts, Ueber einige neue organische Verbindungen des Siliciums und das Atomgewicht dieses Elementes, *Justus Liebigs Ann. Chem.* **1863**, *127*, 28-32.
[25] N. R. Thomas, Frederic Stanley Kipping—Pioneer in Silicon Chemistry: His Life & Legacy, *Silicon* **2010**, *2*, 187-193.
[26] R. West, M. J. Fink, J. Michl, Tetramesityldisilene, a Stable Compound Containing a Silicon-Silicon Double Bond, *Science* **1981**, *214*, 1343-1344.
[27] Z. Feng, S. Tang, Y. Su, X. Wang, Recent advances in stable main group element radicals: preparation and characterization, *Chem. Soc. Rev.* **2022**, *51*, 5930-5973.
[28] S. Fujimori, S. Inoue, in *Comprehensive Organometallic Chemistry IV* (Eds.: G. Parkin, K. Meyer, D. O'hare), Elsevier, Oxford, **2022**, pp. 1-51.
[29] S. Yao, A. Saddington, Y. Xiong, M. Driess, Chelating Bis-silylenes As Powerful Ligands To Enable Unusual Low-Valent Main-Group Element Functions, *Acc. Chem. Res.* **2023**, *56*, 475-488.
[30] A. Igau, H. Grutzmacher, A. Baceiredo, G. Bertrand, Analogous .alpha.,.alpha.'-bis-carbenoid, triply bonded species: synthesis of a stable .lambda.3-phosphino carbene-.lambda.5-phosphaacetylene, *J. Am. Chem. Soc.* **1988**, *110*, 6463-6466.
[31] A. J. Arduengo, III, R. L. Harlow, M. Kline, A stable crystalline carbene, *J. Am. Chem. Soc.* **1991**, *113*, 361-363.
[32] A. Doddi, M. Peters, M. Tamm, *N*-Heterocyclic Carbene Adducts of Main Group Elements and Their Use as Ligands in Transition Metal Chemistry, *Chem. Rev.* **2019**, *119*, 6994-7112.
[33] M. N. Hopkinson, C. Richter, M. Schedler, F. Glorius, An overview of N-heterocyclic carbenes, *Nature* **2014**, *510*, 485-496.
[34] D. M. Flanigan, F. Romanov-Michailidis, N. A. White, T. Rovis, Organocatalytic Reactions Enabled by N-Heterocyclic Carbenes, *Chem. Rev.* **2015**, *115*, 9307-9387.
[35] V. Nesterov, D. Reiter, P. Bag, P. Frisch, R. Holzner, A. Porzelt, S. Inoue, NHCs in Main Group Chemistry, *Chem. Rev.* **2018**, *118*, 9678-9842.
[36] E. Peris, Smart N-Heterocyclic Carbene Ligands in Catalysis, *Chem. Rev.* **2018**, *118*, 9988-10031.
[37] Q. Zhao, G. Meng, S. P. Nolan, M. Szostak, N-Heterocyclic Carbene Complexes in C–H Activation Reactions, *Chem. Rev.* **2020**, *120*, 1981-2048.
[38] Y. Mizuhata, T. Sasamori, N. Tokitoh, Stable Heavier Carbene Analogues, *Chem. Rev.* **2009**, *109*, 3479-3511.
[39] W. Kutzelnigg, Orthogonal and non-orthogonal hybrids, *J. Mol. Struct. THEOCHEM* **1988**, *169*, 403-419.
[40] P. Pyykko, Relativistic effects in structural chemistry, *Chem. Rev.* **1988**, *88*, 563-594.
[41] V. S. V. S. N. Swamy, S. Pal, S. Khan, S. S. Sen, Cations and dications of heavier group 14 elements in low oxidation states, *Dalton Trans.* **2015**, *44*, 12903-12923.
[42] Y. Apeloig, R. Pauncz, M. Karni, R. West, W. Steiner, D. Chapman, Why Is Methylene a Ground State Triplet while Silylene Is a Ground State Singlet?, *Organometallics* **2003**, *22*, 3250-3256.

[43] G. Trinquier, Double bonds and bridged structures in the heavier analogs of ethylene, *J. Am. Chem. Soc.* **1990**, *112*, 2130-2137.
[44] M. Driess, H. Grützmacher, Main Group Element Analogues of Carbenes, Olefins, and Small Rings, *Angew. Chem. Int. Ed. Engl.* **1996**, *35*, 828-856.
[45] P. Jutzi, New Element-Carbon (p-p)π Bonds, *Angew. Chem. Int. Ed. Engl.* **1975**, *14*, 232-245.
[46] L. E. Gusel'nikov, N. S. Nametkin, Formation and properties of unstable intermediates containing multiple p.pi.-p.pi. bonded Group 4B metals, *Chem. Rev.* **1979**, *79*, 529-577.
[47] D. E. Goldberg, D. H. Harris, M. F. Lappert, K. M. Thomas, A new synthesis of divalent group 4B alkyls M[CH(SiMe3)2]2(M = Ge or Sn), and the crystal and molecular and molecular strcuture of the tin compound, *J. Chem. Soc., Chem. Commun.* **1976**, 261-262.
[48] E. A. Carter, W. A. Goddard, III, Relation between singlet-triplet gaps and bond energies, *J. Phys. Chem.* **1986**, *90*, 998-1001.
[49] G. Trinquier, J. P. Malrieu, Nonclassical distortions at multiple bonds, *J. Am. Chem. Soc.* **1987**, *109*, 5303-5315.
[50] P. P. Power, π-Bonding and the Lone Pair Effect in Multiple Bonds between Heavier Main Group Elements, *Chem. Rev.* **1999**, *99*, 3463-3504.
[51] R. C. Fischer, P. P. Power, π-Bonding and the Lone Pair Effect in Multiple Bonds Involving Heavier Main Group Elements: Developments in the New Millennium, *Chem. Rev.* **2010**, *110*, 3877-3923.
[52] P. Jiang, P. P. Gaspar, Tri-tert-butylsilyl(triisopropylsilyl)silylene (tBu)3Si−Si−Si(iPr)3 and Chemical Evidence for Its Reactions from a Triplet Electronic State, *J. Am. Chem. Soc.* **2001**, *123*, 8622-8623.
[53] A. Sekiguchi, T. Tanaka, M. Ichinohe, K. Akiyama, S. Tero-Kubota, Bis(tri-tert-butylsilyl)silylene: Triplet Ground State Silylene, *J. Am. Chem. Soc.* **2003**, *125*, 4962-4963.
[54] S. Ashenagar, M. Z. Kassaee, New triplet silylenes M − Si − M' − X along with some unusual cyclic forms (M = Li, Na, and K; M′ = Be, Mg, and Ca; X = F, Cl, and Br), *Turk. J. Chem.* **2018**, *42*, 974-987.
[55] L. Zhu, J. Zhang, C. Cui, Intramolecular cyclopropanation of alkali-metal-substituted silylene with the aryl substituent of an N-heterocyclic framework, *Inorg. Chem.* **2019**, *58*, 12007-12010.
[56] A. Sekiguchi, T. Tanaka, M. Ichinohe, K. Akiyama, P. P. Gaspar, Tri-tert-butylsilylsilylenes with Alkali Metal Substituents (tBu3Si)SiM (M = Li, K): Electronically and Sterically Accessible Triplet Ground States, *J. Am. Chem. Soc.* **2008**, *130*, 426-427.
[57] F. S. Kipping, J. E. Sands, XCIII.—Organic derivatives of silicon. Part XXV. Saturated and unsaturated silicohydrocarbons, Si4Ph8, *J. Chem. Soc., Trans.* **1921**, *119*, 830-847.
[58] R. Schwarz, G. Pietsoh, Versuche zur Darstellung des Siliciumdichlorides, *Z. Anorg. Allg. Chem.* **1937**, *232*, 249-256.
[59] R. K. Asundi, M. Karim, R. Samuel, Emission bands of $SiCl_2$ and $SnCl_2$, *Proc. Phys. Soc.* **1938**, *50*, 581.
[60] P. S. Skell, E. J. Goldstein, Dimethylsilene: CH_3SiCH_3, *J. Am. Chem. Soc.* **1964**, *86*, 1442-1443.
[61] T. J. Drahnak, J. Michl, R. West, Dimethylsilylene, $(CH_3)_2Si$, *J. Am. Chem. Soc.* **1979**, *101*, 5427-5428.
[62] P. Jutzi, D. Kanne, C. Krüger, Decamethylsilicocene-synthesis and structure, *Angew. Chem. Int. Ed. Engl.* **1986**, *25*, 164-164.

[63] M. Denk, R. Lennon, R. Hayashi, R. West, A. V. Belyakov, H. P. Verne, A. Haaland, M. Wagner, N. Metzler, Synthesis and Structure of a Stable Silylene, *J. Am. Chem. Soc.* **1994**, *116*, 2691-2692.

[64] M. Denk, J. C. Green, N. Metzler, M. Wagner, Electronic structure of a stable silylene: photoelectron spectra and theoretical calculations of Si(NRCHCHNR), Si(NRCH2CH2NR) and SiH2(NRCHCHNR), *J. Chem. Soc. Dalton Trans.* **1994**, 2405-2410.

[65] B. Gehrhus, M. F. Lappert, J. Heinicke, R. Boese, D. Bläser, Synthesis, structures and reactions of new thermally stable silylenes, *J. Chem. Soc., Chem. Commun.* **1995**, 1931-1932.

[66] M. Kira, S. Ishida, T. Iwamoto, C. Kabuto, The First Isolable Dialkylsilylene, *J. Am. Chem. Soc.* **1999**, *121*, 9722-9723.

[67] T. Abe, R. Tanaka, S. Ishida, M. Kira, T. Iwamoto, New Isolable Dialkylsilylene and Its Isolable Dimer That Equilibrate in Solution, *J. Am. Chem. Soc.* **2012**, *134*, 20029-20032.

[68] R. Kobayashi, S. Ishida, T. Iwamoto, An Isolable Silicon Analogue of a Ketone that Contains an Unperturbed Si=O Double Bond, *Angew. Chem. Int. Ed.* **2019**, *58*, 9425-9428.

[69] G.-H. Lee, R. West, T. Müller, Bis[bis(trimethylsilyl)amino]silylene, an Unstable Divalent Silicon Compound, *J. Am. Chem. Soc.* **2003**, *125*, 8114-8115.

[70] M. Driess, S. Yao, M. Brym, C. van Wüllen, D. Lentz, A New Type of N-Heterocyclic Silylene with Ambivalent Reactivity, *J. Am. Chem. Soc.* **2006**, *128*, 9628-9629.

[71] Y. Wang, Y. Xie, P. Wei, R. B. King, H. F. Schaefer, P. von R. Schleyer, G. H. Robinson, A Stable Silicon(0) Compound with a Si=Si Double Bond, *Science* **2008**, *321*, 1069-1071.

[72] M. Chen, Y. Wang, Y. Xie, P. Wei, R. J. Gilliard Jr, N. A. Schwartz, H. F. Schaefer Iii, P. v. R. Schleyer, G. H. Robinson, Dynamic Complexation of Copper(I) Chloride by Carbene-Stabilized Disilicon, *Chem. Eur. J.* **2014**, *20*, 9208-9211.

[73] H. P. Hickox, Y. Wang, Y. Xie, M. Chen, P. Wei, H. F. Schaefer Iii, G. H. Robinson, Transition-Metal-Mediated Cleavage of a Si=Si Double Bond, *Angew. Chem. Int. Ed.* **2015**, *54*, 10267-10270.

[74] K. C. Mondal, P. P. Samuel, H. W. Roesky, R. R. Aysin, L. A. Leites, S. Neudeck, J. Lübben, B. Dittrich, N. Holzmann, M. Hermann, G. Frenking, One-Electron-Mediated Rearrangements of 2,3-Disiladicarbene, *J. Am. Chem. Soc.* **2014**, *136*, 8919-8922.

[75] K. C. Mondal, S. Roy, B. Dittrich, D. M. Andrada, G. Frenking, H. W. Roesky, A Triatomic Silicon(0) Cluster Stabilized by a Cyclic Alkyl(amino) Carbene, *Angew. Chem. Int. Ed.* **2016**, *55*, 3158-3161.

[76] M. Asay, S. Inoue, M. Driess, Aromatic Ylide-Stabilized Carbocyclic Silylene, *Angew. Chem. Int. Ed.* **2011**, *50*, 9589-9592.

[77] A. V. Protchenko, K. H. Birjkumar, D. Dange, A. D. Schwarz, D. Vidovic, C. Jones, N. Kaltsoyannis, P. Mountford, S. Aldridge, A stable two-coordinate acyclic silylene, *J. Am. Chem. Soc.* **2012**, *134*, 6500-6503.

[78] B. D. Rekken, T. M. Brown, J. C. Fettinger, H. M. Tuononen, P. P. Power, Isolation of a stable, acyclic, two-coordinate silylene, *J. Am. Chem. Soc.* **2012**, *134*, 6504-6507.

[79] T. Kosai, S. Ishida, T. Iwamoto, A two-coordinate cyclic (alkyl)(amino)silylene: Balancing thermal stability and reactivity, *Angew. Chem. Int. Ed.* **2016**, *55*, 15554-15558.

[80] V. Lavallo, Y. Canac, C. Präsang, B. Donnadieu, G. Bertrand, Stable Cyclic (Alkyl)(Amino)Carbenes as Rigid or Flexible, Bulky, Electron-Rich Ligands for Transition-Metal Catalysts: A Quaternary Carbon Atom Makes the Difference, *Angew. Chem. Int. Ed.* **2005**, *44*, 5705-5709.

[81] I. Alvarado-Beltran, A. Baceiredo, N. Saffon-Merceron, V. Branchadell, T. Kato, Cyclic Amino(Ylide) Silylene: A Stable Heterocyclic Silylene with Strongly Electron-Donating Character, *Angew. Chem. Int. Ed.* **2016**, *55*, 16141-16144.

[82] A. Rosas-Sánchez, I. Alvarado-Beltran, A. Baceiredo, N. Saffon-Merceron, S. Massou, V. Branchadell, T. Kato, Exceptionally Strong Electron-Donating Ability of Bora-Ylide Substituent vis-à-vis Silylene and Silylium Ion, *Angew. Chem. Int. Ed.* **2017**, *56*, 10549-10554.

[83] I. Alvarado-Beltran, A. Rosas-Sánchez, A. Baceiredo, N. Saffon-Merceron, V. Branchadell, T. Kato, A Fairly Stable Crystalline Silanone, *Angew. Chem. Int. Ed.* **2017**, *56*, 10481-10485.

[84] A. Rosas-Sánchez, I. Alvarado-Beltran, A. Baceiredo, N. Saffon-Merceron, S. Massou, D. Hashizume, V. Branchadell, T. Kato, Cyclic (Amino)(Phosphonium Bora-Ylide)Silanone: A Remarkable Room-Temperature-Persistent Silanone, *Angew. Chem. Int. Ed.* **2017**, *56*, 15916-15920.

[85] S. Takahashi, E. Bellan, A. Baceiredo, N. Saffon-Merceron, S. Massou, N. Nakata, D. Hashizume, V. Branchadell, T. Kato, A Stable N-Hetero-Rh-Metallacyclic Silylene, *Angew. Chem. Int. Ed.* **2019**, *58*, 10310-10314.

[86] N. Weyer, M. Heinz, J. I. Schweizer, C. Bruhn, M. C. Holthausen, U. Siemeling, A Stable N-Heterocyclic Silylene with a 1,1′-Ferrocenediyl Backbone, *Angew. Chem. Int. Ed.* **2021**, *60*, 2624-2628.

[87] J. Keuter, A. Hepp, A. Massolle, J. Neugebauer, C. Mück-Lichtenfeld, F. Lips, Synthesis and Reactivity of a Neutral Homocyclic Silylene, *Angew. Chem. Int. Ed.* **2022**, *61*, e202114485.

[88] S. P. Green, C. Jones, A. Stasch, Stable Magnesium(I) Compounds with Mg-Mg Bonds, *Science* **2007**, *318*, 1754-1757.

[89] A. V. Protchenko, A. D. Schwarz, M. P. Blake, C. Jones, N. Kaltsoyannis, P. Mountford, S. Aldridge, A generic one-pot route to acyclic two-coordinate silylenes from silicon(IV) precursors: Synthesis and structural characterization of a silylsilylene, *Angew. Chem. Int. Ed.* **2013**, *52*, 568-571.

[90] B. D. Rekken, T. M. Brown, J. C. Fettinger, F. Lips, H. M. Tuononen, R. H. Herber, P. P. Power, Dispersion sorces and counterintuitive steric effects in main group molecules: Heavier Group 14 (Si–Pb) dichalcogenolate carbene analogues with Sub-90° interligand bond angles, *J. Am. Chem. Soc.* **2013**, *135*, 10134-10148.

[91] T. J. Hadlington, J. A. B. Abdalla, R. Tirfoin, S. Aldridge, C. Jones, Stabilization of a two-coordinate, acyclic diaminosilylene (ADASi): Completion of the series of isolable diaminotetrylenes, :E(NR_2)$_2$ (E = group 14 element), *Chem. Commun.* **2016**, *52*, 1717-1720.

[92] R. S. Ghadwal, H. W. Roesky, S. Merkel, J. Henn, D. Stalke, Lewis Base Stabilized Dichlorosilylene, *Angew. Chem. Int. Ed.* **2009**, *48*, 5683-5686.

[93] D. Wendel, A. Porzelt, F. A. D. Herz, D. Sarkar, C. Jandl, S. Inoue, B. Rieger, From Si(II) to Si(IV) and back: Reversible intramolecular carbon–carbon bond activation by an acyclic iminosilylene, *J. Am. Chem. Soc.* **2017**, *139*, 8134-8137.

[94] D. Wendel, D. Reiter, A. Porzelt, P. J. Altmann, S. Inoue, B. Rieger, Silicon and oxygen's bond of affection: An acyclic three-coordinate silanone and its transformation to an iminosiloxysilylene, *J. Am. Chem. Soc.* **2017**, *139*, 17193-17198.

[95] Y. K. Loh, L. Ying, M. Á. Fuentes, D. C. H. Do, S. Aldridge, An N-heterocyclic boryloxy ligand isoelectronic with N-heterocyclic imines: Access to an acyclic dioxysilylene and its heavier congeners, *Angew. Chem. Int. Ed.* **2019**, *58*, 4847-4851.

[96] M. M. D. Roy, M. J. Ferguson, R. McDonald, Y. Zhou, E. Rivard, A vinyl silylsilylene and its activation of strong homo- and heteroatomic bonds, *Chem. Sci.* **2019**, *10*, 6476-6481.

[97] M. M. D. Roy, S. R. Baird, E. Dornsiepen, L. A. Paul, L. Miao, M. J. Ferguson, Y. Zhou, I. Siewert, E. Rivard, A stable homoleptic divinyl tetrelene series, *Chem. Eur. J.* **2021**, *27*, 8572-8579.
[98] S. Raoufmoghaddam, Y.-P. Zhou, Y. Wang, M. Driess, N-heterocyclic silylenes as powerful steering ligands in catalysis, *J. Organomet. Chem.* **2017**, *829*, 2-10.
[99] L. Wang, Y. Li, Z. Li, M. Kira, Isolable silylenes and their diverse reactivity, *Coord. Chem. Rev.* **2022**, *457*, 214413.
[100] Y.-P. Zhou, M. Driess, Isolable silylene ligands can boost efficiencies and selectivities in metal-mediated catalysis, *Angew. Chem. Int. Ed.* **2019**, *58*, 3715-3728.
[101] P. P. Power, Main-group elements as transition metals, *Nature* **2010**, *463*, 171-177.
[102] Z. Dong, Z. Li, X. Liu, C. Yan, N. Wei, M. Kira, T. Müller, Dihydrogen Splitting Using Dialkylsilylene-Based Frustrated Lewis Pairs, *Chem. Asian J.* **2017**, *12*, 1204-1207.
[103] D. Reiter, R. Holzner, A. Porzelt, P. J. Altmann, P. Frisch, S. Inoue, Disilene–silylene interconversion: A synthetically accessible acyclic bis(silyl)silylene, *J. Am. Chem. Soc.* **2019**, *141*, 13536-13546.
[104] N. Tokitoh, H. Suzuki, R. Okazaki, K. Ogawa, Synthesis, structure, and reactivity of extremely hindered disilenes: the first example of thermal dissociation of a disilene into a silylene, *J. Am. Chem. Soc.* **1993**, *115*, 10428-10429.
[105] F. Lips, J. C. Fettinger, A. Mansikkamäki, H. M. Tuononen, P. P. Power, Reversible Complexation of Ethylene by a Silylene under Ambient Conditions, *J. Am. Chem. Soc.* **2014**, *136*, 634-637.
[106] F. Lips, A. Mansikkamäki, J. C. Fettinger, H. M. Tuononen, P. P. Power, Reactions of Alkenes and Alkynes with an Acyclic Silylene and Heavier Tetrylenes under Ambient Conditions, *Organometallics* **2014**, *33*, 6253-6258.
[107] R. Rodriguez, D. Gau, T. Kato, N. Saffon-Merceron, A. De Cózar, F. P. Cossío, A. Baceiredo, Reversible Binding of Ethylene to Silylene–Phosphine Complexes at Room Temperature, *Angew. Chem. Int. Ed.* **2011**, *50*, 10414-10416.
[108] D. Wendel, W. Eisenreich, C. Jandl, A. Pöthig, B. Rieger, Reactivity of an Acyclic Silylsilylene toward Ethylene: Migratory Insertion into the Si–Si Bond, *Organometallics* **2016**, *35*, 1-4.
[109] T. Eisner, A. Kostenko, F. Hanusch, S. Inoue, Room temperature observable interconversion between Si(IV) and Si(II) via reversible intramolecular insertion into an aromatic C-C bond, *Chem. Eur. J.* **2022**, e202202330.
[110] R. Nougué, S. Takahashi, A. Baceiredo, N. Saffon-Merceron, V. Branchadell, T. Kato, Reversible Isomerization Between Silacyclopropyl Cation and Cyclic (Alkyl)(Amino)Silylene, *Angew. Chem. Int. Ed.* **2023**, *62*, e202215394.
[111] A. V. Protchenko, M. P. Blake, A. D. Schwarz, C. Jones, P. Mountford, S. Aldridge, Reactivity of Boryl- and Silyl-Substituted Carbenoids toward Alkynes: Insertion and Cycloaddition Chemistry, *Organometallics* **2015**, *34*, 2126-2129.
[112] B. Blom, M. Driess, in *Functional Molecular Silicon Compounds II: Low Oxidation States* (Ed.: D. Scheschkewitz), Springer International Publishing, Cham, **2014**, pp. 85-123.
[113] X. F. Wu, B. X. Han, K. L. Ding ,Z. M. Liu, in *The Chemical Transformations of C1 Compounds*, Wiley-VCH, Weinheim, **2022**.
[114] M. Vogt, J. E. Bennett, Y. Huang, C. Wu, W. F. Schneider, J. F. Brennecke, B. L. Ashfeld, Solid-State Covalent Capture of CO2 by Using N-Heterocyclic Carbenes, *Chem. Eur. J.* **2013**, *19*, 11134-11138.
[115] L. Yang, H. Wang, Recent Advances in Carbon Dioxide Capture, Fixation, and Activation by using N-Heterocyclic Carbenes, *ChemSusChem* **2014**, *7*, 962-998.
[116] J. A. Kelly, F. J. Kiefer, A. Kostenko, S. Inoue, in *Advances in Inorganic Chemistry, Vol. 82* (Eds.: K. Meyer, R. van Eldik), Academic Press, **2023**, pp. 157-187.

[117] E. J. Kuhlmann, J. J. Alexander, Carbon monoxide insertion into transition metal-carbon sigma-bonds, *Coord. Chem. Rev.* **1980**, *33*, 195-225.
[118] L. D. Durfee, I. P. Rothwell, Chemistry of .eta.2-acyl, .eta.2-iminoacyl and related functional groups, *Chem. Rev.* **1988**, *88*, 1059-1079.
[119] G. J. Sunley, D. J. Watson, High productivity methanol carbonylation catalysis using iridium: The Cativa™ process for the manufacture of acetic acid, *Catalysis Today* **2000**, *58*, 293-307.
[120] A. N. Desnoyer, J. A. Love, Recent advances in well-defined, late transition metal complexes that make and/or break C–N, C–O and C–S bonds, *Chem. Soc. Rev.* **2017**, *46*, 197-238.
[121] V. Lavallo, Y. Canac, B. Donnadieu, W. W. Schoeller, G. Bertrand, CO Fixation to Stable Acyclic and Cyclic Alkyl Amino Carbenes: Stable Amino Ketenes with a Small HOMO–LUMO Gap, *Angew. Chem. Int. Ed.* **2006**, *45*, 3488-3491.
[122] C. Ganesamoorthy, J. Schoening, C. Wölper, L. Song, P. R. Schreiner, S. Schulz, A silicon–carbonyl complex stable at room temperature, *Nat. Chem.* **2020**, *12*, 608-614.
[123] D. Reiter, R. Holzner, A. Porzelt, P. Frisch, S. Inoue, Silylated silicon–carbonyl complexes as mimics of ubiquitous transition-metal carbonyls, *Nat. Chem.* **2020**, *12*, 1131-1135.
[124] S. Fujimori, A. Kostenko, R. Scopelliti, S. Inoue, Synthesis, isolation and application of a sila-ketenyl anion, *Nat. Syn.* **2023**, *2*, 688-694.
[125] M. Weidenbruch, B. Brand-Roth, S. Pohl, W. Saak, A Cyclodimeric Silaketenimine, *Angew. Chem. Int. Ed. Engl.* **1990**, *29*, 90-92.
[126] N. Takeda, H. Suzuki, N. Tokitoh, R. Okazaki, S. Nagase, Reaction of a Sterically Hindered Silylene with Isocyanides: The First Stable Silylene−Lewis Base Complexes, *J. Am. Chem. Soc.* **1997**, *119*, 1456-1457.
[127] N. Takeda, T. Kajiwara, H. Suzuki, R. Okazaki, N. Tokitoh, Synthesis and Properties of the First Stable Silylene–Isocyanide Complexes, *Chem. Eur. J.* **2003**, *9*, 3530-3543.
[128] S. Mukhopadhyay, A. G. Patro, R. S. Vadavi, S. Nembenna, Coordination Chemistry of Main Group Metals with Organic Isocyanides, *Eur. J. Inorg. Chem.* **2022**, *2022*, e202200469.
[129] Y. Zhao, Y. Chen, L. Zhang, J. Li, Y. Peng, Z. Chen, L. Jiang, H. Zhu, Homocoupling of Isocyanide at the Si(II) Center of Borylaminoamidinatosilylene, *Inorg. Chem.* **2022**, *61*, 5215-5223.
[130] T. Abe, T. Iwamoto, C. Kabuto, M. Kira, Synthesis, Structure, and Bonding of Stable Dialkylsilaketenimines, *J. Am. Chem. Soc.* **2006**, *128*, 4228-4229.
[131] E. Buchner, T. Curtius, Ueber die einwirkung von diazoessigäther auf aromatische kohlenwasserstoffe, *Ber. Dtsch. Chem. Ges.* **1885**, *18*, 2377-2379.
[132] E. Buchner, T. Curtius, Synthese von ketonsäureäthern aus aldehyden und diazoessigäther, *Ber. Dtsch. Chem. Ges.* **1885**, *18*, 2371-2377.
[133] S. E. Reisman, R. R. Nani, S. Levin, Buchner and beyond: Arene cyclopropanation as applied to natural product total synthesis, *Synlett* **2011**, *2011*, 2437-2442.
[134] A. Ford, H. Miel, A. Ring, C. N. Slattery, A. R. Maguire, M. A. McKervey, Modern Organic Synthesis with α-Diazocarbonyl Compounds, *Chem. Rev.* **2015**, *115*, 9981-10080.
[135] W. v. E. Doering, G. Laber, R. Vonderwahl, N. F. Chamberlain, R. B. Williams, The structure of the Buchner acids, *J. Am. Chem. Soc.* **1956**, *78*, 5448-5448.
[136] A. J. Anciaux, A. Demonceau, A. F. Noels, A. J. Hubert, R. Warin, P. Teyssie, Transition-metal-catalyzed reactions of diazo compounds. 2. Addition to aromatic molecules: Catalysis of Buchner's synthesis of cycloheptatrienes, *J. Org. Chem.* **1981**, *46*, 873-876.

[137] L. Wang, J. Ma, E. Si, Z. Duan, Recent Advances in Luminescent Annulated Borepins, Silepins, and Phosphepins, *Synthesis* **2020**, *53*, 623-635.
[138] T. Janosik, R. Berg, Chemistry of silepins and their analogs containing group 14 elements, *Arkivoc* **2021**, *2020*, 379-400.
[139] H. Gilman, S. G. Cottis, W. H. Atwell, Some Diels-Alder Adducts of 1,1,2,3,4,5-Hexaphenyl-1-silacyclopentadiene, *J. Am. Chem. Soc.* **1964**, *86*, 5584-5588.
[140] L. Birkofer, H. Haddad, 3.3-Diphenyl-3H-3-benzosilepin, *Chem. Ber.* **1969**, *102*, 432-434.
[141] T. J. Barton, W. E. Volz, J. L. Johnson, 1, 1-Dimethyl-1-sila-2, 3: 6, 7-dibenzocycloheptatriene. A dibenzosilepin, *J. Org. Chem.* **1971**, *36*, 3365-3367.
[142] F. K. Cartledge, P. D. Mollère, 5,5-dimethyl-5H-dibenzo[b,f]silepin: A 14π-electron silicon heterocycle, *J. Organomet. Chem.* **1971**, *26*, 175-181.
[143] T. Nishinaga, K. Komatsu, N. Sugita, 1,1-Dimethylsila-, -germa-, and -stannacycloheptatrienes Fully Annelated with Bicyclo[2.2.2]octene: Syntheses, Structures, and Properties, *J. Org. Chem.* **1995**, *60*, 1309-1314.
[144] H. Sohn, J. Merritt, D. R. Powell, R. West, A new spirocyclic system: Synthesis of a silaspirotropylidene, *Organometallics* **1997**, *16*, 5133-5134.
[145] T. Nishinaga, Y. Izukawa, K. Komatsu, Effects of Substituents on Silicon upon the Ring Inversion of Silepins Annelated with Bicyclo[2.2.2]octene Frameworks, *Chem. Lett.* **1998**, *27*, 269-270.
[146] T. Nishinaga, Y. Izukawa, K. Komatsu, The first silatropylium iron stabilized by rigid σ-frameworks: Preparation, properties, and some reactions, *Tetrahedron* **2001**, *57*, 3645-3656.
[147] H. Shirani, T. Janosik, Synthesis of Fused 1-Sila-, 1-Germa-, and 1-Selenacyclohepta-2,4,6-trienes, *Organometallics* **2008**, *27*, 3960-3963.
[148] T. Matsuda, S. Sato, Synthesis of Dibenzoheteropines of Group 13–16 Elements via Ring-Closing Metathesis, *J. Org. Chem.* **2013**, *78*, 3329-3335.
[149] V. Blasco, J. Murga, E. Falomir, M. Carda, S. Royo, A. C. Cuñat, J. F. Sanz-Cervera, J. A. Marco, Synthesis and biological evaluation of cyclic derivatives of combretastatin A-4 containing group 14 elements, *Org. Bio. Chem.* **2018**, *16*, 5859-5870.
[150] T. Shibata, N. Uno, T. Sasaki, H. Takano, T. Sato, K. S. Kanyiva, Ir-Catalyzed Synthesis of Substituted Tribenzosilepins by Dehydrogenative C–H/Si–H Coupling, *J. Org. Chem.* **2018**, *83*, 3426-3432.
[151] K. Takamoto, S. Yoshioka, H. Fujioka, M. Arisawa, Palladium-Catalyzed Seven-Membered Silacycle Construction: 1,7-Enyne Hydroxycyclization To Give a Benzosilepine Skeleton, *Org. Lett.* **2018**, *20*, 1773-1776.
[152] Y. Dong, K. Sekine, Y. Kuninobu, Facile synthesis of tribenzosilepins from terphenyls and dihydrosilanes by electrophilic double silylation, *Chem. Commun.* **2021**, *57*, 7007-7010.
[153] T. Tsuda, S.-M. Choi, R. Shintani, Palladium-Catalyzed Synthesis of Dibenzosilepin Derivatives via 1,n-Palladium Migration Coupled with anti-Carbopalladation of Alkyne, *J. Am. Chem. Soc.* **2021**, *143*, 1641-1650.
[154] L. G. Mercier, S. Furukawa, W. E. Piers, A. Wakamiya, S. Yamaguchi, M. Parvez, R. W. Harrington, W. Clegg, Design, Synthesis, and Characterization of Functionalized Silepins: High Quantum Yield Blue Emitters, *Organometallics* **2011**, *30*, 1719-1729.
[155] M. E. Volpin, Y. D. Koreshkov, V. G. Dulova, D. N. Kursanov, Three-membered heteroaromatic compounds—I, *Tetrahedron* **1962**, *18*, 107-122.
[156] T. J. Barton, R. C. Kippenhan Jr, A. J. Nelson, Synthesis of 1, 1-dimethyl-2, 7-diphenyl-1-silacyclohepta-2, 4, 6-triene. Nonannulated silepin, *J. Am. Chem. Soc.* **1974**, *96*, 2272-2273.

[157] O. Ermer, F. G. Klaerner, M. Wette, Planarization of unsaturated rings. Cycloheptatriene with a planar seven-membered ring, *J. Am. Chem. Soc.* **1986**, *108*, 4908-4911.
[158] H. Jansen, J. C. Slootweg, K. Lammertsma, Valence isomerization of cyclohepta-1,3,5-triene and its heteroelement analogues, *Beilstein J. Org. Chem.* **2011**, *7*, 1713-1721.
[159] Z. Chen, H. Jiao, J. I. Wu, R. Herges, S. B. Zhang, P. v. R. Schleyer, Homobenzene: Homoaromaticity and Homoantiaromaticity in Cycloheptatrienes, *J. Phys. Chem. A* **2008**, *112*, 10586-10594.
[160] F. A. L. Anet, Ring inversion in cycloheptatriene, *J. Am. Chem. Soc.* **1964**, *86*, 458-460.
[161] F. R. Jensen, L. A. Smith, The Structure and interconversion of cycloheptatriene, *J. Am. Chem. Soc.* **1964**, *86*, 956-957.
[162] H. Suzuki, N. Tokitoh, R. Okazaki, A novel reactivity of a silylene: The first examples of [1 + 2] cycloaddition with aromatic compounds, *J. Am. Chem. Soc.* **1994**, *116*, 11572-11573.
[163] M. Kira, S. Ishida, T. Iwamoto, C. Kabuto, Excited-state reactions of an isolable silylene with aromatic compounds, *J. Am. Chem. Soc.* **2002**, *124*, 3830-3831.
[164] M. Kira, S. Ishida, T. Iwamoto, A. de Meijere, M. Fujitsuka, O. Ito, The singlet excited state of a stable dialkylsilylene is responsible for its photoreactions, *Angew. Chem. Int. Ed.* **2004**, *43*, 4510-4512.
[165] J. Y. Liu, T. Eisner, S. Inoue, B. Rieger, Isolation of a New Silepin with an Imine Ligand Based on Cyclic Alkyl Amino Carbene, *Eur. J. Inorg. Chem.* **2023**, *n/a*, e202300568.
[166] L. G. Mercier, W. E. Piers, M. Parvez, Benzo- and Naphthoborepins: Blue-Emitting Boron Analogues of Higher Acenes, *Angew. Chem. Int. Ed.* **2009**, *48*, 6108-6111.
[167] Y. Adachi, F. Arai, F. Jäkle, Extended conjugated borenium dimers via late stage functionalization of air-stable borepinium ions, *Chem. Commun.* **2020**, *56*, 5119-5122.
[168] S. Murthy, Y. Nagano, J. Beauchamp, Electron impact ionization of phenylsilane. Evidence for the formation of phenylsilyl and silacycloheptatrienyl cations, *J. Am. Chem. Soc.* **1992**, *114*, 3573-3574.
[169] G. A. Olah, G. Rasul, L. Heiliger, J. Bausch, G. K. S. Prakash, Continued search for elusive persistent trivalent organosilyl cations: the claimed trimethylsilyl cation revisited. Attempted preparation of cyclic and halogen-bridged organosilicenium ions, *J. Am. Chem. Soc.* **1992**, *114*, 7737-7742.
[170] T. Nishinaga, Y. Izukawa, K. Komatsu, The First Cyclic π-Conjugated Silylium Ion: The Silatropylium Ion Annelated with Rigid σ-Frameworks, *J. Am. Chem. Soc.* **2000**, *122*, 9312-9313.
[171] M. Ludwig, D. Franz, A. Espinosa Ferao, M. Bolte, F. Hanusch, S. Inoue, Anions featuring an aluminium–silicon core with alumanyl silanide and aluminata-silene characteristics, *Nat. Chem.* **2023**, *15*, 1452-1460.
[172] S. Ito, Y. Ishii, K. Ishimura, T. Kuwabara, A new strategy for hyperconjugative antiaromatic compounds utilizing negative charges: a dibenzo[b,f]silepinyl dianion, *Chem. Commun.* **2021**, *57*, 11330-11333.
[173] T. Ochiai, D. Franz, S. Inoue, Applications of *N*-heterocyclic imines in main group chemistry, *Chem. Soc. Rev.* **2016**, *45*, 6327-6344.
[174] N. Kuhn, U. Abram, C. Maichle-Mößmer, J. Wiethoff, Derivate des Imidazols. XXIV [1].$[Li_{12}O_2Cl_2(ImN)_8(THF)_4]$ · 8 THF: Ein Peroxo-Komplex des Lithiums mit neuartiger Käfigstruktur, *Z. Anorg. Allg. Chem.* **1997**, *623*, 1121-1124.
[175] N. Kuhn, R. Fawzi, M. Steimann, J. Wiethoff, Derivate des Imidazols. XXIII. 2-Iminoimidazolin-Derivate des Magnesiums und Aluminiums, *Z. Anorg. Allg. Chem.* **1997**, *623*, 554-560.
[176] N. Kuhn, R. Fawzi, M. Steimann, J. Wiethoff, Derivate des Imidazols. XXII. Imidazoliniminato-Komplexe des Titans. Synthese und Kristallstrukturen von

[(ImN)$TiCl_3$]$_2$ und [(ImN)$TiCl_3$ · 2 MeCN] (ImN = 1,3-Dimethylimidazolin-2-imino), *Z. Anorg. Allg. Chem.* **1997**, *623*, 769-774.

[177] T. K. Panda, A. G. Trambitas, T. Bannenberg, C. G. Hrib, S. Randoll, P. G. Jones, M. Tamm, Imidazolin-2-iminato Complexes of Rare Earth Metals with Very Short Metal−Nitrogen Bonds: Experimental and Theoretical Studies, *Inorg. Chem.* **2009**, *48*, 5462-5472.

[178] R. Kinjo, B. Donnadieu, G. Bertrand, Isolation of a Carbene-Stabilized Phosphorus Mononitride and Its Radical Cation ($PN^{+\cdot}$), *Angew. Chem. Int. Ed.* **2010**, *49*, 5930-5933.

[179] O. Back, B. Donnadieu, M. von Hopffgarten, S. Klein, R. Tonner, G. Frenking, G. Bertrand, *N*-Heterocyclic carbenes versus transition metals for stabilizing phosphinyl radicals, *Chem. Sci.* **2011**, *2*, 858-861.

[180] F. Dielmann, O. Back, M. Henry-Ellinger, P. Jerabek, G. Frenking, G. Bertrand, A Crystalline Singlet Phosphinonitrene: A Nitrogen Atom–Transfer Agent, *Science* **2012**, *337*, 1526-1528.

[181] F. Dielmann, C. E. Moore, A. L. Rheingold, G. Bertrand, Crystalline, Lewis Base-Free, Cationic Phosphoranimines (Iminophosphonium Salts), *J. Am. Chem. Soc.* **2013**, *135*, 14071-14073.

[182] F. Dielmann, D. M. Andrada, G. Frenking, G. Bertrand, Isolation of Bridging and Terminal Coinage Metal–Nitrene Complexes, *J. Am. Chem. Soc.* **2014**, *136*, 3800-3802.

[183] F. Dielmann, G. Bertrand, Reactivity of a Stable Phosphinonitrene towards Small Molecules, *Chem. Eur. J.* **2015**, *21*, 191-198.

[184] T.-F. Leung, D. Jiang, M.-C. Wu, D. Xiao, W.-M. Ching, G. P. A. Yap, T. Yang, L. Zhao, T.-G. Ong, G. Frenking, Isolable dicarbon stabilized by a single phosphine ligand, *Nat. Chem.* **2021**, *13*, 89-93.

[185] S. Inoue, K. Leszczyńska, An Acyclic Imino-Substituted Silylene: Synthesis, Isolation, and its Facile Conversion into a Zwitterionic Silaimine, *Angew. Chem. Int. Ed.* **2012**, *51*, 8589-8593.

[186] M. W. Lui, C. Merten, M. J. Ferguson, R. McDonald, Y. Xu, E. Rivard, Contrasting Reactivities of Silicon and Germanium Complexes Supported by an N-Heterocyclic Guanidine Ligand, *Inorg. Chem.* **2015**, *54*, 2040-2049.

[187] T. Ochiai, D. Franz, E. Irran, S. Inoue, Formation of an Imino-Stabilized Cyclic Tin(II) Cation from an Amino(imino)stannylene, *Chem. Eur. J.* **2015**, *21*, 6704-6707.

[188] T. Ochiai, D. Franz, X.-N. Wu, S. Inoue, Isolation of a germanium(ii) cation and a germylene iron carbonyl complex utilizing an imidazolin-2-iminato ligand, *Dalton Trans.* **2015**, *44*, 10952-10956.

[189] D. Franz, T. Szilvási, A. Pöthig, S. Inoue, Isolation of an *N*-Heterocyclic Carbene Complex of a Borasilene, *Chem. Eur. J.* **2019**, *25*, 11036-11041.

[190] D. Franz, T. Szilvási, E. Irran, S. Inoue, A monotopic aluminum telluride with an Al=Te double bond stabilized by N-heterocyclic carbenes, *Nat. Commun.* **2015**, *6*, 10037.

[191] T. Ochiai, D. Franz, X.-N. Wu, E. Irran, S. Inoue, A tin analogue of carbenoid: isolation and reactivity of a lithium bis(imidazolin-2-imino)stannylenoid, *Angew. Chem. Int. Ed.* **2016**, *55*, 6983-6987.

[192] T. Ochiai, T. Szilvási, D. Franz, E. Irran, S. Inoue, Isolation and structure of germylene-germyliumylidenes stabilized by *N*-heterocyclic imines, *Angew. Chem. Int. Ed.* **2016**, *55*, 11619-11624.

[193] D. Franz, L. Sirtl, A. Pöthig, S. Inoue, Aluminum Hydrides Stabilized by *N*-Heterocyclic Imines as Catalysts for Hydroborations with Pinacolborane, *Z. Anorg. Allg. Chem.* **2016**, *642*, 1245-1250.

[194] D. Franz, C. Jandl, C. Stark, S. Inoue, Catalytic CO_2 Reduction with Boron- and Aluminum Hydrides, *ChemCatChem* **2019**, *11*, 5275-5281.

[195] M. W. Lui, N. R. Paisley, R. McDonald, M. J. Ferguson, E. Rivard, Metal-Free Dehydrogenation of Amine-Boranes by Tunable *N*-Heterocyclic Iminoboranes, *Chem. Eur. J.* **2016**, *22*, 2134-2145.
[196] C. Weetman, N. Ito, M. Unno, F. Hanusch, S. Inoue, in *Inorganics, Vol. 7*, **2019**.
[197] M. A. Wünsche, P. Mehlmann, T. Witteler, F. Buß, P. Rathmann, F. Dielmann, Imidazolin-2-ylidenaminophosphines as Highly Electron-Rich Ligands for Transition-Metal Catalysts, *Angew. Chem. Int. Ed.* **2015**, *54*, 11857-11860.
[198] F. Buß, P. Mehlmann, C. Mück-Lichtenfeld, K. Bergander, F. Dielmann, Reversible Carbon Dioxide Binding by Simple Lewis Base Adducts with Electron-Rich Phosphines, *J. Am. Chem. Soc.* **2016**, *138*, 1840-1843.
[199] P. Mehlmann, T. Witteler, L. F. B. Wilm, F. Dielmann, Isolation, characterization and reactivity of three-coordinate phosphorus dications isoelectronic to alanes and silylium cations, *Nat. Chem.* **2019**, *11*, 1139-1143.
[200] M. A. Wünsche, T. Witteler, F. Dielmann, Lewis Base Free Oxophosphonium Ions: Tunable, Trigonal-Planar Lewis Acids, *Angew. Chem. Int. Ed.* **2018**, *57*, 7234-7239.
[201] Y. K. Loh, M. Ángeles Fuentes, P. Vasko, S. Aldridge, Successive Protonation of an *N*-Heterocyclic Imine Derived Carbonyl: Superelectrophilic Dication Versus Masked Acylium Ion, *Angew. Chem. Int. Ed.* **2018**, *57*, 16559-16563.
[202] X.-X. Zhao, T. Szilvási, F. Hanusch, S. Inoue, An Isolable Three-Coordinate Germanone and Its Reactivity, *Chem. Eur. J.* **2021**, *27*, 15914-15917.
[203] S. Qiu, X. Zhang, C. Hu, H. Chu, Q. Li, D. A. Ruiz, L. L. Liu, C.-H. Tung, L. Kong, Unveiling Hetero-Enyne Reactivity of Aryliminoboranes: Dearomative Hetero-Diels–Alder-Like Reactions, *Angew. Chem. Int. Ed.* **2022**, *61*, e202205814.
[204] J. Li, Z. Lu, L. L. Liu, A Free Phosphaborene Stable at Room Temperature, *J. Am. Chem. Soc.* **2022**, *144*, 23691-23697.
[205] D. Wendel, T. Szilvási, C. Jandl, S. Inoue, B. Rieger, Twist of a silicon–silicon double bond: Selective anti-addition of hydrogen to an iminodisilene, *J. Am. Chem. Soc.* **2017**, *139*, 9156-9159.
[206] D. Wendel, T. Szilvási, D. Henschel, P. J. Altmann, C. Jandl, S. Inoue, B. Rieger, Precise activation of ammonia and dioxide by an iminodisilene, *Angew. Chem. Int. Ed.* **2018**, *57*, 14575-14579.
[207] R. Holzner, A. Porzelt, U. S. Karaca, F. Kiefer, P. Frisch, D. Wendel, M. C. Holthausen, S. Inoue, Imino(silyl)disilenes: application in versatile bond activation, reversible oxidation and thermal isomerization, *Dalton Trans.* **2021**, *50*, 8785-8793.
[208] S. Du, H. Jia, H. Rong, H. Song, C. Cui, Z. Mo, Synthesis and Reactivity of N-Heterocyclic Silylene Stabilized Disilicon(0) Complexes, *Angew. Chem. Int. Ed.* **2022**, *61*, e202115570.
[209] S. Du, F. Cao, X. Chen, H. Rong, H. Song, Z. Mo, A silylene-stabilized ditin(0) complex and its conversion to methylditin cation and distannavinylidene, *Nat. Commun.* **2023**, *14*, 7474.